Applications of Aziridinium Ylides for the Formation of *N*-heterocycles and Progress Toward the Total Synthesis of Jogyamycin

By

Kate A. Nicastri

A dissertation submitted in partial fulfillment of

the requirements for the degree of

Doctor of Philosophy

(Chemistry)

at the

UNIVERSITY OF WISCONSIN-MADISON

2022

Date of final oral examination: 03/17/2022

The dissertation is approved by the following members of the Final Oral Committee:

Jennifer M. Schomaker, Professor, Organic Chemistry

Tehshik P. Yoon, Professor, Organic Chemistry

Steven D. Burke, Professor, Organic Chemistry

Jeff D. Martell, Assistant Professor, Chemical Biology/Materials Chemistry

This work is dedicated to my mentors. Throughout my life and academic journey, I have been privileged to learn from and be guided by many – thank you.

Abstract

Amines are a prominent motif in natural products, agrochemicals, and pharmaceuticals. In the pharmaceutical sector alone 84% of approved, structurally unique drugs contain at least one nitrogen atom. Given the utility of amines, methods and synthetic routes that generate complex amines are highly sought after. The first section of this work will entail the development of methods for the preparation of densely functionalized and stereochemically complex dehydropiperidines (**Chapter 2**) and dehydromorpholines (**Chapter 3**) through the intermediacy of aziridinium ylides. The development of these methods has enabled the application of aziridinium ylides for the formation of C–C, C–N, and C–O bonds and has led to several mechanistic discoveries that will prove insightful for the expansion of this chemistry.

The second part of this work will be focused on progress toward the total synthesis of jogyamycin (**Chapter 5**). Jogyamycin is a member of the aminocyclopentitol class of natural products most notably recognized for its high antiprotozoal activity against the parasites responsible for malaria and African trypanosomiasis (sleeping sickness). This complex aminated natural product possesses a heteroatom-bearing stereocenter at each cyclic carbon, three contiguous amine stereocenters, and three quaternary stereocenters. Given its dense functionality and high level of complexity, a total synthesis of jogyamycin has so far eluded synthetic chemists. In this section, a new approach toward the total synthesis of jogyamycin will be discussed which includes a key tandem Ichikawa/Winstein rearrangement that sets adjacent amine stereocenters in a single step.

Acknowledgements

I'd like to start by acknowledging my committee, especially Professor Jennifer Schomaker for taking me on as a graduate student and providing me space in her laboratory for the past 5 years. Jen has facilitated my growth as a scientist and given me the opportunity to explore my intellectual curiosities while guiding me through some challenging but fascinating scientific questions. I'd like to thank Professor Steven Burke for the many conversations about my projects. Even though Professor Burke retired, he still found time to answer my emails and elected to stay on my committee – for that I am extremely grateful. I'd also like to acknowledge Professors Tehshik Yoon and Jeffery Martell both of whom have greatly contributed to my growth as a scientist and pushed me to continually improve at every requirement and milestone. To Dr. Nick Hill, working with you has been one of my greatest joys of graduate school. I'm so thankful for your mentorship and support. To Professors Kevin Quinn and Andre Isaacs, as well as Mr. Albert Reid thank you for seeing my potential early on. Lastly, thank you to all present and past members of the Schomaker group who have all contributed to the scientist I am today. I would especially like to thank Dr. Nels Gerstner who saw my potential as an excited first-year graduate student and mentored me throughout my graduate career. I look forward to hearing about your successes in the future.

I'd next like to thank my family. I am the product of the village that raised me. There is much I could say to each and every one of you, but perhaps what I find most important for all of you to know is that I carry a part of each of you with me. To all of my parents, yes, all six (parents, stepparents, and in-laws), to my brothers, sister, brother-in-law, sisters-in-law, their children, and my fiancé: thank you for showing me what it means to be in community with those you love. It is the imperfections of our family that I love the most. Experiencing life with you all has been the universe's greatest gift – thank you.

To all of my friends, I would not have made it to this moment without you. Graduate school has gifted me coworkers that have turned into lifelong friends. To Yun and Emily, I look forward to seeing what you all accomplish in the world. To Logan, who has earned the loving title of my "work husband," thank you for relentlessly challenging me to become a better scientist and for your friendship. To Veronica and Cole, you have unequivocally changed my life. Thank you for all of the support, Sunday dinners, pastry wars, kitty cuddles, and hours-upon-hours of conversation. I'm not sure I have the vocabulary to describe exactly what you both mean to me but, what I can say is that what we share is rare – thank you for being chosen family, I love you.

Table of Contents

Abstract ii

Acknowledgements iii

Table of Contents iv

Abbreviations and Acronyms vii

List of Figures, Schemes, and Tables xiii

Chapter 1

Introduction to carbene transfer and ammonium ylides

1.1 Introduction to Carbene Transfer of Onium Ylides

1.2 Introduction to Carbene Transfer of Ammonium Ylides

1.3 Early Examples of Aziridinium Ylides in the Literature

1.4 Schomaker Group's Contributions to Aziridinium Ylide Formation and Ring Expansion

1.5 Conclusion

1.6 References

Chapter 2

Intermolecular [3+3] Ring-Expansion of Aziridines to Dehydropiperidines through the Intermediacy of Aziridinium Ylides

2.1 Introduction to piperidines and Previous Methods that Access these Motifs by Leveraging Aziridines

2.2 Initial Results

2.3 Optimized Results and Reaction Scope

2.4 Mechanistic Studies

2.5 Other Reaction Derivatives and Post-Synthetic Modifications to Demonstrate Product Utility

2.6 Conclusion

2.7 References

2.8 Experimental Details

2.9 Spectra

2.10 Experimental Details References

Chapter 3

Tunable Aziridinium Ylide Reactivity: Non-covalent Interactions Enable Divergent Product Outcomes

3.1 Introduction

3.2 Initial explorations of diverse carbene precursors

3.3 Controlling Product Outcomes with Temperature

3.4 Controlling Reaction Outcomes by Applying Bond Rotation Data

3.5 Application of Symmetric Diketone Precursors for the Formation of Dehydromorpholines

3.6 Conclusion

3.7 References

3.8 Experimental Details

3.9 Spectra

3.10 Experimental Details References

Chapter 4

Strategies for the Syntheses of Pactamycin and Jogyamycin

4.1 Introduction to Aminocylopentitols

4.2 Syntheses of Pactamycin

4.2.1 Hanessian's Total Synthesis of Pactamycin

4.2.2 Johnson's Total Synthesis of Pactamycin

4.2.3 Concluding Thoughts

4.3 Approaches toward the Core of Jogyamycin

4.3.1 Trost's Progress Toward the Synthesis of Jogyamycin

4.3.2 Schomaker Group: Allene Aziridination Approach

4.3.3 Schomaker Group: Schomaker Group Overman/Ichikawa Approach

4.4.1 Introduction to the Ichikawa/Winstein Approach

4.4.2 The Winstein Rearrangement

4.4.3 Schomaker's Tandem Ichikawa/Winstein Rearrangement Strategy to Set C1 and C2 Simultaneously

4.5 Conclusion

4.6 References

Chapter 5

Progress Toward the Total Synthesis of Jogyamycin: an Ichikawa/Winstein Rearrangement Strategy

5.1 Ichikawa/Winstein Rearrangement Retrosynthetic Analysis

5.2 Progress on the Ichikawa/Winstein Rearrangement Route to Intermediate **5.1**

5.3 Attempts at Allylic Functionalization of Compound **5.1**

5.4 Attempts at Epoxidation of Compound **5.1**

5.5 Revised Dihydroxylation End Game Strategy

5.6 Investigation of Late-Stage C-H Activation Chemistry (Hartwig)

5.7 Incorporation of C6 Primary Alcohol at Outset

5.8 Overall Thought and Conclusions

5.9 References

5.10 Experimental Details

5.11 Spectra

5.12 Experimental Details References

Abbreviations and Acronyms

(S,S)-tBuBOX	(*S,S*)-2,2'-Isopropylidene-bis(4-*tert*-butyl-2-oxazoline)
1,2-DCE	ethylene chloride
ab q	ab quartet
Ac	acetate
AgOTF	silver triflate
Bipy	bipyridine
Bn	benzyl
Boc	tert-butyl carbamate
BOMCl	benzyl chloromethyl ether

Br s	broad singlet
BRSM	based on recovered starting material
Cbz	benzyl carbamate
CSA	camphor sulfonic acid
$Cu(acac)_2$	Copper(II) acetylacetonate
$Cu(hfacac)_2$	Copper(II) hexafluoroacetylacetonate
DBU	1,8-diazabicyclo[5.40]undec-7-ene
Ddd	doublet of doublet of doublets
Dddd	doublet of doublet of doublet of doublets
DDQ	2,3-Dichloro-5,6-dicyano-1,4-benzoquinone
DFT	density functional theory
DIBAL-H	diisobutylaluminum hydride
DMA	N,N-dimethylacetamide
DMAP	N,N-dimethylpyridin-4-amine
Dmbox	dimethyl box
DMDO	dimethyldioxirane
DMF	dimethyl formamide
DMP	Dess-Martin periodinane
DMSO	dimethyl sulfoxide

dr	diastereomeric ratio
dt	doublet of triplets
dtd	doublet of triplet of doublets
dtt	doublet of triplet of triplets
EDA	ethyl diazoacetate
EDC	N-(3-Dimethylaminopropyl)-N’-ethylcarbodiimide hydrochloride
ee	enantiomeric excess
eq.	equivalent
er	*enantiomeric ratio*
Et	ethyl
EtOAc	ethyl acetate
EtOH	ethanol
EWG	electron withdrawing group
G-II	Grubbs-II
Hex	Hexane
IBX	2-iodoxybenzoic acid
INT	intermediate
iPr	isopropyl

Kcarb	potassium carbonate
Kcal	kilo calorie
KHMDS	potassium hexamethyldisilazide
LDA	lithium diisopropyl amide
LiHMDS	lithium hexamethyldisilazide
LP	lone pair
M	metal
m	meta
m-CPBA	meta-chloroperoxybenzoic acid
Me	methyl
MeCN	acetonitrile
MeLi	methyl lithium
MeOH	methanol
MHz	mega hertz
mM	milli molar
MS	mass spectrometery
MSA	methyl salicylic acid
MsCl	mesyl chloride

NaHMDS	sodium hexamethyldisilazide
Nbe	norbornene
NBO	natural bond order
n-BuLi	n-butyl lithium
NCI	non-covalent interaction
nM	nanomolar
NMO	4-methylmorpholine N-oxide
NMR	nuclear magnetic resonance
o	ortho
p	para
PDC	pyridinium dichromate
PG	protecting group
Ph	phenyl
PhIO	iodosobenzene
PhMe	toluene
PMB	4-methoxybenzyl
Pyr.	pyridine
q	quartet

rac	racemic
RRCM	relay ring-closing metathesis
RSG	radical stabilizing group
SES	2-(trimethylsilyl)eethanesulfonyl
SOPT	second-order perturbation theory
T	triplet
TAI	trichloroacetyl isocyanate
TASF	tris(dimethylamino)sulfonium difluorotrimethylsilicate
TBAF	tetra-n-butyl ammonium fluoride
TBDPSCl	tert-Butyl(chloro)diphenyl silane
TBHP	tert-Butyl hydrogen peroxide
TBS	tert-Butyldimethyl silane
TBSOTf	tert-Butyldimethylsilyl trifluoromethanesulfonate
tBuLi	tert-Butyl lithium
td	triplet of doublets
TEMPO	2,2,6,6-tetramethyl piperidine 1-oxyl
TES	triethyl silyl
TESCl	triethyl silyl chloride

Tf_2O	triflic anhydride
TFA	trifluoroacetic acid
TFPAA	trifluoro peracetic acid
THF	tetrahydrofuran
TMM	trimethylenemethane
TMS	trimethyl silyl
TMSCl	trimethyl silyl chloride
UHP	urea hydrogen peroxide
VT	variable temperature
μM	micromolar

List of Schemes, Figures, and Tables

Figure 1.1. Metallocarbene-derived ylide formation and subsequent transformations. 3

Figure 1.2. a. General representation of ammonium ylides. b. General structures of both sp^2 and sp^3 nitrogen ylides. 4

Figure 1.3. a. Base-mediated generation of ammonium ylides. b. Generation of ammonium ylides *via* reaction with a metal-supported carbene. 4

Figure 1.4. a. General [2.3]-sigmatriopic rearrangement of allylic amines. b. [1,2]-Stevens shift. c. N-H insertion reaction *via* protic ammonium ylides. d. Electrophilic trapping of a protic ammonium ylide (cyclization is shown but can present as a multi-component reaction). 5

Figure 1.5. a. Example aziridinium ylide b. Pyramidal inversion. 6

Scheme 1.1. Seminal report of aziridinium ylides by Watanabe. 7

Scheme 1.2. Intramolecular [2,3]-sigmatropic rearrangement of vinyl aziridine to indolizidine type compounds. 8

Scheme 1.3. Intramolecular [2,3]-sigmatropic rearrangement and competitive [1,5]-hydrogen shift of vinyl aziridine. 9

Scheme 1.4. Bicyclic aziridines generated by silver nitrene transfer catalysis. 10

Scheme 1.5. Scope and mechanistic studies of [3+1]-ring expansion to furnish bicyclic methylene azetidines *via* the intermediacy of an aziridinium ylide. 11

Figure 2.1. Selected examples of transition metal-catalyzed ring expansions of aziridines to *N*-heterocycles. 23

Scheme 2.1. Proposed reactivity 24

Scheme 2.2. Initial results with saturated bicyclic aziridines 25

Table 2.1. Scope of ring-expansion with various aziridines 26

Table 2.2. Scope of ring-expansion with various styrenyl aziridines 27

Figure 2.2. Computed reaction profile for the process involving aziridine **2.1b** 28

Scheme 2.3. Enantiotransfer experiment using sequential silver-catalyzed transfer and Rh-mediated aziridinium ylide formation. 32

Scheme 2.4. Streamlined sequential nitrene/carbene transfer 32

Scheme 2.5. Post synthetic modifications. 33

Scheme 2.6. Dehydropiperidine formation using diazoacetates derived from biomolecules. 34

Figure S-2.1. Racemic standard for (*S,R*)-**2.1c.** 69

Figure S-2.2. Scalemic aziridine (*S,R*)-**2.1c** utilized in the synthesis of (*R,R,R*)-**2.6ca**. 70

Figure S-2.3. Racemic standard for piperidine (*R,R,R*)-**2.6ca**. 71

Figure S-2.4. Scalemic piperidine (*R,R,R*)-**2.6ca**. 71

Figure S-2.5. A molecular drawing of **2.6cc** shown with 50% probability ellipsoids. All H atoms are omitted. 79

Figure S-2.6. A molecular drawing of one organic molecule from **2.6cc** shown with 50% ellipsoids. The other molecule and all hydrogen atoms are omitted. 80

Figure S-2.7. A molecular drawing of the overlay of the two molecules from **2.6cc** shown with 50% ellipsoids. The molecule with suffix "A" was inverted and drawn in green. 80

Table S-1. Crystal data and structure refinement for **2.6cc**. 80

Table S-2.2. Fractional Atomic Coordinates ($\times 10^4$) and equivalent isotropic displacement parameters ($Å^2 \times 10^3$) for **2.6cc**. U_{eq} is defined as 1/3 of the trace of the orthogonalized U_{IJ} tensor. 81

Table S-2.3. Anisotropic Displacement Parameters ($Å^2 \times 10^3$) for **2.6cc**. The anisotropic displacement factor exponent takes the form: $-2\pi^2[h^2a^{*2}U_{11}+2hka^*b^*U_{12}+\ldots]$. 83

Table S-2.4. Bond lengths for **2.6cc**. 85

Table S-2.5. Bond angles for **2.6cc**. 87

Table S-2.6. Torsion angles for **2.6cc**. 88

Table S-2.7. Hydrogen atom coordinates ($Å \times 10^4$) and isotropic displacement parameters ($Å^2 \times 10^3$) for **2.6cc**. 90

Figure S-2.8. Computed (SCM(CH_2Cl_2)-B3LYP-D3/def2-SVP level) intrinsic reaction coordinate for the transformation of **TS2'** into **2.6ba**. 92

Scheme 3.1. Prior work in aziridnium ylide chemistry and new divergent reactivity. 214

Scheme 3.2. Ring expansions of 3.1 with donor-acceptor diazoketone carbene precursors 215

Figure 3.1. a. Computed reaction energy profiles for formation of **3.3a** and **3.4a**. 217
b. Contour plots (top) of the reduced density gradient isosurfaces (density cutoff of 0.04 a.u.) for intermediate **INT2**.

Scheme 3.3 a. Controlling product distribution using temperature. b. Computed reaction profile (relative free energies are given in kcal/mol) for intermediate **INT4**. **c.** Scope of the process. 219

Figure 3.2. Computed barriers for C–N bond rotation in aziridinium ylides from diverse carbene precursors. 221

Scheme 3.4. Competing cheletropic extrusion/ring expansion to dehydromorpholines. See caption to **Figure 1** for computational details. 224

Figure 3.3. ^{1}H NMR time course data for the reaction of **3.1** and **3.2e**. 225

Scheme 3.5. Dehydromorpholine formation from symmetric carbene precursors. 227

Figure S-3.1. Racemic bicyclic aziridine **3.15** HPLC data. 257

Figure S-3.2. Enantioenriched bicyclic aziridine (*S,R*)-**3.15** HPLC data. 257

Figure S-3.3. Racemic morpholin **3.15f** HPLC data. 258

Figure S-3.4. Enantioenriched morpholine (*S,R*)-**3.15f** HPLC data 259

Figure S-3.5. Limitations of reaction scope. 260

Figure S-3.6. NMR time course studies of the transformation of **3.1** and **3.2e** to **3.3e**, **3.4e** and **3.5e**. 261

Figure S-3.7. Zoom-in of relevant peaks. 262

Figure S-3.8. HSQC spectrum of reaction aliquot (transformation of **3.1** and **3.2e** to **3.3e**, **3.4e** and **3.5e**). 263

Figure S-3.9. 1D-TOCSY of reaction aliquot (**2h**). Irradiation of the apparent t at 4.69 ppm reveals the full chain for the unique compound proposed to be compound **3.3e**. 264

Figure S-3.10. A molecular drawing of the first symmetry-independent molecule in **3.3a** shown with 50% probability ellipsoids. 266

Figure S-3.11. A molecular drawing of the second symmetry-independent molecule in **3.3a** shown with 50% probability ellipsoids. 266

Figure S-3.12. An overlay of the two symmetry-independent molecules in **3.3a** shown with 50% probability ellipsoids. One of the enantiomers was inverted to demonstrate the conformation similarity. 267

Table S-1. Crystal data and structure refinement for **3.3a**. 267

Table S-3.2. Fractional atomic coordinates ($\times 10^4$) and equivalent isotropic displacement parameters ($Å^2 \times 10^3$) for **3.3a**. U_{eq} is defined as 1/3 of the trace of the orthogonalised U_{IJ} tensor. 268

Table S-3.3. Anisotropic displacement parameters ($Å^2 \times 10^3$) for **3.3a**. The anisotropic displacement factor exponent takes the form: $-2\pi^2[h^2a^{*2}U_{11}+2hka^*b^*U_{12}+\ldots]$. 269

Table S-3.4. Bond lengths for **3.3a**. 270

Table S-3.5. Bond angles for **3.3a**. 270

Table S-3.6. Torsion angles for **3.3a**. 270

Table S-3.7. Hydrogen atom coordinates ($Å \times 10^4$) and isotropic displacement parameters ($Å^2 \times 10^3$) for **3.3a**. 273

Figure S-3.13. A molecular drawing of **3.4e** shown with 50% probability ellipsoids. 275

Table S-3.8. Crystal data and structure refinement for **3.4e.** 275

Table S-3.9. Fractional atomic coordinates ($\times 10^4$) and equivalent isotropic displacement parameters ($Å^2 \times 10^3$) for **3.4e**. U_{eq} is defined as 1/3 of the trace of the orthogonalized U_{IJ} tensor. 276

Table S-3.10. Anisotropic displacement parameters ($Å^2 \times 10^3$) for **3.4e**. The anisotropic displacement factor exponent takes the form: $2\pi^2[h^2a^{*2}U_{11}+2hka^*b^*U_{12}+\ldots]$. 277

Table S-3.11. Bond lengths for **3.4e**. 277

Table S-3.12. Bond angles for **3.4e.** 278

Table S-3.13. Torsion angles for **3.4e**. 278

Table S-3.14. Hydrogen atom coordinates (Å×10^4) and isotropic displacement parameters (Å^2×10^3) for **3.4e**. 279

Figure S-3.14. Contour plots of the reduced density gradient isosurfaces for intermediate **INT2-Rh** and associated SOPT-NBO stabilizing energy. 280

Figure S-3.15. Computed (SMD-B3LYP-D3/def2-SVP level) alternative pathways from ylide **INT6**. Relative free energies DG, at 298 K) are given in kcal/mol. 281

Figure 4.1. The aminocyclopentitol family of natural products and genetically engineered analogues. 403

Figure 4.2. Biological activity of the aminocyclopentitol family and genetically engineered analogues. 404

Scheme 4.1. a. Retrosynthetic analysis of Hanessian's route to pactamycin **4.1** b. Forward route to pactamycin **4.1.** 407

Scheme 4.2. Johnson's partial route to pactamycin. 409

Scheme 4.3. Retrosynthetic analysis of Johnson's successful route to pactamycin **4.1** b. Forward route of Johnson's successful synthesis of pactamycin **4.1.** 411

Scheme 4.4. a. Retrosynthetic analysis of Trost's partial synthesis of jogyamycin **4.2** b. Forward synthesis of Trost's partial synthesis of jogyamycin **4.2.** 414

Scheme 4.5. Second half of Trost's partial synthesis of jogyamycin **4.2.** 415

Scheme 4.6. a. Retrosynthetic analysis to Schomaker's allene aziridination strategy to the core of jogyamycin **4.2** b. Forward route to the core of jogyamycin **4.2.** 417

Scheme 4.7. a. Retrosynthetic analysis of Schomaker's Ichikawa/Overman rearrangement strategy to jogyamycin **4.2** b. Forward route to the core of jogyamycin **4.2.** 420

Scheme 4.8. Failed Overman and Ichikawa reactions. 422

Scheme 4.9. a. The Winstein rearrangement b. ^{15}N labeling experiment to unambiguously identify the [3,3]-sigmatropic mechanism of the Winstein rearrangement. 424

Scheme 4.10. Schomaker's tandem Ichikawa/Winstein rearrangement strategy to set C1 and C2 simultaneously. 425

Scheme 5.1. Retrosynthetic analysis of the Ichikawa/Winstein rearrangement route. 430

Scheme 5.2. Aldol condensation and protection to form conjugated ester **5.4.** 431

Scheme 5.3. Organometallic addition for the synthesis of methyl ketones. 432

Scheme 5.4. Organometallic addition to ketone **5.8** for the formation of the C5 stereocenter. 433

Scheme 5.5. RRCM of **5.11** for formation of the core of jogyamycin **4.2.** 434

Scheme 5.6. Azidation and protecting group manipulation for the formation of Ichikawa precursor **5.2.** 435

Scheme 5.7. Tandem Ichikawa/Winstein rearrangement and hypothesized by-product formation. 436

Scheme 5.8. End game strategy via allylic functionalization of the C4 methyl group. 437

Scheme 5.9. Attempted allylic oxidation of **5.1** and **5.2.** 438

Scheme 5.10. Temperature and base stability studies of **5.1.** 439

Scheme 5.11. Harsher allylic oxidation conditions applied to **5.1.** 440

Scheme 5.12. Attempted allylic oxidation on C5-BOM deprotected **5.29.** 440

Scheme 5.13. Potential mechanism of urea decomposition *via* oxidants. 441

Scheme 5.14. Attempts at olefin oxidation of intermediate **5.1.** 442

Scheme 5.15. Exposure of **5.1** to TFPAA for C3/C4 olefin oxidation. 442

Scheme 5.16. Attempts at Metal-Catalyzed Epoxidation Reactions of **5.1.** 443

Scheme 5.17. Attempts at olefin oxidation of amine **5.32** with TFPAA. 443

Scheme 5.18. Attempts at olefin oxidation with OsO_4. 444

Scheme 5.19. Olefin dihydroxylation with RuO_4. 445

Scheme 5.20. New dihydroxylation end game strategy. 446

Scheme 5.21. Acetate protection of diol **5.39.** 447

Scheme 5.22. Attempts at elimination of the C4 tertiary alcohol of **5.41.** 448

Scheme 5.23. Attempts at C4 tertiary alcohol elimination of **5.41** *via* mesylate formation. 449

Scheme 5.24. Attempts to access the C4 tertiary alcohol by oxidation of the C2 alcohol in **5.41.** 450

Scheme 5.25. Possible alternative late-stage oxidation strategy, Hartwig unactivated C-H oxidation conditions. 450

Scheme 5.26. Suggested substrates for Hartwig's C-H activation chemistry. 451

Scheme 5.27. Hartwig C–H activation chemistry on tertiary azide **5.48.** 451

Scheme 5.28. Hartwig CH activation chemistry on urea **5.47.** 452

Scheme 5.29. Hartwig CH activation chemistry on aldol product **5.49.** 453

Scheme. 5.30. Incorporation of the C6 alcohol at the outset, proposed application of the Fleming-Tamao reaction. 454

Scheme 5.31. Synthesis of the Fleming-Tamao substrate**.** 455

Scheme 5.32. Attempted aldol reaction with **5.53**. 455

Chapter 1. Introduction to Aziridinium Ylides

Portions of this chapter have been published and reprinted with permission from:

Dequina, H. J.*; **Nicastri, K. A.***; Schomaker, J. M. Chapter One - Additions of N, O, and S Heteroatoms to Metal-Supported Carbenes: Mechanism and Synthetic Applications in Modern Organic Chemistry. In *Advances in Organometallic Chemistry*; Pérez, P. J., Ed.; Academic Press, 2021, Vol. 76, pp. 1–100

Copyright © 2022 Elsevier Inc. All rights reserved

1.1 Introduction to Carbene Transfer of Onium Ylides

Carbene transfer reactions comprise a useful class of transformations for the formation of new C–C or C–X bonds, particularly in the construction of complex carbo- and heterocyclic motifs present in diverse bioactive small molecules and natural products. These reactions are typically conducted in the presence of transition metal catalysts which facilitate access to the desired metal carbene intermediates from bench-stable precursors and enables some control over carbene reactivity via the choice of metal and ligand. Metal carbenes derived from α-diazocarbonyl compounds are among the most common, as they display high electrophilicity, allowing them to readily react with nucleophiles to generate versatile ylide intermediates.[1] An ylide is a molecular species containing a negatively charged carbon atom adjacent to a positively charged heteroatom (referred to as an 'onium' group).[2] Synthetic applications of ylides were not widely explored until after the pioneering work of Wittig in 1953, where phosphonium ylides were employed for the preparation of alkenes from aldehydes and ketones.[3]

The general process of ylide formation between a metal carbene complex and a Lewis base begins with a double umpolung of the carbenic carbon (**Figure 1.1**).[2] The metal complex, generally derived from a copper(I) or dirhodium(II) catalyst, behaves as a Lewis acid and accepts electrons from the diazo carbon at its vacant coordination site; since the turn of the century, the breadth of metal complexes aiding in productive carbene transfer has been extended to include those of ruthenium[4-11], iron[12-17], palladium[18-20], silver[21-24], and cobalt.[25-33] Electron back-donation from the metal complex to the carbenic carbon and the concomitant loss of dinitrogen generates the metal carbene species (**Figure 1.1**). In its capacity as a Lewis acid, the metal carbene intermediate can then accept electrons from the heteroatom of a Lewis base to generate the metal-associated ylide, which can subsequently dissociate to furnish the free ylide species. Common Lewis bases reported

to add to metal-supported carbenes to furnish ylides include amines, ethers, and sulfides; ylide formation can occur in either an inter- or intramolecular fashion. These versatile ylide intermediates can undergo a host of subsequent transformations, including rearrangements ([1,2]-Stevens and [2,3]-sigmatropic rearrangements),[34-35] X−H insertions, as well as multicomponent reactions (MCRs)[36] to provide a powerful synthetic approach toward the rapid construction of structurally complex products.

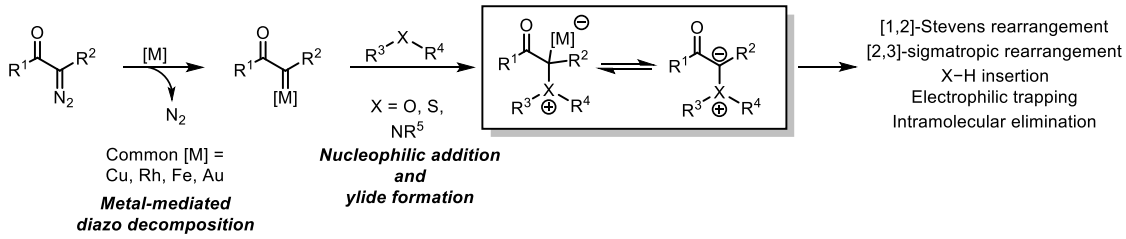


Figure 1.1 – Metallocarbene-derived ylide formation and subsequent transformations.

1.2 Introduction to Carbene Transfer of Ammonium Ylides

Nitrogen ylides are a subset of onium ylides that contain a positively charged nitrogen atom adjacent to a carbanion (**Figure 1.2a**). The hybridization of the nitrogen atom plays a significant role in the resultant reactivity;[37-39] as such, this general structure can be further defined by subdividing the ylides into *N*-sp^2 and *N*-sp^3 ylides. The *N*-sp^2 ylides include azomethine, pyridinium, and triazolium ylides (**Figure 1.2b, left**).[40-42] In contrast, ammonium ylides contain a sp^3-hybridized nitrogen atom adjacent to a carbanionic site (**Figure 1.2b, right**).

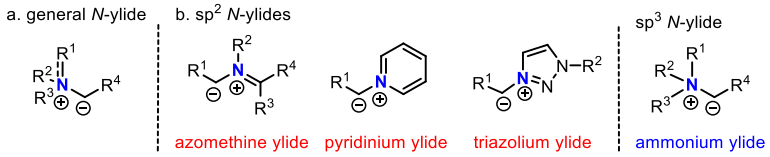


Figure 1.2 – a. General representation of ammonium ylides. b. General structures of both sp^2 and sp^3 nitrogen ylides.

Ammonium ylides are commonly generated in two ways. The first approach involves base-induced deprotonation of a quaternary ammonium salt in situ to deliver the corresponding ylide (**Figure 1.3a**). An extensive body of work has been reported in this area in recent years and its application in asymmetric cyclization reactions has been recently reviewed.[39] A second approach to generate ammonium ylides involves the reaction between an amine and a metal-supported carbene (**Figure 1.3b**). These reactions are less well-explored than base-induced ammonium ylide formations but do offer unique opportunities to expand novel chemical space and generate complex molecules in a relatively rapid fashion.

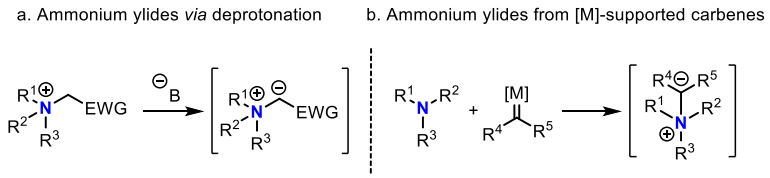


Figure 1.3 – a. Base-mediated generation of ammonium ylides b. Generation of ammonium ylides *via* reaction with a metal-supported carbene.

Reactions of ammonium ylides generated via the reaction of an amine with a metal-supported carbene can be divided into four categories (**Figure 1.4**). One class of reactions involves rearrangement processes that include [2,3]-sigmatropic, [1,2]-Stevens rearrangements, and other lesser-known sigmatropic-like transformations. A [2,3]-sigmatropic rearrangement is a pericyclic reaction in which an onium group, in this case, an amine, substituted with an allyl group reacts

with a metal-supported carbene to furnish an ammonium ylide. The initial *N*-allyl group is transposed to the anionic ylide carbon to furnish the rearrangement product (**Figure 1.4a**). In contrast, [1,2]-Stevens rearrangements are symmetry-forbidden and are hypothesized to occur

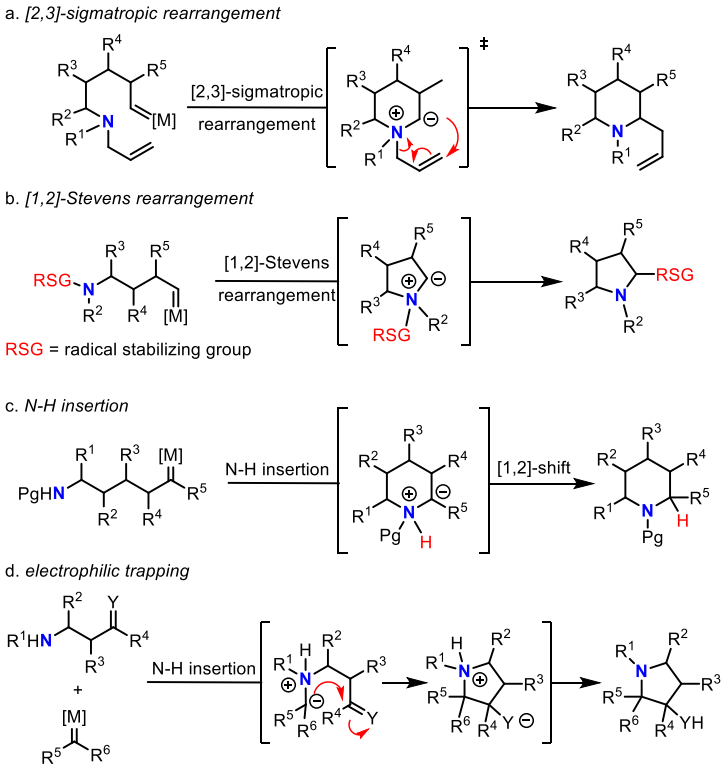


Figure 1.4 – a. General [2,3]-sigmatropic rearrangement of allylic amines. b. [1,2]-Stevens shift. **c**. N-H insertion reaction *via* protic ammonium ylides. d. Electrophilic trapping of a protic ammonium ylide (cyclization is shown but can present as a multi-component reaction).

through stepwise radical pathways (**Figure 1.4b**). For this reason, the [1,2]-Stevens rearrangement can occur on many different types of amines as long as the reaction proceeds in the presence of a radical-stabilizing group. The reaction of metal-supported carbenes with secondary amines is another common way to generate protic ammonium ylides. These intermediates can undergo two divergent reaction pathways that involve either N-H insertion or electrophilic trapping. N-H insertion occurs when the ammonium ylide intermediate undergoes a [1,2]-shift to deliver a new

amine product (**Figure 1.4c**). In contrast, if a protic ammonium ylide is intercepted with an electrophile before the [1,2]-shift, a delayed proton transfer can yield products resulting from intramolecular cyclizations or novel multi-component reactions (**Figure 1.4d**, intramolecular cyclization pictured).

The remainder of this chapter will focus on the generation of aziridinium ylides, a subset of ammonium ylides (**Figure 1.5a**). In contrast to their acyclic counterparts, aziridinium ylides are embedded in a highly strained ring, where the bonding constraints of the aziridine increases the free energy to pyramidal inversion of the nitrogen; often this rate is slow enough to measure using variable temperature (VT) or dynamic NMR spectroscopy (**Figure 1.5b**).[43] The presence of two invertomers that slowly interconvert (compared to free amines) hinders the ability to selectively form and engage aziridinium ylides in secondary reactions and has limited their applications in the synthesis of complex *N*-heterocycles. The following section will focus on the challenges and successes associated with employing aziridinium ylides in the syntheses of diverse *N*-heterocycles.

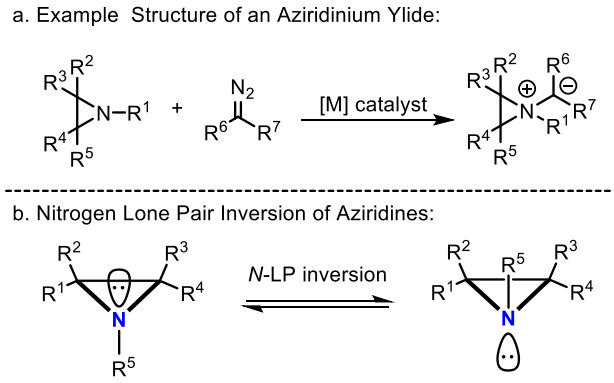
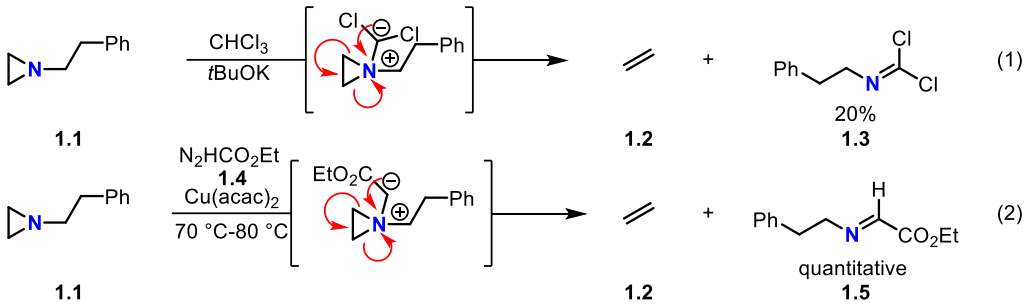


Figure 1.5 – a. Example aziridinium ylide b. Pyramidal inversion.

1.3 Early Examples of Aziridinium Ylides in the Literature

The first mention of an aziridinium ylide in the literature was by Watanabe in 1972.[44] In this seminal work, Watanabe examined the reaction of an alkyl aziridine **1.1** with a dichlorocarbene which furnished ethylene **1.2** and imine **1.3 (Scheme 1.1 eq. 1)**; hypothesized to occur through a cheletropic extrusion mechanism. Unfortunately, the use of highly reactive dichlorocarbenes led to low yields and competing side reactions. Later, Watanabe recognized that off-target reactivity could be controlled by employing a metal catalyst such as $Cu(acac)_2$. When the same reaction was performed with ethyl diazoacetate (EDA) **1.4** ethylene **1.2** and the corresponding imine **1.5** were generated in quantitative yield (**Scheme 1.1 eq. 2**). Although a step forward in the use of aziridinium ylides as reactive intermediates in synthesis, the authors never found a way to circumvent the undesired cheletropic extrusion process in favor of a productive ring expansion or cyclization.

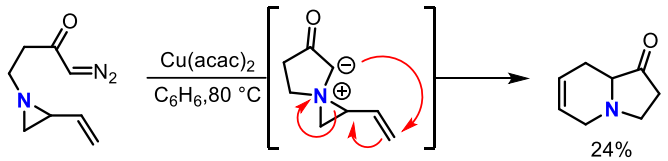
Scheme 1.1 – Seminal report of aziridinium ylides by Watanabe.



In 2001, Clark reported an aziridinium ylide-mediated ring expansion of vinyl aziridines to the corresponding indolizidine product.[45] In this reaction, vinyl aziridine **1.6** underwent intramolecular aziridinium ylide formation in the presence of $Cu(acac)_2$ to furnish indolizidine **1.7,** presumably via a [2,3]-sigmatropic rearrangement (**Scheme 1.2**). The authors attributed the modest yield to the instability of the vinyl aziridine, mentioning that the substrate decomposed within one day when it was stored under argon at -30 ˚C. Another possibility for low-yield is off-

target reactivity of the intermediate aziridinium ylide, or further reaction of the indolizidine product although this is never specifically mentioned.

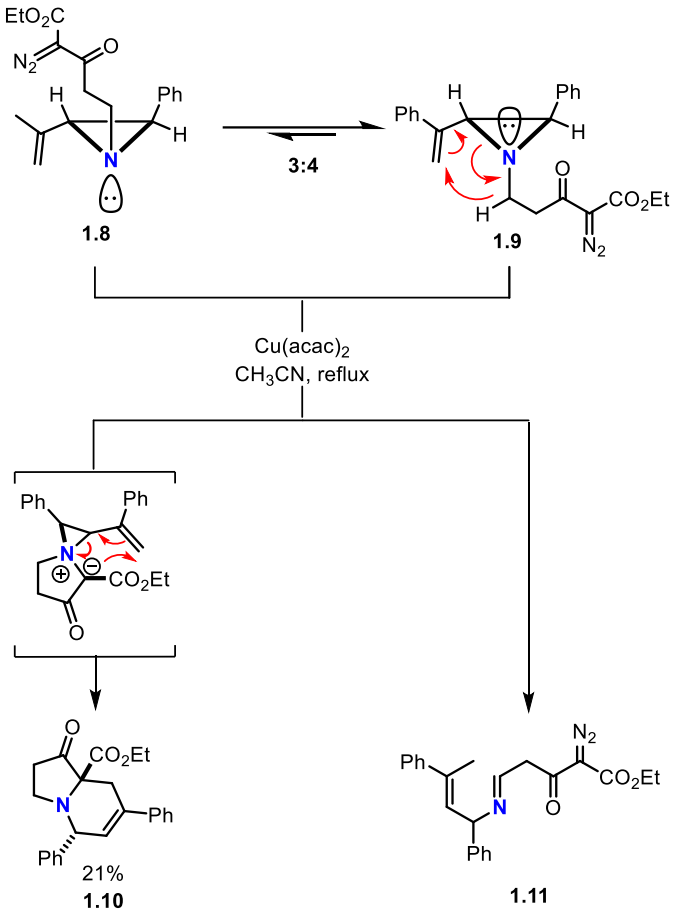
Scheme 1.2 – Intramolecular [2,3]-sigmatropic rearrangement of vinyl aziridine to indolizidine type compounds.



1.6 **1.7**

In 2004, Rowlands disclosed a single example of aziridine ring expansion through the intermediacy of an aziridinium ylide.[46] In this report, the authors specified that the desired vinyl aziridine exists as a 3:4 mixture of nitrogen invertomers (**1.8:1.9**) favoring the invertomer bearing a *syn* relationship between the appendant nitrogen alkyl chain and the vinyl substituent. When this aziridine was exposed to $Cu(acac)_2$ in refluxing acetonitrile, only 21% of the desired [2,3]-sigmatropic rearrangement **1.10** was observed (**Scheme 1.3**). The low yield was attributed to the mixture of nitrogen invertomers, as only the minor invertomer possessed the required geometry for rearrangement. The remainder of the mass-balance was accounted for by a competitive 1,5-hydride shift of the major invertomer to furnish imine **1.11.** As this rearrangement proceeded before nitrogen lone-pair inversion could occur, the remainder of the mass balance was accounted for by this off-target reactivity. Rowland's work highlights the importance of nitrogen lone pair inversion for productive ylide formation. To generate a successful reaction, one must either generate substrates that do not undergo lone-pair inversion, or design aziridine substrates that can undergo fast lone-pair inversion to outcompete off-target reactivity.

Scheme 1.3 – Intramolecular [2,3]-sigmatropic rearrangement and competitive [1,5]-hydrogen shift of vinyl aziridines.

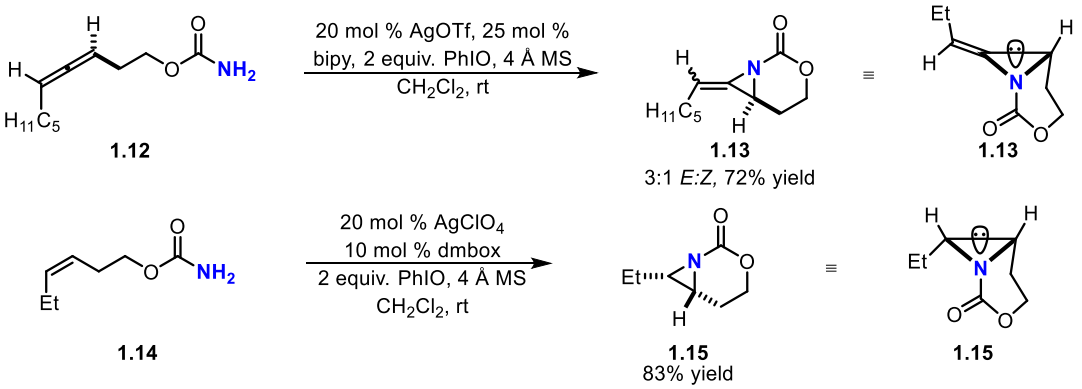


1.4 Schomaker Group's Contribution to Aziridinium Ylide Formation and Ring Expansion

The Schomaker group has reported methods to generate aziridines using silver nitrene transfer catalysis.[48] Selective access to both bicyclic methylene aziridines (**1.13)**, and saturated bicyclic aziridines, (**1.15)**, can be achieved from simple homoallylic allenes (**1.12)** and homoallylic alkenes (**1.14)** (**Scheme 1.4**). Importantly, these aziridines have characteristics that make them stand out as excellent substrates for aziridinium ylide formation. The nitrogen lone pair is ~sp^3 hybridized and does not undergo effective conjugation with the carbamate tether. As a result, the carbamate behaves as a σ-electron-withdrawing group, which has been reported to raise the barrier

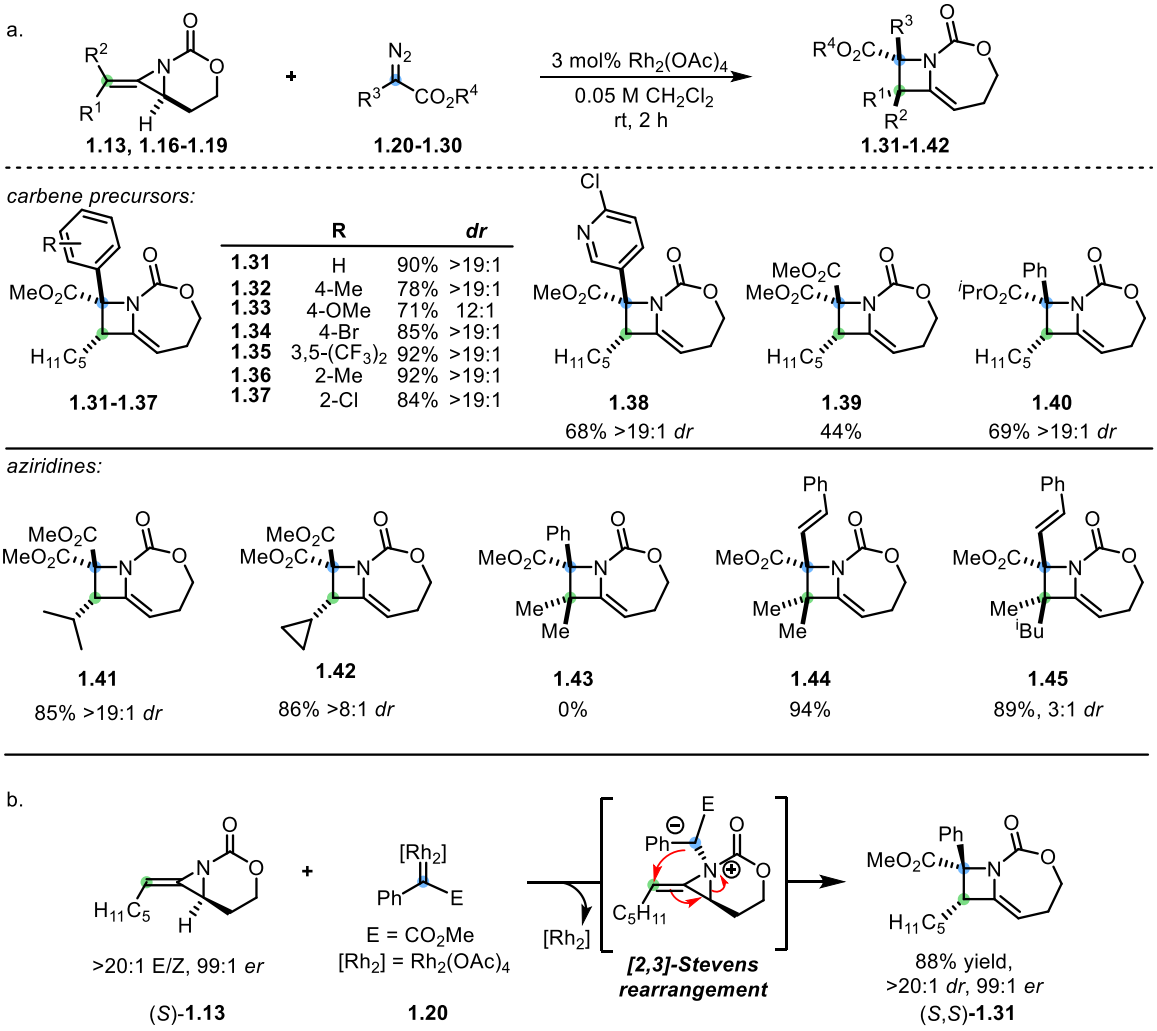
to *N*-pyramidal inversion.[47] Additionally, the geometric constraint imposed by the bicyclic nature of the tether raises the nitrogen inversion barrier;[47] an effect observed in rigid cyclic amines such as sparteine and Tröger's base.[49,50] Both of these unique structural characteristics work synergistically to furnish a set of substrates that do not undergo observable nitrogen inversion. We hypothesized that by using substrates incapable of *N*-lone pair inversion that we could generate diastereomerically pure aziridinium ylides that avoid off-target reactivity and generate synthetically useful ring-expansion products.

Scheme 1.4 – Bicyclic aziridines generated by silver nitrene transfer catalysis.



In 2017, the Schomaker group reported that bicyclic methylene aziridines such as **1.13, 1.16-1.19** could be transformed to highly substituted methylene azetidines **1.31-1.42** via an intermolecular [3+1] ring expansion reaction with donor/acceptor carbenes (**Scheme 1.5a**).[51] The key aziridinium ylide intermediate was generated by nucleophilic addition of the methylene aziridine nitrogen to a rhodium-bound carbene (**Scheme 1.5b**); as previously noted, successful ylide formation benefited from the electron-withdrawing groups on the nitrogen and the structural rigidity imparted by the bicyclic nature of the aziridine to deliver these products in high yield and *dr*.

Scheme 1.5 – Scope and mechanistic studies of [3+1]-ring expansion to furnish bicyclic methylene azetidines *via* the intermediacy of an aziridinium ylide.



This reaction displayed a broad substrate scope in comparison to the reactions described above. Differentially substituted aryl groups on the carbene precursors did not have a significant effect on the reaction outcome, furnishing methylene azetidines all in high yield and *dr* (**Scheme 1.5a**). This method could also be extended to carbenes derived from iodonium ylides such as **1.28** to deliver **1.39**: expanding the number of viable carbene sources applicable in this chemistry. Aziridine

substitution was also variable with both isopropyl (**1.41**) and cyclopropane substitutions (**1.42**) being tolerated. Steric hindrance prevented the formation of methylene azetidines from terminally disubstituted aziridines such as **1.18/1.19** , however, fully substituted methylene azetidines **1.44** and **1.45** could be obtained upon modification of the carbene precursor to a less hindered styrenyl diazoester partner. Although the *dr* is somewhat variable when employing styrenyl diazoacetate **1.19**, it is important to note that reactions with styrenyl diazoesters did not appear to furnish any additional [n+1] ring expansions, reinforcing the uniquely high selectivity of this transformation.

Studies with exogenous TEMPO gave no change in selectivity in the reaction and application of a cyclopropane ring of **1.17** (**Scheme 1.5a**) did not yield any cyclopropane ring-opened products suggesting against a radical-based mechanism. In addition, the reaction of enantiopure **1.13** demonstrates excellent chirality transfer from the aziridine stereocenter before its ablation (**Scheme 1.5b**). An initially proposed mechanism involved a 2-amidoallyl cation; however, upon further computational studies, the most likely pathway was concluded to involve a highly asynchronous, concerted [2,3]-Stevens rearrangement.[52]

Overall, the strained bicyclic framework of methylene aziridines and the unique reactivity of aziridinium ylides allowed for an efficient and stereospecific transformation to forge two new C−C and C−N bonds, as well as two adjacent stereocenters. This work represents the first synthetically useful intermolecular transformation of aziridinium ylides to furnish highly substituted and diastereomerically pure *N*-heterocycles.

1.5 Conclusion

Aziridinium ylides are underutilized intermediates for the synthesis of *N*-heterocycles. Many of the challenges associated with leveraging them in synthetically useful ways have

stemmed from the high reactivity of the intermediate ylides and the challenges associated with forming them selectively. The Schomaker group has shown that with careful manipulation and understanding of aziridine scaffolds that this reactivity can be controlled, and more importantly, leveraged to deliver highly diastereomerically pure and complex *N*-heterocycles such as methylene azetidines. The following chapters will contain two additional reports of *N*-heterocycle formation *via* the intermediacy of aziridinium ylides that expand both the synthetic utility and mechanistic understanding in this field of chemistry.

1.6 References

(1) Ford, A.; Miel, H.; Ring, A.; Slattery, C. N.; Maguire, A. R.; McKervey, M. A. Modern Organic Synthesis with α-Diazocarbonyl Compounds. *Chem. Rev.* **2015**, *115*, 9981–10080.

(2) Padwa, Albert.; Hornbuckle, S. F. Ylide Formation from the Reaction of Carbenes and Carbenoids with Heteroatom Lone Pairs. *Chem. Rev.* **1991**, *91*, 263–309.

(3) Wittig, G.; Geissler, G. Zur Reaktionsweise Des Pentaphenyl-Phosphors Und Einiger Derivate. *Justus Liebigs Ann. Chem.* **1953**, *580*, 44–57.

(4) Simonneaux, G.; Galardon, E.; Paul-Roth, C.; Gulea, M.; Masson, S. Ruthenium–Porphyrin-Catalyzed Carbenoid Addition to Allylic Compounds: Application to [2,3]-Sigmatropic Rearrangements of Ylides. *J. Organomet. Chem.* **2001**, *617–618*, 360–363.

(5) Zhou, C.-Y.; Yu, W.-Y.; Chan, P. W. H.; Che, C.-M. Ruthenium Porphyrin Catalyzed Tandem Sulfonium/Ammonium Ylide Formation and [2,3]-Sigmatropic Rearrangement. A Concise Synthesis of (±)-Platynecine. *J. Org. Chem.* **2004**, *69*, 7072–7082.

(6) Ho, C.-M.; Zhang, J.-L.; Zhou, C.-Y.; Chan, O.-Y.; Yan, J. J.; Zhang, F.-Y.; Huang, J.-S.; Che, C.-M. A Water-Soluble Ruthenium Glycosylated Porphyrin Catalyst for Carbenoid Transfer Reactions in Aqueous Media with Applications in Bioconjugation Reactions. *J. Am. Chem. Soc.* **2010**, *132*, 1886–1894.

(7) Koduri, N. D.; Scott, H.; Hileman, B.; Cox, J. D.; Coffin, M.; Glicksberg, L.; Hussaini, S. R. Ruthenium Catalyzed Synthesis of Enaminones. *Org. Lett.* **2012**, *14*, 440–443.

(8) Koduri, N. D.; Wang, Z.; Cannell, G.; Cooley, K.; Lemma, T. M.; Miao, K.; Nguyen, M.; Frohock, B.; Castaneda, M.; Scott, H.; Albinescu, D.; Hussaini, S. R. Enaminones via Ruthenium-Catalyzed Coupling of Thioamides and α-Diazocarbonyl Compounds. *J. Org. Chem.* **2014**, *79*, 7405–7414.

(9) Egger, L.; Guénée, L.; Bürgi, T.; Lacour, J. Regioselective and Enantiospecific Synthesis of Dioxepines by (Cyclopentadienyl)Ruthenium-Catalyzed Condensations of Diazocarbonyls and Oxetanes. *Adv. Synth. Catal.* **2017**, *359*, 2918–2923.

(10) Wang, M.-Z.; Xu, H.-W.; Liu, Y.; Wong, M.-K.; Che, C.-M. Stereoselective Synthesis of Multifunctionalized 1,2,4-Triazolidines by a Ruthenium Porphyrin-Catalyzed Three-Component Coupling Reaction. *Adv. Synth. Catal.* **2006**, *348*, 2391–2396.

(11) Xu, H.-W.; Li, G.-Y.; Wong, M.-K.; Che, C.-M. Asymmetric Synthesis of Multifunctionalized Pyrrolines by a Ruthenium Porphyrin-Catalyzed Three-Component Coupling Reaction. *Org. Lett.* **2005**, *7*, 5349–5352.

(12) Aviv, I.; Gross, Z. Iron(III) Corroles and Porphyrins as Superior Catalysts for the Reactions of Diazoacetates with Nitrogen- or Sulfur-Containing Nucleophilic Substrates: Synthetic Uses and Mechanistic Insights. *Chem. Eur. J* **2008**, *14* (13), 3995–4005.

(13) Hock, K. J.; Mertens, L.; Hommelsheim, R.; Spitzner, R.; Koenigs, R. M. Enabling Iron Catalyzed Doyle–Kirmse Rearrangement Reactions with in situ Generated Diazo Compounds. *Chem. Commun.* **2017**, *53*, 6577–6580.

(14) Holzwarth, M. S.; Alt, I.; Plietker, B. Catalytic Activation of Diazo Compounds Using Electron-Rich, Defined Iron Complexes for Carbene-Transfer Reactions. *Angew. Chem, Int. Ed.* **2012**, *51*, 5351–5354.

(15) Carter, D. S.; Van Vranken, D. L. Iron-Catalyzed Doyle−Kirmse Reaction of Allyl Sulfides with (Trimethylsilyl)Diazomethane. *Org. Lett.* **2000**, *2*, 1303–1305.

(16) Prabharasuth, R.; Van Vranken, D. L. Iron-Catalyzed Reaction of Propargyl Sulfides and Trimethylsilyldiazomethane. *J. Org. Chem.* **2001**, *66*, 5256–5258.

(17) Zhu, S.-F.; Zhou, Q.-L. Iron-Catalyzed Transformations of Diazo Compounds. *National Science Review* **2014**, *1*, 580–603.

(18) Zhu, C.; Chen, P.; Zhu, R.; Lin, Z.; Wu, W.; Jiang, H. C=N Bond Formation via Palladium-Catalyzed Carbene Insertion into N=N Bonds: Inhibiting the General 1,2-Migration Process of Ylide Intermediates. *Chem. Commun.* **2017**, *53*, 2697–2700.

(19) Jiang, H.; Chen, F.; Zhu, C.; Zhu, R.; Zeng, H.; Liu, C.; Wu, W. Two C–O Bond Formations on a Carbenic Carbon: Palladium-Catalyzed Coupling of N-Tosylhydrazones and Benzo-1,2-Quinones to Construct Benzodioxoles. *Org. Lett.* **2018**, *20*, 3166–3169.

(20) Greenman, K. L.; Carter, D. S.; Van Vranken, D. L. Palladium-Catalyzed Insertion Reactions of Trimethylsilyldiazomethane. *Tetrahedron* **2001**, *57*, 5219–5225.

(21) Urbano, J.; Belderraín, T. R.; Nicasio, M. C.; Trofimenko, S.; Díaz-Requejo, M. M.; Pérez, P. J. Functionalization of Primary Carbon−Hydrogen Bonds of Alkanes by Carbene Insertion with a Silver-Based Catalyst. *Organometallics* **2005**, *24*, 1528–1532.

(22) Krishnamoorthy, P.; Browning, R. G.; Singh, S.; Sivappa, R.; Lovely, C. J.; Dias, H. V. R. Silver-Catalyzed [2,3]-Rearrangement of Halonium Ylides Derived from Allyl and Propargyl Halides and Alkyl Diazoacetates. *Chem. Commun.* **2007**, 731–733.

(23) Caballero Ana; Despagnet-Ayoub Emmanuelle; Mar Díaz-Requejo M.; Díaz-Rodríguez Alba; González-Núñez María Elena; Mello Rossella; Muñoz Bianca K.; Ojo Wilfried-Solo; Asensio Gregorio; Etienne Michel; Pérez Pedro J. Silver-Catalyzed C-C Bond Formation between Methane and Ethyl Diazoacetate in Supercritical CO_2. *Science* **2011**, *332*, 835–838.

(24) Davies, P. W.; Albrecht, S. J.-C.; Assanelli, G. Silver-Catalysed Doyle–Kirmse Reaction of Allyl and Propargyl Sulfides. *Org. Biomol. Chem.* **2009**, *7*, 1276–1279.

(25) Lankelma, M.; Olivares, A. M.; de Bruin, B. [Co(TPP)]-Catalyzed Formation of Substituted Piperidines. *Chemistry* **2019**, *25*, 5658–5663.

(26) Dzik, W. I.; Xu, X.; Zhang, X. P.; Reek, J. N. H.; de Bruin, B. 'Carbene Radicals' in CoII(Por)-Catalyzed Olefin Cyclopropanation. *J. Am. Chem. Soc.* **2010**, *132*, 10891–10902.

(27) Das, B. G.; Chirila, A.; Tromp, M.; Reek, J. N. H.; de Bruin, B. Co^{III}–Carbene Radical Approach to Substituted 1H-Indenes. *J. Am. Chem. Soc.* **2016**, *138*, 8968–8975.

(28) Lu, H.; Dzik, W. I.; Xu, X.; Wojtas, L.; de Bruin, B.; Zhang, X. P. Experimental Evidence for Cobalt(III)-Carbene Radicals: Key Intermediates in Cobalt(II)-Based Metalloradical Cyclopropanation. *J. Am. Chem. Soc.* **2011**, *133*, 8518–8521.

(29) Chen, Y.; Zhang, X. P. Asymmetric Cyclopropanation of Styrenes Catalyzed by Metal Complexes of D2-Symmetrical Chiral Porphyrin: Superiority of Cobalt over Iron. *J. Org. Chem.* **2007**, *72*, 5931–5934.

(30) Huang, L.; Chen, Y.; Gao, G.-Y.; Zhang, X. P. Diastereoselective and Enantioselective Cyclopropanation of Alkenes Catalyzed by Cobalt Porphyrins. *J. Org. Chem.* **2003**, *68*, 8179–8184.

(31) Skaggs, A. J.; Lin, E. Y.; Jamison, T. F. Cobalt Cluster-Containing Carbonyl Ylides for Catalytic, Three-Component Assembly of Oxygen Heterocycles. *Org. Lett.* **2002**, *4*, 2277–2280.

(32) Fukuda, T.; Irie, R.; Katsuki, T. Catalytic and Asymmetric [2,3]-Sigmatropic Rearrangement: Co(III)-Salen Catalyzed S-Ylide Formation from Allyl Aryl Sulfides and Their Rearrangement. *Tetrahedron* **1999**, *55*, 649–664.

(33) Fukuda, T.; Katsuki, T. Co(III)-Salen Catalyzed Carbenoid Reaction: Stereoselective [2,3]Sigmatropic Rearrangement of S-Ylides Derived from Allyl Aryl Sulfides. *Tetrahedron Lett.* **1997**, *38*, 3435–3438.

(34) Sweeney, J. B. Sigmatropic Rearrangements of 'Onium' Ylids. *Chem. Soc. Rev.* **2009**, *38*, 1027–1038.

(35) Sheng, Z.; Zhang, Z.; Chu, C.; Zhang, Y.; Wang, J. Transition Metal-Catalyzed [2,3]-Sigmatropic Rearrangements of Ylides: An Update of the Most Recent Advances. *Tetrahedron* **2017**, *73*, 4011–4022.

(36) Guo, X.; Hu, W. Novel Multicomponent Reactions via Trapping of Protic Onium Ylides with Electrophiles. *Acc. Chem. Res.* **2013**, *46*, 2427–2440.

(37) Bur, S.; Padwa, A. Ammonium Ylides as Building Blocks for Alkaloid Synthesis. In *Modern Tools for the Synthesis of Complex Bioactive Molecules*; John Wiley & Sons, Ltd, 2012; pp 433–484.

(38) Fu, Y.; Wang, H.-J.; Chong, S.-S.; Guo, Q.-X.; Liu, L. An Extensive Ylide Thermodynamic Stability Scale Predicted by First-Principle Calculations. *J. Org. Chem.* **2009**, *74*, 810–819.

(39) Aggarwal, V. K.; Harvey, J. N.; Robiette, R. On the Importance of Leaving Group Ability in Reactions of Ammonium, Oxonium, Phosphonium, and Sulfonium Ylides. *Angew. Chem, Int. Ed.* **2005**, *44*, 5468–5471.

(40) Coldham, I.; Hufton, R. Intramolecular Dipolar Cycloaddition Reactions of Azomethine Ylides. *Chem. Rev.* **2005**, *105*, 2765–2810.

(41) Moderhack, D. N-Ylides of 1,2,3-Triazoles and Tetrazoles – An Overview. *Heterocycles* **2014**, *89*, 2053–2089.

(42) Sowmiah, S.; Esperança, J. M. S. S.; Rebelo, L. P. N.; Afonso, C. A. M. Pyridinium Salts: From Synthesis to Reactivity and Applications. *Org. Chem. Front.* **2018**, *5*, 453–493.

(43) a. de Loera, D.; Liu, F.; Houk, K. N.; Garcia-Garibay, M. A. Aziridine Nitrogen Inversion by Dynamic NMR: Activation Parameters in a Fused Bicyclic Structure. *J. Org. Chem.* **2013**, *78*, 11623–11626. b. Anet, F. A. L.; Osyany, J. M. Nuclear Magnetic Resonance Spectra and Nitrogen Inversion in 1-Acylaziridines. *J. Am. Chem. Soc.* **1967**, *89*, 352–356. c. Bottini, A. T.; Roberts, J. D. Nuclear Magnetic Resonance Spectra. Nitrogen Inversion Rates of N-Substituted Aziridines (Ethylenimines) *J. Am. Chem. Soc.* **1958**, *80*, 5203–5208.

(44) 15. Hata, Y.; Watanabe, M. Fragmentation Reaction of Aziridinium Ylids. II. *Tetrahedron Lett.* **1972**, *13*, 4659–4660.

(45) Clark, J. S.; Hodgson, P. B.; Goldsmith, M. D.; Blake, A. J.; Cooke, P. A.; Street, L. J. Rearrangement of Ammonium Ylides Produced by Intramolecular Reaction of Catalytically Generated Metal Carbenoids. Part 2. Stereoselective Synthesis of Bicyclic Amines. *J. Chem. Soc., Perkin Trans. 1* **2001**, 3325–3337.

(46) Rowlands, G. J.; Kentish Barnes, W. Studies on the [2,3]-Stevens Rearrangement of Aziridinium Ions. *Tetrahedron Lett.* **2004**, *45*, 5347–5350.

(47) Rauk, A.; Allen, L. C.; Mislow, K. Pyramidal Inversion. *Angew. Chem. Int. Ed.* **1970**, *9*, 400–414.

(48) a. Ju, M.; Weatherly, C. D.; Guzei, I. A.; Schomaker, J. M. Chemo- and Enantioselective Intramolecular Silver-Catalyzed Aziridinations. *Angew. Chem, Int. Ed.* **2017**, *56*, 9944–9948. b. Rigoli, J. W.; Weatherly, C. D.; Alderson, J. M.; Vo, B. T.; Schomaker, J. M. Tunable, Chemoselective Amination via Silver Catalysis. *J. Am. Chem. Soc.* **2013**, *135*, 17238–17241. c. Rigoli, J. W.; Weatherly, C. D.; Vo, B. T.; Neale, S.; Meis, A. R.; Schomaker, J. M. Chemoselective Allene Aziridination via Ag(I) Catalysis. *Org. Lett.* **2013**, *15*, 290–293.

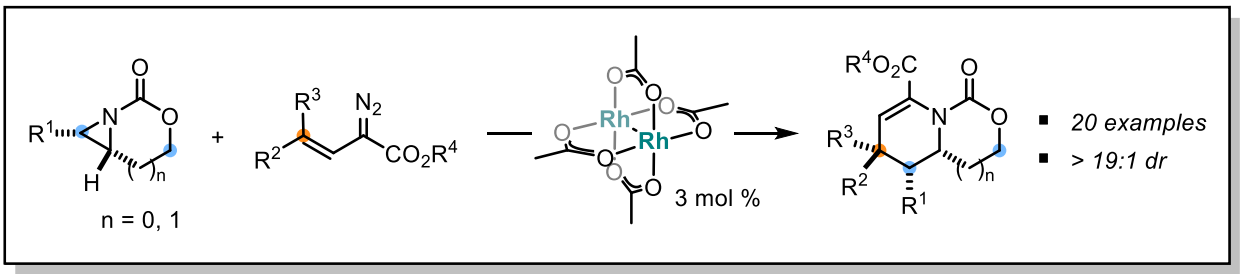
(49) Couch, J. F. Isolation of Sparteine from Lupinus Barbiger. *J. Am. Chem. Soc.* **1932**, *54*, 1691–1692.

(50) Tröger, J. Ueber Einige Mittelst Nascirenden Formaldehydes Entstehende Basen. *J. Prakt. Chem.* **1887**, *36*, 225–245.

(51) Schmid, S. C.; Guzei, I. A.; Schomaker, J. M. A Stereoselective [3+1] Ring Expansion for the Synthesis of Highly Substituted Methylene Azetidines. *Angew. Chem, Int. Ed.* **2017**, *56*, 12229–12233.

(52) Schmid, S. C.; Guzei, I. A.; Fernández, I.; Schomaker, J. M. Ring Expansion of Bicyclic Methyleneaziridines via Concerted, Near-Barrierless [2,3]-Stevens Rearrangements of Aziridinium Ylides. *ACS Catal.* **2018**, *8*, 7907–7914.

Chapter 2. Intermolecular [3+3] Ring-Expansion of Aziridines to Dehydropiperidines through the Intermediacy of Aziridinium Ylides



The following chapter has been published in an open-access journal:

Eshon, J.*; **Nicastri, K. A.***; Schmid, S. C.; Raskopf, W. T.; Guzei, I. A.; Fernández, I.; Schomaker, J. M. *Nat. Commun.* **2020**, *11*, 1273–1281. *Indicates co-first authorship.

2.1 Introduction to Piperidines and Previous Methods that Access these Motifs by Leveraging Aziridines

Piperidines rank as the most prominent *N*-heterocyclic pharmacophore in current drugs on the market, appearing in ~55% of all FDA-approved drugs containing at least one *N*-heterocycle.[1] Convergent methods that unite multiple reactive fragments, particularly hetero-[4+2] cycloadditions, deliver substituted dehydropiperidines in enantioenriched form;[2,3] however, critical substrate and/or catalyst control over regio- and stereoselectivity is challenging and often results in a narrow scope. Traditional preparations of stereodefined piperidines using intramolecular S_N2-type reactions require selective installation of functional groups prior to ring closure, resulting in lower efficiency, modularity, and step economy as the desired target's complexity increases.[1]

Aziridines are an ideal starting material for conversion to larger nitrogenated heterocycles. They are easily accessible from a variety of alkenes by nitrene transfer or from simple manipulations of epoxides; methods for asymmetric aziridination enable these strained rings to be prepared with substantial stereochemical and substitutional complexity.[4] An attractive feature of aziridines is their ring strain, ensuring a favorable thermodynamic driving force for ring-opening reactions. **Figure 2.1** illustrates a selection of transition metal-catalyzed aziridine ring expansions that give rise to 4-to-7 membered *N*-heterocycles.[5-8] For example, Alper and others have achieved metal-catalyzed carbonylations of aziridines to yield valuable β-lactams, although good regioselectivity depends on the substitution pattern of the three-membered ring.[5j] Njardarson has described a series of Cu-catalyzed aziridine expansions to pyrrolidines and related rings; while these reactions are often stereospecific, they are largely limited to intramolecular examples.[5e-g]

Scattered examples describing the conversion of aziridines to piperidines, dehydropiperidines, and azepines are known, but these reactions are also intramolecular or have limited scope.[5i,k,6]

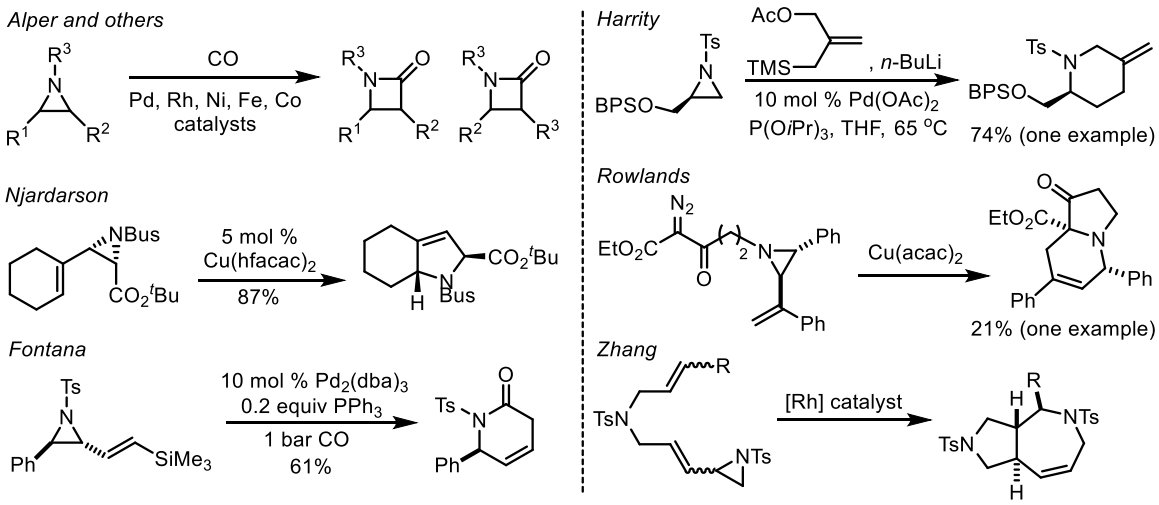


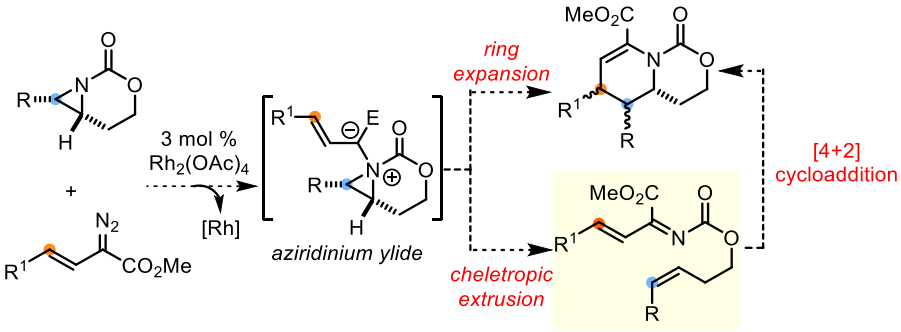
Figure 2.1 – Selected examples of transition metal-catalyzed ring expansions of aziridines to *N*-heterocycles.

As noted in **Figure 2.1**, aziridines are often highly engineered to achieve effective ring expansions. In particular, the inclusion of a vinyl group in the aziridine frequently provides the kinetic impetus to drive successful metal-mediated isomerizations and other functionalizations.[5d-f,i-k, 6] However, utilizing unbiased aziridines for stereocontrolled expansions to larger *N*-heterocycles can be challenging, as epimerization or racemization of the aziridine must be avoided to successfully relay stereochemical information at sp^3 stereocenters to the product with excellent fidelity.[8] Despite these difficulties, the ease of aziridine preparation and their strain-loaded reactivity make them attractive scaffolds for the discovery of new reactivity.[4]

A less common approach is to engage an aziridine and a simple coupling partner in the formation of an aziridinium ylide which could undergo a stereocontrolled, and ideally stereospecific, ring expansion reaction. We hypothesized this could be achieved via an

intermolecular ring expansion between simple bicyclic aziridines and Rh-supported vinyl carbenes (**Scheme 2.1, top**). The intermediacy of an unusual aziridinium ylide species would be followed by either a stereospecific rearrangement that secures access to enantioenriched novel *N*-heterocyclic products or a subsequent [4+2] cycloaddition which may occur after a cheletropic extrusion (**Scheme 2.1**, **bottom**).

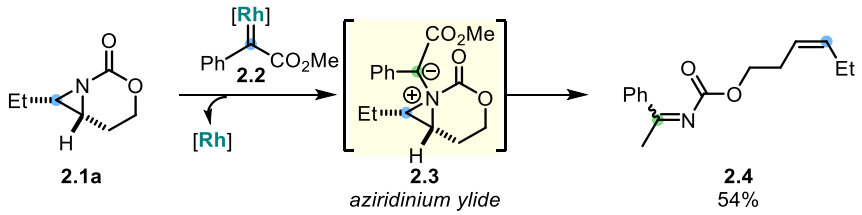
Scheme 2.1 – Proposed reactivity.



2.2 Initial Results

We previously leveraged the unusual strain in methyleneaziridines[9] to achieve a formal [3+1] reaction to furnish azetidines upon exposure to rhodium-supported carbenes (**Chapter 1, Scheme 1.5**).[10,11] Unfortunately, removing the exocyclic alkene to attempt the reaction with less-biased **2.1a** (**Scheme 2.2**) only furnished **2.4**, presumably via **2.3**, a pathway also observed by Watanabe[7] in a Cu-catalyzed reaction of an aziridine and ethyl diazoacetate (**Chapter 1, Scheme 1.1**). Given this reaction outcome, we hypothesized incorporating additional unsaturation into an amphiphilic carbene precursor, may enable our desired reactivity (**Scheme 2.1**).

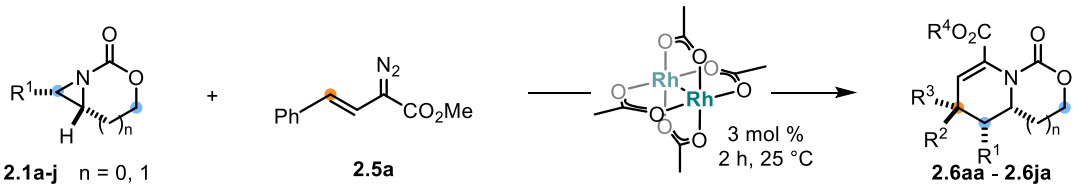
Scheme 2.2 – Initial results with saturated bicyclic aziridines.

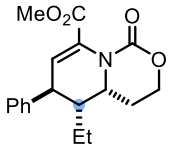
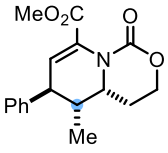
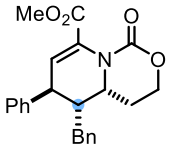
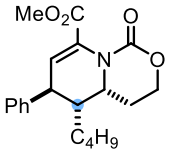
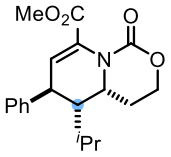
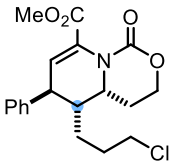
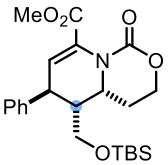
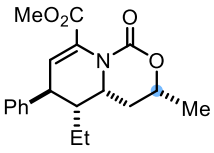
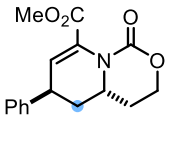
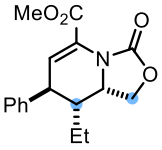


2.3 Optimized Results and Reaction Scope

Reaction of *cis*-alkene-derived aziridine **2.1a** with Davies' styrenyl diazoacetate[12] **2.5a** under dirhodium catalysis produced **2.6aa** in 74% yield and in excellent >19:1 diastereoselectivity (**Table 2.1**). Optimization of conditions for the [3+3] aziridine ring expansion showed that the simple dirhodium paddlewheel complex $Rh_2(OAc)_4$ was the superior catalyst using slow addition of the vinyl diazoacetate. With these conditions in hand, the aziridine scope was further explored using **2.5a** as the vinyl carbene precursor. Linear alkyl groups on the aziridines **2.1a-d**, including benzyl, methyl, ethyl, and *n*-butyl, gave good yields of the products **2.6aa-2.6da** in high *dr*. ^{1}H NMR spectroscopy indicated a *dr* of at least >19:1 for the dehydropiperidine products; minor amounts of the presumed diastereomers were noted. Increasing the bulk of the substituent on the aziridine to an isopropyl group in **2.1e** furnished **2.6ea** in 71% yield and excellent *dr*. Alkyl chloride and ether functionalities were also well-tolerated to deliver dehydropiperidines **2.6fa** and

Table 2.1 – Scope of ring-expansion with various aziridines.



 **2.6aa** 74%[a], >19:1 *dr*	 **2.6ba** 66%[a], 19:1 *dr*	 **2.6ca** 75%[a], >19:1 *dr*	 **2.6da** 92%, >19:1 *dr*	 **2.6ea** 71%[a], >19:1 *dr*
 **2.6fa** 69%[a], >19:1 *dr*	 **2.6ga** 84%, >19:1 *dr*	 **2.6ha** 74%, >19:1 *dr*	 **2.6ia** 67%, >19:1 *dr*	 **2.6ja** 54%, >19:1 *dr*

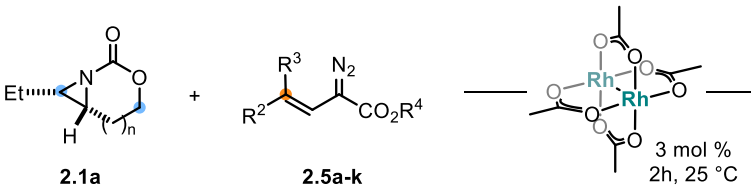
[a] Conditions: 3 mol % $Rh_2(OAc)_4$, 0.05 M CH_2Cl_2, rt, slow addition of diazocetate as a solution in CH_2Cl_2. [b] NMR yield.

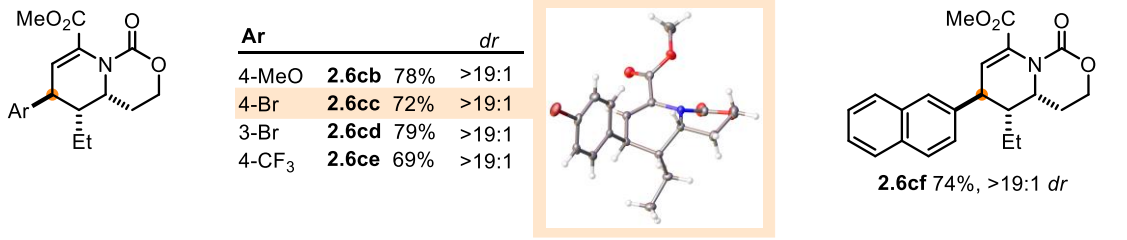
2.6ga. Alkyl substitution α to the carbamate tether in **2.1h** (*dr* >19:1) gave a 74% yield of **2.6ha** as a single diastereomer. Aziridine **2.1i**, unsubstituted at the terminal carbon, gave **2.6ia** in 67% yield and >19:1 *dr*. Finally, it was not necessary to have the carbamate contained in a six-membered ring, as the [5,3]-bicyclic aziridine **2.1j** (R^1 = Et, n = 0) gave the [5.6]-bicyclic ring **2.6ja** in 54% yield and in >19:1 *dr*.

We next examined the scope of the carbene precursor using ethyl-substituted aziridine **2.1a** (**Table 2.2**). The impact of the electronics of a series of phenyl-substituted diazoacetates **2.5a-2.5f** was investigated first. Similar yields were obtained for **2.6ca** and **2.6cb-2.6cc**, irrespective of whether the diazoester carbene precursor contains electron-donating or neutral substituents, suggesting there is little effect of the electronics of the styrene on the reaction outcome. A single crystal X-ray structure of **2.6cc** established the relative stereochemical configuration in the heterocycle product (see expansion for **2.6cc**), confirming earlier nOe studies. Moving the Br to

the *meta* position in **2.5d** resulted in a similar 79% yield of **2.6cd**. Diazoester **2.5e**, bearing a strongly electron-withdrawing trifluoromethyl group, gave a 69% yield of **2.6ce**, also in good *dr*, providing a convenient way to introduce valuable fluorine into the piperidine product. Carbene transfer of the naphthyl-substituted **2.5f** provided **2.6cf** in similar yield and *dr* as compared to **2.6ca**. It was not necessary to employ a styrenyl-derived diazoester, as a series of β-alkyl-substituted diazoesters **2.5g-i** all resulted in good yields of dehydropiperidines **2.6cg-2.6ci** as single diastereomers as determined by ^{1}H NMR. The furan-substituted **2.5j** gave **2.6cj** in only 14% isolated yield, as these oxygen heterocycles have been reported to be reactive in the presence of metal-supported carbenoids.[13,14] Bulking up the methyl ester on the diazoester to a cyclohexyl ester was also successful, producing **2.6ck** in 56% yield and >19:1 *dr*.

Table 2.2 – Scope of ring-expansion with various styrenyl diazoacetates.





[a] Conditions: 3 mol % $Rh_2(OAc)_4$, 0.05 M CH_2Cl_2, rt, slow addition of diazocetate as a solution in CH_2Cl_2. [b] NMR yield.

2.4 Mechanistic Studies

The difficulty of studying carbene transfer using traditional kinetics, particularly when slow addition is required, led us to turn to DFT calculations[15] to gain more insight into the mechanism of the ring expansion (**Figure 2.2**). The pathway involving the reaction of the methyl-substituted aziridine **2.1b** and the [Rh_2]-carbenoid derived from diazoacetate **2.5a** to furnish piperidine **2.6ba** was explored. Nucleophilic attack of the aziridine nitrogen atom on the carbon of the Rh-supported carbenoid occurs as the first step, forming aziridinium ylide **INT1** via transition state **TS1**.[10,11] A saddle point was associated with dissociation of the dirhodium catalyst from the nitrogen to produce zwitterion **INT2**, where the negative charge is fully delocalized into the allylic system (**see inset in Figure 2.2**). Two fates were envisaged for this species, one involving a cheletropic extrusion/aza-Diels-Alder reaction, hypothesized based on initial data (**Scheme 2.1**), and the other a ring-opening/ring-closing sequence to furnish the observed **2.6ba**. In the former case, **INT2** forms azadiene **INT3** through a cheletropic extrusion reaction (via **TS2**), followed by a concerted aza-Diels-Alder cycloaddition (via **TS3**). Experimentally, we found that subjecting enantioenriched (*S,R*)-**2.1c**[16] to the standard reaction conditions resulted in transfer of the *ee* to unsaturated piperidine (*R,R,R*)-**2.6ca** with good fidelity (**Figure 2.2, bottom**). Thus, our initial hypothesis of cheletropic extrusion cannot account for the observed enantioretention in the reaction of (*S,R*)-**2.1c** to (*R,R,R*)-**2ca**; in addition, the height of the barrier of **TS3** relative to **INT3** argues against the aza-Diels-Alder reaction proceeding at room temperature.

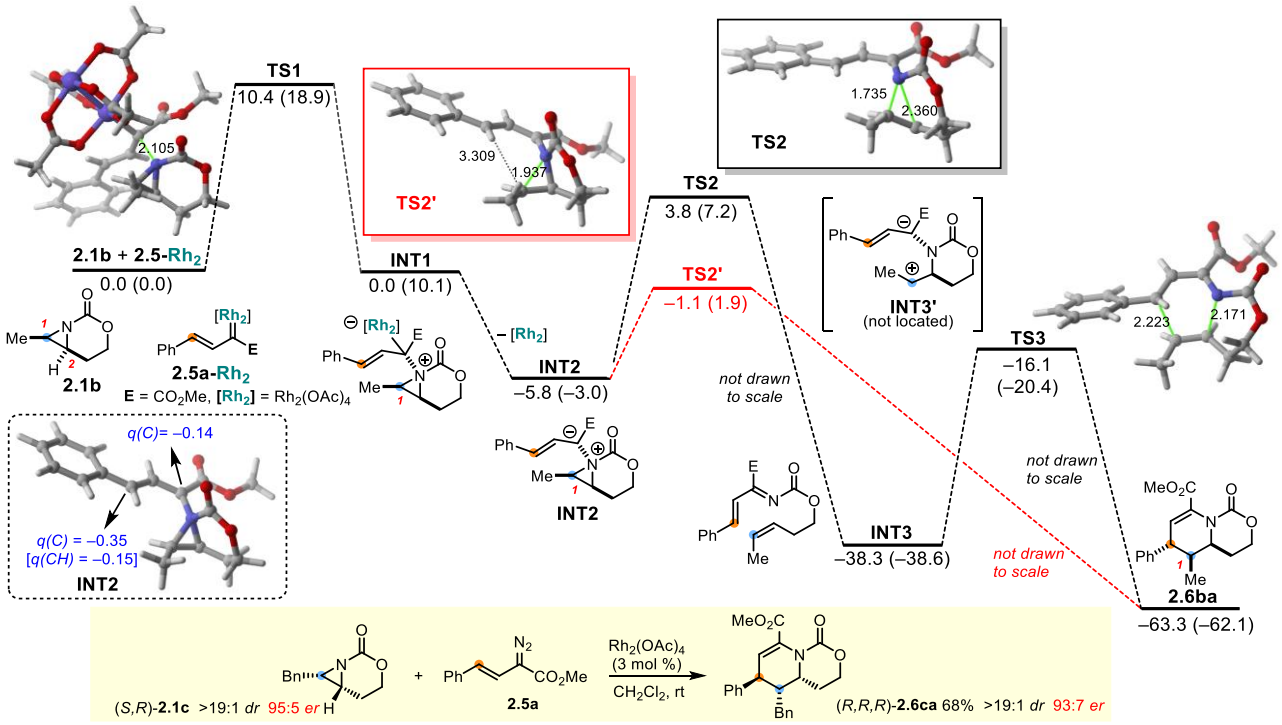


Figure 2.2. – Computed reaction profile for the process involving aziridine **2.1b** and Rh_2-bound carbene **2.5a**-Rh_2. Relative free energies (ΔG, computed at 298.15 K and 1 M) and bond distances are given in kcal/mol and Å, respectively. All data have been computed at the SMD(CH_2Cl_2)-B3LYP-D3/def2-SVP level. Values within parentheses were computed at the SMD(CH_2Cl_2)-B3LYP-D3/def2-TZVPP//SMD(CH_2Cl_2)-B3LYP-D3/def2-SVP level of theory.

Based on these observations, a pathway involving a pseudo-[1,4]-sigmatropic rearrangement of **INT2** via **TS2'**, is favored as: (i) it proceeds with a lower barrier than the alternative cheletropic extrusion ($\Delta\Delta G^{\neq}$ = 5.3 kcal/mol), (ii) enables delocalization of the negative charge of the ylide through the vinyl group to produce the observed dehydropiperidine, and (iii) directly parlays absolute and relative stereochemical information from the aziridine into the product.[17,18,26] Most importantly, computational studies support our experimental observations of chirality transfer from aziridine (*S,R*)-**2.1c** to the product (*R,R,R*)-**2.6ca**.[17,18]

As earlier hypothesized, it appears the unique carbamate tether is critical to the high *dr* associated with **2.6ba**. As the stereochemistry that is set during the initial formation of the aziridinium ylide is subsequently transferred to **2.6ba**, it is imperative that **2.1b** does not undergo pyramidal inversion following attack of the aziridine on the Rh-supported carbene. While the electron-withdrawing carbamate in the tether may contribute to the lack of pyramidal inversion, the bicyclic nature of the substrate likely plays a key role in restricting conformational flexibility.[19] The retention of stereochemistry at the internal aziridine carbon C1 of **2.1b** in the heterocycle **2.6ba** also bears further comment. Invoking an intramolecular S_N2 attack on C1 in **INT-2** (**Figure 2.2**) to close the ring would invert the stereochemistry at C1; in addition, even if the negative charge resides on the benzylic carbon, this π orbital cannot overlap effectively with the σ* of the aziridinium ylide. The relative stereochemistry of **2.6cc**, obtained by single X-ray crystallography, rules out the possibility of an S_N2 mechanism. We also considered the fact that Stevens rearrangements involving ammonium ylides can potentially proceed through diradical intermediates;[20] however, the chirality transfer from aziridine (*S,R*)-**2.1c** to the product (*R,R,R*)-**2.6ca** means that a solvent cage would have to be involved to explain this experimental result.

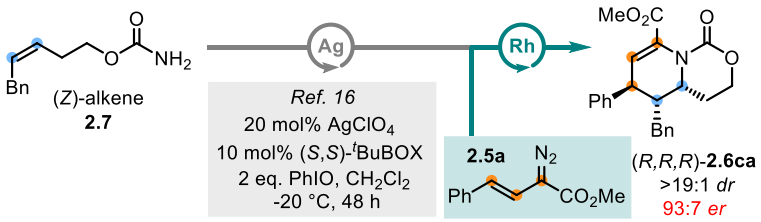
Finally, we considered an unusual stereoretentive nucleophilic substitution; examples of this rare mechanism include the chlorination of secondary alcohols with thionyl chloride (S_N1) and benzylic substitution in supramolecular cavities.[21] Computations on our system suggested that a stereoretentive 'S_N1-like' mechanism might be operative. Firstly, **TS2'** is comprised mainly of C-N bond breakage at the external C1-N bond, which elongates to 1.937 Å. This contrasts to the bond-breaking sequence in **TS2**, where the internal bicyclic C2-N bond shows more elongation at 2.360 Å, as compared to the C1-N bond (1.735 Å). Thus, even though both **TS2** and **TS2'** can be described as relatively low-barrier, early transition states, the extent to which the C-N bond breaks

appears biased. Secondly, consistent with our experimental results, **TS2'** predicts that ring-opening of the C1-N aziridine bond and subsequent C-C bond formation proceeds with retention, due to the stereochemical relationship established between the nitrogen and the carbon substituents on the aziridine during formation of the aziridinium ylide. The Me-bearing C1 of the original aziridine **2.1b** is essentially a full carbocation, with nearly complete C-N rupture in **TS2'** just prior to the ring closure. We are unaware of any other non-metal induced aziridine substitutions of this type that occur with retention of configuration, highlighting the unique nature of tethered aziridine opening of the bicyclic aziridinium ylide intermediate.

2.5 Other Reaction Derivatives and Post-Synthetic Modifications to Demonstrate Product Utility

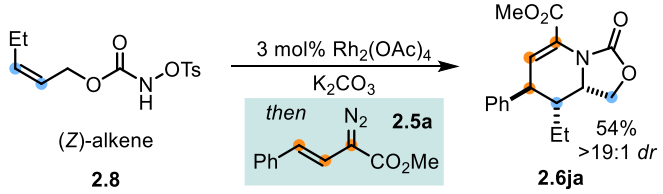
The synthetic utility of the sequential nitrene/carbene transfer reaction could be amplified by running it in tandem with asymmetric alkene aziridination to form enantioenriched piperidines over two steps. In 2017, we disclosed an asymmetric aziridination protocol using silver bisoxazoline (BOX) complexes to enact intramolecular aziridination of homoallylic carbamate esters to achieve high enantioselectivities with a cost-effective catalyst.[16] Application of our asymmetric aziridination to the carbamate of (3Z)-3-penten-5-phenyl-1-ol **2.7** gave enantioenriched (*S,R*)-**2.1c** in 95:5 *er.* Treatment of (*S,R*)-**2.1c** under the standard reaction conditions gives (*R,R,R*)-**2.6ca** with minimal loss of *ee* **(Scheme 2.3)**.

Scheme 2.3 – Enantiotransfer experiment using sequential silver-catalyzed nitrene transfer and Rh-mediated aziridinium ylide formation.



Alternatively, a single catalyst could be used to accomplish the sequential nitrene/carbene transfer. Preparation of the allylic *N*-tosyloxycarbamate ester **2.8**, according to the method described by Lebel and coworkers,[22] followed by treatment with $Rh_2(OAc)_4$ and K_2CO_3 generated the intermediate [5,3]-bicyclic aziridine. Filtration and solvent exchange, followed by slow addition of **2.5a**, gave the unsaturated piperidine **2.6ja** in 54% and >19:1 *dr* (**Scheme 2.4**).

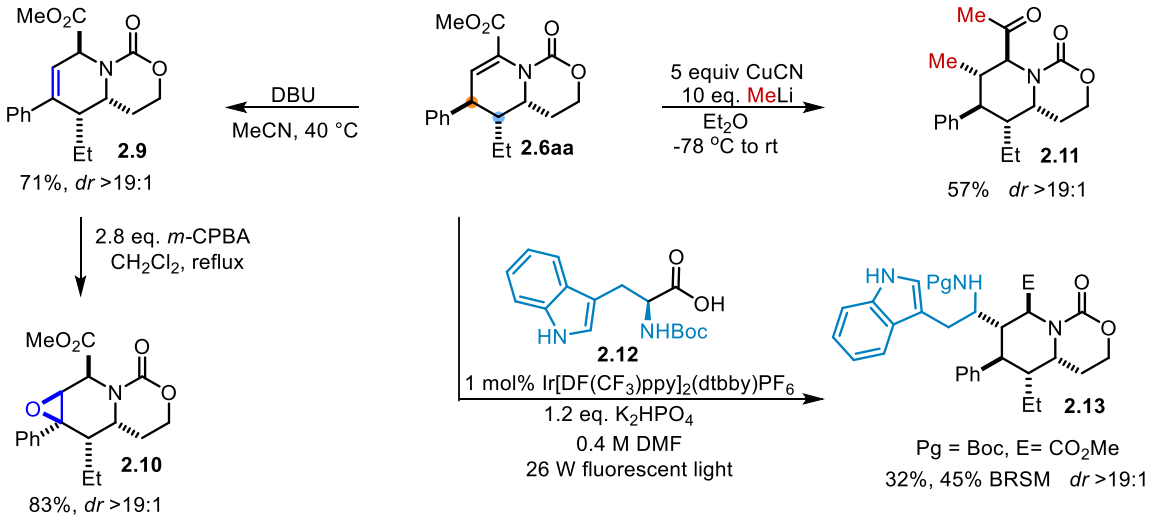
Scheme 2.4 – Streamlined sequential nitrene/carbene transfer.



Further functionalization of the unsaturated piperidine **2.6aa** provides fully substituted, stereochemically rich piperidines in just two steps from the bicyclic aziridine (**Scheme 2.5**). Treatment of **2.6aa** with a higher order cuprate furnished **2.11** in 57% yield and >19:1 *dr* through a diastereoselective conjugate addition reaction.[23] In an initial effort to expand the conjugate addition reaction to include other heteroatom nucleophiles, we found treatment of **2.6aa** with DBU and various nucleophiles did not furnish a conjugate addition product, but rather produced styrene **2.9** in 71% yield and excellent *dr*. Further treatment of **2.9** with *m*CPBA yielded epoxide **2.10** in

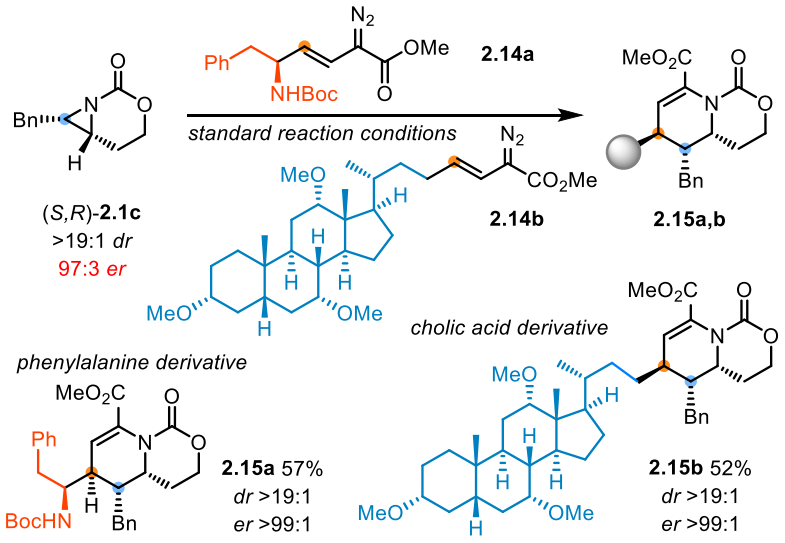
equally good yield and *dr*. Furthermore, inspired by MacMillan and co-workers,[24] **2.6aa** was found to undergo a radical Michael addition with Boc-protected tryptophan **2.12** to yield fully elaborated piperidine **2.13** in 32% yield as a single diastereomer. Although the yield was modest, this transformation rapidly builds complexity in two steps from a simple aziridine.

Scheme 2.5 – Post synthetic modifications.



Finally, the mild reaction conditions and the transfer of the stereochemical information in the aziridine (*S,R*)-**2.1c** to (*R,R,R*)-**2.6ca** with good fidelity promoted us to explore the potential of this chemistry to append biomolecules to our unsaturated piperidine scaffolds. D-Phenylalanine and cholic acid were transformed into suitable diazoesters **2.14a** and **2.14b** (**Scheme 2.5**), then subjected to treatment with (*S,R*)-**2.1c** (94% *ee*) under the standard reaction conditions. The products **2.15a** and **2.15b** were obtained in good yields, with excellent diastereoselectivities and enantiomeric ratios. We envisage this strategy could be effectively applied to explorations of new bioactive chemical space uncovered through fragment-based screening approaches.

Scheme 2.6 – Dehydropiperidine formation using diazoacetates derived from biomolecules.



2.6 Conclusion

In conclusion, aziridinium ylides, accessed in high diastereoselectivity from the intermolecular reaction of simple aziridines with metal-bound vinyl carbenes, are shown to be efficient intermediates for the conversion of small ring heterocycles to complex piperidines, a privileged motif in bioactive compounds. DFT computations, in tandem with transfer of chirality experiments, revealed that the ylides undergo a concerted, asynchronous, pseudo-[1,4]-sigmatropic rearrangement to yield products in high diastereoselectivity and with retention of *ee* installed in the aziridine precursor. Surprisingly, this chemistry is the first to bypass deleterious cheletropic extrusion using unbiased aziridines, suggesting that rearrangements of other strained ylides can likewise be controlled in a productive fashion. Additionally, this mechanism proceeds with retention at the C-C bond, a unique consequence of the S_N1-like closing of the vinyl anion tether.

2.7 References

(1) Vitaku, E.; Smith, D. T.; Njardarson, J. T. Analysis of the Structural Diversity, Substitution Patterns, and Frequency of Nitrogen Heterocycles Among U.S. FDA-Approved Pharmaceuticals. *J. Med. Chem.* **2014**, *57*, 10257–10274.

(2) (a) Ma, C.; Gu, J.; Teng, B.; Zhou, Q.; Li, R.; Chen, Y. C. 1-Azadienes as Regio- and Chemoselective Dienophiles in Aminocatalytic Asymmetric Diels-Alder Reaction. *Org. Lett.* **2013**, *15*, 6206–6209. (b) Jarrige, L.; Blanchard, F.; Masson, G. Enantioselective Organocatalytic Intramolecular Aza-Diels-Alder Reaction. *Angew. Chem., Int. Ed.* **2017**, *56*, 10573–10576. (c) Wang, H.; Zhou, W.; Tao, M.; Hu, A.; Zhang, J. Functionalized Tetrahydropyridines by Enantioselective Phosphine-Catalyzed Aza-[4+2] Cycloaddition of N-Sulfonyl-1-aza-1,3-dienes with Vinyl Ketones. *Org. Lett.* **2017**, *19*, 1710–1713. (d) He, M.; Struble, J.R.; Bode, J.W. Highly Enantioselective Azadiene Diels-Alder Reactions Catalyzed by Chiral N-Heterocyclic Carbenes. *J. Am. Chem. Soc.* **2006**, *128*, 8418–8420. (e) Chu, J.C.; Dalton, D.M.; Rovis, T. Zn-Catalyzed Enantio- and Diastereoselective Formal [4+2] Cycloaddition Involving Two Electron-deficient Partners: Asymmetric Synthesis of Piperidines from 1-Azadienes and Nitro-alkenes. *J. Am. Chem. Soc.* **2015**, *137*, 4445–4452.

(3) For selected examples of the synthesis of complex piperidines see: (a) Bossharth, E.; Desbordes, P.; Monteiro, N.; Balme, G. Palladium-mediated Three-component Synthesis of Furo[2,3-b]pyridones by One-pot Coupling of 3-Iodopyridones, Alkynes, and Organic Halides. *Org. Lett.* **2003**, *5*, 2441-2444. (b) Shu, C.; Liebeskind, L. S. Enantiocontrolled Synthesis of 2,6-Disubstituted Piperidines by Desymmetrization of *meso*-η-(3,4,5)-Dihydropyridinylmolybdenum Complexes. Application to the Total Synthesis of (-)-Dihydropinidine and (-)-Andrachcinidine. *J.*

Am. Chem. Soc. **2003**, *125*, 2878–2879. (c) Fayol, A.; Zhu, J. Synthesis of Polysubstituted 4,5,6,7-Tetrahydrofuro[2,3-c]pyridines by a Novel Multicomponent Reaction. *Org. Lett.* **2004**, *6*, 115–118. (d) Zhu, W.; Mena, M.; Jnoff, E.; Sun, N.; Pasau, P.; Ghosez, L. Multicomponent Reactions for the Synthesis of Complex Piperidine Scaffolds. *Angew. Chem., Int. Ed.* **2009**, *48*, 5880–5883. (e) Jakubec, P.; Cockfield, D. M.; Helliwell, M.; Raftery, J.; Dixon D. J. Stereoselective, Nitro-mannich/Lactamization Cascades for the Direct Synthesis of Heavily Decorated 5-Nitropiperidin-2-ones and Related Heterocycles. *Beilstein J. Org. Chem.* **2012**, *8*, 567–578. (f) Kubota, K.; Watanabe, Y.; Hayama, K.; Ito H. Enantioselective Synthesis of Chiral Piperidines *via* the Stepwise Dearomatization/Borylation of Pyridines. *J. Am. Chem. Soc.* **2016**, *138*, 4338−4341.

(4) For selected references on the asymmetric syntheses of epoxides and aziridines, see: (a) Katsuki, T.; Martin, V. Asymmetric Epoxidation of Allylic Alcohols: the Katsuki–Sharpless Epoxidation Reaction. *Org. Reactions* **2004**, *48*, pp.1–299. (b) Zhang, W.; Loebach, J. L.; Wilson, S. R.; Jacobsen, E. N. Enantioselective Epoxidation of Unfunctionalized Olefins Catalyzed by Salen Manganese Complexes. *J. Am. Chem. Soc.* **1990**, *112*, 2801–2803. (c) Katsuki, T.; Sharpless, K. B. The First Practical Method for Asymmetric Epoxidation. *J. Am. Chem. Soc.* **1980**, *102*, 5974–5976. (d) Li, Z.; Conser, K. R.; Jacobsen, E. N. Asymmetric Alkene Aziridination with Readily Available Chiral Diimine-based Catalysts. *J. Am. Chem. Soc.* **1993**, *115*, 5326–5327. (e) Evans, D. A.; Faul, M. M.; Bilodeau, M. T.; Anderson, B. A.; Barnes, D. M. Bis (oxazoline)-Copper Complexes as Chiral Catalysts for the Enantioselective Aziridination of Olefins. *J. Am. Chem. Soc.* **1993**, *115*, 5328–5329.

(5) For selected references on ring expansions of aziridines, see: (a) Ghorai, M. K.; Bhattacharyya, A.; Das, S.; Chauhan, N. Ring expansions of activated aziridines and azetidines. *In Synthesis of 4- to 7-membered heterocycles by ring expansion*. Springer, 2015, pp. 49–142. (b) Davoli, P.; Moretti, I.; Prati, F.; Alper, H. Carbonylation of Silylated Hydroxymethyl Aziridines to β-Lactams. *J. Org. Chem.* **1999**, *64*, 518–521. c) Ghorai, M. K.; Shukla, D.; Bhattacharyya, A. Syntheses of Chiral β-and γ-Amino Ethers, Morpholines, and their Homologues via Nucleophilic Ring-Opening of Chiral Activated Aziridines and Azetidines. *J. Org. Chem.* **2012**, *77*, 3740–3753. (d) Schomaker, J. M.; Bhattacharjee, S.; Yan, J.; Borhan, B. Diastereomerically and Enantiomerically Pure 2,3-Disubstituted Pyrrolidines from 2,3-Aziridin-1-ols Using a Sulfoxonium Ylide: A One-carbon Homologative Relay Ring Expansion. *J. Am. Chem. Soc*. **2007**, *129*, 1996–2003. (e) Ilardi, E. A.; Njardarson, J. T. Ring Expansions of Vinyloxiranes, -Thiiranes, and -Aziridines: Synthetic Approaches, Challenges, and Catalytic Success Stories. *J. Org. Chem.* **2013**, *78*, 9533–9540. (f) Brichacek, M.; Navarro Villalobos, M.; Plichta, A.; Njardarson, J. T. Stereospecific Ring Expansion of Chiral Vinyl Aziridines. *Org. Lett.* **2011**, *13*, 1110–1113. (g) Mack, D. J.; Njardarson, J. T. Recent Advances in the Metal-Catalyzed Ring Expansions of Three-and Four-Membered Rings. *ACS Catal.* **2013**, *3*, 272–286. (h) D'hooghe, M.; Ha, H. J. *Synthesis of 4-to 7-Membered Heterocycles by Ring Expansion.* Topics in Heterocyclic Chemistry, **2016**. (i) Provoost, O. Y.; Hazelwood, A. J.; Harrity, J. P. Pd-catalysed [3+3] Annelations in the Stereoselective Synthesis of Indolizidines. *Beilstein J. Org. Chem.* **2007**, *3*. (j) Piens, N.; D'hooghe, M. Carbonylation of Aziridines as a Powerful Tool for the Synthesis of Functionalized β-Lactams. *Eur. J. Org. Chem.* **2017**, 5943–5960. (k) Feng, J.; Lin, T.; Wu, H.; Zhang, J. Modular Access to the Stereoisomers of Fused Bicyclic Azepines: Rhodium-catalyzed Intramolecular Stereospecific

Hetero-[5+2] Cycloaddition of Vinyl Aziridines and Alkenes. *Angew. Chem., Int. Ed.* **2015**, *54*, 15854–15858.

(6) Kentish Barnes, W.; Rowlands, G. J. Studies on the [2,3]-Stevens Rearrangement of Aziridinium Ions. *Tetrahedron Lett.* **2004**, *45*, 5347–5350.

(7) Hata, Y.; Watanabe, M. Fragmentation reaction of aziridinium ylides. *Tetrahedron Lett.* **1972**, 46, 4659–4660.

(8) (a) Dolfen, J.; Kenis, S.; Van Hecke, K.; De Kimpe, N.; D'hooghe, M. Selective Synthesis of Functionalized Trifluoromethylated Pyrrolidines, Piperidines, and Azepanes Starting from 1-Tosyl-2-(trifluoromethyl) Aziridine. *Chem. Eur. J.* **2014**, *20*, 10650–10653. (b) Coldham, I.; Collis, A. J.; Mould, R. J.; Rathmell, R. E. Ring Expansion of Aziridines to Piperidines using the Aza-Wittig Rearrangement. *Tetrahedron Lett.* **1995**, *36*, 3557–3560. (c) Vervisch, K.; D'hooghe, M.; Törnroos, K. W.; De Kimpe, N. Synthesis of Stereodefined Piperidines from Aziridines and their Transformation into Conformationally Constrained Amino Acids, Amino Alcohols and 2,7-Diazabicyclo[3.3.1]nonanes. *J. Org. Chem.* **2010**, *75*, 7734–7744. (d) Jarvis, S. B.; Charette, A.B. Synthesis of Enantiopure Substituted Piperidines via an Aziridinium Ring Expansion. *Org. Lett.* **2011**, *13*, 3830–3833.

(9) For previous work on bicyclic methylene aziridines see: (a) Boralsky, L. A.; Marston, D.; Grigg, R. D.; Hershberger, J. C.; Schomaker, J. M. Allene Functionalization *via* Bicyclic Methyleneaziridines. *Org. Lett.* **2011**, *13*, 1924–1927. (b) Rigoli, J. W.; Boralsky, L. A.; Hershberger, J. R.; Marston, D.; Meis, A. R.; Guzei, I. A.; Schomaker, J. M. 1,4-Diazaspiro[2.2]pentanes as a Flexible Platform for the Synthesis of Diamine-bearing Stereotriads.

J. Org. Chem. **2012**, *77*, 2446–2455. (c) Weatherly, C. D.; Rigoli, J. W.; Schomaker, J. M. Synthesis of 1,3-Diaminated Stereotriads *via* Rearrangement of 1,4-Diazaspiro[2.2]pentanes. *Org. Lett.* **2012**, *14*, 1704–1707. (d) Adams, C. S.; Boralsky, L. A.; Guzei, I. A.; Schomaker, J. M. Modular Functionalization of Allenes to Aminated Stereotriads. *J. Am. Chem. Soc.* **2012**, *134*, 10807–10810. (e) Rigoli, J. W.; Guzei, I. A.; Schomaker, J. M. Aminodiols *via* Stereocontrolled Oxidation of Methyleneaziridines. *Org. Lett.* **2014**, *16*, 1696–1699. (f) Adams, C. S.; Grigg, R. D.; Schomaker, J. M. Complete Stereodivergence in the Synthesis of 2-Amino-1,3-diols from Allenes. *Chem. Sci.* **2014**, *5*, 3046–3056. (g) Burke, E. G.; Schomaker, J. M. Oxidative Allene Amination for the Synthesis of Azetidin-3-ones. *Angew. Chem., Int. Ed.* **2015**, *54*, 12097–12101. (h) Gerstner, N. C.; Adams, C. S.; Tretbar, M.; Schomaker, J. M. Stereocontrolled Syntheses of Seven-Membered Carbocycles by Tandem Allene Aziridination/[4+3] Reaction. *Angew. Chem., Int. Ed.* **2016**, *128*, 13434–13437. (i) Adams, C. S.; Weatherly, C. D.; Burke, E. G.; Schomaker, J. M. The Conversion of Allenes to Strained Three-membered Heterocycles. *Chem. Soc. Rev.* **2014**, *43*, 3136–316.

(10) Schmid, S. C.; Guzei, I. A.; Schomaker, J. M. A Stereoselective [3+1] Ring Expansion for the Synthesis of Highly Substituted Methylene Azetidines. *Angew. Chem., Int. Ed.* **2017**, *56*, 12229–12233.

(11) Schmid, S. C.; Guzei, I.; Fernandez, I.; Schomaker, J. M. Ring Expansion of Bicyclic Methyleneaziridines via Concerted, Near-barrierless [2,3]-Stevens Rearrangement. *ACS Catal.* **2018**, *8*, 7907–7914.

(12) Davies, H. M.; Morton, D. Guiding Principles for Site Selective and Stereoselective Intermolecular C–H Functionalization by Donor/acceptor Rhodium Carbenes. *Chem. Soc. Rev.* **2011**, *40*, 1857–1869.

(13) Ahmend, G.; Churchhill, M. R.; Davies, H. L. M. Asymmetric Synthesis of Highly Functionalized 8-Oxabicyclo[3.2.1]octene Derivatives. *J. Am. Chem. Soc.* **1996**, *118*, 10774–10782.

(14) Yang, J.; Manning, J. R.; Davies, H. M. L. Direct Synthesis of Methyl 2-Diazo-4-aryl-3-butenoates and their Application to the Enantioselective Synthesis of 4-Aryl-4-(1-naphthyl)-2-butenoates. *Tetrahedron Asymmetry.* **2006**, *17*, 665–673.

(15) See Computational Details in the Supporting Information.

(16) Ju, M.; Weatherly, C. D.; Guzei, I. A.; Schomaker, J. M. Chemo- and Enantioselective Intramolecular Silver-catalyzed Aziridinations. *Angew. Chem., Int. Ed*. **2017**, *56*, 9944–9948.

(17) Zwitterion **INT3'** could not be located on the potential energy surface. Indeed, intrinsic reaction calculations (IRCs) starting from **TS2'** show the final closing of the C-C bond to form the piperidine exists on a plateau-like energy pathway, where ring closure only begins to occur following completion of the C-N bond rupture.

(18) Similar effects have been noted in ring expansions of epoxides: (a) Achard, T.; Tortoreto, C.; Poblador-Bahamonde, A. I.; Guénée, L.; Bürgi, T.; Lacour, J. [CpRu]-Catalyzed Carbene Insertions into Epoxides: 1,4-Dioxene Synthesis through Sn1-like Chemistry with Retention of Configuration. *Angew. Chem., Int. Ed.* **2014**, *53*, 6140–6144. (b) Ma, X.; Pan, S.; Wang, H.; Chen, W. Rhodium-catalyzed Transannulation of *N*-Sulfonyl-1,2,3-triazoles and Epoxides: Regioselective synthesis of Substituted 3,4-Dihydro-2*H*-1,4-oxazines. *Org. Lett.* **2014**, *16*, 4554–4557.

(19) (a) Atkinson R. S. 3-Acetoxyaminoquinazolinones (QNHPAc) as Aziridinating Agents: Ring-Opening of N-(Q)-Substituted Aziridines *Tetrahedron* **1999**, *55*, 1519-1559 (b) Roohi, H.; Deyhimi F.; Ebrahimi, A. Nitrogen-inversion in some Aziridine Type Compounds: Structural and Kinetic Investigations by Ab Initio Methods *J. Mol. Struct.* **2001**, *535* 247–256 (c) Sweeney, J.B. Aziridines: Epoxides' Ugly Cousins? *Chem. Soc. Rev*., **2002**, *31*, 247–258.

(20) Bhakat, S. The Controversial Reaction Mechanism of the Stevens Rearrangement: A Review. J. Chem. Pharm. Res. **2011**, 3, 115–121.

(21) For other examples of stereoretentive nucleophilic substitutions, see: (a) Müller, P.; Rossier, J. Solvent Effects on the Steric Course of the Solvolysis of Tertiary Acyclic Derivatives. *J. Chem. Soc. Perk. Trans. 2* **2000**, 2232–2239. (b) Zhao, C.; Toste, F. D.; Raymond, K. N.; Bergman, R. G. Nucleophilic Substitution Catalyzed by a Supramolecular Cavity Proceeds with Retention of Absolute Stereochemistry. *J. Am. Chem. Soc.* **2014**, *136*, 14409–14412.

(22) Lebel, H.; Lectard, S.; Parmentier, M. Copper-catalyzed Alkene Aziridination with *N*-Tosyloxycarbamates. *Org. Lett.* **2007**, *9*, 4797–4800.

(23) (a) Toyooka, N.; Fukutome, A.; Nemoto, H.; Daly, J. W.; Spande, T. F.; Garraffo, H. M.; Kaneko, T. Synthesis of alkaloid 223A and a structural revision. *Org. Lett.* **2002**, *4*, 1715-1717. (b) Okada, T.; Yamamoto, T.; Kato, D.; Kawasaki, M.; Saporito, R. A.; Toyooka, N. Synthesis of 8-Deoxypumiliotoxin 193H and 9-Deoxyhomopumiliotoxin 207O. *Tetrahedron Lett.* **2018**, *59*, 3797–3800. (c) Toyooka, N.; Fukutome, A.; Shinoda, H.; Nemoto, H. Stereodivergent Synthesis of the 2,3,5,6-Tetrasubstituted Piperidine Ring System: an Application to the Synthesis of Alkaloids 223A and 205B from Poison Frogs. *Tetrahedron* **2004**, *60*, 6197–6216.

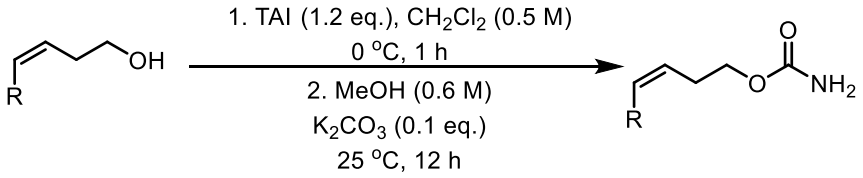
(24) Chu, L.; Ohta, C.; Zuo, Z.; MacMillan, D. W. C. Carboxylic Acids as a Traceless Activation Group for Conjugate Additions: A Three-Step Synthesis of (±)-Pregabalin. *J. Am. Chem. Soc.* **2014**, *136*, 10886–10889.

2.8 Experimental Details

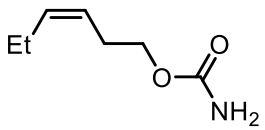
Unless otherwise specified, all reactions were run under an inert atmosphere of N_2. Glassware was either oven-dried overnight at 130 °C or flame-dried under a stream of dry nitrogen prior to use. Unless otherwise specified, reagents were used as obtained from the vendor without further purification. Procedures for compounds requiring purification were obtained from "Purification of Laboratory Chemicals".[1a] Dichloromethane and acetonitrile were dried over CaH_2 and freshly distilled prior to use. All other solvents were also purified in accordance with methods reported in "Purification of Laboratory Chemicals".[1a] Analytical thin layer chromatography (TLC) was performed utilizing pre-coated silica gel 60 F_{254} plates containing a fluorescent indicator, while preparative chromatography was performed using SilicaFlash P60 silica gel (230-400 mesh) via Still's method.[1b] The mobile phases for column chromatography varied depending on the substrate; however, hexanes/ether, hexanes/ethyl acetate, or toluene/ethyl acetate were commonly employed. Columns were typically run using a gradient method, beginning with 100% of the less polar eluent and gradually increasing the polarity with the other solvent. For reactions producing products without a UV signature, a potassium permanganate stain or CAM stain was employed to visualize the reaction products. ^{1}H NMR and ^{13}C NMR spectra were obtained using Bruker Avance-400, Bruker Avance-500 or Varian Inova-600 NMR spectrometers. For ^{1}H NMR, chemical shifts are reported relative to residual protiated solvent peaks (δ 7.26, 2.49, 7.15 and 4.80 ppm for $CDCl_3$, $(CD_3)_2SO$, C_6D_6 and CD_3OD respectively). ^{13}C NMR spectra were measured at either 125 MHz or 150 MHz on the same instruments noted above for recording ^{1}H NMR spectra. Chemical shifts were again reported in accordance to residual protiated solvent peaks (δ 77.1, 39.5, 128.0 and 49.0 ppm for $CDCl_3$, $(CD_3)_2SO$, C_6D_6, and CD_3OD, respectively). Accurate mass measurements were acquired at the University of Wisconsin, Madison using a Micromass LCT (electrospray ionization, time-of-flight analyzer or electron impact methods). The NMR and Mass Spectrometry facilities are funded by the NSF (CHE-1048642), the NIH (S10 OD012245, 1S10 OD020022-1), the Bender Fund, UW2020, and the University of Wisconsin-Madison.

2.8.1 Substrate Synthesis

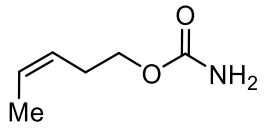
Preparation of carbamate aziridine precursors. All carbamates, if not explicitly mentioned in the subsequent section, were synthesized according to reported literature procedures.[2]



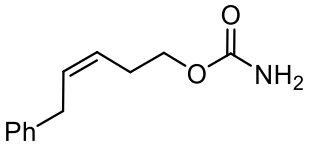
General procedure for carbamate formation. The homoallylic alcohol (1 eq.) was dissolved in CH_2Cl_2 (0.5 M) and cooled to 0 ˚C. Trichloroacetyl isocyanate (TAI) (1.2 eq.) was then added dropwise to the cooled solution. The reaction was stirred at 0 ˚C until TLC indicated complete consumption of the starting material (usually ~1 h). The solvent was then removed under reduced pressure and the crude reaction mixture was dissolved in MeOH (0.6 M). K_2CO_3 (0.1 eq.) was added in a single portion, and the mixture was stirred at room temperature until TLC indicated complete consumption of the starting material, generally overnight. Saturated aqueous NH_4Cl was added to quench the reaction and the mixture was extracted with three portions of CH_2Cl_2. The combined organic phases were washed with brine. The crude product was then diluted with CH_2Cl_2 (0.05 M) and 1 M aqueous NaOH solution (10 mL/mmol) was added. The biphasic solution was vigorously stirred for 30 min to remove the trichloroacetamide impurity. *Note: it is imperative that this step is done carefully. If not, it is likely that the aziridination will not proceed to completion.* The mixture was extracted with three portions of CH_2Cl_2. The combined organic phases were washed with brine, dried over Na_2SO_4 and concentrated under reduced pressure. The crude product was purified by silica gel column chromatography (generally, 40% EtOAc/ Hexanes).



Carbamate precursor to Compound 2.6a. Following the general procedure, the reaction to furnish the carbamate precursor to **2.6a** was conducted on 22.1 mmol scale. The product was purified by silica gel flash column chromatography (0% to 50% EtOAc/Hex) to yield **2.6a** as a white solid (2.92 g, 92% yield).^{1}H NMR (500 MHz, $CDCl_3$) δ 5.50 (dtt, *J* = 10.5, 7.2, 1.6 Hz, 1H), 5.32 (dtt, *J* = 10.6, 7.3, 1.6 Hz, 1H), 4.68 (brs, 1H), 4.06 (t, *J* = 6.9 Hz, 2H), 2.37 (dt, *J* = 8.2, 6.3 Hz, 2H), 2.06 (dt, 7.5, 7.6 Hz); (app p, *J* = 7.5, 1.5 Hz, 2H), 0.96 (t, *J* = 7.5 Hz, 2H). ^{13}C NMR (126 MHz, $CDCl_3$) δ 157.0, 134.6, 123.8, 64.7, 27.0, 20.6, 14.2. *m/z* matched already published data.[2]

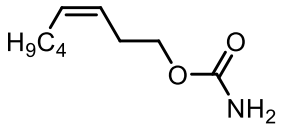


Carbamate precursor to Compound 2.1b. Following the general procedure, the reaction to furnish carbamate precursor to **2.1b** was conducted on 1.2 mmol scale. The product was purified by silica gel flash column chromatography (10% to 50% Et_2O/Pentane) to yield **2.1b** as a white solid (154.0 mg, 92% yield). The minor NMR impurity is the isomerized *trans* product, which can be carried on, as it is unreactive in the carbene transfer reaction. ^{1}H NMR (500 MHz, $CDCl_3$) δ 5.58 (m, 1H), 5.38 (dtq, *J* = 10.8, 7.3, 1.9 Hz, 1H), 4.58 (br s, 2H), 4.07 (t, *J* = 6.9 Hz, 2H), 2.39 (dt, 7.0, 7.0 Hz); (app q, *J* = 7.0 Hz, 2H), 1.64 (dd, *J* = 6.8, 1.7 Hz, 3H). δ ^{13}C NMR (126 MHz, $CDCl_3$) δ 156.9, 126.8, 125.3, 64.6, 26.8, 12.9. HRMS (ESI) *m/z* calculated for $C_6H_{11}NO_2$ $[M+ Na+]^+$ 152.0862; found, 152.0863.

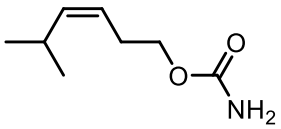


Carbamate precursor to Compound 2.1c. Following the general procedure, the reaction to furnish the carbamate precursor to **2.1c** was conducted on 10 mmol scale. The product was purified by silica gel flash column chromatography (20% to 50% EtOAc/Hex) to yield **2.1c** as a white solid (1.81g, 88% yield). ^{1}H NMR (500 MHz, $CDCl_3$) δ 7.31 – 7.27 (m, 2H), 7.22 – 7.17

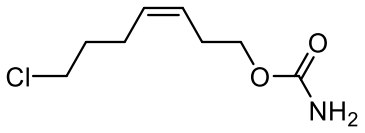
(m, 3H), 5.72 (dtt, *J* = 10.8, 7.5, 1.6 Hz, 1H), 5.52 (dtt, *J* = 10.7, 7.3, 1.7 Hz, 1H), 4.55 (br s, 2H), 4.12 (t, *J* = 6.7 Hz, 2H), 3.43 (dd, *J* = 7.5, 1.5 Hz, 2H), 2.50 (tdd, *J* = 6.8, 6.8, 1.8 Hz); (app qd, *J* = 6.8, 1.8 Hz). ^{13}C NMR (126 MHz, $CDCl_3$) δ 156.9, 140.8, 131.1, 128.6, 128.5, 126.1, 125.8, 64.6, 33.6, 27.3. HRMS (ESI) *m/z* calculated for $C_{12}H_{15}NO_2$ $[M+H]^+$ 206.1176; found, 206.1173.



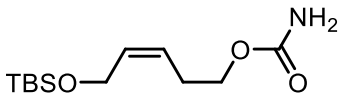
Carbamate precursor to Compound 2.1d. Following the general procedure, the reaction to furnish the carbamate precursor to **2.1d** was conducted on a 15.7 mmol scale. The product was purified by silica gel flash column chromatography (40% EtOAc/Hex) to yield **2.1d** as a white solid (1.19 g, 44% yield). ^{1}H NMR (500 MHz, $CDCl_3$) ^{1}H NMR (500 MHz, $CDCl_3$) δ 5.61 – 5.46 (m, 1H), 5.43 – 5.28 (m, 1H), 4.56 (br s, 2H), 4.06 (t, *J* = 6.9 Hz, 2H), 2.59 – 2.35 (m, 2H), 2.05 (m, 2H), 1.44 – 1.28 (m, 4H), 1.03 – 0.80 (m, 3H). ^{13}C NMR (126 MHz, $CDCl_3$) δ 157.0, 133.1, 124.5, 64.9, 31.9, 27.3, 27.2, 22.5, 14.1. HRMS (ESI) *m/z* calculated for $C_9H_{17}NO_2$ $[M+H]^+$ 172.1332; found, 172.1330.



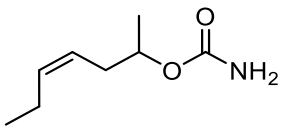
Carbamate precursor to Compound 2.1e. Following the general procedure, the reaction to furnish carbamate precursor to **2.1e** was conducted on a 6.02 mmol scale. The product was purified by silica gel flash column chromatography (40% ethyl acetate/ hexanes) to yield **2.1e** as a white solid (0.69 g, 73% yield). ^{1}H NMR (500 MHz, $CDCl_3$) δ 5.34 (ddt, *J* = 11.0, 9.4, 1.5 Hz, 1H), 5.23 (dt, *J* = 10.7, 7.2 Hz, 1H), 4.53 (br s, 2H), 4.06 (t, *J* = 6.9 Hz, 2H), 2.60 (m, 1H), 2.39 (qd, *J* = 7.0, 1.5 Hz, 2H), 0.96 (d, *J* = 6.6 Hz, 6H).^{13}C NMR (126 MHz, $CDCl_3$) δ 156.9, 140.4, 121.9, 64.8, 27.2, 26.6, 23.1. HRMS (ESI) *m/z* calculated for $C_8H_{15}NO_2$ $[M+H]^+$ 158.1176; found, 158.1175.



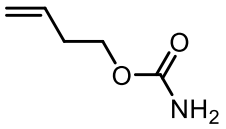
Carbamate precursor to Compound 2.1f. Following the general procedure, the product to furnish carbamate precursor to **2.1f** was conducted on a 4.6 mmol scale. The product was purified by silica gel flash column chromatography (30% EtOAc/Hex) to yield **2.1f** as a white solid (830.0 mg, 95% yield) ^{1}H NMR (500 MHz, $CDCl_3$) δ 5.54 – 5.27 (m, 2H), 4.60 (br s, 2H), 4.08 (t, *J* = 6.8 Hz, 2H), 3.54 (t, *J* = 6.5 Hz, 2H), 2.51 – 2.33 (m, 2H), 2.33 – 2.17 (m, 2H), 1.93 – 1.74 (m, 2H). ^{13}C NMR (126 MHz, $CDCl_3$) δ 156.7, 130.5, 126.3, 64.5, 44.4, 32.2, 27.1, 24.4. HRMS (ESI) *m/z* calculated for $C_8H_{14}NO_2$ $[M+H]^+$ 192.0786; found, 192.0784.



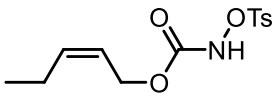
Carbamate precursor to Compound 2.1g. Following the general procedure, the reaction to furnish carbamate precursor to compound **2.1g** was conducted on a 0.50 mmol scale. The product was purified by silica gel flash column chromatography (0% to 50% EtOAc/CH2Cl2) to yield **2.1g** as a clear oil (104.1 mg, 87% yield). ^{1}H NMR (500 MHz, $CDCl_3$) δ 5.65 (m, 1H), 5.43 (dtt, *J* = 10.9, 7.4, 1.7 Hz, 1H), 4.60 (br s, 2H), 4.24 (ddt, *J* = 6.2, 1.7, 0.8 Hz, 2H), 4.07 (dd, 4.07 *J* = 6.8, 6.8 Hz, 2H); (app t, *J* = 6.8 Hz, 2H), 2.39 (dtd, *J* = 7.6, 6.7, 1.7 Hz, 2H), 0.90 (s, 9H), 0.07 (s, 6H).^{13}C NMR (126 MHz, $CDCl_3$) δ ^{13}C NMR (126 MHz, Chloroform-*d*) δ 156.9, 132.6, 125.7, 64.5, 59.6, 27.6, 26.1, -5.0. HRMS (ESI) *m/z* calculated for $C_{12}H_{25}NO_3Si$ $[M+H]^+$ 260.1674; found, 260.1674.



Carbamate precursor to Compound 2.1h. Following the general procedure, the reaction to furnish carbamate precursor to compound **2.1h** was conducted on a 12.2 mmol scale. The product was purified by silica gel flash column chromatography (20% to 50% EtOAc/Hex) to yield **2.1h** as a yellow low-melting solid (1.17g, 61% yield). ^{1}H NMR (500 MHz, $CDCl_3$) δ 5.63 – 5.40 (m, 1H), 5.40 – 5.11 (m, 1H), (4.81 dq *J* = 6.3, 6.3 Hz); (app h, *J* = 6.3 Hz, 1H), 4.60 (br s, 2H), 2.41 – 2.30 (m, 1H), 2.30 – 2.21 (m, 1H), 2.11 – 2.00 (m, 2H), 1.22 (d, *J* = 6.3 Hz, 3H), 0.96 (t, *J* = 7.5 Hz, 3H). δ ^{13}C NMR (126 MHz, $CDCl_3$) δ 156.7, 134.6, 123.7, 71.6, 33.8, 20.8, 19.8, 14.3. HRMS (ESI) *m/z* calculated for $C_8H_{15}NO_2$ $[M+Na]^+$ 180.0995; found, 180.0994.

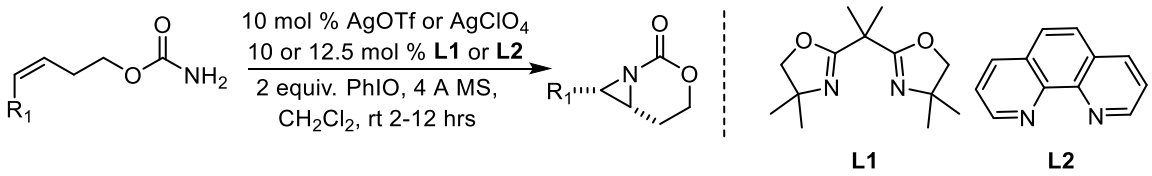


Carbamate precursor to Compound 2.1i. Following the general procedure, the reaction to furnish the carbamate precursor to **2.1i** was conducted on 1.39 mmol scale. The product purified by silica gel flash column chromatography (30% EtOAc/Hex) to yield **2.1i** as a clear oil (90.3 mg, 60 % yield) ^{1}H NMR (500 MHz, $CDCl_3$) δ 5.78 (ddt, *J* = 17.0, 10.3, 6.7 Hz, 1H), 5.22 – 5.02 (m, 2H), 4.80 (br s, 2H), 4.11 (t, *J* = 6.8 Hz, 2H), 2.38 (dddt , *J* = 6.7, 6.7, 6.7, 1.4 Hz);(app qt, *J* = 6.7, 1.4 Hz, 2H). ^{13}C NMR (126 MHz, $CDCl_3$) δ 157.2, 134.2, 117.3, 64.3, 33.5. HRMS (ESI) *m/z* calculated for $C_5H_9NO_2$ $[M+H]^+$ 116.0706; found, 116.0705.

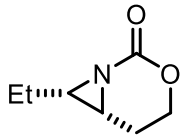


Carbamate precursor to Compound 2.1j. The *N*-tosyl carbamate was synthesized following Lebel's reported preparation.[3] ^{1}H NMR (500 MHz, $CDCl_3$) δ 7.89 – 7.86 (m, 2H), 7.77 (br s, 1H), 7.36 (d, *J* = 8.1 Hz, 2H), 5.62 (dtt, *J* = 10.3, 7.5, 1.4 Hz, 1H), 5.29 (dtt, *J* = 10.4, 7.0, 1.6 Hz, 1H), 4.56 (dd, *J* = 7.0, 1.2 Hz, 2H), 2.46 (s, 3H), 2.04 (qdd, *J* = 7.6 Hz, 7.6 Hz, 1.6 Hz); (app pd, *J* = 7.6, 1.6 Hz),0.96 (t, *J* = 7.5 Hz, 3H). ^{13}C NMR (126 MHz, $CDCl_3$) δ 155.5, 146.2, 138.2, 130.5, 129.9, 129.7, 121.5, 62.8, 21.9, 21.0, 14.1. δ HRMS (ESI) *m/z* calculated for $C_{13}H_{17}NO_5S$ $[M+NH_4]^+$ 317.1166; found, 317.1166.

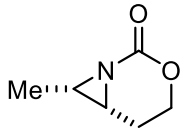
Preparation of aziridine precursors. All aziridines, if not explicitly mentioned in the subsequent section, were synthesized according to reported literature procedures.[2]



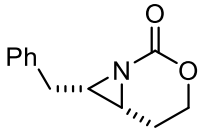
General procedure for silver-catalyzed aziridination of homoallylic carbamates. A cooled, flame-dried round bottom flask was charged with $AgClO_4$ or AgOTf (0.1 eq.) and dimethyl bisoxazoline **L1** or 1,10-phenanthroline ligand **L2** (0.1 eq.). Dry CH_2Cl_2 (0.05 M) was added to the round-bottom and the mixture was stirred vigorously for 15 minutes. *Note: Both **L1** and **L2** will furnish the aziridine product. **L2** may result in varying ratios of aziridine to C-H insertion product if the metal/ligand ratio is not carefully measured to be 1:1.*[2] ***L1** is the preferable ligand, as the ratio of metal/ligand is not as important to the aziridine/C-H insertion product ratio. However, **L2** is a good commercially available alternative if **L1** is unavailable.* After 15 minutes of pre-stirring, powdered 4Å molecular sieves (1g of sieves /mmol of substrate) were added. After 5 minutes, the carbamate ester (1 eq.) and iodosobenzene (2 eq.) were added. The reaction was then capped, covered in aluminum foil (if AgOTf is used), and allowed to stir at room temperature for 2-12 h. After TLC indicated complete consumption of the starting material, the reaction mixture was filtered over celite and concentrated. The crude mixture was then purified by column chromatography – once with a gradient elution of 0-2.5% MeOH/CH_2Cl_2, followed by a second column with a gradient elution of 0-50% EtOAc/hexanes or 5% EtOAc/CH_2Cl_2. *Note*: *omitting the first plug with CH_2Cl_2 leaves silver byproducts in the mixture, which, upon concentration, can degrade the aziridine over time or cause decreased reactivity in the subsequent carbene transfer reaction.* The compounds were stored at -20 or -78 ˚C to prevent decomposition. All aziridines not described below were prepared according to published literature procedures.



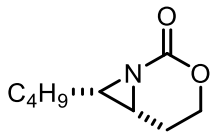
Compound 2.1a. Following the general procedure, the aziridination reaction to furnish **2.1a** was conducted on 6.98 mmol scale. The product was purified by silica gel flash column chromatography (0-2.5% MeOH/CH_2Cl_2, then 0 to 5% EtOAc/CH_2Cl_2) to yield **2.1a** as a white solid (0.660 g, 67%). ^{1}H NMR (500 MHz, $CDCl_3$) δ 4.41 – 4.27 (m, 2H), 2.84 (ddd, *J* = 9.0, 6.9, 4.9 Hz, 1H), 2.57 (dt, *J* = 8.3, 5.2 Hz, 1H), 2.16 (dddd, *J* = 14.7, 7.0, 2.0, 2.0 Hz, 1H); app ddt, *J* = 14.7, 7.0, 2.0 Hz, 1H), 1.83 (dqd, *J* = 14.4, 7.3, 5.3 Hz, 1H), 1.44 (dddd, *J* = 14.3, 12.1, 9.0, 4.9 Hz, 1H), 1.29 – 1.14 (m, 1H), 1.07 (t, *J* = 7.3 Hz, 3H). ^{13}C NMR (126 MHz, $CDCl_3$) δ 158.7, 68.0, 44.0, 37.3, 19.0 (d, *J* = 2.0 Hz), 10.9. HRMS (ESI) *m/z* matched already published data.[2]



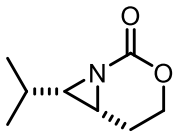
Compound 2.1b. Following the general procedure, the aziridination reaction to furnish **2.1b** was conducted on a 0.97 mmol scale. The product was purified by silica gel flash column chromatography (0-2.5% MeOH/CH_2Cl_2, then 0% to 50% EtOAc/Hexanes) to yield **2.1b** as a clear oil (65.2 mg, 53%). ^{1}H NMR (500 MHz, $CDCl_3$) δ 4.39 (ddd, *J* = 12.4, 10.4, 2.2 Hz, 1H), 4.34 (ddd, *J* = 10.5, 4.6, 1.7 Hz, 1H), 2.89 (ddd, *J* = 8.9, 7.0, 4.9 Hz, 1H), 2.81 – 2.72 (m, 1H), 2.18 (dddd 14.7, 6.9, 2.0, 2.0 Hz, 1H); (app ddt, *J* = 14.7, 6.9, 2.0 Hz, 1H), 1.55 – 1.44 (m, 1H), 1.29 (d, *J* = 6.0 Hz, 3H). ^{13}C NMR (126 MHz, $CDCl_3$) δ 158.5, 67.7, 38.3, 37.6, 18.9, 10.2 HRMS (ESI) *m/z* calculated for $C_6H_9NO_2[M+H]^+$ 128.0706; found, 128.0704.



Compound 2.1c. Following the general procedure, the aziridination reaction to furnish **2.1c** was conducted on 0.48 mmol scale. The product was purified by silica gel flash column chromatography (0-2.5% MeOH/CH_2Cl_2, then 0 to 5% EtOAc/CH_2Cl_2) to yield **2.1c** as a white solid (84.9 mg, 86%). ^{1}H NMR (500 MHz, $CDCl_3$ δ 7.34 (tt, *J* = 8.1, 1.5 Hz, 2H), 7.30 – 7.27 (m, 1H), 7.25 – 7.22 (m, 2H), 4.50 – 4.39 (m, 2H), 3.34 (dd, *J* = 15.4, 3.9 Hz, 1H), 2.98 (ddd, *J* = 8.9, 6.8, 4.8 Hz, 1H), 2.90 (ddd, *J* = 10.1, 4.8, 3.9 Hz, 1H), 2.41 (dd, *J* = 15.3, 10.1 Hz, 1H), 2.29 (dddd *J* = 14.6, 6.8, 1.9, 1.9 Hz, 1H);(app ddt, *J* = 14.6, 6.8, 1.9 Hz, 1H), 1.69 (dddd, *J* = 14.4, 12.1, 8.9, 4.7 Hz, 1H). ^{13}C NMR (126 MHz, $CDCl_3$) δ 158.6, 136.7, 129.0, 128.5, 127.2, 68.1, 42.8, 37.8, 31.1, 19.7. HRMS (ESI) *m/z* calculated for $C_{12}H_{13}NO_2[M+H]^+$ 204.1019; found, 204.1020.

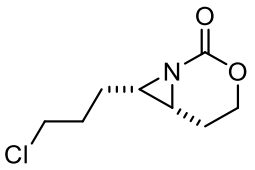


Compound 2.1d. Following the general procedure, the aziridination reaction to furnish **2.1d** was conducted on a 2.16 mmol scale. The product was purified by silica gel flash column chromatography (2.5% MeOH/CH_2Cl_2 and 5% EtOAc/CH_2Cl_2) to yield **2.1d** as a clear oil (208.5 mg, 57%). ^{1}H NMR (500 MHz, $CDCl_3$) δ 4.48 – 4.29 (m, 2H), 2.87 (ddd, *J* = 8.9, 6.9, 4.9 Hz, 1H), 2.63 (dt, *J* = 9.4, 4.9 Hz, 1H), 2.18 (ddt, *J* = 14.6, 6.9, 2.0 Hz, 1H), 1.88 (ddt, *J* = 14.2, 9.6, 5.2 Hz, 1H), 1.63 – 1.32 (m, 5H), 1.16 (dtd, *J* = 14.6, 9.2, 5.2 Hz, 1H), 0.92 (t, *J* = 7.0 Hz, 3H). ^{13}C NMR (126 MHz, $CDCl_3$) δ 158.8, 68.0, 42.9, 37.5, 28.8, 25.2, 22.6, 19.3, 14.1. HRMS (ESI) *m/z* calculated for $C_9H_{15}NO_2$ $[M+H]^+$ 170.1176; found, 170.1174.

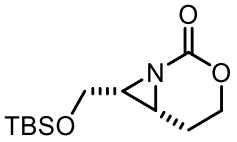


Compound 2.1e. Following the general procedure, the aziridination reaction to furnish **2.1e** was conducted on a 2.05 mmol scale. The product was purified by silica gel flash column

chromatography (2.5% MeOH/CH_2Cl_2 and 5% EtOAc/CH_2Cl_2) to yield **2.1e** as a white solid (0.316 g, 95%). ^{1}H NMR (500 MHz, $CDCl_3$) δ 4.45 – 4.22 (m, 2H), 2.81 (ddd, *J* = 9.1, 6.8, 5.0 Hz, 1H), 2.38 (dd, *J* = 9.9, 5.0 Hz, 1H), 2.19 (dddd, *J* = 14.6, 6.8, 2.0, 2.0 Hz, 1H); (app ddt, *J* = 14.6, 6.8, 2.0 Hz, 1H), 1.62 – 1.35 (m, 2H), 1.30 (d, *J* = 6.4 Hz, 3H), 1.01 (d, *J* = 6.7 Hz, 3H).^{13}C NMR (126 MHz, $CDCl_3$) δ 158.5, 67.7, 49.4, 36.9, 26.9, 20.1, 20.0, 19.6. HRMS-(ESI) *m/z* calculated for $C_8H_{13}NO_4$ $[M+Na]^+$ 156.1019; found, 156.1019.

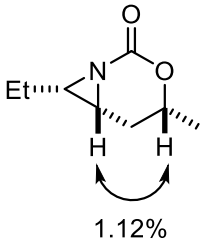


Compound 2.1f. Following the general procedure, the aziridination reaction to furnish **2.1f** was conducted on 0.42 mmol scale. The product was purified by silica gel flash column chromatography (2.5% MeOH/CH_2Cl_2 and then 0 to 50% EtOAc/Hexanes) to yield **2.1f** as a colorless oil (49.7 mg, 62%). ^{1}H NMR (500 MHz, $CDCl_3$) δ 4.46 – 4.33 (m, 2H), 3.63 (ddd, *J* = 11.0, 6.8, 5.2 Hz, 1H), 3.55 (ddd, *J* = 11.0, 7.6, 5.2 Hz, 1H), 2.90 (ddd, *J* = 9.0, 6.9, 4.9 Hz, 1H), 2.65 (ddd, *J* = 7.5, 6.0, 4.9 Hz, 1H), 2.30 – 2.11 (m, 2H), 1.97 – 1.87 (m, 1H), 1.83 (dddd, *J* = 14.5, 9.6, 5.9, 4.8 Hz, 1H), 1.65 – 1.47 (m, 2H). ^{13}C NMR (126 MHz, $CDCl_3$) δ 158.6, 68.0, 44.3, 42.0, 37.4, 29.6, 23.2, 19.3 HRMS (ESI) *m/z* calculated for $C_8H_{12}ClNO_2[M+H]^+$ 190.0629; found, 190.0630.

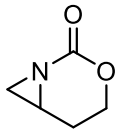


Compound 2.1g. Following the general procedure, the aziridination reaction to furnish **2.1g** was conducted on 1.01 mmol scale. The product was purified by silica gel flash column chromatography (2.5% MeOH/CH_2Cl_2 and 5% EtOAc/CH_2Cl_2) to yield **2.1g** as a colorless oil

(226.0 mg, 87%). ^{1}H NMR (500 MHz, $CDCl_3$) δ 4.40 – 4.24 (m, 2H), 4.13 (dd, *J* = 11.8, 3.6 Hz, 1H), 3.39 (dd, *J* = 11.8, 8.4 Hz, 1H), 2.83 (ddd, *J* = 9.0, 7.0, 4.8 Hz, 1H), 2.70 (ddd, *J* = 8.4, 4.8, 3.5 Hz, 1H), 2.13 (dddd, *J* = 14.7, 6.9, 2.0, 2.0 Hz, 1H); (ap ddt, *J* = 14.7, 6.9, 2.0 Hz, 1H), 1.68 (dddd, *J* = 14.7, 12.2, 8.9, 4.7 Hz, 1H), 0.82 (s, 9H), 0.01 (s, 6H). ^{13}C NMR (126 MHz, $CDCl_3$) δ 158.3, 68.1, 58.5, 41.7, 37.4, 25.8, 19.0, -5.4. HRMS-(ESI) *m/z* calculated for $C_{12}H_{23}NO_3Si$ $[M+H]^+$ 258.1520; found, 258.1518.



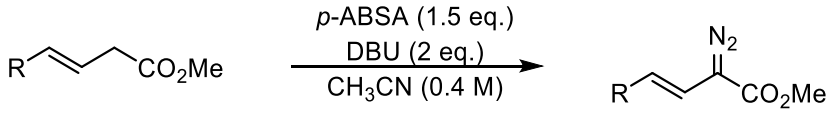
Compound 2.1h. Following the general procedure, the aziridination reaction to furnish **2.1h** was conducted on 2.7 mmol scale. The product was purified by silica gel flash column chromatography (2.5% MeOH/CH_2Cl_2 and then 0 to 20% EtOAc/CH_2Cl_2) to yield **2.1h** as a colorless oil (174.1 mg, 38%). The minor diastereomer was separated *via* automated flash chromatography using the 5% EtOAc/CH_2Cl_2 solvent system. ^{1}H NMR (500 MHz, $CDCl_3$) δ 4.57 (dqd, *J* = 11.1, 6.3, 2.1 Hz, 1H), 2.82 (ddd, *J* = 9.0, 6.9, 4.9 Hz, 1H), 2.61 (dt, *J* = 8.3, 5.1 Hz, 1H), 2.18 (ddd, *J* = 14.4, 6.9, 2.1 Hz, 1H), 1.86 (ddd, *J* = 14.4, 7.3, 5.4 Hz, 1H), 1.37 (d, *J* = 6.2 Hz, 3H), 1.30 – 1.12 (m, 2H),1.10 (t, *J* = 7.4 Hz, 3H). ^{13}C NMR (126 MHz, $CDCl_3$) δ 159.2, 75.8, 44.8, 37.1, 26.2, 20.7, 19.1, 10.9 HRMS-(ESI) *m/z* calculated for $C_8H_{13}NO_2[M+H]^+$ 156.1019; found, 156.1015.



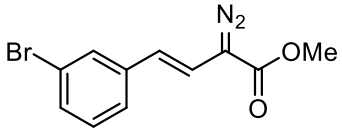
Compound 2.1i. Following the general procedure, the aziridination reaction to furnish **2.1i** was conducted on 1.74 mmol scale. The product was purified by silica gel flash column chromatography (0-2.5% MeOH/CH_2Cl_2 and then 0 to 70% EtOAc/Hexanes) to yield **2.1i** as a

colorless oil (53.8 mg, 27%). ^{1}H NMR (500 MHz, $CDCl_3$) δ 4.45 (ddd, *J* = 12.5, 10.6, 2.0 Hz, 1H), 4.33 (ddd, *J* = 10.6, 4.1, 1.9 Hz, 1H), 2.81 (ddt, *J* = 8.4, 6.1, 4.0 Hz, 1H), 2.55 (app d, *J* = 4.4 Hz, 1H), 2.42 (dddd *J* = 14.7, 6.1 Hz, 1.9, 1.9 Hz 1H); (app ddt, *J* = 14.7, 6.1 Hz, 1.9 Hz, 1H), 2.07 (app d, *J* = 3.6 Hz, 1H), 1.36 (dddd, *J* = 14.6, 12.6, 8.7, 4.1 Hz, 1H). ^{13}C NMR (126 MHz, $CDCl_3$) δ 160.91, 68.10, 35.24, 33.91, 25.51. HRMS-(ESI) *m/z* calculated for $C_5H_7NO_2[M+H]^+$ 114.0550; found, 114.0548.

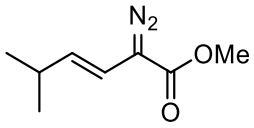
Preparation of diazoesters. All diazoester compounds, if not directly mentioned in the subsequent section, were synthesized according to the reported literature procedures and characterized as described therein.[4] Frequently, the signal-to-noise ratio for the diazo-carbon is not intense enough to be seen on ^{13}C NMR due to quadrupolar broadening.



A flame-dried, round bottom flask was placed under N_2 and charged with ester (1 eq., brought to 0.2 M in CH_3CN). *p*-ABSA (1.2 eq.) was then added in a single portion and the mixture cooled to 0 °C. After 5 minutes of cooling, freshly distilled DBU (2.0 eq.) was added dropwise to the mixture. This reaction was allowed to warm up to room temperature and stir until the TLC indicated completion. Once complete, the CH_3CN was removed under reduced pressure at room temperature. *Note: diazoesters are heat-sensitive and can become explosive if they are heated too high.* The concentrated mixture was then taken back up in ether and transferred to a separatory funnel. The organics were then washed twice with saturated aqueous NH_4Cl, dried with $MgSO_4$ and concentrated *in vacuo*. The residue was subjected to silica gel flash column chromatography (generally, 2% Et_2O/pentane to 10% Et_2O/pentane).

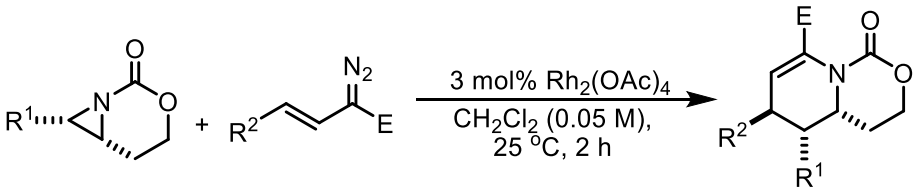


Compound 2.5d. Following a procedure published by Davies and coworkers[5a] from the corresponding aldehyde, the reaction to furnish diazoester **2.5d** was conducted on 10 mmol scale. The product was purified by silica gel flash column chromatography (2% Et_2O/Pentane to 10% Et_2O/Pentane) to yield **2.5d** as an orange solid (950.0 mg, 34%). ^{1}H NMR (500 MHz, $CDCl_3$) δ 7.50 (t, *J* = 1.9 Hz, 1H), 7.32 (ddd, *J* = 7.8, 1.9, 1.0 Hz, 1H), 7.27 (s, 1H), 7.18 (t, *J* = 7.8 Hz, 1H), 6.50 (d, *J* = 16.3 Hz, 1H), 6.13 (d, *J* = 16.3 Hz, 1H), 3.86 (s, 3H). ^{13}C NMR (126 MHz, $CDCl_3$) δ 165.4, 139.1, 130.3, 130.0, 128.8, 124.6, 123.1, 121.5, 113.4, 52.6, $C_{11}H_9BrN_2O_2[M+H]^+$ 280.9920; found, 280.9919.



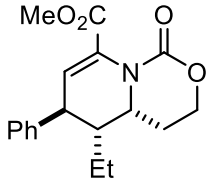
Compound 2.5g. Following the procedure described above, the reaction to furnish diazoester **2.5g** was conducted on 8.44 mmol scale. The product was purified by silica gel flash column chromatography (2% Et_2O/Pentane to 10% Et_2O/Pentane) to yield **2.5g** as a red oil (980.6 mg, 69%). ^{1}H NMR (500 MHz, $CDCl_3$) δ 5.69 (dd, *J* = 15.9, 1.4 Hz, 1H), 5.29 (dd, *J* = 15.9, 6.7 Hz, 1H), 3.80 (s, 3H), 2.44 (hd, *J* = 6.7, 1.4 Hz, 1H), 1.03 (d, *J* = 6.8 Hz, 6H). ^{13}C NMR (126 MHz, $CDCl_3$) δ 166.1, 132.6, 109.2, 52.1, 31.40, 22.5. $C_8H_{12}N_2O_2$ $[M+H]^+$ 169.0972; found, 169.0969.

2.8.2 General Procedure for Piperidine Synthesis.

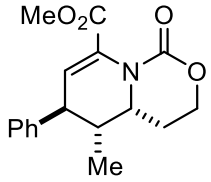


A flame-dried round bottom flask was placed under nitrogen and charged with $Rh_2(OAc)_4$ (0.03 eq.), followed by a solution of the aziridine (0.1 M in dry CH_2Cl_2). *Note: Upon the addition of aziridine, a color change of green to purple will be observed. This does not signify catalyst death; rather, experiments show that if this color change is not observed, the reaction is less likely to proceed*. To this mixture was added a solution of the diazoester compound (1.2 eq., brought to 0.1 M in CH_2Cl_2) dropwise over 2 h using a syringe pump. The conversion was

checked by TLC and NMR after the addition was complete; once all the starting material had been consumed, the reaction was concentrated and loaded directly onto silica for column chromatography (0% to 50% EtOAc/Hexanes). *Note: The R_f differences between the aziridine and the piperidine product can be very small.*

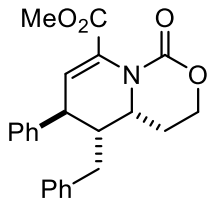


Compound 2.6aa. Following the general procedure, the carbene transfer to furnish **2.6aa** was conducted on 1.00 mmol scale. The product was purified by silica gel flash column chromatography (0 to 50% EtOAc/hexanes, 10% increments) to yield **2.6aa** as a white solid (237.9 mg, 75% yield, >19:1 *dr*). ^{1}H NMR (500 MHz, $CDCl_3$) δ 7.35 (t, *J* = 7.6 Hz, 2H), 7.27 (d, *J* = 8.3 Hz, 1H), 7.20 – 7.14 (m, 2H), 6.12 (dd, *J* = 4.6, 1.4 Hz, 1H), 4.33 – 4.24 (m, 2H), 3.84 (s, 3H), 3.72 (ddd, *J* = 10.1, 8.1, 1.7 Hz, 1H), 3.66 (d, *J* = 4.6 Hz, 1H), 2.12 – 2.01 (m, 1H), 1.90 (dddd, *J* = 14.3, 8.1, 2.0, 2.0 Hz, 1H); (app ddt, *J* = 14.3, 8.1, 2.0 Hz, 1H), 1.65 – 1.54 (m, 3H), 1.16 – 1.13 (m, 3H). ^{13}C NMR (126 MHz, $CDCl_3$) δ 164.2, 152.7, 143.3, 133.3, 128.7, 128.3, 126.9, 120.3, 64.6, 52.5, 51.7, 47.0, 41.8, 25.5, 19.0, 12.2 HRMS (ESI) *m/z* calculated for $C_{18}H_{21}NO_4[M+H]^+$ 316.1543; found, 316.1541.

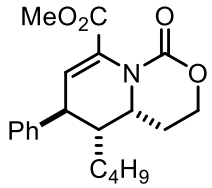


Compound 2.6ba. Following the general procedure, the carbene transfer to furnish **2.6ba** was conducted on 0.20 mmol scale. The product was purified by silica gel flash column chromatography (0 to 50% EtOAc/Hexanes, 10% increments) to yield **2.6ba** as a white solid (38.4 mg, 65% yield, >19:1 *dr*). ^{1}H NMR (500 MHz, $CDCl_3$) δ 7.35 (dd, *J* = 8.3, 6.9 Hz, 2H), 7.29 – 7.27 (m, 1H), 7.24 – 7.13 (m, 2H), 6.11 (dd, *J* = 4.6, 1.5 Hz, 1H), 4.35 – 4.23 (m, 2H),

3.85 (s, 3H), 3.70 (ddd, *J* = 10.4, 7.9, 1.8 Hz, 1H), 3.44 (d, *J* = 4.6 Hz, 1H), 2.08 – 1.93 (m, 2H), 1.88 (dddd, *J* = 14.3, 7.8, 2.1, 2.1 Hz, 1H); (app ddt, *J* = 14.3, 7.8, 2.1 Hz, 1H), 1.07 (d, *J* = 6.9 Hz, 3H). ^{13}C NMR (126 MHz, $CDCl_3$) δ 164.5, 152.9, 143.5, 133.0, 128.9, 128.4, 127.2, 120.1, 64.7, 52.7, 51.9, 46.1, 39.1, 25.9, 13.9. HRMS (ESI) *m/z* calculated for $C_{17}H_{19}NO_4$ $[2M+NH_4]^+$; 620.2966 found, 620.2973.

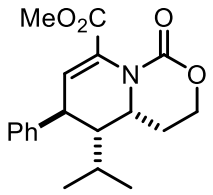


Compound 2.6ca. Following the general procedure, the carbene transfer to furnish **2.6ca** was conducted on 0.1 mmol scale. The product was purified by silica gel flash column chromatography (0 to 50% EtOAc/hexanes, 10% increments) to yield **2.6ca** as a white solid (30.8 mg, 76% yield, >19:1 *dr*). ^{1}H NMR (500 MHz, $CDCl_3$) δ 7.38 (t, *J* = 7.5 Hz, 2H), 7.32 – 7.27 (m, 1H), 7.26 – 7.23 (m, 4H), 7.23 – 7.18 (m, 1H), 6.87 (dd, *J* = 7.0, 1.9 Hz, 2H), 6.12 (dd, *J* = 4.6, 1.4 Hz, 1H), 4.45 – 4.25 (m, 2H), 3.87 (s, 3H), 3.87 – 3.81 (m, 1H), 3.50 (d, *J* = 4.6 Hz, 1H), 2.98 (dd, *J* = 13.7, 3.0 Hz, 1H), 2.34 – 2.20 (m, 2H), 2.13 (m, 1H), 2.02 (dddd, *J* = 14.2, 8.0, 2.0, 2.0 Hz, 1H); (app ddt, *J* = 14.2, 8.0, 2.0 Hz, 1H).^{13}C NMR (126 MHz, $CDCl_3$) δ 164.1, 152.6, 143.1, 139.0, 133.3, 129.3, 128.8, 128.6, 128.1, 126.9, 126.6, 120.0, 64.6, 52.6, 51.6, 46.7, 41.0, 32.6, 25.5. HRMS (ESI) *m/z* calculated for $C_{23}H_{23}NO_4$ [M+H]+ 378.1700; found, 378.1696.

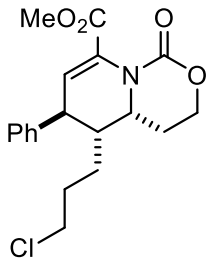


Compound 2.6da. Following the general procedure, the carbene transfer to furnish **2.6da** was conducted on 0.29 mmol scale. The product was purified by silica gel flash column

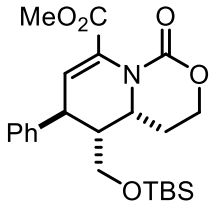
chromatography (0 to 40% EtOAc/Hexanes, 10% increments) to yield **2.6da** as a white solid (91.6 mg, 92% yield, >19:1 *dr*). ^{1}H NMR (500 MHz, $CDCl_3$) δ 7.35 (t, *J* = 7.5 Hz, 3H), 7.20 – 7.13 (m, 2H), 6.11 (dd, *J* = 4.6, 1.5 Hz, 1H), 4.33 – 4.25 (m, 2H), 3.84 (s, 3H), 3.76 – 3.67 (m, 1H), 3.63 (d, *J* = 4.6 Hz, 1H), 2.05 (dt, *J* = 14.2, 5.0 Hz, 1H), 1.89 (dddd, *J* = 14.3, 8.0, 2.0, 2.0 Hz, 1H); (app ddt, *J* = 14.3, 8.0, 2.0 Hz, 1H), 1.75 – 1.60 (m, 2H), 1.53 – 1.33 (m, 5H), 1.15 (dddd, *J* = 13.7, 10.4, 8.9, 4.6 Hz, 1H), 0.95 (t, *J* = 6.9 Hz, 3H). ^{13}C NMR (126 MHz, $CDCl_3$) δ 164.3, 152.7, 143.4, 133.3, 128.7, 128.3, 127.0, 120.4, 64.6, 52.5, 51.7, 45.1, 42.6, 30.1, 25.9, 25.5, 22.8, 14.1. HRMS (ESI) *m/z* calculated for $C_{20}H_{25}NO_4$ $[M+H]^+$ 344.1856; found, 344.1853.



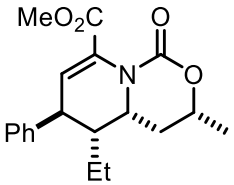
Compound 2.6ea. Following the general procedure, the carbene transfer to furnish **2.6ea** was conducted on 0.32 mmol scale. The product was purified by silica gel flash column chromatography (0 to 40% EtOAc/Hexanes, 10% increments) to yield **2.6ea** as a white solid (74.2 mg, 70% yield, >19:1 *dr*). ^{1}H NMR (500 MHz, $CDCl_3$) δ 7.34 (dd, *J* = 8.2, 7.0 Hz, 2H), 7.25 (d, *J* = 7.4 Hz, 1H), 7.21 – 7.16 (m, 2H), 6.13 (dd, *J* = 4.3, 1.2 Hz, 1H), 4.37 – 4.29 (m, 2H), 3.83 (m, 4H), 3.63 (d, *J* = 4.4 Hz, 1H), 2.27 (dddd *J* = 14.2, 11.3, 8.4, 8.4, 1H); (app ddt, *J* = 14.2, 11.3, 8.4 Hz, 1H), 2.15 (heptd, *J* = 6.9, 2.3 Hz, 1H), 1.86 (dddd *J* = 14.3, 7.4, 2.0, 2.0, 1H); (app ddt, *J* = 14.3, 7.4, 2.0 Hz, 1H), 1.72 (ddd *J* = 2.5, 2.5, 1.1 Hz, 1H); (app td, *J* = 2.5, 1.1 Hz, 1H), 1.18 (d, *J* = 6.8 Hz, 3H), 0.91 (d, *J* = 6.9 Hz, 3H). ^{13}C NMR (126 MHz, $CDCl_3$) δ 164.3, 151.9, 144.6, 133.4, 128.8, 128.0, 126.8, 121.8, 64.8, 52.5, 52.2, 49.5, 37.9, 25.7, 25.1, 24.1, 17.4.



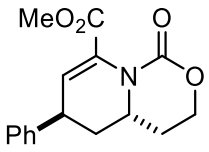
Compound 2.6fa. Following the general procedure, the carbene transfer to furnish **2.6fa** was conducted on 0.1 mmol scale. The product was purified by silica gel flash chromatography (0 to 50% EtOAc/Hexanes, 10% increments) to yield compound **2.6fa** as a white solid (25.1 mg, 69% yield, >19:1 *dr*). ^{1}H NMR (500 MHz, $CDCl_3$) δ 7.36 (t, *J* = 7.6 Hz, 2H), 7.30 – 7.27 (m, 1H), 7.17 – 7.14 (m, 2H), 6.11 (dd, *J* = 4.7, 1.5 Hz, 1H), 4.35 – 4.26 (m, 2H), 3.85 (s, 3H), 3.75 (ddd, *J* = 10.3, 8.2, 1.7 Hz, 1H), 3.64 – 3.50 (m, 3H), 2.25 – 2.12 (m, 1H), 2.12 – 2.03 (m, 1H), 1.97 – 1.84 (m, 2H), 1.78 – 1.65 (m, 1H), 1.26 (tt, *J* = 10.1, 4.7 Hz, 2H). ^{13}C NMR (126 MHz, $CDCl_3$) δ 164.1, 152.5, 142.9, 133.4, 128.8, 128.2, 127.1, 119.8, 64.5, 52.6, 51.5, 44.3, 44.2, 42.6, 30.7, 25.5, 23.6. HRMS (ESI) *m/z* calculated for $C_{19}H_{22}ClNO_4$ [M+H]+ 364.1310; found, 364.1306.



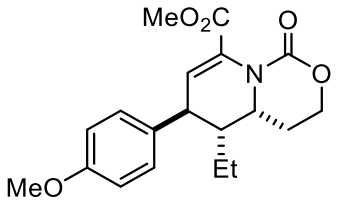
Compound 2.6ga. Following the general procedure, the carbene transfer to furnish **2.6ga** was conducted on 0.19 mmol scale. The product was purified by silica gel flash column chromatography (0 to 40% EtOAc/Hexanes, 10% increments) to yield **2.6ga** as a white solid (70.6 mg, 74% yield, >19:1 *dr*). ^{1}H NMR (500 MHz, $CDCl_3$) δ 7.39 – 7.30 (m, 2H), 7.28 (m, 1H), 7.21 – 7.11 (m, 2H), 6.11 (dd, *J* = 4.6, 1.5 Hz, 1H), 4.28 (m, 2 H), 3.87 – 3.71 (m, 5H), 3.46 (dd, *J* = 10.3, 8.4 Hz, 1H), 2.31 (dddd *J* = 14.4, 11.1, 8.6, 8.6 Hz, 1H); (app ddt, *J* = 14.4, 11.1, 8.6 Hz, 1H), 2.06 (ddd, *J* = 9.1, 5.4, 1.8 Hz, 1H), 1.93 (dddd, *J* = 14.4, 7.8, 2.0 Hz, 1H); (app ddt, *J* = 14.4, 7.8, 2.0 Hz, 1H), 0.93 (s, 9H), 0.08 (s, 6H). ^{13}C NMR (126 MHz, $CDCl_3$) δ 164.4, 152.3, 143.5, 133.2, 128.9, 128.4, 127.1, 120.4, 64.9, 60.8, 52.7, 50.9, 47.7, 40.6, 26.0, 0.2, -5.3. HRMS (ESI) *m/z* calculated for $C_{23}H_{33}NO_5Si$ $[M+H]^+$ 432.2201; found, 432.2201.



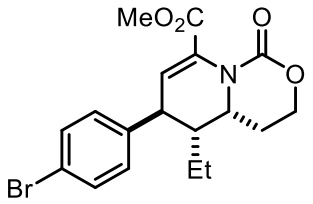
Compound 2.6ha. Following the general procedure, the carbene transfer to furnish **2.6ha** was conducted on 0.1 mmol scale. The product was purified by silica gel flash column chromatography (0 to 35% EtOAc/Hexanes, 10% increments) to yield compound **2.6ha** as a colorless waxy solid (24.0 mg, 72% yield, >19:1 *dr*). A residual minor NMR impurity results from the difficulty of separating the C-H insertion product from the aziridine product in the preceding step. ^{1}H NMR (500 MHz, $CDCl_3$) δ 7.34 (dd, *J* = 8.2, 7.0 Hz, 2H), 7.27 (d, *J* = 1.4 Hz, 1H), 7.22 – 7.03 (m, 2H), 6.10 (dd, *J* = 4.6, 1.4 Hz, 1H), 4.49 (dqd, *J* = 12.5, 6.3, 1.9 Hz, 1H), 3.84 (s, 3H), 3.71 – 3.66 (m, 1H), 3.65 (d, *J* = 4.6 Hz, 1H), 1.90 (ddd, *J* = 14.0, 8.0, 2.0 Hz, 1H), 1.77 (dt, *J* = 14.0, 11.1 Hz, 1H),1.62 – 1.53 (m, 2H), 1.37 (d, *J* = 6.2 Hz, 3H), 1.19 – 1.11 (m, 4H). ^{13}C NMR (126 MHz, $CDCl_3$) δ 164.5, 152.8, 143.5, 133.4, 128.8, 128.4, 127.0, 120.3, 72.1, 52.6, 51.4, 47.1, 42.0, 32.7, 20.3, 19.1, 12.3 HRMS (ESI) *m/z* calculated $C_{19}H_{23}NO_4$ [M+H]+ 330.1700; found, 330.1698.



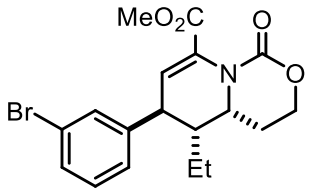
Compound 2.6ia. Following the general procedure, the carbene transfer to furnish **2.6ia** was conducted on 0.17 mmol scale. The product was purified by silica gel flash column chromatography (0 to 50% EtOAc/Hexanes, 10% increments) to yield **2.6ia** as a white solid (33.8 mg, 67% yield, >19:1 *dr*). ^{1}H NMR (500 MHz, $CDCl_3$) δ 7.43 – 7.32 (m, 2H), 7.28 (d, *J* = 7.4 Hz, 1H), 7.21 – 7.16 (m, 2H), 6.17 (dd, *J* = 4.3, 1.3 Hz, 1H), 4.38 – 4.23 (m, 2H), 3.84 (s, 3H), 3.72 (ddd, *J* = 6.1, 4.4, 1.6 Hz, 1H), 3.63 (tdd, *J* = 10.5, 6.7, 2.9 Hz, 1H), 2.12 (dddd, *J* = 14.3, 6.7, 2.1, 2.1 Hz, 1H); (app ddt, *J* = 14.3, 6.7, 2.1 Hz, 1H), 2.09 – 1.95 (m, 2H), 1.90 – 1.73 (m, 1H). ^{13}C NMR (126 MHz, $CDCl_3$) δ 164.7, 151.5, 143.7, 133.1, 128.8, 127.9, 127.1, 121.9, 64.7, 52.5, 49.1, 38.5, 37.2, 29.3. HRMS (ESI) *m/z* calculated for $C_{16}H_{17}NO_4$ $[M+H]^+$ 287.1230; found, 287.1225.



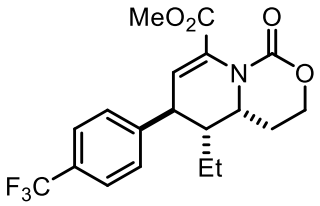
Compound 2.6cb. Following the general procedure, the carbene transfer to furnish **2.6cb** was conducted on 0.16 mmol scale. The product was purified by silica gel flash column chromatography (0 to 50% EtOAc/hexanes, 10% increments) to yield compound **2.6cb** as a white solid (42.9 mg, 78% yield, >19:1 *dr*). ^{1}H NMR (500 MHz, $CDCl_3$) δ 7.08 (d, *J* = 8.6 Hz, 2H), 6.87 (d, *J* = 8.7 Hz, 2H), 6.10 (dd, *J* = 4.6, 1.4 Hz, 1H), 4.39 – 4.21 (m, 2H), 3.84 (s, 3H), 3.80 (s, 3H), 3.70 (ddd, *J* = 10.1, 8.1, 1.6 Hz, 1H), 3.60 (d, *J* = 4.6 Hz, 1H), 2.06 (dddd *J* = 14.2, 10.7, 10.7, 6.6 Hz, 1H); (app dtd, *J* = 14.2, 10.7, 6.6 Hz, 1H), 1.89 (dddd, *J* = 14.3, 8.1, 2.0, 2.0 Hz, 1H); (app ddt, *J* = 14.3, 8.1, 2.0 Hz, 1H), 1.66 – 1.49 (m, 2H), 1.15 – 1.10 (m, 4H). ^{13}C NMR (126 MHz, $CDCl_3$) δ 164.3, 158.5, 152.7, 135.4, 133.0, 129.3, 120.7, 114.0, 64.6, 55.3, 52.5, 51.6, 47.2, 41.0, 25.5, 18.9, 12.2 HRMS (ESI) *m/z* calculated for $C_{19}H_{23}NO_5$ [M+H+] 346.1640; found, 346.1646.



Compound 2.6cc. Following the general procedure, the carbene transfer to furnish **2.6cc** was conducted on 0.35 mmol scale. The product was purified by silica gel flash column chromatography (0 to 40% EtOAc/Hexanes, 10% increments) to yield **2.6cc** as a white solid (90.6 mg, 72% yield, >19:1 *dr*). ^{1}H NMR (500 MHz, $CDCl_3$) δ 7.51 – 7.39 (m, 2H), 7.09 – 7.02 (m, 2H), 6.06 (dd, *J* = 4.6, 1.5 Hz, 1H), 4.34 – 4.24 (m, 2H), 3.84 (s, 3H), 3.65 (ddd, *J* = 10.3, 8.2, 1.6 Hz, 1H), 3.61 (d, *J* = 4.6 Hz, 1H), 2.13 – 2.01 (m, 1H), 1.90 (m, , 1H), 1.65 – 1.52 (m, 3H), 1.16 – 1.11 (m, 3H). ^{13}C NMR (126 MHz, $CDCl_3$) δ 164.3, 152.7, 142.5, 133.8, 132.0, 130.2, 121.1, 119.6, 64.7, 52.8, 51.8, 47.1, 41.4, 25.7, 19.1, 12.3. HRMS (ESI) *m/z* calculated for $C_{18}H_{20}BrNO_4$ $[M+Na]^+$ 416.0468; found, 416.0461.

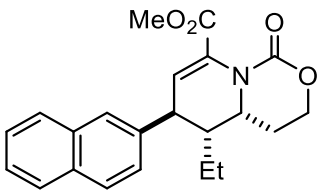


Compound 2.6cd. Following the general procedure, the carbene transfer to furnish **2.6cd** was conducted on 0.12 mmol scale. The product was purified by silica gel flash chromatography (0 to 50% EtOAc/hexanes, 10% increments) to yield **2.6cd** as a white solid (34.6 mg, 73% yield, >19:1 *dr*). ^{1}H NMR (500 MHz, $CDCl_3$) δ 7.40 (dt, *J* = 8.4, 1.2 Hz, 1H), 7.29 (d, *J* = 1.9 Hz, 1H), 7.22 (t, *J* = 7.8 Hz, 1H), 7.10 (dt, *J* = 7.7, 1.4 Hz, 1H), 6.05 (dd, *J* = 4.6, 1.5 Hz, 1H), 4.42 – 4.24 (m, 2H), 3.84 (s, 3H), 3.67 (ddd, *J* = 10.2, 8.1, 1.6 Hz, 1H), 3.62 (d, *J* = 4.6 Hz, 1H), 2.07 (dddd *J* = 14.3, 11.0, 11.0, 5.9 Hz, 1H);(app dtd, *J* = 14.3, 11.0, 5.9 Hz, 1H), 1.92 (dddd *J* = 14.3, 8.1, 2.0, 2.0 Hz, 1H); (app ddt, *J* = 14.3, 8.1, 2.0 Hz, 1H), 1.66 – 1.53 (m, 2H), 1.13 (m, 4H). ^{13}C NMR (126 MHz, $CDCl_3$) δ 164.2, 152.8, 145.9, 134.0, 131.4, 130.4, 130.3, 127.2, 123.1, 119.3, 64.7, 52.8, 51.9, 47.1, 41.6, 25.6, 19.1, 12.3. HRMS (ESI) *m/z* calculated for $C_{18}H_{20}BrNO_4$ $[2M+NH_4]+$ 804.1490; found, 804.1501.

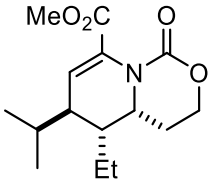


Compound 2.6ce. Following the general procedure, the carbene transfer to furnish **2.6ce** was conducted on 0.25 mmol scale using 4 mol% of $Rh_2(OAc)_4$. The product was purified by silica gel flash column chromatography (0 to 40% EtOAc/Hexanes, 10% increments) to yield **2.6ce** as a white solid (67.8 mg, 69% yield, >19:1 *dr*). ^{1}H NMR (500 MHz, $CDCl_3$) δ 7.61 (d, *J* = 8.1 Hz, 2H), 7.30 (d, *J* = 8.0 Hz, 2H), 6.08 (dd, *J* = 4.6, 1.4 Hz, 1H), 4.31 (m, 2H), 3.84 (s, 3H), 3.72 (d, *J* = 4.6 Hz, 1H), 3.67 (ddd, *J* = 10.1, 8.1, 1.6 Hz, 1H), 2.12 – 2.05 (m, 1H), 1.92 (dddd *J* = 14.3, 8.1, 2.0, 2.0 Hz, 1H); (app ddt, *J* = 14.3, 8.1, 2.0 Hz, 1H), 1.67 – 1.56 (m, 2H), 1.21 – 1.12 (m, 3H). ^{13}C NMR (126 MHz, $CDCl_3$) δ 164.2, 152.7, 147.5, 134.0, 129.5, 128.8, 125.8, 119.1, 64.7,

52.7, 51.8, 46.9, 41.7, 25.5, 19.1, 12.2. HRMS (ESI) *m/z* calculated for $C_{19}H_{20}F_3NO_4$ [M+H]+ 384.1417; found, 384.1407.

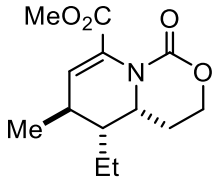


Compound 2.6cf. Following the general procedure, the carbene transfer to furnish **2.6cf** was conducted on 0.1 mmol scale. The product was purified by silica gel flash chromatography (0 to 50% EtOAc/hexanes, 10% increments) to yield **2.6cf** as a white solid (28.4 mg, 78% yield, >19:1 *dr*). ^{1}H NMR (500 MHz, $CDCl_3$) δ 7.98 – 7.61 (m, 3H), 7.62 – 7.41 (m, 3H), 7.31 (dd, *J* = 8.5, 1.9 Hz, 1H), 6.23 (dd, *J* = 4.6, 1.5 Hz, 1H), 4.37 – 4.22 (m, 2H), 3.89 (s, 3H), 3.81 (d, *J* = 4.6 Hz, 1H), 3.76 (ddd, *J* = 10.2, 8.2, 1.7 Hz, 1H), 2.17 – 1.98 (m, 1H), 1.84 (dddd, *J* = 14.2, 8.1, 2.0, 2.0 Hz, 1H); (app ddt, *J* = 14.2, 8.1, 2.0 Hz, 1H), 1.73 – 1.67 (m, 1H), 1.68 – 1.58 (m, 1H), 1.24 – 1.16 (m, 4H). ^{13}C NMR (126 MHz, $CDCl_3$) δ 164.4, 152.9, 140.8, 133.7, 133.3, 132.4, 128.8, 127.9, 127.7, 127.1, 126.7, 126.6, 126.2, 120.4, 64.7, 52.7, 51.8, 46.8, 42.0, 25.6, 19.1, 12.3. HRMS (ESI) *m/z* calculated for $C_{22}H_{23}NO_4$ [M+H]+ 366.1700; found, 366.1697.

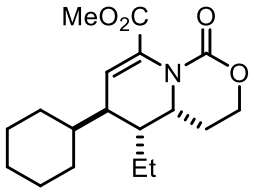


Compound 2.6cg. Following the general procedure, the carbene transfer to furnish **2.6cg** was conducted on 0.18 mmol scale. The product was purified by silica gel flash chromatography (0 to 50% EtOAc/hexanes, 10% increments) to yield (0 to 50% EtOAc/hexanes, 10% increments) **2.6cg** as a white solid (38.0 mg, 75% yield, >19:1 *dr*). ^{1}H NMR (500 MHz, $CDCl_3$) δ 6.11 (dd, *J* = 4.5, 1.5 Hz, 1H), 4.31 (dd, *J* = 8.8, 2.2 Hz, 2H), 3.78 (s, 3H), 3.67 (ddd, *J* = 10.3, 8.2, 1.8 Hz, 1H), 2.14 (ddt, *J* = 14.3, 10.4, 8.6 Hz, 1H), 2.06 (ddt, *J* = 14.2, 8.3, 2.2 Hz, 1H), 1.89 (dd, *J* = 8.3, 4.5 Hz, 1H), 1.66 – 1.56 (m, 1H), 1.49 (m, 2H), 1.02 (d, *J* = 6.7 Hz, 3H), 0.96 (d, *J* = 6.6 Hz,

3H), 0.95 – 0.90 (m, 4H).^{13}C NMR (126 MHz, $CDCl_3$) δ 164.3, 152.7, 131.2, 123.6, 64.6, 53.7, 52.3, 43.7, 41.0, 33.0, 25.8, 21.1, 20.7, 19.0, 11.7 HRMS (ESI) *m/z* calculated for $C_{15}H_{23}NO_4$ $[M+H]^+$ 282.1700; found, 282.1698.

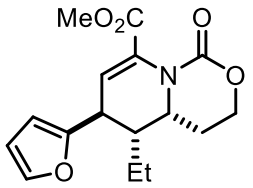


Compound 2.6ch. Following the general procedure, the carbene transfer to furnish **2.6ch** was conducted on 0.18 mmol scale. The product was purified by silica gel flash column chromatography (0 to 50% EtOAc/hexanes, 10% increments) to yield **2.6ch** as a white solid (30.5 mg, 69% yield, >19:1 *dr*). ^{1}H NMR (500 MHz, $CDCl_3$) δ 6.02 (dd, *J* = 4.5, 1.4 Hz, 1H), 4.41 – 4.26 (m, 2H), 3.77 (s, 3H), 3.73 (ddd, *J* = 10.2, 8.2, 1.7 Hz, 1H), 2.41 (qd, *J* = 7.2, 4.4 Hz, 1H), 2.23 – 2.02 (m, 2H), 1.49 (dddd 13.4, 7.1, 3.9, 3.9 Hz, 1H); (app ddt, *J* = 13.4, 7.1, 3.9 Hz, 1H), 1.35 (m, 1H), 1.09 (d, *J* = 7.2 Hz, 3H), 0.94 (m, 4H).^{13}C NMR (126 MHz, $CDCl_3$) δ 164.4, 152.9, 130.9, 126.4, 64.7, 52.6, 52.5, 45.0, 31.3, 25.9, 21.8, 19.1, 12.1 HRMS (ESI) *m/z* calculated for $C_{13}H_{19}NO_4$ [M+H]+ 254.1387; found, 254.1385.

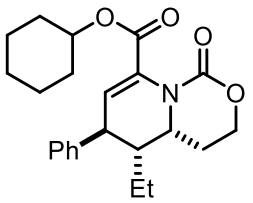


Compound 2.6ci. Following the general procedure, the carbene transfer to furnish **2.6ci** was conducted on 0.35 mmol scale. The product was purified by silica gel flash column chromatography (0 to 50% EtOAc/Hexanes, 10% increments) to yield **2.6ci** as a white solid (77.3 mg, 70% yield, >19:1 *dr*). ^{1}H NMR (500 MHz, $CDCl_3$) δ 6.10 (dd, *J* = 4.6, 1.4 Hz, 1H), 4.31 (dd, *J* = 7.7, 1.9 Hz, 2H), 3.78 (s, 3H), 3.68 (ddd, *J* = 10.2, 8.2, 1.7 Hz, 1H), 2.17 – 2.06 (m, 1H), 1.97 (dd, *J* = 7.7, 4.5 Hz, 1H), 1.88 – 1.44 (m, 9H), 1.33 – 1.07 (m, 6H), 1.00 – 0.86 (m, 4H). ^{13}C NMR (126 MHz, $CDCl_3$) δ 164.5, 152.9, 131.3, 123.8, 64.8, 54.1, 52.5, 43.0, 42.7,

41.0, 31.5, 31.2, 26.5, 26.0, 19.2, 12.0. HRMS (ESI) *m/z* calculated for $C_{18}H_{27}NO_4$ $[M+H]^+$ 322.2013; found, 322.2010.



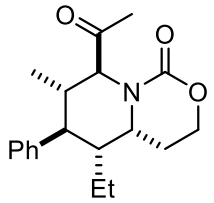
Compound 2.6cj. Following the general procedure, the carbene transfer to furnish **2.6cj** was conducted on 0.35 mmol scale. The product was purified by silica gel flash column chromatography (0 to 50% EtOAc/Hexanes, 10% increments) to yield **2.6cj** as a yellow solid (15.7 mg, 14% yield, >19:1 *dr*). ^{1}H NMR (500 MHz, $CDCl_3$) δ 7.36 (dd, *J* = 1.9, 0.8 Hz, 1H), 6.31 (dd, *J* = 3.2, 1.9 Hz, 1H), 6.08 (dd, *J* = 4.6, 1.4 Hz, 1H), 6.03 (dd, *J* = 3.2, 0.9 Hz, 1H), 4.43 – 4.23 (m, 2H), 3.84 – 3.74 (m, 4H), 3.65 (d, *J* = 4.7 Hz, 1H), 2.15 – 2.05 (m, 2H), 2.01 (dddd, *J* = 14.3, 8.2, 2.1, 2.1 Hz, 1H); (app ddt, *J* = 14.3, 8.2, 2.1 Hz, 1H), 1.90 – 1.80 (m, 1H), 1.62 – 1.49 (m, 2H), 1.12 – 1.02 (m, 3H). ^{13}C NMR (126 MHz, $CDCl_3$) δ 164.3, 155.4, 142.2, 133.3, 118.2, 110.4, 107.4, 64.8, 53.2, 52.7, 43.0, 36.4, 25.7, 18.6, 12.1. HRMS (ESI) *m/z* calculated for $C_{16}H_{19}NO_5$ $[M+H]^+$ 306.1336; found, 306.1331.



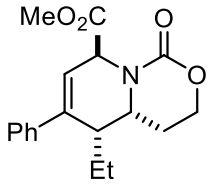
Compound 2.6ck. Following the general procedure, the carbene transfer to furnish **2.6ck** was conducted on 0.25 mmol scale. The product was purified by silica gel flash column chromatography (0 to 50% EtOAc/Hexanes, 10% increments) to yield **2.6ck** as a white solid (52.9 mg, 56% yield, >19:1 *dr*). ^{1}H NMR (500 MHz, $CDCl_3$) δ 7.35 (dd, *J* = 8.2, 6.9 Hz, 2H), 7.30 – 7.26 (m, 1H), 7.19 – 7.13 (m, 2H), 6.10 (dd, *J* = 4.6, 1.4 Hz, 1H), 4.91 (tt, *J* = 8.9, 3.9 Hz, 1H), 4.31 – 4.25 (m, 2H), 3.72 (ddd, *J* = 10.4, 8.2, 1.5 Hz, 1H), 3.65 (d, *J* = 4.5 Hz, 1H), 2.13 – 1.85 (m, 1H), 1.75 (m, 2H), 1.66 – 1.46 (m, 6H), 1.45 – 1.34 (m, 2 H), 1.33 – 1.16 (m, 2H), 1.15 (m, 3H). ^{13}C NMR (126 MHz, $CDCl_3$) δ 163.3, 152.8, 143.8, 134.2, 128.9, 128.5, 127.0, 120.1,

64.7, 51.9, 47.3, 42.0, 31.7, 31.5, 25.8, 25.6, 24.0, 19.2, 12.4, 0.2. HRMS (ESI) *m/z* calculated for $C_{23}H_{29}NO_4$ $[M+H]^+$ 384.2169; found, 384.2165.

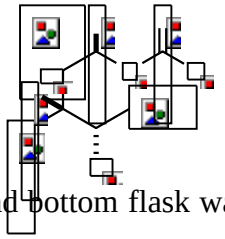
2.8.3. Piperidine derivatizations



Compound 2.11. In accordance with literature conditions,[6] a flame-dried round bottom flask was charged with piperidine **2.6aa (**0.23 mmol, 1 eq.) and diluted to 0.01 M with freshly distilled ether. This solution was cooled to -78 ˚C and allowed to stir while a second flame-dried round bottom flask was charged with CuCN (1.2 mmol, 5 eq.) and diluted with 12 mL of freshly distilled ether (0.1 M) and cooled to -35 ˚C. To the flask containing CuCN was added a solution of MeLi dropwise (1.5 mL, 1.6 M solution in Et_2O, 10 eq.). After five minutes, the mixture was warmed up to 0 ˚C and allowed to stir for 30 additional minutes. After this period, the solution was cannula transferred to the cooled mixture of **2.6aa** in Et_2O. After five minutes, the reaction mixture was allowed to warm to room temperature and stirred until TLC indicated complete consumption of the starting material. The reaction was then quenched with saturated NH_4Cl and diluted with CH_2Cl_2. This biphasic mixture was filtered to remove solids and the resulting biphasic mixture was transferred to a separatory funnel. The layers were separated, and the aqueous layer extracted with three portions of CH_2Cl_2. The organics were combined, dried with Na_2SO_4, and the volatiles concentrated *in vacuo* and purified by silica gel flash chromatography (0 to 20% EtOAc/CH_2Cl_2, 10% increments) to yield **2.11** as a light-yellow oil (42.0 mg 57% yield). ^{1}H NMR (500 MHz, $CDCl_3$) δ 7.38 – 7.29 (m, 2H), 7.26 – 7.20 (m, 1H), 7.19 – 7.14 (m, 2H), 4.41 (d, *J* = 7.6 Hz, 1H), 4.39 – 4.35 (m, 1H), 4.35 – 4.26 (m, 2H), 2.48 (ddd, *J* = 14.0, 6.8, 3.4 Hz, 1H), 2.34 (s, 3H), 2.17 (dd, *J* = 10.6, 6.8 Hz, 1H), 2.13 – 2.02 (m, 1H), 1.96 (ddt, *J* = 13.8, 5.4, 2.8 Hz, 1H), 1.77 (qd, *J* = 6.9, 4.6 Hz, 1H), 1.40 – 1.30 (m, 1H), 1.12 (dt, *J* = 14.3, 7.2 Hz, 1H), 0.93 – 0.81 (m, 6H). ^{13}C NMR (126 MHz, $CDCl_3$) δ 208.5, 154.8, 144.4, 128.9, 127.9, 126.9, 66.7, 65.4, 52.9, 50.2, 45.0, 36.8, 29.4, 24.1, 23.1, 18.3, 11.6. HRMS (ESI) *m/z* calculated for $C_{19}H_{25}NO_3$ $[M+H]^+$ 316.1907; found, 316.108.

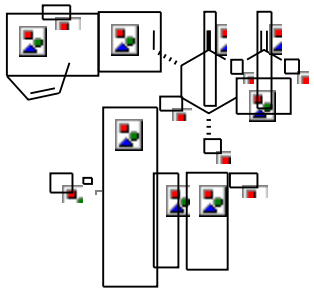


Compound 2.9. A flame-dried round bottom flask was charged with piperidine **2.6aa** and diluted with MeCN (0.10 mmol). To this solution was added DBU, dropwise (0.95 mmol, 3 eq.). This mixture was heated to 50 °C and was allowed to stir until TLC indicated completion (approximately 18 h). After TLC indicated complete consumption of the starting material the solution was cooled to room temperature and quenched with saturated NH_4Cl^+ and extracted with three portions of EtOAc. The combined organic layers were dried with Na_2SO_4, concentrated under reduced pressure and purified by silica gel flash column chromatography (0 to 60% EtOAc/Hexanes) to yield **Compound 2.9** as a viscous light-yellow oil (75.3 mg, 74% yield). ^{1}H NMR (500 MHz, $CDCl_3$) δ 7.36 (d, J = 4.3 Hz, 4H), 7.32 (dd, J = 4.9, 3.7 Hz, 1H), 6.08 (d, J = 3.8 Hz, 1H), 5.28 (d, *J* = 3.8 Hz, 1H), 4.44 – 4.29 (m, 2H), 4.01 (ddd, *J* = 9.6, 6.1, 3.2 Hz, 1H), 3.76 (s, 3H), 2.77 (m, 1H), 2.29 (dddd *J* = 14.3, 9.8, 9.8, 4.6 Hz, 1H); (app dtd, *J* = 14.3, 9.8, 4.6 Hz, 1H), 2.15 (dddd, J = 13.7, 6.5, 4.1, 2.8 Hz, 1H), 1.57 (m, 2H), 0.76 (t, J = 7.5 Hz, 3H). ^{13}C NMR (126 MHz, $CDCl_3$) δ 170.7, 154.8, 142.8, 140.0, 128.8, 128.2, 126.1, 118.6, 64.8, 57.1, 53.9, 52.8, 41.3, 25.6, 21.8, 11.8 δ HRMS (ESI) m/z calculated for $C_{18}H_{21}NO_4$ $[M+H]^+$ 316.1543; found, 316.1540.



Compound 2.10 To a flame dried round bottom flask was added **Compound 2.9**, CH_2Cl_2 (0.05 M), and *m*CPBA (2.8 eq. 0.22 mmol). The round bottom flask was fitted with a reflux condenser and allowed to stir at reflux until TLC indicated complete consumption of the starting material. Once complete, the reaction was quenched with H_2O and diluted with CH_2Cl_2. The biphasic mixture was transferred to a separatory funnel and the layers separated. The aqueous layer was extracted with three portions of CH_2Cl_2 and the combined organics dried over $MgSO_4$. The volatiles were then concentrated under reduced pressure and purified by silica gel flash column chromatography (0 to 60% EtOAc/Hexanes) to yield **2.10** as an off-white solid (21.7 mg, 83%

yield). ^{1}H NMR (500 MHz, $CDCl_3$) δ 7.48 – 7.34 (m, 5H), 5.17 (d, *J* = 3.6 Hz, 1H), 4.42 – 4.28 (m, 2H), 4.16 (ddd, *J* = 11.2, 6.1, 2.8 Hz, 1H), 4.06 (dd, *J* = 3.6, 1.0 Hz, 1H), 3.82 (s, 3H), 2.24 (m, 1H), 2.20 – 2.09 (m, 1H), 1.95 (ddt, *J* = 13.9, 5.9, 2.5 Hz, 1H), 1.48 (dtd, *J* = 9.7, 7.5, 4.0 Hz, 2H), 0.76 (t, *J* = 7.6 Hz, 3H). ^{13}C NMR (126 MHz, $CDCl_3$) δ 169.2, 154.6,137.4, 129.1, 128.9, 127.7, 65.1, 64.8, 56.0, 54.8, 53.0, 50.7, 43.0, 25.5, 19.0, 12.8. HRMS (ESI) m/z calculated for $C_{18}H_{21}NO_5$ $[M+H]^+$ 332.1493; found, 332.1484.



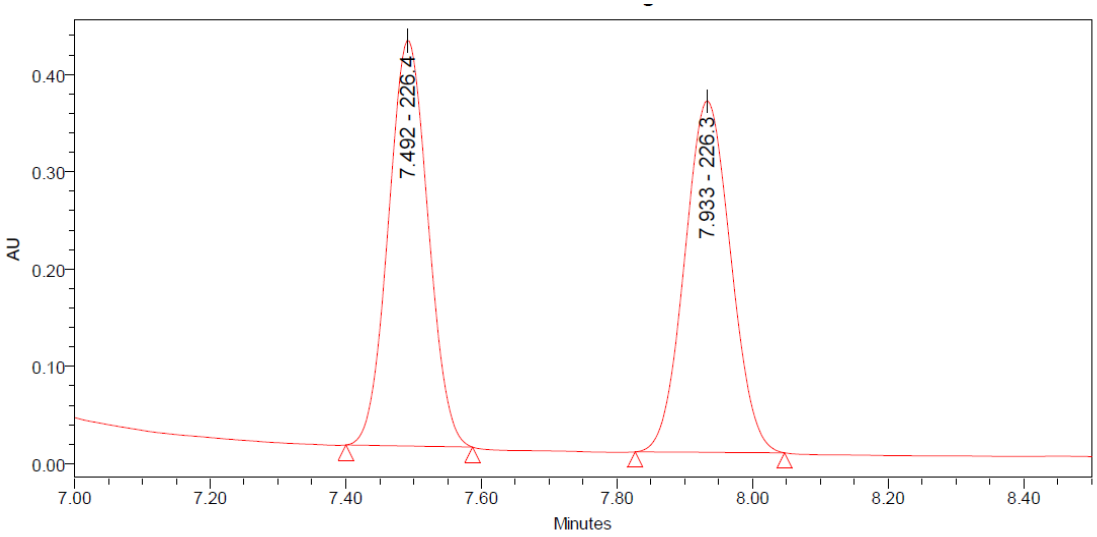
Compound 2.13 In accordance with literature conditions,[27] to a flame dried vial equipped with a Teflon septum was added piperidine **2.6aa**, Compound **2.12**, $Ir[DF(CF_3)ppy]_2(dtbby)PF_6$ (0.01 eq., 1.1 mg), K_2HPO_4 (1.2 eq., 20.9 mg), and DMF (0.4 M). The reaction mixture was degassed *via* a stream of nitrogen for 15 minutes and then irradiated with a 26W fluorescent lamp (2 cm from light source). After 36 hours the reaction mixture was diluted with saturated aqueous $NaHCO_3$ solution and extracted with three portions of Et_2O. The combined organics were washed with water and brine, then dried with $MgSO_4$. The crude material was concentrated under reduced pressure and purified by silica gel flash column chromatography (20 to 100% EtOAc/Hex) to yield **2.13** as a light-yellow solid (18.0 mg, 32% yield, 45% yield BRSM). The remainder of the mass balance appeared to be a Boc deprotected-10 with no other products or diastereomer detected *via* NMR. ^{1}H NMR (500 MHz, $CDCl_3$) δ 7.86 (s, 1H), 7.32 (d, *J* = 7.9 Hz, 1H), 7.24 (d, *J* = 8.1 Hz, 1H), 7.19 (t, *J* = 7.4 Hz, 2H), 7.14 (d, *J* = 7.1 Hz, 1H), 7.12 – 7.07 (m, 2H), 6.94 (t, *J* = 7.5 Hz, 1H), 6.59 (d, *J* = 2.4 Hz, 1H), 5.31 – 5.28 (m, 1H), 4.49 – 4.42 (m, 1H), 4.36 (td, *J* = 11.2, 4.3 Hz, 1H), 4.22 – 4.13 (m, 1H), 4.14 – 4.04 (m, 1H), 3.85 (bs, 1H), 3.73 (s, 3H), 2.90 (dd, *J* = 15.1, 7.2 Hz, 1H), 2.86 – 2.72 (m, 2H), 2.49 (dd, *J* = 12.6, 9.8 Hz, 1H), 1.90 (m, 2H), 1.75 (td, *J* = 13.1, 12.1, 5.6 Hz, 1H), 1.63 (bs, 1H), 1.42 (s, 9H), 1.07 – 0.97 (m, 1H), 0.92 – 0.80 (m, 1H), 0.67 (t, *J* = 7.4 Hz, 3H).^{13}C NMR (126 MHz, $CDCl_3$) δ 173.2, 156.5, 154.2, 141.8, 136.1, 129.0, 128.6, 127.6, 126.7, 122.1, 121.8, 119.3, 118.9, 112.1, 110.8, 78.8, 66.7,

53.9, 53.0, 52.7, 50.8, 49.4, 43.1, 40.6, 29.9, 28.6, 22.3, 22.0, 11.6. HRMS (ESI) m/z calculated for $C_{33}H_{41}N_3O_6$ [M+H]+ 576.3068; found, 576.3063.

2.8.4 Transfer of Chirality Experiments

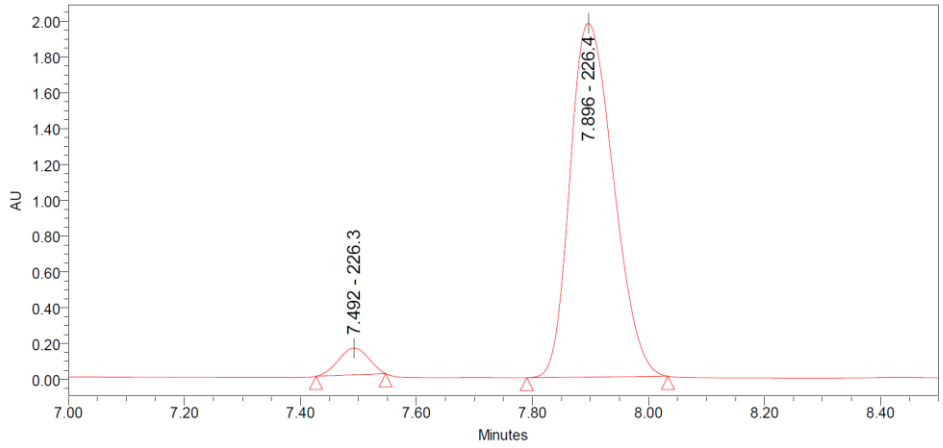
The enantioenriched bicyclic aziridine (*S,R*)-**2.1c** was synthesized as described above and its enantiopurity determined by SFC/MS. SFC/MS analyses were performed on a Waters ACQUITY UPC^2 equipped with ACQUITY UPC^2 PDA and ACQUITY QDa Detector. A CHIRALPAK IC-3 column (3mm ID × 150 mm L, 3 µm PS) was used for enantioselective separations. The eluent was a mixture (97:3 CO_2/ iPrOH) with a flow rate of 0.8 mL/min at 40 °C with an ABPR at 2200 psi.

Figure S-2.1. Racemic standard for (*S,R*)-**2.1c**



Peak #	Retention Time	Area	% Area
1	7.492	1694026	49.8%
2	7.933	1704523	50.2%

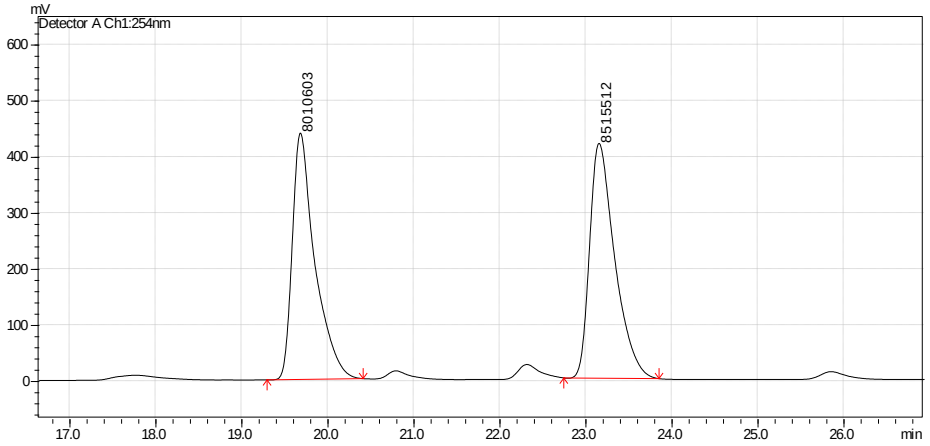
Figure S-2.2. Scalemic aziridine (*S*,*R*)-**2.1c** utilized in the synthesis of (*R*,*R*,*R*)-**2.6ca.**



Peak #	Retention Time	Area	% Area
1	7.492	605058	5.5%
2	7.896	10330501	94.5%

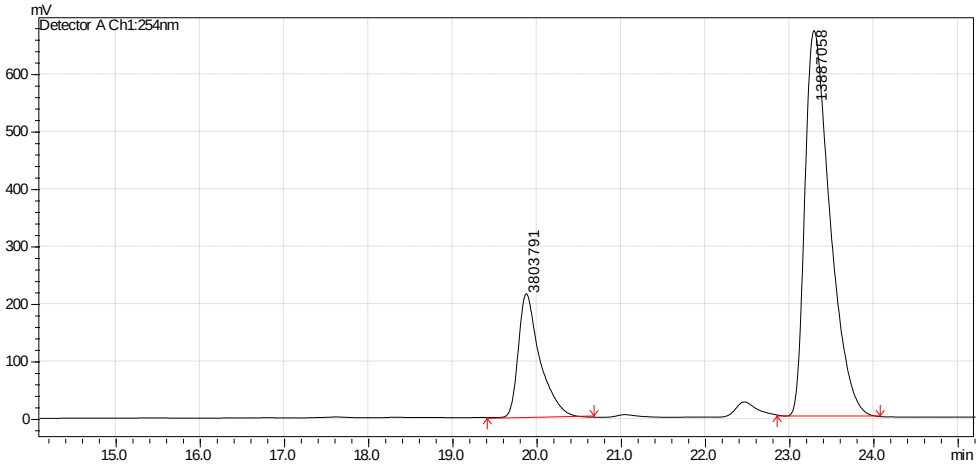
HPLC conditions – chromatograms of piperidine products were acquired on a Shimadzu Prominence HPLC equipped with a Chiracel AD-H column. Flow rate: 1.00 mL/min.; Oven temp 25.0 °C for compound **2.1c**, (*rac*)-**2.1c**, and scalemic (*S*,*R*)-**2.1c**; Solvent: 5:95 *i*PrOH:hexane, increasing to 30:70 *i*PrOH:hexane over 30 minutes. The eluent was held at the more polar composition for another 20 minutes to complete the analysis. Detector: UV @ 254 nm:

Figure S-2.3. Racemic piperidine (*R,R,R*)-**2.6ca.**



Peak #	Retention Time	Area	% Area
1	19.676	8010603	48.5%
2	23.148	8515512	51.5%

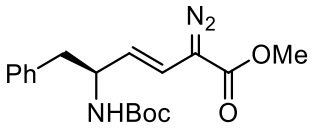
Figure S-2.4. Scalemic piperidine (*R,R,R*)-**2.6ca.**



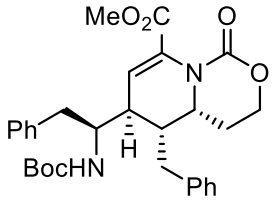
Peak #	Retention Time	Area	% Area
1	19.870	3803791	21.5%
2	23.218	13887058	78.5%

2.8.5 Piperidine Analogues of Select Biomolecules

The following molecules shown are synthetic intermediates accessed in pursuit of **2.15a** and **2.15b**, as well as characterization data regarding **2.15a** and **2.15b**. All intermediates not shown are known compounds and were synthesized according to published literature procedures and characterized therein.[5-7]

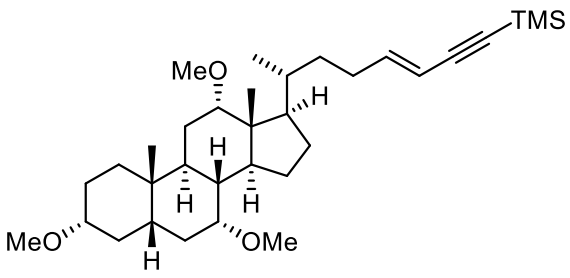


Compound 2.14a. Following the general procedure provided in Section **2.8.1** the reaction to furnish diazoester **2.14a** was conducted on 2.50 mmol scale utilizing 10 eq. of *p*-ABSA and 2.6 eq. of DBU. The product was purified by silica gel flash column chromatography (30% Et_2O/pentane) to yield **2.14a** as a red oil (741.1 mg, 86% yield). ^{1}H NMR (500 MHz, $CDCl_3$) δ 7.22 (td, *J* = 7.2, 6.3, 1.4 Hz, 2H), 7.18 – 7.12 (m, 1H), 7.09 (dd, *J* = 7.0, 1.8 Hz, 2H), 5.92 – 5.73 (m, 1H), 5.26 (dd, *J* = 15.8, 5.0 Hz, 1H), 4.45 (s, 2H), 3.72 (s, 3H), 2.78 (d, *J* = 5.7 Hz, 2H), 1.33 (s, 9H). ^{13}C NMR (126 MHz, $CDCl_3$) δ 164.5, 154.0, 136.1, 128.4, 127.4, 125.6, 123.2, 112.5, 52.0, 51.1, 40.9, 27.3. HRMS (ESI) *m/z* calculated for $C_{18}H_{23}N_3O_4$ $[M+NH_4]^+$ 363.2027; found, 363.2025.

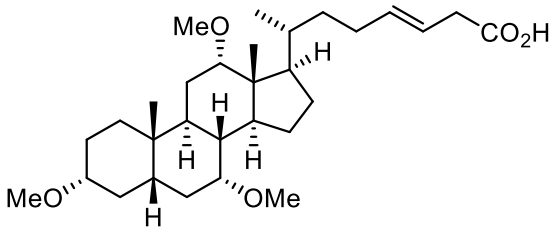


Compound 2.15a. The general procedure was followed, utilizing (*S*,*R*)-**2.1c** as the substrate. The carbene transfer to furnish **2.15a** was conducted on 0.1 mmol scale. The product was purified by silica gel flash chromatography (0 to 30% EtOAc/CH_2Cl_2, 10% increments) to yield **7b** as a white solid (24.4 mg, 47%, >19:1 *dr*). ^{1}H NMR (500 MHz, $CDCl_3$) δ 7.25 – 7.18 (m, 3H), 7.16 – 7.13 (m, 3H), 7.03 (d, *J* = 7.2 Hz, 2H), 6.78 (dd, *J* = 6.5, 2.9 Hz, 2H), 6.00 (d, *J* = 4.3 Hz, 1H), 4.41 – 4.34 (m, 2H), 4.25 (d, *J* = 10.1 Hz, 1H), 4.02 (dd, *J* = 10.4, 8.3 Hz, 1H), 3.81 (s, 3H), 3.76 (q, *J* = 5.7 Hz, 1H), 2.91 – 2.82 (m, 1H), 2.58 (qd, *J* = 14.1, 6.9 Hz, 2H), 2.36 – 2.19

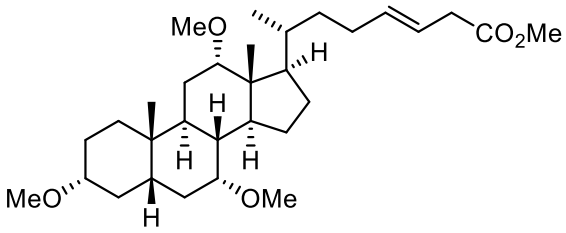
(m, 3H), 2.13 (dd, *J* = 14.2, 8.3 Hz, 1H), 1.36 (s, 9H). ^{13}C NMR (126 MHz, $CDCl_3$) δ 164.0, 155.4, 152.6, 138.5, 136.7, 133.6, 129.1, 128.9, 128.7, 128.6, 126.6, 126.5, 79.8, 64.7, 55.9, 53.9, 52.5, 42.8, 39.2, 38.7, 32.5, 29.7, 28.2, 25.7 HRMS (ESI) *m/z* calculated for $C_{30}H_{36}N_2O_6$ $[2M+NH_4]^+$ 1058.5485; found, 1058.5497.



Compound S1. In accordance with literature conditions,[5] the reaction to furnish ene-yne **S1** was conducted on a 4.94 mmol scale. The product was purified *via* automated flash chromatography using a 0-10% gradient of EtOAc/CH_2Cl_2 to yield **S1** as clear viscous oil. This was isolated as an inseparable mixture of *trans* and *cis*-isomers, with only the major *trans* product characterized (1.32 g, 51%, 4:1 *trans:cis*). ^{1}H NMR (500 MHz, C_6D_6) δ 6.27 (dt, *J* = 15.8, 7.1 Hz, 1H), 5.60 (dt, *J* = 16.0, 1.5 Hz, 1H), 3.26 (s, 3H), 3.23 (s, 1H), 3.07 (s, 1H), 3.05 (s, 3H), 3.02 (s, 3H), 2.96 (tt, *J* = 11.0, 4.2 Hz, 1H), 2.56 – 2.40 (m, 3H), 2.31 (td, *J* = 12.3, 4.4 Hz, 1H), 2.07 (q, *J* = 9.8 Hz, 1H), 1.98 (tt, *J* = 11.3, 5.6 Hz, 1H), 1.88 – 1.70 (m, 7H), 1.57 – 1.48 (m, 3H), 1.48 – 1.35 (m, 5H), 1.30 (ddq, *J* = 10.2, 6.8, 2.9 Hz, 2H), 1.26 – 1.18 (m, 1H), 1.13 – 1.01 (m, 4H), 0.58 (s, 3H), 0.42 (s, 3H), 0.22 (s, 9H). ^{13}C NMR (126 MHz, C_6D_6) δ 147.0, 110.3, 105.3, 92.8, 82.0, 81.0, 77.4, 55.8, 55.4, 46.8, 46.6, 42.9, 42.4, 40.2, 35.8, 35.5, 35.3, 35.2, 30.1, 28.4, 28.1, 27.8, 27.6, 23.7, 23.3, 22.3, 17.8, 12.7, 0.2. HRMS (ESI) *m/z* calculated for $C_{33}H_{56}O_3Si$ $[M+NH_4]^+$ 546.4337; found, 546.336.

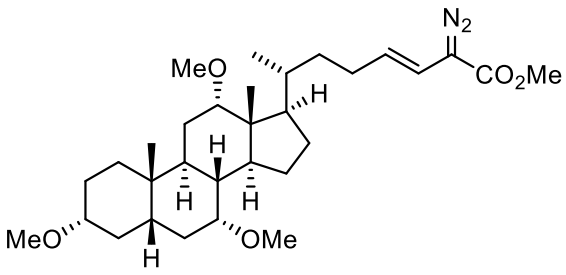


Compound S2. In accordance with literature conditions,[8] the hydroboration oxidation reaction of ene-yne **S1** to furnish carboxylic acid **S2** was conducted on a 2.5 mmol scale. The product was purified by acid-base extraction to remove the cyclohexanol impurity and was isolated as a white solid. The crude material was utilized in the next reaction (0.834 g, 67%, 6:1 *trans:cis*). Over integration in the ^{1}H NMR is attributed to the *cis*-isomer. ^{1}H NMR (500 MHz, C_6D_6) δ 5.60 – 5.51 (m, 1H), 5.39 (dt, *J* = 14.6, 6.7 Hz, 1H), 3.28 (d, *J* = 3.0 Hz, 1H), 3.27 (s, 3H), 3.08 (s, 3H), 3.06 – 3.04 (m, 1H), 3.04 (s, 3H), 2.97 (tt, *J* = 11.5, 4.6 Hz, 1H), 2.81 (d, *J* = 6.9 Hz, 2H), 2.56 – 2.42 (m, 2H), 2.33 (td, *J* = 12.3, 4.2 Hz, 1H), 2.17 (q, *J* = 9.8 Hz, 1H), 2.12 – 2.03 (m, 1H), 1.97 – 1.70 (m, 8H), 1.70 – 1.60 (m, 3H), 1.61 – 1.28 (m, 9H), 1.28 – 1.19 (m, 2H), 1.13 – 1.02 (m, 3H), 0.98 (d, *J* = 6.6 Hz, 3H), 0.87 (s, 3H), 0.65 (s, 3H). ^{13}C NMR (126 MHz, C_6D_6) δ 176.6, 135.8, 121.6, 82.2, 81.2, 77.6, 56.0, 55.6, 55.5, 47.1, 46.8, 43.0, 42.6, 40.4, 38.0, 36.0, 35.9, 35.9, 35.4, 35.4, 29.8, 28.6, 28.3, 28.1, 27.8, 24.0, 23.4, 22.5, 18.1, 13.0. HRMS (ESI) *m/z* calculated for $C_{30}H_{50}O_5$ $[M^-H]^-$ 489.3586; found, 489.3584.

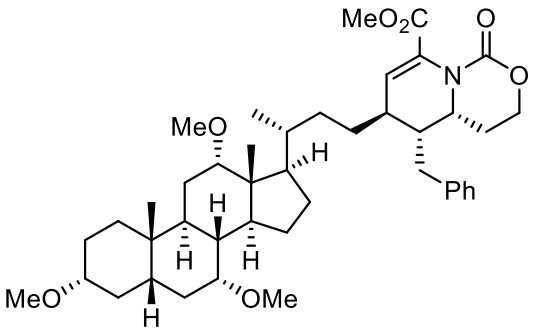


Compound S3. Carboxylic acid **S2** (1.70 mmol, 1 eq.) was dissolved in 10 mL of MeOH (0.6 M), 0.1 mL of H_2SO_4 (1.88 mmol, 1.1 eq.) was added, and the mixture allowed to stir until TLC indicated completion. The reaction was poured into a solution of saturated aqueous $NaHCO_3$ and extracted with three portions of Et_2O. The combined organics were then dried over $MgSO_4$ and concentrated *in vacuo*. The crude material was purified *via* silica column flash chromatography using a 0-20% gradient of EtOAc/Pentanes to yield methyl ester **S3** as clear viscous oil (0.53 g, 65%, 6:1 *trans:cis*). ^{1}H NMR (500 MHz, C_6D_6) δ 5.65 (dt, *J* = 14.6, 6.9 Hz, 1H), 5.45 (dd, *J* = 14.7, 7.3 Hz, 1H), 3.32 (s, 3H), 3.28 (s, 2H), 3.27 (s, 3H), 3.07 (s, 3H), 3.03 (s, 3H), 2.97 (tt, *J* = 11.1, 3.6 Hz, 1H), 2.88 (d, *J* = 6.9 Hz, 2H), 2.48 (dt, *J* = 19.8, 12.6 Hz, 2H), 2.33 (td, *J* = 12.4, 4.1 Hz, 1H), 2.24 – 2.06 (m, 2H), 2.00 – 1.68 (m, 6H), 1.64 (ddt, *J* = 12.3, 9.7, 4.5 Hz, 2H), 1.59 – 1.32 (m, 6H), 1.28 – 1.12 (m, 3H), 1.12 – 1.01 (m, 2H), 0.98 (d, *J* = 6.5 Hz, 3H), 0.87 (s, 3H), 0.65 (s, 3H), ^{13}C NMR (126 MHz,C_6D_6) δ 171.75, 135.2, 122.1, 82.0, 81.0, 77.4, 55.8, 55.4,

55.3, 51.2, 47.0, 46.6, 42.9, 42.4, 40.2, 4.2, 35.9, 35.8, 35.7, 35.2, 29.6, 28.4, 28.1, 29.0 27.5, 23.7, 23.2, 22.3, 17.9, 12.7. HRMS (ESI) *m/z* calculated for $C_{31}H_{52}O_5$ $[M+NH_4]^+$ 522.4153; found, 522.4152.

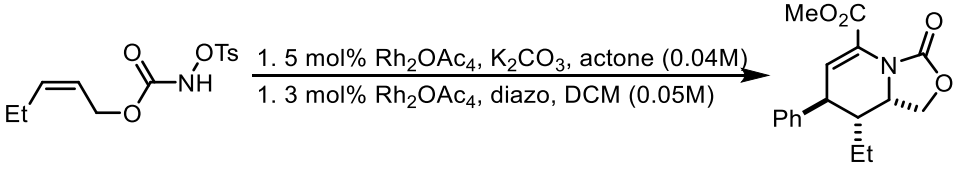


Compound 2.14b. Following the general preparation provided in section **2.8.1** the reaction to furnish diazoester **2.14b** was conducted on methyl ester **S3** (1.0 mmol) utilizing 10 eq. of *p*-ABSA, and 2.6 equiv of DBU. The product was purified by silica gel flash column chromatography (30% Et_2O/pentane) to yield **2.14b** as an orange solid (0.200 g, 38%, all *trans*). *Note: if compound was left of vacuum for longer than a period of 1-2 h the sample began to noticeably decompose*. *For best results, the diazoester compound should be freshly made*. ^{1}H NMR (500 MHz, C_6D_6). ^{1}H NMR δ 5.86 (d, *J* = 15.8 Hz, 1H), 5.21 (dt, *J* = 14.8, 6.9 Hz, 1H), 3.33 (s, 3H), 3.28 (d, *J* = 2.9 Hz, 1H), 3.26 (s, 3H), 3.09 (s, 3H), 3.06 (d, *J* = 4.1 Hz, 1H), 3.04 (s, 3H), 2.97 (tt, *J* = 11.1, 4.1 Hz, 1H), 2.56 – 2.41 (m, 3H), 2.33 (td, *J* = 12.3, 4.4 Hz, 1H), 2.21 – 2.10 (m, 2H), 2.05 – 1.93 (m, 1H), 1.90 – 1.70 (m, 6H), 1.65 (m, 3H), 1.57 – 1.34 (m, 5H), 1.30 – 1.17 (m, 2H), 1.18 – 1.02 (m, 2H), 0.98 (d, *J* = 6.5 Hz, 3H), 0.97 – 0.88 (m, 1H), 0.87 (s, 3H) 0.64 (s, 3H). ^{13}C NMR (126 MHz, C_6D_6) δ 165.4, 129.7, 126.6, 112.0, 82.0, 81.0, 77.4, 55.0, 55.4., 55.3, 51.5, 46.8, 46.6, 42.9, 42.4, 40.2, 36.2, 35.8, 35.7, 35.2, 30.0, 28.4, 28.1, 28.0, 27.5, 23.7, 23.2, 22.3, 18.0, 12.70. HRMS (ESI) *m/z* calculated for $C_{31}H_{50}N_2O_5$ $[M+NH_4]^+$; 548.4058 found, 548.4053.



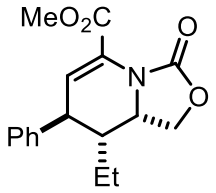
Compound 2.15b. The general procedure was followed, utilizing (*S*,*R*)-**2.1c** as the substrate. The carbene transfer to furnish **2.15b** was conducted on 0.12 mmol scale. The product was purified by silica gel flash chromatography (0 to 50% EtOAc/Hexanes, 10% increments) to yield **2.15b** as a white solid (44.0 mg, 52%, >19:1 *dr*). ^{1}H NMR (500 MHz, CD_3CN) δ 7.29 – 7.16 (m, 3H), 7.16 – 7.05 (m, 2H), 5.91 (dd, *J* = 4.5, 1.3 Hz, 1H), 4.37 – 4.11 (m, 2H), 3.77 (td, *J* = 9.0, 8.1, 1.5 Hz, 1H), 3.62 (s, 3H), 3.24 (t, *J* = 2.8 Hz, 1H), 3.17 (s, 3H), 3.12 (s, 3H), 3.12 (s, 3H), 3.06 (q, *J* = 3.1 Hz, 1H), 2.91 – 2.84 (m, 1H), 2.83 – 2.79 (m, 1H), 2.78 – 2.72 (m, 1H), 2.46 – 2.36 (m, 1H), 2.17 (dddd, *J* = 15.2, 8.7, 5.1, 2.6 Hz, 1H), 1.92 – 1.80 (m, 8H), 1.76 – 1.48 (m, 6H), 1.45 – 1.32 (m, 3H), 1.28 – 0.83 (m, 8H), 0.82 – 0.81 (m, 1H), 0.80 (s, 3H), 0.69 (d, *J* = 6.6 Hz, 3H), 0.52 (s, 3H). ^{13}C NMR (126 MHz, CD_3CN) δ 165.2, 153.6, 140.8, 131.9, 130.2, 129.6, 129.3, 125.4, 82.8, 81.1, 78.2, 69.3, 66.0, 56.1, 56.0, 55.5, 54.0, 52.6, 47.5, 46.8, 43.4, 43.3, 42.6, 40.3, 37.4, 36.3, 35.8, 35.5, 33.8, 33.2, 32.9, 31.7, 28.6, 28.5, 28.1, 27.7, 26.3, 23.8, 23.1, 22.6, 20.0, 18.1, 12.7. HRMS (ESI) *m/z* calculated for $C_{43}H_{63}NO_7$ $[M+NH_4]^+$ 723.4943; found, 723.4945.

2.8.6 One-pot Nitrene-carbene Transfer Reaction



A flame-dried, round bottom flask was placed under nitrogen and charged with $Rh_2(OAc)_4$ (4.20 mg, 0.01 mmol, 0.05 eq.), *N*-tosyl carbamate (50.00 mg, 0.17 mmol, 1 eq.), K_2CO_3 (0.184 g, 1.17 mmol, 7 eq.) and acetone (4.2 mL, 0.04 M).[3] The mixture was stirred vigorously at room

temperature for 16 h (TLC was used to determine when the reaction was complete). Once the starting material was consumed, the reaction mixture was passed through a plug of celite to remove K_2CO_3. The filter pad was washed with EtOAc and the volatiles removed under reduced pressure. The resulting oil was diluted with CH_2Cl_2 (3.5 mL, 0.05 M) and $Rh_2(OAc)_4$ (2.2 mg, 0.01 mmol, 0.03 eq). To this mixture was added a solution of the diazoester compound (40.5 mg, 0.20 mmol, 1.2 eq.) dropwise over 2 h using a syringe pump. The conversion was checked by TLC and NMR after the addition was finished; once the reaction was complete, it was concentrated and loaded directly onto silica for column chromatography (0% to 40% ethyl acetate/hexanes).



Compound 2.6ja. Following the general procedure, the nitrene and carbene transfer to furnish **2.6ja** was conducted on 0.17 mmol scale. The product was purified by silica gel flash column chromatography (0 to 40% EtOAc/Hexanes, 10% increments) to yield **2.6ja** as a white solid (53.6 mg, 54% yield, >19:1 *dr*). ^{1}H NMR (500 MHz, $CDCl_3$) δ 7.36 (d, *J* = 7.3 Hz, 2H), 7.28 (d, *J* = 7.3 Hz, 1H), 7.15 – 7.10 (m, 2H), 6.24 (dd, *J* = 4.9, 1.1 Hz, 1H), 4.49 (dd, *J* = 8.8, 8.8 Hz, 1H); (app t, *J* = 8.8 Hz, 1H), 4.16 (dd, *J* = 9.2, 2.5 Hz, 1H), 3.90 (s, 4H), 3.65 (d, *J* = 5.0 Hz, 1H), 1.70 – 1.57 (m, 2H), 1.17 (t, *J* = 3.8 Hz, 4H).^{13}C NMR (126 MHz, $CDCl_3$) δ 163.2, 155.1, 142.5, 130.3, 129.0, 128.4, 127.3, 121.6, 65.4, 52.8, 51.7, 46.1, 41.5, 18.9, 12.3. HRMS (ESI) *m/z* calculated for $C_{17}H_{19}NO_4$ $[M+H]^+$ 302.1387; found, 302.1384.

2.8.7 X-Crystallographic Information for 2.6cc.

Data Collection

A colorless crystal with approximate dimensions 0.20 x 0.15 x 0.11 mm^3 was selected under oil under ambient conditions and attached to the tip of a MiTeGen MicroMount©. The crystal was mounted in a stream of cold nitrogen at 100(1) K and centered in the X-ray beam by using a video camera.

The crystal evaluation and data collection were performed on a Bruker SMART APEXII diffractometer with Cu K_α (λ = 1.54178 Å) radiation and the diffractometer to crystal distance of 4.03 cm .[8]

The initial cell constants were obtained from three series of ω scans at different starting angles. Each series consisted of 41 frames collected at intervals of 0.6º in a 25º range about ω with the exposure time of 10 seconds per frame. The reflections were successfully indexed by an automated indexing routine built in the APEX3 program. The final cell constants were calculated from a set of 9913 strong reflections from the actual data collection.

The data were collected by using the full sphere data collection routine to survey the reciprocal space to the extent of a full sphere to a resolution of 0.81 Å. A total of 24327 data were harvested by collecting 14 sets of frames with 0.5º scans in ω and φ with an exposure time 10 sec per frame. These highly redundant datasets were corrected for Lorentz and polarization effects. The absorption correction was based on fitting a function to the empirical transmission surface as sampled by multiple equivalent measurements.[9]

Structure Solution and Refinement

The systematic absences in the diffraction data were consistent for the space groups $P\bar{1}$ and *P*1. The *E*-statistics strongly suggested the centrosymmetric space group $P\bar{1}$ that yielded chemically reasonable and computationally stable results of refinement.[10-15]

A successful solution by the direct methods provided most non-hydrogen atoms from the *E*-map. The remaining non-hydrogen atoms were located in an alternating series of least-squares cycles and difference Fourier maps. All non-hydrogen atoms were refined with anisotropic displacement coefficients. All hydrogen atoms were included in the structure factor calculation at idealized positions and were allowed to ride on the neighboring atoms with relative isotropic displacement coefficients.

There are two organic molecules per asymmetric unit. These molecules each have three chiral centers and are enantiomers of each other, therefore the second molecule was labeled with the suffix “A”. The chiral centers are C3 - *S*, C4 - *S*, and C5 - *R* for the first molecule, and C3A-*R*, C4A - *R*, and C5A - *S* for the second.

The final least-squares refinement of 437 parameters against 6575 data resulted in residuals *R* (based on F^2 for $I \geq 2\sigma$) and *wR* (based on F^2 for all data) of 0.0249 and 0.0659, respectively. The final difference Fourier map was featureless.

Summary

Crystal Data for $C_{18}H_{20}BrNO_4$ (M =394.26 g/mol): triclinic, space group $P\bar{1}$ (no. 2), a = 7.2645(4) Å, b = 15.1045(15) Å, c = 17.5158(14) Å, α = 65.499(5)°, β = 84.097(5)°, γ = 82.736(4)°, V = 1732.1(2) Å^3, Z = 4, T = 100.02 K, μ(CuKα) = 3.422 mm^{-1}, *Dcalc* = 1.512 g/cm^3, 24314 reflections measured (5.554° ≤ 2Θ ≤ 144.264°), 6575 unique (R_{int} = 0.0222, R_{sigma} = 0.0190) which were used in all calculations. The final R_1 was 0.0249 (I > 2σ(I)) and wR_2 was 0.0659 (all data).

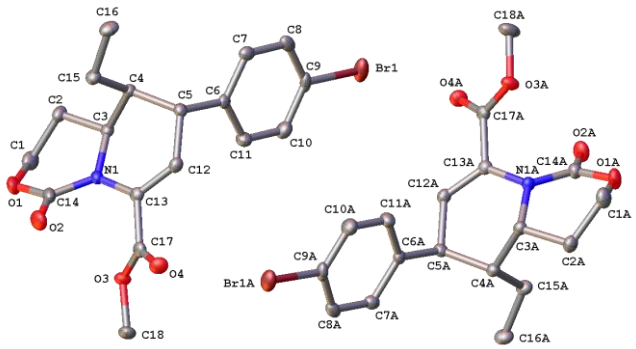


Figure S-2.5. A molecular drawing of **2.6cc** shown with 50% probability ellipsoids. All H atoms are omitted.

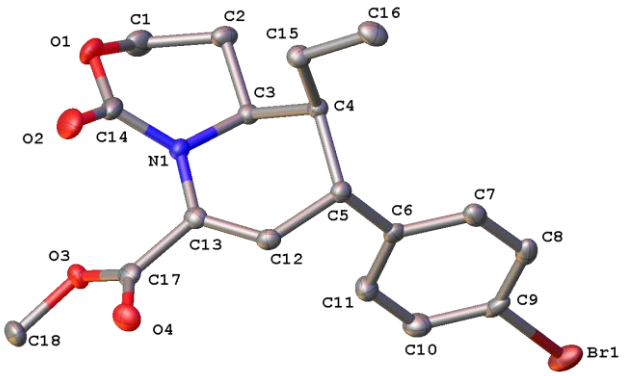


Figure S-2.6. A molecular drawing of one organic molecule from **2.6cc** shown with 50% ellipsoids. The other molecule and all hydrogen atoms are omitted.

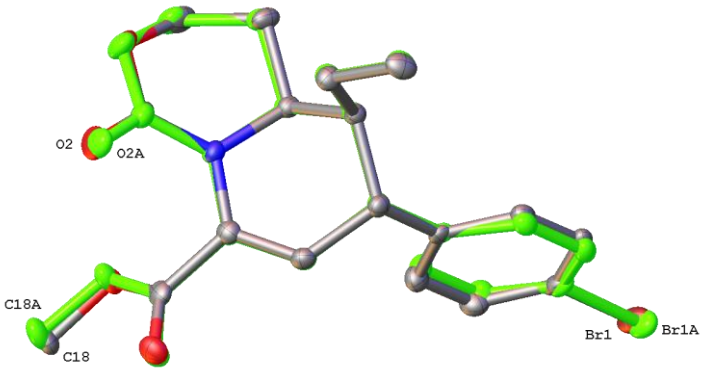


Figure S-2.7. A molecular drawing of the overlay of the two molecules from **2.6cc** shown with 50% ellipsoids. The molecule with suffix "A" was inverted and drawn in green.

Table S-2.1. Crystal data and structure refinement for **2.6cc**.

Identification code	**2.6cc**
Empirical formula	$C_{18}H_{20}BrNO_4$
Formula weight	394.26
Temperature/K	100.02
Crystal system	triclinic
Space group	$P\bar{1}$
a/Å	7.2645(4)
b/Å	15.1045(15)

c/Å	17.5158(14)
α/°	65.499(5)
β/°	84.097(5)
γ/°	82.736(4)
Volume/Å^3	1732.1(2)
Z	4
ρ_{calc}g/cm^3	1.512
μ/mm^{-1}	3.422
F(000)	808.0
Crystal size/mm^3	0.203 × 0.154 × 0.108
Radiation	CuKα (λ = 1.54178)
2Θ range for data collection/°	5.554 to 144.264
Index ranges	-8 ≤ h ≤ 8, -18 ≤ k ≤ 18, -21 ≤ l ≤ 20
Reflections collected	24314
Independent reflections	6575 [R_{int} = 0.0222, R_{sigma} = 0.0190]
Data/restraints/parameters	6575/0/437
Goodness-of-fit on F^2	1.021
Final R indexes [I>=2σ (I)]	R_1 = 0.0249, wR_2 = 0.0643
Final R indexes [all data]	R_1 = 0.0273, wR_2 = 0.0659
Largest diff. peak/hole / e Å^{-3}	0.43/-0.48

Table S-2.2. Fractional Atomic Coordinates (×10^4) and Equivalent Isotropic Displacement Parameters (Å^2×10^3) for **2.6cc**. U_{eq} is defined as 1/3 of of the trace of the orthogonalised U_{IJ} tensor.

Atom	***x***	***y***	***z***	**U(eq)**
Br1	9180.5(2)	7210.2(2)	3815.2(2)	31.44(7)

O1	4946.8(19)	3932.8(9)	9846.0(8)	30.2(3)
O2	2007.7(19)	4038.4(10)	9558.1(8)	32.6(3)
O3	1629.4(15)	6100.0(8)	8450.2(7)	20.3(2)
O4	-379.0(15)	5671.9(9)	7795.9(8)	23.6(2)
N1	4161.7(18)	4562.9(9)	8462.8(8)	15.9(3)
C1	6790(3)	4214.5(14)	9488.7(12)	28.5(4)
C2	7341(2)	3818.3(11)	8830.1(10)	19.5(3)
C3	6022(2)	4326.4(10)	8117.3(9)	14.8(3)
C4	5798(2)	3744.1(10)	7595.1(9)	14.6(3)
C5	4599(2)	4395.7(11)	6844.7(10)	15.6(3)
C6	5718(2)	5096.4(11)	6110.5(9)	15.3(3)
C7	6793(2)	4754.8(12)	5562.9(10)	18.3(3)
C8	7821(2)	5370.2(13)	4879.3(10)	20.5(3)
C9	7790(2)	6343.3(12)	4748.5(10)	21.4(3)
C10	6753(2)	6703.9(12)	5281.3(11)	24.1(3)
C11	5711(2)	6080.7(12)	5956.7(11)	21.4(3)
C12	2954(2)	4916.6(11)	7130.5(10)	16.3(3)
C13	2762(2)	4961.2(11)	7878.7(10)	16.1(3)
C14	3608(3)	4161.8(12)	9302.0(10)	23.0(3)
C15	4937(2)	2775.4(11)	8111.7(10)	18.1(3)
C16	5174(2)	2088.5(12)	7660.7(11)	22.7(3)
C17	1140(2)	5586.8(11)	8049.4(10)	18.2(3)
C18	158(2)	6769.9(12)	8588.1(11)	23.9(3)
Br1A	473.8(2)	7575.1(2)	6100.8(2)	29.44(6)
O1A	5567.6(17)	11359.3(9)	157.8(7)	26.3(3)
O2A	8357.2(16)	11257.7(9)	608.3(8)	27.2(3)
O3A	8705.3(15)	9150.7(9)	1472.8(7)	22.2(2)

O4A	10433.5(15)	9341.1(9)	2379.6(8)	22.4(2)
N1A	6034.0(17)	10544.1(9)	1573.4(8)	15.2(3)
C1A	3710(2)	11034.1(14)	397.9(11)	25.5(4)
C2A	2907(2)	11291.0(12)	1115.7(10)	19.9(3)
C3A	4092(2)	10723.6(11)	1872.1(9)	14.7(3)
C4A	4117(2)	11224.1(11)	2478.6(10)	15.0(3)
C5A	5210(2)	10523.5(11)	3250.8(10)	15.6(3)
C6A	4029(2)	9796.7(11)	3933.4(10)	15.5(3)
C7A	3065(2)	10052.1(12)	4556.7(10)	18.1(3)
C8A	2005(2)	9398.9(12)	5200.6(10)	20.1(3)
C9A	1886(2)	8486.6(12)	5212.9(10)	20.5(3)
C10A	2800(2)	8216.6(12)	4598.3(11)	23.6(3)
C11A	3877(2)	8871.0(12)	3966.3(10)	20.9(3)
C12A	6926(2)	10025.4(11)	2987.6(10)	16.1(3)
C13A	7304(2)	10074.8(11)	2210.6(10)	15.2(3)
C14A	6753(2)	11073.6(12)	776.0(10)	19.8(3)
C15A	4970(2)	12210.3(11)	2061.5(10)	19.1(3)
C16A	4586(2)	12812.5(12)	2589.5(11)	22.9(3)
C17A	9007(2)	9502.2(11)	2032.2(10)	17.0(3)
C18A	10271(3)	8570.5(15)	1279.2(12)	31.4(4)

Table S-2.3. Anisotropic Displacement Parameters ($Å^2 \times 10^3$) for 2**.6cc**. The Anisotropic displacement factor exponent takes the form: $-2\pi^2[h^2a^{*2}U_{11}+2hka^*b^*U_{12}+\ldots]$.

Atom	U_{11}	U_{22}	U_{33}	U_{23}	U_{13}	U_{12}
Br1	20.46(10)	36.89(11)	20.84(11)	3.93(8)	0.54(7)	-2.80(7)
O1	42.3(8)	32.2(7)	12.7(6)	-8.2(5)	-4.7(5)	7.3(6)
O2	35.5(7)	31.8(7)	20.0(7)	-3.4(5)	10.3(5)	-1.5(5)
O3	19.6(6)	21.6(5)	20.3(6)	-11.0(5)	0.7(4)	3.3(4)
O4	16.3(6)	25.1(6)	27.9(7)	-10.0(5)	1.5(5)	-1.6(4)
N1	19.8(7)	14.7(6)	12.5(7)	-5.3(5)	-0.6(5)	0.0(5)
C1	37.5(10)	28.8(9)	22.5(10)	-13.2(8)	-13.0(7)	4.2(7)
C2	24.3(8)	16.6(7)	18.4(8)	-7.2(6)	-8.1(6)	1.3(6)
C3	17.3(7)	12.7(7)	14.3(8)	-5.4(6)	-1.7(6)	-0.5(5)
C4	16.3(7)	13.4(7)	14.0(8)	-5.7(6)	-1.3(6)	-0.3(5)
C5	18.0(7)	15.8(7)	13.7(8)	-6.8(6)	-1.9(6)	-1.1(6)
C6	16.8(7)	17.1(7)	11.4(8)	-5.0(6)	-4.9(6)	0.7(6)
C7	17.1(8)	20.6(7)	19.4(9)	-10.5(7)	-5.3(6)	2.5(6)
C8	14.4(7)	32.0(9)	16.1(8)	-11.5(7)	-3.1(6)	1.9(6)
C9	16.2(8)	27.3(8)	11.5(8)	1.5(6)	-2.1(6)	-1.8(6)
C10	26.4(9)	18.2(8)	23.4(9)	-4.6(7)	-1.7(7)	-0.7(6)
C11	26.2(8)	19.2(8)	19.4(9)	-9.5(7)	0.1(6)	0.2(6)
C12	14.9(7)	16.1(7)	16.6(8)	-4.9(6)	-3.0(6)	-0.9(6)
C13	16.4(7)	13.8(7)	16.4(8)	-4.3(6)	0.6(6)	-3.1(6)
C14	35.1(10)	16.5(7)	13.5(8)	-4.1(6)	0.2(7)	2.8(7)
C15	21.4(8)	14.6(7)	18.4(8)	-6.6(6)	-1.8(6)	-2.1(6)
C16	24.1(8)	16.3(7)	30.9(10)	-12.3(7)	-6.2(7)	0.4(6)
C17	19.7(8)	16.5(7)	13.8(8)	-2.2(6)	3.7(6)	-3.2(6)
C18	22.9(8)	25.0(8)	22.1(9)	-11.2(7)	2.5(6)	6.5(7)
Br1A	24.27(10)	29.54(10)	21.57(11)	1.44(8)	4.20(7)	-3.43(7)
O1A	24.9(6)	33.7(7)	13.3(6)	-2.9(5)	-2.0(5)	-1.3(5)

O2A	20.9(6)	33.7(7)	19.8(6)	-4.2(5)	4.3(5)	-5.3(5)
O3A	18.5(6)	29.1(6)	22.8(6)	-16.1(5)	-1.6(4)	4.7(5)
O4A	14.4(5)	27.6(6)	24.5(6)	-10.5(5)	-2.0(4)	0.9(4)
N1A	14.2(6)	16.7(6)	13.4(7)	-5.1(5)	-1.3(5)	-0.2(5)
C1A	25.0(9)	31.8(9)	18.1(9)	-7.3(7)	-6.6(7)	-2.6(7)
C2A	18.3(8)	20.4(7)	18.5(9)	-5.0(7)	-5.3(6)	0.0(6)
C3A	12.7(7)	15.0(7)	14.8(8)	-4.7(6)	-0.6(6)	-1.0(5)
C4A	15.0(7)	13.7(7)	15.2(8)	-5.0(6)	0.3(6)	-1.0(5)
C5A	16.9(7)	16.1(7)	15.3(8)	-8.2(6)	-0.6(6)	-1.3(6)
C6A	16.8(7)	16.5(7)	12.5(8)	-5.3(6)	-4.1(6)	1.8(6)
C7A	16.7(7)	20.7(7)	18.9(8)	-10.5(7)	-3.5(6)	1.5(6)
C8A	15.8(8)	29.7(8)	15.2(8)	-10.4(7)	-1.9(6)	2.6(6)
C9A	16.8(7)	24.3(8)	12.3(8)	0.5(6)	0.0(6)	-2.4(6)
C10A	28.9(9)	17.4(7)	22.4(9)	-6.2(7)	0.5(7)	-2.6(6)
C11A	28.0(9)	18.8(7)	16.8(8)	-9.1(7)	1.4(6)	-1.2(6)
C12A	15.3(7)	15.9(7)	16.4(8)	-5.4(6)	-3.3(6)	-1.2(6)
C13A	14.6(7)	14.0(7)	16.5(8)	-5.2(6)	-0.7(6)	-2.8(5)
C14A	22.7(8)	19.7(7)	14.5(8)	-5.3(6)	-0.5(6)	0.1(6)
C15A	20.3(8)	14.6(7)	21.7(9)	-6.8(6)	1.4(6)	-3.1(6)
C16A	24.0(8)	17.2(7)	28.8(9)	-11.0(7)	0.0(7)	-2.5(6)
C17A	16.7(8)	16.5(7)	14.9(8)	-3.8(6)	2.0(6)	-2.7(6)
C18A	25.0(9)	43.3(11)	31.6(11)	-24.8(9)	-1.2(7)	10.2(8)

Table S-2.4. Bond Lengths for **2.6cc**.

Atom	**Atom**	**Length/Å**	**Atom**	**Atom**	**Length/Å**
Br1	C9	1.9044(16)	Br1A	C9A	1.9026(16)

O1	C1	1.455(2)	O1A	C1A	1.456(2)
O1	C14	1.344(2)	O1A	C14A	1.345(2)
O2	C14	1.211(2)	O2A	C14A	1.211(2)
O3	C17	1.339(2)	O3A	C17A	1.3397(19)
O3	C18	1.4493(18)	O3A	C18A	1.4460(19)
O4	C17	1.204(2)	O4A	C17A	1.203(2)
N1	C3	1.4865(19)	N1A	C3A	1.4857(19)
N1	C13	1.411(2)	N1A	C13A	1.411(2)
N1	C14	1.375(2)	N1A	C14A	1.376(2)
C1	C2	1.505(2)	C1A	C2A	1.506(2)
C2	C3	1.527(2)	C2A	C3A	1.529(2)
C3	C4	1.5397(19)	C3A	C4A	1.541(2)
C4	C5	1.550(2)	C4A	C5A	1.549(2)
C4	C15	1.539(2)	C4A	C15A	1.541(2)
C5	C6	1.520(2)	C5A	C6A	1.520(2)
C5	C12	1.504(2)	C5A	C12A	1.505(2)
C6	C7	1.397(2)	C6A	C7A	1.398(2)
C6	C11	1.396(2)	C6A	C11A	1.393(2)
C7	C8	1.387(2)	C7A	C8A	1.389(2)
C8	C9	1.388(2)	C8A	C9A	1.383(2)
C9	C10	1.382(2)	C9A	C10A	1.384(2)
C10	C11	1.389(2)	C10A	C11A	1.388(2)
C12	C13	1.332(2)	C12A	C13A	1.333(2)
C13	C17	1.500(2)	C13A	C17A	1.500(2)
C15	C16	1.529(2)	C15A	C16A	1.530(2)

Table S-2.5. Bond Angles for **2.6cc**.

Atom	Atom	Atom	Angle/°	Atom	Atom	Atom	Angle/°
C14	O1	C1	116.72(13)	C14A	O1A	C1A	116.81(13)
C17	O3	C18	114.96(13)	C17A	O3A	C18A	115.05(13)
C13	N1	C3	115.39(12)	C13A	N1A	C3A	115.21(12)
C14	N1	C3	123.84(13)	C14A	N1A	C3A	123.50(13)
C14	N1	C13	117.64(13)	C14A	N1A	C13A	117.29(13)
O1	C1	C2	108.38(14)	O1A	C1A	C2A	108.84(13)
C1	C2	C3	108.09(13)	C1A	C2A	C3A	108.60(13)
N1	C3	C2	109.59(12)	N1A	C3A	C2A	109.40(12)
N1	C3	C4	108.98(12)	N1A	C3A	C4A	108.62(12)
C2	C3	C4	114.87(12)	C2A	C3A	C4A	114.86(12)
C3	C4	C5	108.70(12)	C3A	C4A	C5A	108.87(12)
C15	C4	C3	113.10(12)	C3A	C4A	C15A	112.74(12)
C15	C4	C5	110.39(12)	C15A	C4A	C5A	110.17(12)
C6	C5	C4	112.77(12)	C6A	C5A	C4A	113.53(12)
C12	C5	C4	110.44(12)	C12A	C5A	C4A	111.01(12)
C12	C5	C6	112.15(12)	C12A	C5A	C6A	111.96(12)
C7	C6	C5	119.48(13)	C7A	C6A	C5A	119.60(13)
C11	C6	C5	122.34(14)	C11A	C6A	C5A	122.16(14)
C11	C6	C7	118.18(15)	C11A	C6A	C7A	118.24(15)
C8	C7	C6	121.48(15)	C8A	C7A	C6A	121.19(14)
C7	C8	C9	118.77(14)	C9A	C8A	C7A	118.97(14)
C8	C9	Br1	119.94(13)	C8A	C9A	Br1A	119.52(12)
C10	C9	Br1	118.80(13)	C8A	C9A	C10A	121.27(15)
C10	C9	C8	121.25(15)	C10A	C9A	Br1A	119.21(13)
C9	C10	C11	119.25(15)	C9A	C10A	C11A	119.12(15)

C10	C11	C6	121.05(15)	C10A	C11A	C6A	121.20(15)
C13	C12	C5	124.16(14)	C13A	C12A	C5A	124.02(14)
N1	C13	C17	118.67(13)	N1A	C13A	C17A	118.14(13)
C12	C13	N1	122.20(14)	C12A	C13A	N1A	122.02(14)
C12	C13	C17	118.44(14)	C12A	C13A	C17A	119.31(14)
O1	C14	N1	116.33(15)	O1A	C14A	N1A	115.82(14)
O2	C14	O1	120.18(15)	O2A	C14A	O1A	119.95(15)
O2	C14	N1	123.45(16)	O2A	C14A	N1A	124.18(15)
C16	C15	C4	112.58(13)	C16A	C15A	C4A	112.46(13)
O3	C17	C13	111.84(13)	O3A	C17A	C13A	111.54(13)
O4	C17	O3	124.29(14)	O4A	C17A	O3A	124.39(14)
O4	C17	C13	123.62(14)	O4A	C17A	C13A	123.98(14)

Table S-2.6. Torsion Angles for **2.6cc**.

A	**B**	**C**	**D**	**Angle/°**	**A**	**B**	**C**	**D**	**Angle/°**
Br1	C9	C10	C11	179.03(12)	Br1A	C9A	C10A	C11A	-177.94(13)
O1	C1	C2	C3	65.08(17)	O1A	C1A	C2A	C3A	-63.65(17)
N1	C3	C4	C5	62.67(15)	N1A	C3A	C4A	C5A	-62.53(15)
N1	C3	C4	C15	-60.29(16)	N1A	C3A	C4A	C15A	60.04(16)
N1	C13	C17	O3	33.16(19)	N1A	C13A	C17A	O3A	-28.31(18)
N1	C13	C17	O4	-152.32(15)	N1A	C13A	C17A	O4A	155.02(15)
C1	O1	C14	O2	-172.58(15)	C1A	O1A	C14A	O2A	174.46(15)
C1	O1	C14	N1	5.4(2)	C1A	O1A	C14A	N1A	-3.1(2)
C1	C2	C3	N1	-31.90(17)	C1A	C2A	C3A	N1A	29.20(17)
C1	C2	C3	C4	-154.95(14)	C1A	C2A	C3A	C4A	151.62(13)
C2	C3	C4	C5	-173.95(13)	C2A	C3A	C4A	C5A	174.63(12)

C2	C3	C4	C15	63.09(17)	C2A	C3A	C4A	C15A	-62.81(17)
C3	N1	C13	C12	15.2(2)	C3A	N1A	C13A	C12A	-16.7(2)
C3	N1	C13	C17	-155.16(13)	C3A	N1A	C13A	C17A	154.89(13)
C3	N1	C14	O1	31.4(2)	C3A	N1A	C14A	O1A	-35.5(2)
C3	N1	C14	O2	-150.75(15)	C3A	N1A	C14A	O2A	147.12(16)
C3	C4	C5	C6	82.22(15)	C3A	C4A	C5A	C6A	-85.40(15)
C3	C4	C5	C12	-44.14(16)	C3A	C4A	C5A	C12A	41.77(16)
C3	C4	C15	C16	-165.30(13)	C3A	C4A	C15A	C16A	166.54(13)
C4	C5	C6	C7	79.54(17)	C4A	C5A	C6A	C7A	-88.25(16)
C4	C5	C6	C11	-100.75(16)	C4A	C5A	C6A	C11A	92.25(17)
C4	C5	C12	C13	12.2(2)	C4A	C5A	C12A	C13A	-9.0(2)
C5	C4	C15	C16	72.67(16)	C5A	C4A	C15A	C16A	-71.62(16)
C5	C6	C7	C8	179.30(13)	C5A	C6A	C7A	C8A	-178.58(14)
C5	C6	C11	C10	179.84(15)	C5A	C6A	C11A	C10A	179.60(15)
C5	C12	C13	N1	3.8(2)	C5A	C12A	C13A	N1A	-5.2(2)
C5	C12	C13	C17	174.16(13)	C5A	C12A	C13A	C17A	-176.63(13)
C6	C5	C12	C13	-114.50(16)	C6A	C5A	C12A	C13A	119.07(16)
C6	C7	C8	C9	0.8(2)	C6A	C7A	C8A	C9A	-1.0(2)
C7	C6	C11	C10	-0.4(2)	C7A	C6A	C11A	C10A	0.1(2)
C7	C8	C9	Br1	-179.87(11)	C7A	C8A	C9A	Br1A	178.95(12)
C7	C8	C9	C10	-0.3(2)	C7A	C8A	C9A	C10A	0.0(2)
C8	C9	C10	C11	-0.5(3)	C8A	C9A	C10A	C11A	1.0(3)
C9	C10	C11	C6	0.9(3)	C9A	C10A	C11A	C6A	-1.1(3)
C11	C6	C7	C8	-0.4(2)	C11A	C6A	C7A	C8A	0.9(2)
C12	C5	C6	C7	-155.02(14)	C12A	C5A	C6A	C7A	145.08(14)
C12	C5	C6	C11	24.7(2)	C12A	C5A	C6A	C11A	-34.4(2)
C12	C13	C17	O3	-137.58(15)	C12A	C13A	C17A	O3A	143.49(14)

C12	C13	C17	O4	36.9(2)	C12A	C13A	C17A	O4A	-33.2(2)
C13	N1	C3	C2	-174.83(12)	C13A	N1A	C3A	C2A	176.42(12)
C13	N1	C3	C4	-48.35(16)	C13A	N1A	C3A	C4A	50.34(16)
C13	N1	C14	O1	-169.58(13)	C13A	N1A	C14A	O1A	168.14(13)
C13	N1	C14	O2	8.3(2)	C13A	N1A	C14A	O2A	-9.3(2)
C14	O1	C1	C2	-53.16(18)	C14A	O1A	C1A	C2A	51.90(19)
C14	N1	C3	C2	-15.38(19)	C14A	N1A	C3A	C2A	19.59(19)
C14	N1	C3	C4	111.10(16)	C14A	N1A	C3A	C4A	-106.49(15)
C14	N1	C13	C12	-145.56(15)	C14A	N1A	C13A	C12A	141.66(15)
C14	N1	C13	C17	44.06(19)	C14A	N1A	C13A	C17A	-46.77(18)
C15	C4	C5	C6	-153.20(12)	C15A	C4A	C5A	C6A	150.50(12)
C15	C4	C5	C12	80.45(15)	C15A	C4A	C5A	C12A	-82.33(15)
C18	O3	C17	O4	1.7(2)	C18A	O3A	C17A	O4A	-2.1(2)
C18	O3	C17	C13	176.17(13)	C18A	O3A	C17A	C13A	-178.72(14)

Table S-2.7. Hydrogen Atom Coordinates (Å×10^4) and Isotropic Displacement Parameters (Å^2×10^3) for **2.6cc**.

Atom	***x***	***y***	***z***	**U(eq)**
H1A	7694.31	3945.88	9934.18	34
H1B	6778.64	4935.32	9233.16	34
H2A	7256.98	3103.7	9074.83	23
H2B	8638.67	3945.22	8614.22	23
H3	6520.46	4956.78	7728.48	18
H4	7057.81	3590.82	7365.83	17
H5	4099.91	3950.08	6640.75	19
H7	6820.13	4085.97	5660.7	22

H8	8533.77	5130.09	4507.54	25
H10	6751.56	7370.32	5186.97	29
H11	4981.9	6328.44	6319.66	26
H12	1991.81	5233.86	6753.53	20
H15A	5528.49	2444.7	8656.79	22
H15B	3595.97	2916.75	8229.19	22
H16A	4480.04	2383.55	7149.07	34
H16B	4698.41	1463.56	8032.27	34
H16C	6494.16	1977.91	7511.54	34
H18A	-362.55	7207.62	8050.55	36
H18B	663.15	7156.25	8835.88	36
H18C	-820.49	6398.89	8970.98	36
H1AA	3769.66	10318.84	571.25	31
H1AB	2910.46	11356.94	-85.84	31
H2AA	1608.5	11117.81	1261.01	24
H2AB	2905	12001.95	952.44	24
H3A	3589.83	10075.52	2195.75	18
H4A	2807.07	11344.63	2676.95	18
H5A	5644.95	10939.71	3503.2	19
H7A	3137.38	10683.73	4539.54	22
H8A	1371.44	9576.3	5625.93	24
H10A	2690.24	7591.4	4608.81	28
H11A	4524.02	8684.5	3548.41	25
H12A	7792.48	9652.85	3400.38	19
H15C	6330.3	12088.65	1973.43	23
H15D	4454.12	12590.37	1503.81	23
H16D	5102.92	13443.41	2287.79	34

H16E	5167.09	12458.8	3128	34
H16F	3241.29	12921.15	2690.8	34
H18D	9972.18	8402.48	825.27	47
H18E	10540.24	7970.33	1779.94	47
H18F	11359.84	8945.51	1101.32	47

2.8.8 Computational Methods.

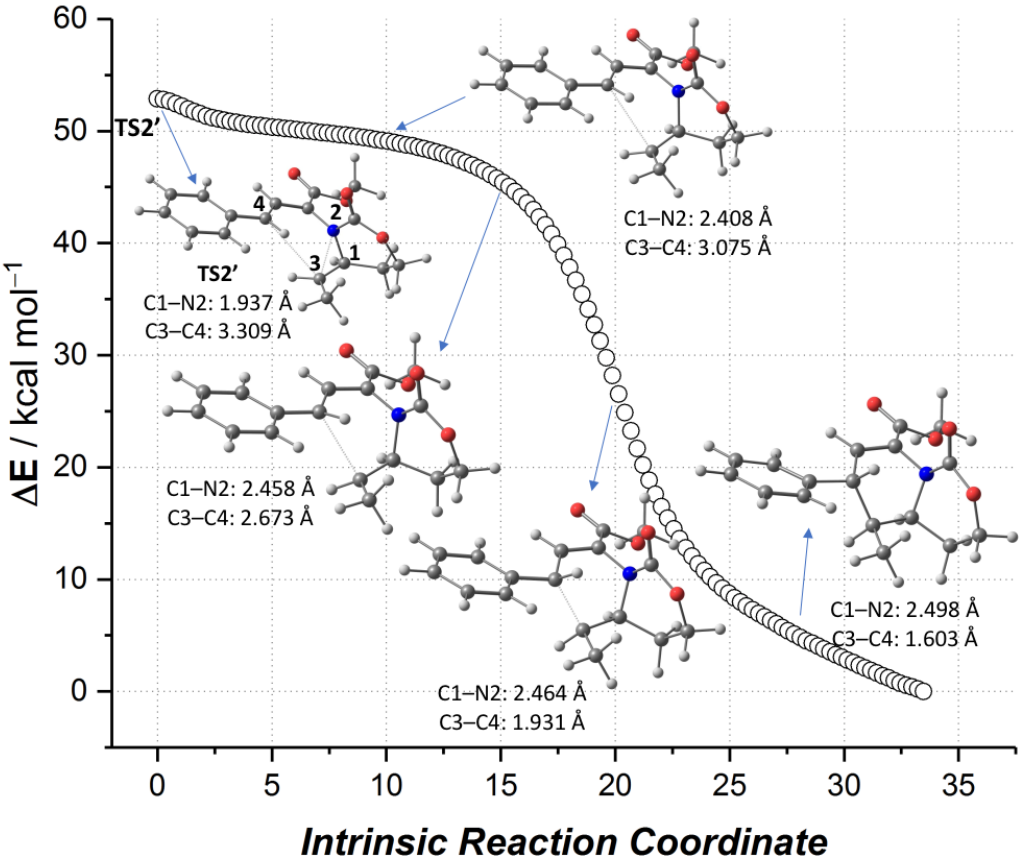


Figure S-2.8. Computed (SCM(CH_2Cl_2)-B3LYP-D3/def2-SVP level) intrinsic reaction coordinate for the transformation of **TS2'** into **2.6ba**.

Computational Details

All the calculations reported in this paper were performed with the Gaussian 09 suite of programs.[16] Electron correlation was partially taken into account using the hybrid functional usually denoted as B3LYP[17] in conjunction with the D3 dispersion correction suggested by Grimme et al.[18] using the standard double- ζ quality def2-SVP[19] basis set for all atoms. The SMD continuum model was used to model the effects of the solvent (CH_2Cl_2). This level is denoted SMD(CH_2Cl_2)-B3LYP-D3/def2-SVP. Geometries were fully optimized in solution without any geometry or symmetry constraints. Reactants, intermediates, and products were characterized by frequency calculations,[20] and have positive definite Hessian matrices. Transition structures (TS's) show only one negative eigenvalue in their diagonalized force constant matrices, and their associated eigenvectors were confirmed to correspond to the motion along the reaction coordinate under consideration using the Intrinsic Reaction Coordinate (IRC) method.[21] Frequency calculations were also used to determine the difference between the potential (E) and Gibbs (G) energies, G −E, which contains the zero-point, thermal, and entropy energies. Potential energies were refined, E_{sol}, by means of single point (SP) calculations at the same level with a larger basis set, def2-TZVPP, [19] where all elements were described with a triple-ζ + polarization quality basis set. This level is denoted SMD(CH_2Cl_2)-B3LYP-D3/def2-TZVPP//SMD(CH_2Cl_2)-B3LYP-D3/def2-SVP. The ΔG and $\Delta G^{\ddagger}$ values given in the text were obtained from the Gibbs energy in solution, G_{sol}, which was calculated by adding the thermochemistry corrections, G − E, to the refined SP energies, E_{sol}, i.e., $G_{sol} = E_{sol} + G - E$. Cartesian coordinates (in Å) and total energies (in a.u.) of all the stationary points discussed in the text. All calculations have been performed at the SMD(CH_2Cl_2)-B3LYP-D3/def2-TZVPP//SMD(CH_2Cl_2)-B3LYP-D3/def2-SVP level.

2.1b, E = -439.426005

N	0.262344000	-0.539114000	-0.948473000
C	0.848806000	0.795236000	-0.891354000
C	1.583461000	-0.383547000	-0.320214000
H	1.209079000	1.138283000	-1.868937000
C	0.104868000	1.866386000	-0.112266000
C	-1.045236000	1.299079000	0.724484000
O	-1.687216000	0.161318000	0.109043000
C	-0.886730000	-0.877142000	-0.241211000

O	-1.217593000	-2.017801000	-0.020856000
H	-0.707954000	0.995664000	1.728914000
H	-1.838113000	2.046650000	0.858032000
H	0.784812000	2.436048000	0.541734000
H	-0.304495000	2.575161000	-0.847857000
H	2.392151000	-0.783004000	-0.945054000
C	1.781988000	-0.639707000	1.151603000
H	1.020096000	-0.160260000	1.780849000
H	1.754373000	-1.722168000	1.356808000
H	2.769158000	-0.262542000	1.463080000

2.5-Rh_2, E = -1711.649206

Rh	0.466384000	0.261091000	0.002211000
C	-0.921406000	1.726662000	0.051352000
Rh	2.143460000	-1.548448000	0.016834000
O	1.031665000	-2.429618000	1.518524000
C	-0.036508000	-1.887091000	1.915309000
O	-0.512866000	-0.786395000	1.481126000
O	3.171180000	-0.438473000	1.423076000
C	2.706427000	0.668584000	1.816805000
O	1.627105000	1.207294000	1.408682000
O	0.973308000	-2.511985000	-1.387086000
C	-0.085317000	-1.967712000	-1.805624000
O	-0.535128000	-0.835002000	-1.427935000
O	3.115392000	-0.531635000	-1.492077000
C	2.643516000	0.563299000	-1.913119000
O	1.589194000	1.132230000	-1.484998000
C	3.362053000	1.245204000	-3.049706000
H	4.435006000	1.011529000	-3.021870000
H	2.949865000	0.863075000	-3.998852000
H	3.199433000	2.330865000	-3.016806000
C	-0.893070000	-2.682607000	-2.857986000
H	-0.760636000	-2.158675000	-3.818966000
H	-0.562613000	-3.723527000	-2.965897000
H	-1.962635000	-2.642307000	-2.603889000
C	3.460634000	1.406317000	2.892893000

H	4.535678000	1.190555000	2.826800000
H	3.274389000	2.486678000	2.828429000
H	3.097061000	1.051623000	3.872175000
C	-0.821723000	-2.561953000	3.010089000
H	-0.479079000	-3.593822000	3.159316000
H	-0.680993000	-1.995072000	3.945149000
H	-1.894736000	-2.542704000	2.769068000
C	-2.321491000	1.603928000	0.055330000
H	-2.927013000	2.513946000	0.146065000
C	-2.960129000	0.378729000	-0.038198000
H	-2.329235000	-0.506859000	-0.115992000
C	-4.380833000	0.135519000	-0.044399000
C	-5.351660000	1.164610000	0.052484000
C	-4.821986000	-1.207422000	-0.147100000
C	-6.706634000	0.853875000	0.046297000
C	-6.180508000	-1.512682000	-0.153711000
C	-7.124260000	-0.482580000	-0.056288000
H	-5.039461000	2.207509000	0.132151000
H	-4.078154000	-2.005423000	-0.220092000
H	-7.448725000	1.652385000	0.121049000
H	-6.508173000	-2.551821000	-0.233512000
H	-8.191534000	-0.718927000	-0.060761000
C	-0.389108000	3.092521000	0.276553000
O	-0.409681000	3.609455000	1.375222000
O	0.132593000	3.651397000	-0.814353000
C	0.767162000	4.926551000	-0.644158000
H	0.054698000	5.674557000	-0.263200000
H	1.611817000	4.844713000	0.057102000
H	1.129000000	5.222121000	-1.636888000

TS1, E = -2151.068188

Rh	0.751513000	-0.216715000	0.158461000
C	-1.027164000	0.649616000	0.885287000
N	-1.523895000	2.220884000	-0.424767000
C	-2.890828000	2.109258000	-0.980991000
C	-1.703743000	1.783865000	-1.826935000

H	-3.409076000	1.225799000	-0.599860000
C	-3.774646000	3.344961000	-0.997127000
C	-3.035507000	4.635940000	-0.637811000
O	-1.957455000	4.389202000	0.295512000
C	-1.015887000	3.546976000	-0.189994000
O	0.107047000	3.888910000	-0.409943000
H	-2.609140000	5.129818000	-1.526774000
H	-3.703175000	5.351984000	-0.142399000
H	-4.261835000	3.458012000	-1.978707000
H	-4.571763000	3.174067000	-0.258774000
Rh	2.876961000	-1.279549000	-0.522855000
O	2.235361000	-2.966833000	0.485012000
C	1.128943000	-2.955118000	1.096373000
O	0.330430000	-1.968013000	1.166881000
O	3.694027000	-0.537550000	1.220959000
C	2.992663000	0.189539000	1.980636000
O	1.773341000	0.498321000	1.793330000
O	1.899645000	-1.936229000	-2.223234000
C	0.674506000	-1.683640000	-2.383180000
O	-0.057490000	-1.022394000	-1.575310000
O	3.344325000	0.492887000	-1.477729000
C	2.479400000	1.417636000	-1.514619000
O	1.335789000	1.384499000	-0.967449000
C	2.806334000	2.660595000	-2.303426000
H	3.883916000	2.871794000	-2.259666000
H	2.537919000	2.484022000	-3.358601000
H	2.220061000	3.508137000	-1.926599000
C	-0.011308000	-2.204230000	-3.621242000
H	0.704223000	-2.695975000	-4.292189000
H	-0.792671000	-2.922520000	-3.324958000
H	-0.509370000	-1.373212000	-4.144154000
C	3.642102000	0.772246000	3.210824000
H	3.776947000	1.855669000	3.059049000
H	2.983185000	0.636094000	4.081030000
H	4.619894000	0.309263000	3.396104000
C	0.700134000	-4.206421000	1.821530000
H	-0.334323000	-4.458556000	1.542840000

H	1.371071000	-5.044927000	1.595092000
H	0.709744000	-4.011528000	2.906129000
H	-1.489243000	0.714497000	-1.919776000
C	-1.179634000	2.606188000	-2.972941000
H	-1.459241000	3.667613000	-2.919074000
H	-0.083193000	2.534257000	-3.001025000
H	-1.580534000	2.196362000	-3.913319000
C	-2.282024000	-0.082158000	0.927701000
H	-3.034206000	0.268254000	1.644614000
C	-2.543873000	-1.193977000	0.190363000
H	-1.768900000	-1.545543000	-0.491170000
C	-3.761981000	-2.000171000	0.223412000
C	-4.912587000	-1.648339000	0.964975000
C	-3.787415000	-3.199346000	-0.521611000
C	-6.037882000	-2.470069000	0.961950000
C	-4.914457000	-4.022725000	-0.521642000
C	-6.043439000	-3.660670000	0.221010000
H	-4.928167000	-0.722641000	1.543911000
H	-2.904363000	-3.483497000	-1.100597000
H	-6.919996000	-2.183650000	1.540526000
H	-4.913009000	-4.949145000	-1.101581000
H	-6.928567000	-4.302189000	0.222599000
C	-0.790397000	1.384307000	2.167061000
O	-0.989710000	0.839408000	3.236025000
O	-0.289104000	2.611505000	2.055892000
C	0.088708000	3.279835000	3.259600000
H	-0.770083000	3.382873000	3.940903000
H	0.891331000	2.725976000	3.769351000
H	0.448751000	4.270305000	2.953378000

INT1, E = -2151.083394

Rh	0.552639000	-0.412020000	0.176635000
C	-0.583800000	1.501855000	0.728913000
N	-0.162627000	2.592852000	-0.234180000
C	-1.188247000	3.513646000	-0.869402000
C	-0.540403000	2.477203000	-1.710173000
H	-2.189328000	3.267914000	-0.512371000

C	-0.886604000	4.983397000	-0.817794000
C	0.560200000	5.284100000	-1.120845000
O	1.450480000	4.377797000	-0.421308000
C	1.184351000	3.185586000	0.082552000
O	1.966471000	2.596099000	0.755490000
H	0.786661000	5.206420000	-2.192743000
H	0.850277000	6.286621000	-0.780942000
H	-1.531863000	5.510099000	-1.538200000
H	-1.151942000	5.339531000	0.189610000
Rh	1.714589000	-2.472174000	-0.501687000
O	0.371814000	-3.518113000	0.663735000
C	-0.510636000	-2.889214000	1.318438000
O	-0.657759000	-1.628794000	1.339903000
O	2.923721000	-2.206841000	1.146924000
C	2.749027000	-1.201903000	1.901431000
O	1.876073000	-0.298451000	1.744489000
O	0.404187000	-2.581605000	-2.103474000
C	-0.481758000	-1.691652000	-2.249668000
O	-0.654832000	-0.689080000	-1.488298000
O	2.981486000	-1.287218000	-1.619035000
C	2.773568000	-0.040672000	-1.681622000
O	1.842908000	0.583601000	-1.086467000
C	3.683382000	0.777693000	-2.564559000
H	4.661978000	0.289764000	-2.667234000
H	3.229918000	0.853791000	-3.566949000
H	3.800462000	1.792938000	-2.161581000
C	-1.442325000	-1.819628000	-3.406019000
H	-1.466110000	-0.877909000	-3.975371000
H	-1.164470000	-2.652246000	-4.064769000
H	-2.455482000	-1.986608000	-3.005687000
C	3.641467000	-1.093329000	3.113820000
H	4.667979000	-1.393024000	2.858028000
H	3.627865000	-0.074023000	3.521184000
H	3.269211000	-1.788962000	3.884398000
C	-1.503364000	-3.702825000	2.111259000
H	-1.078884000	-4.678563000	2.383026000
H	-1.821295000	-3.155787000	3.009224000

H	-2.391930000	-3.872892000	1.480556000
H	-1.128680000	1.567934000	-1.832385000
C	0.461436000	2.629394000	-2.827099000
H	1.361447000	3.199562000	-2.574578000
H	0.779245000	1.630159000	-3.145895000
H	-0.041370000	3.127324000	-3.671115000
C	-1.931293000	0.915111000	0.652338000
H	-2.076395000	0.328660000	1.562499000
C	-2.940975000	0.853496000	-0.250715000
H	-2.935223000	1.422911000	-1.180954000
C	-4.112281000	-0.021578000	-0.102729000
C	-4.131520000	-1.134461000	0.769784000
C	-5.268256000	0.221668000	-0.877008000
C	-5.263477000	-1.943290000	0.878471000
C	-6.399279000	-0.591465000	-0.769520000
C	-6.407478000	-1.676982000	0.113926000
H	-3.234374000	-1.383684000	1.339708000
H	-5.275269000	1.067432000	-1.571563000
H	-5.248587000	-2.799772000	1.558902000
H	-7.281018000	-0.375420000	-1.379716000
H	-7.290622000	-2.315846000	0.197911000
C	-0.379112000	1.978330000	2.142929000
O	-0.403124000	1.278684000	3.126474000
O	-0.261440000	3.329113000	2.218598000
C	0.043413000	3.879789000	3.503253000
H	-0.737641000	3.622751000	4.234574000
H	1.012878000	3.504736000	3.866472000
H	0.089622000	4.967846000	3.366547000

INT2, E = -1015.282384

C	0.551999000	0.900073000	-0.188694000
N	1.291218000	-0.356331000	-0.158447000
C	2.223648000	-0.664503000	-1.321619000
C	0.965874000	-1.429910000	-1.225566000
H	2.198205000	0.162463000	-2.033650000
C	3.612563000	-1.103175000	-0.956863000
C	3.646624000	-2.026905000	0.238429000

O	2.782986000	-1.564965000	1.310112000
C	1.696346000	-0.823849000	1.203292000
O	1.043180000	-0.500669000	2.147294000
H	3.339366000	-3.050826000	-0.013497000
H	4.647945000	-2.072080000	0.684433000
H	4.070632000	-1.609231000	-1.820943000
H	4.193493000	-0.192347000	-0.751386000
H	0.173093000	-1.029440000	-1.861345000
C	0.748594000	-2.868744000	-0.838433000
H	1.278721000	-3.187546000	0.066573000
H	-0.324046000	-3.048874000	-0.682824000
H	1.084657000	-3.505399000	-1.671955000
C	-0.863137000	0.908104000	-0.139037000
C	1.334374000	2.093090000	-0.089885000
O	0.920973000	3.246893000	-0.104707000
O	2.682470000	1.819123000	0.040120000
C	3.544891000	2.947220000	0.129306000
H	3.500585000	3.561379000	-0.785312000
H	3.285076000	3.586415000	0.988339000
H	4.562280000	2.552326000	0.257952000
C	-1.734808000	-0.138431000	0.011588000
H	-1.333163000	-1.138843000	0.196350000
C	-3.190670000	-0.055663000	0.005372000
C	-3.914857000	1.132128000	-0.271732000
C	-3.954290000	-1.216366000	0.287249000
C	-5.309094000	1.153775000	-0.253648000
H	-3.374801000	2.052438000	-0.507477000
C	-5.349877000	-1.192705000	0.301150000
H	-3.429431000	-2.152546000	0.503079000
C	-6.043444000	-0.006344000	0.032237000
H	-5.833000000	2.089839000	-0.469969000
H	-5.902293000	-2.110502000	0.524686000
H	-7.136351000	0.015152000	0.042068000
H	-1.264791000	1.922108000	-0.237432000

TS2, E = -1015.264461

C	0.442061000	0.843680000	0.190551000
N	1.104025000	-0.324226000	0.333571000
C	2.050918000	-1.167322000	-1.657013000
C	0.923963000	-1.546818000	-0.883962000
H	1.883321000	-0.345410000	-2.358742000
C	3.471498000	-1.503649000	-1.386633000
C	3.693714000	-2.097614000	-0.011546000
O	3.171297000	-1.312560000	1.080461000
C	2.206744000	-0.389707000	1.215314000
O	2.240222000	0.323280000	2.192791000
H	3.269710000	-3.108344000	0.059546000
H	4.769312000	-2.177926000	0.201629000
H	3.874887000	-2.227612000	-2.124650000
H	4.082177000	-0.591001000	-1.507827000
H	-0.012676000	-1.205290000	-1.336901000
C	0.716348000	-2.878577000	-0.180600000
H	1.363085000	-3.021901000	0.693146000
H	-0.322797000	-2.952922000	0.169553000
H	0.897401000	-3.706453000	-0.883566000
C	-0.980545000	0.909194000	0.063915000
C	1.203112000	2.095850000	-0.001919000
O	0.737889000	3.216541000	0.088964000
O	2.489292000	1.859662000	-0.340034000
C	3.341977000	2.999373000	-0.453981000
H	2.963147000	3.705621000	-1.209149000
H	3.422742000	3.523149000	0.511802000
H	4.326450000	2.618944000	-0.755477000
C	-1.850812000	-0.119527000	0.293201000
H	-1.446367000	-1.060653000	0.676554000
C	-3.298131000	-0.089919000	0.117269000
C	-3.994310000	1.017967000	-0.423566000
C	-4.058093000	-1.219931000	0.500004000
C	-5.380657000	0.994624000	-0.562022000
H	-3.442299000	1.904892000	-0.742271000
C	-5.446467000	-1.241501000	0.358033000
H	-3.541969000	-2.088941000	0.918664000
C	-6.117039000	-0.133815000	-0.173232000

H	-5.894889000	1.863626000	-0.981748000
H	-6.009224000	-2.127964000	0.663349000
H	-7.204189000	-0.148046000	-0.286230000
H	-1.361280000	1.886581000	-0.243028000

TS2', E = -1015.274842

C	0.670116000	0.994794000	0.080088000
N	1.337729000	-0.248494000	0.065774000
C	2.178138000	-0.643629000	-1.133166000
C	0.954988000	-1.380866000	-1.458926000
H	2.335631000	0.243951000	-1.749581000
C	3.494612000	-1.261303000	-0.730051000
C	3.327378000	-2.348307000	0.309574000
O	2.311939000	-2.030058000	1.291233000
C	1.455428000	-1.006110000	1.275555000
O	0.808037000	-0.739566000	2.250634000
H	3.042650000	-3.310973000	-0.135350000
H	4.254033000	-2.503100000	0.879827000
H	4.003647000	-1.670628000	-1.615807000
H	4.110009000	-0.439891000	-0.333927000
H	0.196539000	-0.776126000	-1.961278000
C	0.649842000	-2.821187000	-1.259263000
H	-0.357820000	-3.050491000	-1.629772000
H	1.386885000	-3.445732000	-1.795528000
H	0.694095000	-3.130913000	-0.201240000
C	-0.746778000	1.042578000	0.102383000
C	1.456695000	2.199013000	-0.035771000
O	1.019668000	3.341862000	-0.077500000
O	2.805418000	1.949683000	-0.079504000
C	3.650052000	3.092232000	-0.179202000
H	3.440603000	3.671552000	-1.093234000
H	3.524245000	3.759022000	0.688924000
H	4.681199000	2.714443000	-0.209273000
C	-1.607419000	-0.024393000	0.136666000
H	-1.192320000	-1.029011000	0.254013000
C	-3.062390000	0.034998000	0.053388000

C	-3.798257000	1.242609000	-0.047982000
C	-3.807007000	-1.170233000	0.070403000
C	-5.190248000	1.238243000	-0.127071000
H	-3.270822000	2.199358000	-0.064071000
C	-5.200546000	-1.172142000	-0.011729000
H	-3.270447000	-2.120758000	0.150927000
C	-5.906576000	0.032672000	-0.110882000
H	-5.725918000	2.189207000	-0.202873000
H	-5.740760000	-2.123378000	0.004321000
H	-6.997920000	0.034600000	-0.173527000
H	-1.146305000	2.059141000	0.044034000

INT3, E = -1015.335060

N	1.270914000	-0.066270000	-1.148547000
C	1.522818000	1.857512000	1.286335000
C	0.275738000	1.951571000	1.776471000
H	2.092391000	0.952971000	1.524670000
C	2.228135000	2.851299000	0.401651000
C	2.298418000	2.459541000	-1.075763000
O	3.123998000	1.299340000	-1.310045000
C	2.639979000	0.051498000	-1.378632000
O	3.368593000	-0.863521000	-1.700042000
H	1.293637000	2.293973000	-1.489580000
H	2.788671000	3.261616000	-1.647406000
H	1.737500000	3.837263000	0.437841000
H	3.261841000	2.996752000	0.761306000
H	-0.081504000	1.121437000	2.399554000
C	-0.717641000	3.056192000	1.564732000
H	-0.341017000	3.861867000	0.917427000
H	-1.642095000	2.660629000	1.107045000
H	-1.022193000	3.504725000	2.527472000
C	-1.553048000	-0.270349000	-0.580552000
H	-1.168506000	0.654666000	-1.022115000
C	-0.643790000	-1.222734000	-0.254232000
H	-0.939502000	-2.158184000	0.225142000

C	0.785016000	-1.027755000	-0.444357000
C	-2.997730000	-0.320979000	-0.383072000
C	-3.664667000	-1.441314000	0.162803000
C	-3.766045000	0.807349000	-0.744513000
C	-5.046000000	-1.426221000	0.340003000
C	-5.150396000	0.820236000	-0.565132000
C	-5.794249000	-0.296204000	-0.021414000
H	-3.098160000	-2.329763000	0.449202000
H	-3.262797000	1.679218000	-1.171473000
H	-5.547188000	-2.300240000	0.763807000
H	-5.728532000	1.703135000	-0.849405000
H	-6.877974000	-0.289440000	0.121463000
C	1.665738000	-2.051267000	0.262277000
O	1.510214000	-3.241337000	0.134374000
O	2.571429000	-1.470335000	1.044027000
C	3.534939000	-2.329356000	1.675408000
H	3.032620000	-3.090924000	2.290407000
H	4.154229000	-2.824454000	0.912330000
H	4.155003000	-1.678645000	2.303556000

TS3, E = -1015.302020

N	1.396743000	0.390498000	-0.582141000
C	0.650374000	1.368615000	1.206916000
C	-0.753846000	1.257546000	1.183544000
H	1.184648000	0.596508000	1.762839000
C	1.385591000	2.680483000	1.057392000
C	1.933291000	2.954170000	-0.341072000
O	2.972050000	2.044352000	-0.712378000
C	2.680252000	0.743414000	-0.931084000
O	3.507938000	0.029155000	-1.464526000
H	1.126355000	2.923229000	-1.090743000
H	2.402804000	3.947495000	-0.372293000
H	0.733574000	3.528137000	1.322680000
H	2.234626000	2.693644000	1.759300000
H	-1.177472000	0.515965000	1.864903000
C	-1.625171000	2.445519000	0.871864000

H	-1.300815000	2.967764000	-0.042347000
H	-2.676300000	2.152224000	0.743438000
H	-1.593236000	3.179025000	1.698092000
C	-1.267377000	-0.145520000	-0.462806000
H	-0.982349000	0.684545000	-1.112439000
C	-0.320836000	-1.184121000	-0.349221000
H	-0.622170000	-2.191779000	-0.055758000
C	1.034781000	-0.888841000	-0.442555000
C	-2.713802000	-0.376652000	-0.314289000
C	-3.228082000	-1.344653000	0.572570000
C	-3.622824000	0.400675000	-1.059970000
C	-4.604380000	-1.537395000	0.695950000
C	-5.000626000	0.204074000	-0.939139000
C	-5.496024000	-0.765788000	-0.060916000
H	-2.543376000	-1.941303000	1.180088000
H	-3.237860000	1.160160000	-1.745471000
H	-4.986257000	-2.290842000	1.389882000
H	-5.690400000	0.811429000	-1.531051000
H	-6.573981000	-0.918316000	0.037957000
C	2.025633000	-1.976257000	-0.119116000
O	2.007370000	-3.084277000	-0.603088000
O	2.885644000	-1.576595000	0.825423000
C	3.960555000	-2.468783000	1.137390000
H	3.579868000	-3.439813000	1.489967000
H	4.592689000	-2.629465000	0.250253000
H	4.543373000	-1.982097000	1.929491000

2.6ba, E = -1015.378313

N	-1.268351000	-0.432082000	0.140358000
C	-0.129717000	-1.241923000	0.619677000
C	0.799833000	-1.563093000	-0.574881000
H	0.446858000	-0.588142000	1.292481000
C	-0.632295000	-2.414720000	1.462066000
C	-1.900851000	-3.023850000	0.902803000
O	-2.898633000	-2.015445000	0.664663000
C	-2.580648000	-0.860192000	0.052983000

O	-3.448482000	-0.221822000	-0.508748000
H	-1.727643000	-3.564149000	-0.039511000
H	-2.356533000	-3.724856000	1.615397000
H	0.150928000	-3.184101000	1.537908000
H	-0.840131000	-2.053603000	2.481742000
H	1.651093000	-2.134262000	-0.172826000
C	0.141669000	-2.390154000	-1.682417000
H	-0.761772000	-1.897765000	-2.077903000
H	0.841028000	-2.525906000	-2.522419000
H	-0.139760000	-3.393117000	-1.329684000
C	1.354484000	-0.211292000	-1.130563000
H	1.654332000	-0.385260000	-2.177900000
C	0.299624000	0.861279000	-1.141809000
H	0.553535000	1.822353000	-1.594289000
C	-0.904226000	0.743733000	-0.552306000
C	2.615875000	0.235364000	-0.393010000
C	2.577121000	1.131064000	0.687302000
C	3.859351000	-0.302480000	-0.769577000
C	3.745749000	1.471636000	1.379604000
C	5.027247000	0.035803000	-0.081646000
C	4.974582000	0.925676000	0.998432000
H	1.624285000	1.571214000	0.990696000
H	3.909095000	-0.998681000	-1.612279000
H	3.692809000	2.171327000	2.218301000
H	5.984212000	-0.392426000	-0.392551000
H	5.887949000	1.192846000	1.536642000
C	-1.817793000	1.931032000	-0.498665000
O	-1.963769000	2.721967000	-1.402769000
O	-2.370158000	2.066599000	0.713732000
C	-3.341164000	3.106035000	0.857069000
H	-2.899417000	4.093921000	0.653321000
H	-4.185376000	2.942586000	0.168915000
H	-3.691756000	3.058706000	1.896048000

2.9 Experimental References

(1) (a) Armarego, W.L.F.; Chai, C.L.L. Purification of Laboratory Chemicals 6th ed., Elsevier: Burlington, MA, **2009**. (b) Still, W. C.; Kahn, M.; Mitra, A. *J. Org. Chem.* **1978**, *43*, 2923-2925.

(2) Ju, M.; Weatherly, C. D.; Guzei, I. A., Schomaker, J. M. *Angew. Chem. Int. Ed*. **2017**, *56*, 9944-9948.

(3) (a) Lebel, H.; Lectard, S.; Parmentier, M. *Org. Lett.* **2007**, *9*, 4797-4800. (b) Lebel, H.; Huard, K.; Lectard, S. *J. Am. Chem. Soc.* **2005**, *127*, 141989-14199.

(4) (a) Manning, J. R.; Davies, H. M. L. *Org. Synth.* **2007**, *84*, 334-346. (b) Walji, A. M.; Davies, H. M. L. *Angew. Chem. Int. Ed.* **2005**, *44*, 1733-1735.

(5) Johnson, R. L. *J. Med. Chem*. **1984**, *27*, 1351-1354.

(6) Hudspeth, J. P.; Lunney, E. A.; Michniewicz, E. D.; Repine, J. T.; Roark, W. H.; Stier, M. A.; Tinney, F. J.; Woo, P. K. W.; Essenburg, A. D.; Kaltenbronn J. S. *J. Med. Chem.* **1990**, *33*, 838-845.

(7) Jenmalm, A.; Berts, W.; Li, Y. L.; Luthman, K.; Csöregh, I.; Hacksell, U. J. *Org. Chem.* **1994**, *59*, 1139-1148

(8) Bruker-AXS (2016). *APEX3.* Version 2016.5-0. Madison, Wisconsin, USA.

(9) Krause, L., Herbst-Irmer, R., Sheldrick, G. M. & Stalke, D. *J. Appl. Cryst.* **2015**, 48, 3-10.

(10) Sheldrick, G. M. (2013b). *XPREP*. Version 2013/1. Georg-August-Universität Göttingen, Göttingen, Germany.

(11) Sheldrick, G. M. (2013a). The *SHELX* homepage, http://shelx.uni-ac.gwdg.de/SHELX/.

(12) Sheldrick, G. M. *Acta Cryst. A* **2015a**., 71, 3-8.

(13) Sheldrick, G. M. *Acta Cryst. C* **2015b**, 71, 3-8.

(14) Dolomanov, O. V., Bourhis, L. J., Gildea, R. J., Howard, J. A. K. & Puschmann, H. *J. Appl. Crystallogr*. **2009**, *42*, 339-341.

(15) Guzei, I. A. (2007-2013). Programs *Gn*. University of Wisconsin-Madison, Madison, Wisconsin, USA.

(16) Gaussian 09, Revision D.01, Frisch, M. J.; Trucks, G. W.; Schlegel, H. B.; Scuseria, G. E.; Robb, M. A.; Cheeseman, J. R.; Scalmani, G.; Barone, V.; Mennucci, B.; Petersson, G. A.; Nakatsuji, H.; Caricato, M.; Li, X.; Hratchian, H. P.; Izmaylov, A. F.; Bloino, J.; Zheng, G.; Sonnenberg, J. L.; Hada, M.; Ehara, M.; Toyota, K.; Fukuda, R.; Hasegawa, J.; Ishida, M.; Nakajima, T.; Honda, Y.; Kitao, O.; Nakai, H.; Vreven, T.; Montgomery, J. A., Jr.; Peralta, J. E.; Ogliaro, F.; Bearpark, M.; Heyd, J. J.; Brothers, E.; Kudin, K. N.; Staroverov, V. N.; Kobayashi,

R.; Normand, J.; Raghavachari, K.; Rendell, A.; Burant, J. C.; Iyengar, S. S.; Tomasi, J.; Cossi, M.; Rega, N.; Millam, J. M.; Klene, M.; Knox, J. E.; Cross, J. B.; Bakken, V.; Adamo, C.; Jaramillo, J.; Gomperts, R.; Stratmann, R. E.; Yazyev, O.; Austin, A. J.; Cammi, R.; Pomelli, C.; Ochterski, J. W.; Martin, R. L.; Morokuma, K.; Zakrzewski, V. G.; Voth, G. A.; Salvador, P.; Dannenberg, J. J.; Dapprich, S.; Daniels, A. D.; Farkas, Ö.; Foresman, J. B.; Ortiz, J. V.; Cioslowski, J.; Fox, D. J. Gaussian, Inc., Wallingford CT, 2009.

(17) (a) Becke, A. D. *J. Chem. Phys*. **1993**, *98*, 5648-5652 (b) Lee, C.; Yang, W.; Parr, R. G. *Phys. Rev. B.* **1998**, *37*, 785-789 c) Vosko, S. H.; Wilk, L.; Nusair, M. *Can. J. Phys*. **1980**, *58*, 1200-1211.

(18) Grimme, S.; Antony, J.; Ehrlich, S.; Krieg, H. *J. Chem. Phys*. **2010**, *132*, 154104-154123.

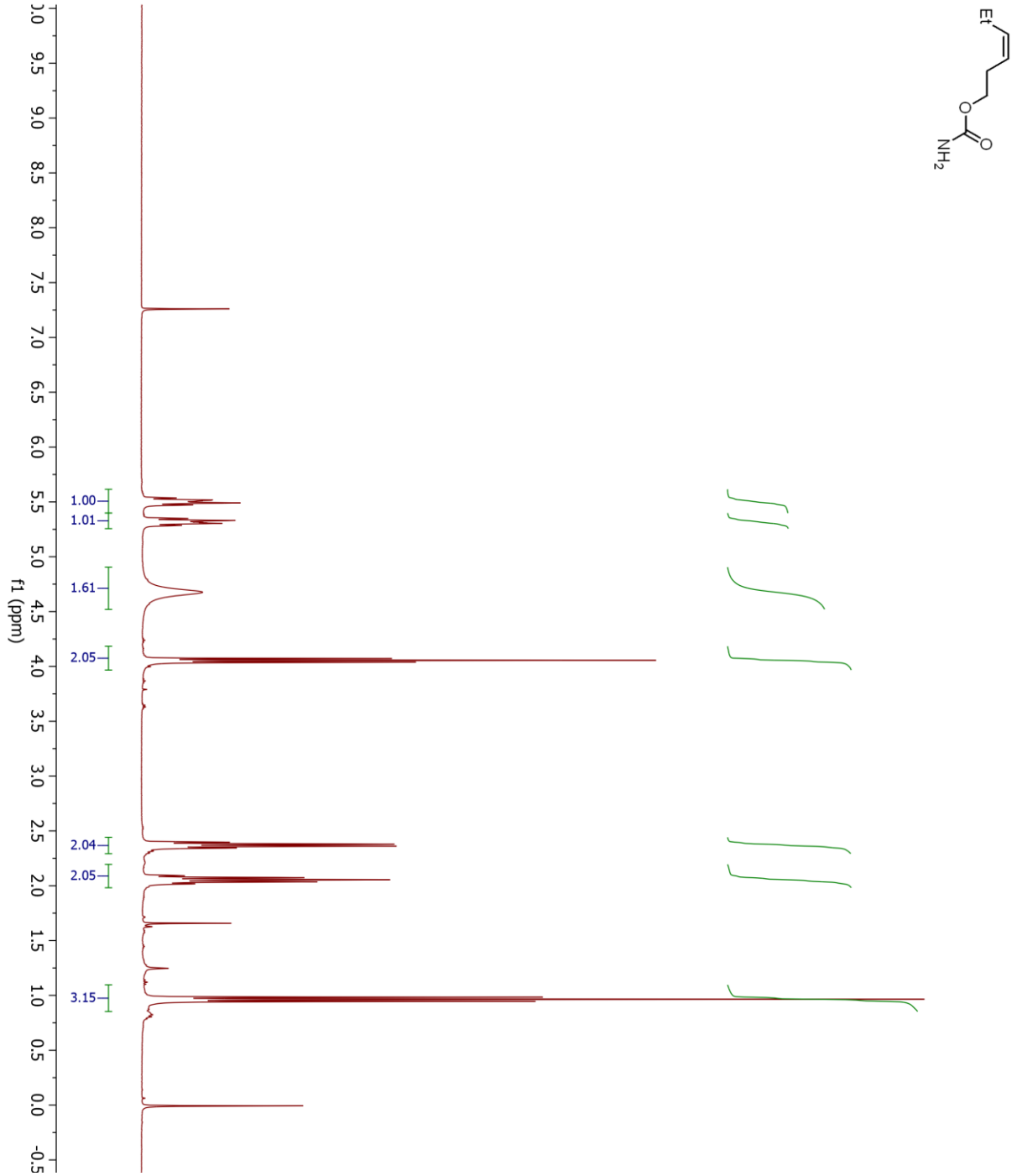
(19) Weigend, F.; Ahlrichs, R. *Phys. Chem. Chem. Phys*. **2005**, *7*, 3297-3305.

(20) McIver, J. W.; Komornicki, A. K. *J. Am. Chem. Soc.* **1972**, *94*, 2625-2633.

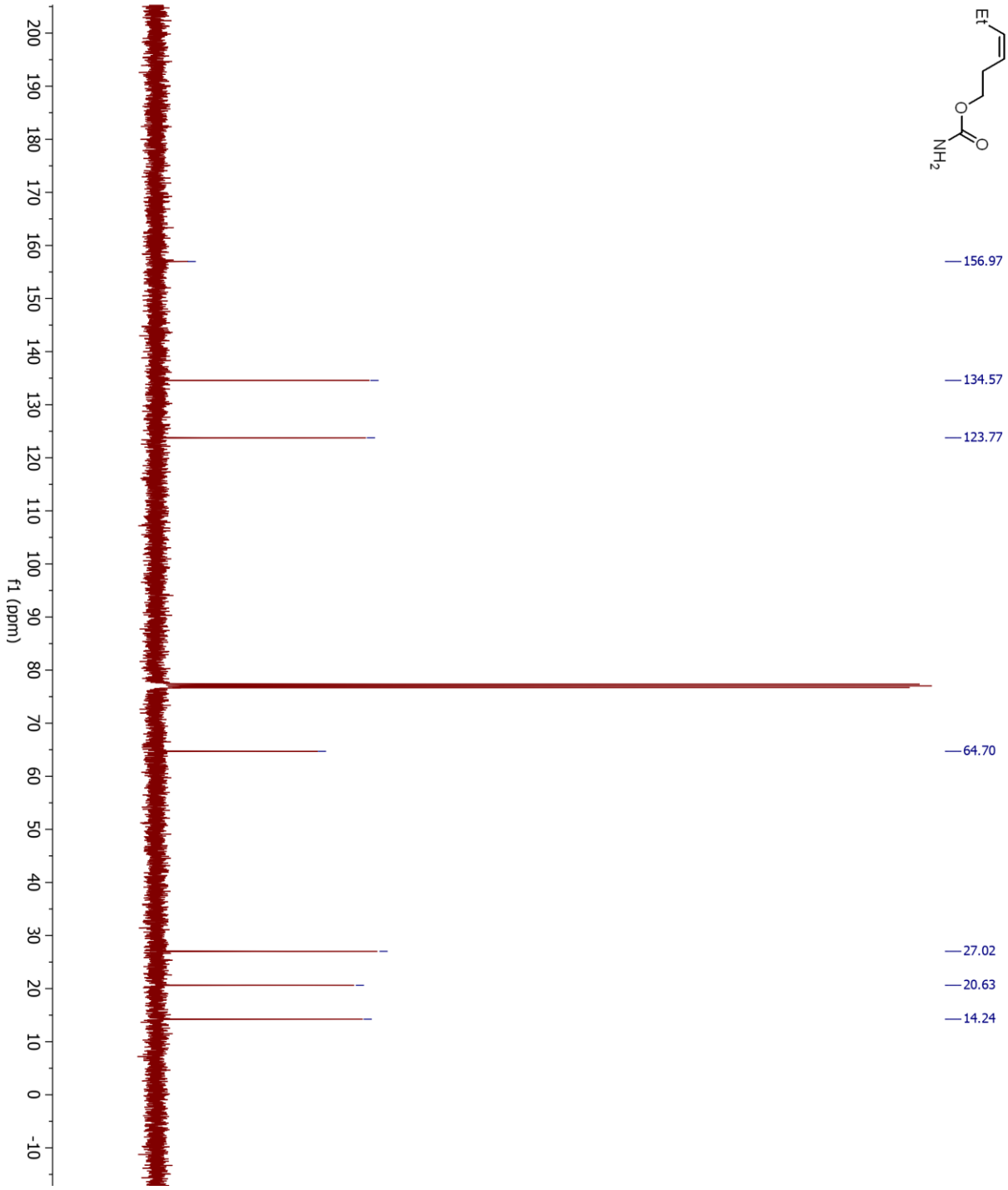
(21) González, C.; Schlegel, H. B. *J. Phys. Chem*. **1990**, *94*, 5523-5527.

2.10 NMR Spectra

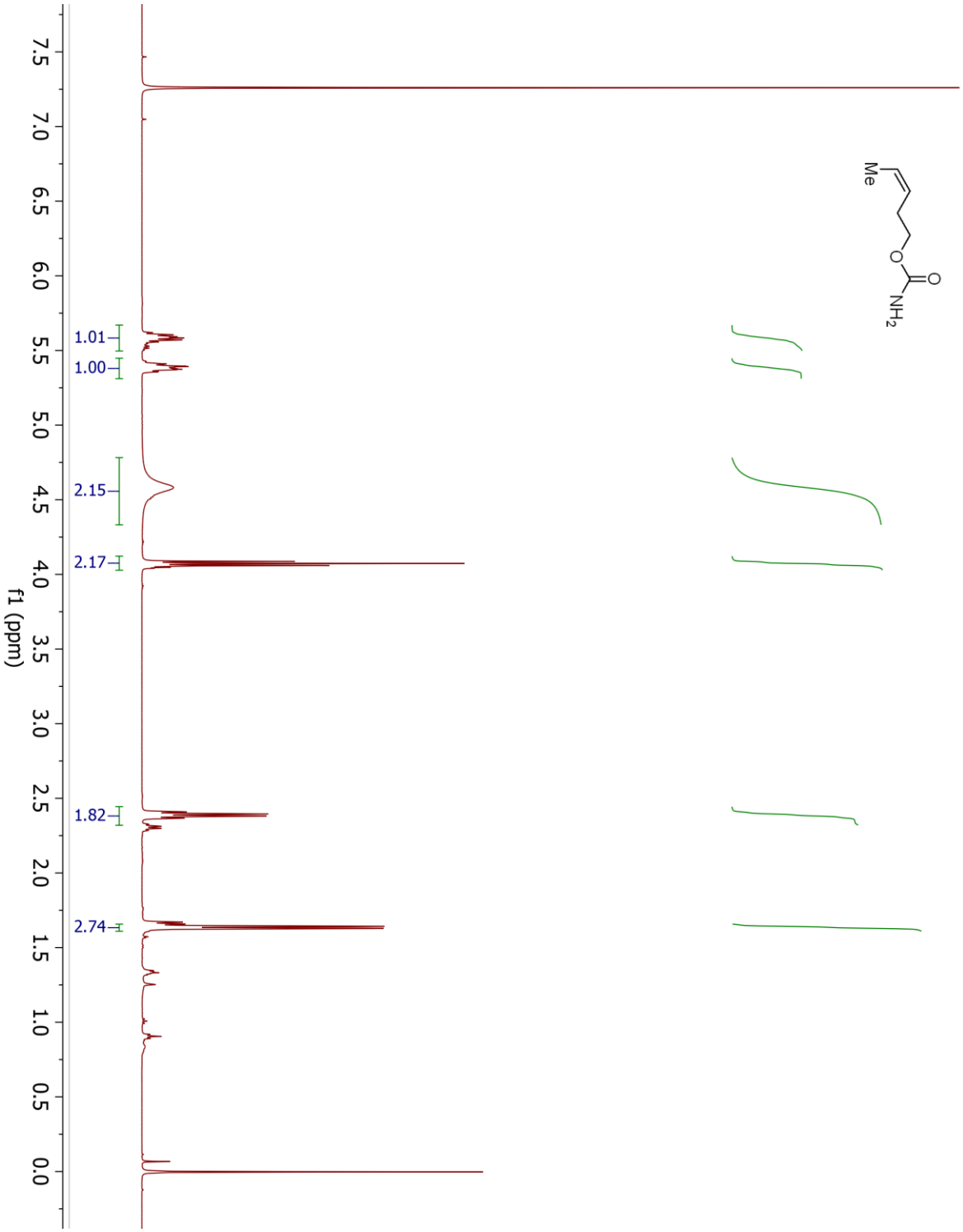
^{1}H NMR (500 MHz, $CDCl_3$) for precursor to compound **2.1a**



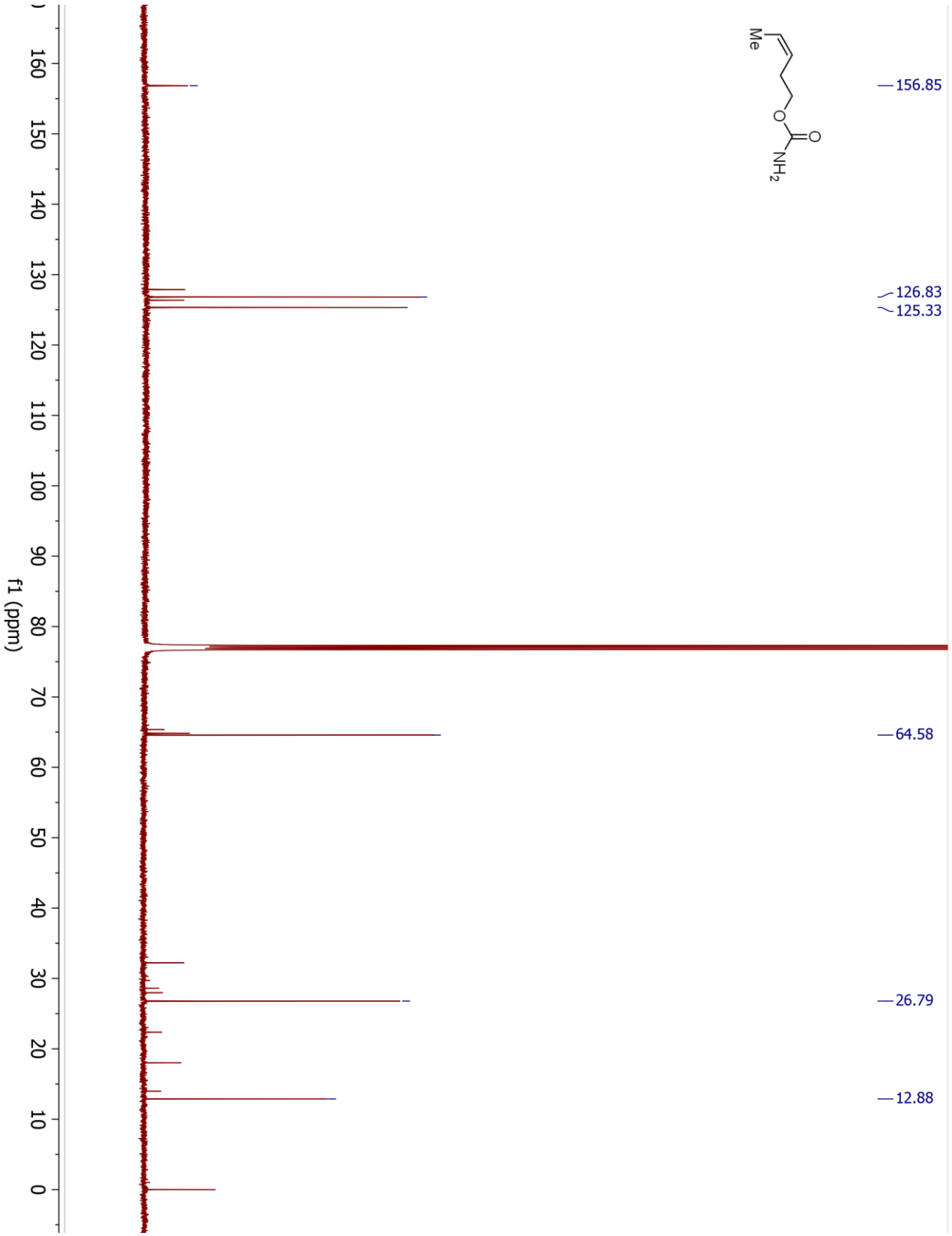
^{13}C NMR (126 MHz, $CDCl_3$) for precursor to compound **2.1a**



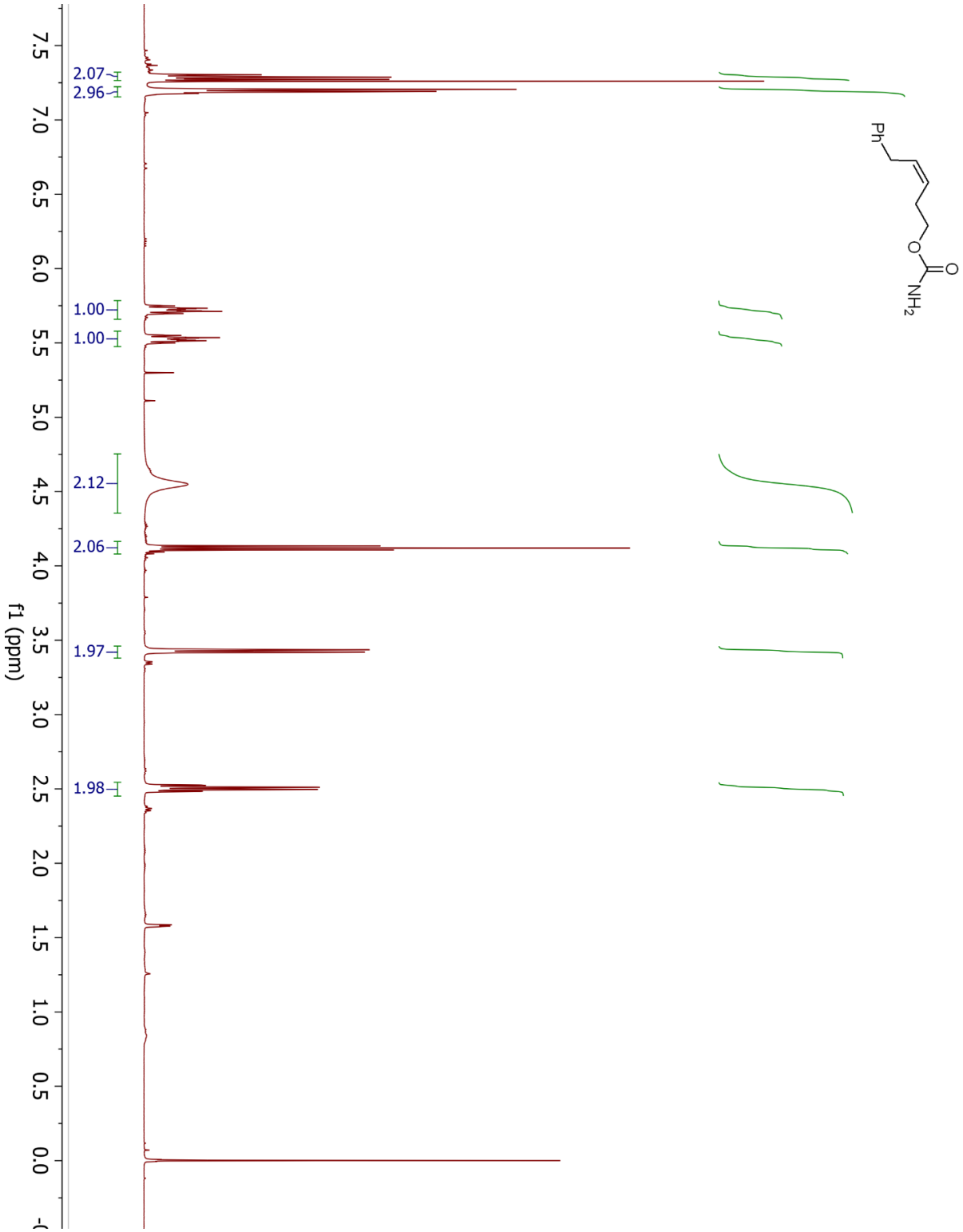
^{1}H NMR (500 MHz, $CDCl_3$) for precursor to compound **2.1b**



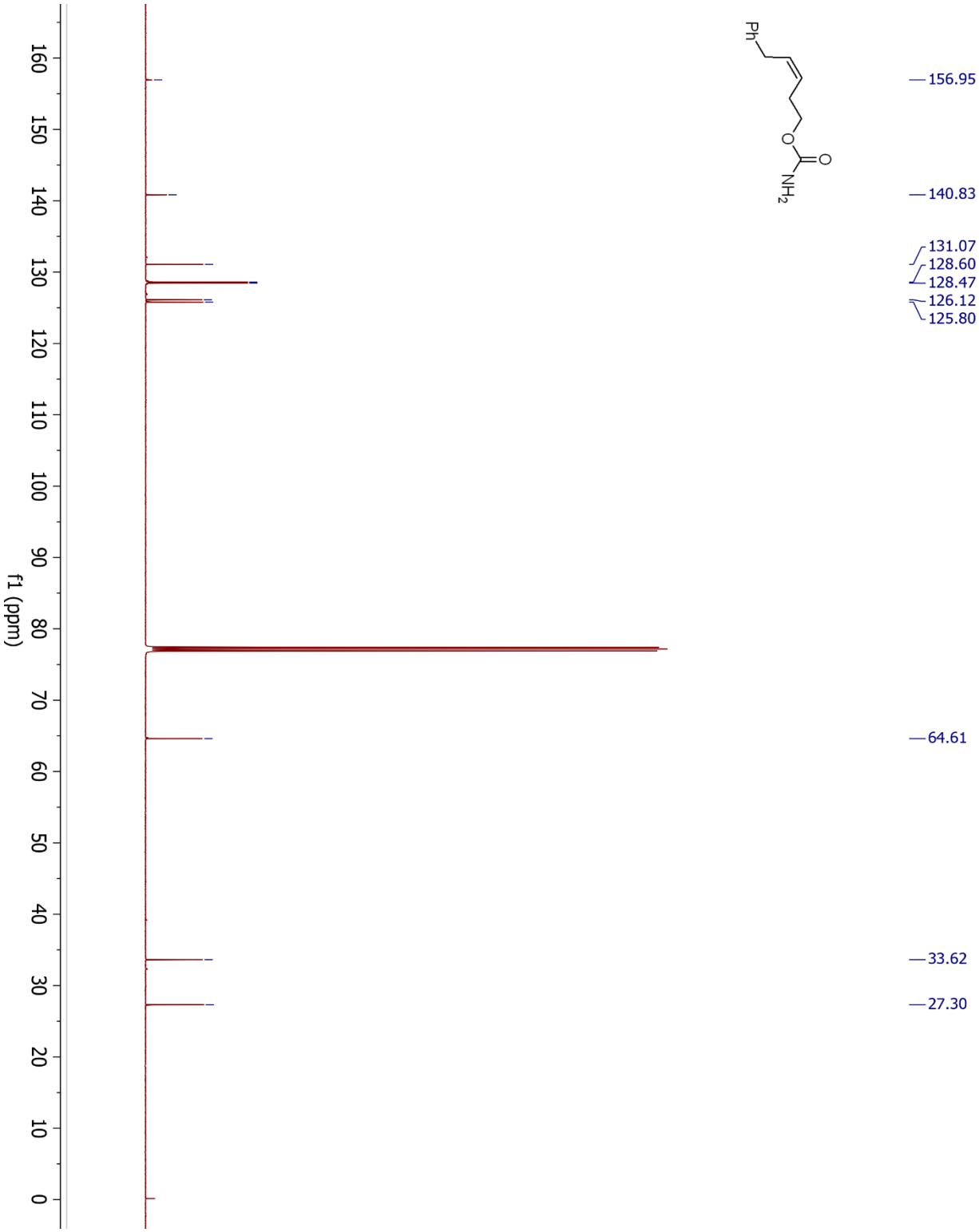
^{13}C NMR (126 MHz, $CDCl_3$) for precursor to compound **2.1b**



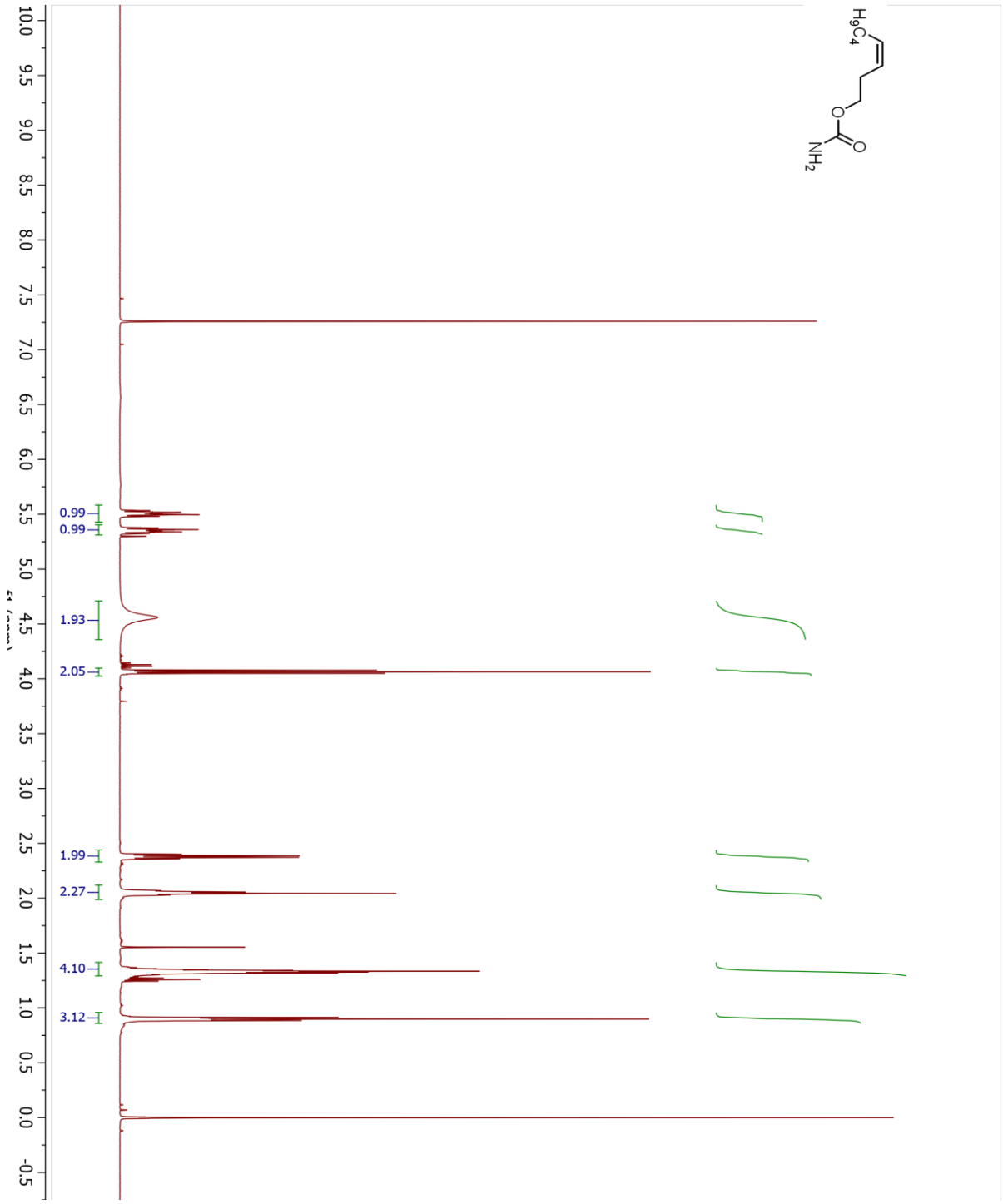
^{1}H NMR (500 MHz, $CDCl_3$) for precursor to compound **2.1c**



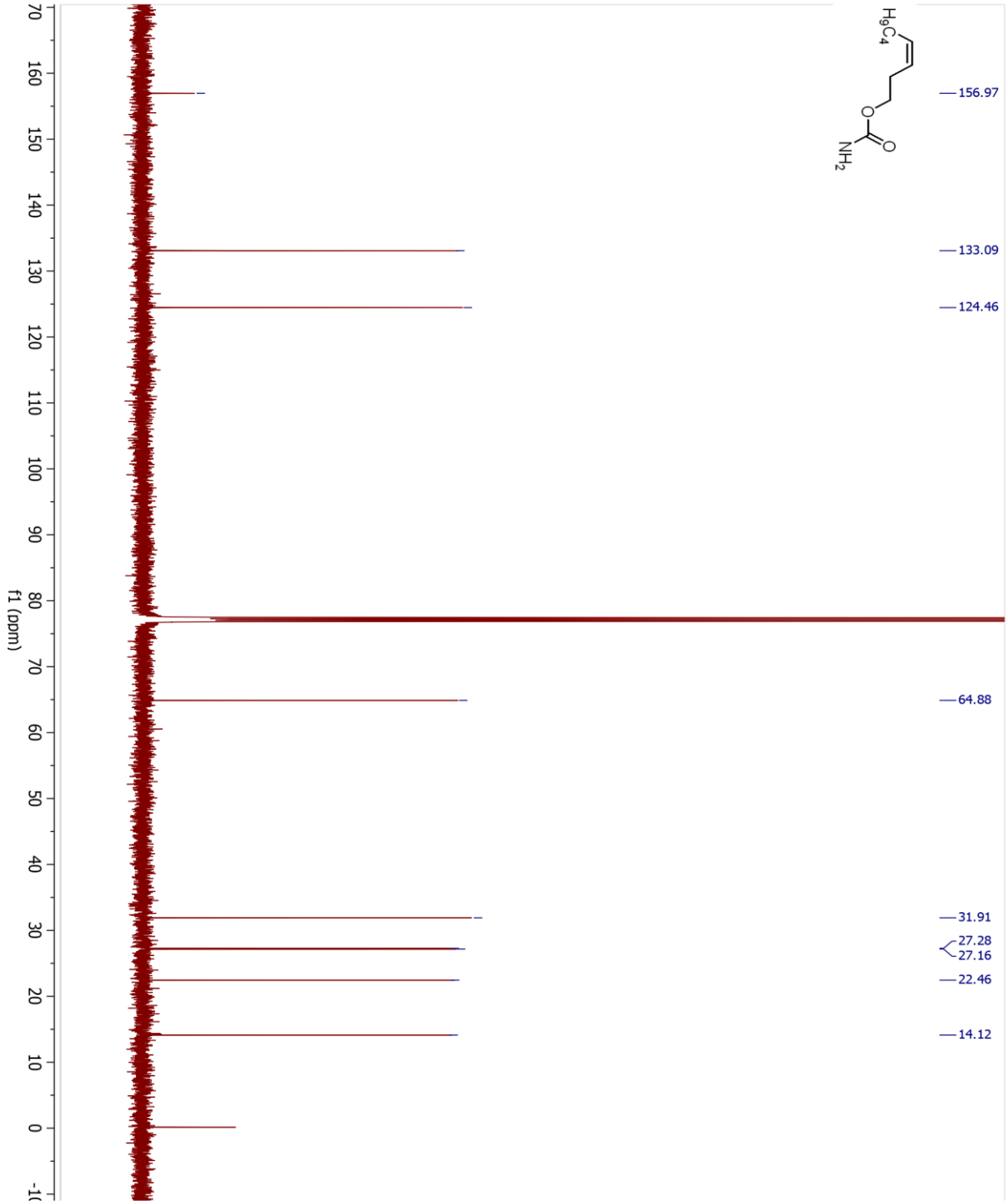
^{13}C NMR (126 MHz, $CDCl_3$) for precursor to compound **2.1c**



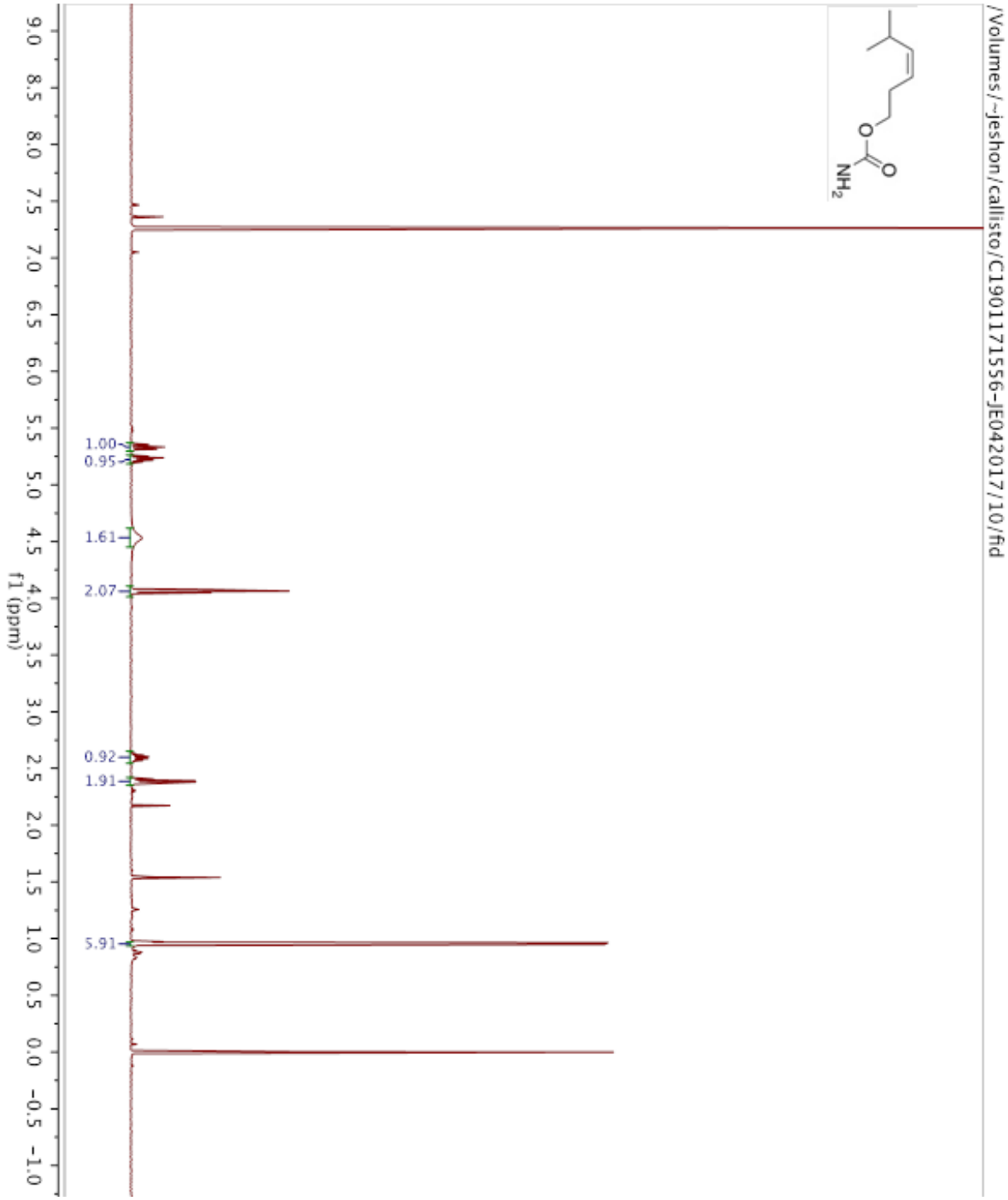
^{1}H NMR (500 MHz, $CDCl_3$) for precursor to compound **2.1d**



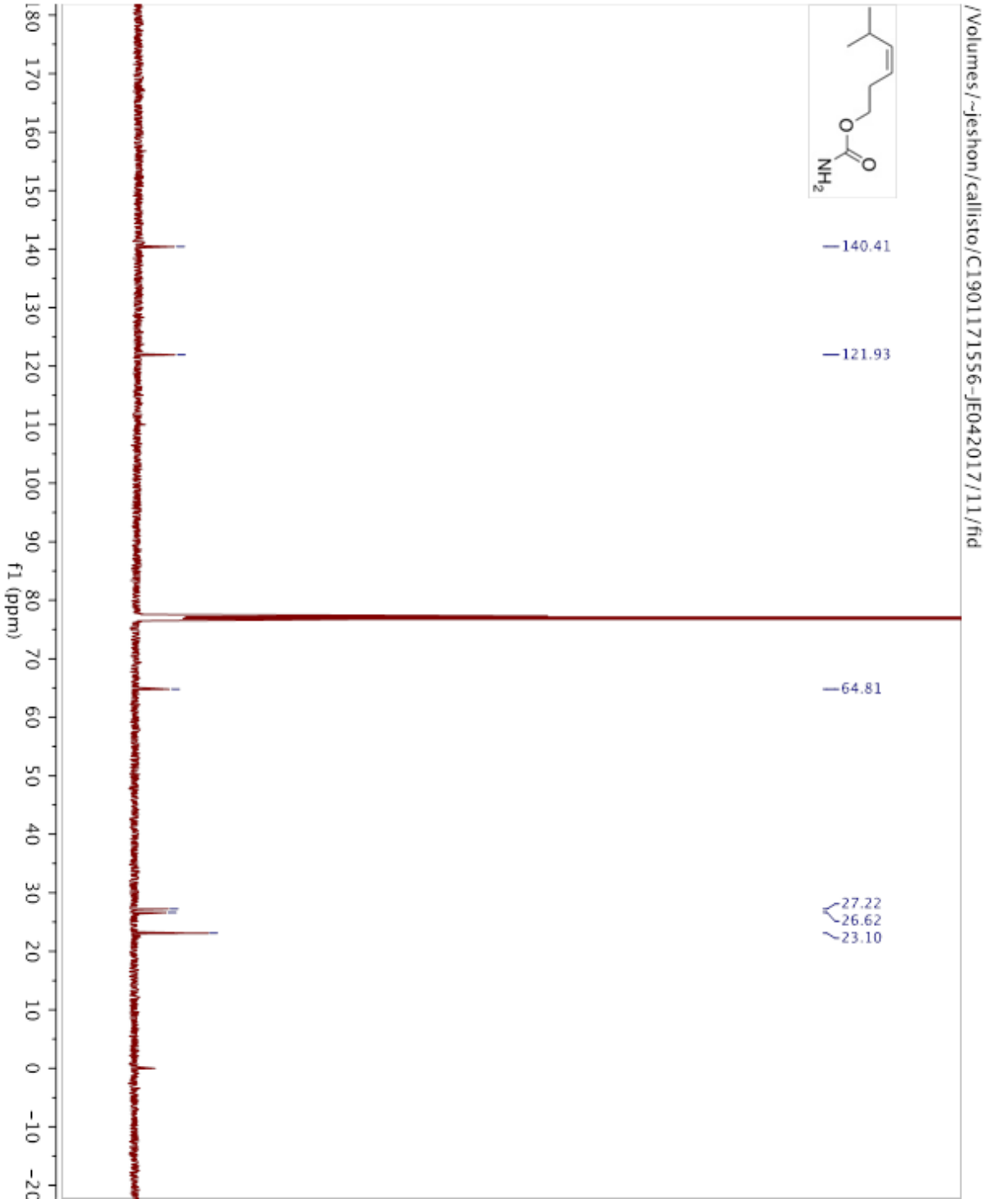
^{13}C NMR (126 MHz, $CDCl_3$) for precursor to compound **2.1d**



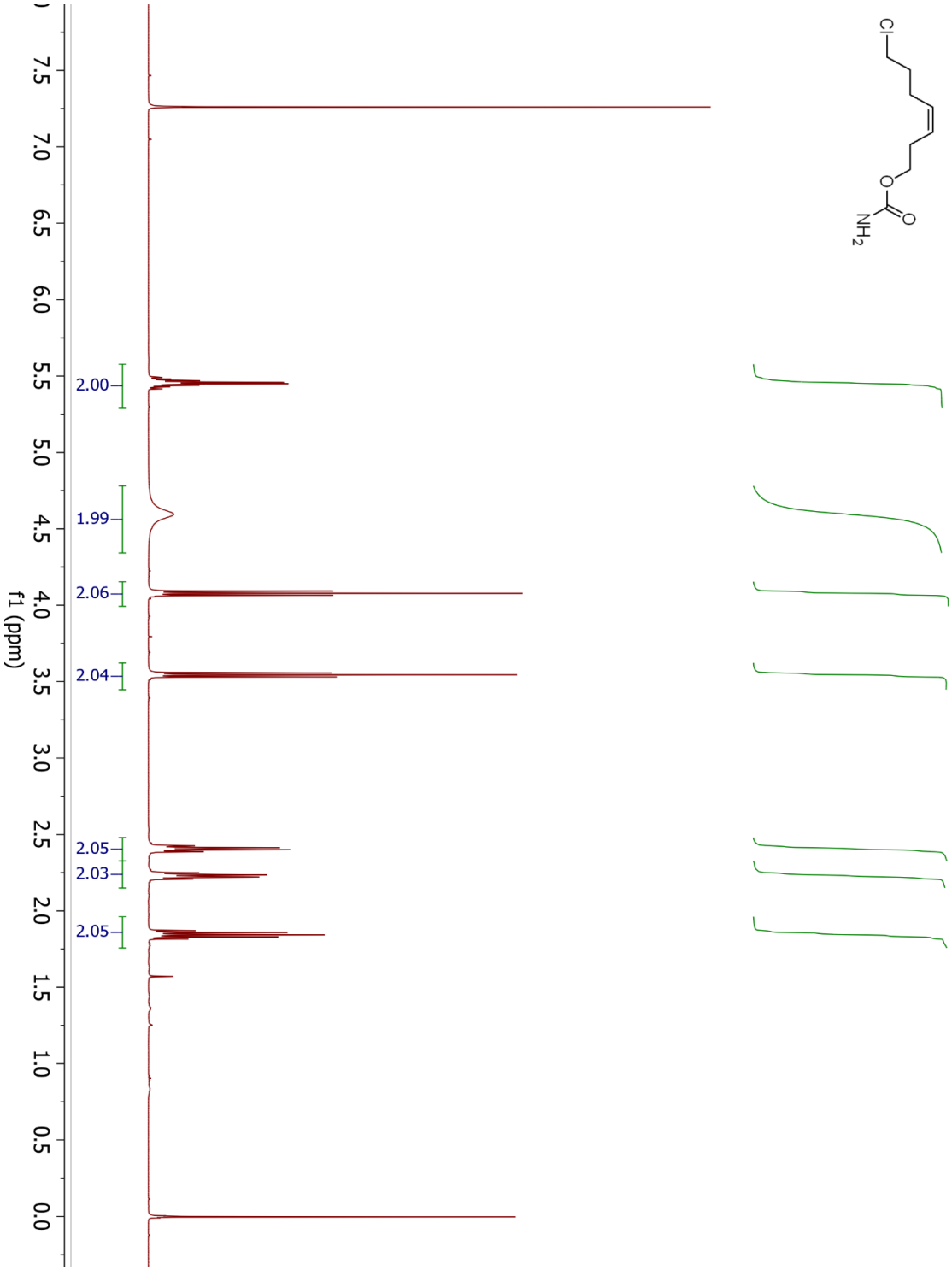
^{1}H NMR (500 MHz, $CDCl_3$) for precursor to compound **2.1e**



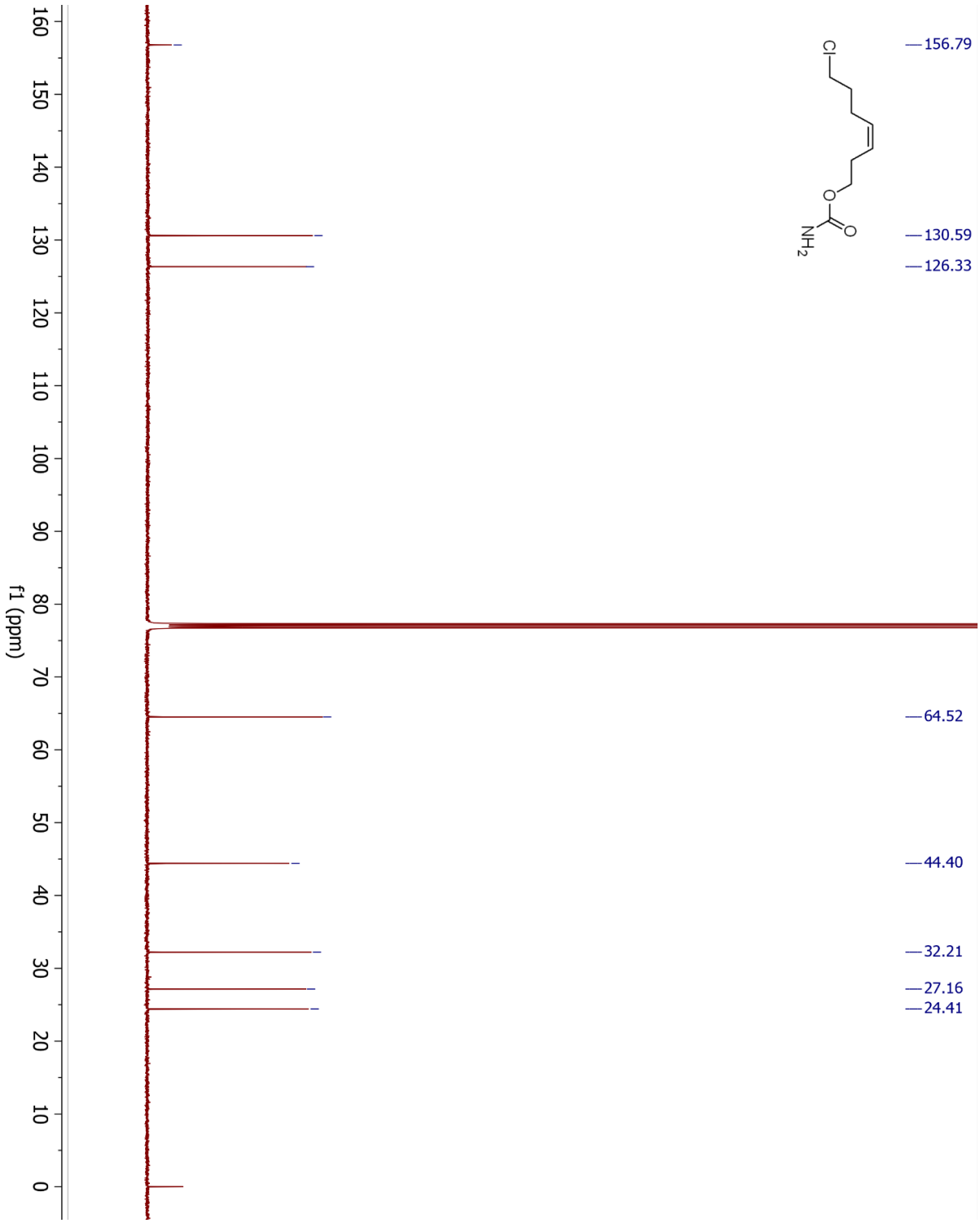
^{13}C NMR (126MHz, $CDCl_3$) for precursor compound **2.1e**



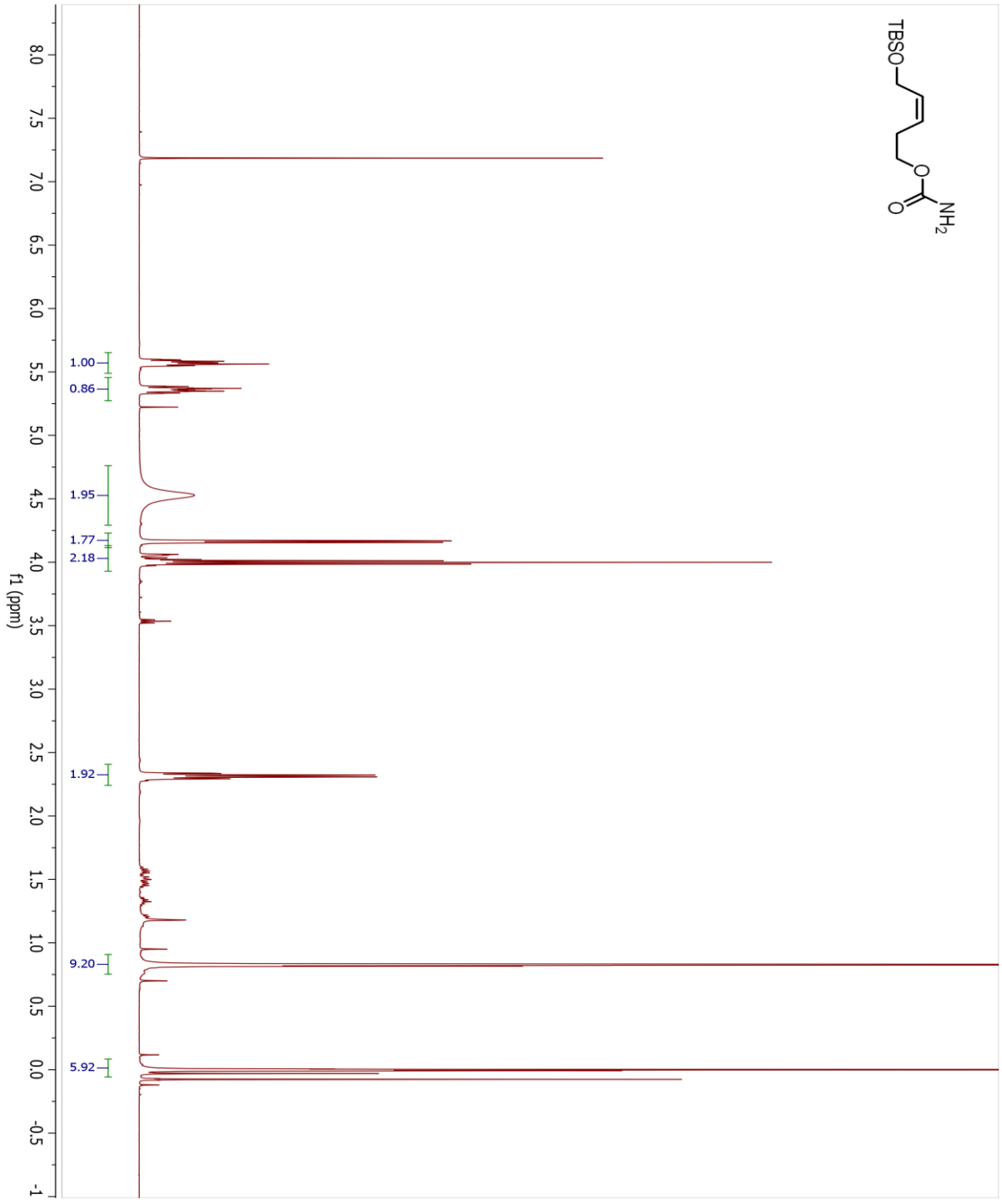
^{1}H NMR (500 MHz, $CDCl_3$) for precursor to compound **2.1f**



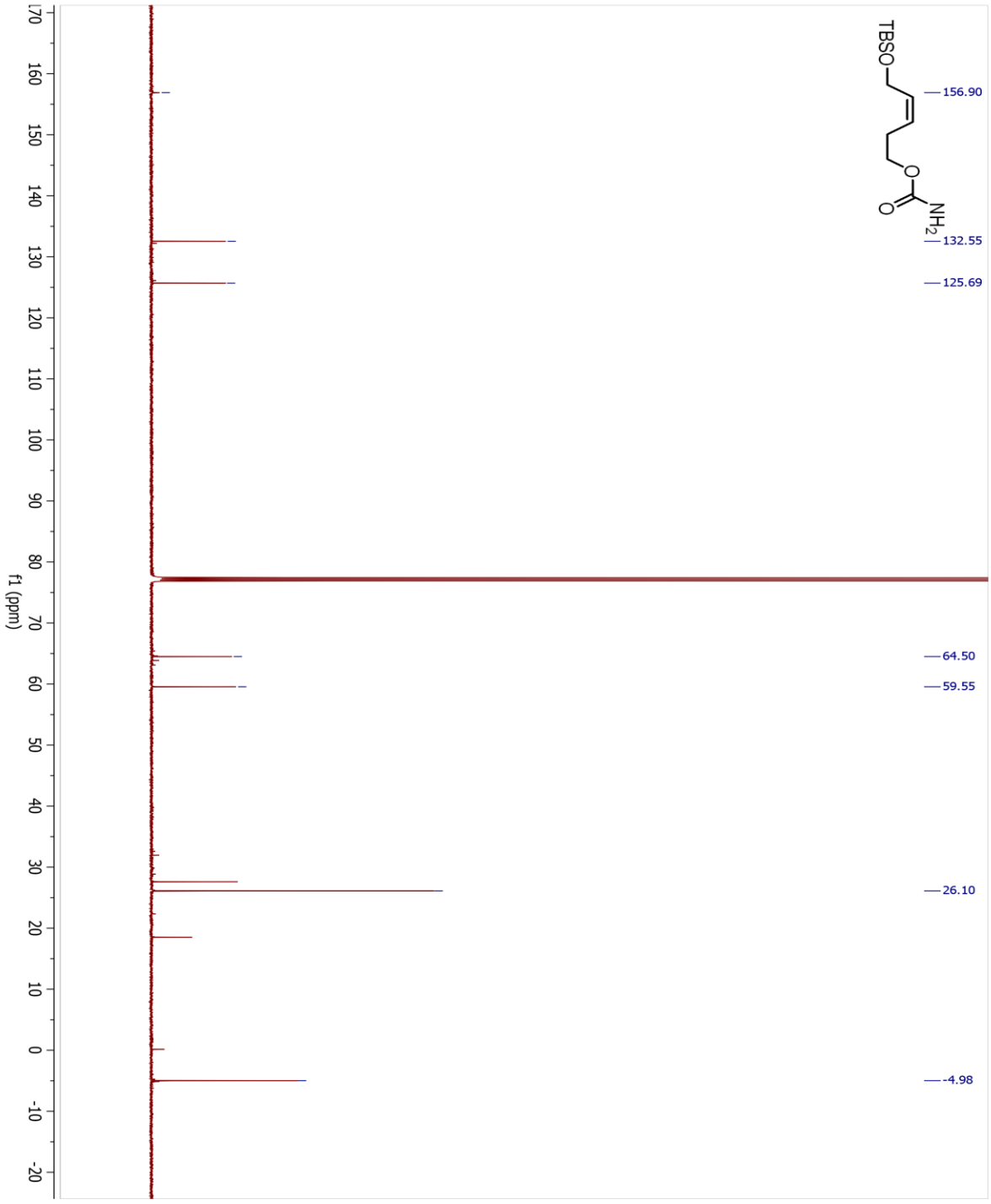
^{13}C NMR (126 MHz, $CDCl_3$) for precursor to compound **2.1f**



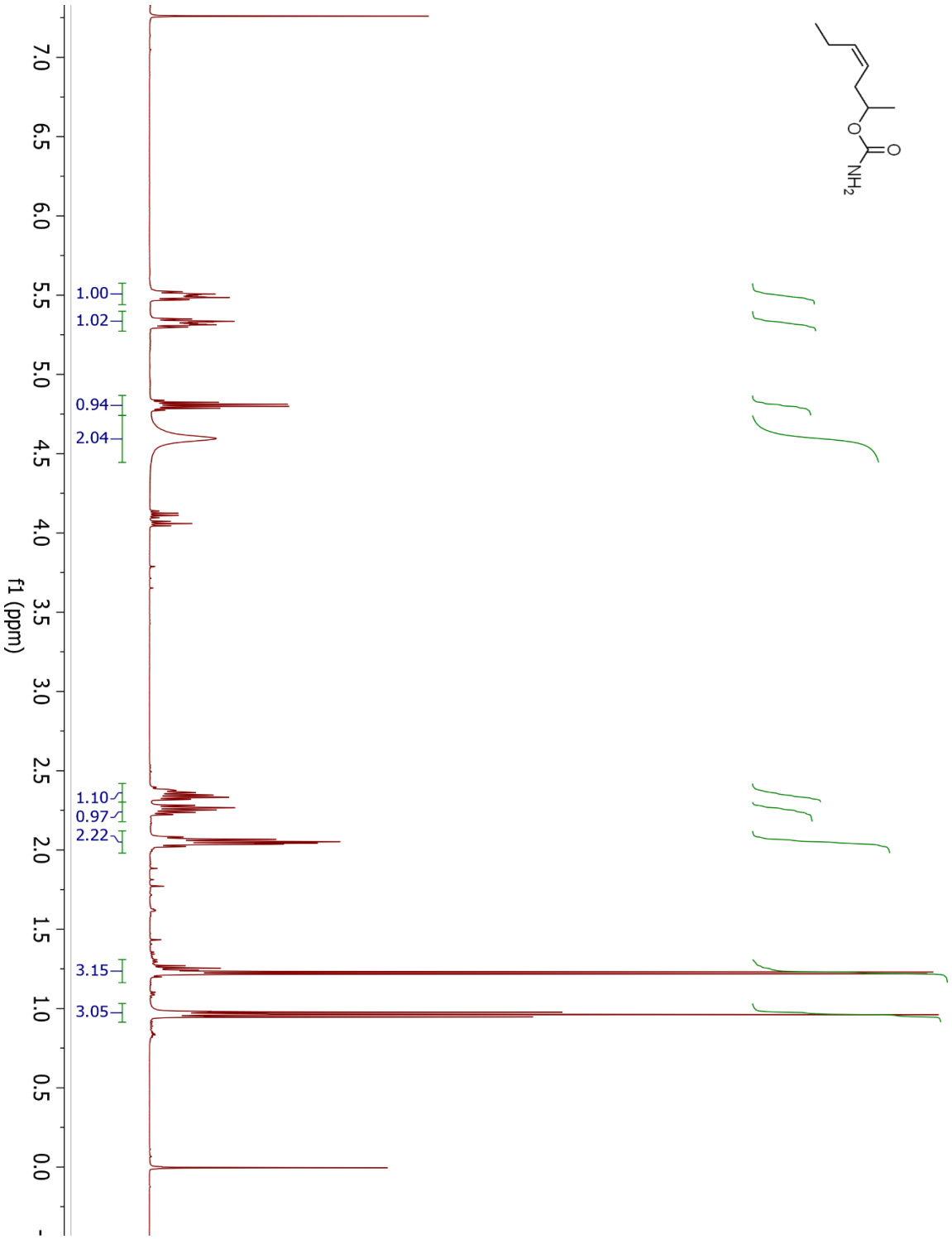
^{1}H NMR (500 MHz, $CDCl_3$) for precursor to compound **2.1g**



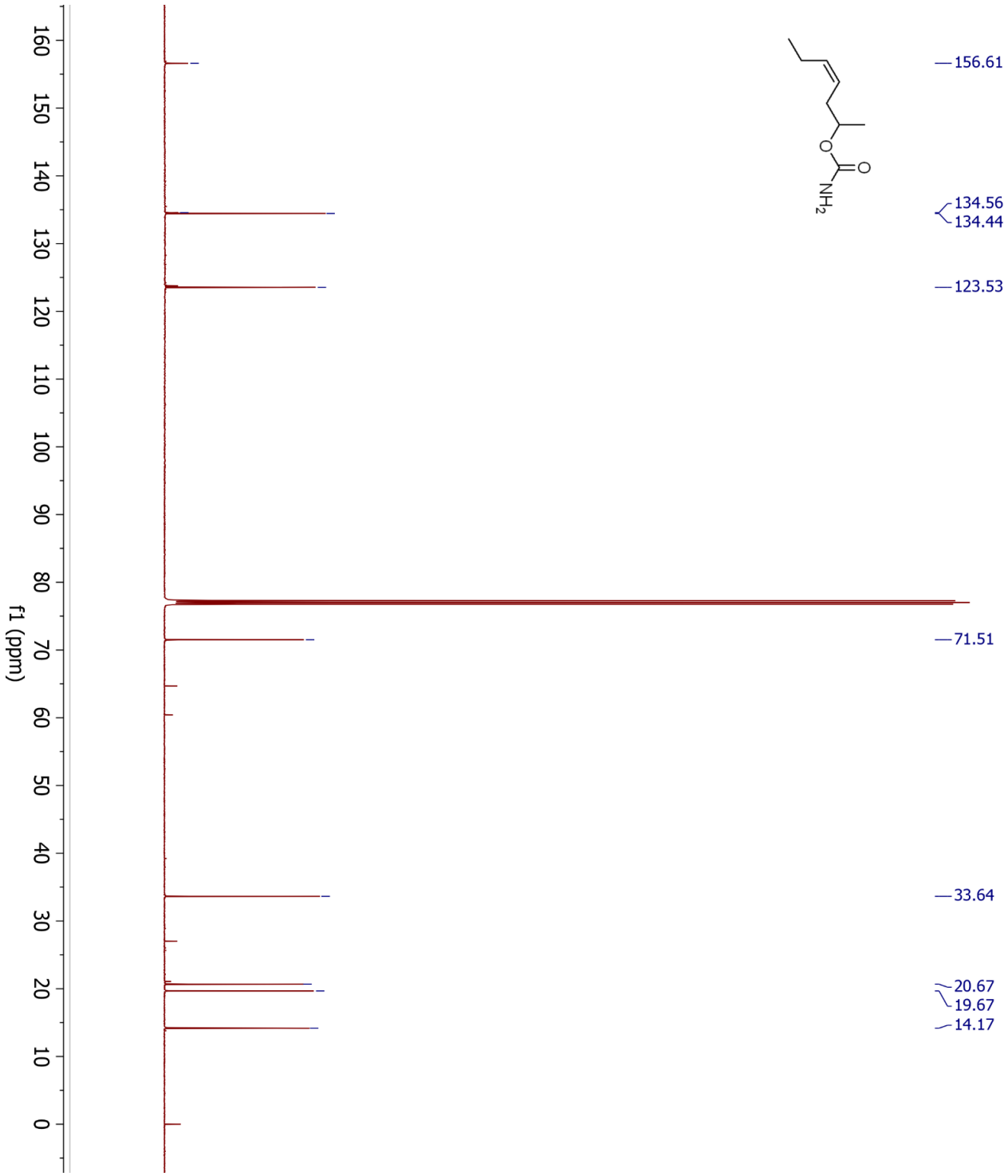
^{13}C NMR (126 MHz, $CDCl_3$) for precursor to compound **2.1g**



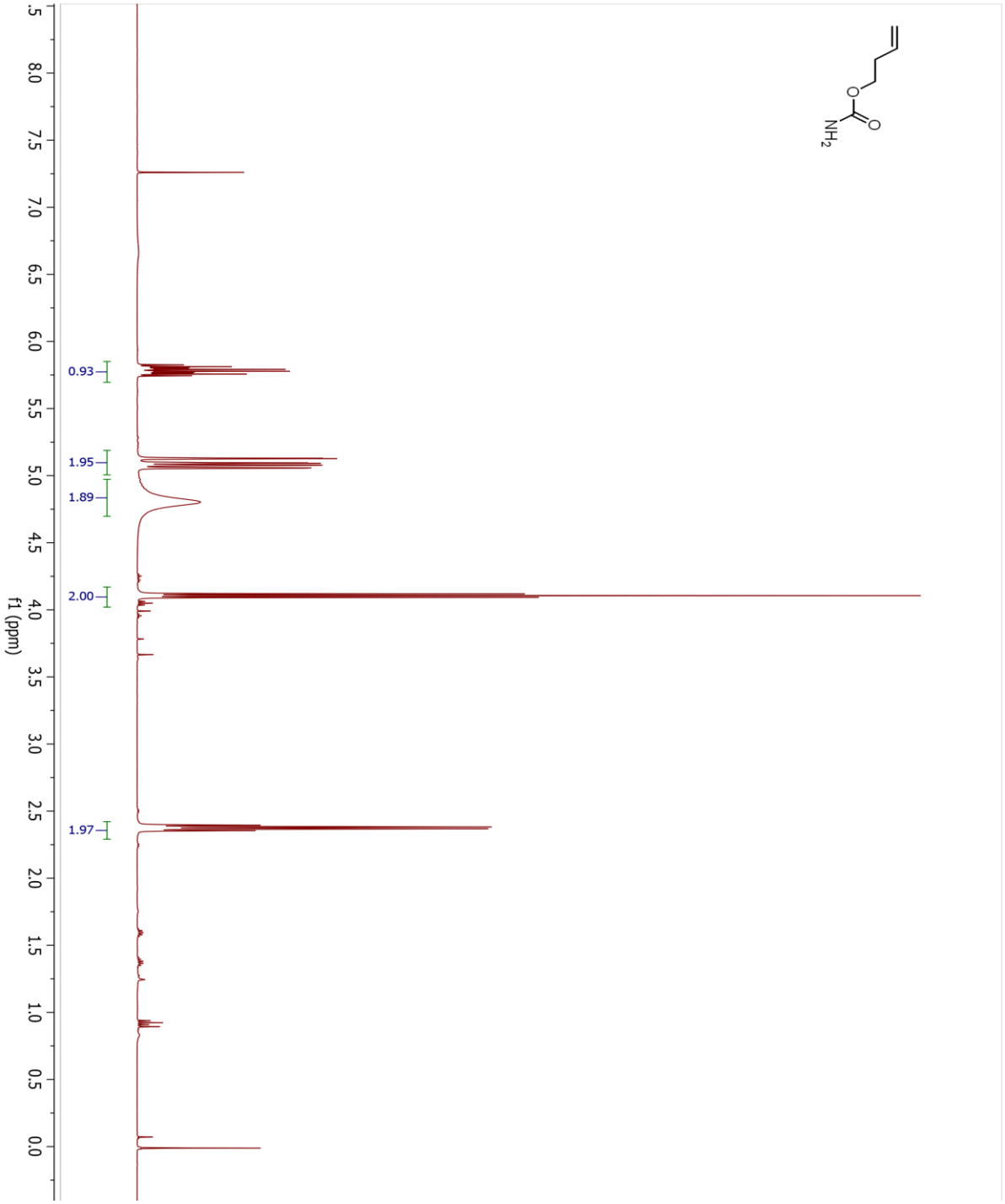
^{1}H NMR (500 MHz, $CDCl_3$) for precursor to compound **2.1h**



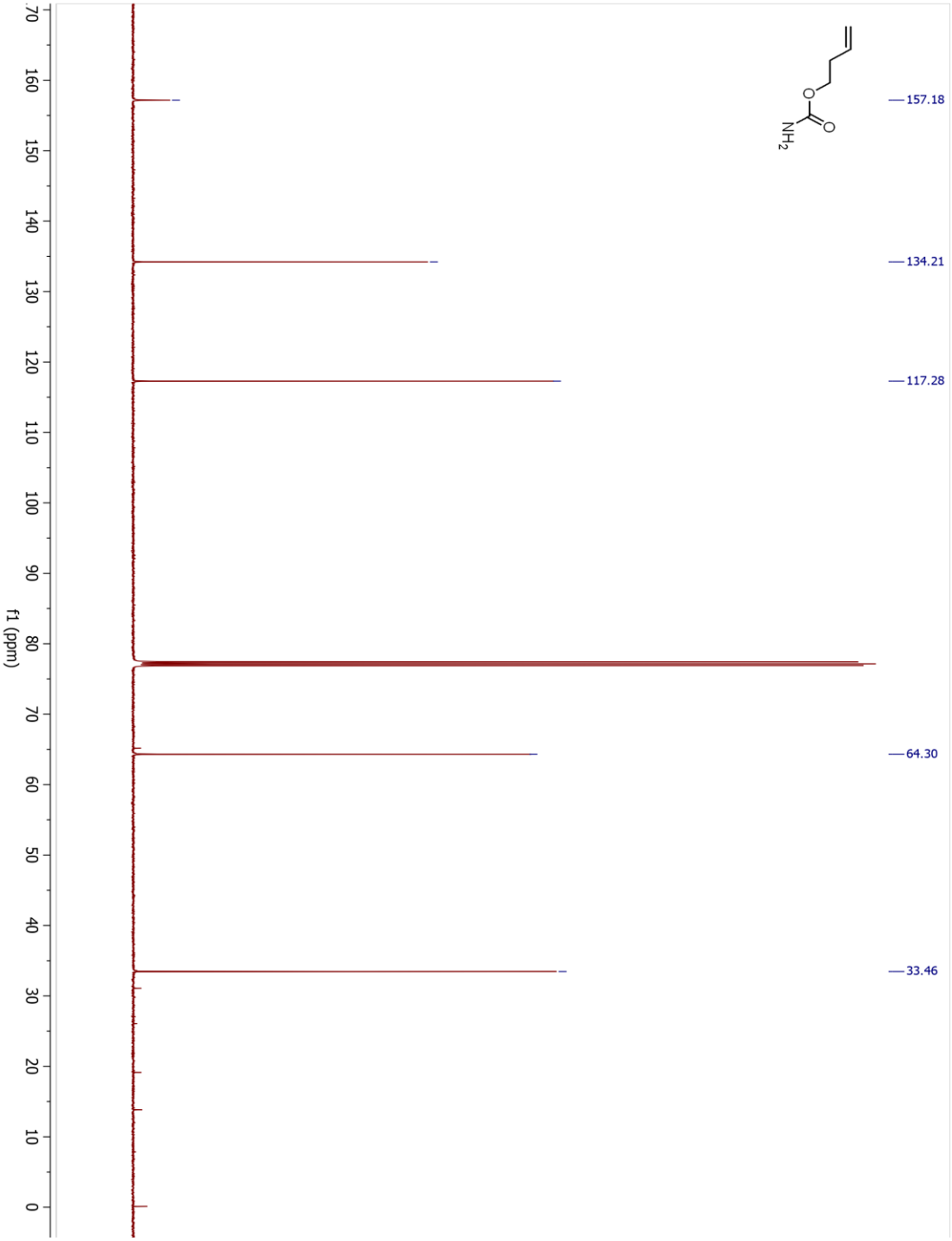
^{13}C NMR (126 MHz, $CDCl_3$) for precursor to compound **2.1h**



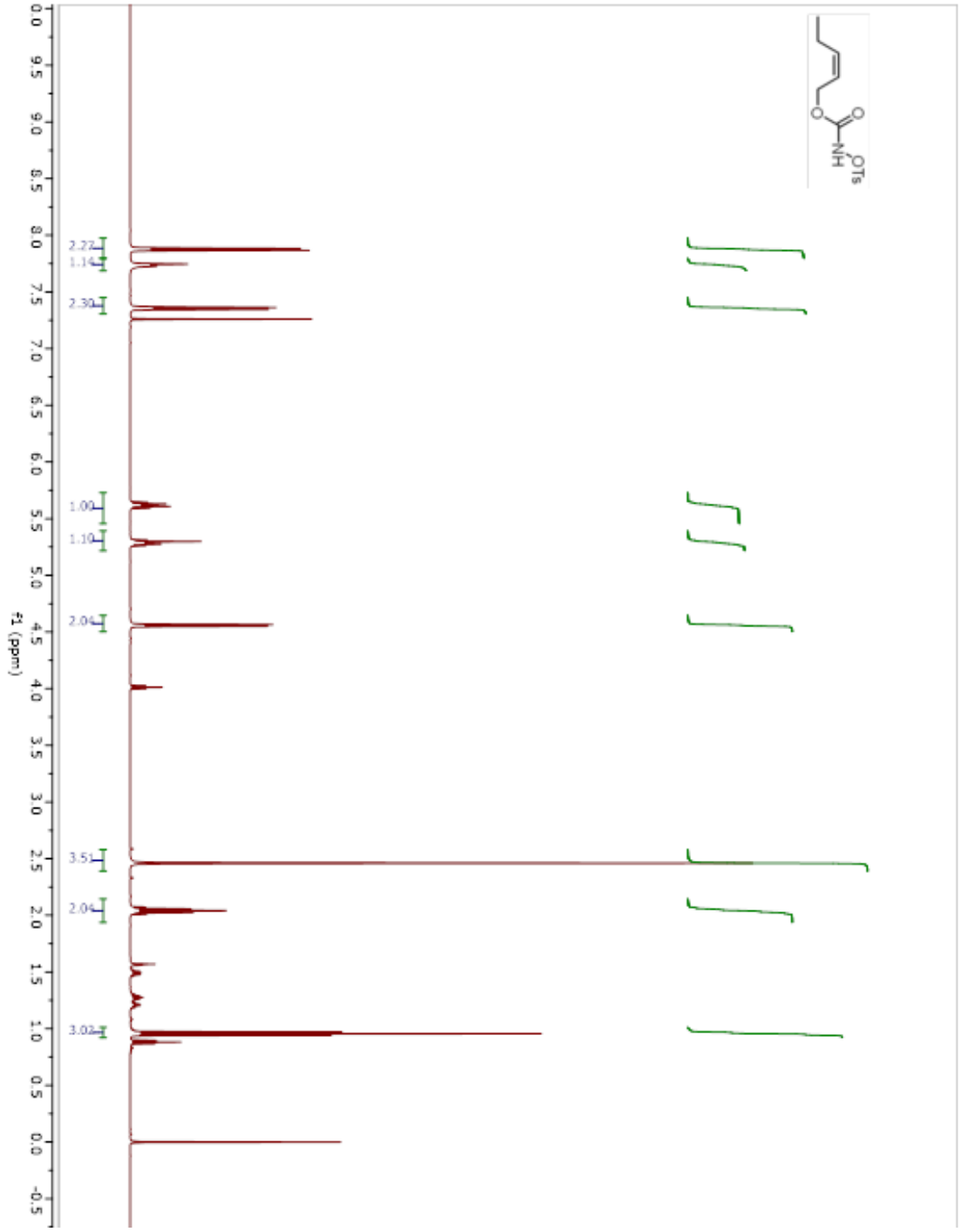
^{1}H NMR (500 MHz, $CDCl_3$) for precursor to compound **2.1i**



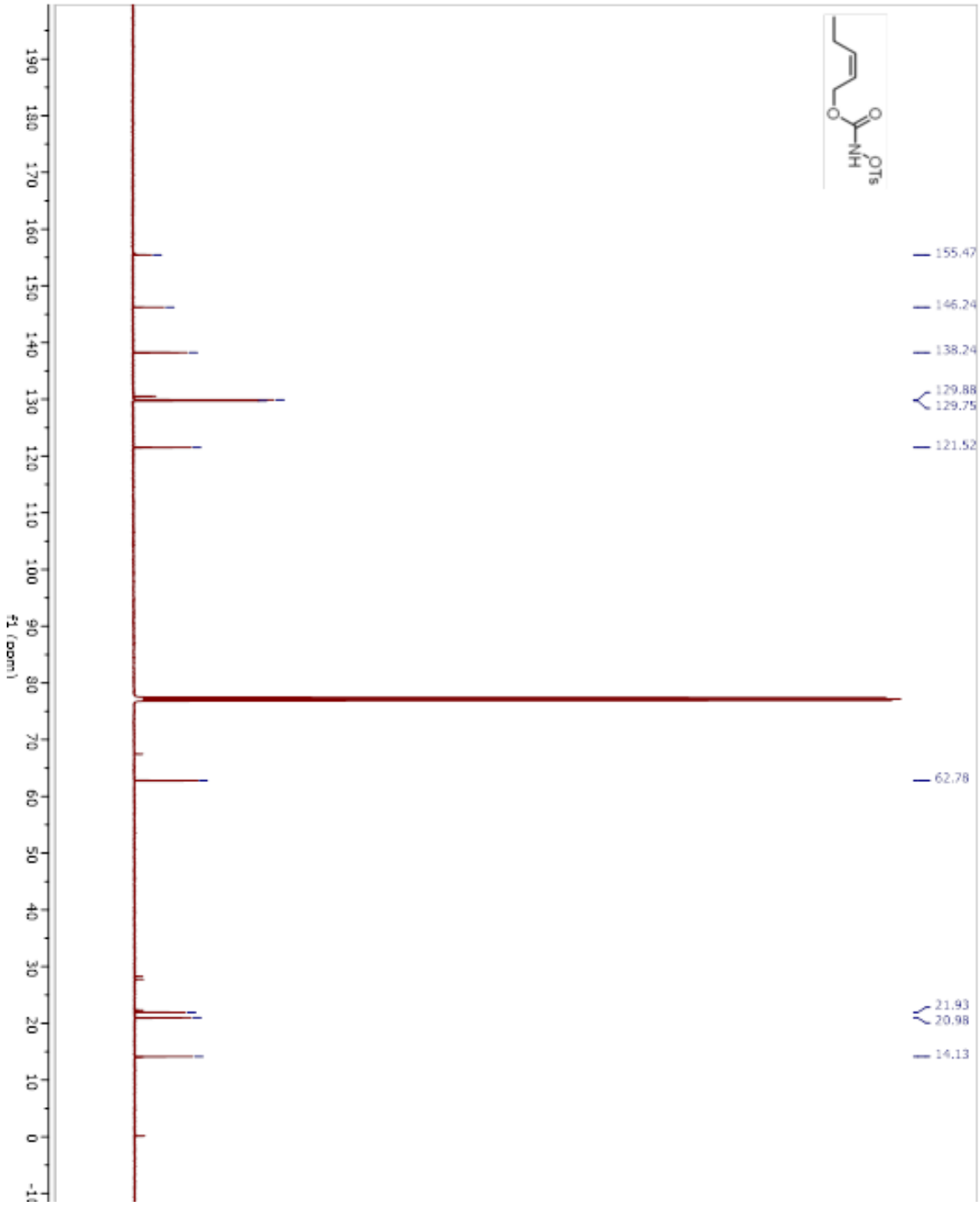
^{13}C NMR (126 MHz, $CDCl_3$) for precursor compound **2.1i**



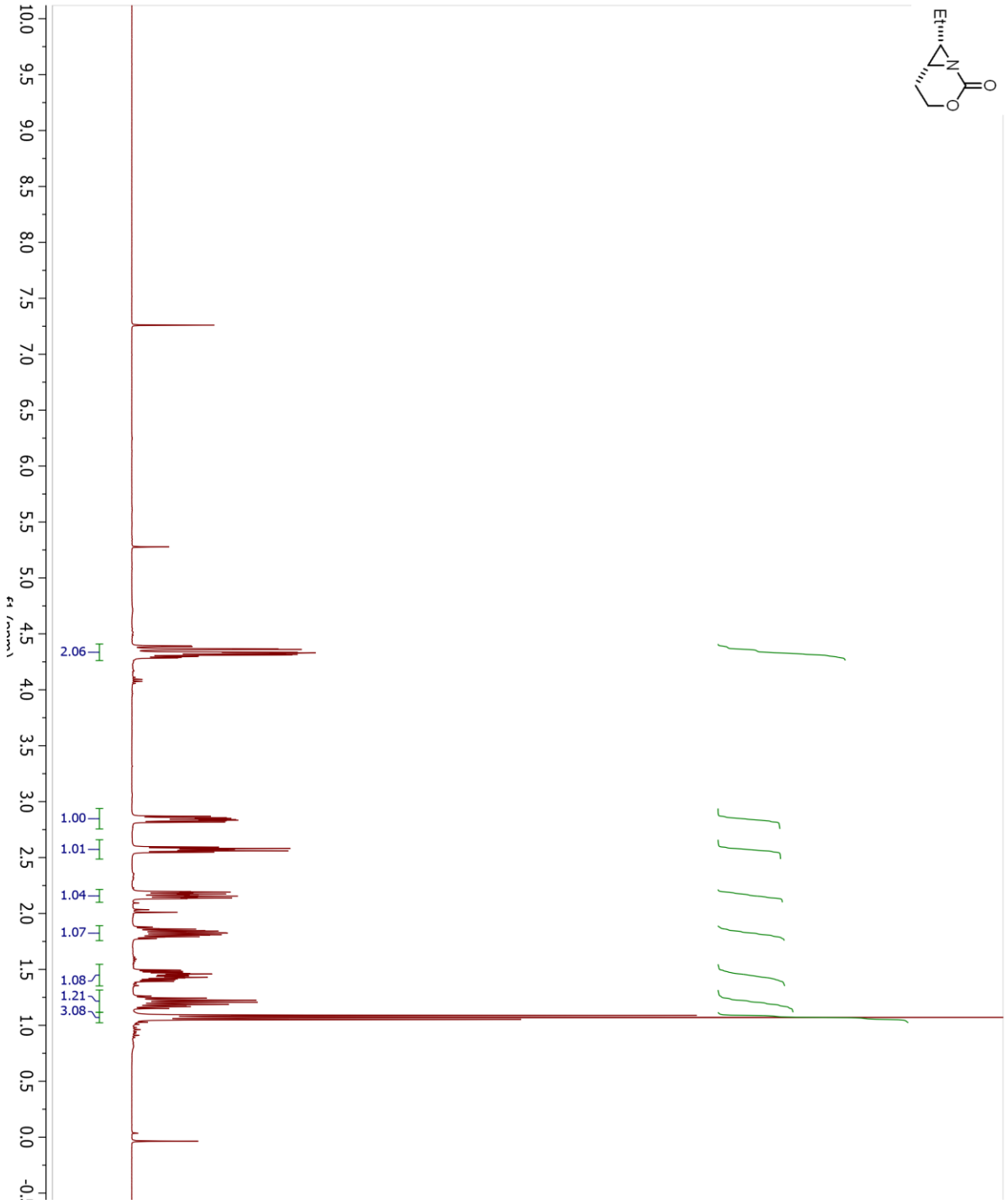
^{1}H NMR (500 MHz, $CDCl_3$) Precursor to compound **2.1j**



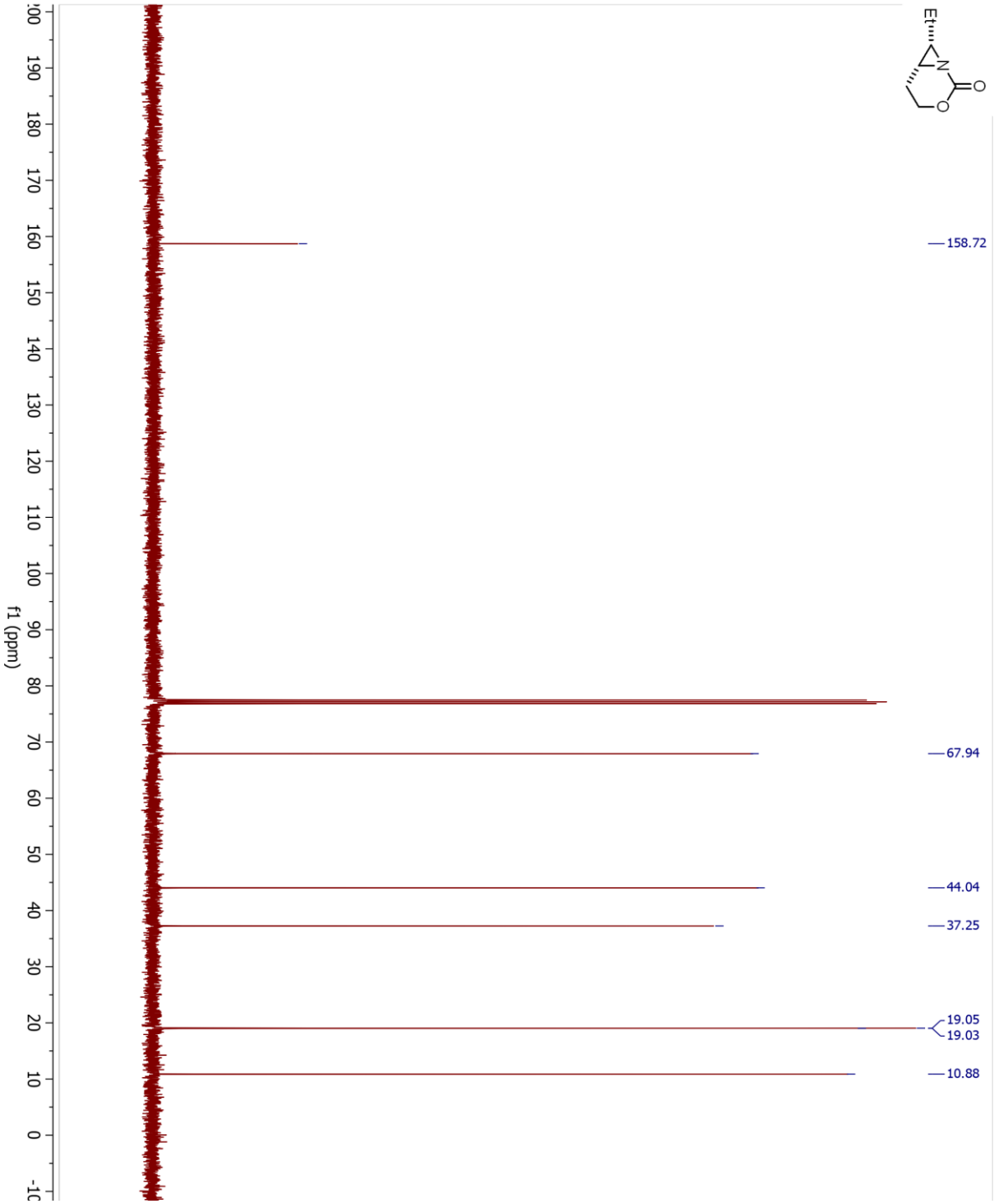
^{13}C NMR (126 MHz, $CDCl_3$) Precursor to compound **2.1j**



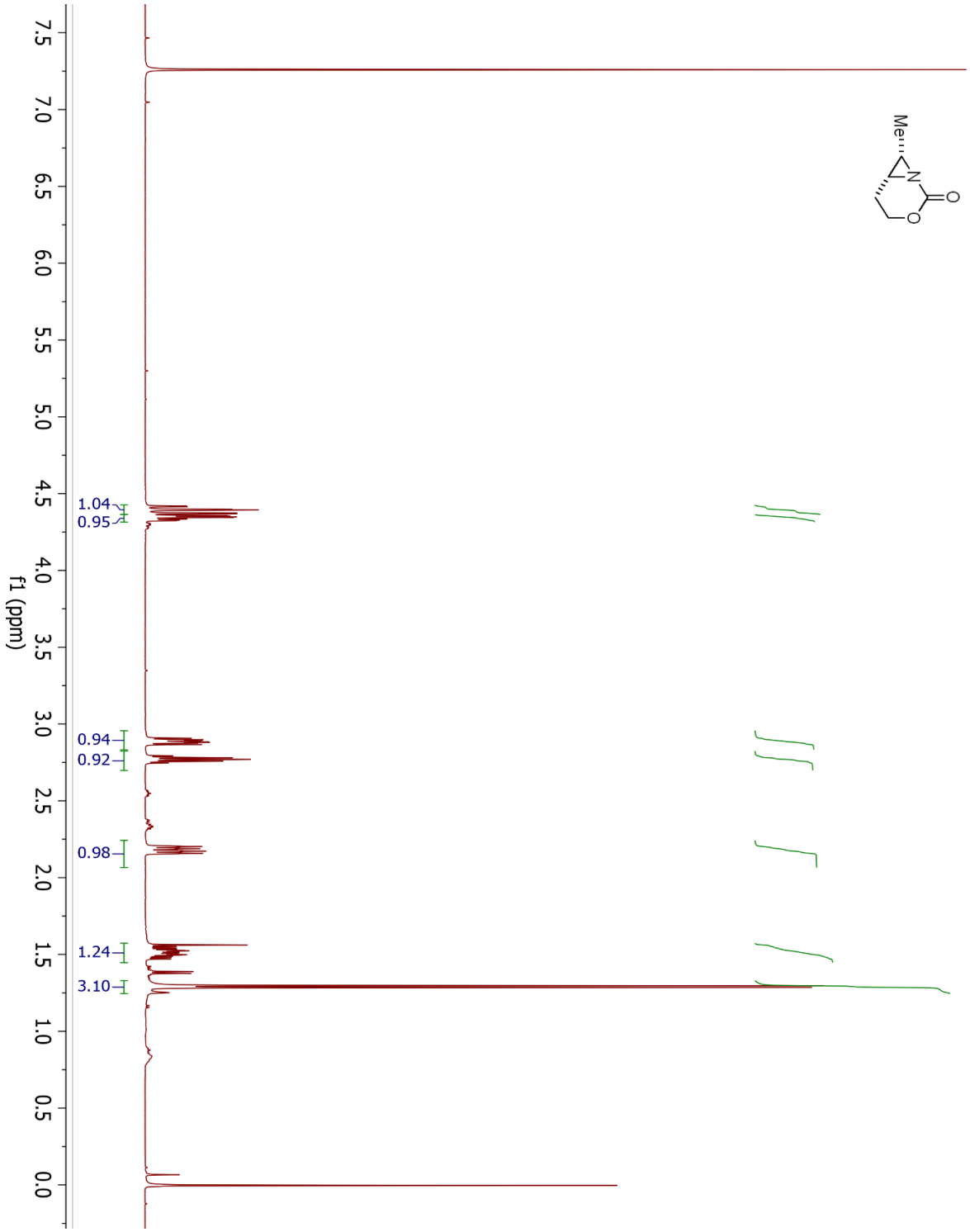
^{1}H NMR (500 MHz, $CDCl_3$) for compound **2.1a**



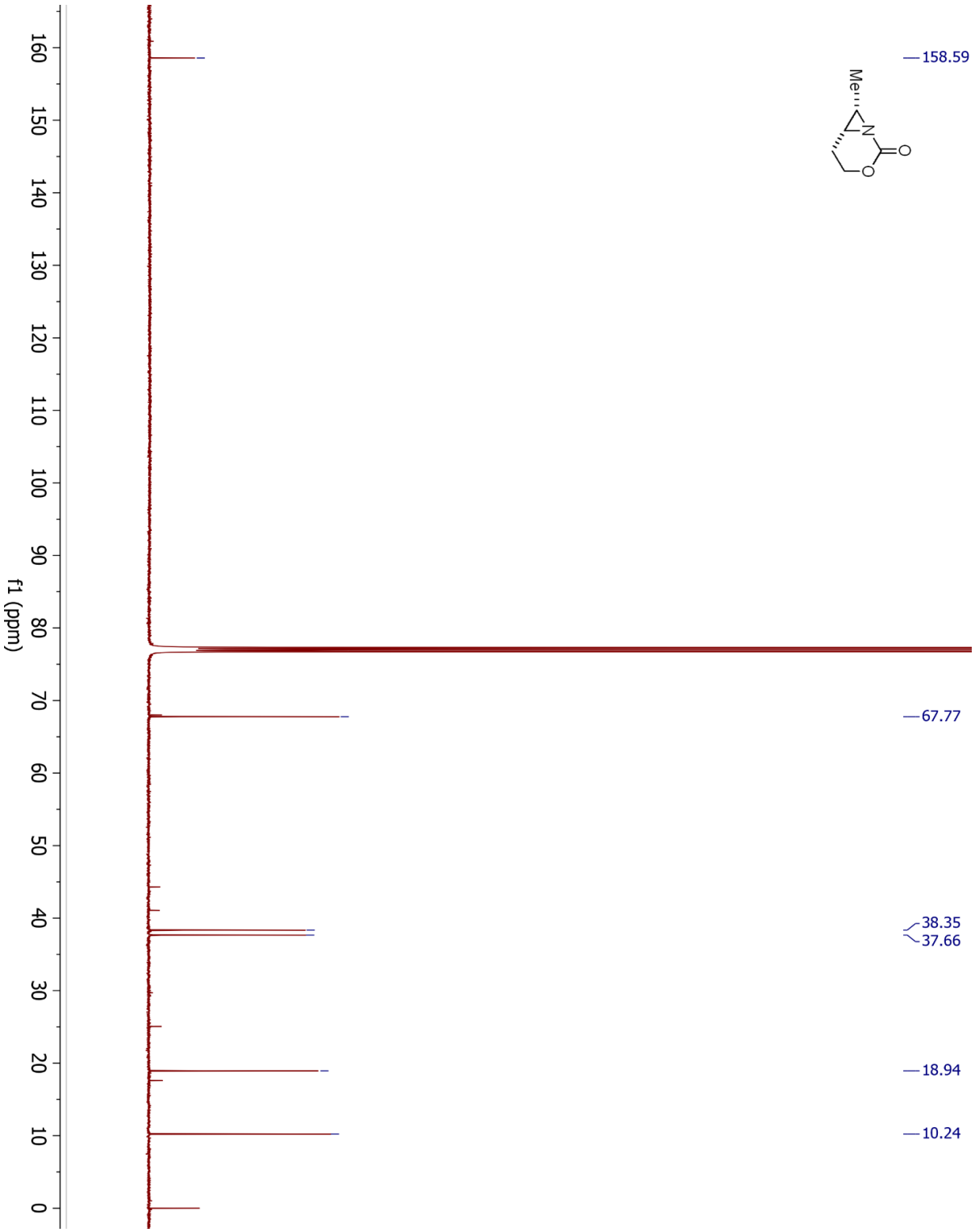
^{13}C NMR (126 MHz, $CDCl_3$) for compound **2.1a**



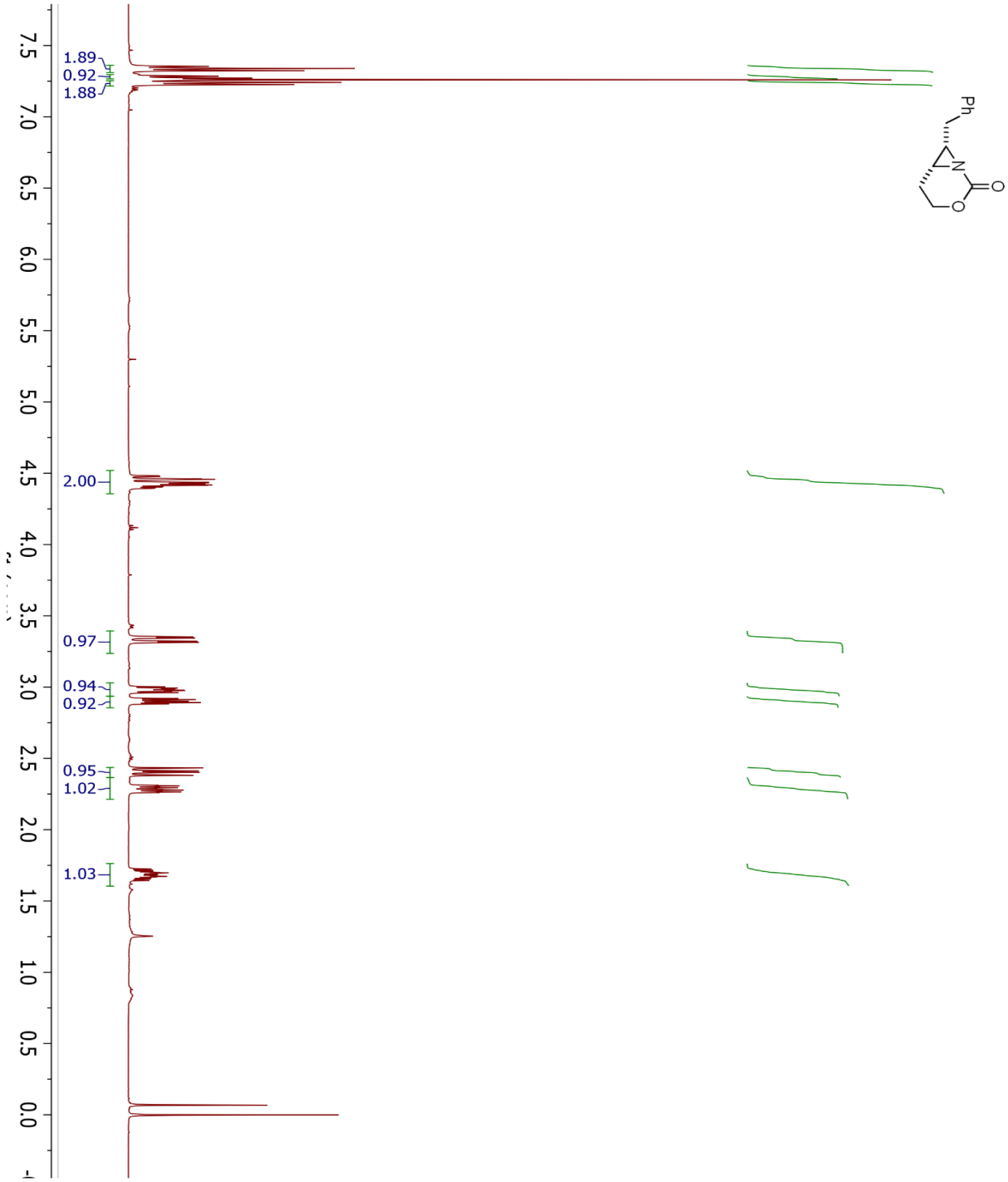
^{1}H NMR (500 MHz, $CDCl_3$) for compound **2.1b**


Me
N
O
O
1.04
0.95
0.94
0.92
0.98
1.24
3.10
f1 (ppm)
7.5
7.0
6.5
6.0
5.5
5.0
4.5
4.0
3.5
3.0
2.5
2.0
1.5
1.0
0.5
0.0

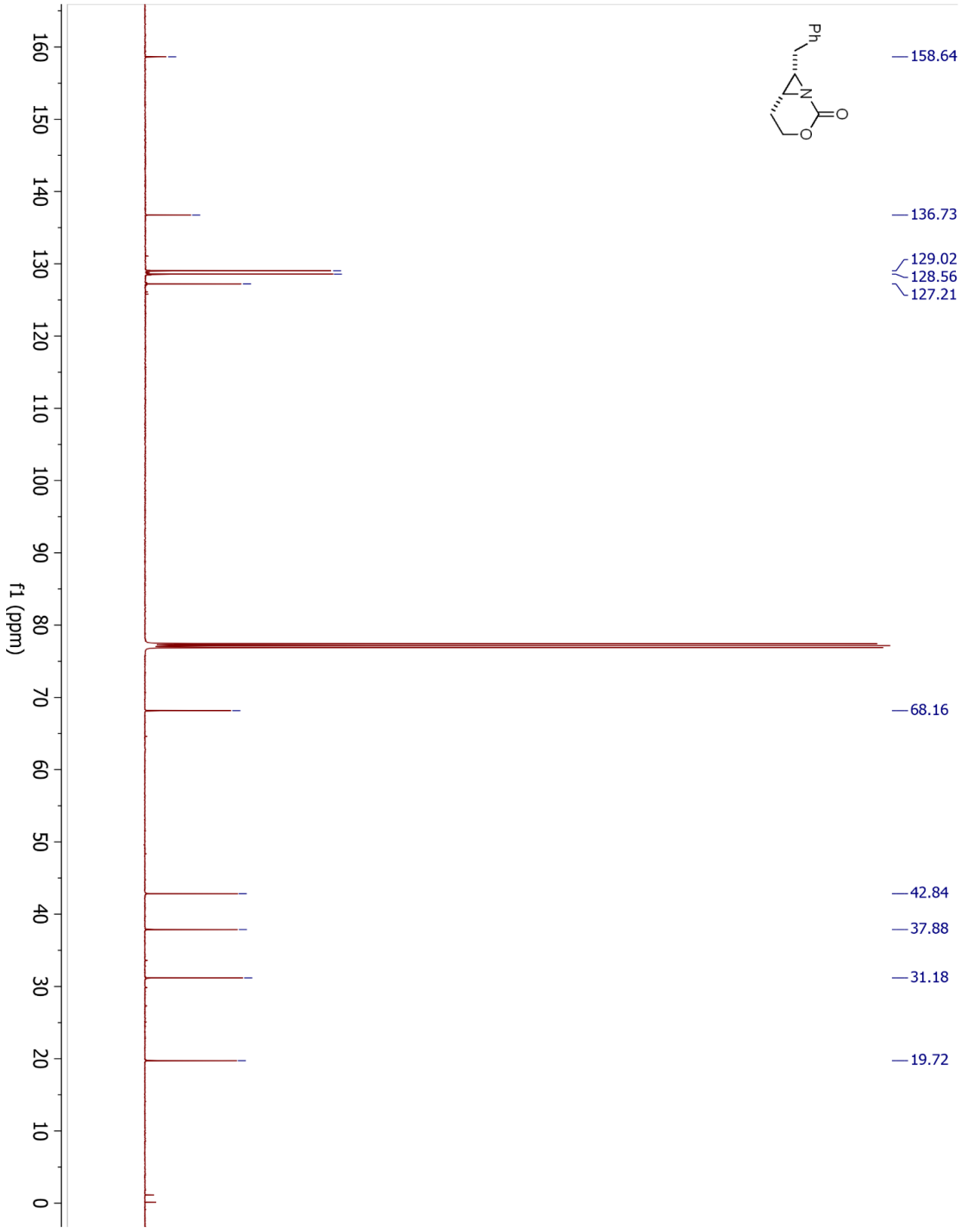
^{13}C NMR (126 MHz, $CDCl_3$) for compound **2.1b**



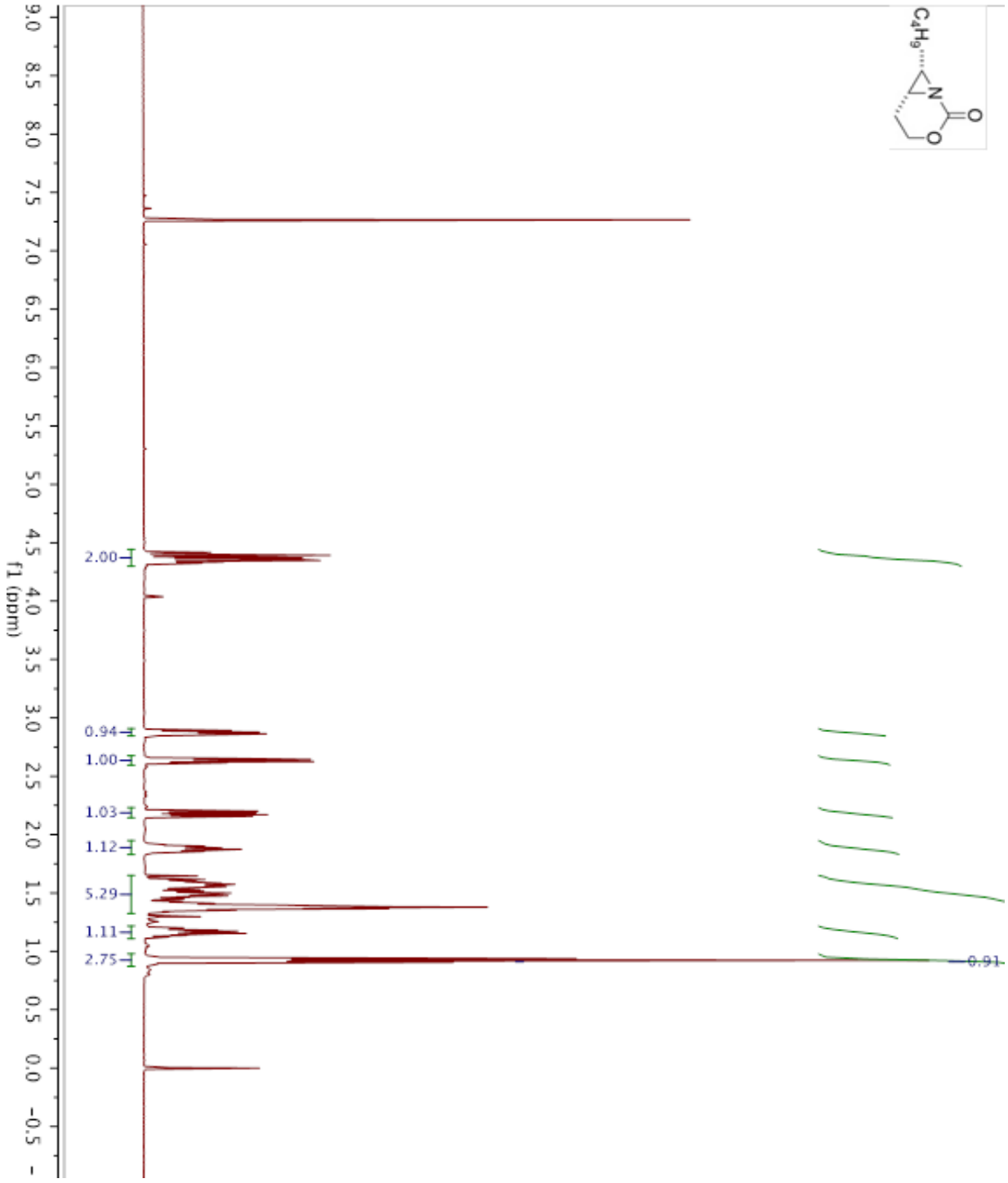
^{1}H NMR (500 MHz, $CDCl_3$) for compound **2.1c**



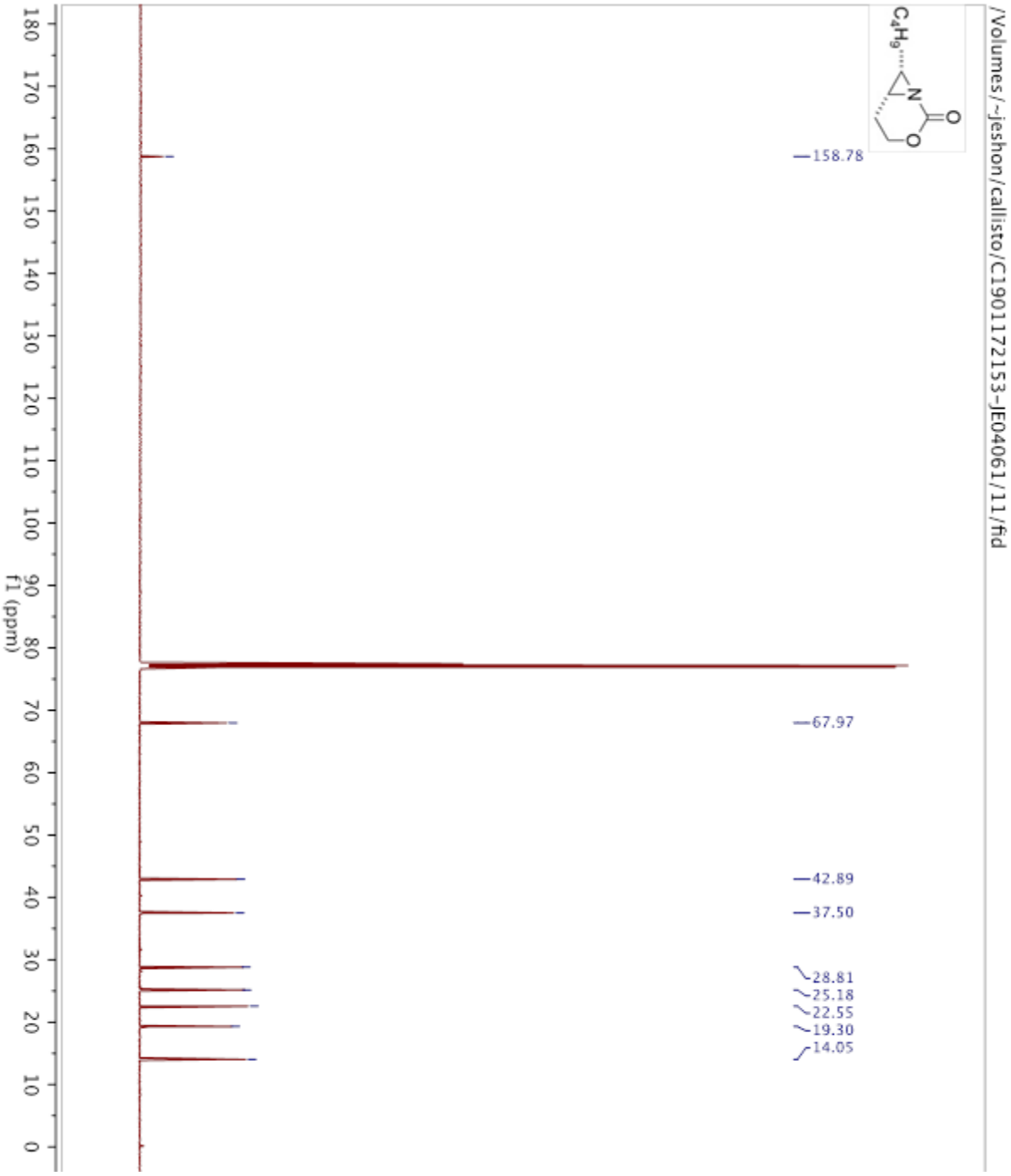
^{13}C NMR (126 MHz, $CDCl_3$) for compound **2.1c**



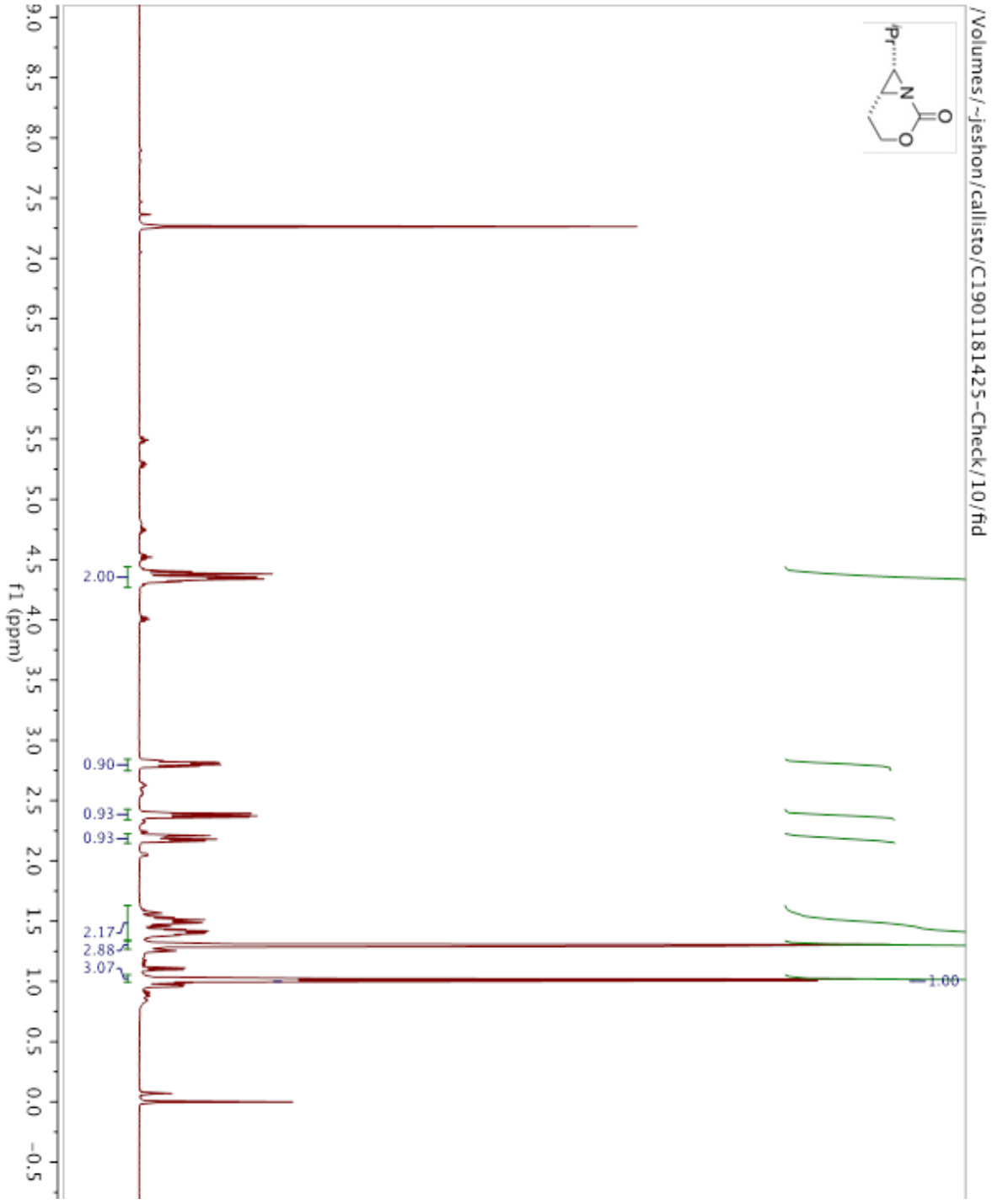
^{1}H NMR (500 MHz, $CDCl_3$) for compound **2.1d**



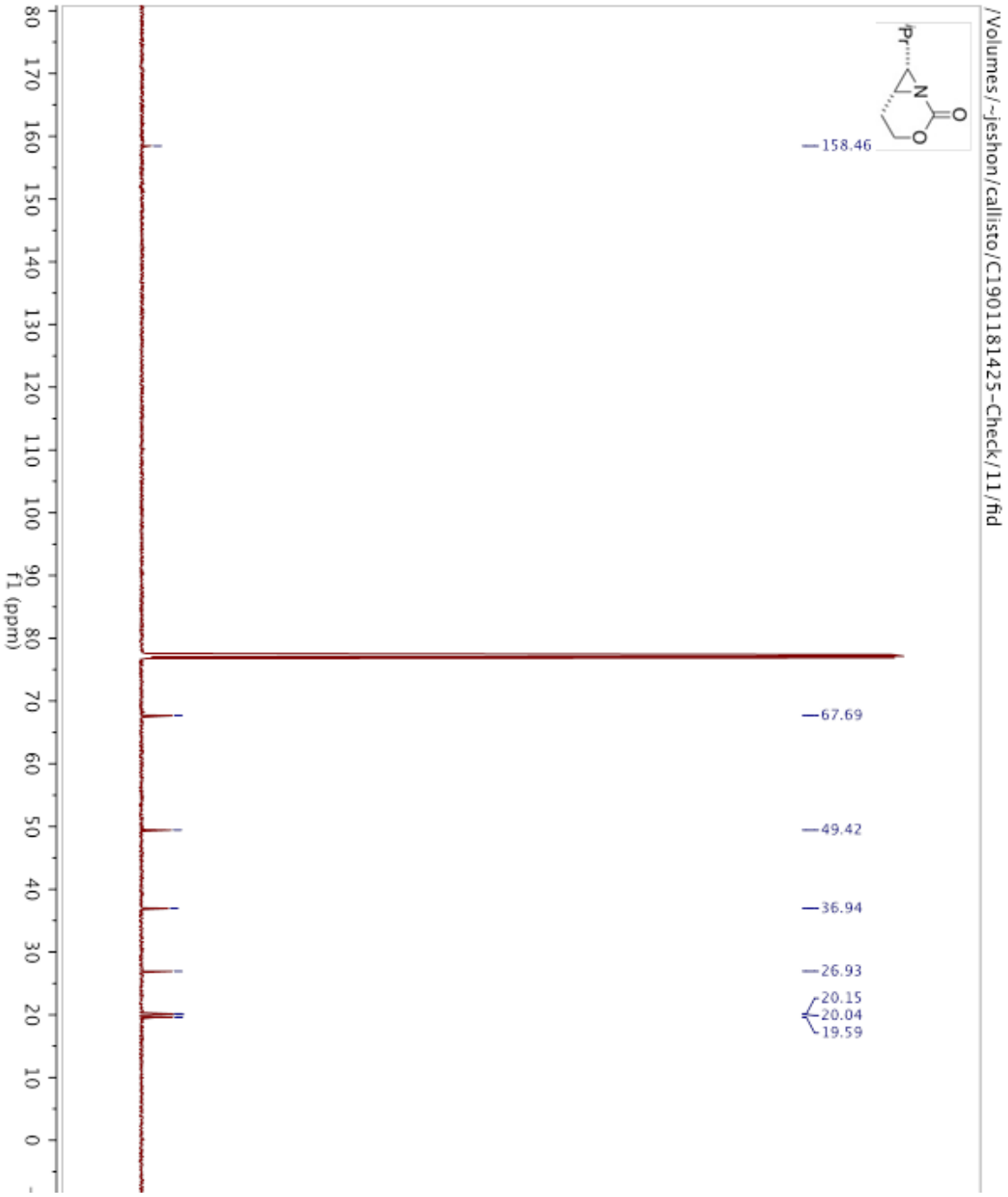
^{13}C NMR (126 MHz, $CDCl_3$) for compound **2.1d**



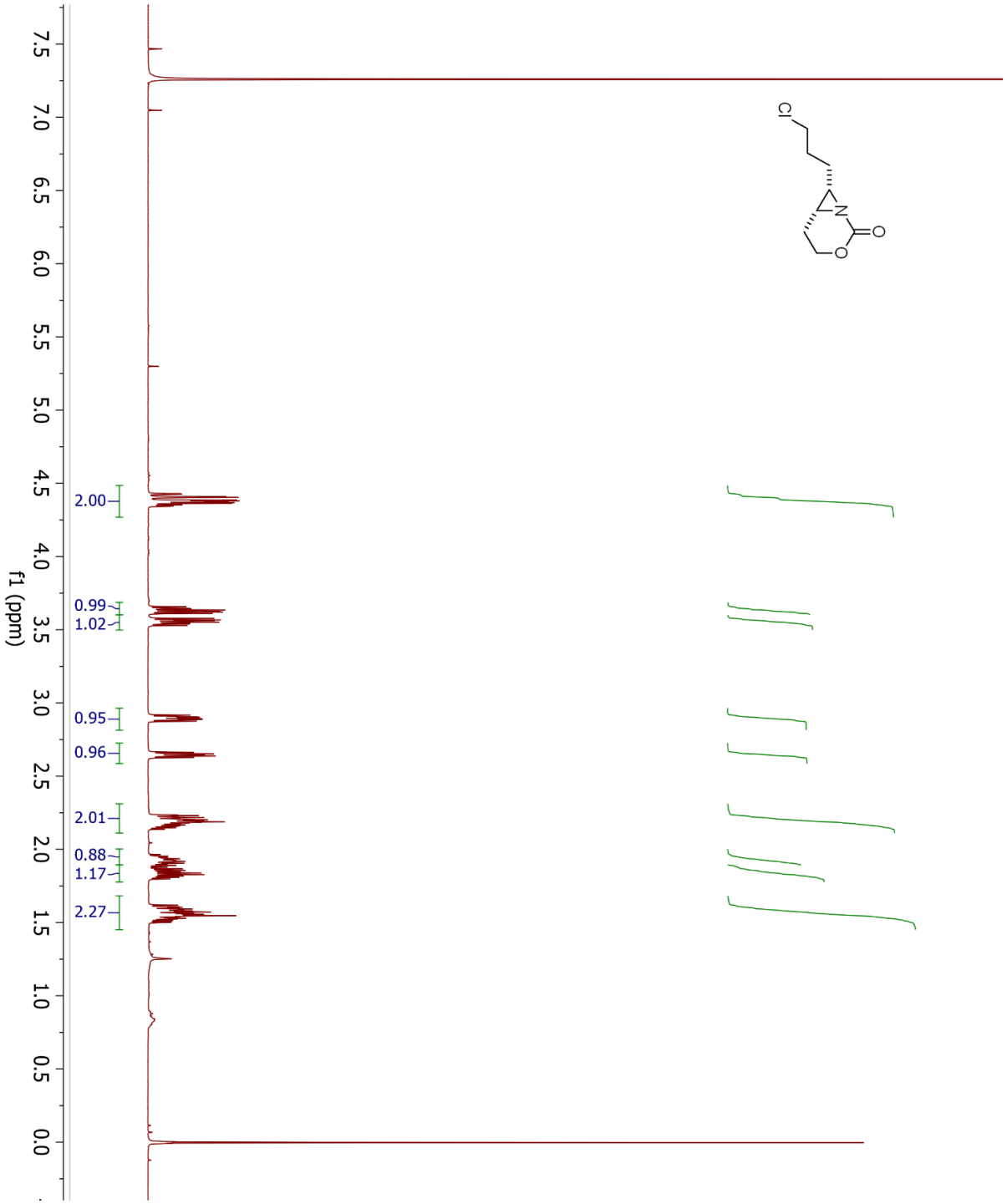
^{1}H NMR (500 MHz, $CDCl_3$) for compound **2.1e**



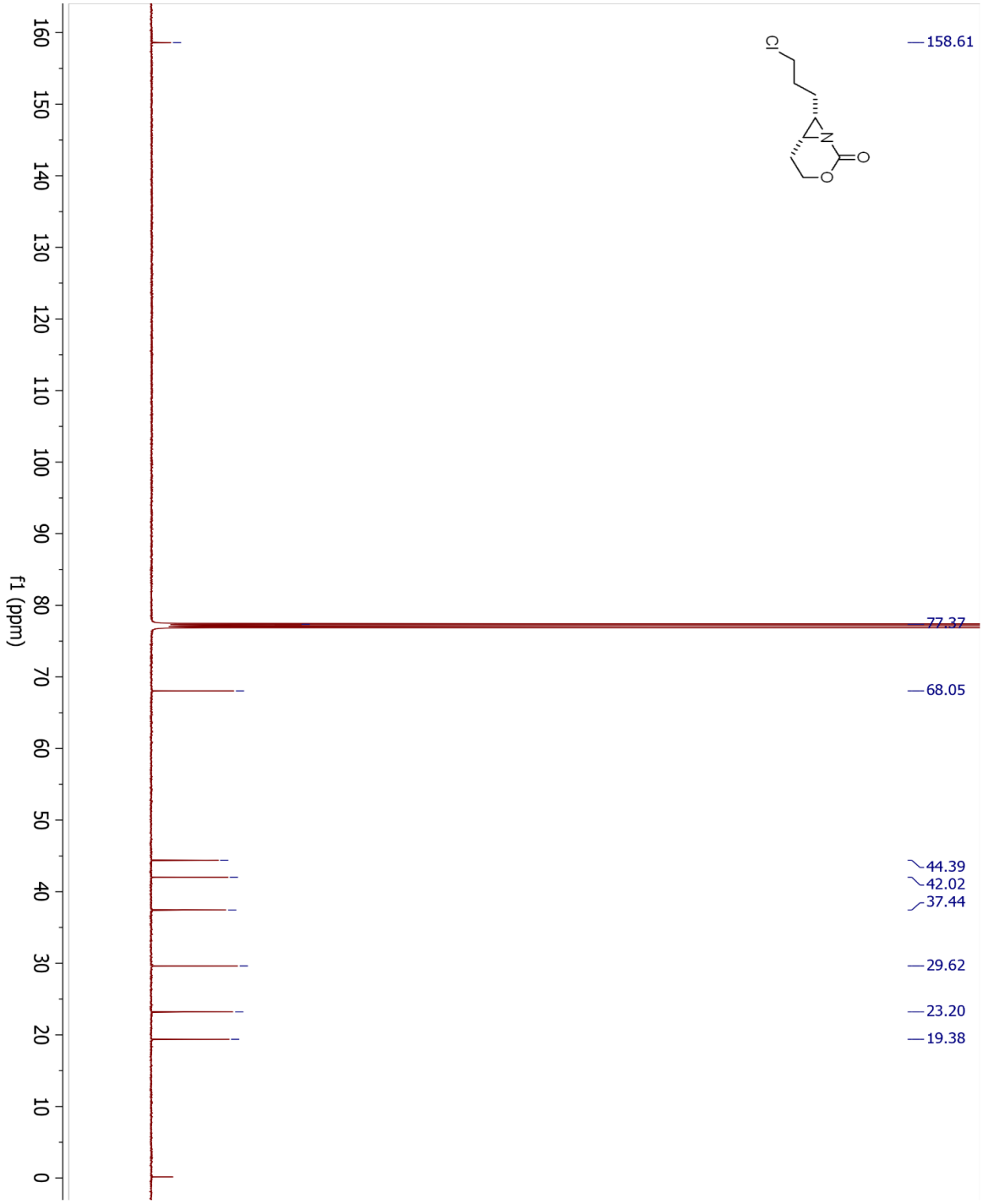
^{13}C NMR (126 MHz, $CDCl_3$) for compound **2.1e**



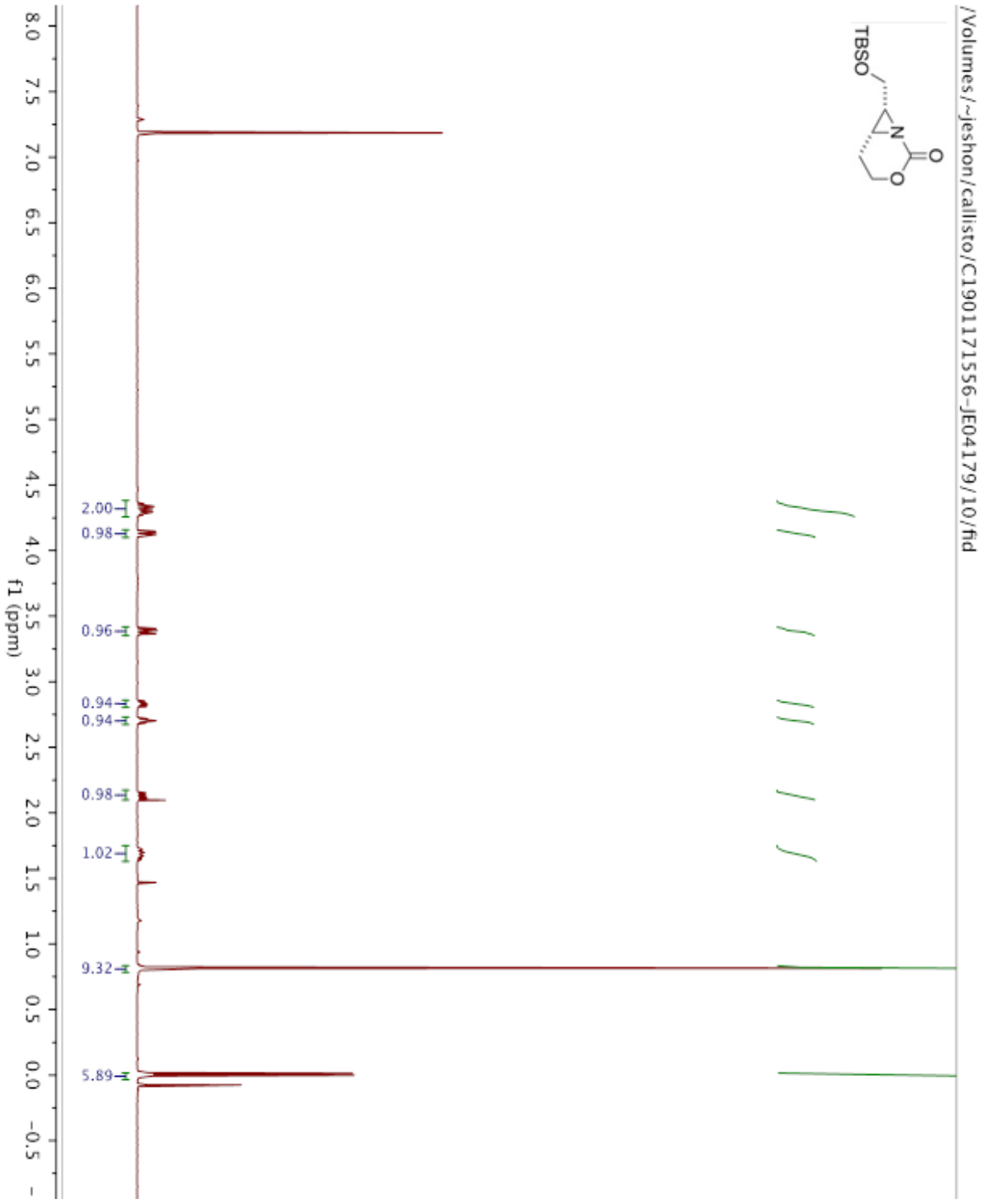
^{1}H NMR (500 MHz, $CDCl_3$) for compound **2.1f**



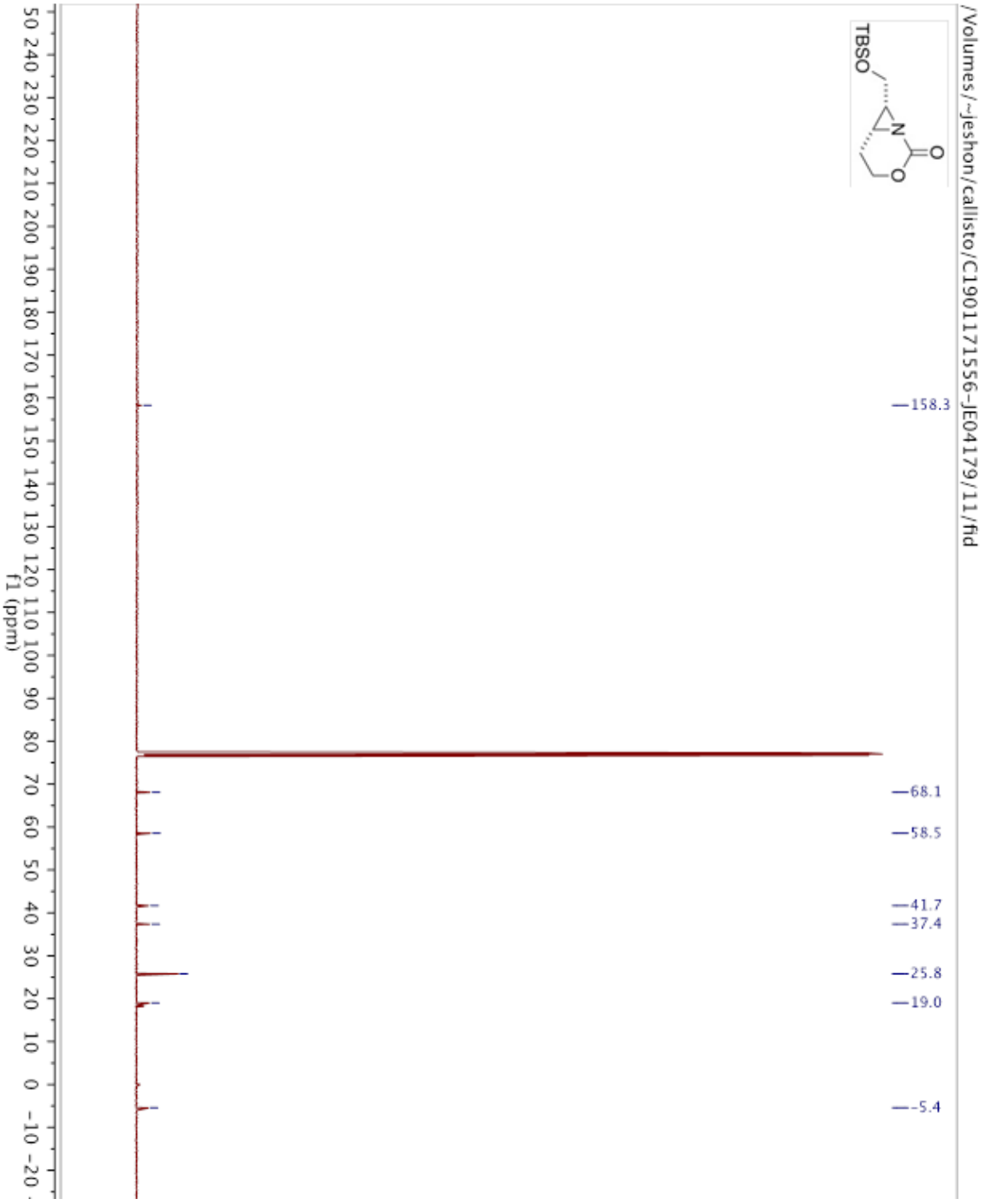
^{13}C NMR (126 MHz, $CDCl_3$) for compound **2.1f.**



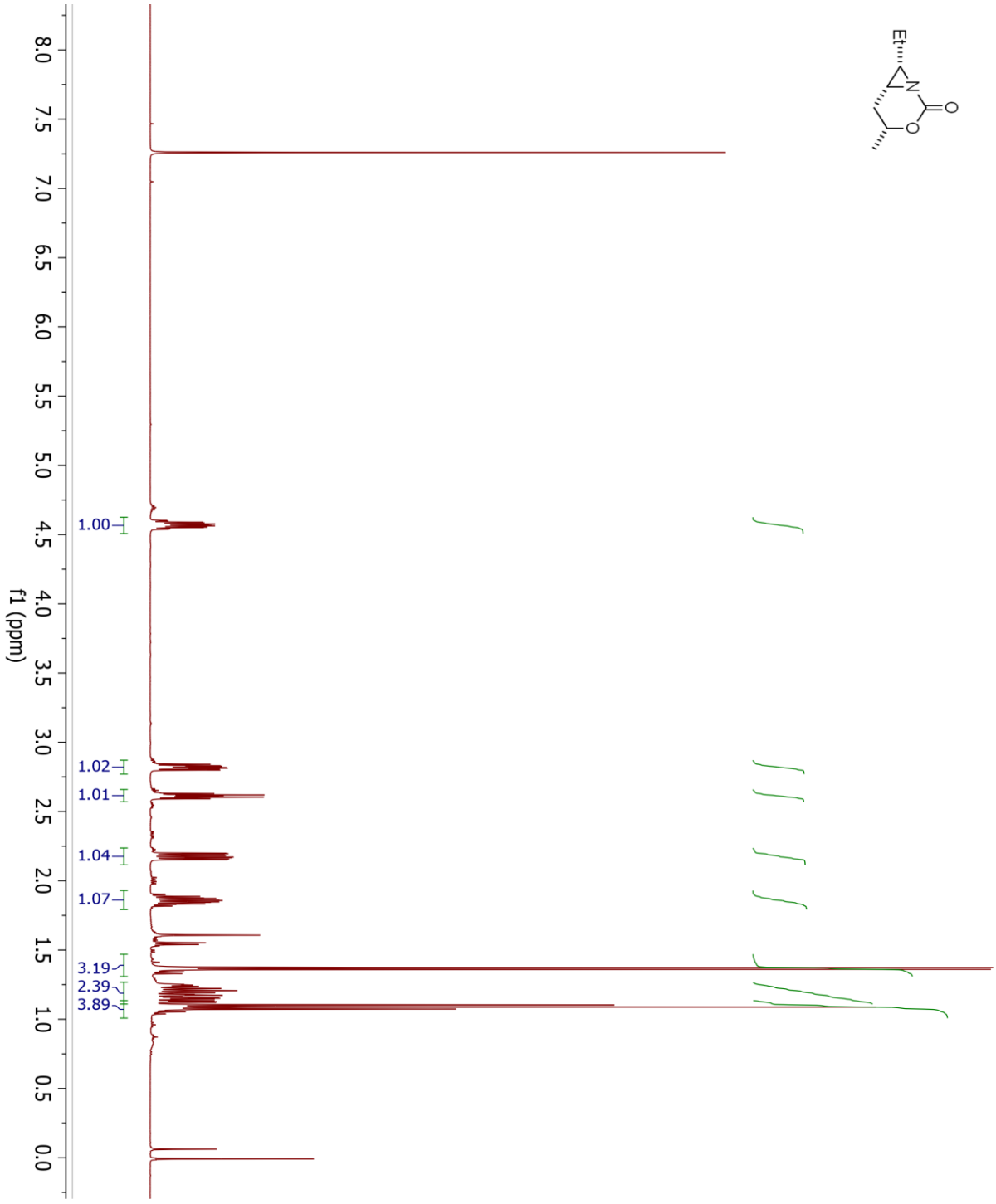
^{1}H NMR (500 MHz, $CDCl_3$) for compound **2.1g**



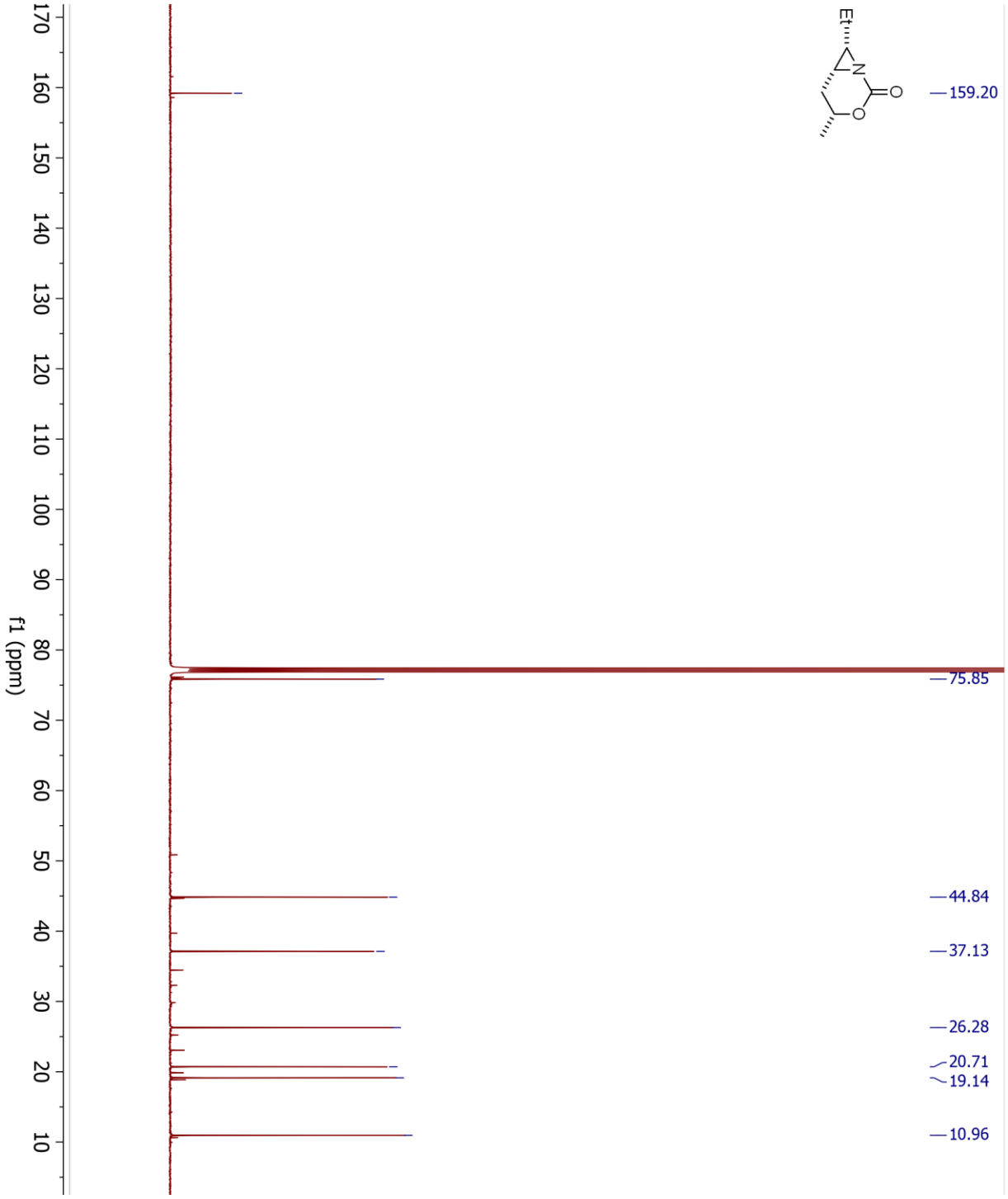
^{13}C NMR (126 MHz, $CDCl_3$) for compound **2.1g**



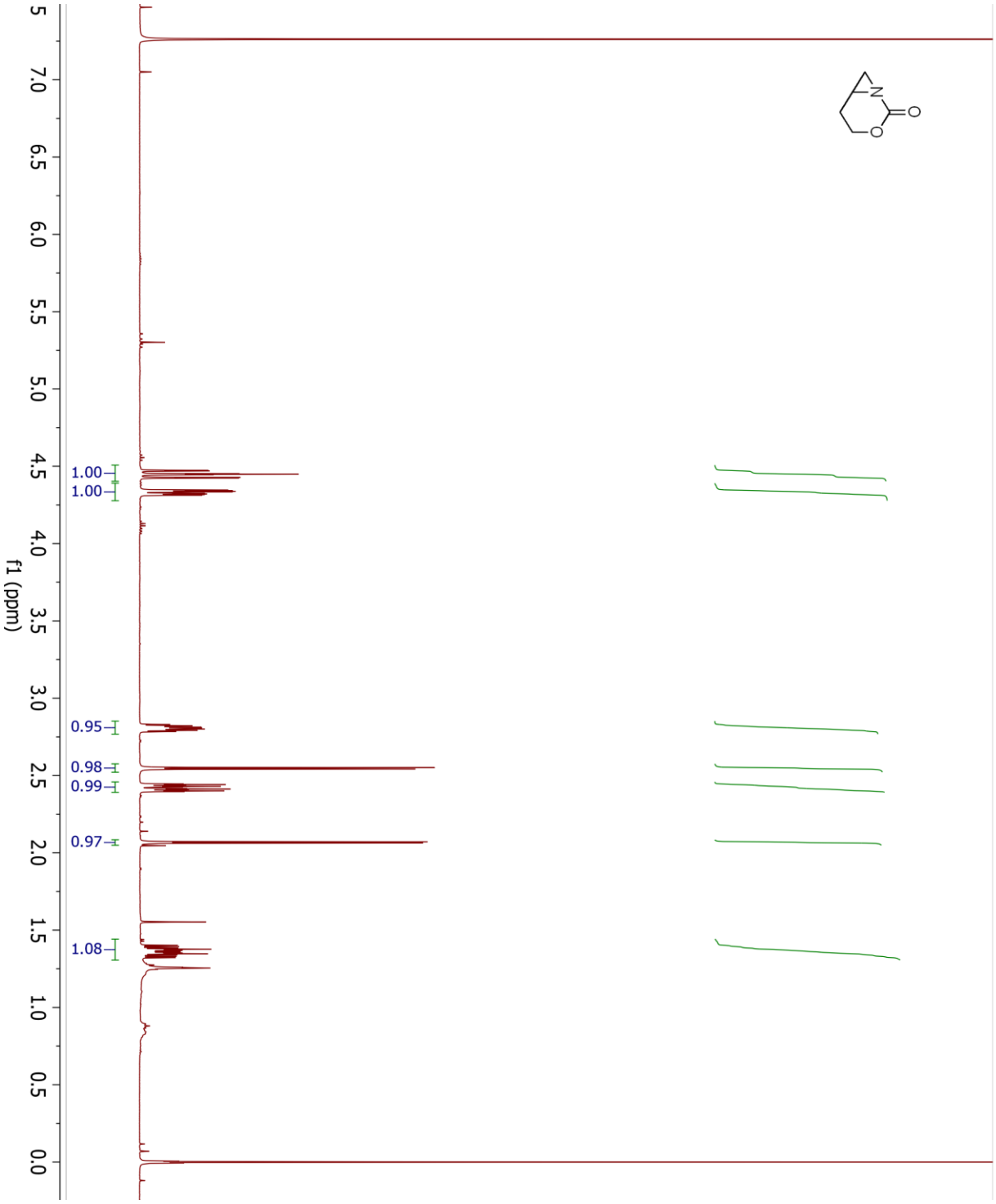
^{1}H NMR (500 MHz, $CDCl_3$) for compound **2.1h**



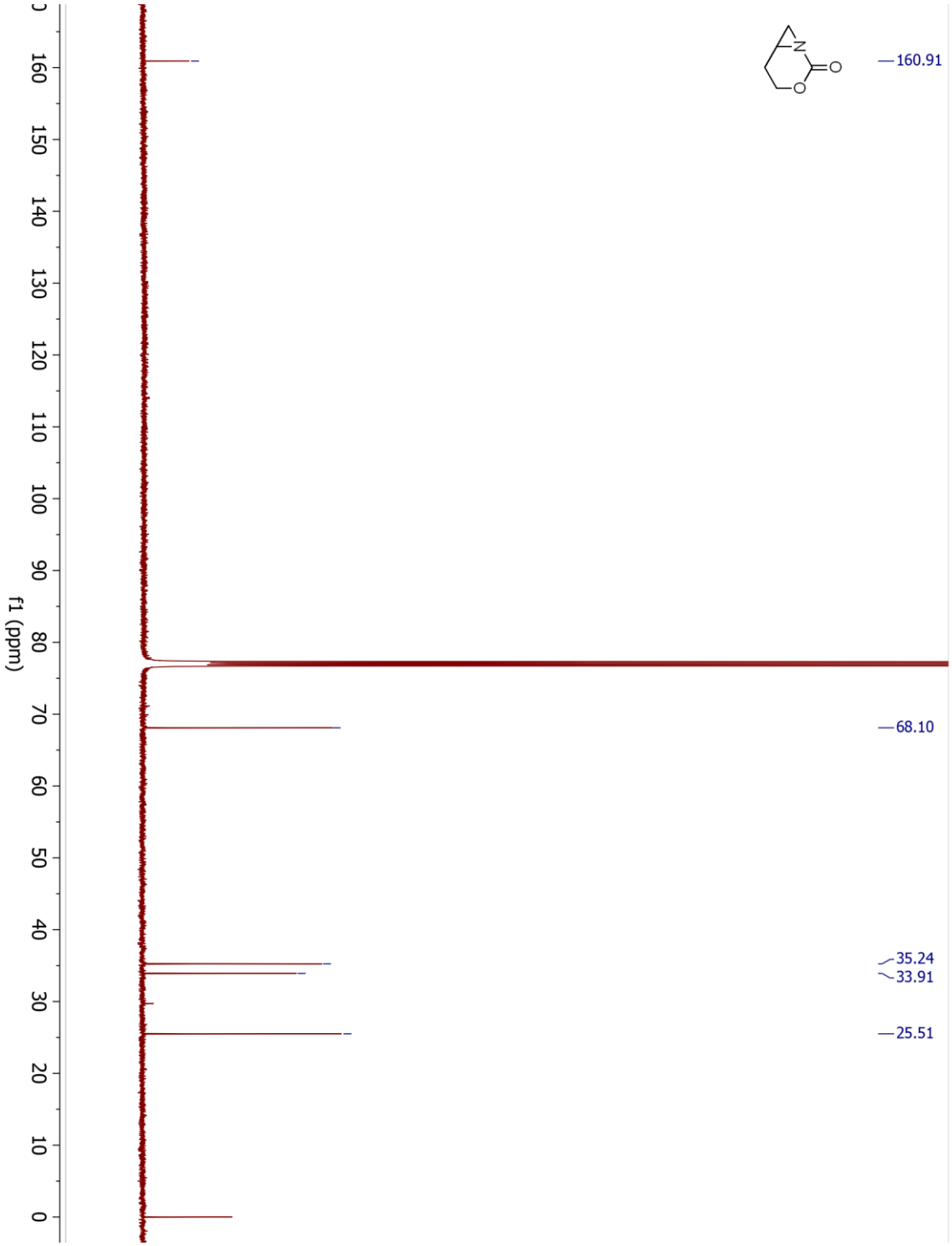
^{13}C NMR (126 MHz, $CDCl_3$) for compound **2.1h**



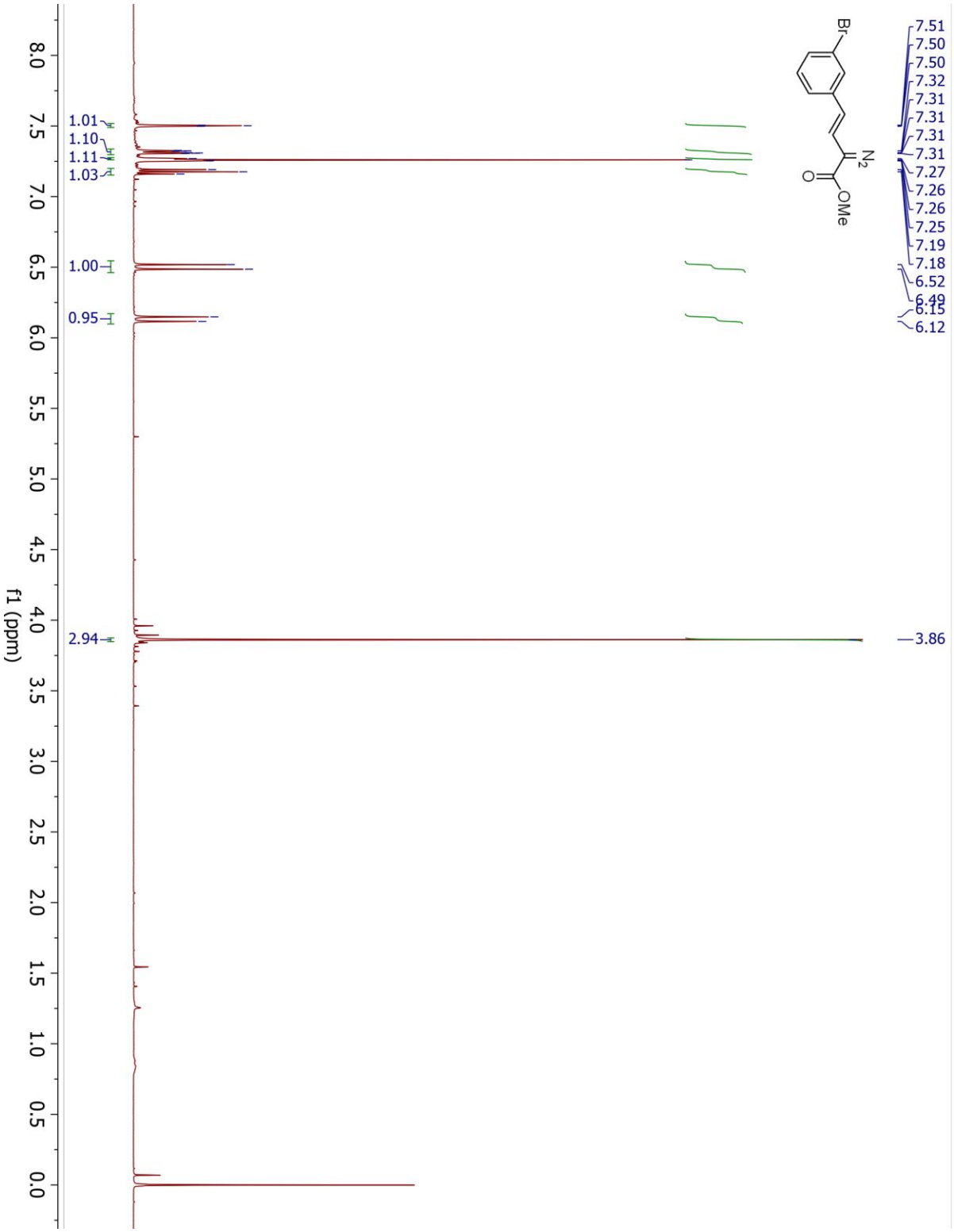
^{1}H NMR (500 MHz, $CDCl_3$) for compound **2.1i**



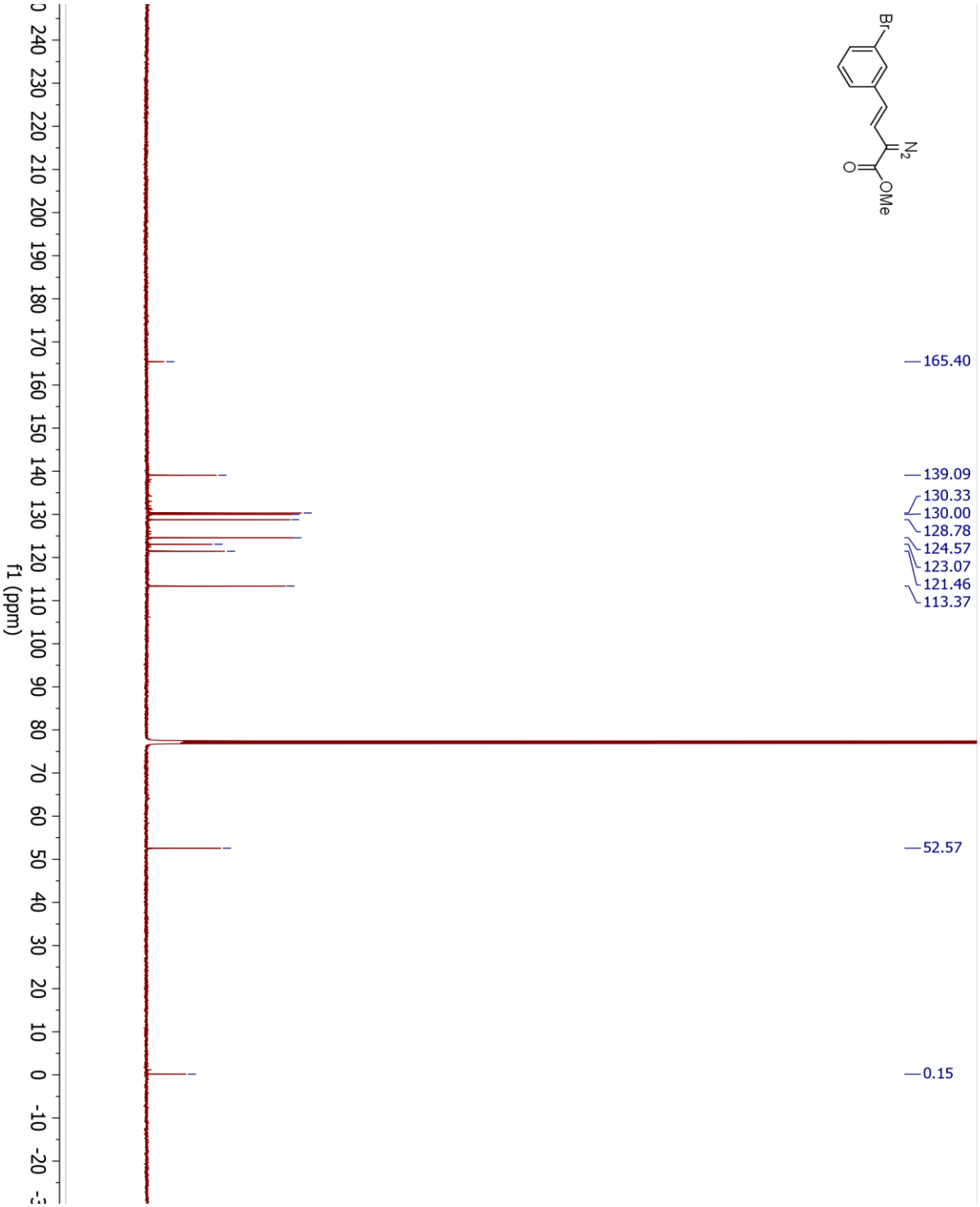
^{13}C NMR (500 MHz, $CDCl_3$) for compound **2.1i**



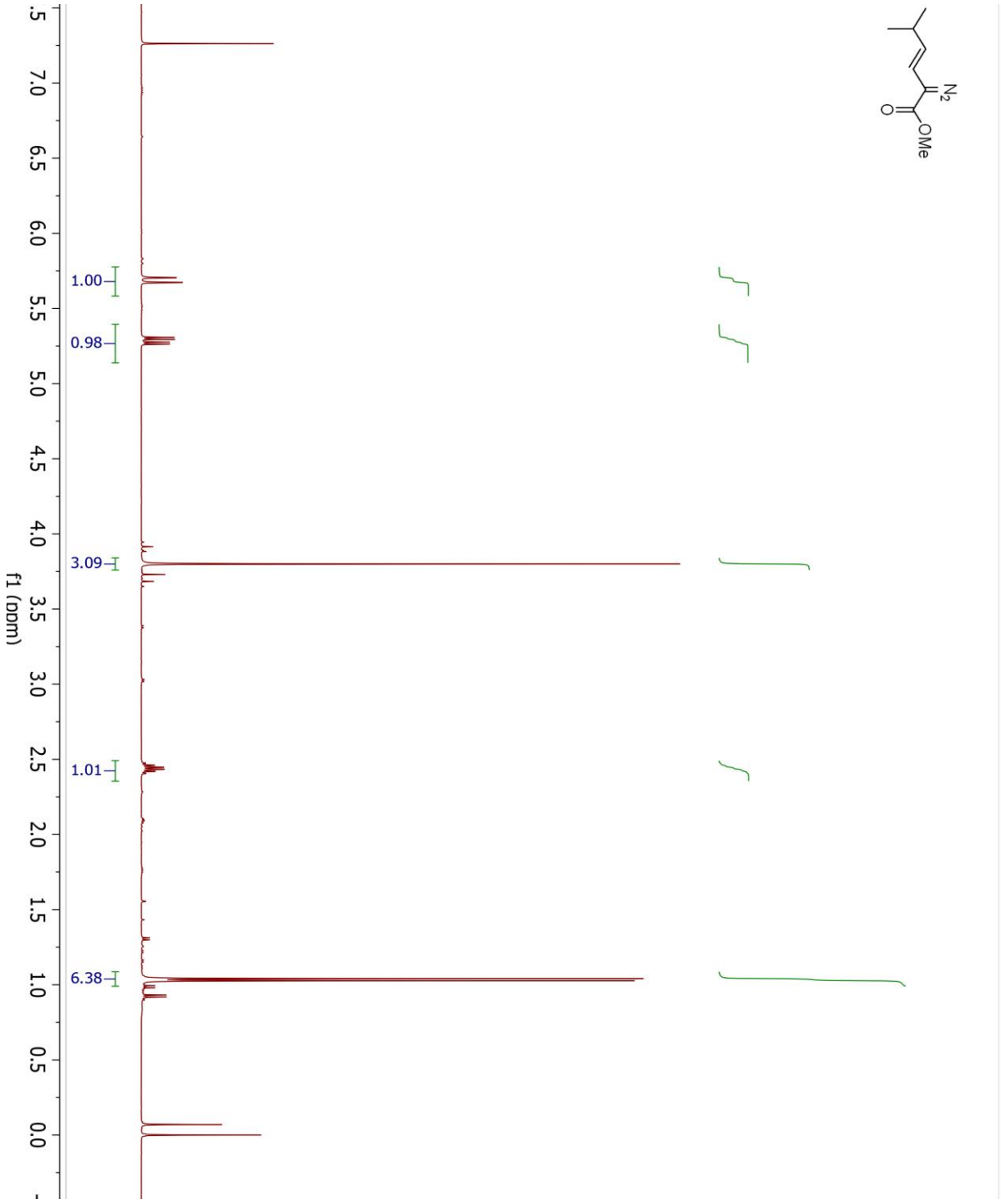
^{1}H NMR (500 MHz, $CDCl_3$) for compound **2.5d**



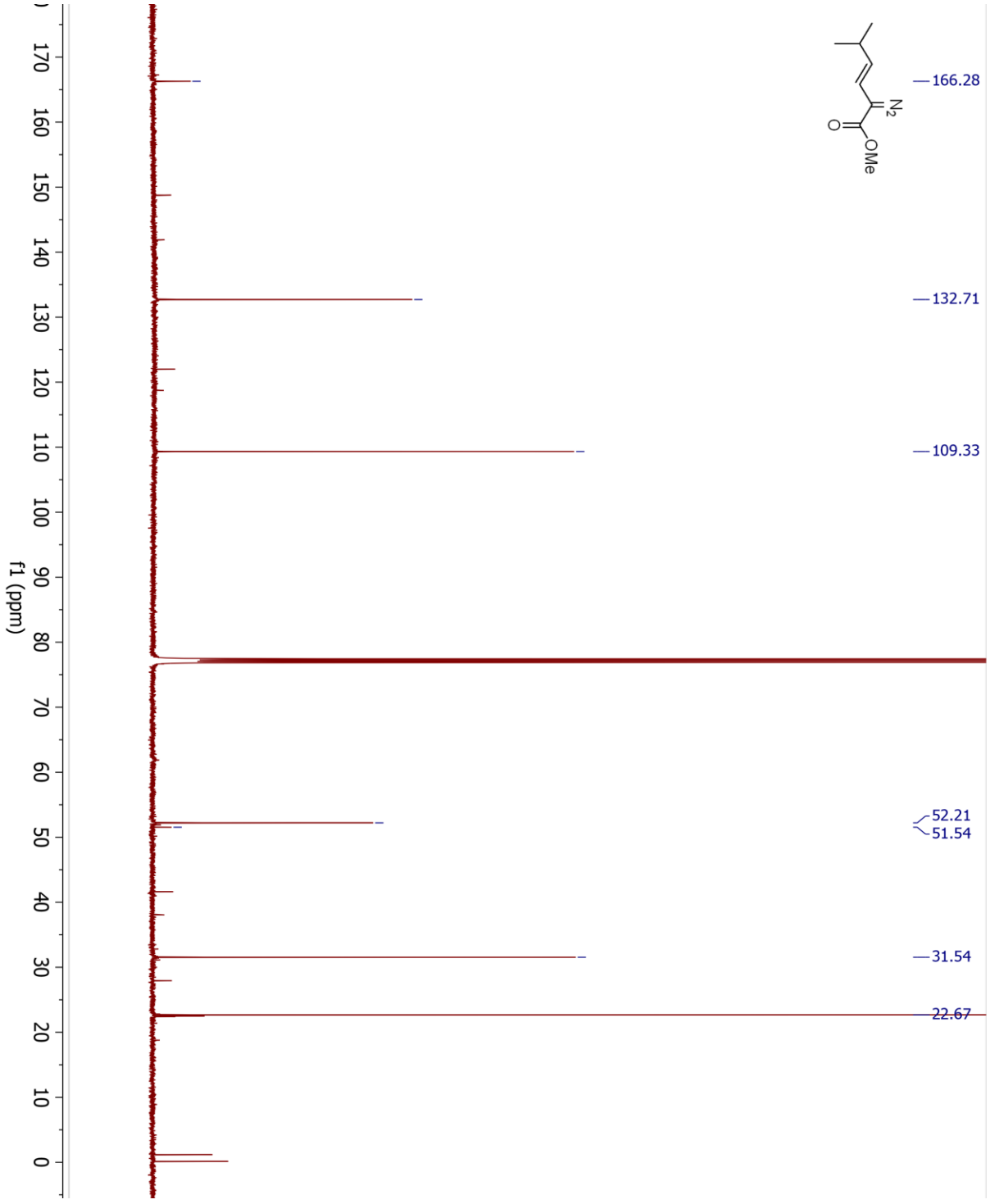
^{13}C NMR (126 MHz, $CDCl_3$) for compound **2.5d**



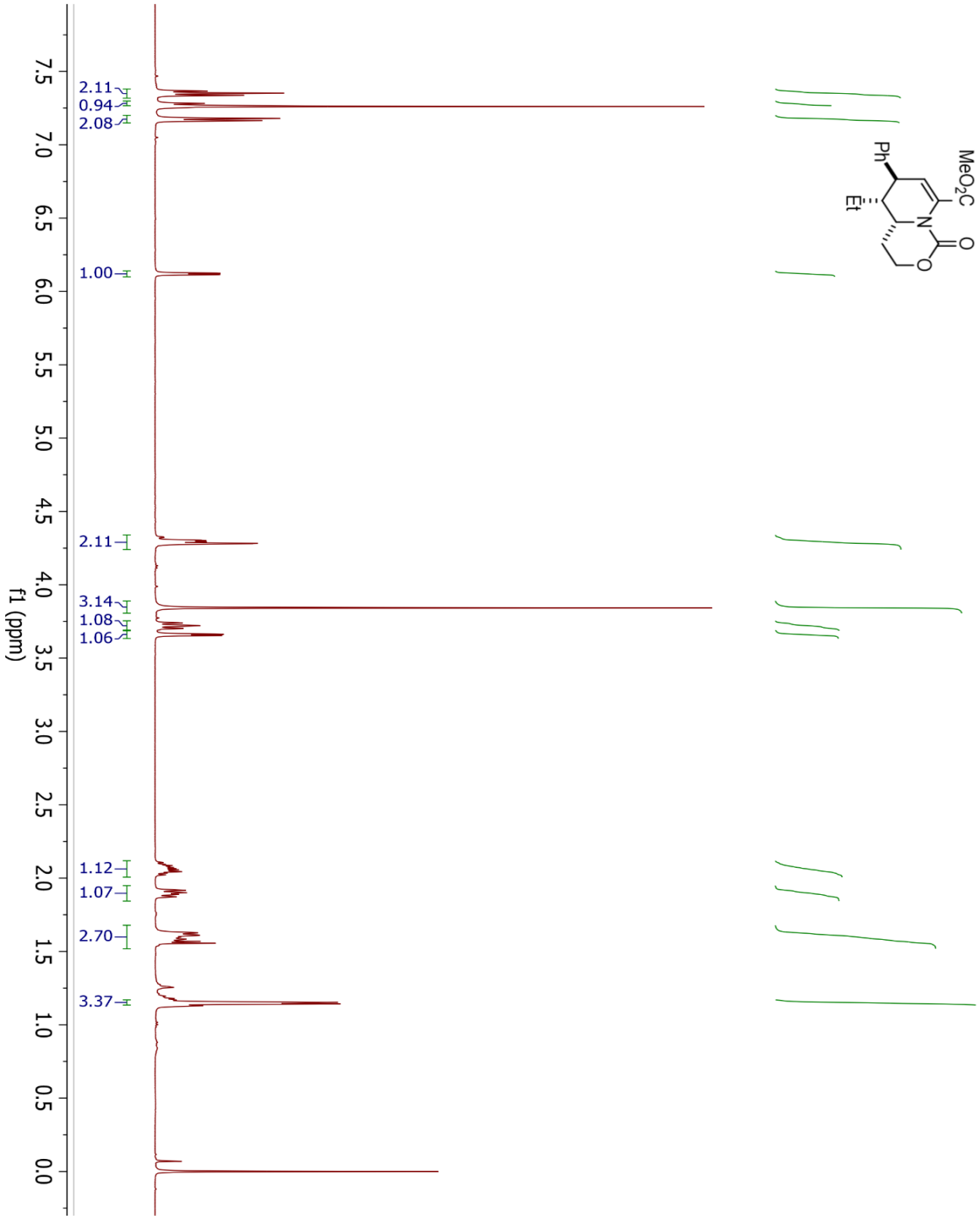
^{1}H NMR (500 MHz, $CDCl_3$) for compound **2.5g**



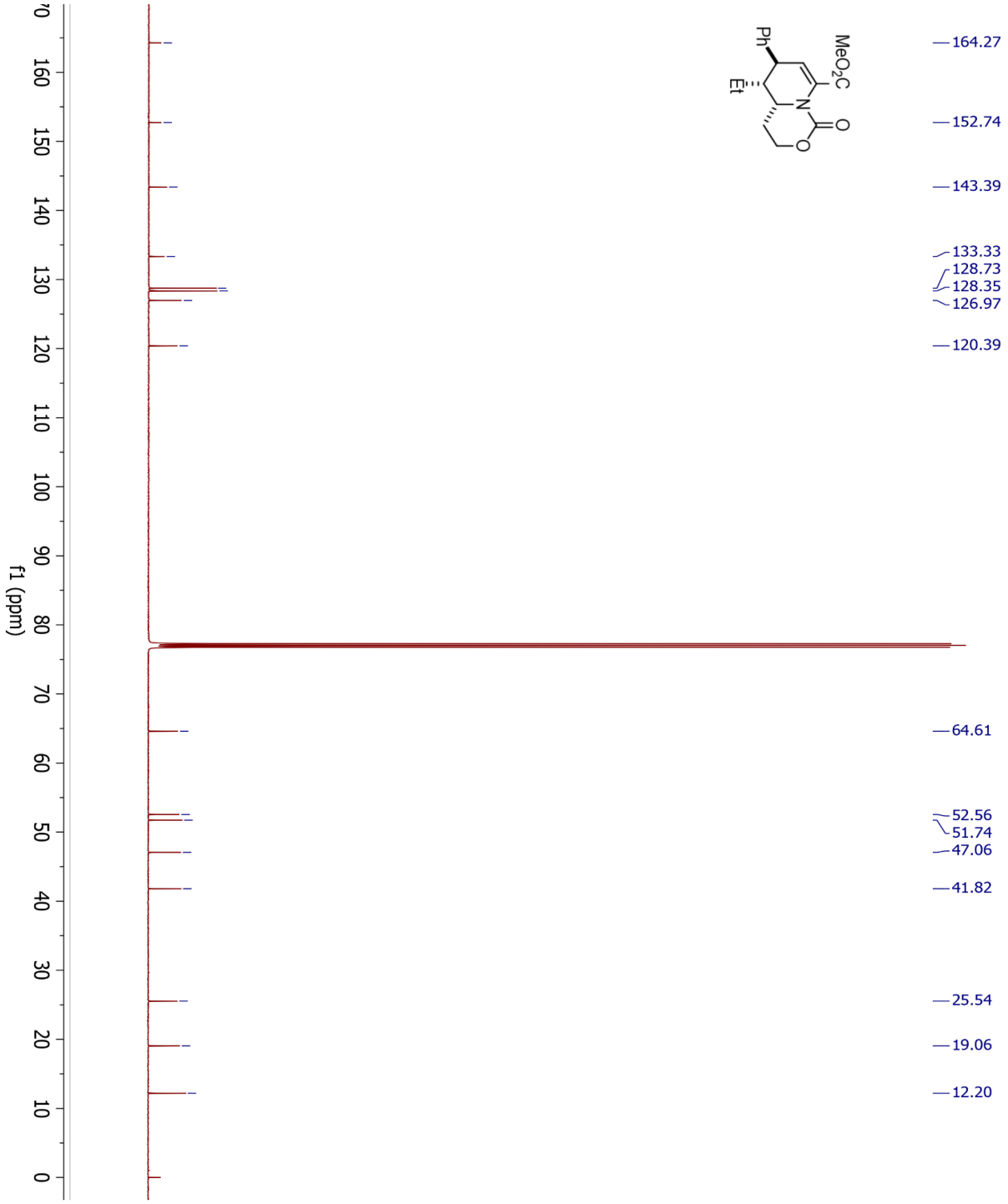
^{13}C NMR (126 MHz, $CDCl_3$) for compound **2.5g**



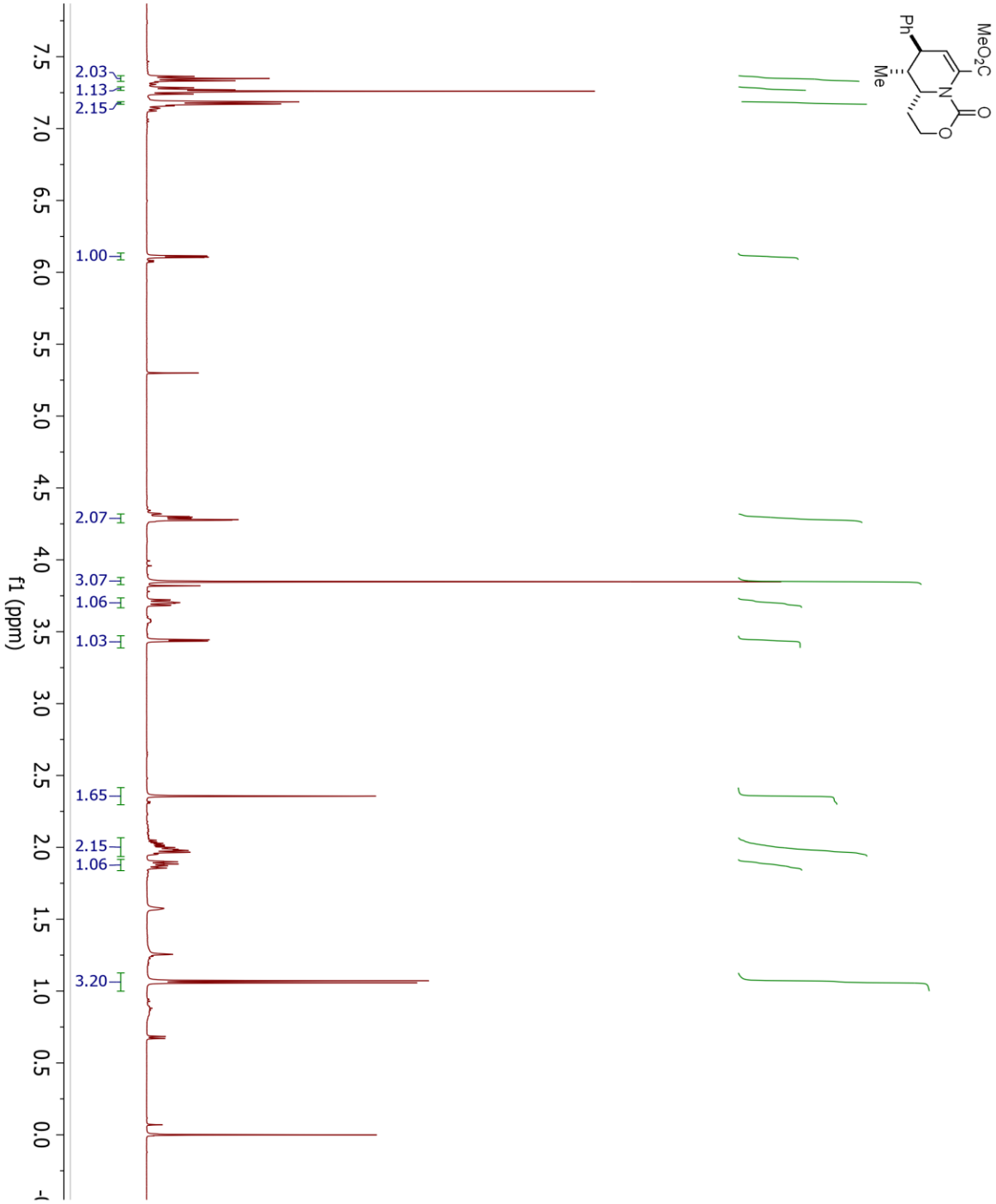
^{1}H NMR (500 MHz, $CDCl_3$) for compound **2.6aa**



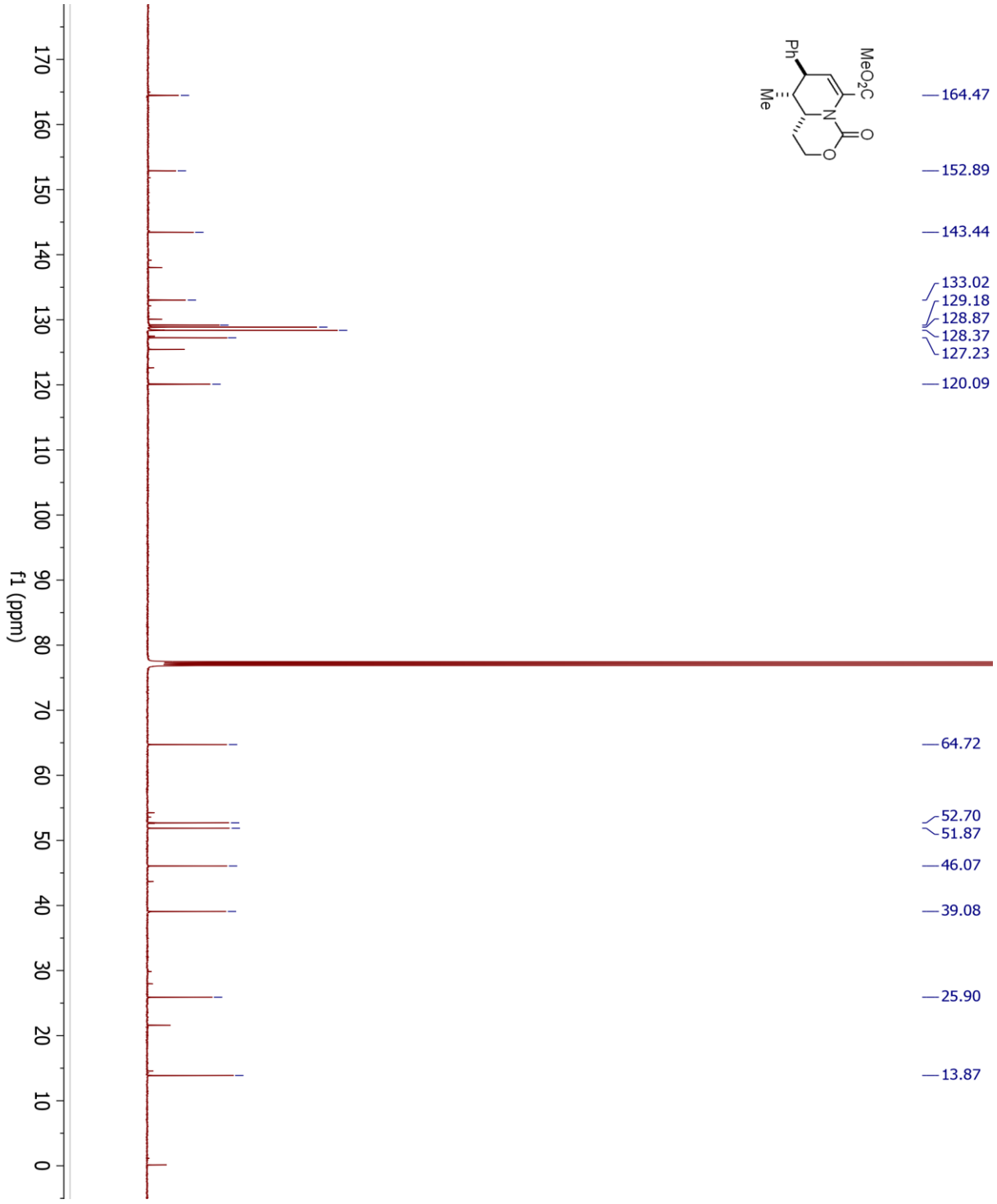
^{13}C NMR (126 MHz, $CDCl_3$) for compound **2.6aa**



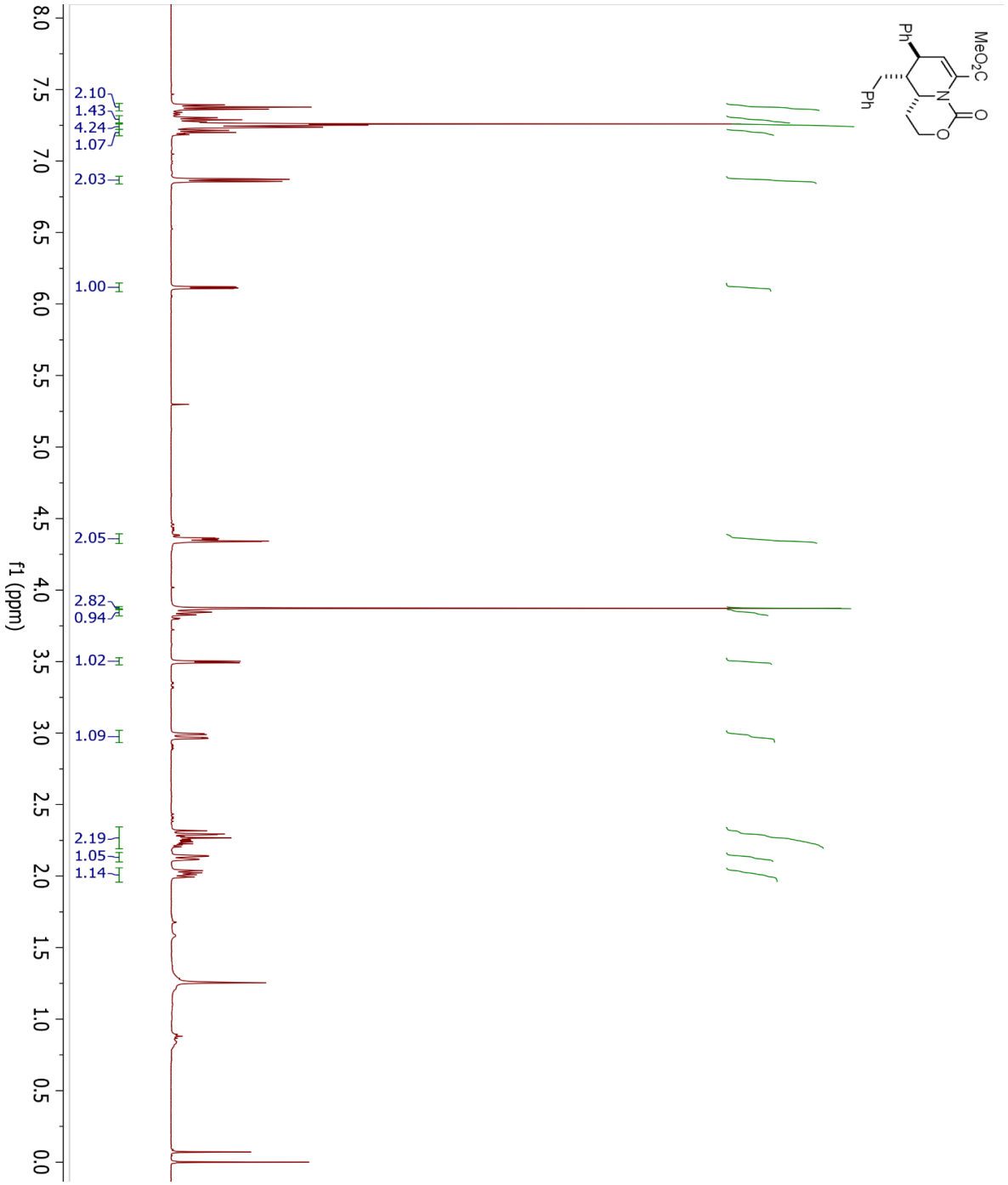
^{1}H NMR (500 MHz, $CDCl_3$) for compound **2.6ba**



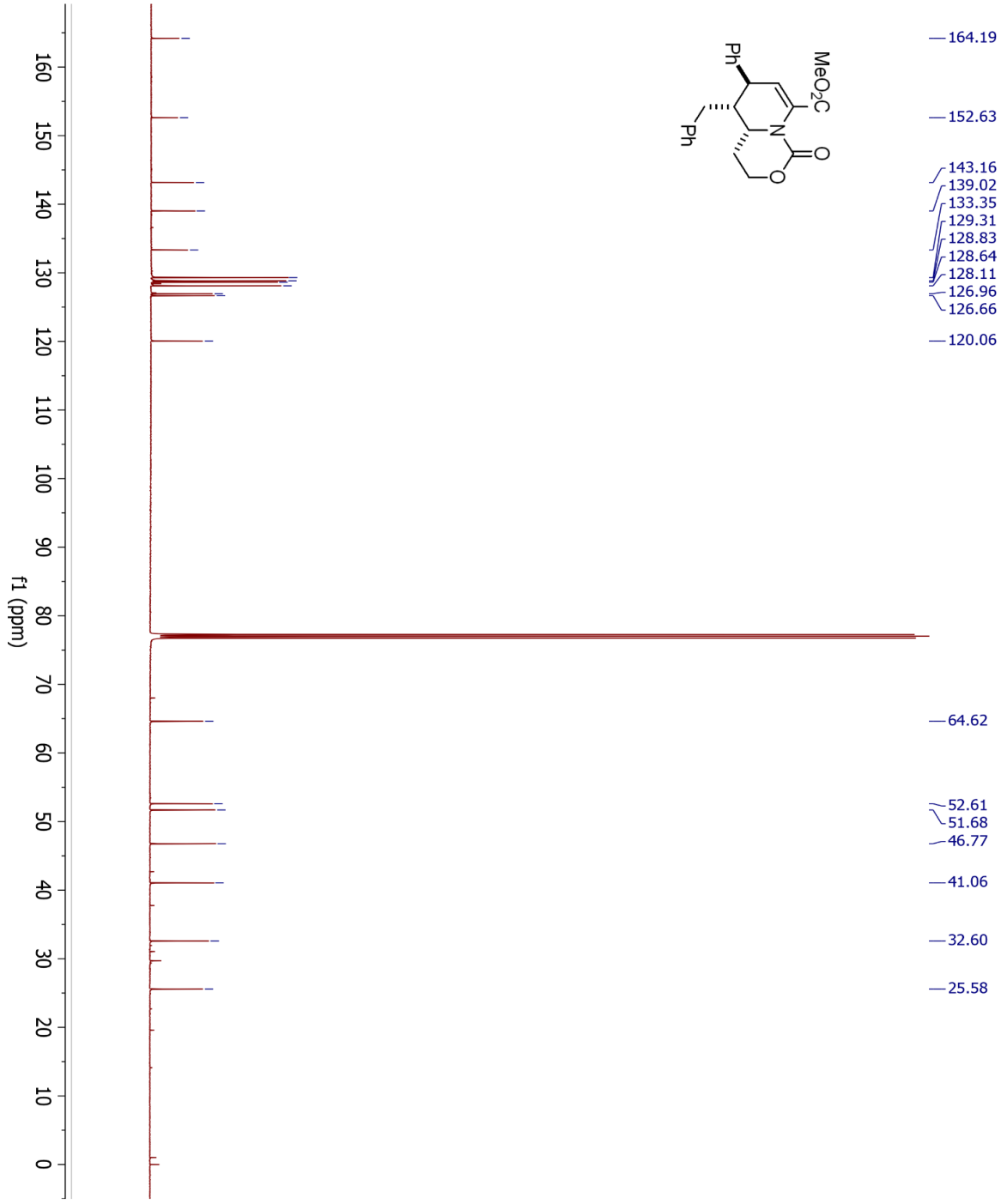
^{13}C NMR (126 MHz, $CDCl_3$) for compound **2.6ba**



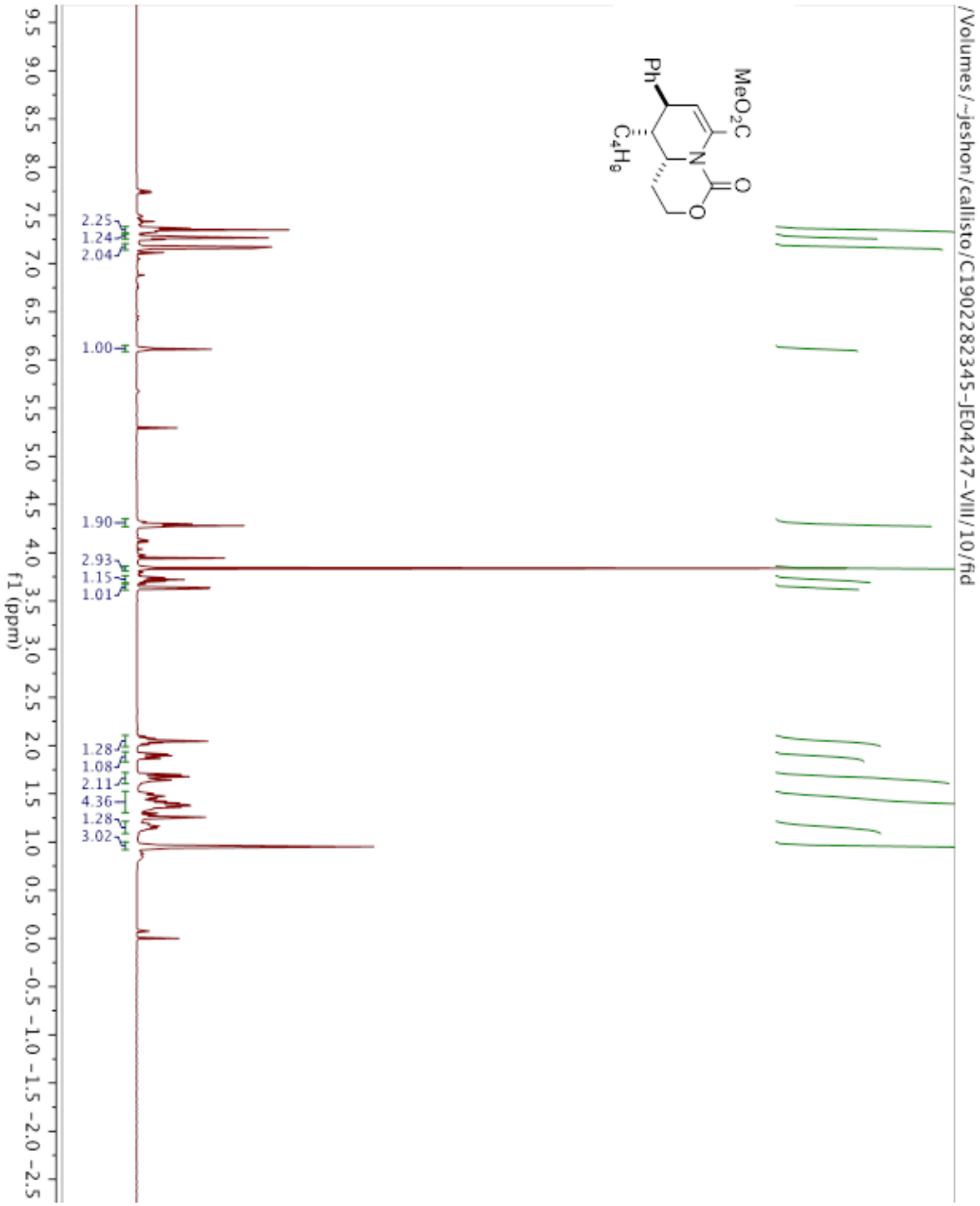
^{1}H NMR (500 MHz, $CDCl_3$) for compound **2.6ca**



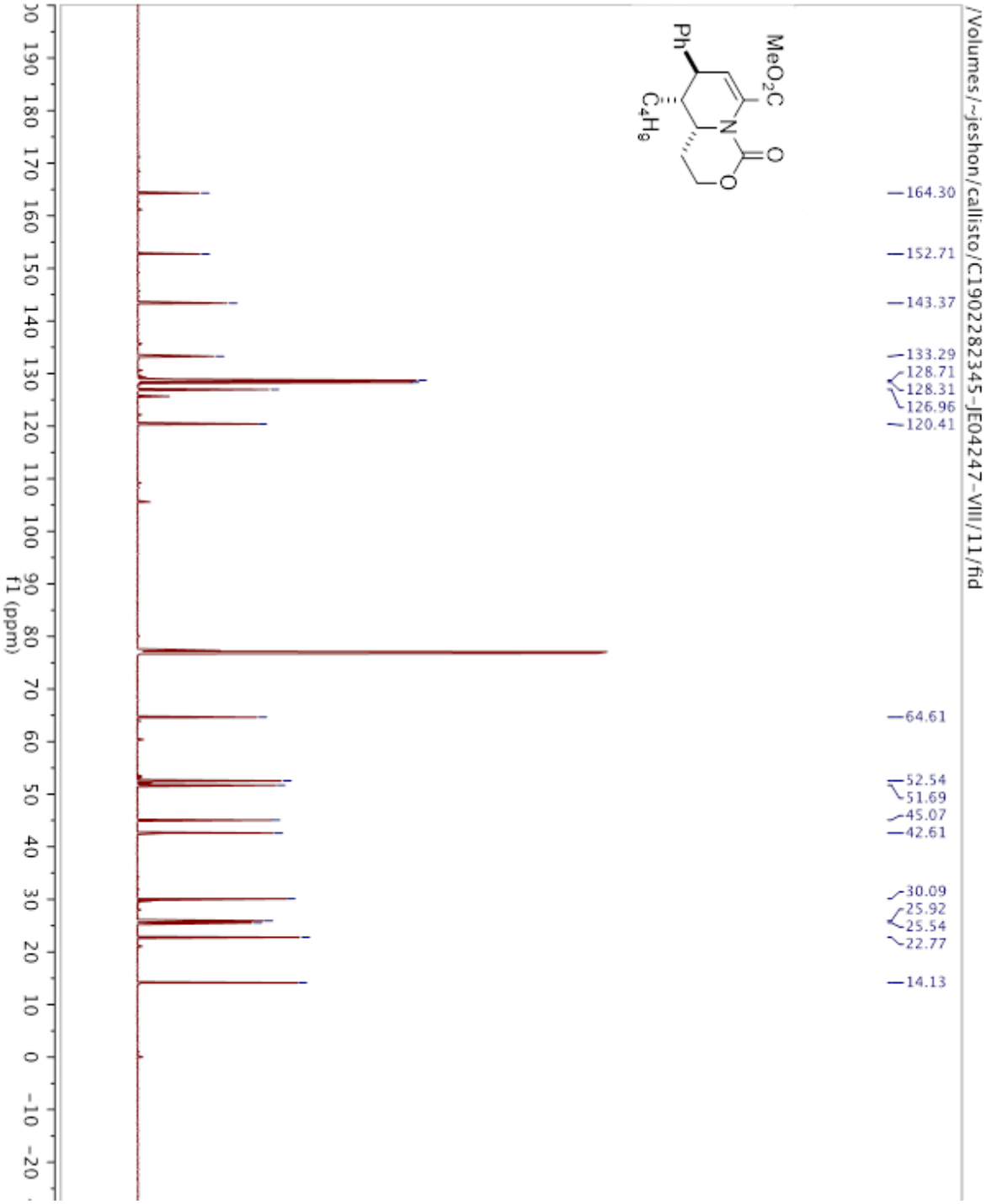
^{13}C NMR (126 MHz, $CDCl_3$) for compound **2.6ca**



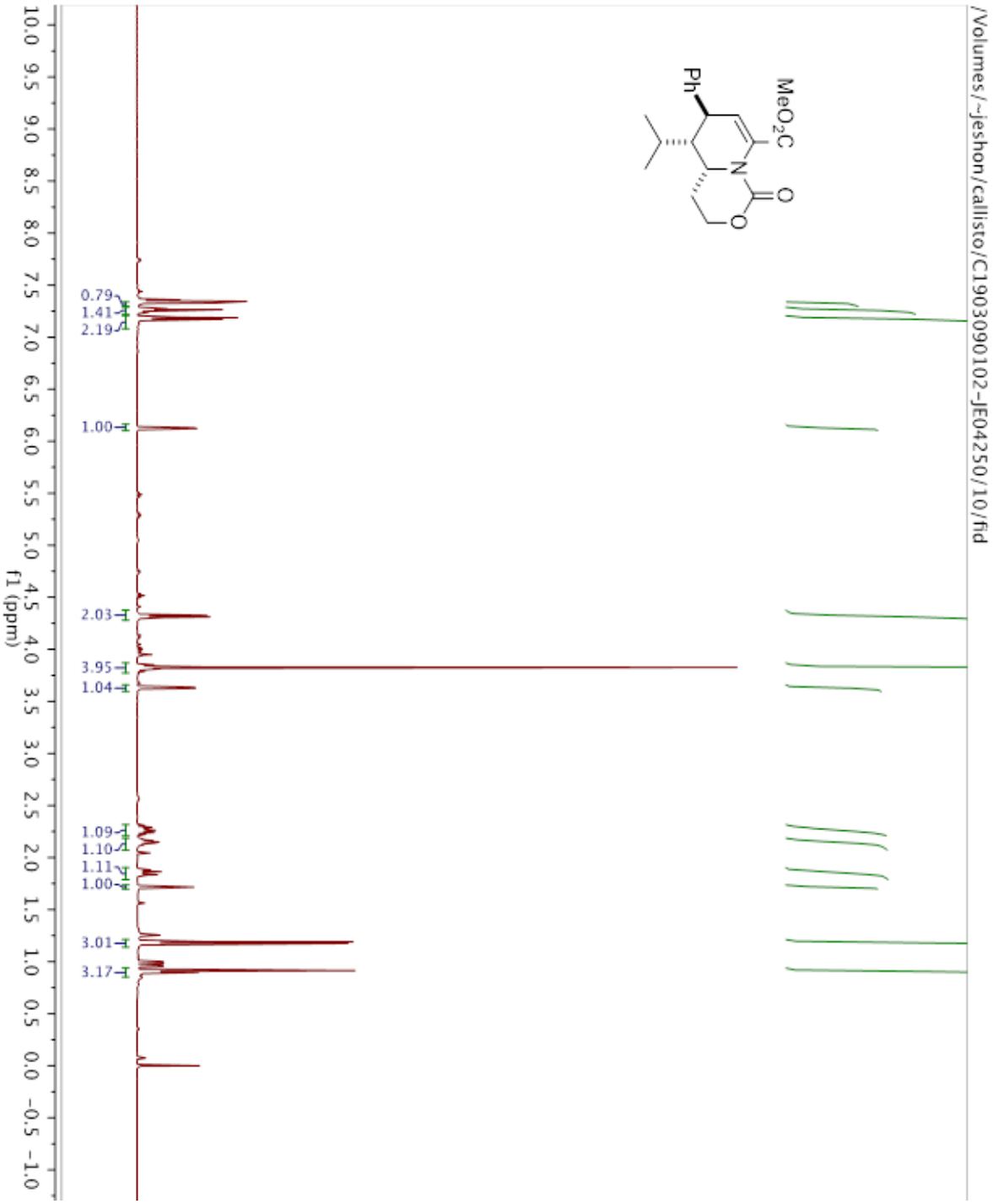
^{1}H NMR (500 MHz, $CDCl_3$) for compound **2.6da**



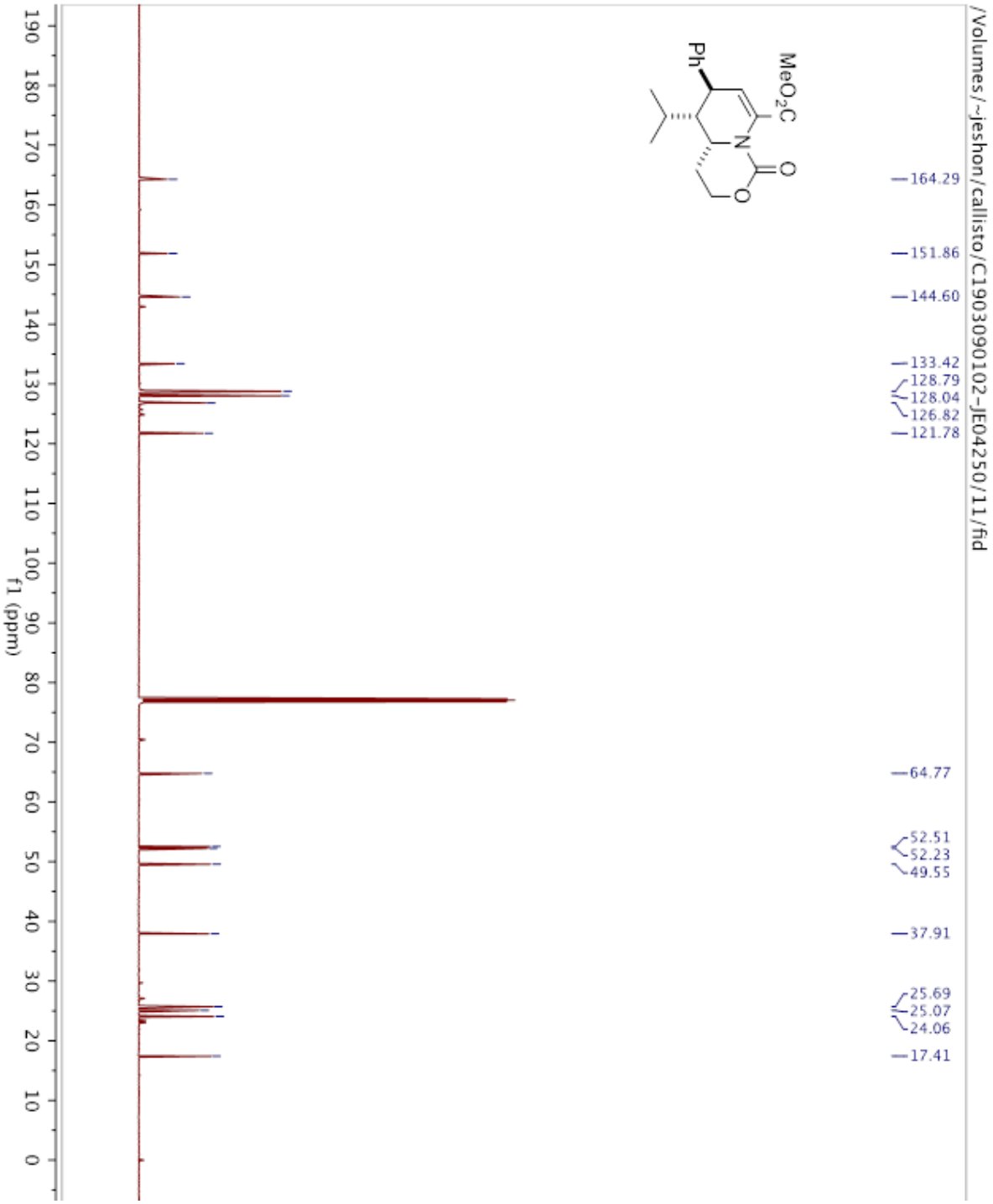
^{13}C NMR (126 MHz, $CDCl_3$) for compound **2.6da**



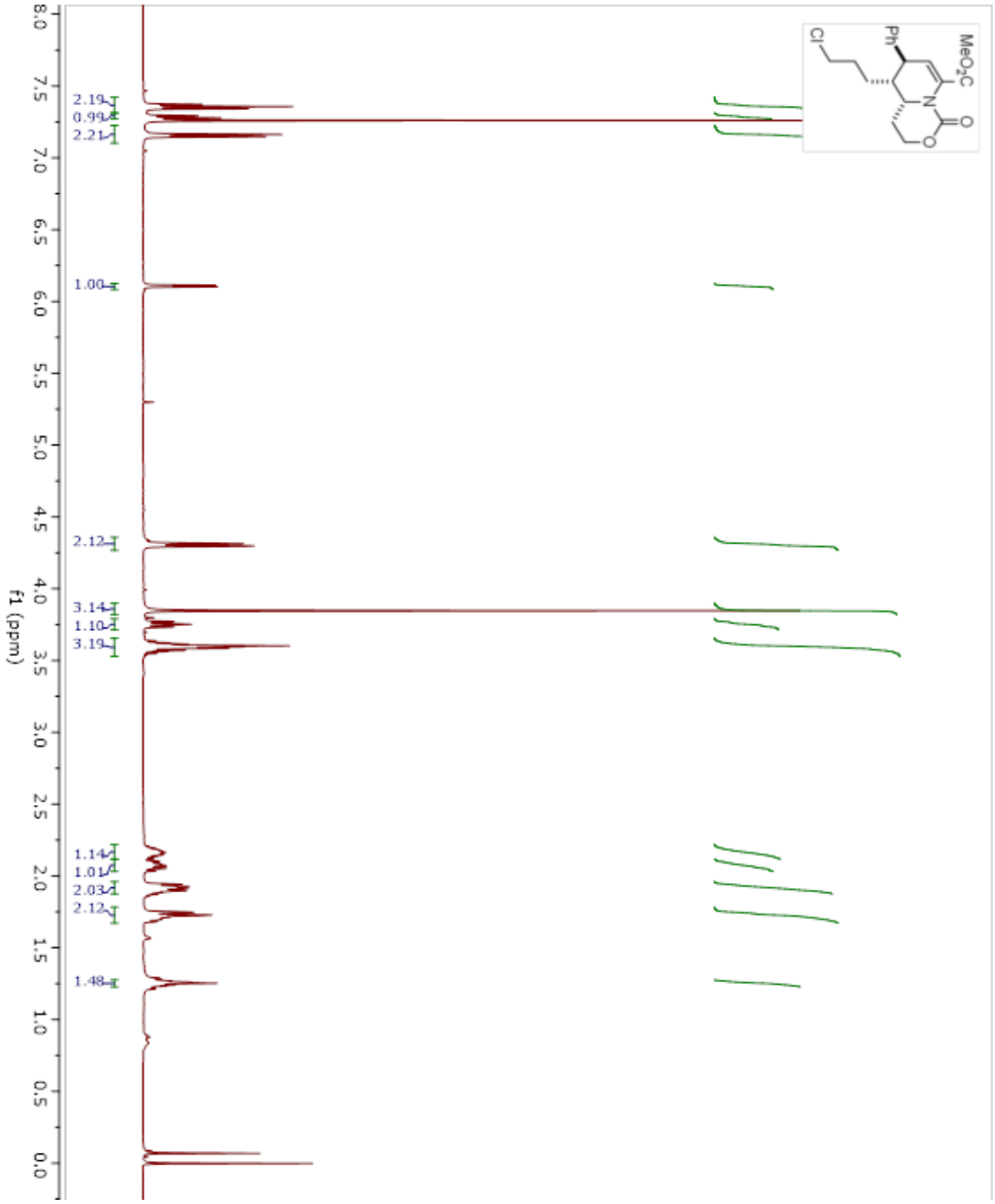
^{1}H NMR (500 MHz, $CDCl_3$) for compound **2.6ea**



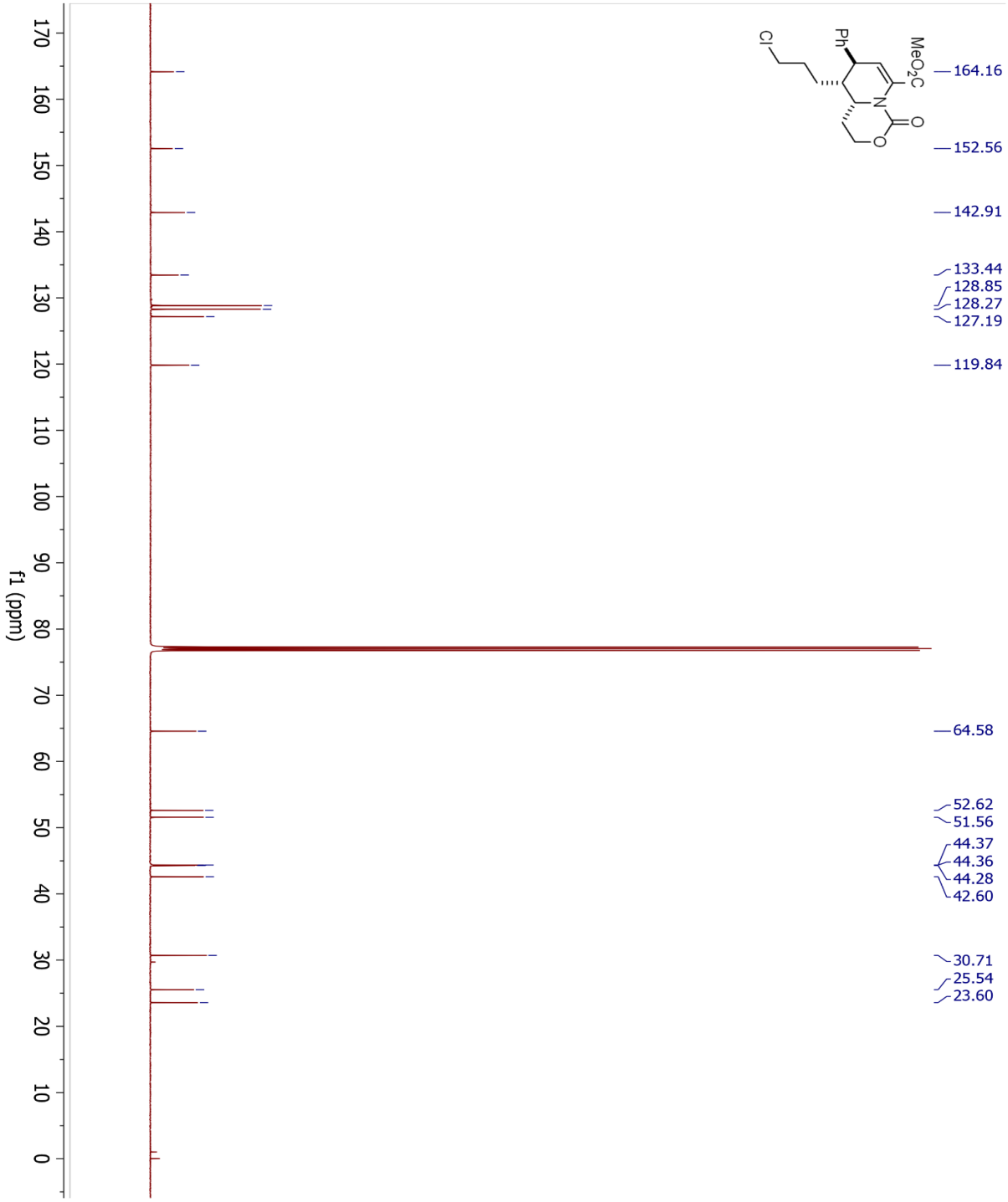
^{13}C NMR (126 MHz, $CDCl_3$) for compound **2.6ea**



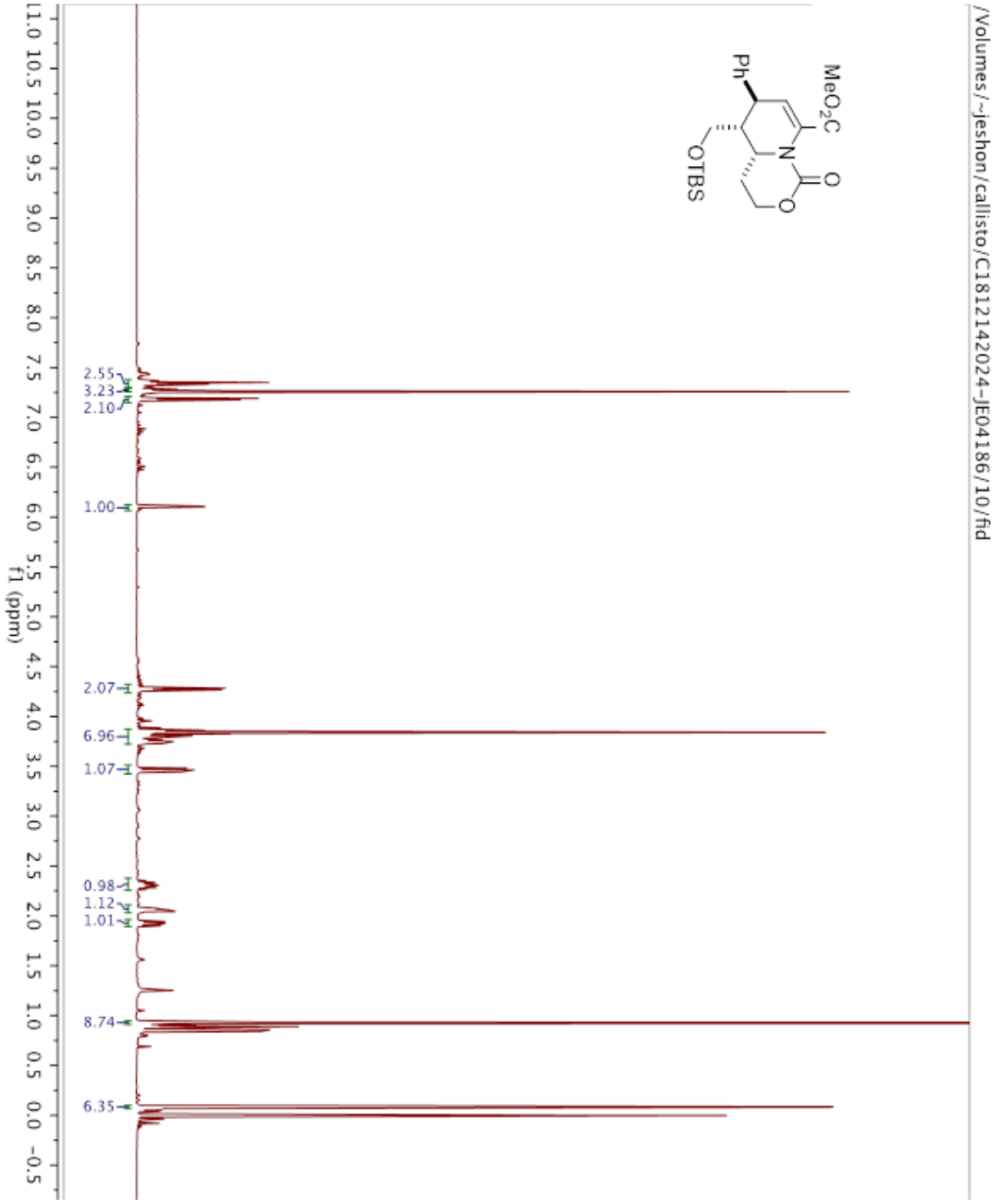
^{1}H NMR (500 MHz, $CDCl_3$) for compound **2.6fa**



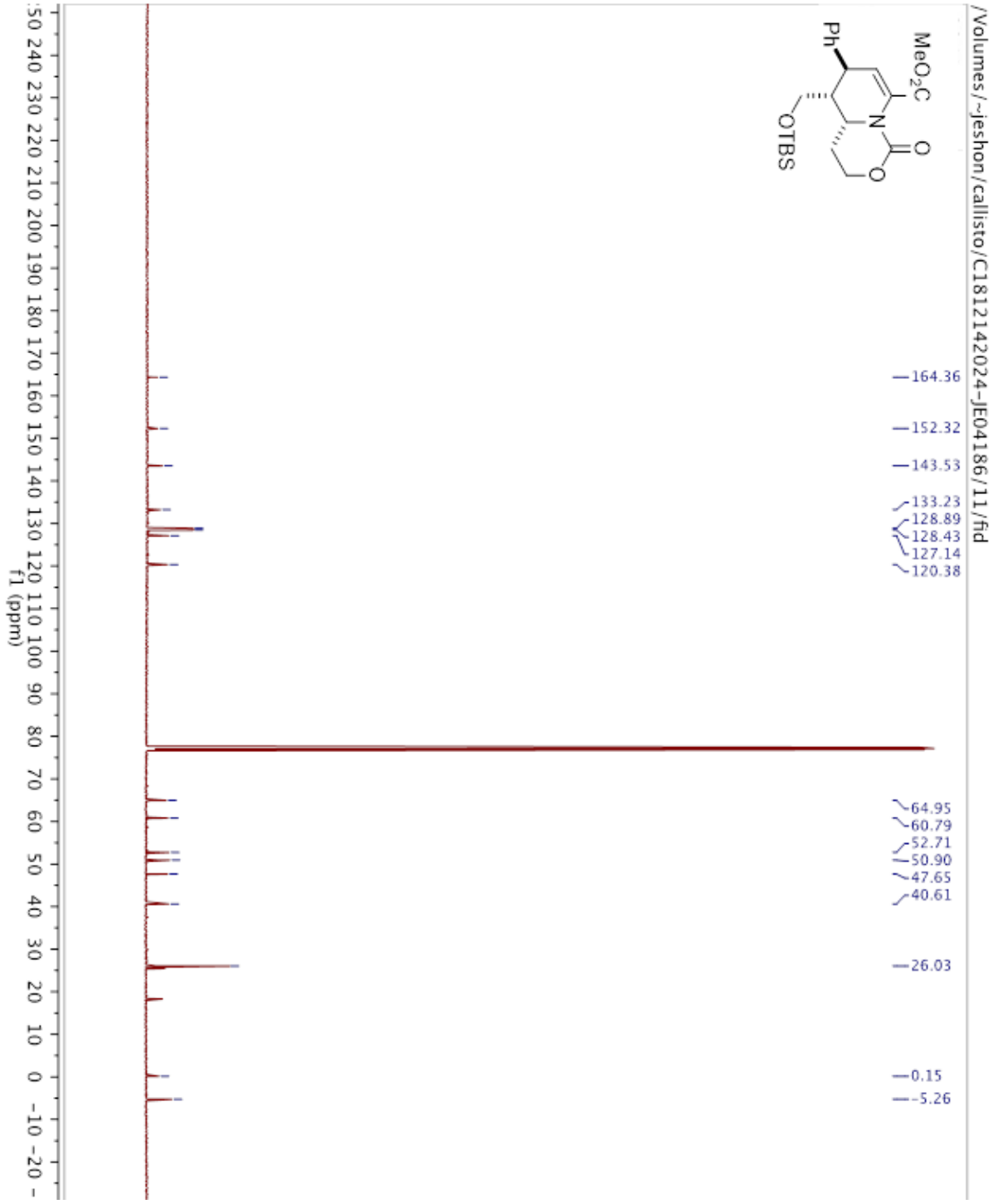
^{13}C NMR (126 MHz, $CDCl_3$) for compound **2.6fa**



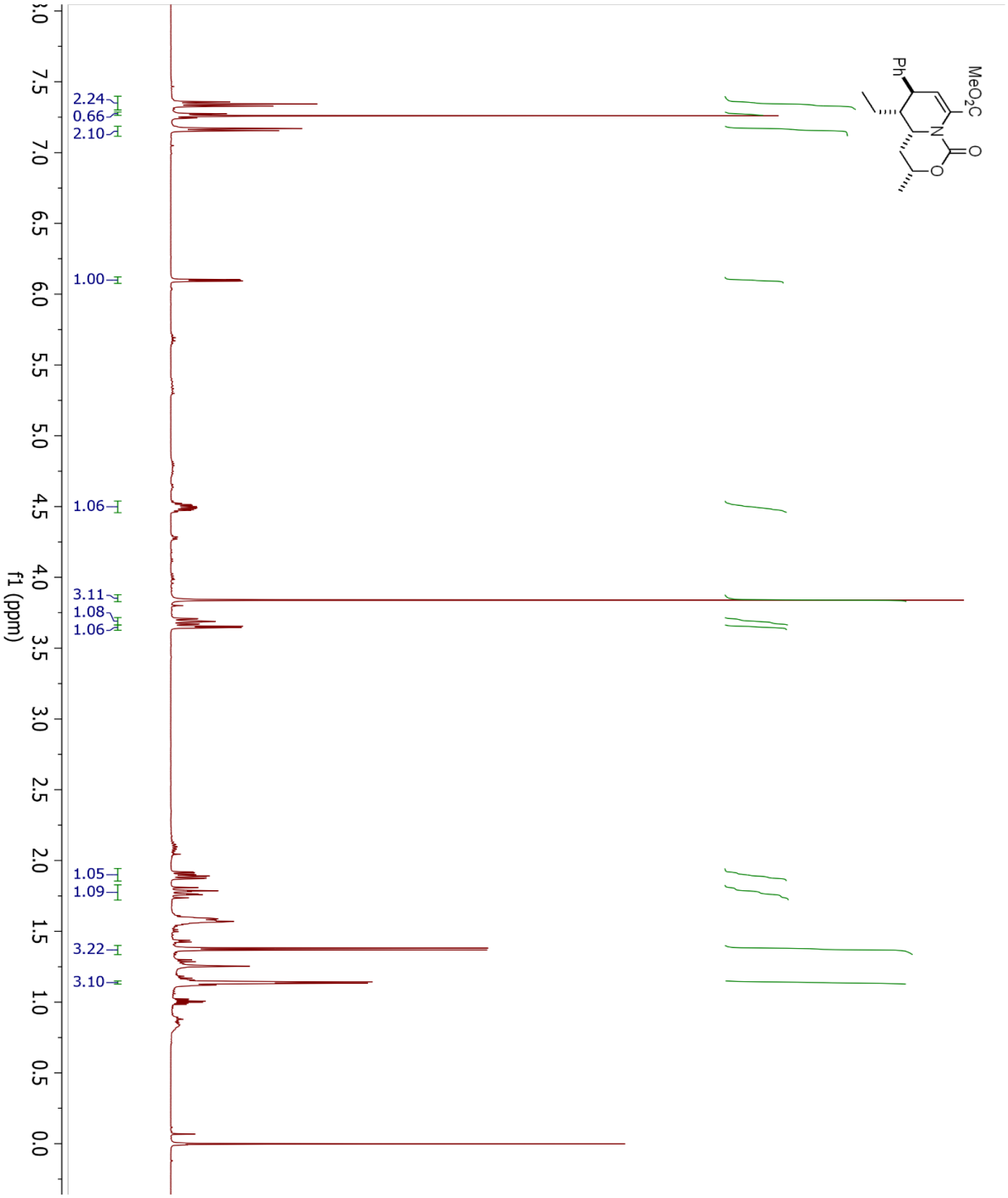
^{1}H NMR (500 MHz, $CDCl_3$) for compound **2.6ga**



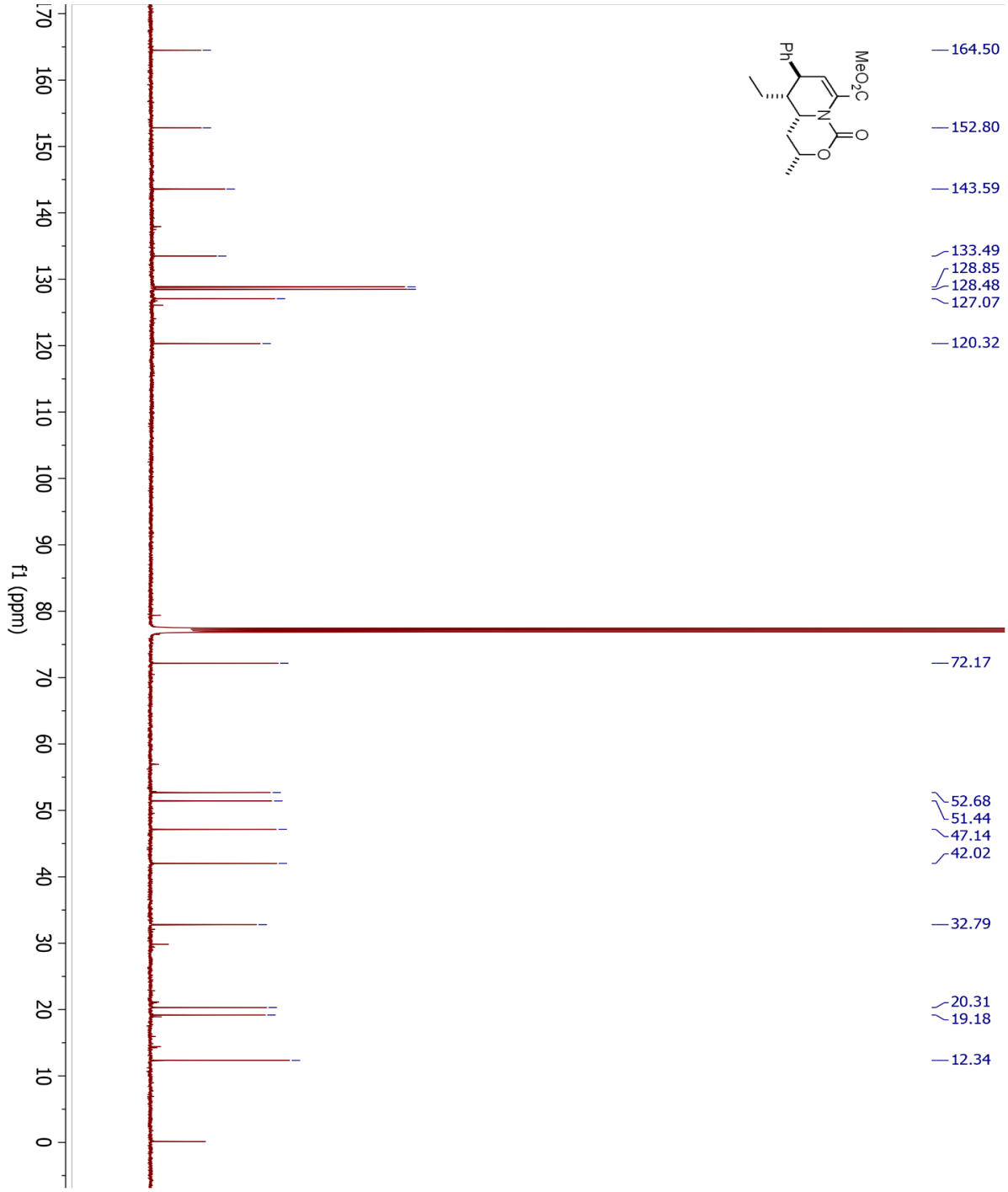
^{13}C NMR (126 MHz, $CDCl_3$) for compound **2.6ga**



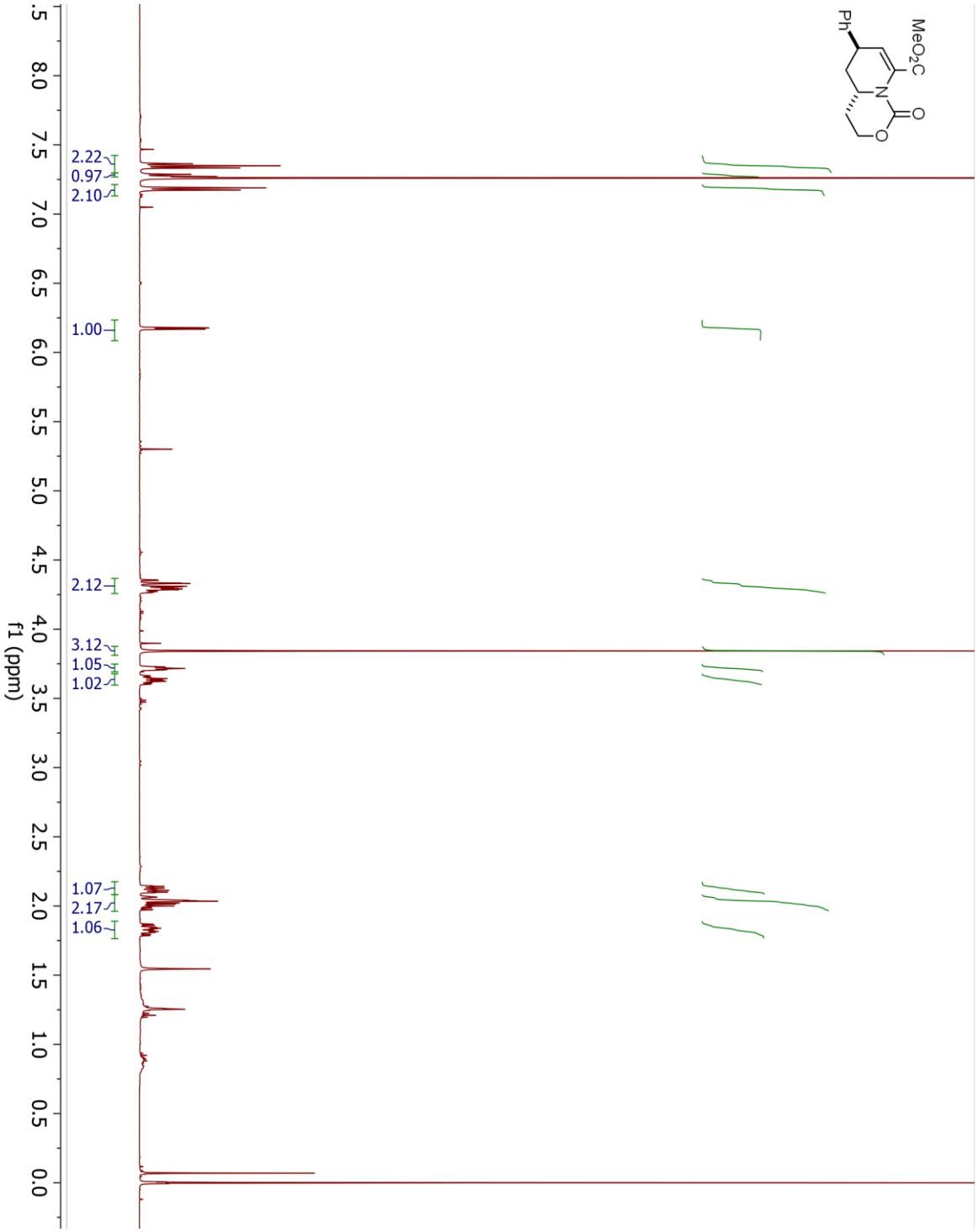
^{1}H NMR (500 MHz, $CDCl_3$) for compound **2.6ha**



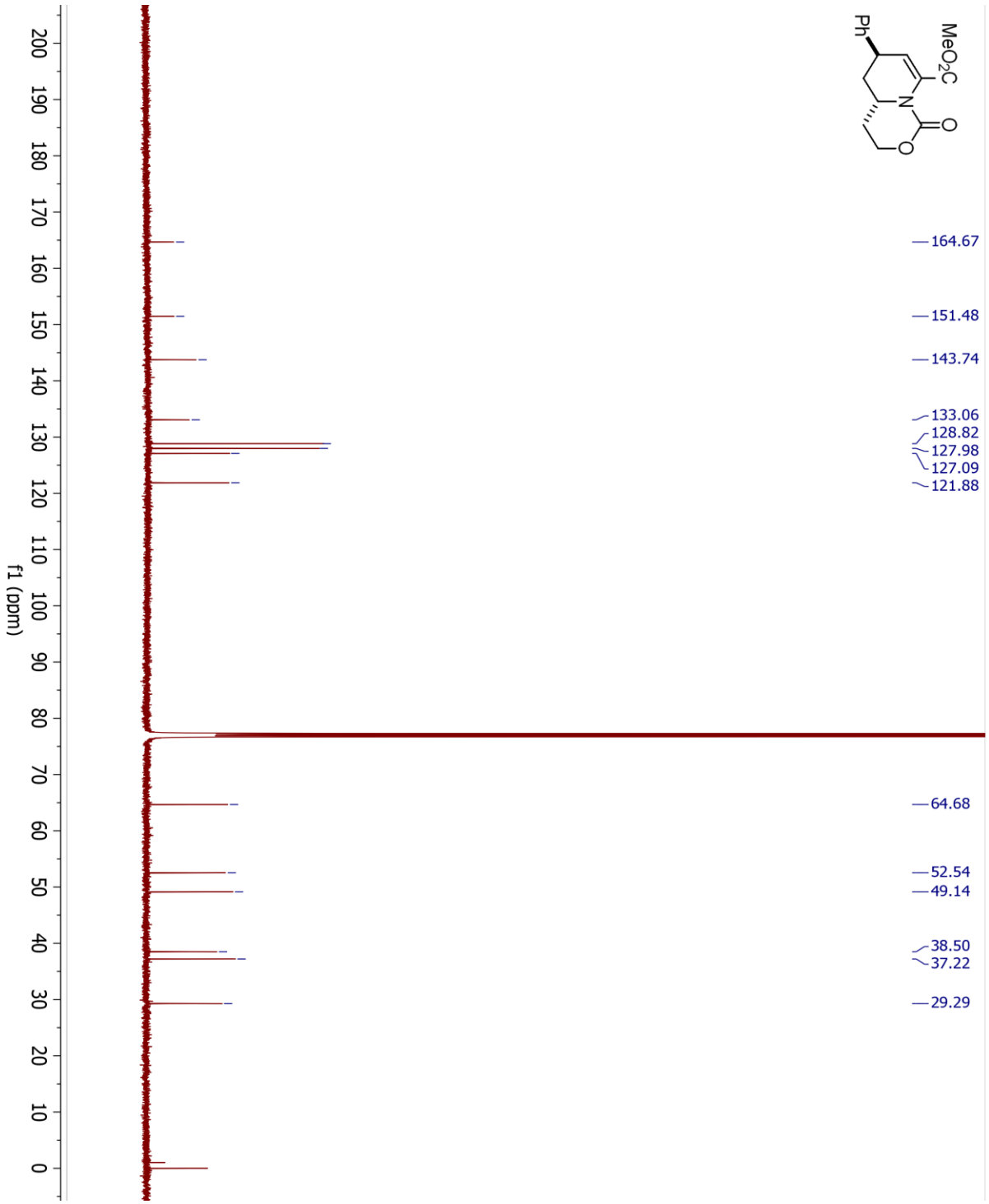
^{13}C NMR (126 MHz, $CDCl_3$) for compound **2.6ha**



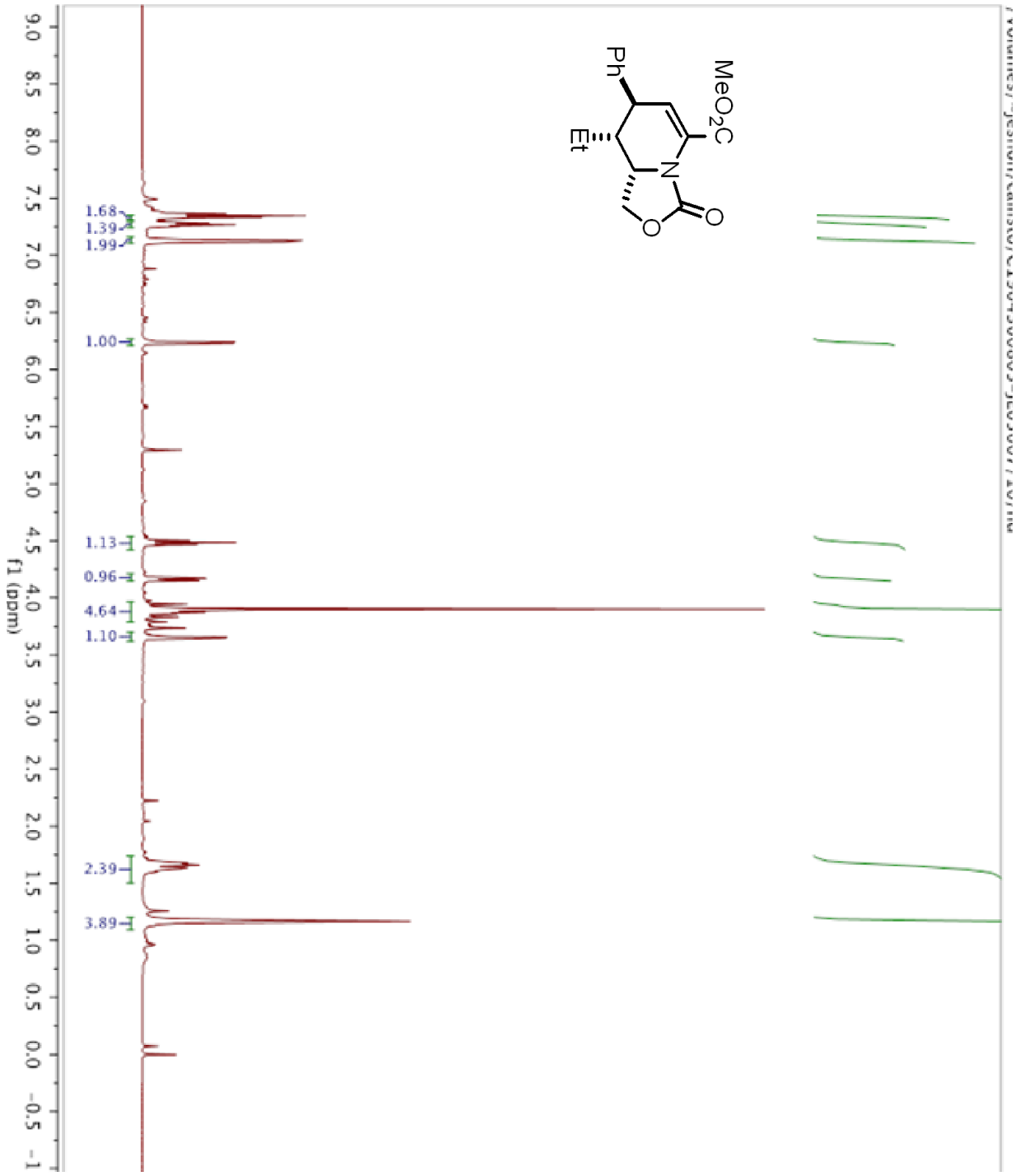
^{1}H NMR (500 MHz, $CDCl_3$) for compound **2.6ia**



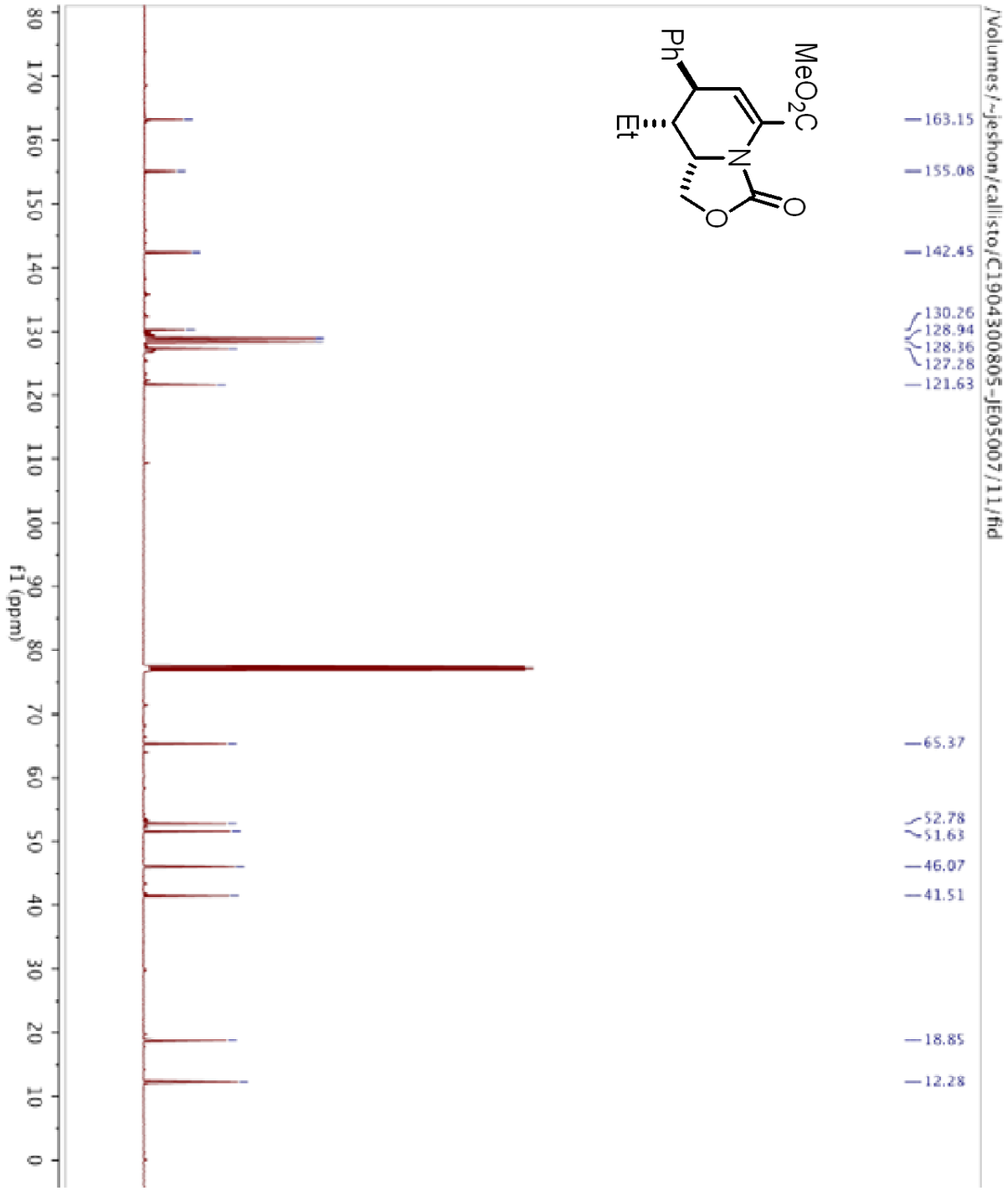
^{13}C NMR (126 MHz, $CDCl_3$) for compound **2.6ia**



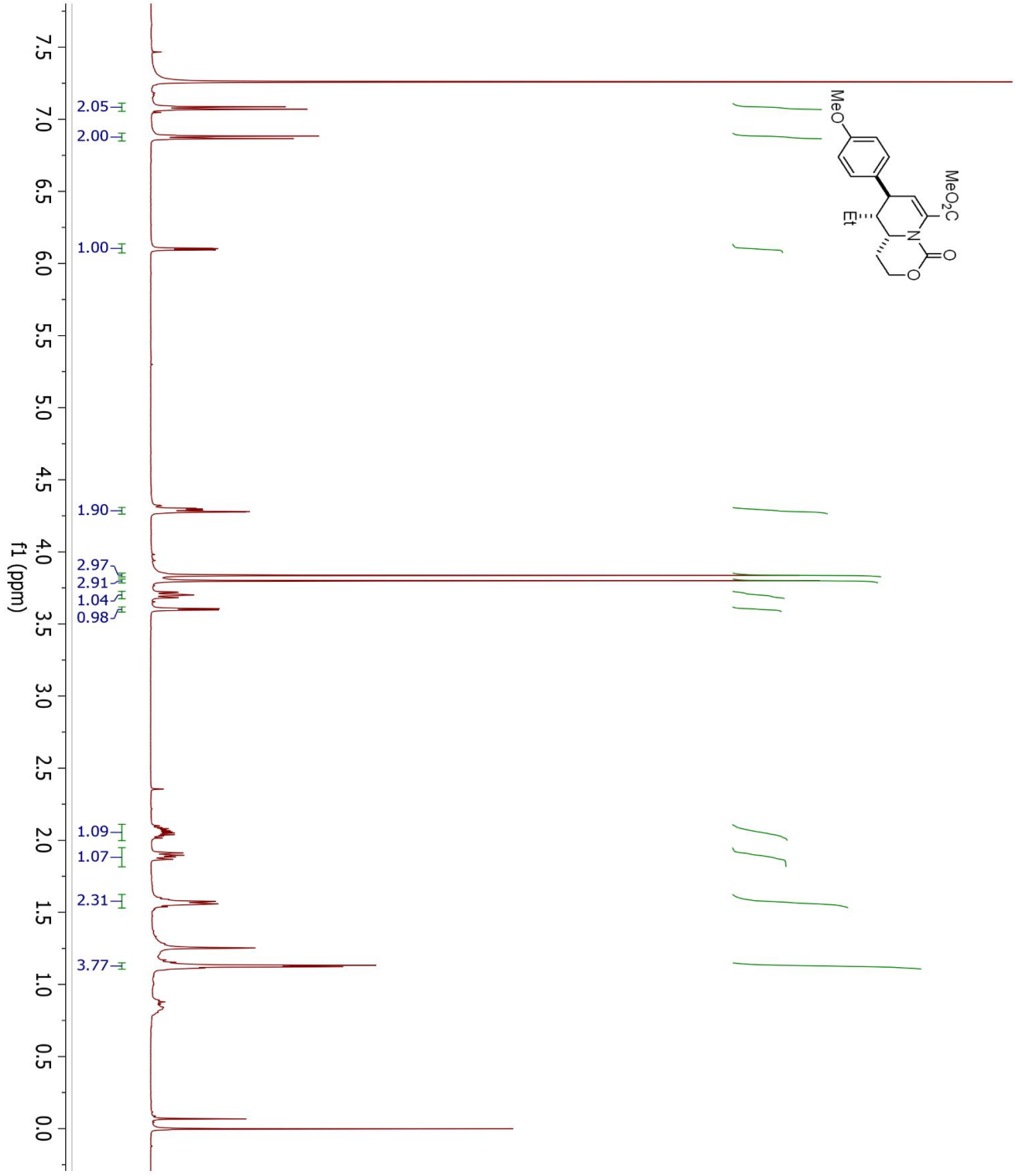
^{1}H NMR (500 MHz, $CDCl_3$) for compound **2.6ja**



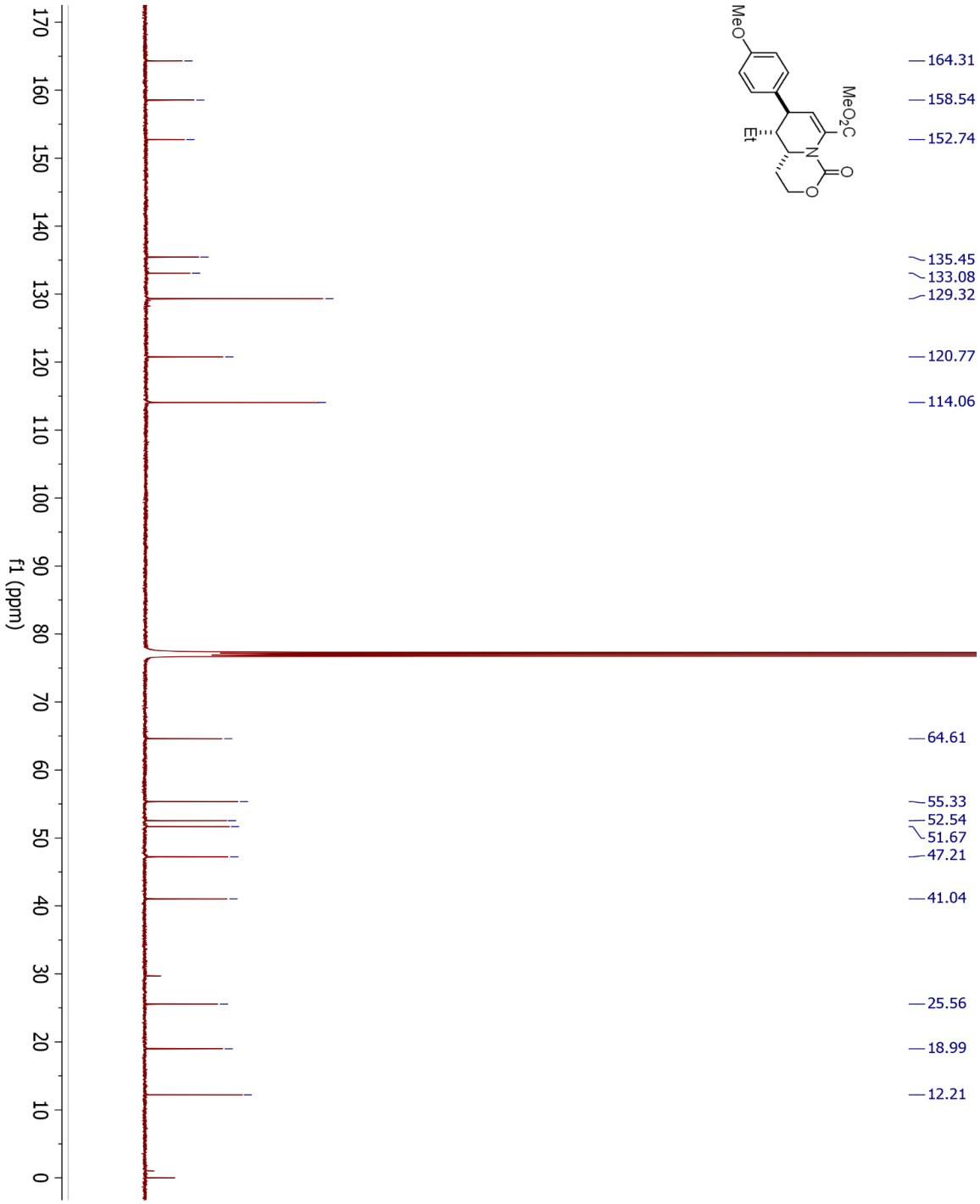
^{13}C NMR (126 MHz, $CDCl_3$) for compound **2.6ja**



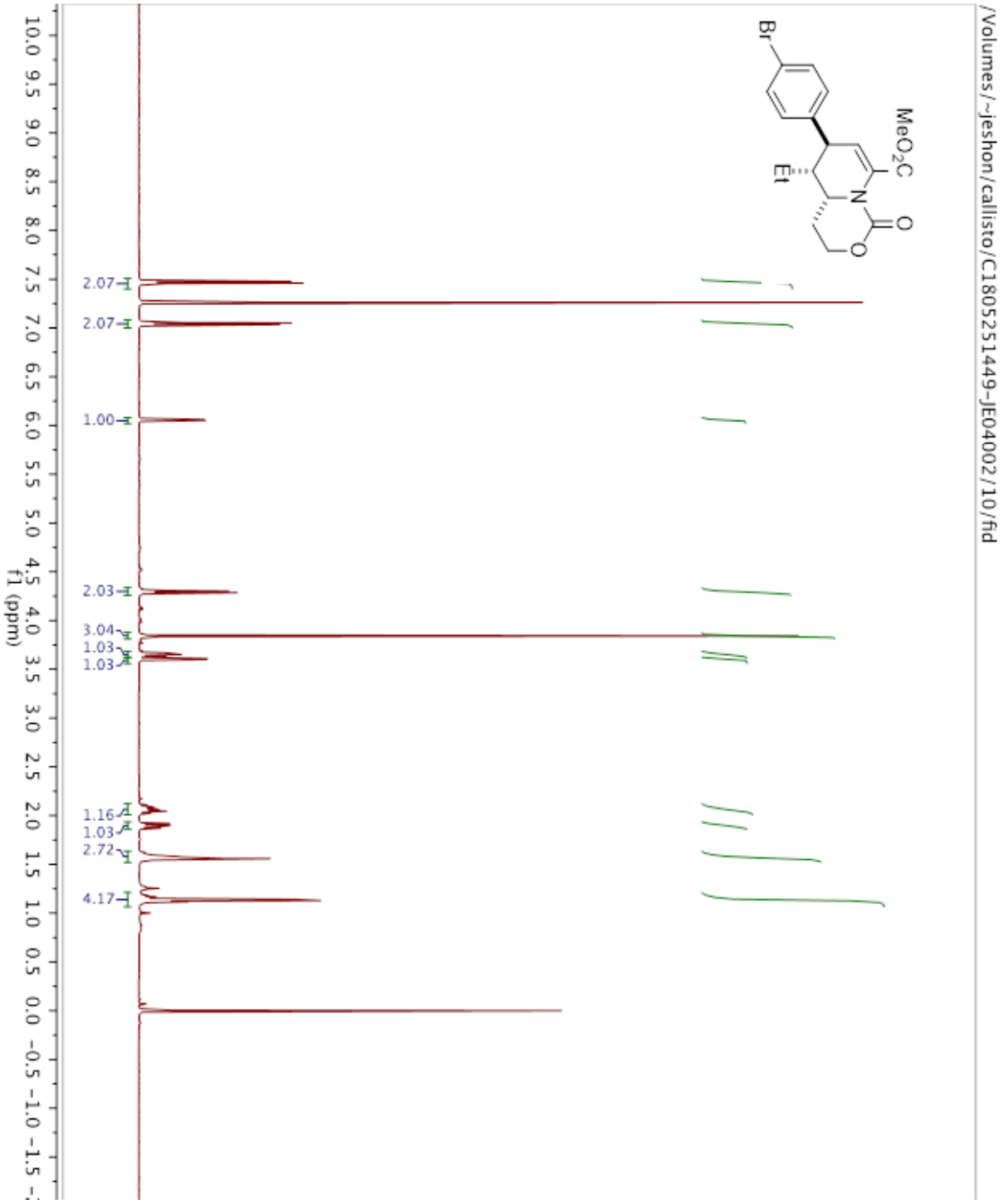
^{1}H NMR (500 MHz, $CDCl_3$) for compound **2.6cb**



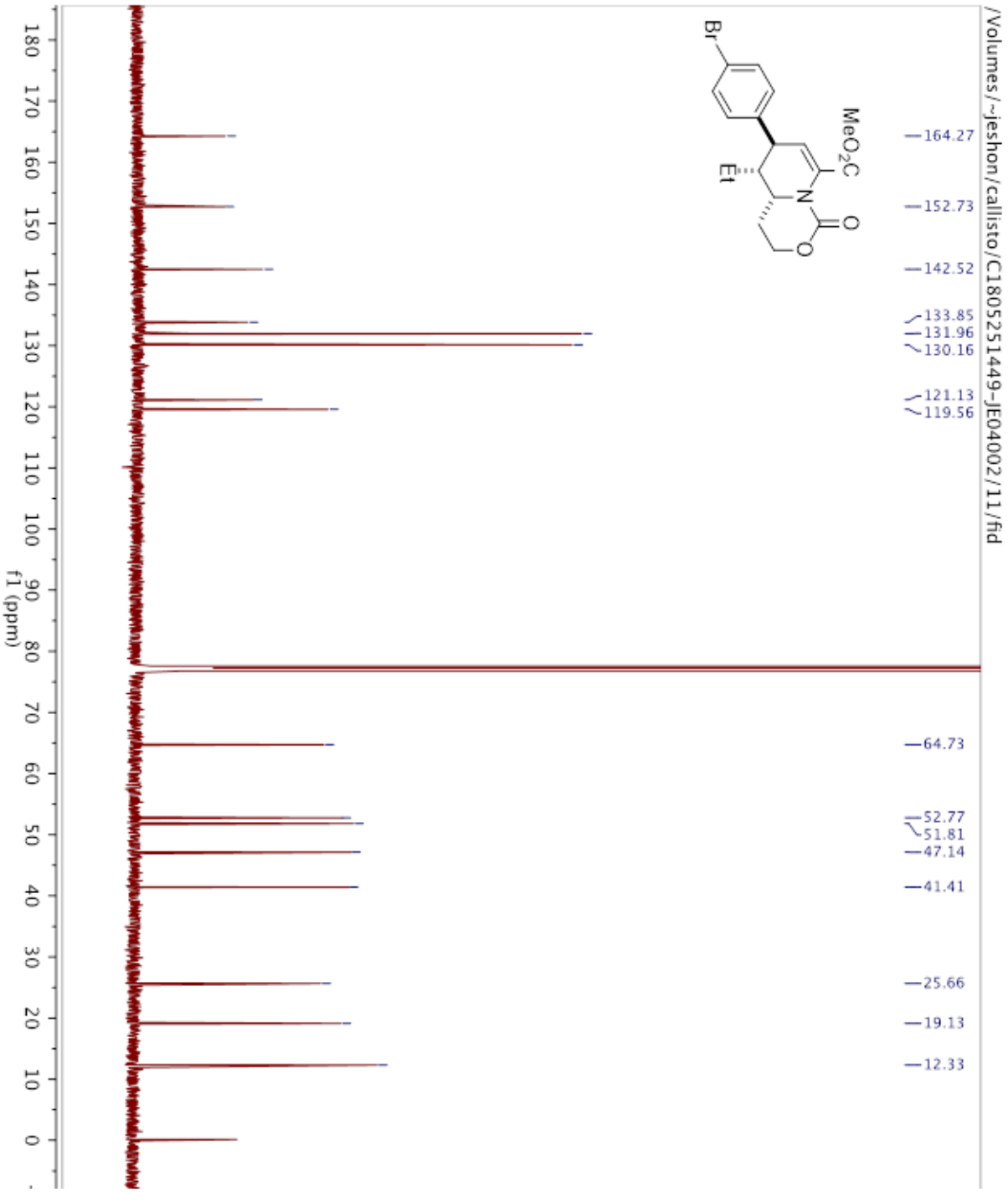
^{13}C NMR (126 MHz, $CDCl_3$) for compound **2.6cb**



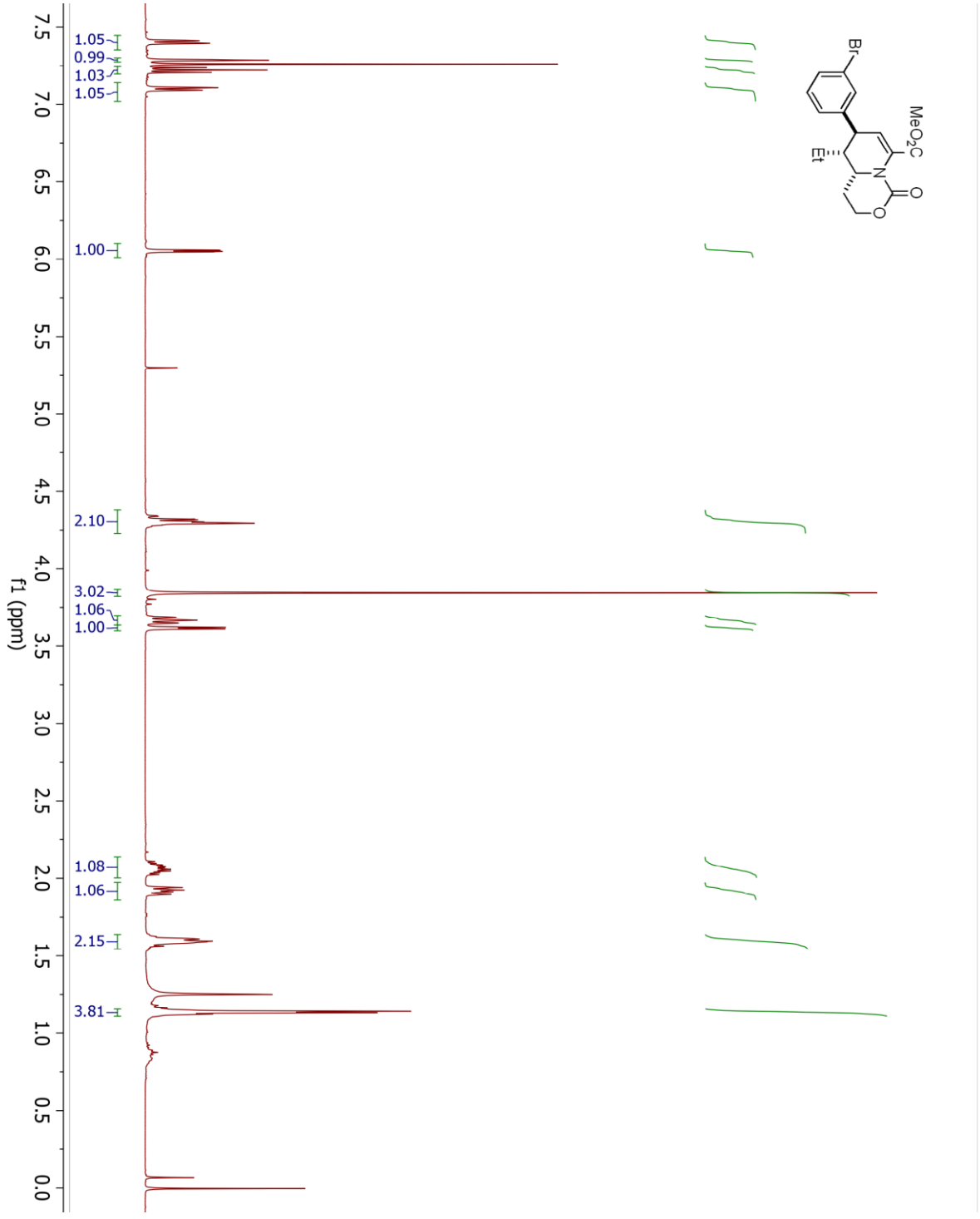
^{1}H NMR (500 MHz, $CDCl_3$) for compound **2.6cc**



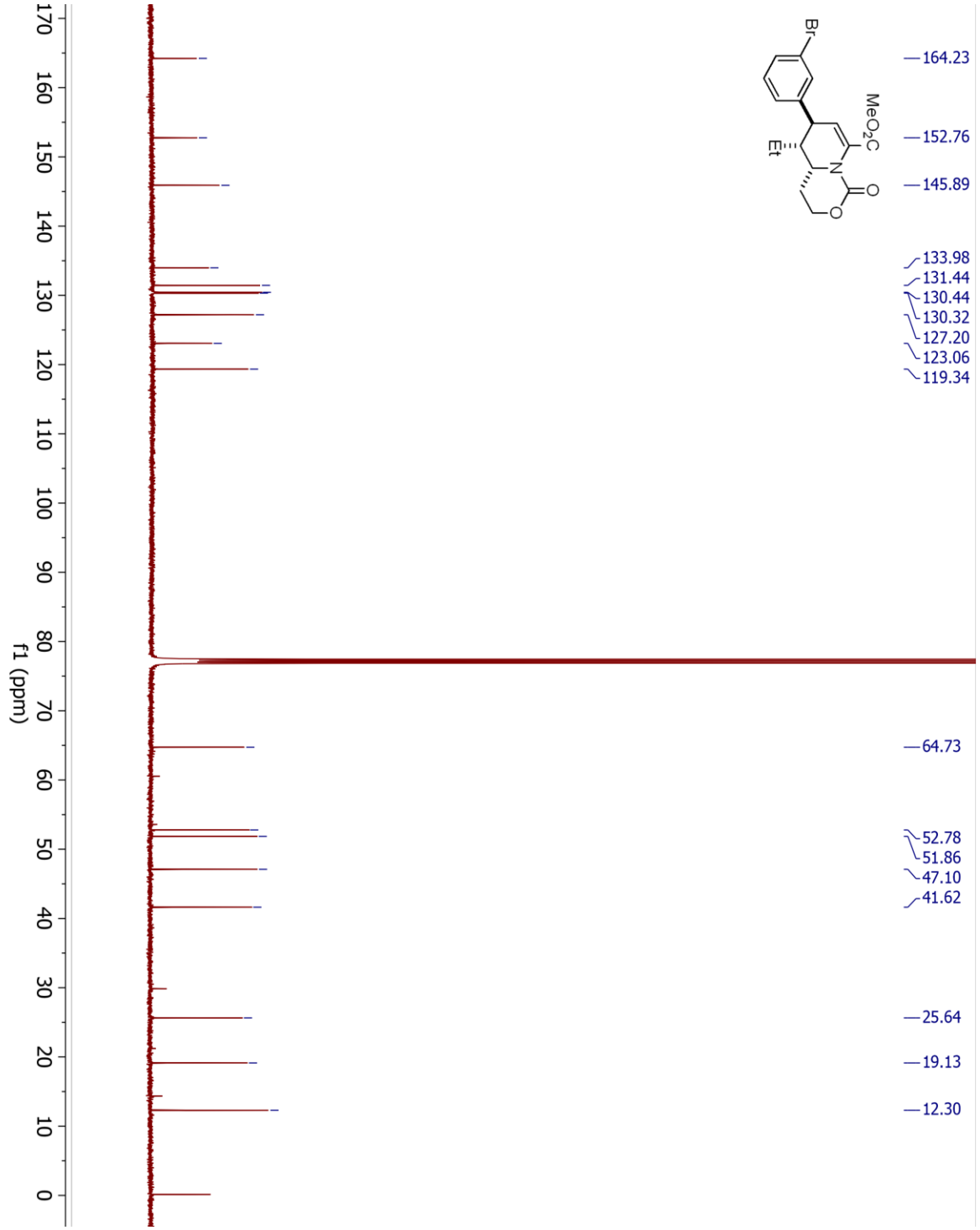
^{13}C NMR (126 MHz, $CDCl_3$) for compound **2.6cc**



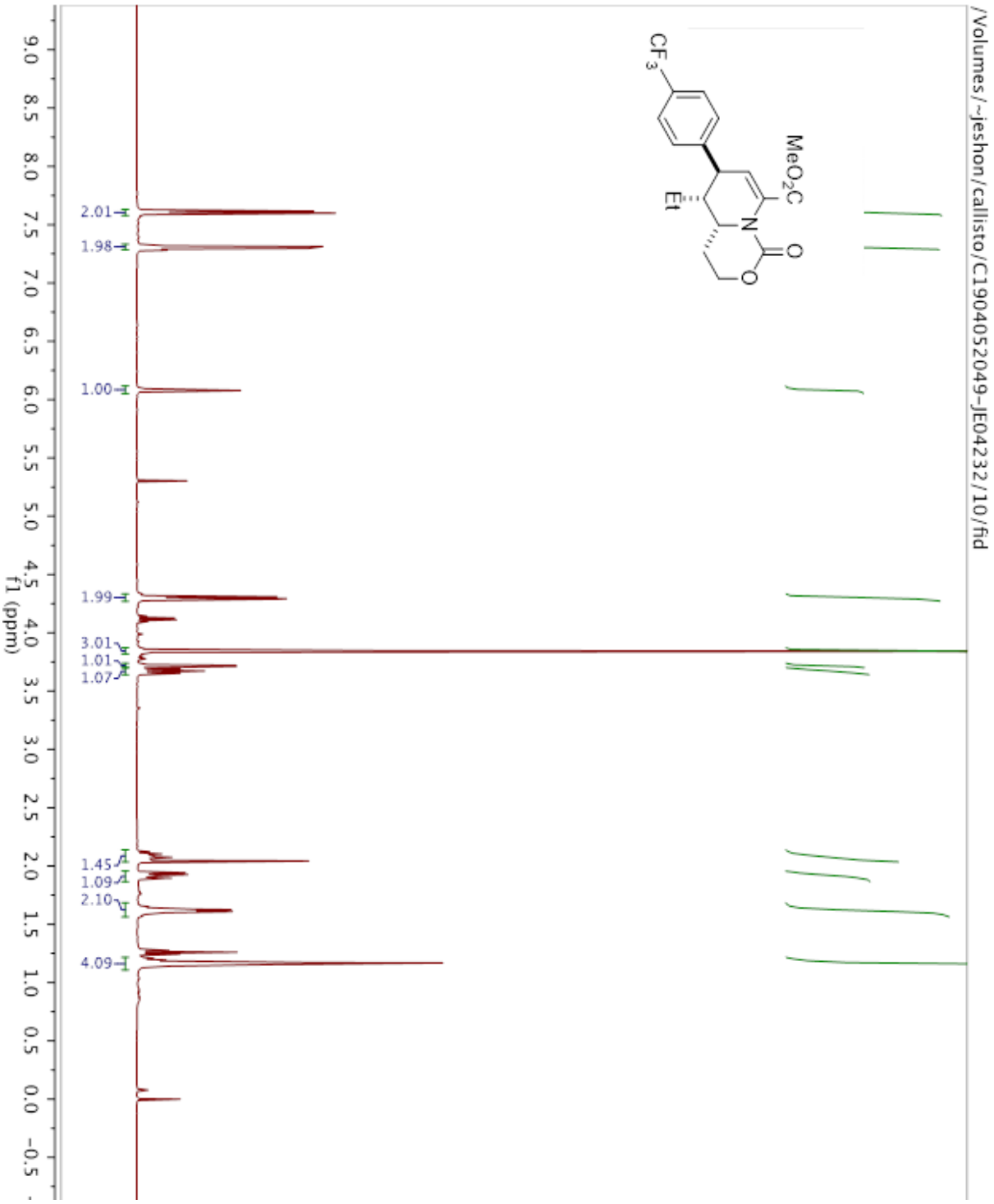
^{1}H NMR (500 MHz, $CDCl_3$) for compound **2.6cd**



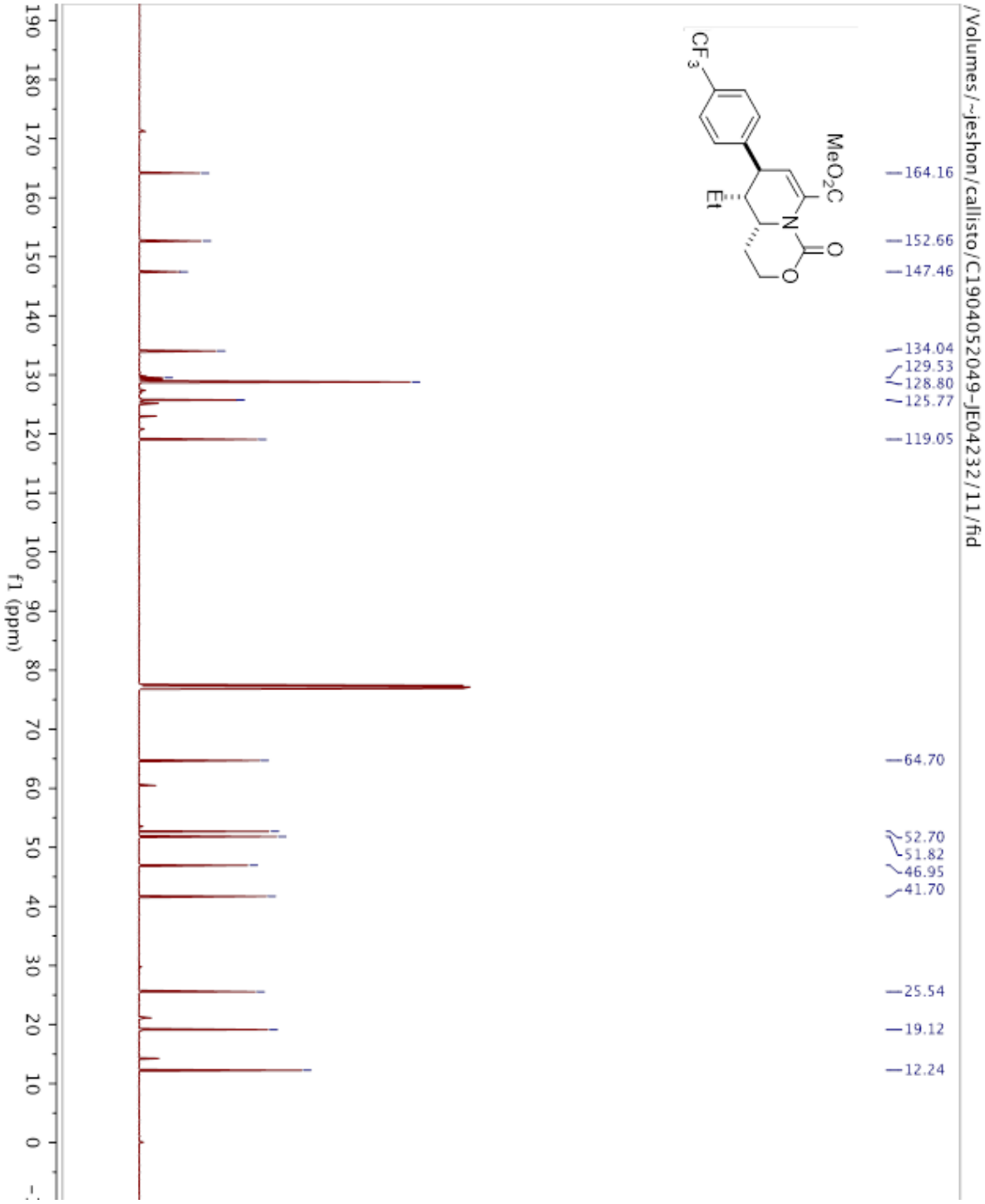
^{13}C NMR (126 MHz, $CDCl_3$) for compound **2.6cd**



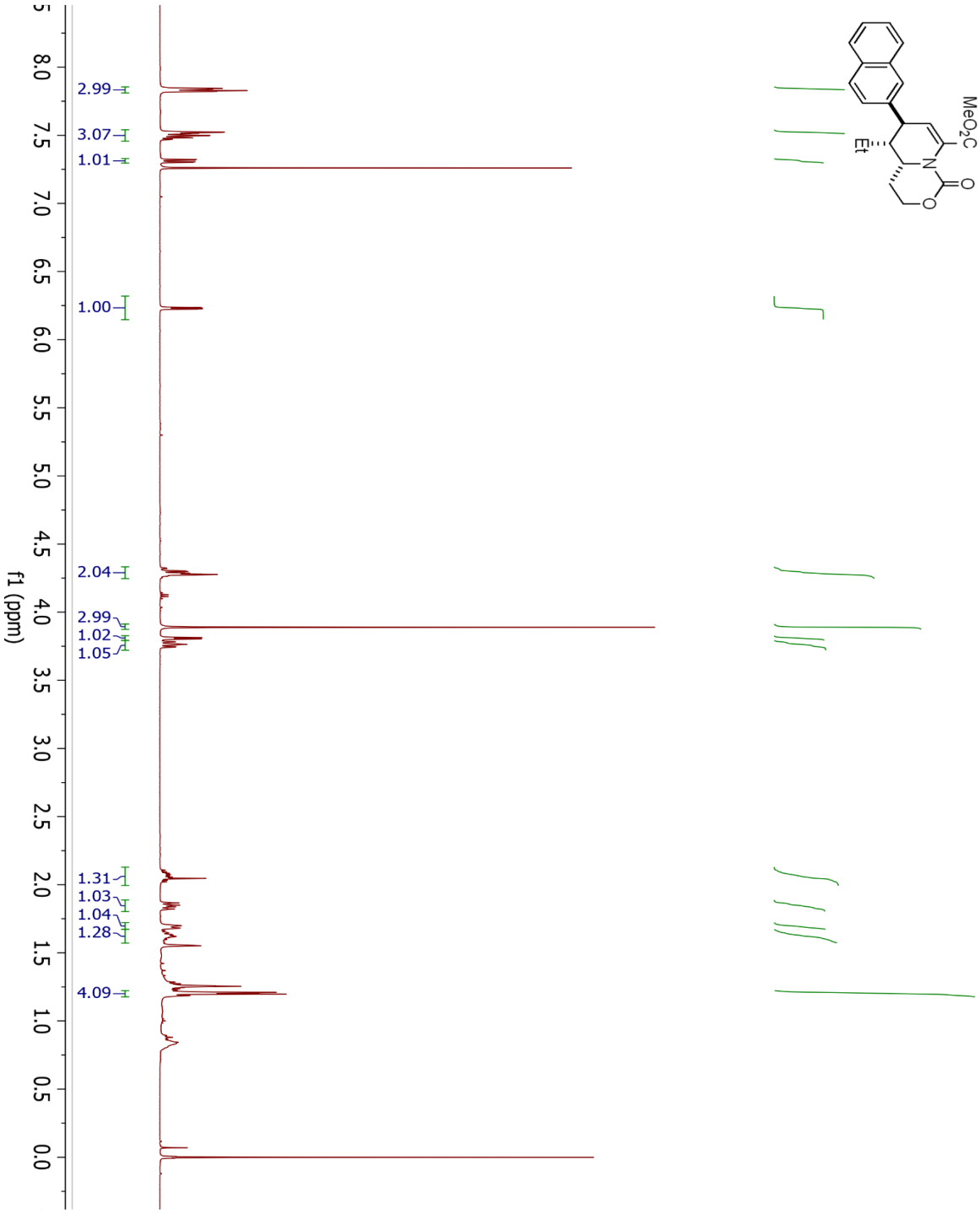
^{1}H NMR (500 MHz, $CDCl_3$) for compound **2.6ce**



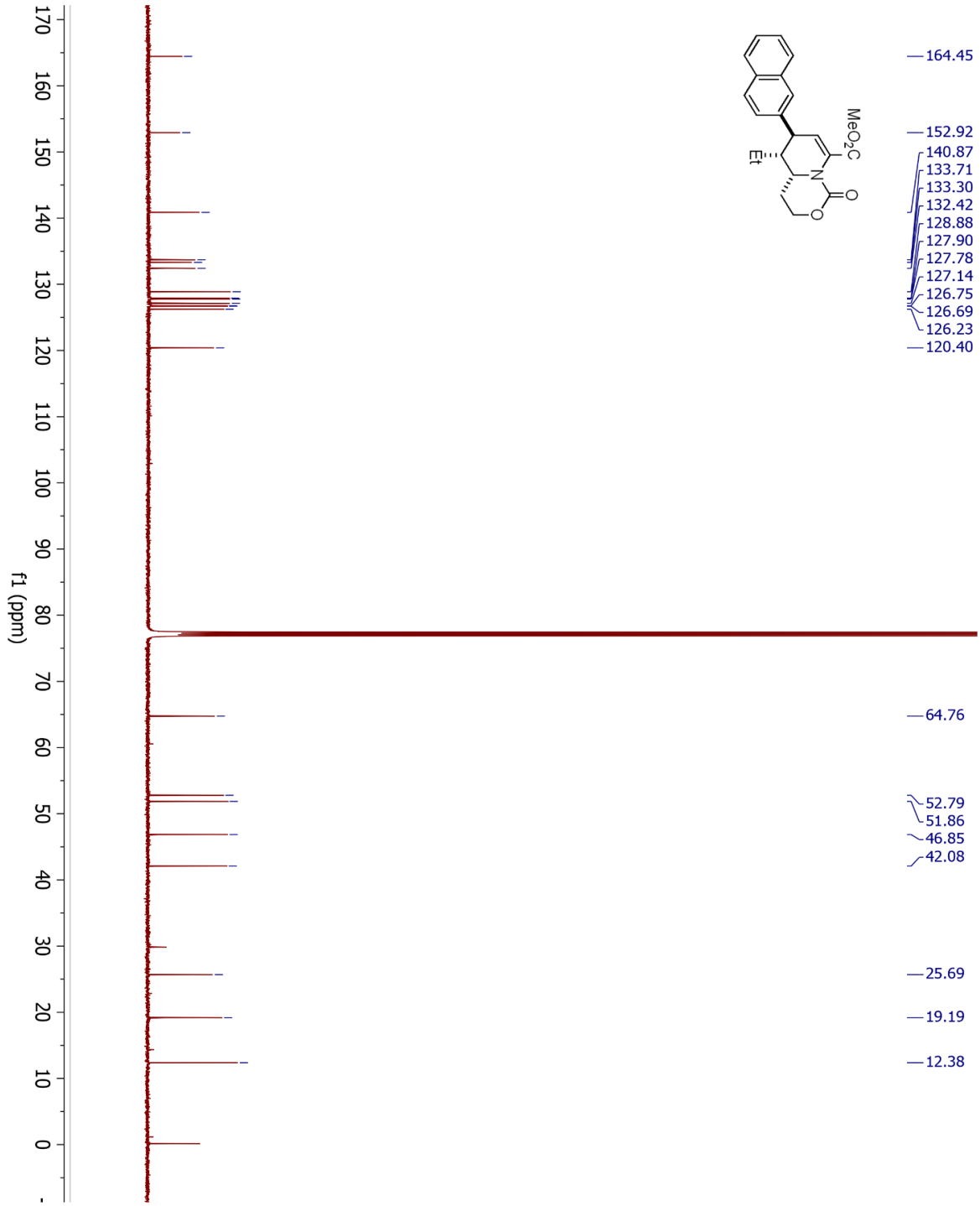
^{13}C NMR (126 MHz, $CDCl_3$) for compound **2.6ce**



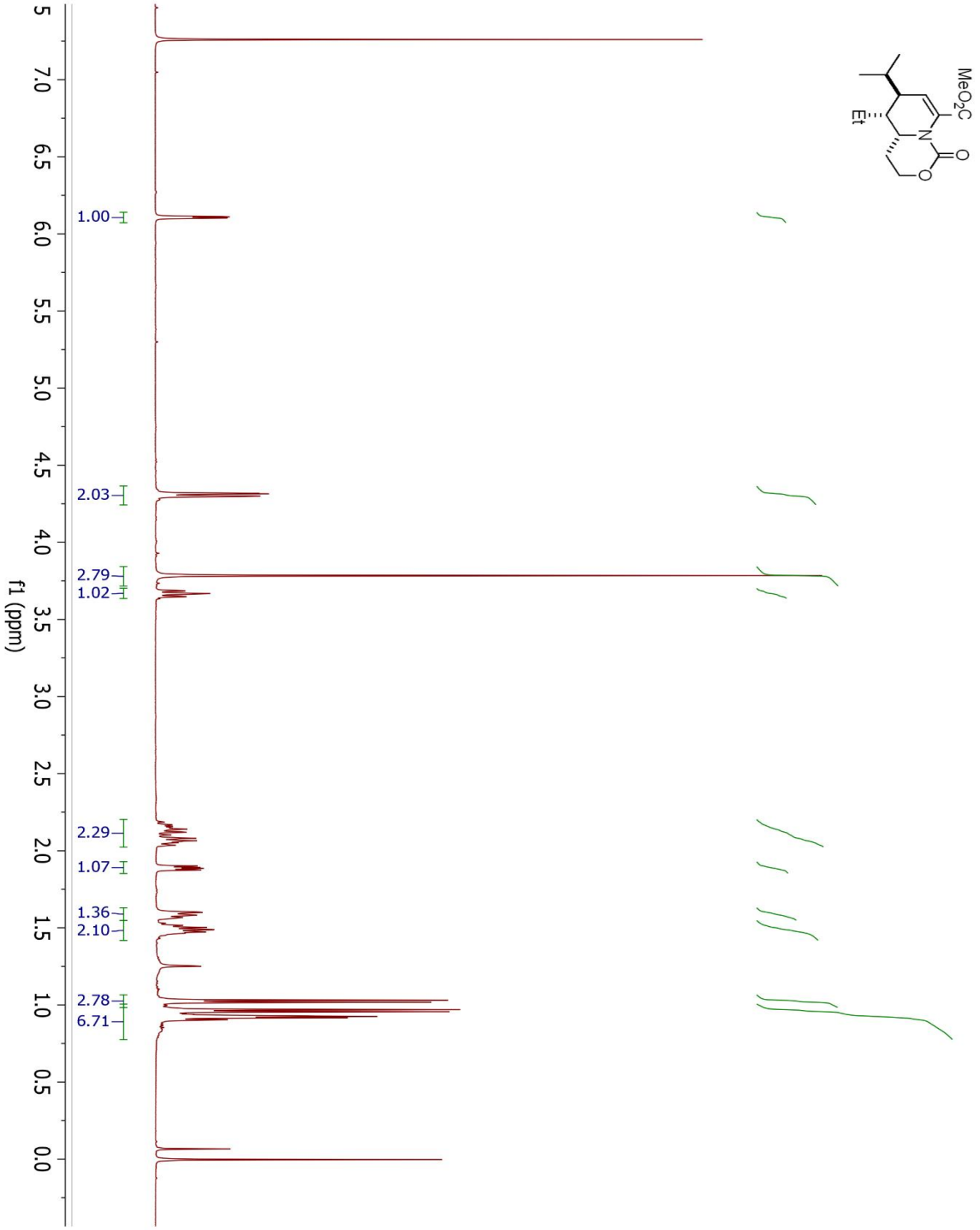
^{1}H NMR (500 MHz, $CDCl_3$) for compound **2.6cf**



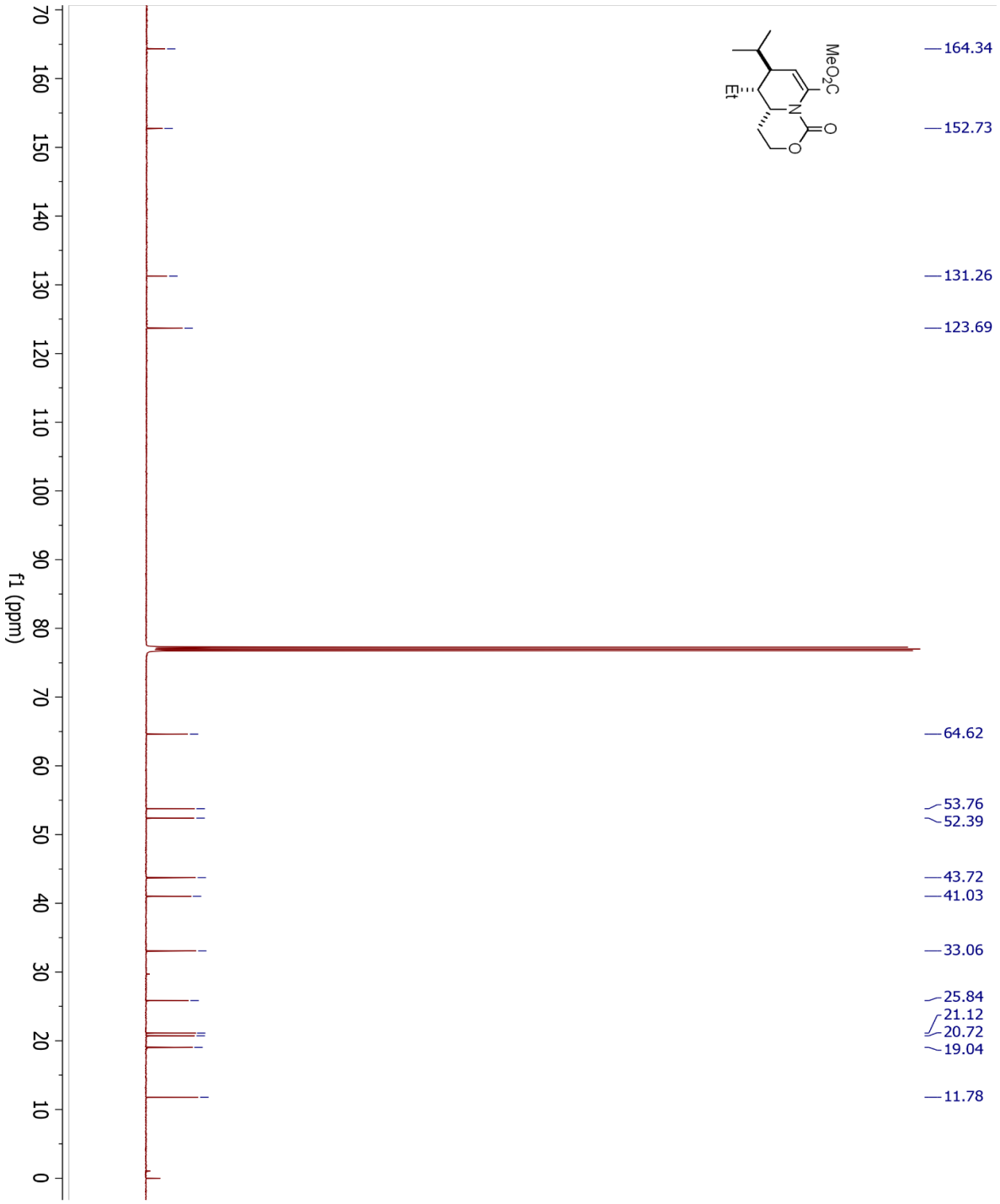
^{13}C NMR (126 MHz, $CDCl_3$) for compound **2.6cf**



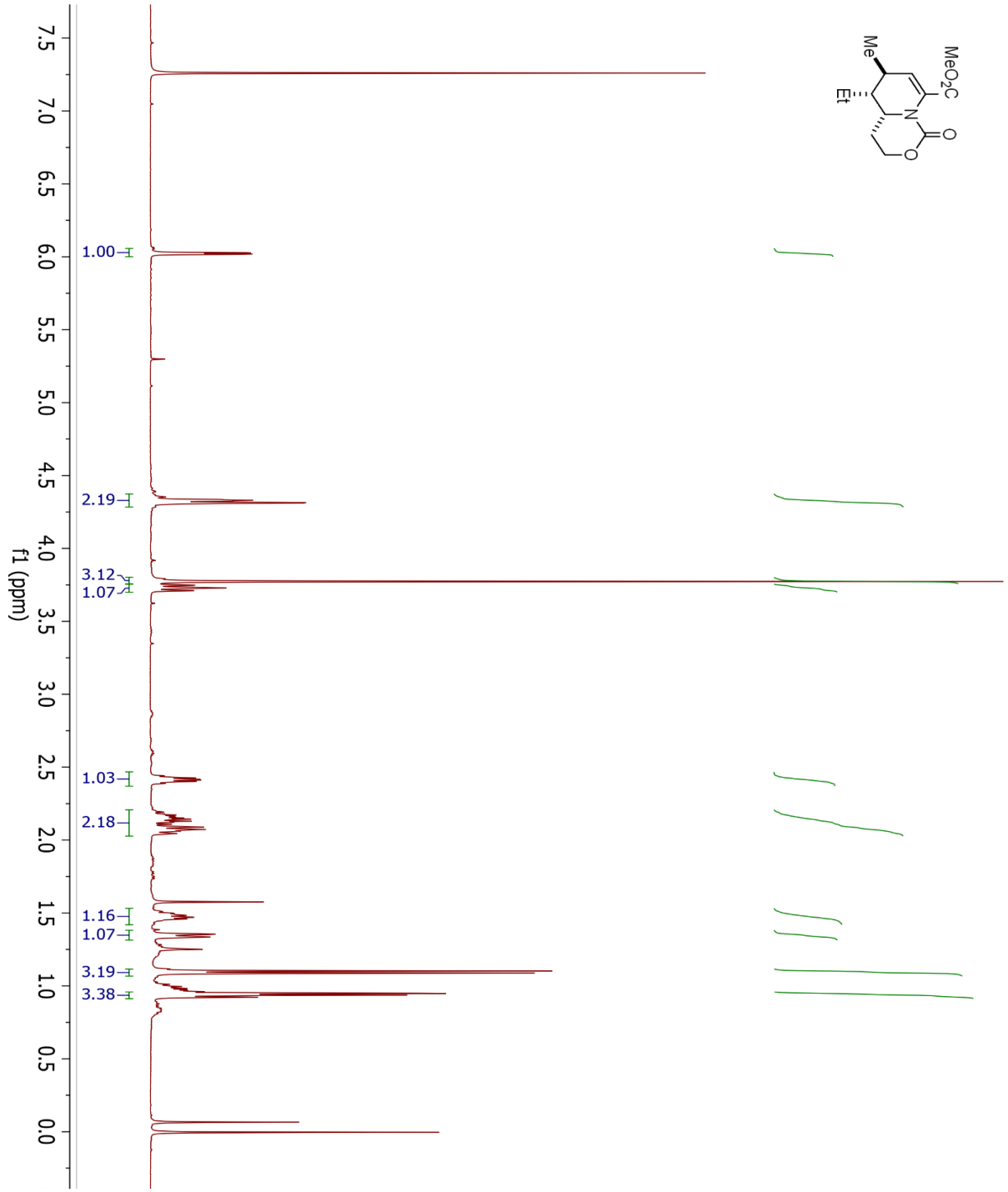
^{1}H NMR (500 MHz, $CDCl_3$) for compound **2.6cg**



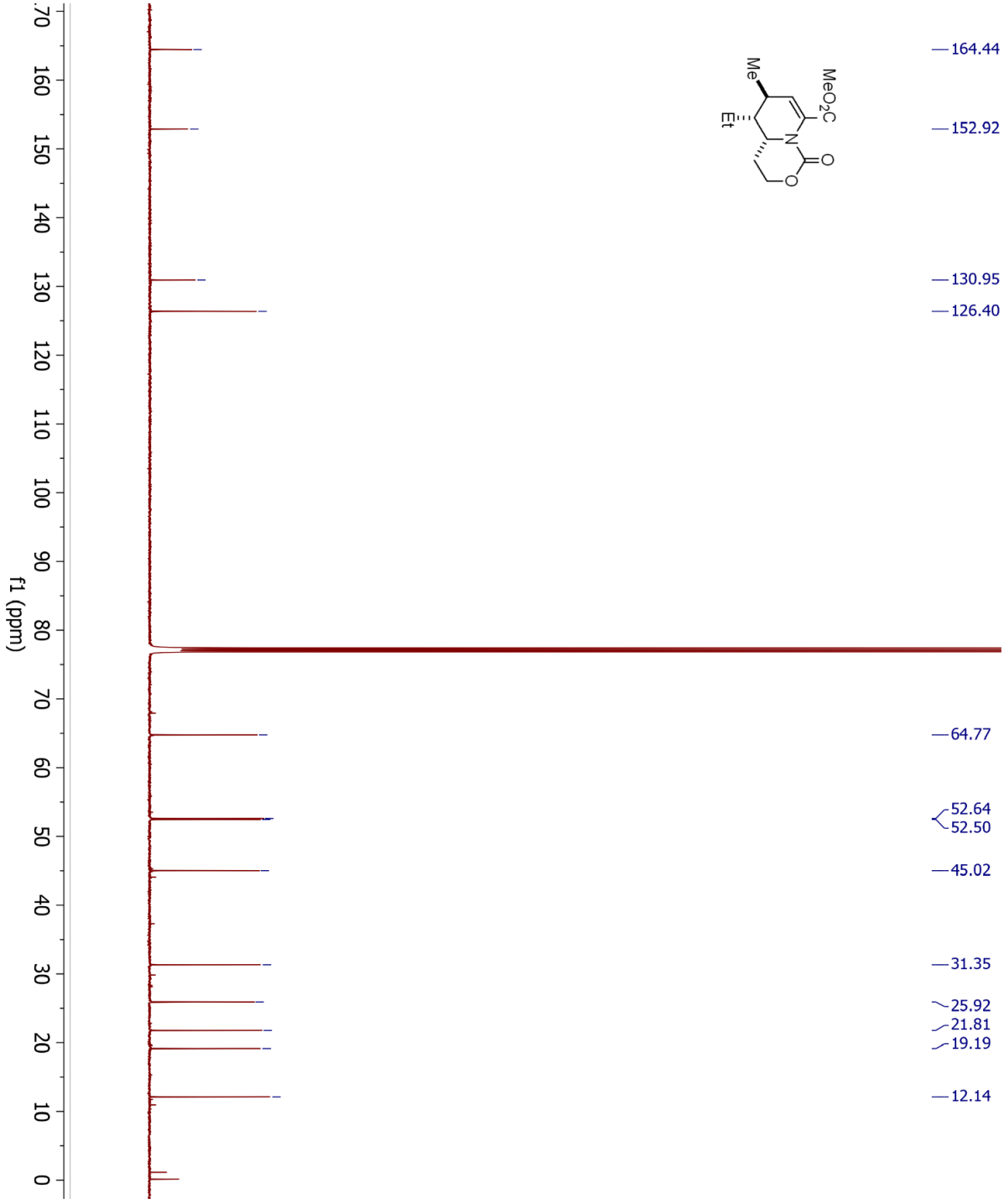
^{13}C NMR (126 MHz, $CDCl_3$) for compound **2.6cg**



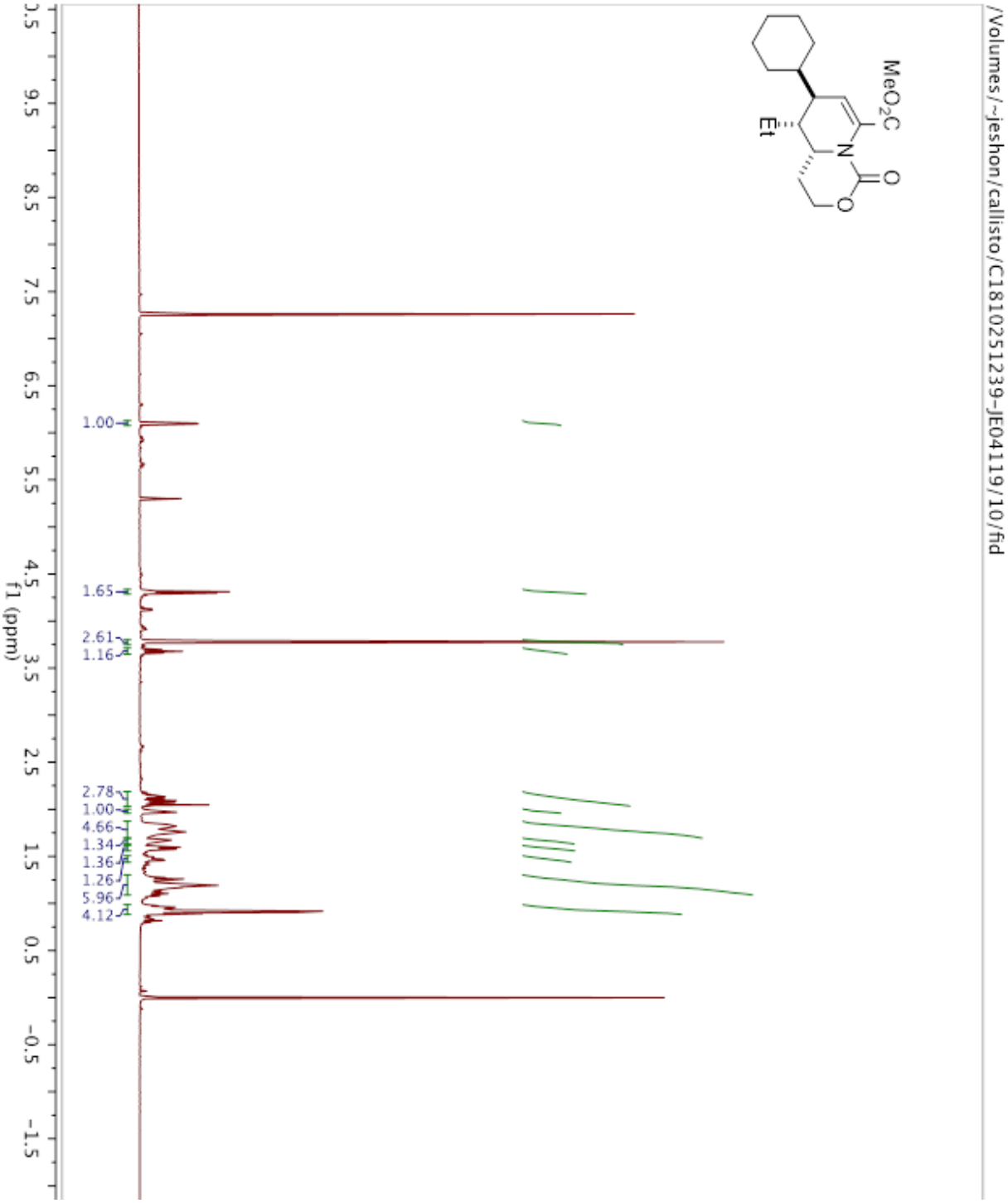
^{1}H NMR (500 MHz, $CDCl_3$) for Compound **2.6ch**



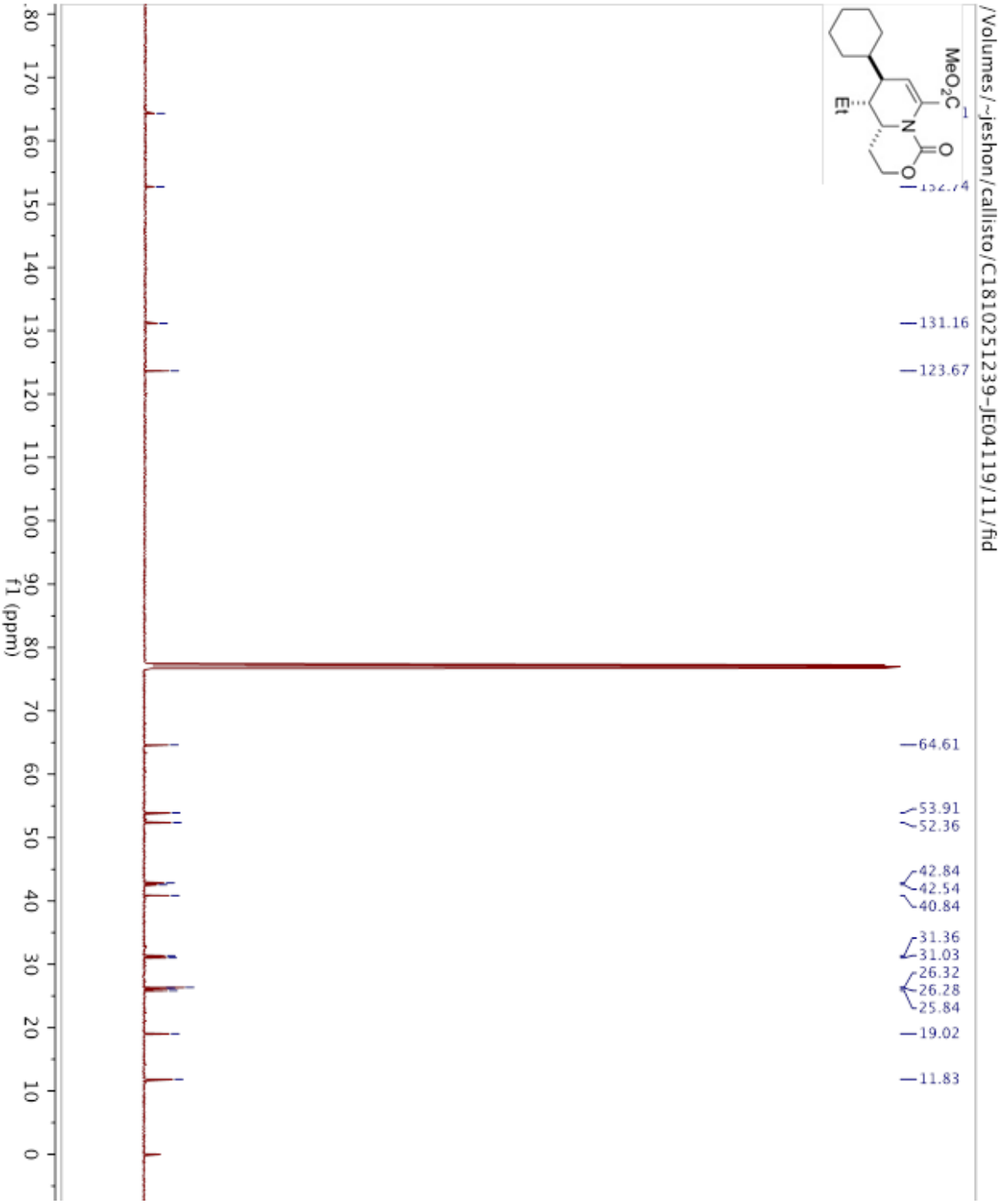
^{13}C NMR (126 MHz, $CDCl_3$) for compound **2.6ch**



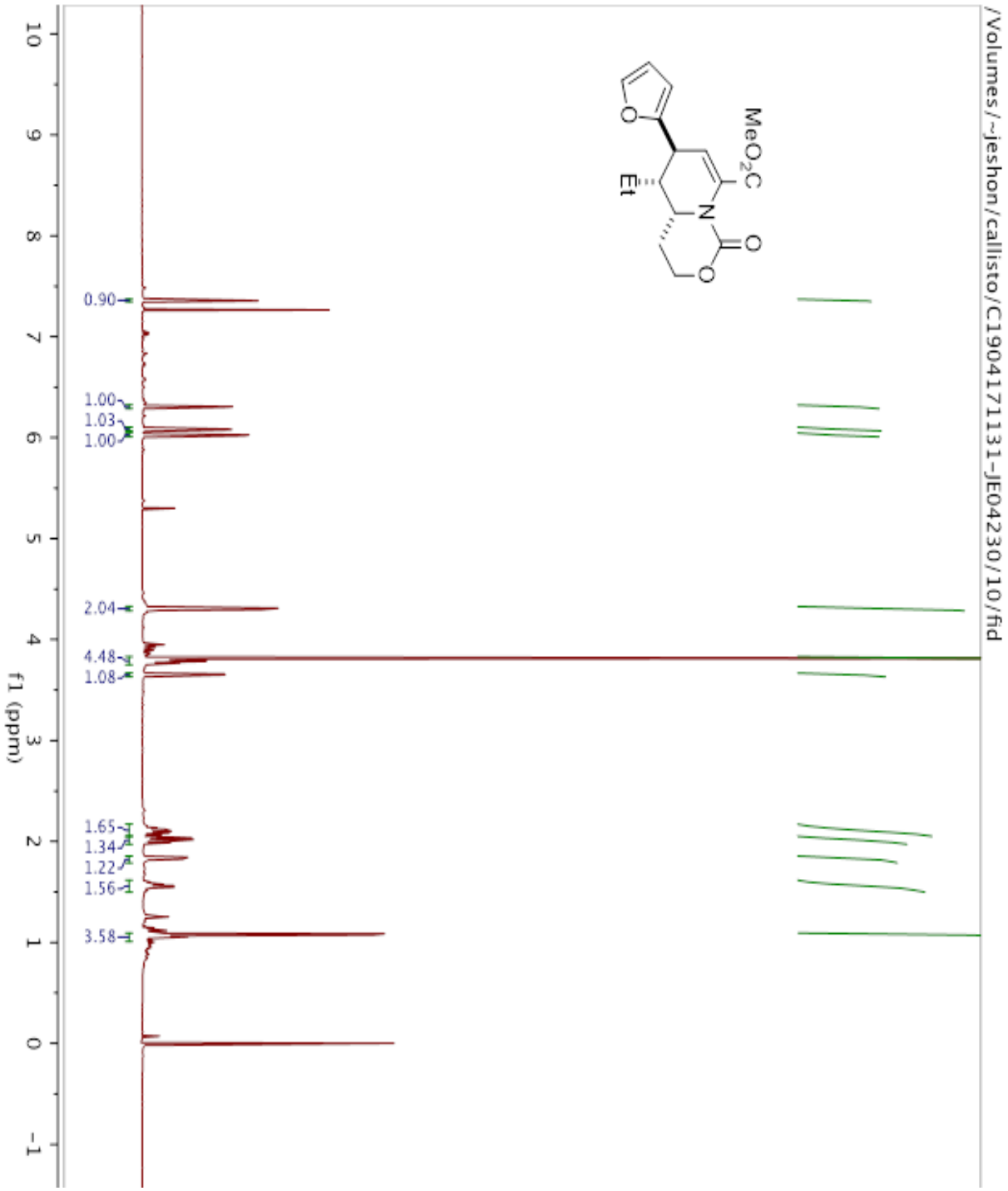
^{1}H NMR (500 MHz, $CDCl_3$) for compound **2.6ci**



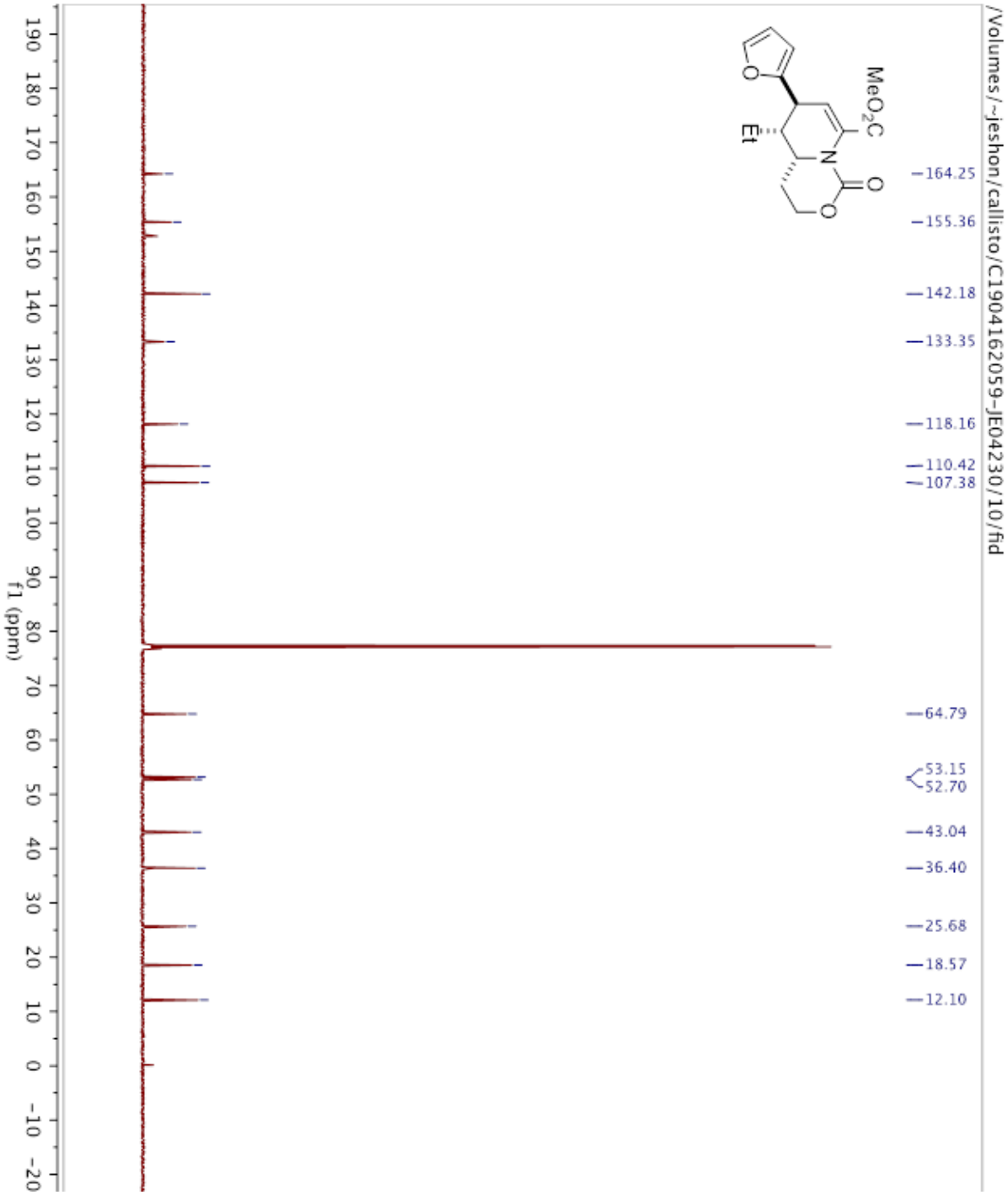
^{13}C NMR (126 MHz, $CDCl_3$) for compound **2.6ci**



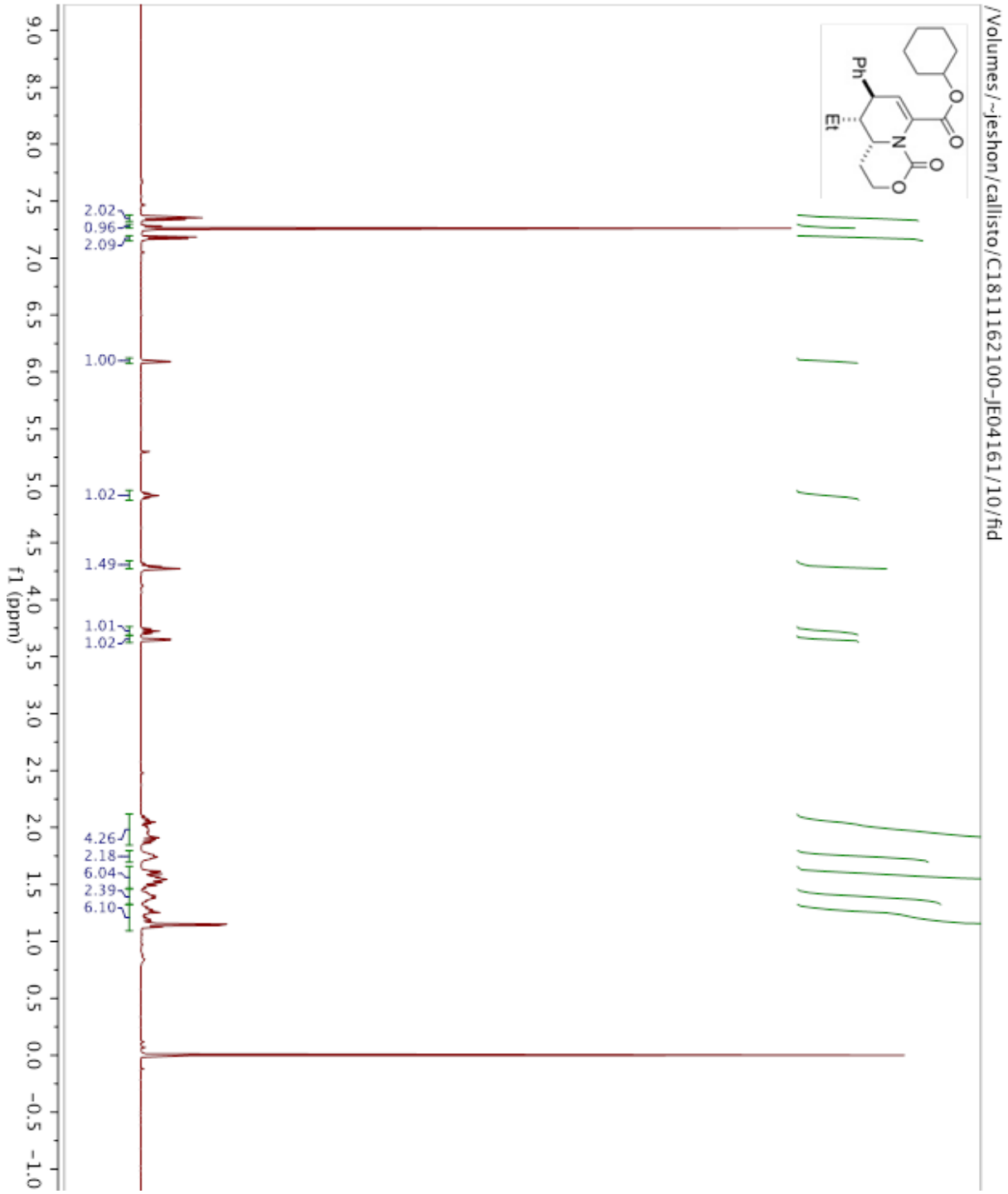
^{1}H NMR (500 MHz, $CDCl_3$) for compound **2.6cj**



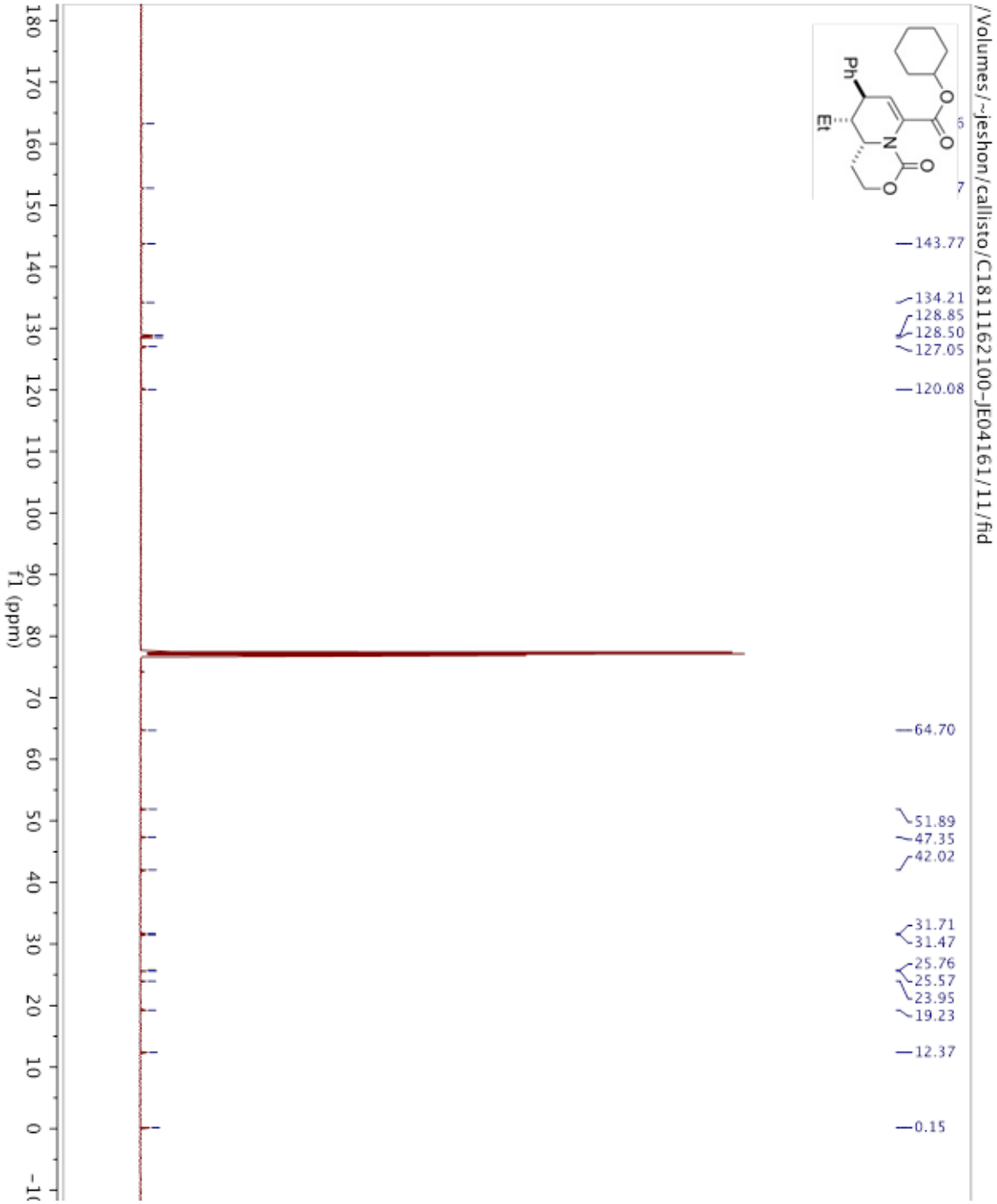
^{13}C NMR (126 MHz, $CDCl_3$) for compound **2.6cj**



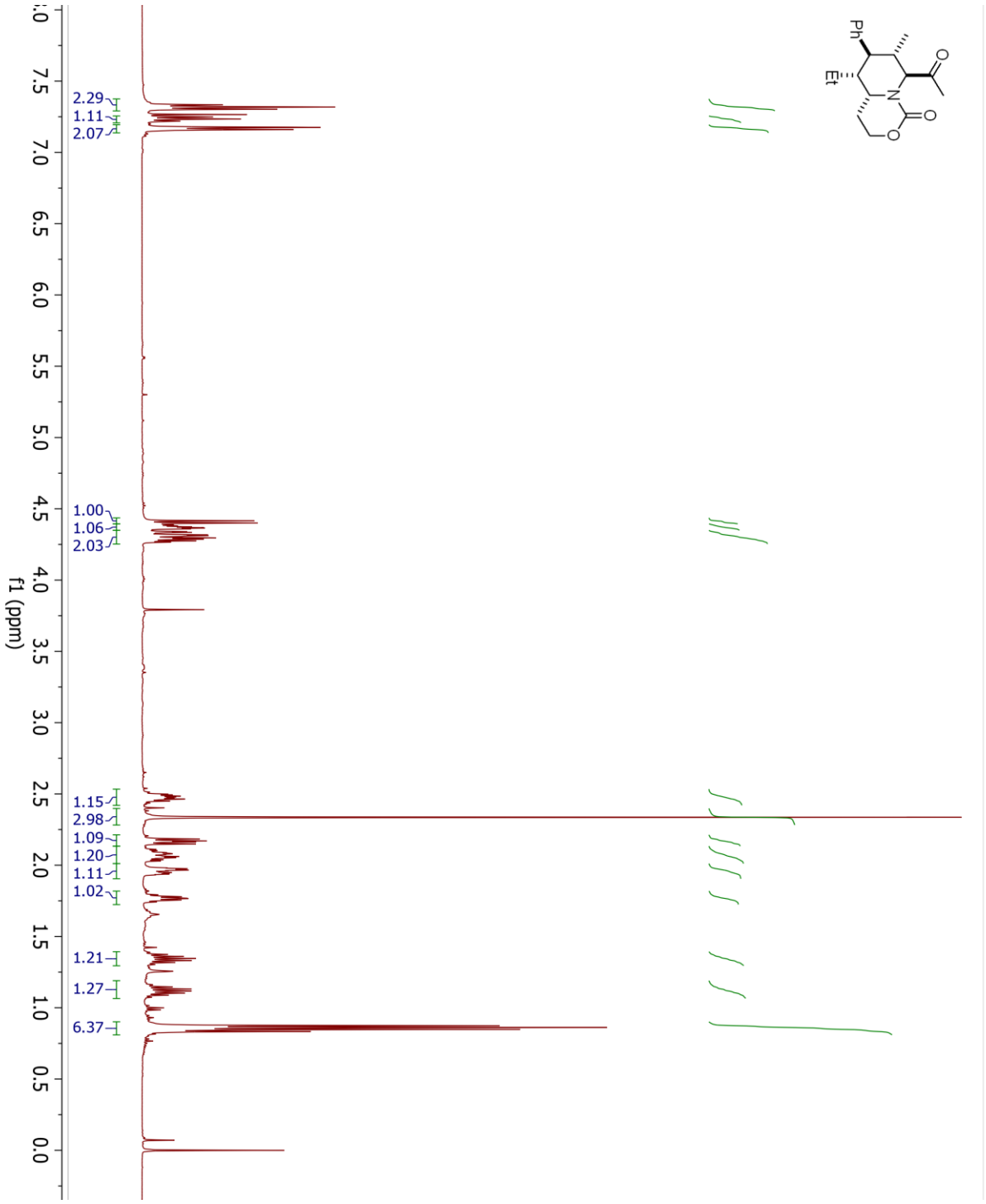
^{1}H NMR (500 MHz, $CDCl_3$) for compound **2.6ck**



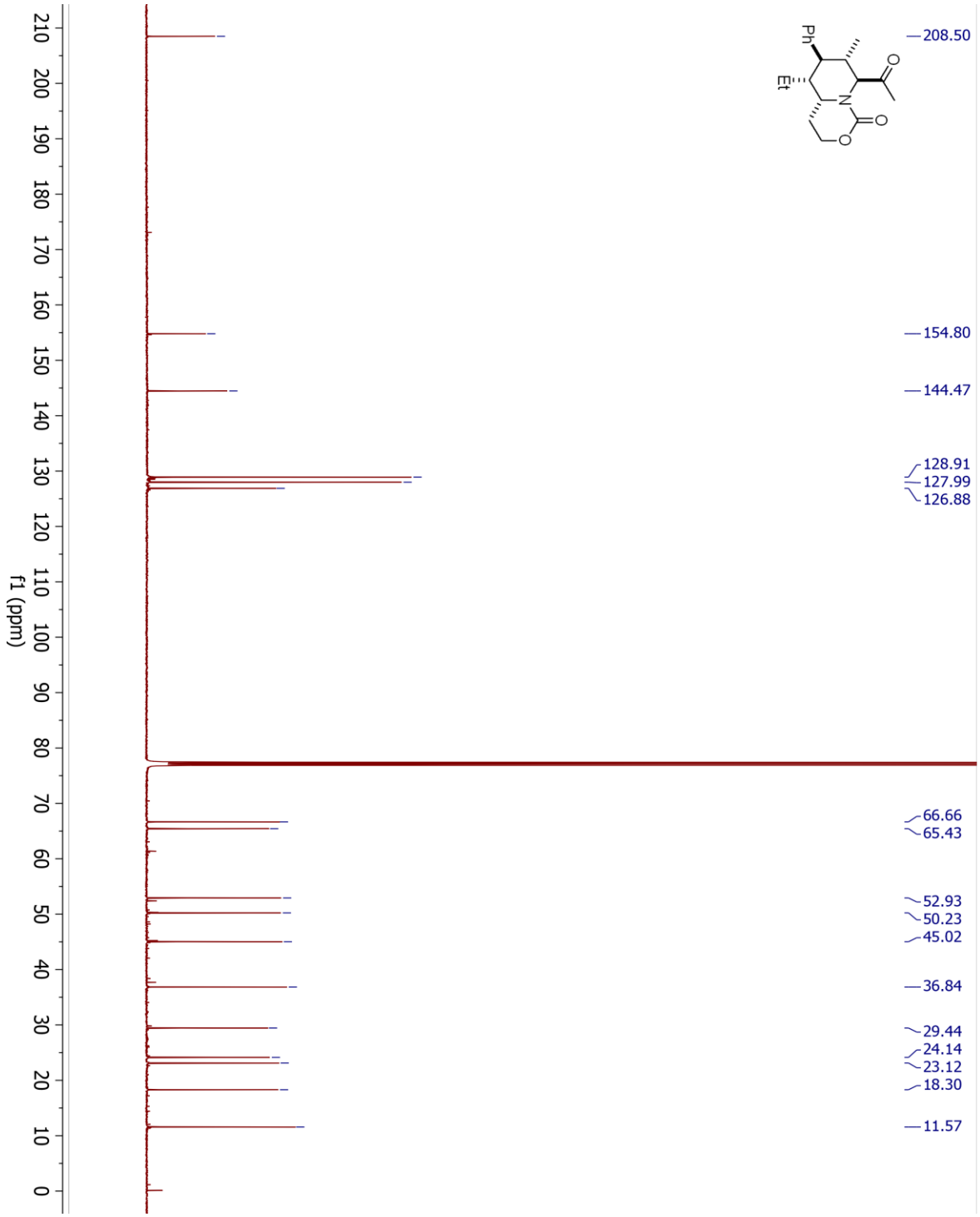
^{13}C NMR (126 MHz, $CDCl_3$) for compound **2.6ck**



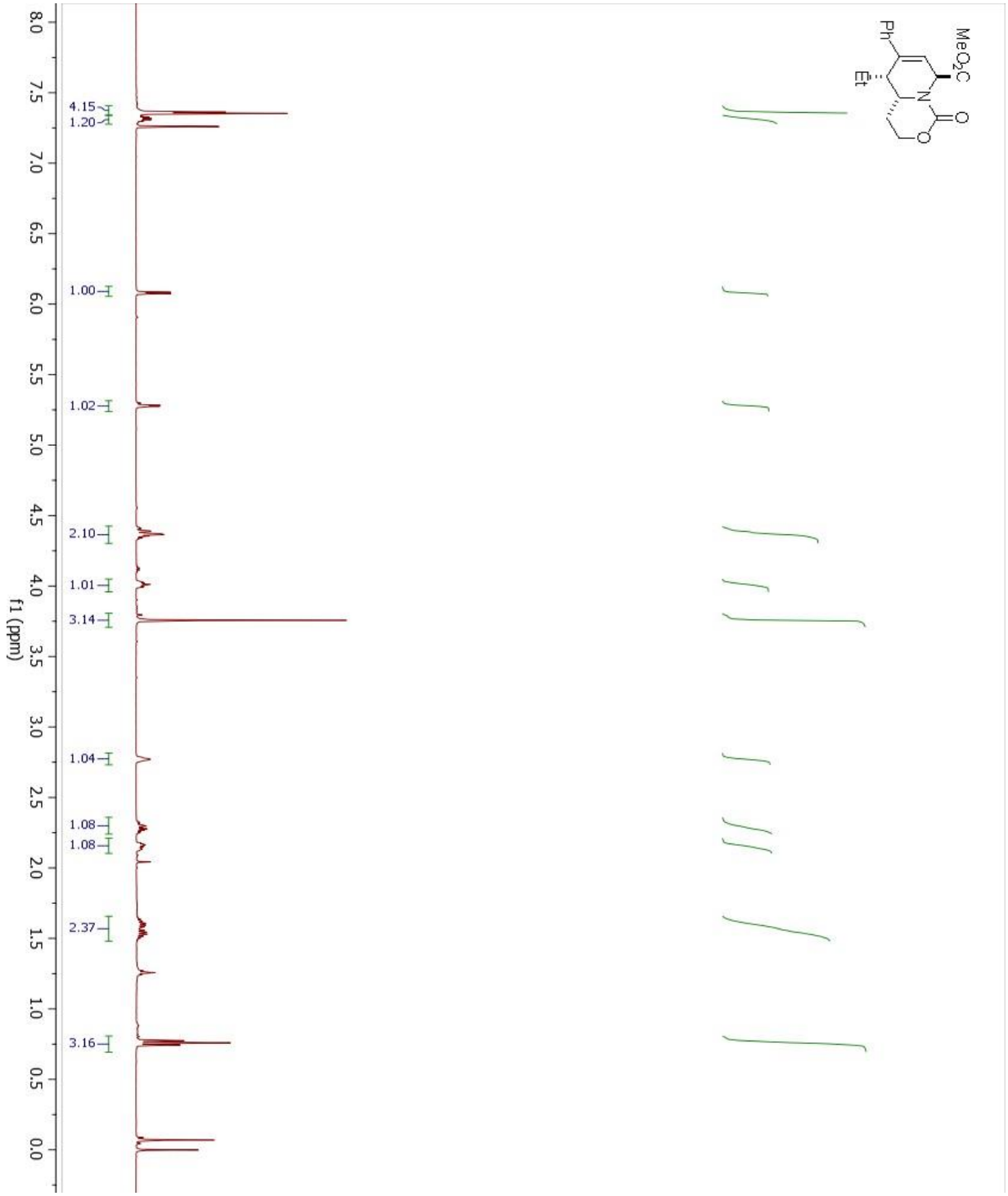
^{1}H NMR (500 MHz, $CDCl_3$) for compound **2.11**



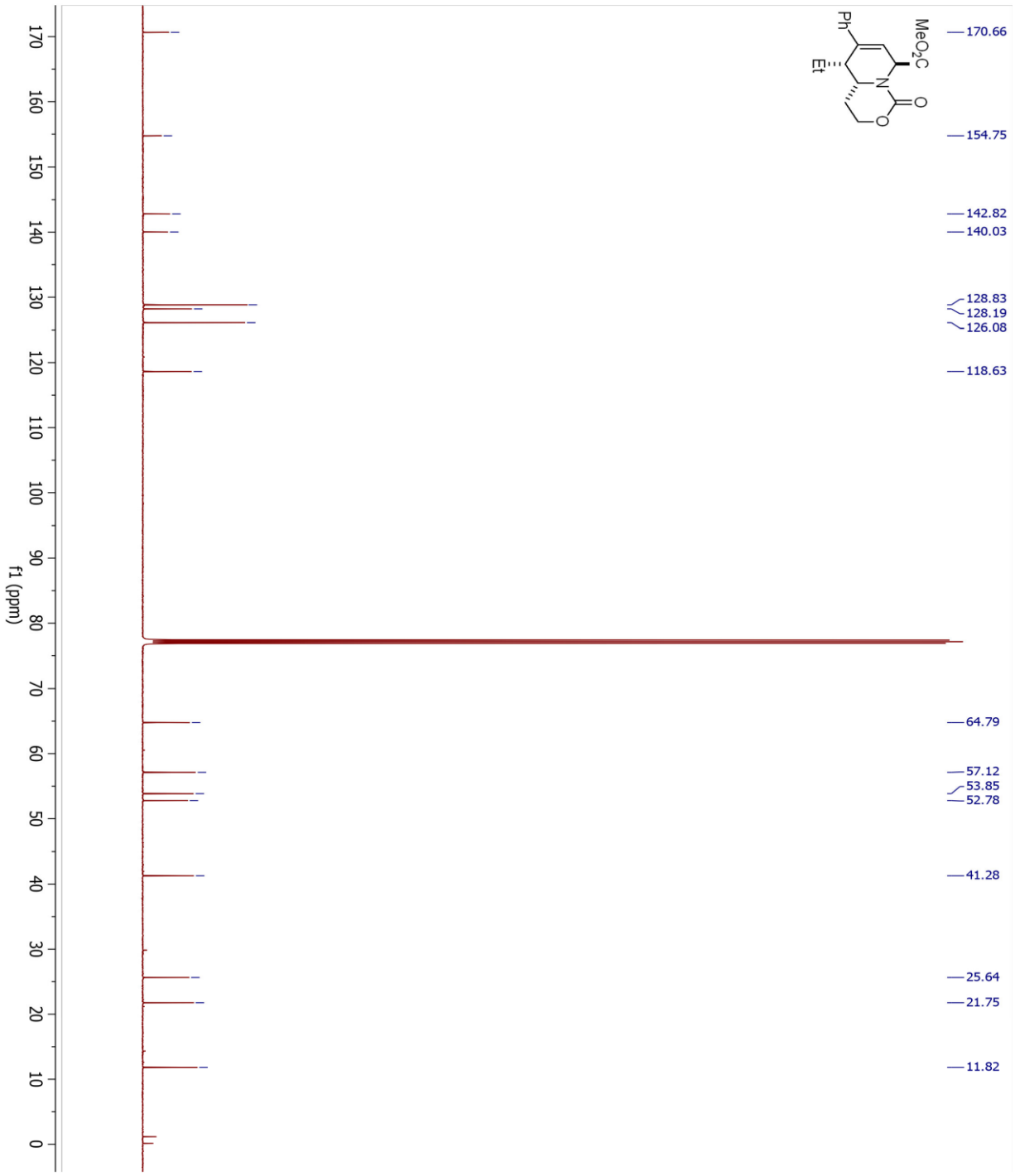
^{13}C NMR (126 MHz, $CDCl_3$) for compound **2.11**



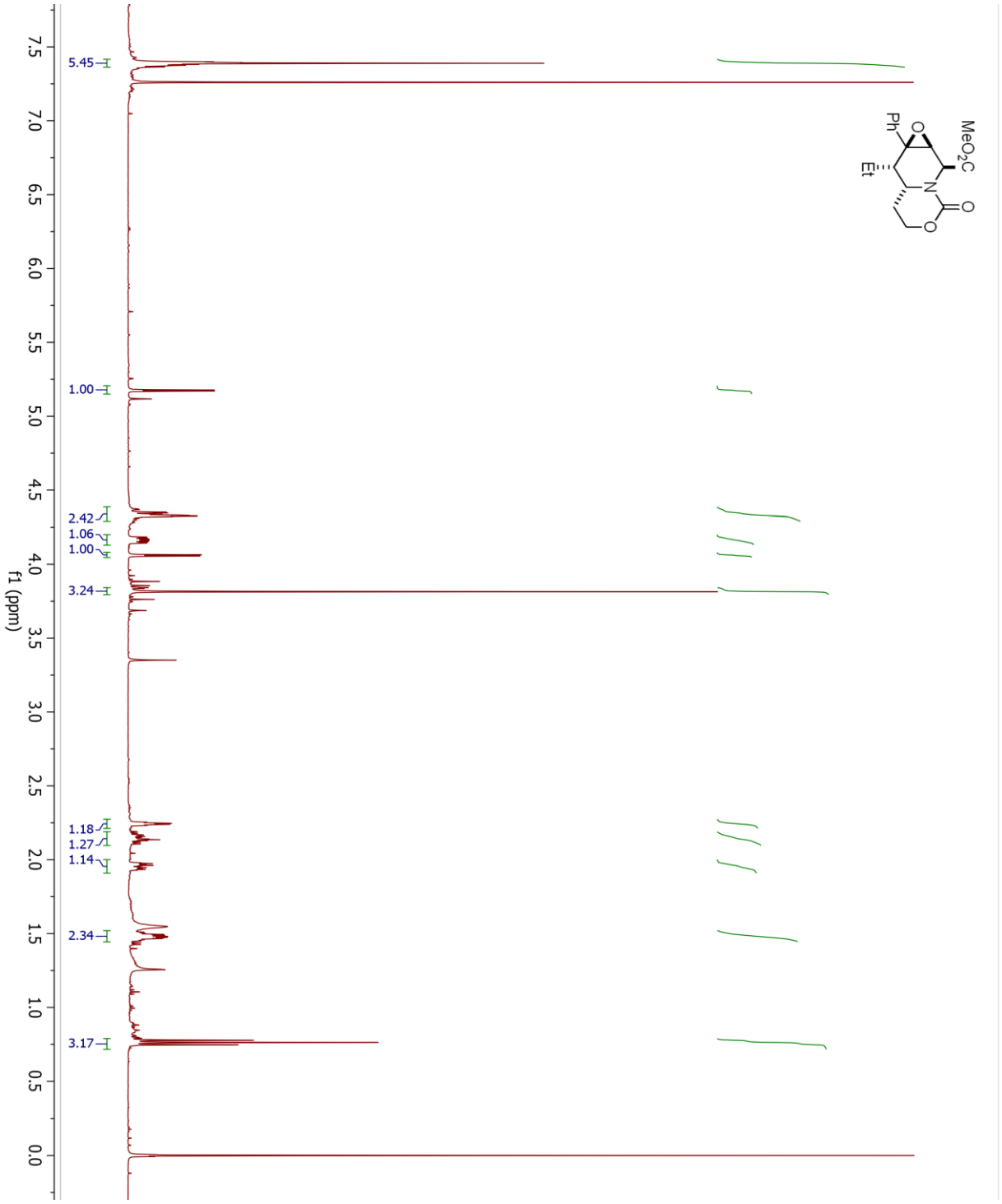
^{1}H NMR (500 MHz, $CDCl_3$) for compound **2.9**



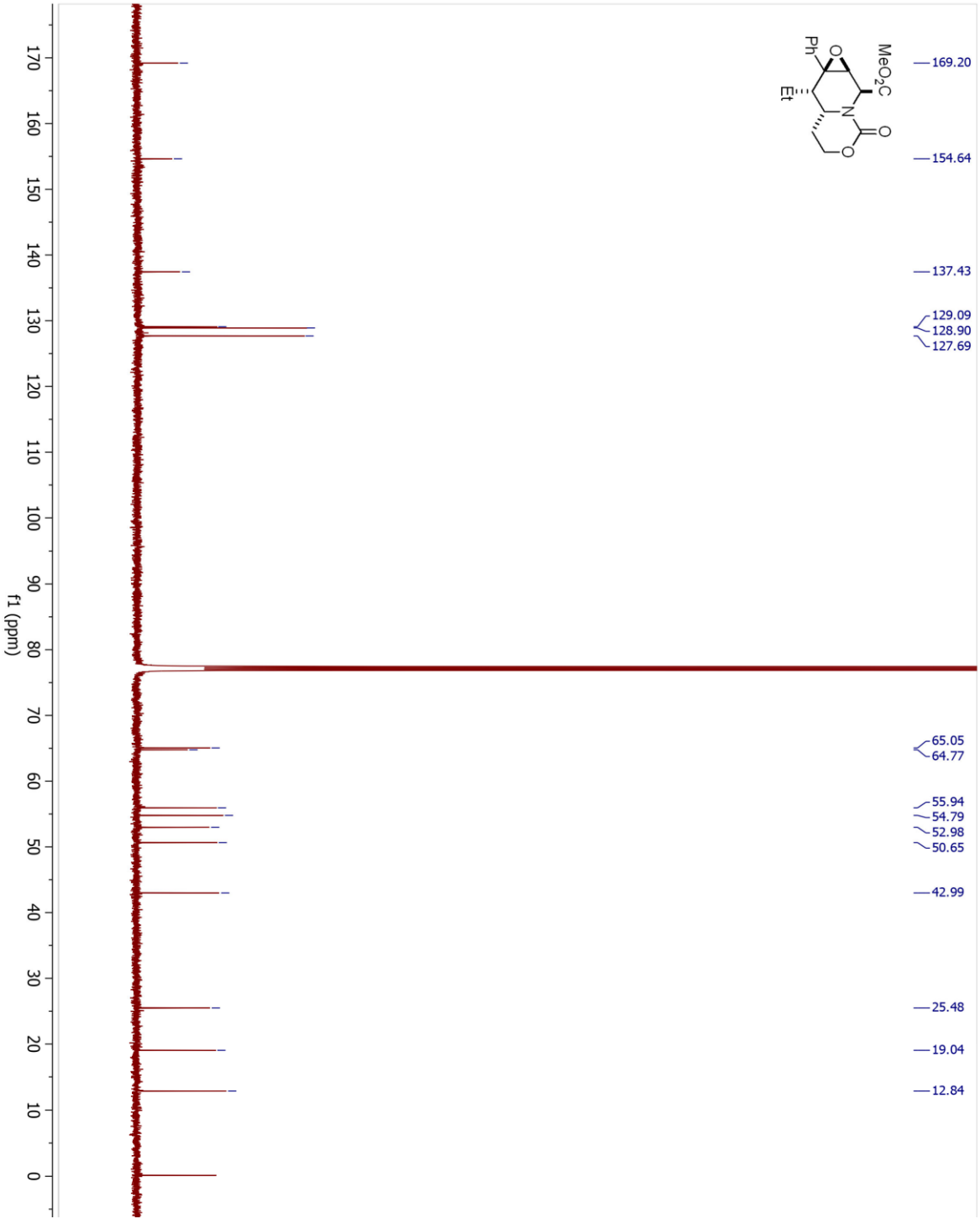
^{13}C NMR (126 MHz, $CDCl_3$) for compound **2.9**



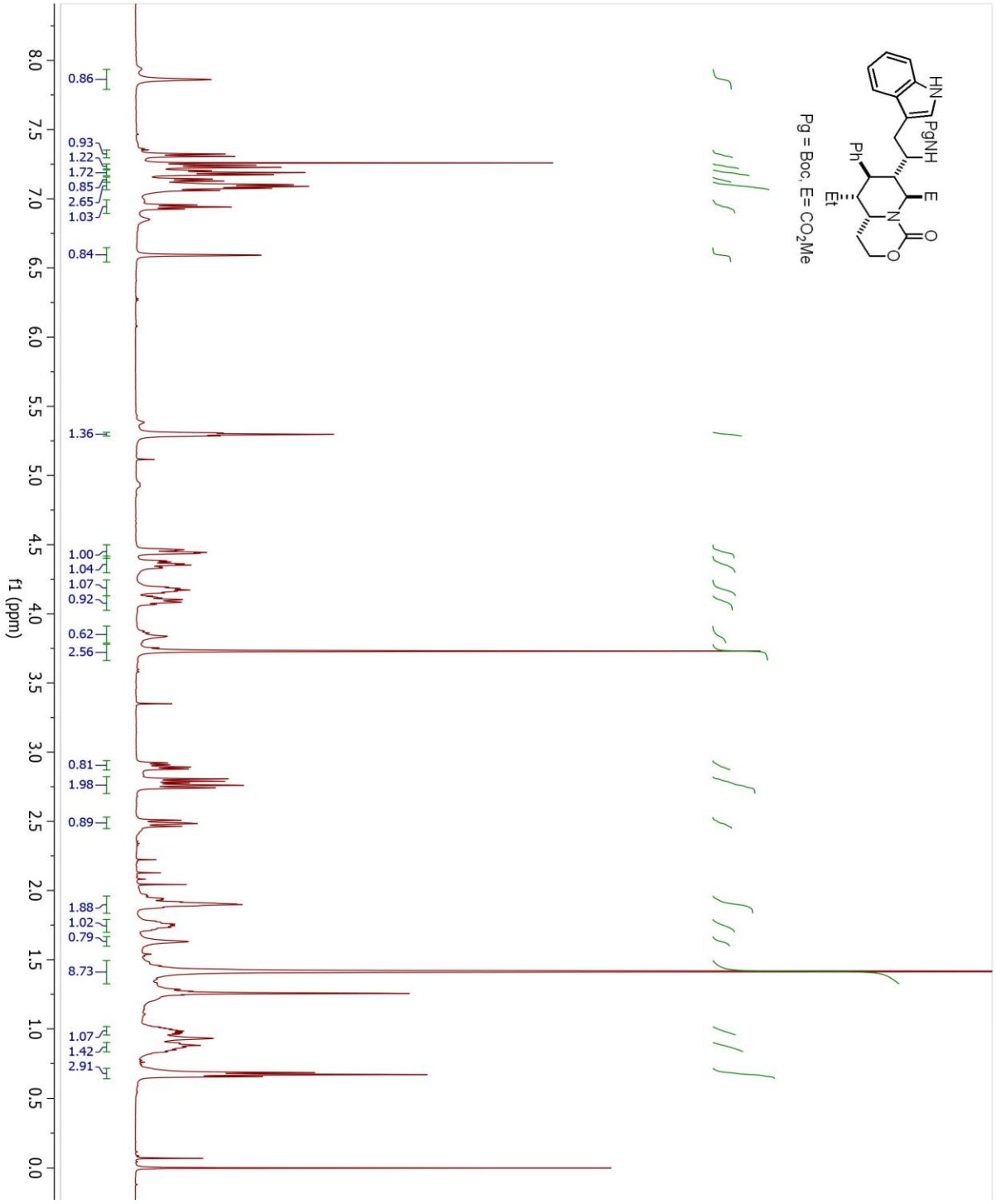
^{1}H NMR (500 MHz, $CDCl_3$) for compound **2.10**



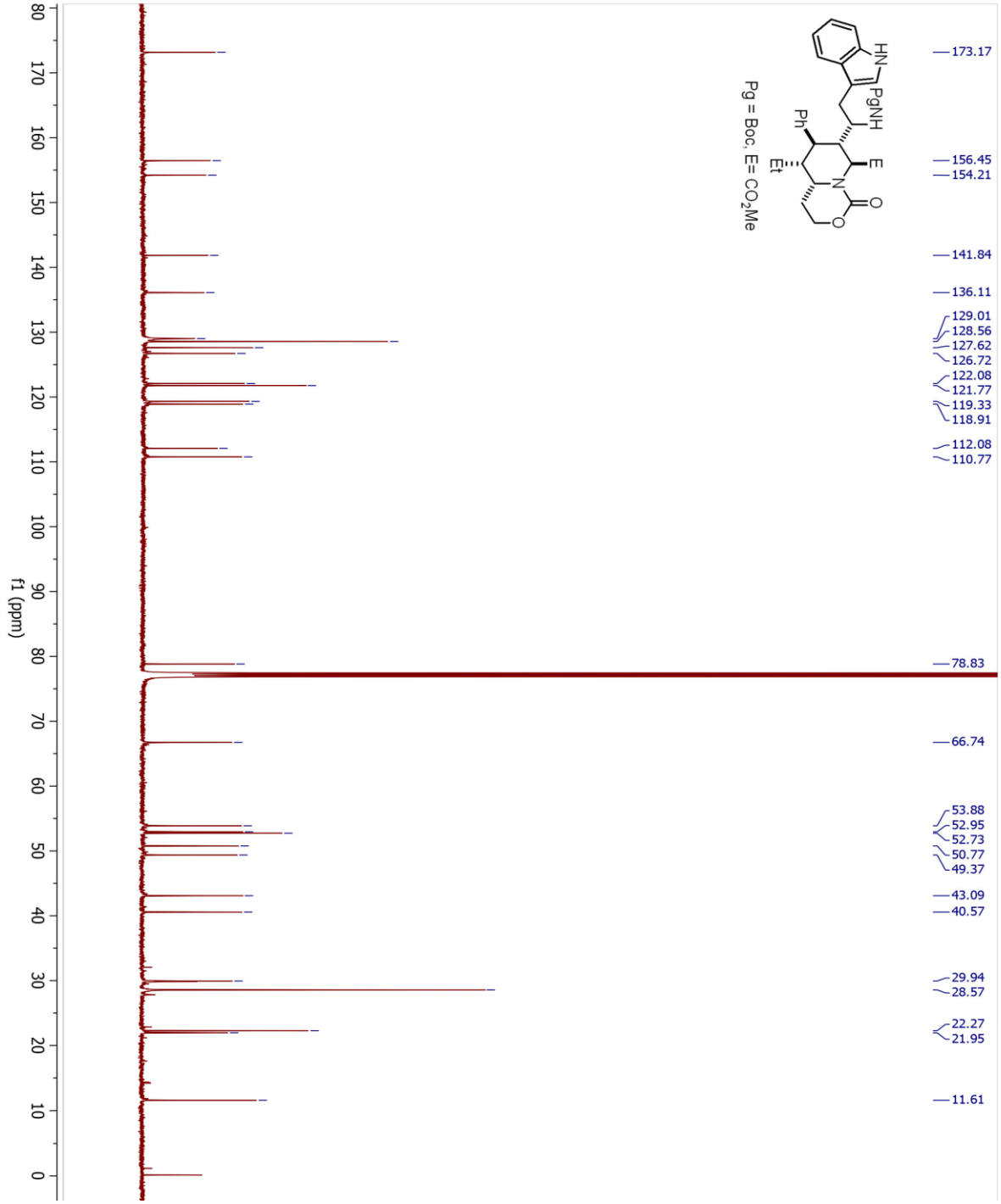
^{13}C NMR (126 MHz, $CDCl_3$) for compound **2.10**



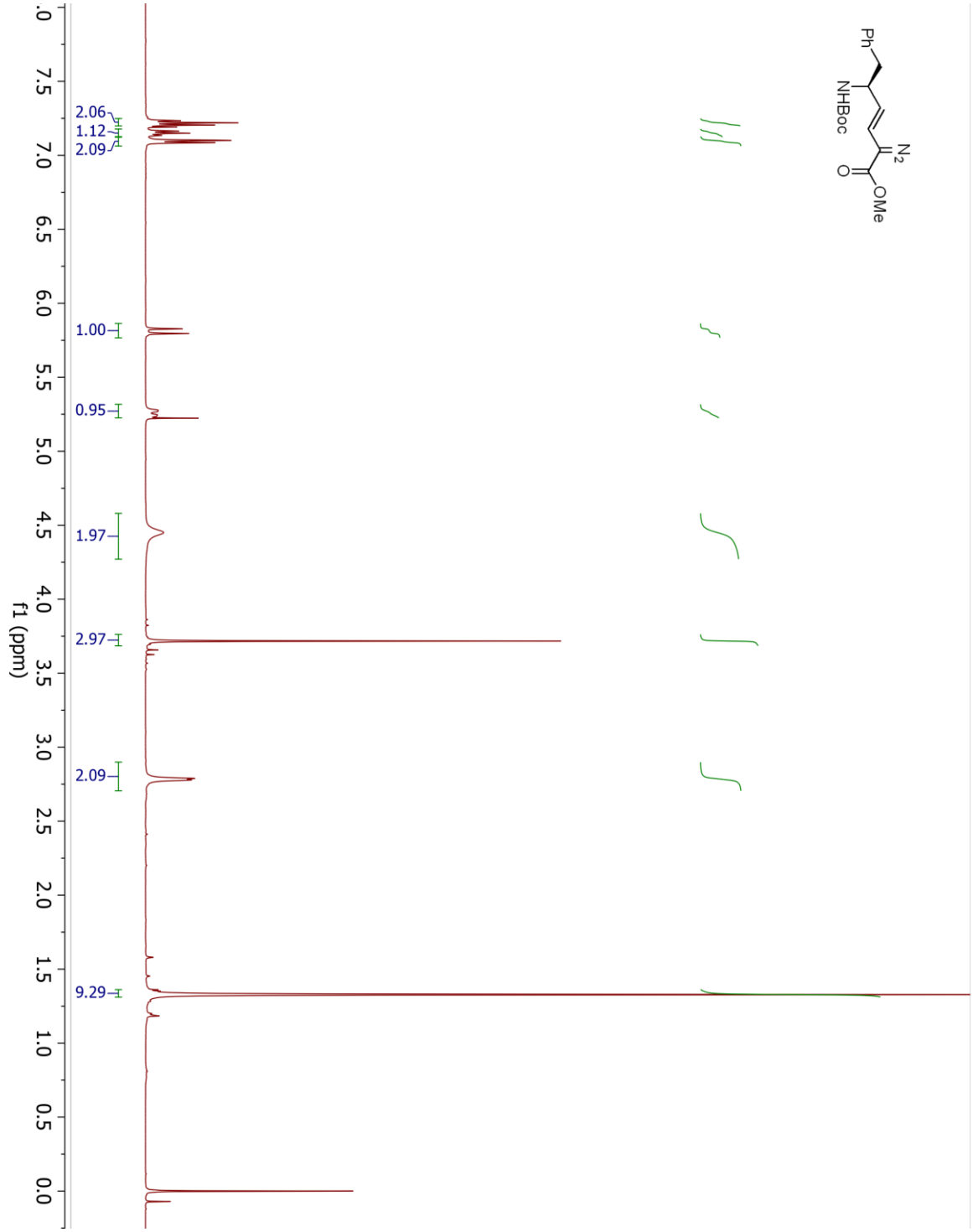
^{1}H NMR (500 MHz, $CDCl_3$) for compound **2.13**



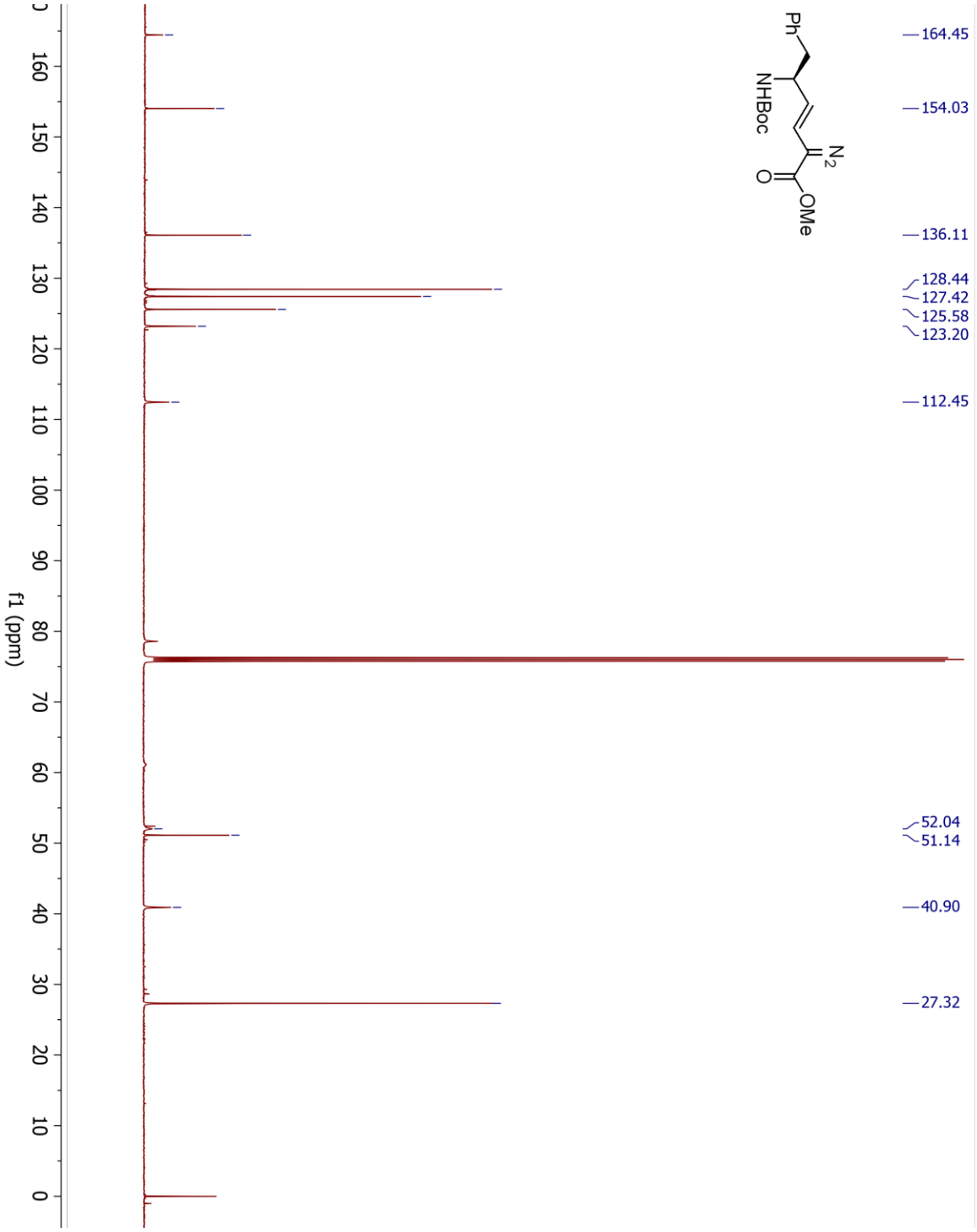
^{13}C NMR (126 MHz, $CDCl_3$) for compound **2.13**



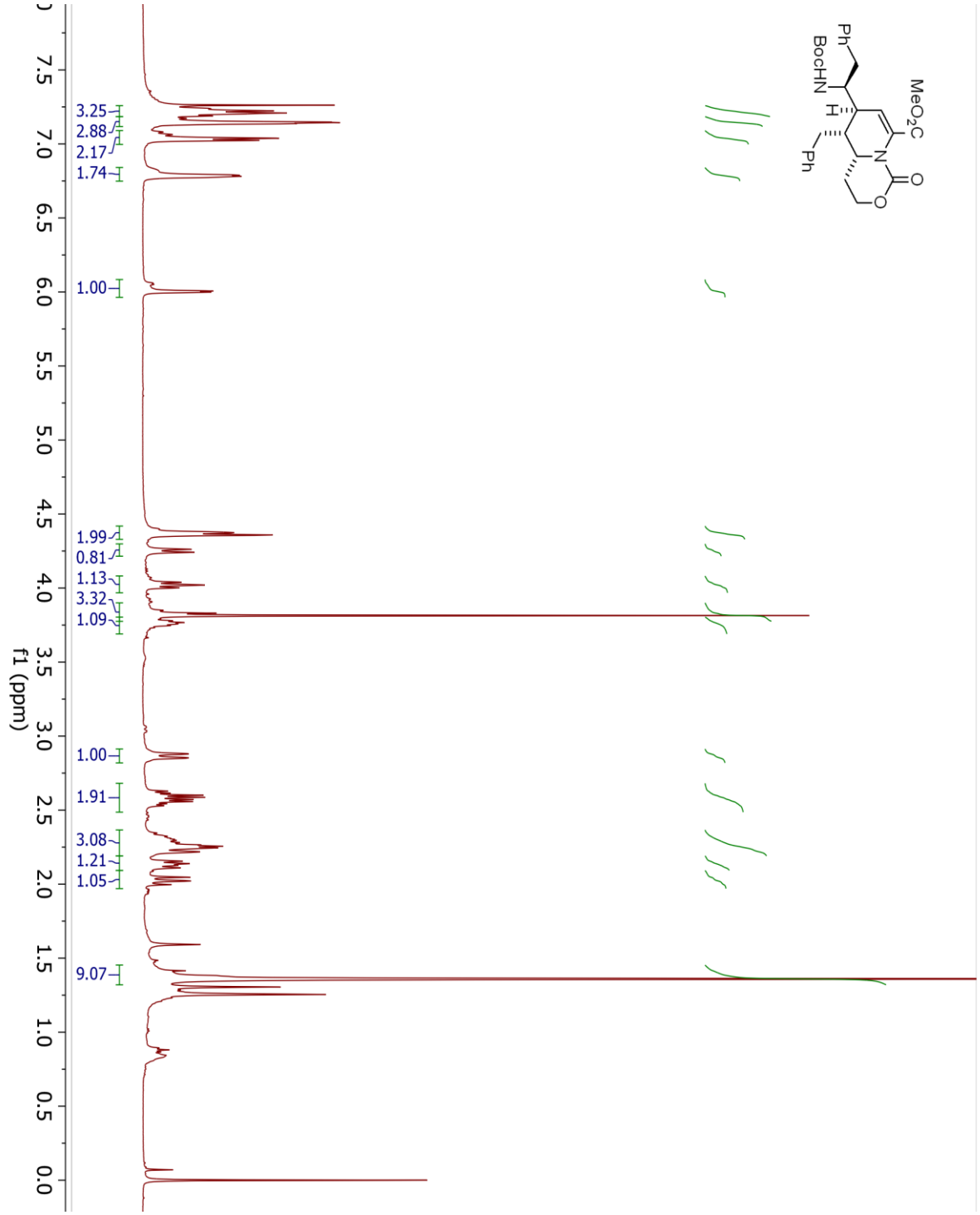
^{1}H NMR (500 MHz, $CDCl_3$) for compound **2.14a**



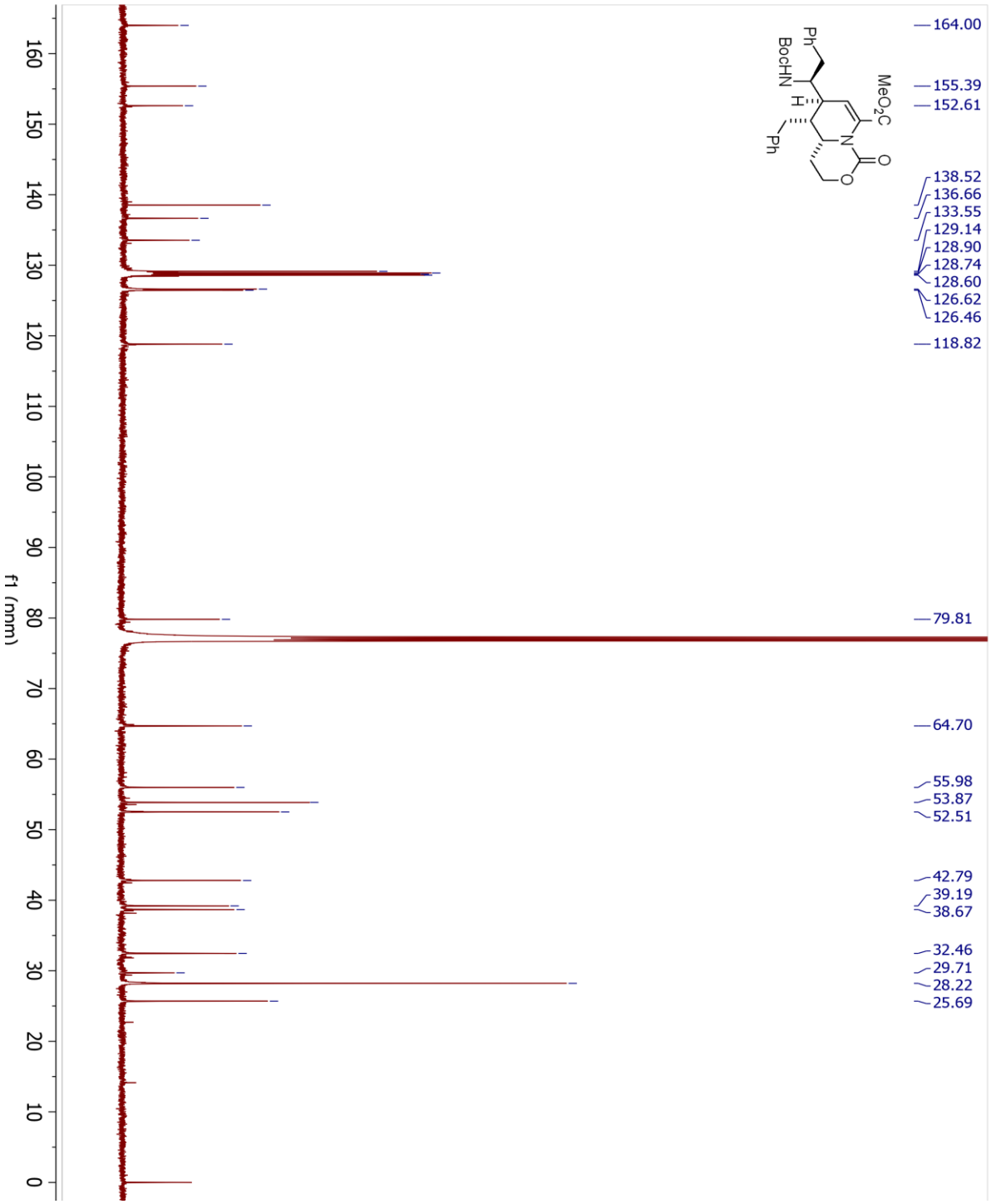
^{13}C NMR (126 MHz, $CDCl_3$) for compound **2.14a**



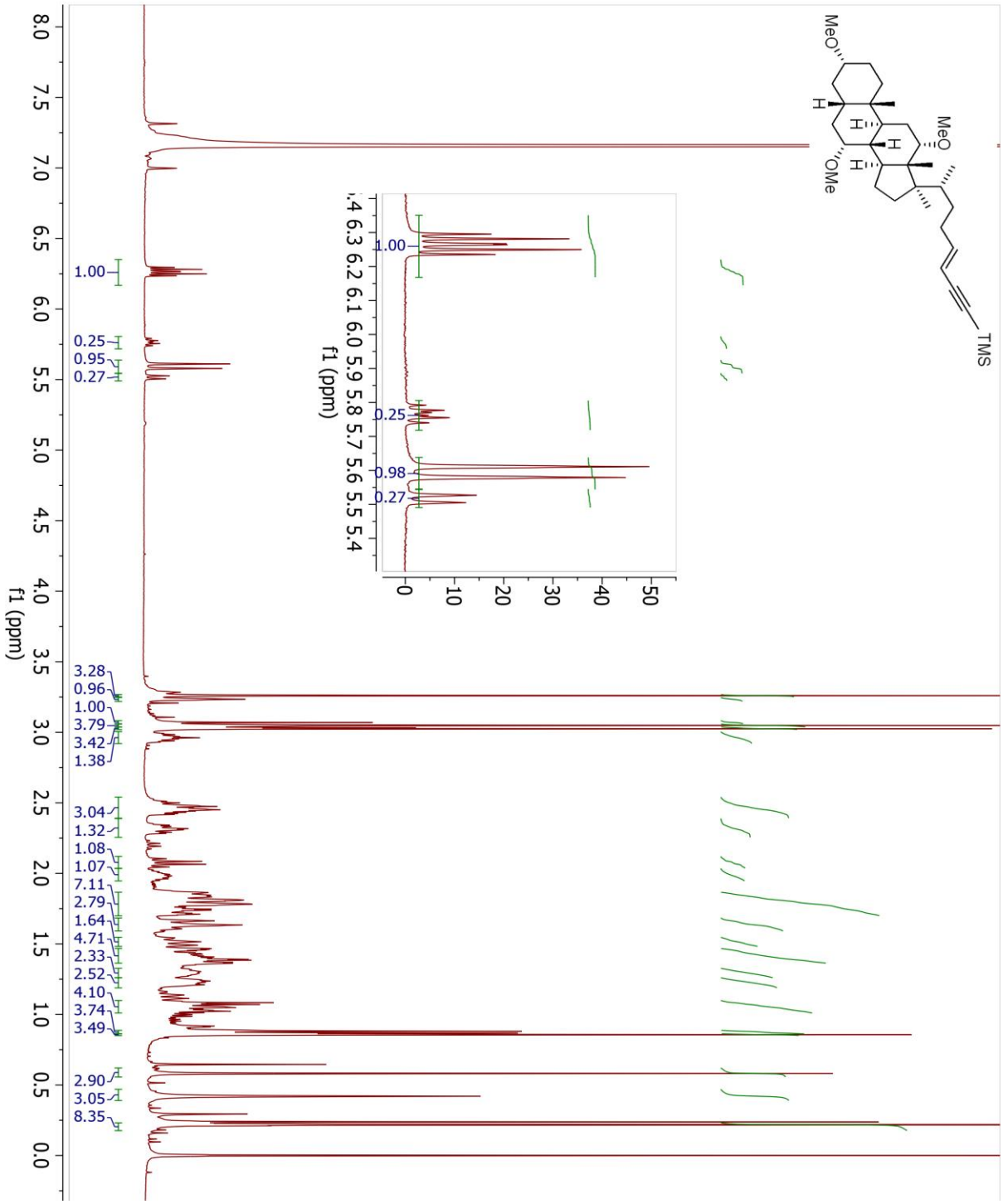
^{1}H NMR (500 MHz, $CDCl_3$) for compound **2.15a**



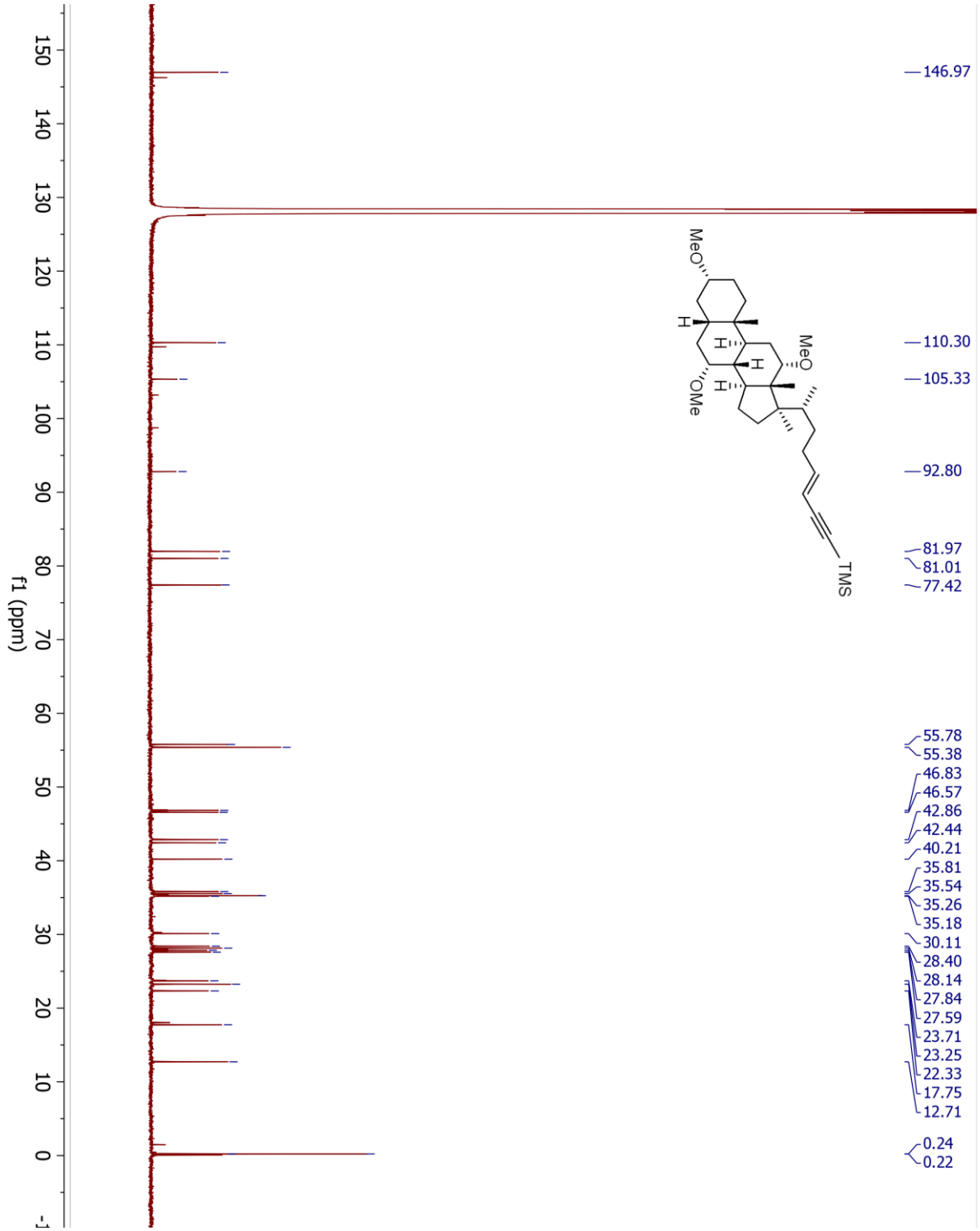
^{13}C NMR (126 MHz, $CDCl_3$) for compound **2.15a**



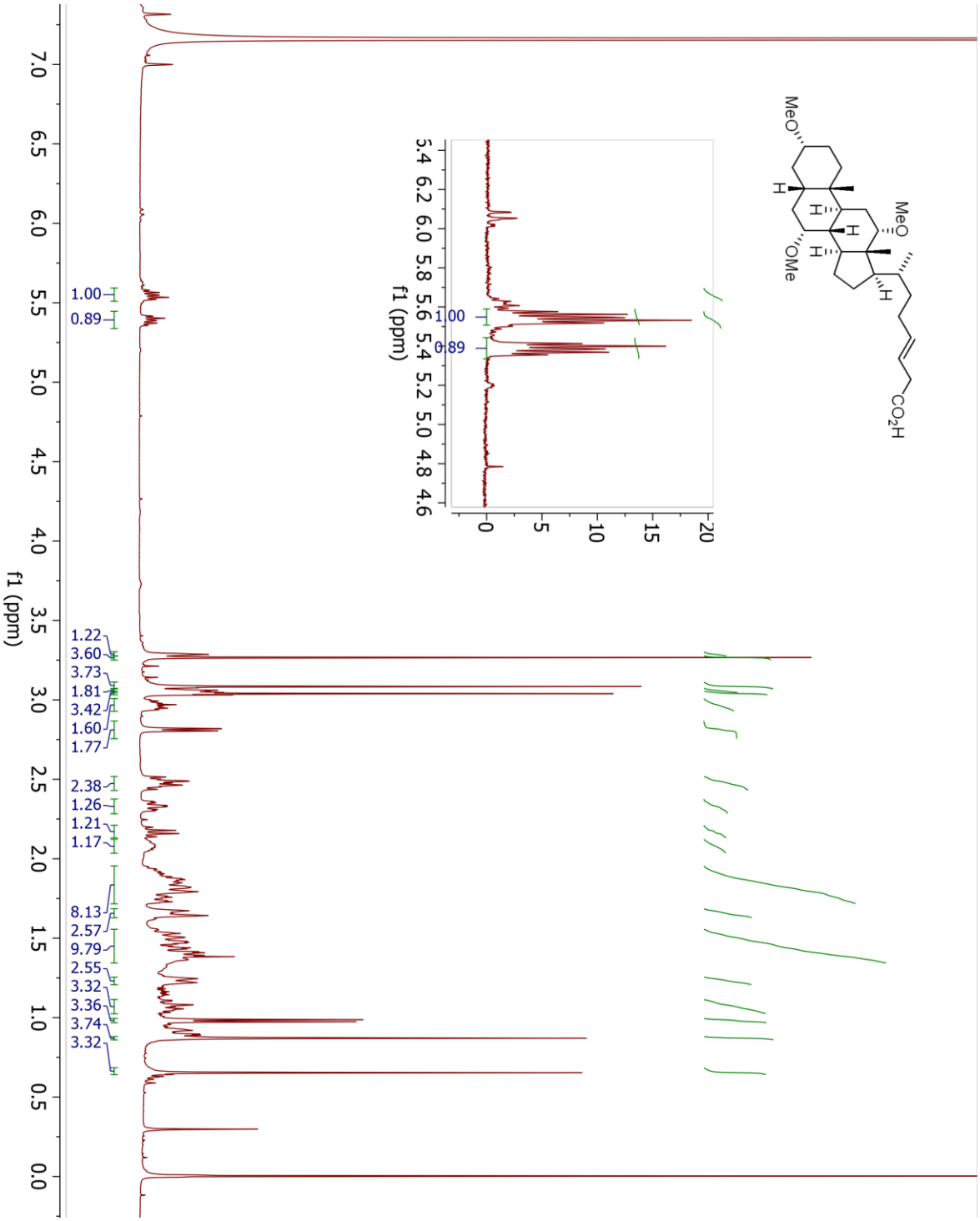
^{1}H NMR (500 MHz, $CDCl_3$) for compound **SI-1**



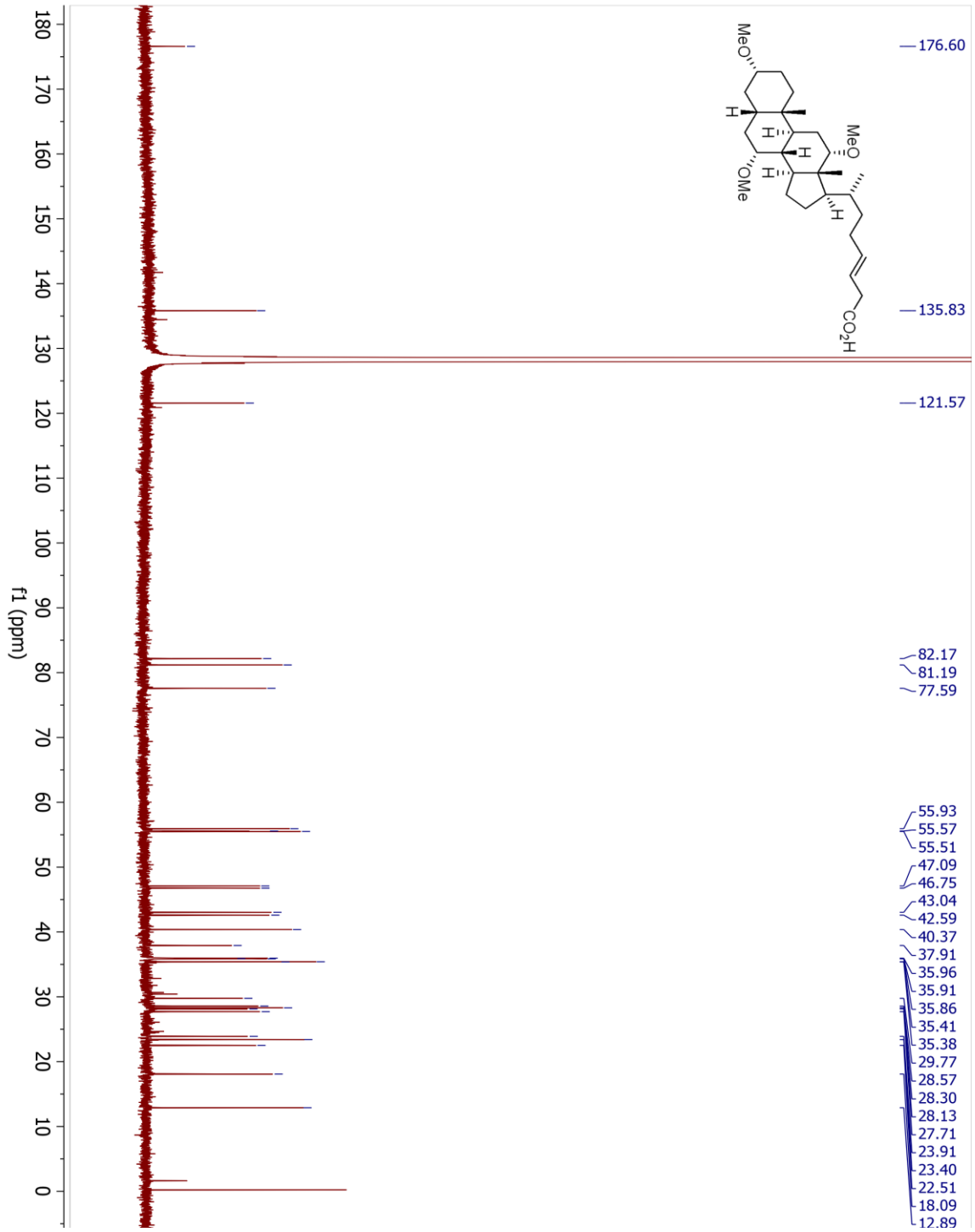
^{13}C NMR (126 MHz, $CDCl_3$) for compound **SI-1**



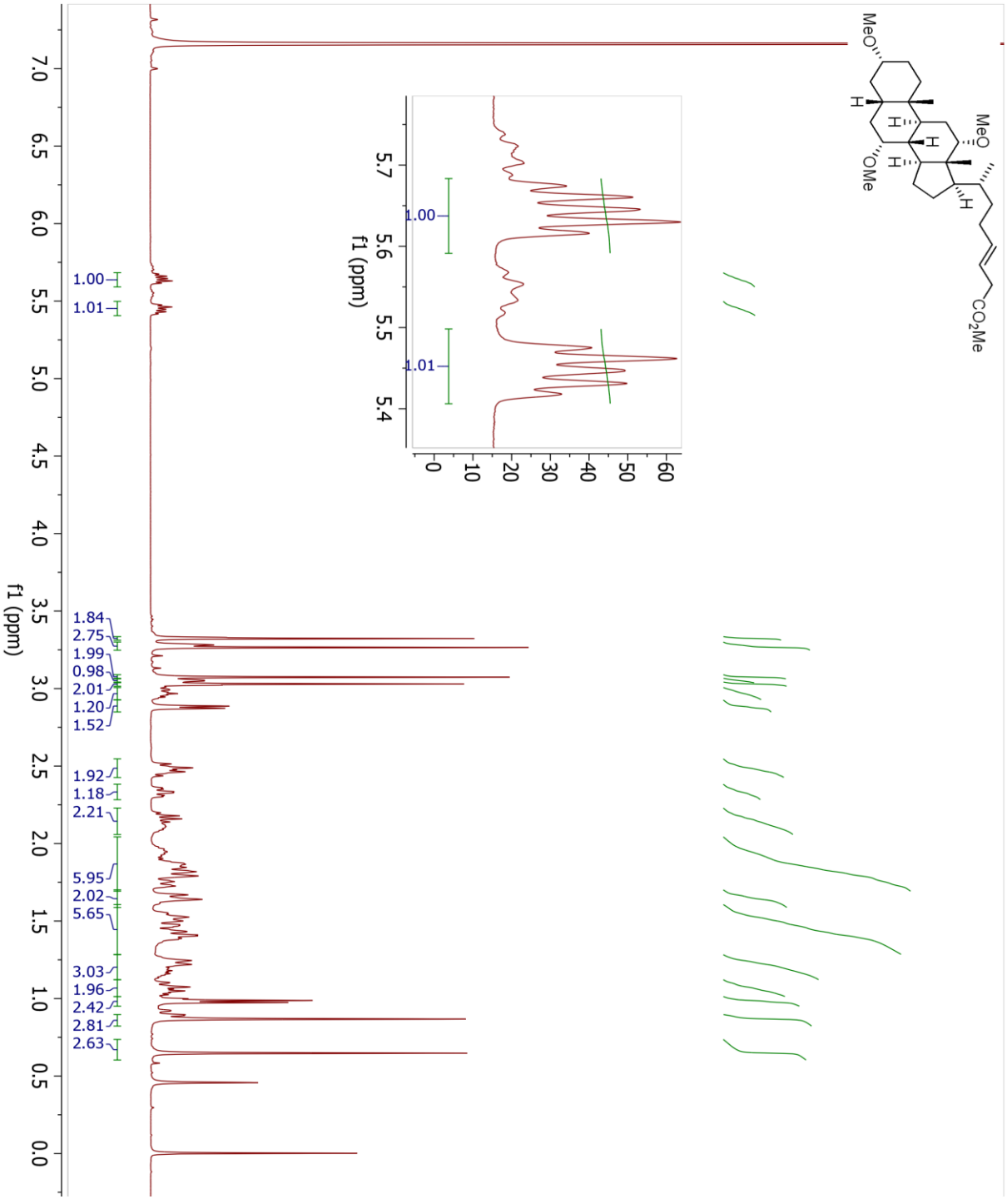
^{1}H NMR (500 MHz, $CDCl_3$) for compound **SI-2**



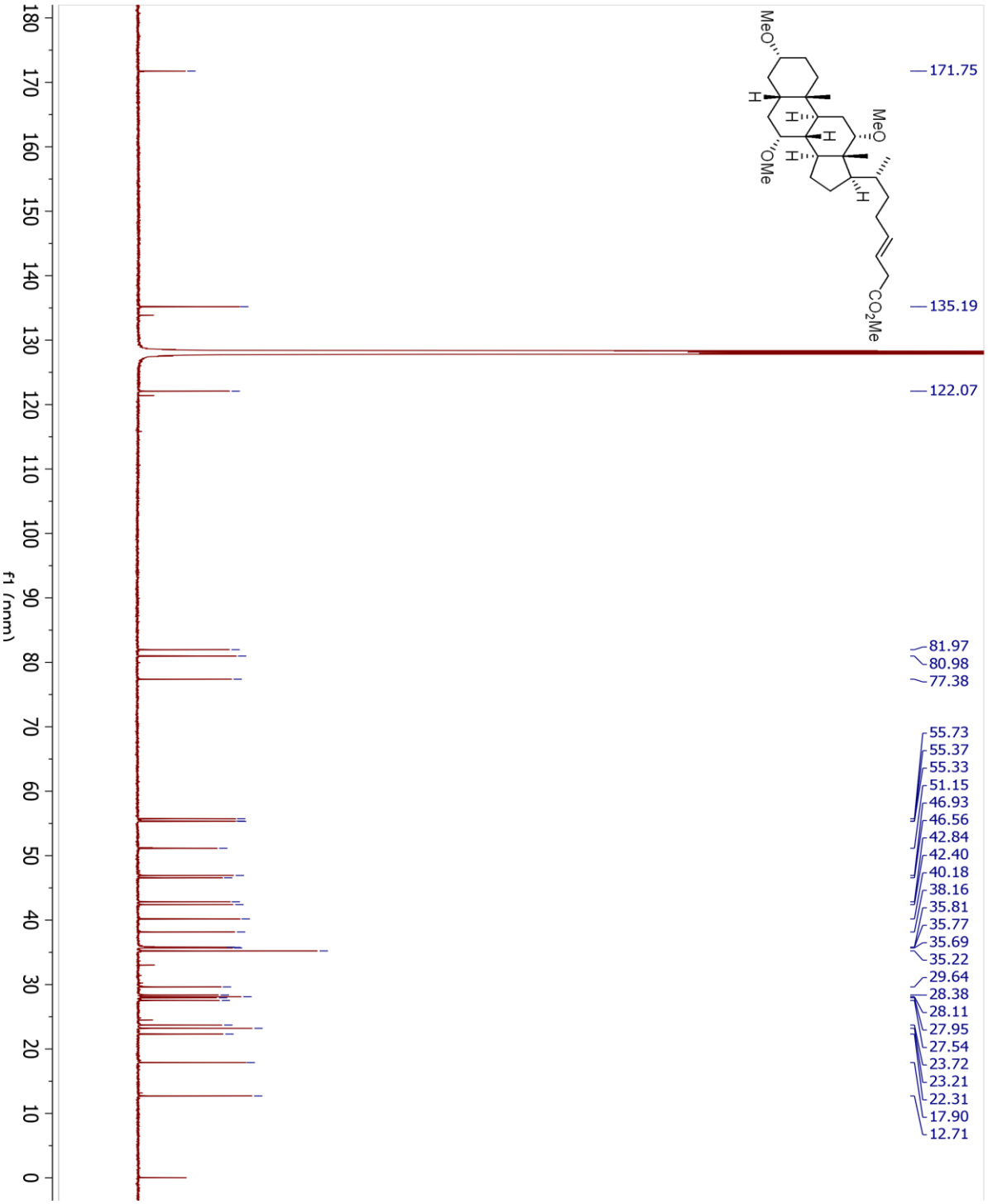
^{13}C NMR (126 MHz, $CDCl_3$) for compound **SI-2**



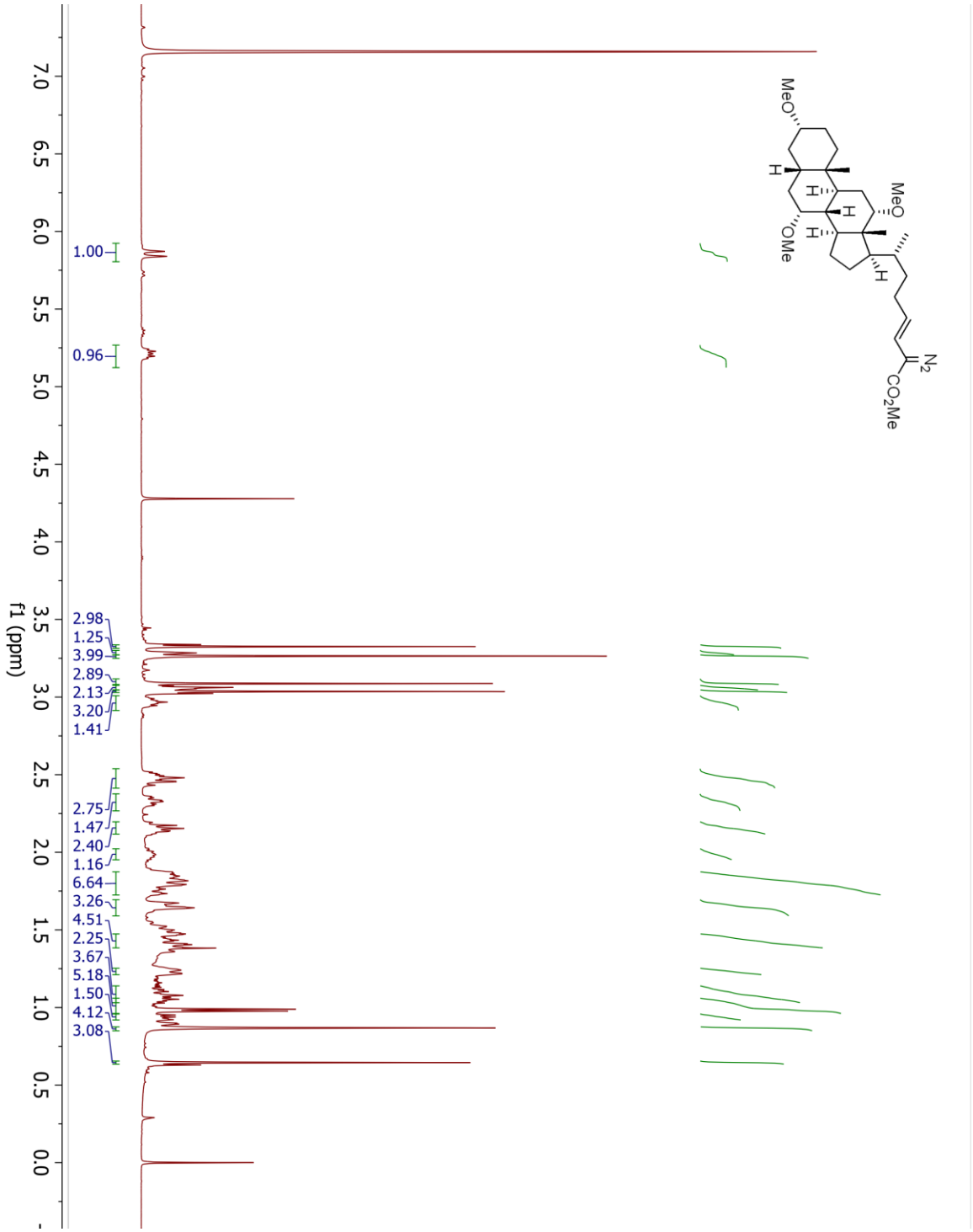
^{1}H NMR (500 MHz, $CDCl_3$) for compound **SI-3**



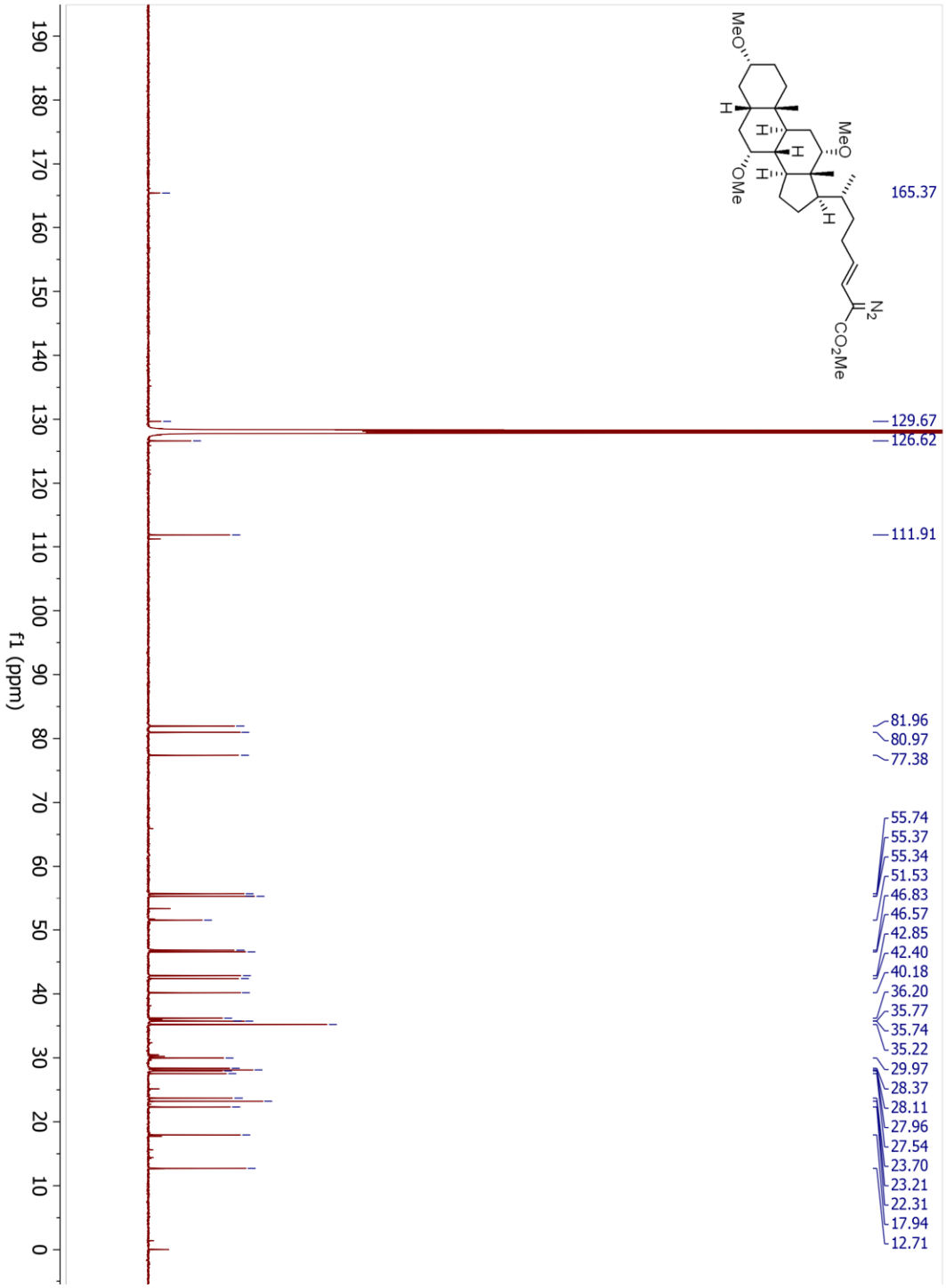
^{13}C NMR (126 MHz, $CDCl_3$) for compound **SI-3**



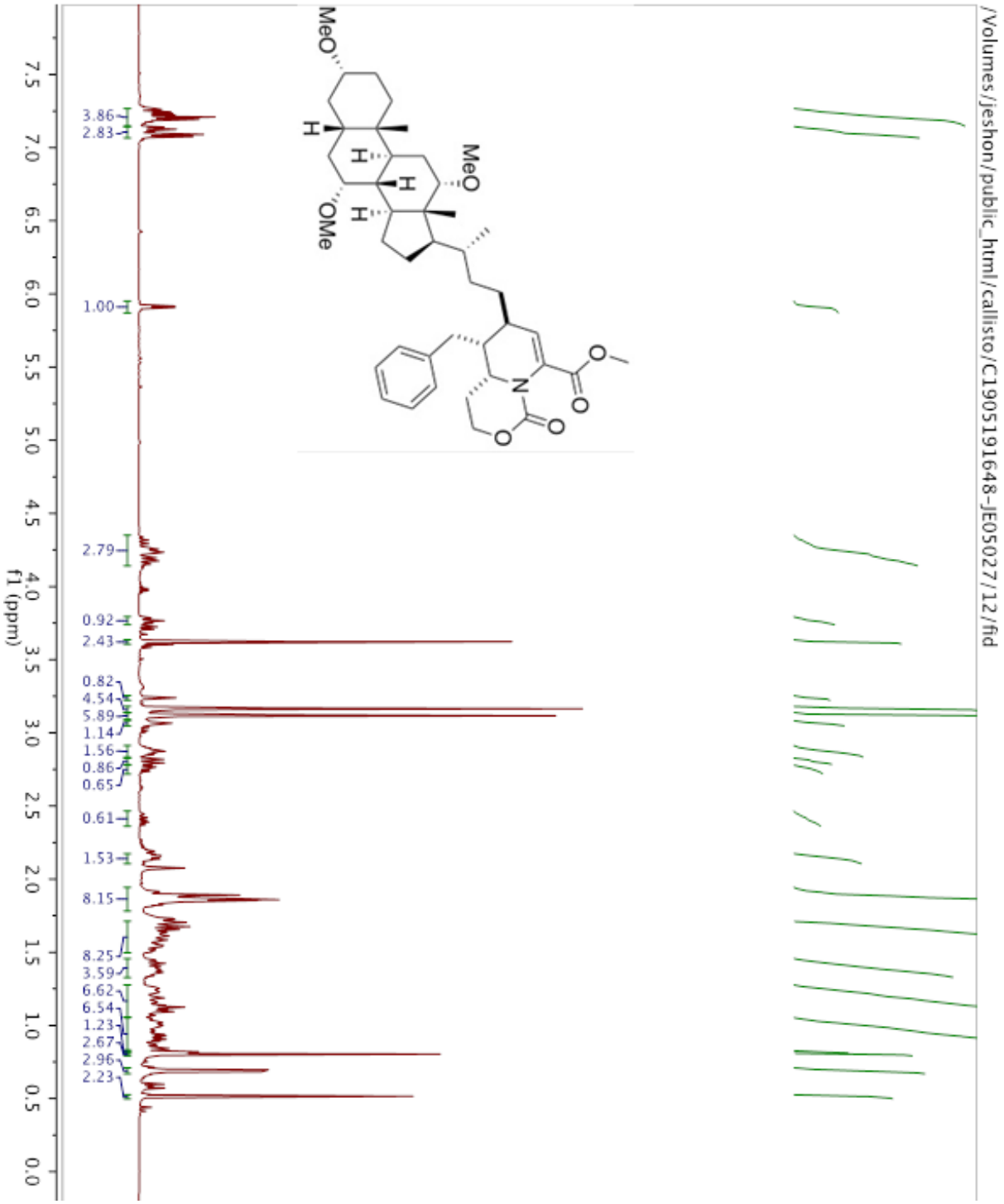
^{1}H NMR (500 MHz, $CDCl_3$) for compound **2.14b**



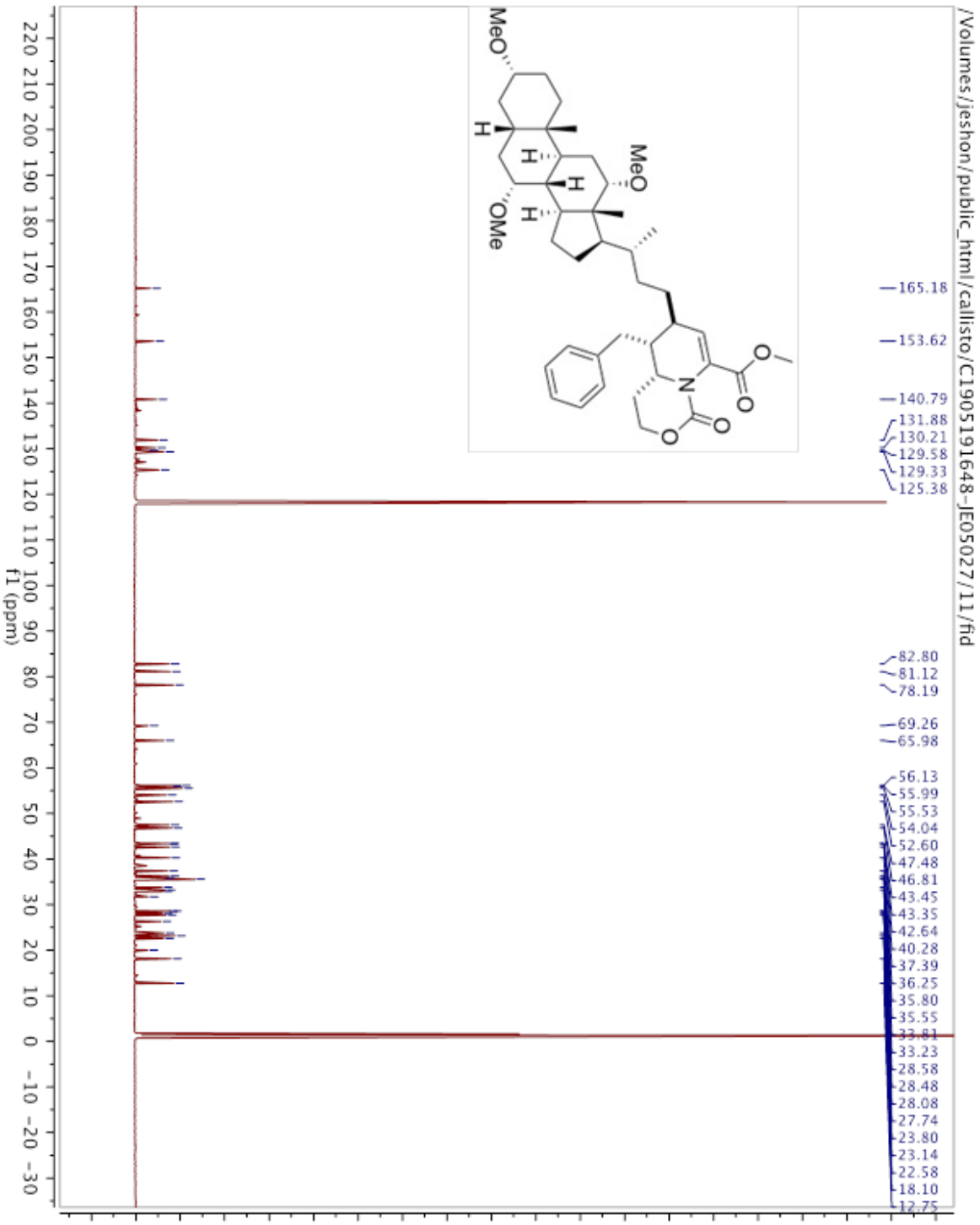
^{13}C NMR (126 MHz, $CDCl_3$) for compound **2.14b**



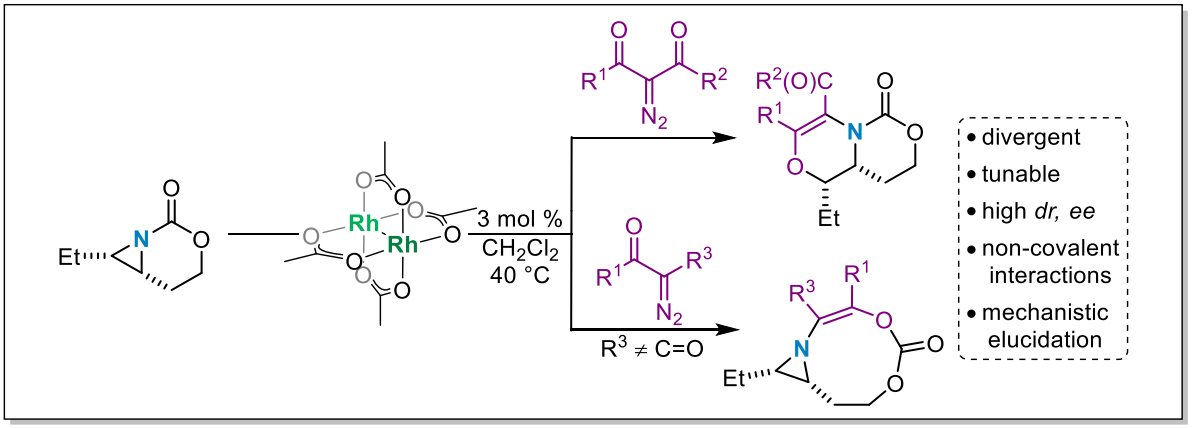
^{1}H NMR (500 MHz, C_6D_6) for compound **2.15b**



^{13}C NMR (126 MHz, C_6D_6) for compound **2.15b**



Chapter 3. Tunable Aziridinium Ylide Reactivity: Non-covalent Interactions Enable Divergent Product Outcomes



This chapter has been published and reprinted with permission from:

Nicastri, K. A.; Zappia, S. A.; Pratt, J. C.; Duncan, J. M.; Guzei, I. A.; Fernández, I.; Schomaker, J. M. Tunable Aziridinium Ylide Reactivity: Noncovalent Interactions Enable Divergent Product Outcomes. *ACS Catal.* **2022**, *12*, 1572–1580.

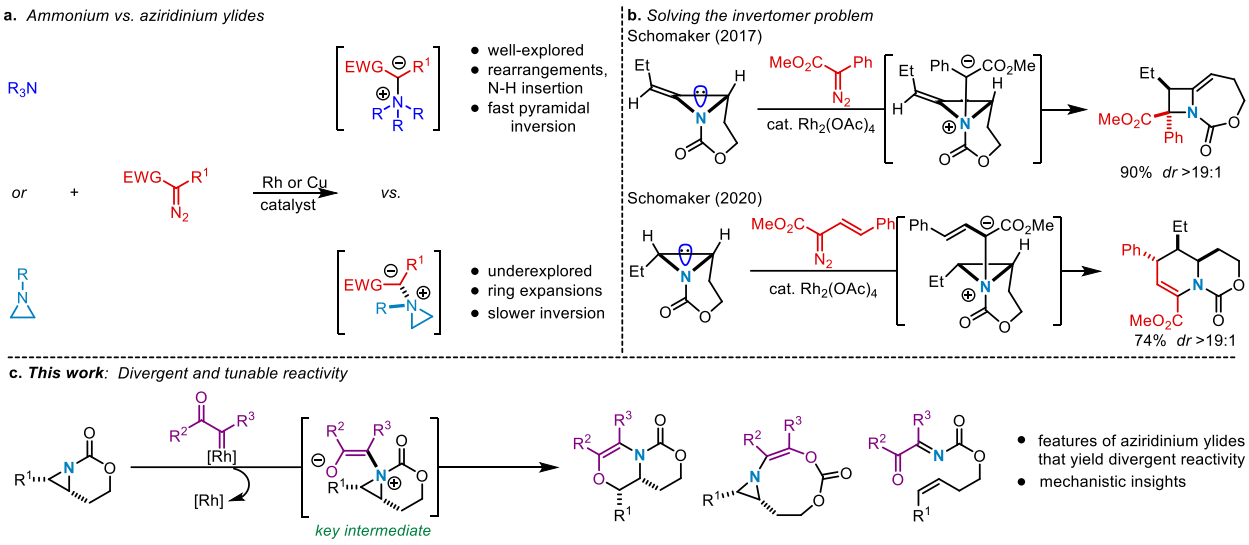
Copyright © 2022 American Chemical Society.

3.1 Introduction

As mentioned in **Chapter 1**, aziridinium ylides[1] represent a unique subclass of ammonium ylides whose reactivity is both poorly understood and underexplored, despite the potential for these intermediates to generate functionalized, stereochemically rich *N*-heterocycles.

In our previous work, we were able to leverage rigid bicyclic aziridines (**Scheme 3.1b**, or **Chapters 1** and **2**), for the synthesis of azetidine[2] and dehydropiperidine[3] products through the intermediacy of aziridinium ylides. In these cases, we avoided off-target decomposition pathways by utilizing substrates that do not undergo *N*-lone pair inversion[4,5]: an issue central to previous attempts to leverage aziridinium ylides for ring expansion reactions.[6-8] Despite the progress we have made, the future development of this type of methodology requires a more detailed understanding of how the identity of the carbene precursor, potential dynamic behavior in the ylide intermediate, and non-covalent interactions may influence the outcome of the reaction. In this chapter, we describe a new method for the synthesis of dehydromorpholines[9-11] by leveraging

Scheme 3.1 – Prior work in aziridinium ylide chemistry and new divergent reactivity.

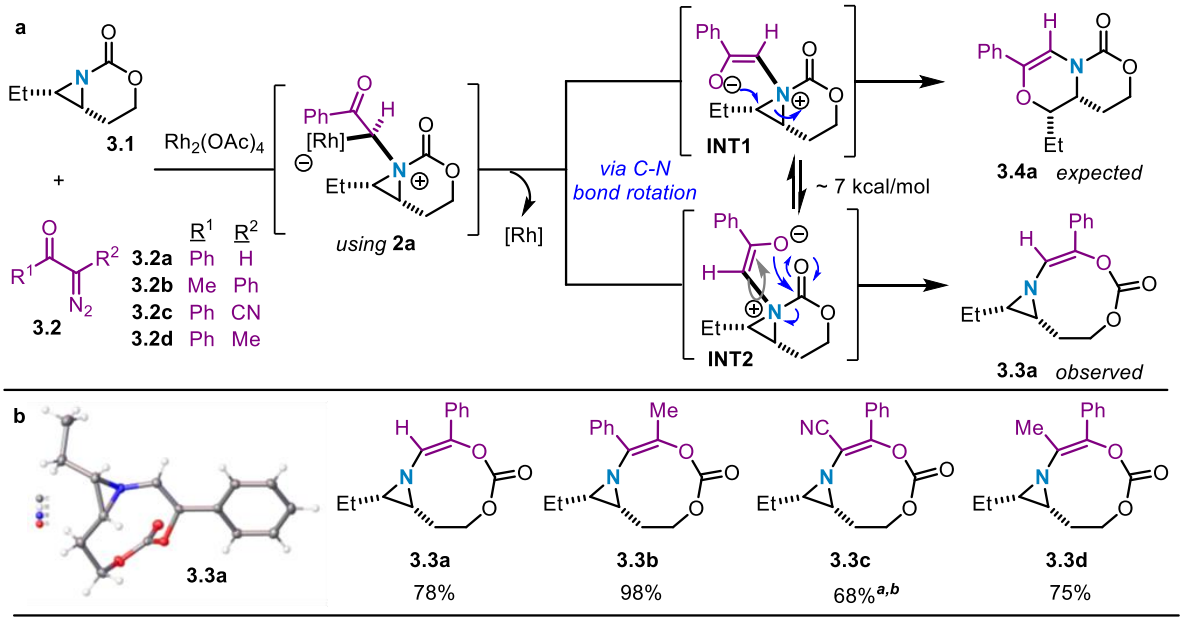


ketone-containing carbenes generated from Rh catalysis (**Scheme 3.1c**). In addition, we report both experimental and computational studies that support our mechanistic hypotheses, provide an explanation for observed divergent reaction pathways, and ways for how they may be controlled.

3.2 Initial Explorations of Diverse Carbene Precursors for Dehydromorpholine Synthesis

In order to assess the possibility of dehydromorpholine formation, we first investigated whether the carbonyl oxygen of a donor-acceptor diazoketone, such as **3.2a**, could serve as a competent nucleophile to open the aziridinium ylide (**Scheme 3.2a**). Only one nucleophilic ketone group is present in **3.2a**; thus, we expected reaction of **3.2a** with **3.1** to furnish **3.4a** in good yield via conformer **INT1**. Surprisingly, treatment of **3.1** with **3.2a** under $Rh_2(OAc)_4$ catalysis gave an unusual [3,9]-aziridine product **3.3a** in 78% yield. Presumably, the 7 kcal/mol barrier to interconversion of aziridinium ylide **INT1** to **INT2** by rotation around the C–N bond (**Scheme**

Scheme 3.2 – Ring expansions of **3.1** with donor-acceptor diazoketone carbene precursors.



Standard conditions: Slow addition of the diazoketone (3.0 equiv) over 3 h to a mixture of 3 mol % $Rh_2(OAc)_4$ and aziridine (1.0 equiv) in CH_2Cl_2 at 40 °C. Yields are given for isolated products. [a] Yields determined by ^{1}H NMR using 1,3,5-trimethoxy-benzene as an internal standard. [b] A small amound of **3.4c** (19%) was also detected in this crude ^{1}H-NMR spectrum

3.2) enables nucleophilic attack of the ketone oxygen on the electrophilic carbonyl of the carbamate tether to furnish **3.3a**. This result was unexpected, as nucleophilic addition to the carbamate tether was not observed in previous syntheses of azetidines or dehydropiperidines from bicyclic aziridines.[20ab,21]

We were curious as to the origin of **3.3a** and hypothesized that the aryl group may be important in biasing the reaction towards this unexpected product. However, exchanging the Ph group of **3.2a** to a Me group in **3.2b** still furnished **3.3b** in an excellent 98% yield (**Scheme 3.2b**). Altering the electronics of R^2 had no effect on product selectivity. Both electron-withdrawing and donating substituents (e.g. CN in **3.2c**, Me in **3.2d**) furnished the [3,9]-aziridine in 75% (**3.3d**) and 68% (**3.3c**) yields, respectively (**Scheme 3.2b**). The consistent product outcome suggested that neither R^1 nor R^2 influences the preferred formation of the [3,9]-aziridine product.

To gain more insight into the formation of **3.3a** at the expense of the expected **3.4a**, Density Functional Theory (DFT) calculations were carried out at the dispersion-corrected SMD(CH_2Cl_2)-B3LYP-D3/def2-SVP level (see computational details in the Supporting Information). **Figure 3.1a** shows the computed reaction profiles leading to the formation of the **3.3a** or **3.4a** from the corresponding free aziridinium ylides, which according to our previous calculations on related systems,[20b,21] derives from the nucleophilic addition of the aziridine **3.2a** to the Rh_2-carbenoid intermediate (formed upon reaction of the diazo-compound and $Rh_2(OAc)_4$). From the data in **Figure 3.1a**, it becomes apparent that metal-free ylide **INT2** involved in the [3,9]-pathway is lower in energy than its analogous intermediate **INT1** involved in the alternative [6,6]-pathway (−4.2 kcal/mol).

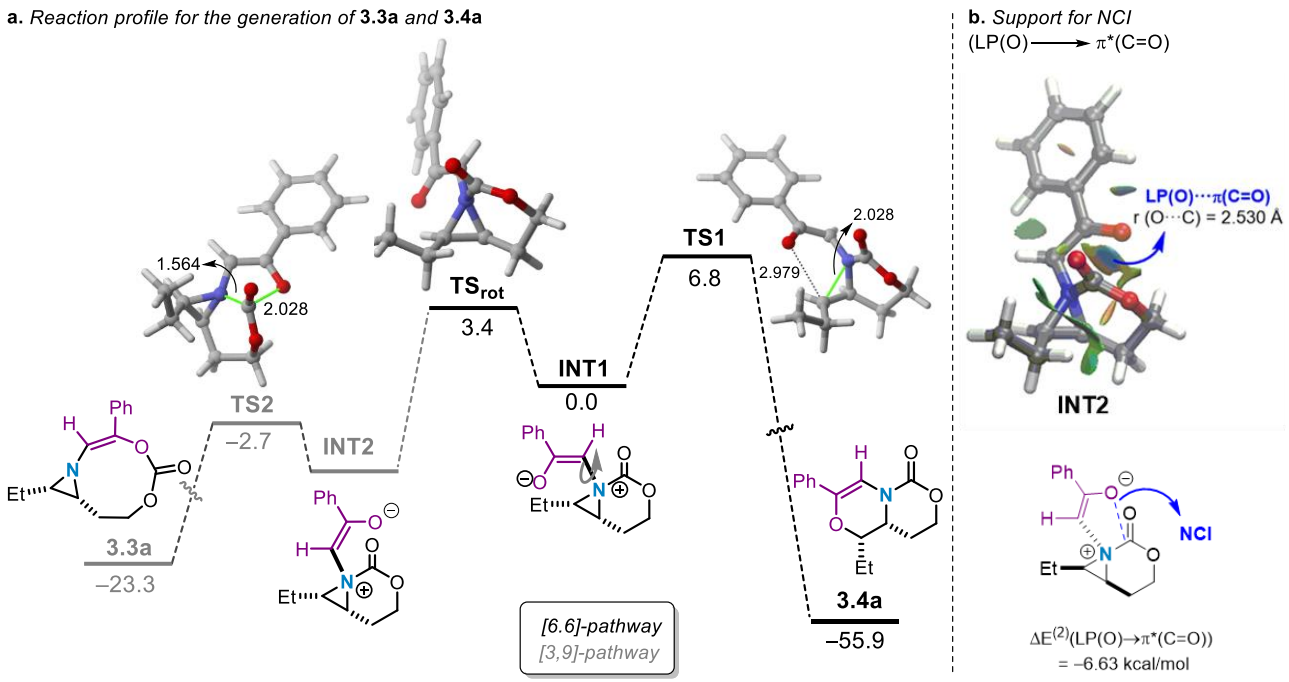


Figure 3.1 – a. Computed reaction energy profiles for formation of **3.3a** and **3.4a**. Relative free energies (DG_{298}, at 298 K) and bond distances are given in kcal/mol and angstroms, respectively. b. Contour plots (top) of the reduced density gradient isosurfaces (density cutoff of 0.04 a.u.) for intermediate **INT2**. The green surfaces indicate attractive noncovalent interactions. Associated SOPT-NBO stabilizing energy (bottom). All data have been computed at the SMD(CH_2Cl_2)B3LYP-D3/def2-SVP level of theory.

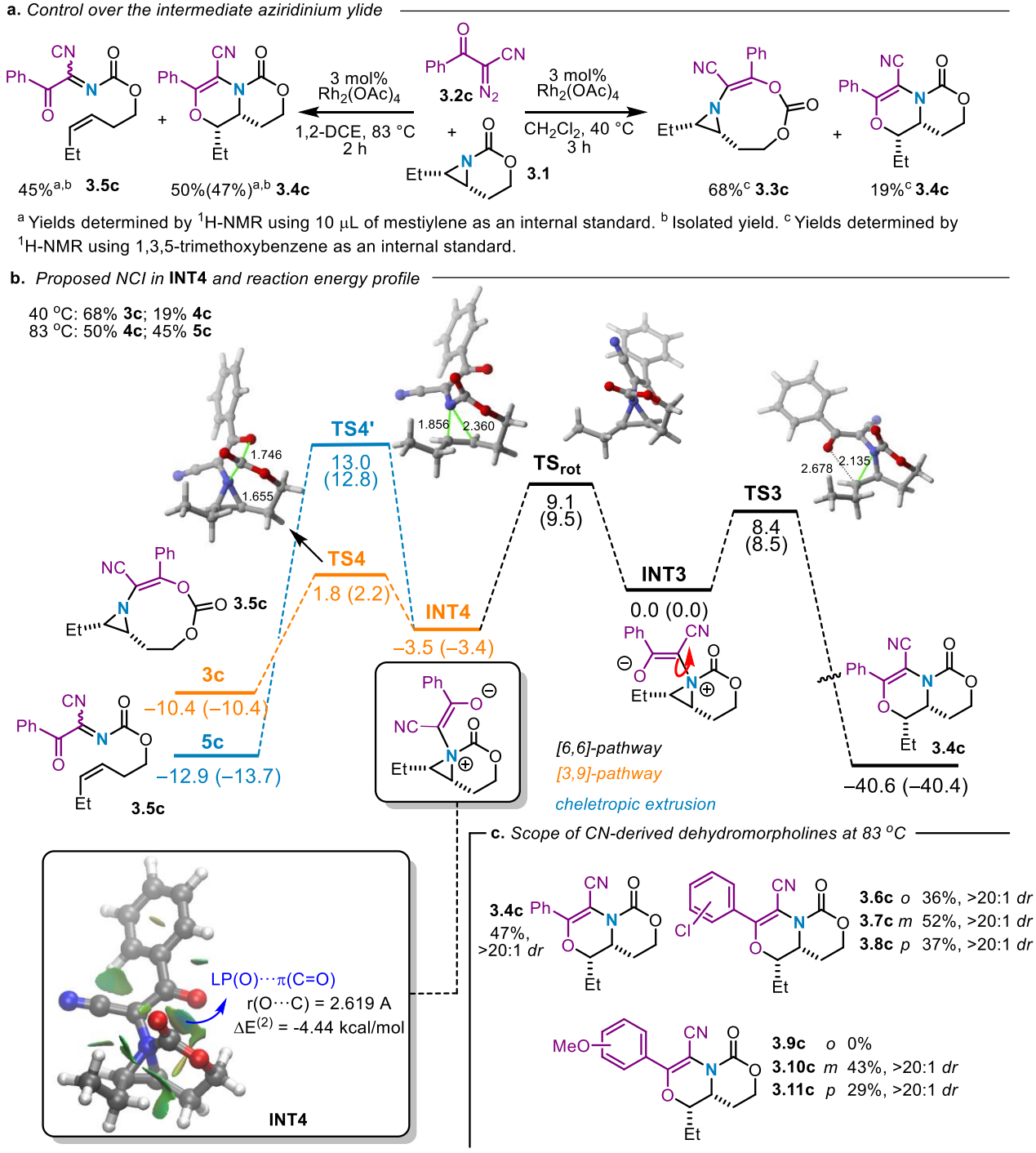
A similar finding was observed in their metal-ylide counterparts ($\Delta\Delta G$ = –5.7). According to the NCIPLOT method, this is in part ascribed to the occurrence of a stabilizing NCI involving the nucleophilic C–O lone pair of the ketone moiety and the electrophilic π*(C=O) molecular orbital of the carbamate, as confirmed for **INT2** (**Figure 3.1b)**The presence of this stabilizing NCI is also supported by the computed short O···C(=O) distance in **INT2** of 2.530 Å, which is markedly shorter than the sum of the van der Waals radii (3.22 Å); this was also confirmed by the associated stabilization energy ($\Delta E^{(2)}$ = –6.63 kcal/mol) computed for the lone pair (LP)(O)→π*(C=O) interaction using the Second-Order Perturbation Theory (SOPT) of the NBO

method (**Figure 3.1b**). Furthermore, the barrier associated with the formation of **3.3a** from **INT2** is 5.3 kcal/mol lower than that associated with the formation of **3.4a** from **INT1** (**Figure 3.1a**). This noticeable difference in the calculated activation energies for the two potential reaction pathways and the occurrence of the NCIs, which show significant stabilization of the key ylide intermediate, leading to the preferred formation of **3.3a** over **3.4a**, despite the fact that the latter species is significantly favored thermodynamically. The barrier to interconversion between **INT1** and **INT2** (7.6 kcal/mol, **Figure 3.1a**) is reinforced by the lower barrier ($\Delta G^{\neq}$ = 1.5 kcal/mol) computed for the generation of the observed product **3.3a**.

3.3 Controlling Product Outcomes with Temperature

Changing the carbene precursor to the CN-containing diazoketone **3.2c** provided the first example of divergence between dehydromorpholine **3.4c** and the [3,9]-aziridine **3.3c**. Standard reaction conditions furnished **3.3c** in 68% yield (by NMR), accompanied by 19% of the dehydromorpholine **3.4c** (**Scheme 3.3a**, right). The 3.6:1 ratio of **3.3c:3.4c** led us to employ computations to probe whether an NCI was also present in the corresponding aziridinium ylide and to estimate the barrier to C–N bond rotation. Computational analysis confirmed the presence of an NCI, where the O···C(=O) distance of **INT4** is predicted to be 2.619 Å (**Scheme 3.3b** compared to 2.530 Å, **Figure 3.1b**), with a stabilizing interaction energy of $\Delta E^{(2)}$ = –4.44 kcal/mol. The balance between the computed barrier to C–N bond rotation between **INT3** and **INT4** of 12.5 kcal/mol and the presence of an NCI leads to a divergent reaction where both **3.3c** and **3.4c** are accessible. These computational observations are reflected in the calculated reaction profile (**Scheme 3.3b**), where both the activation energy barriers leading to **3.3c** and **3.4c** are accessible

Scheme 3.3 – a. Controlling product distribution using temperature. b. Computed reaction profile (relative free energies are given in kcal/mol) at the SMD(CH_2Cl_2)B3LYP-D3/def2-SVP level at 25˚C and 83˚C (values within parentheses) and contour plots of the reduced density gradient isosurfaces (density cutoff of 0.04 a.u.) for intermediate **INT4**. **c.** Scope of the process.



($\Delta G^{\neq}$~8.5 kcal/mol), but slightly higher than that of **3.3a** (**Figure 3.1**, see above). The higher barrier to C–N bond rotation (compared to the analogous ylide **INT2**) is likely a result of charge delocalization across the CN group (as compared to the ketone in **INT2**); nonetheless, it is still low enough to ultimately give rise to the product distribution based on temperature.

The computed reaction profile depicted in **Scheme 3.3b** also shows that the NCI-stabilized ylide **INT4** can undergo a cheletropic extrusion reaction to form the alkene **3.5c**. We hypothesized running the reaction at higher temperatures would: (i) enable facile bond rotation and lead to a greater preference for **3.4c** over the [3,9]-aziridine product **3.3c** and (ii) allow access to the cheletropic extrusion product. To our delight, repeating this reaction at 83 ˚C in 1,2-dichloroethane (**Scheme 3.3a**, left) favored dehydromorpholine **3.4c** formation in 50% yield by ^{1}H-NMR (47% isolated), with the remaining mass balance (45% yield) accounted for by formation of **3.5c**; no [3,9]-aziridine **3.3c** formation was observed. Although full selectivity for **3.4c** would be optimal, this reaction represents the first example where the fate of the aziridinium ylide can be controlled by the reaction conditions and not just the identity of the carbene precursor.

Employing higher temperatures with other cyano-derived diazoketones also proved fruitful (**Scheme 3.3c**). Ketones bearing *ortho*-, *meta*- and *para*-chlorosubstituted benzenes yielded dehydromorpholines **3.6c-3.8c** in moderate yields and excellent *dr* of >20:1. Ketones with *meta*- and *para*-methoxysubstituted benzenes were tolerated to furnish dehydromorpholines **3.10c** and **3.11c** in 43% and 29% yield, respectively. The *ortho*-substituted **3.9c** was not observed under these conditions, possibly due to steric congestion around the reactive site that prevents effective ylide formation.

3.4 Controlling Reaction Outcomes by Applying Bond Rotation Data

Based on our computational analysis of [3,9]-aziridine formation in **Figure 3.1a**, strategies to prohibit NCI formation in the key ylide intermediate were envisaged to promote formation of the desired dehydromorpholines. We hypothesized that raising the barrier to C–N bond rotation in the aziridinium ylide intermediate could 'trap' the kinetically formed conformer(s) and prevent formation of the NCI, potentially favoring a conformer similar to **INT1** (**Scheme 3.2a**). To this end, the barriers for C–N bond rotation in aziridinium ylides generated from reaction of **3.1** with donor-acceptor and acceptor-acceptor carbene precursors **3.2a** and **3.2d-f** were calculated and compared (**Figure 3.2**).

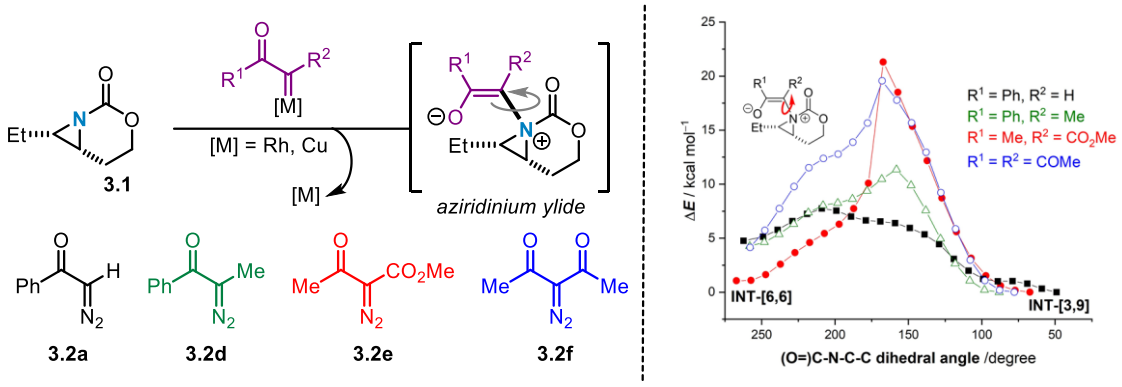


Figure 3.2 – Computed barriers for C–N bond rotation in aziridinium ylides from diverse carbene precursors.

The results suggest that aziridinium ylides arising from reaction of **3.1** with **3.2a** (which experimentally gave [3,9]- aziridines **3.3a**, **Scheme 3.2b**) display a low barrier of ca. 7 kcal/mol to rotation about the C–N bond (black line). The reaction of **3.1** with **3.2d** revealed a higher barrier of 12 kcal/mol (green line) for C–N bond rotation. In contrast, aziridinium ylides formed from

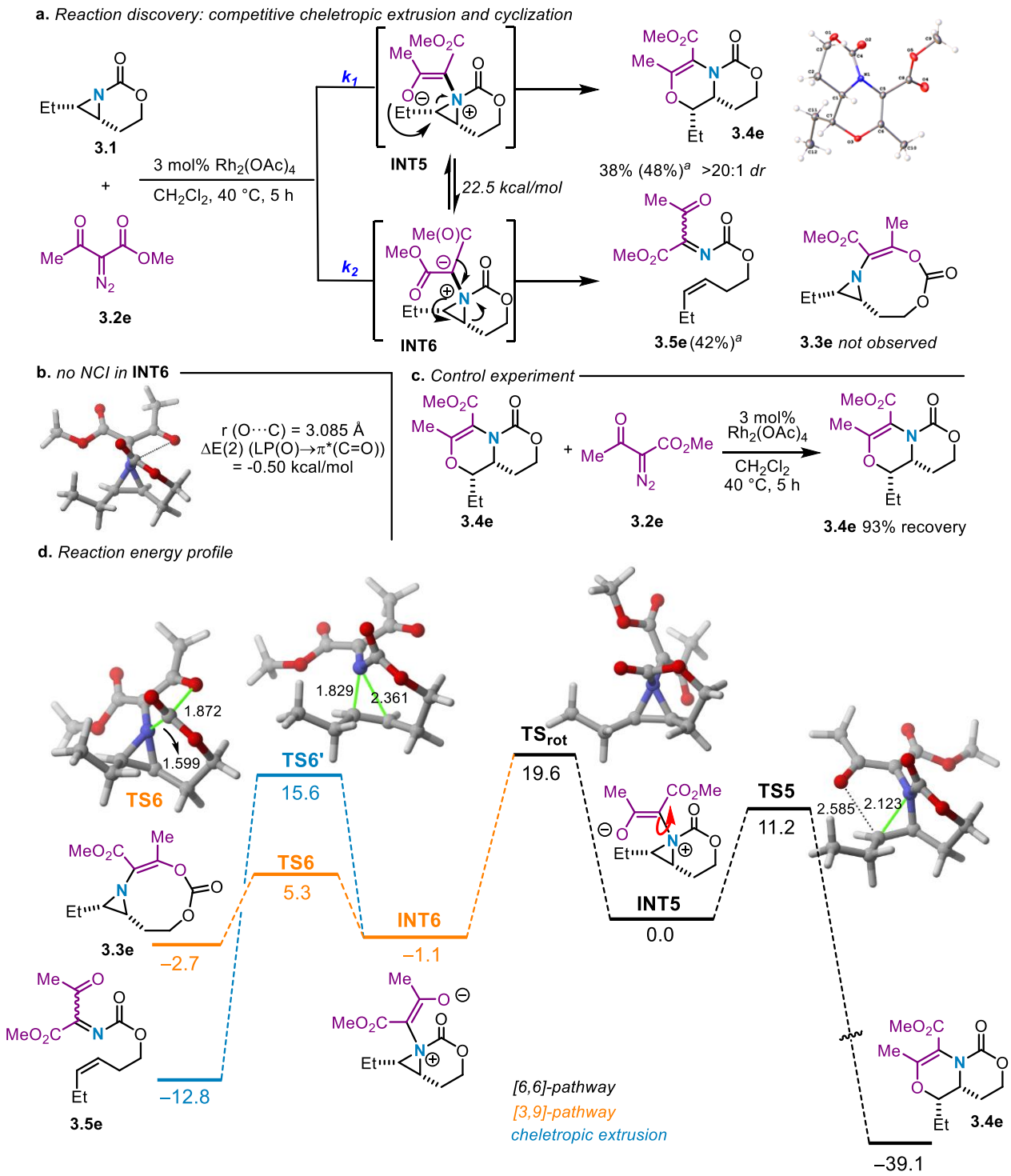
reaction of **3.1** with dicarbonyl-containing diazo compounds **3.2e** and **3.2f** show significantly higher barriers to rotation around the C–N bond at ~23 kcal/mol (red line), and 20 kcal/mol (blue line), respectively. The increased rotational barrier may be attributed to the ability of the enolate of the ylide to be delocalized over both carbonyl-containing groups, providing additional structural rigidity and steric bulk that hinders C–N bond rotation.

To test this hypothesis, aziridine **3.1** was treated with methylacetoacetate-derived **3.2e** and catalytic $Rh_2(OAc)_4$ under optimized conditions (**Scheme 3.4a**, see Supporting Information for details). The dehydromorpholine **3.4e** was obtained in 38% yield (48% by NMR), accompanied by the corresponding cheletropic extrusion product **3.5e** (42% by NMR). Interestingly, no competing [3,9]-aziridine **3.3e** was observed in the crude mixture. Computational analysis of this reaction (**Scheme 3.4b** and **3.4d**) revealed the O···C(=O) distance is much longer for **INT6** (3.085 Å) than for **INT1** (2.530 Å), a distance close to the limit of the sum of the van der Waals radii (3.22 Å). The longer distance is presumably required to accommodate the second C=O from the acceptor-acceptor carbene. This is reflected in the low computed stabilization energy ($\Delta E^{(2)}$ (LP(O)$\rightarrow\pi^*$(C=O)) = −0.50 kcal/mol) which can be considered negligible. This effectively prevents formation of the undesired NCI; as a result, **INT6** and **INT5** are nearly degenerate ($\Delta\Delta G$ ~ 1 kcal/mol), a markedly different scenario from that involving **INT1/INT2** ylides (**Figure 3.1a**, see above).

Although this computational data presents a reasonable scenario for the 1:1 product mixture, we were puzzled why no **3.3e** was observed, considering the predicted energy barrier is only 5.3 kcal/mol compared to 15.6 kcal/mol for **3.5e** (**Scheme 3.4d**). A variety of potential pathways were considered. One possibility invoked a retro-hetero-Diels-Alder reaction of **3.4e** to

give **3.5e**; however, re-exposing **3.4e** under the standard reaction conditions (**Scheme 3.4c**) gave only recovered **3.4e**. Alternatively, **3.5e** might arise from a retro-hetero-Diels-Alder of a product formed by attack of the ester carbonyl on the aziridinium ylide by delocalization of the negative charge in **INT6**. However, computational analysis argues against this pathway, as it shows an energy barrier of 18.9 kcal/mol.

Scheme 3.4 – Competing cheletropic extrusion/ring expansion to dehydromorpholines. See caption to **Figure 1** for computational details.



To experimentally interrogate the origin of **3.5e**, NMR time-course data was collected to identify long-lived reaction intermediates or other products not observed in the final crude mixture. The data (**Figure 3.3**) showed a consistent increase in product **3.4e** over the 4 h reaction period. Interestingly, a small amount of **3.3e** was noted, which increased from 1-2 h, then decreased from

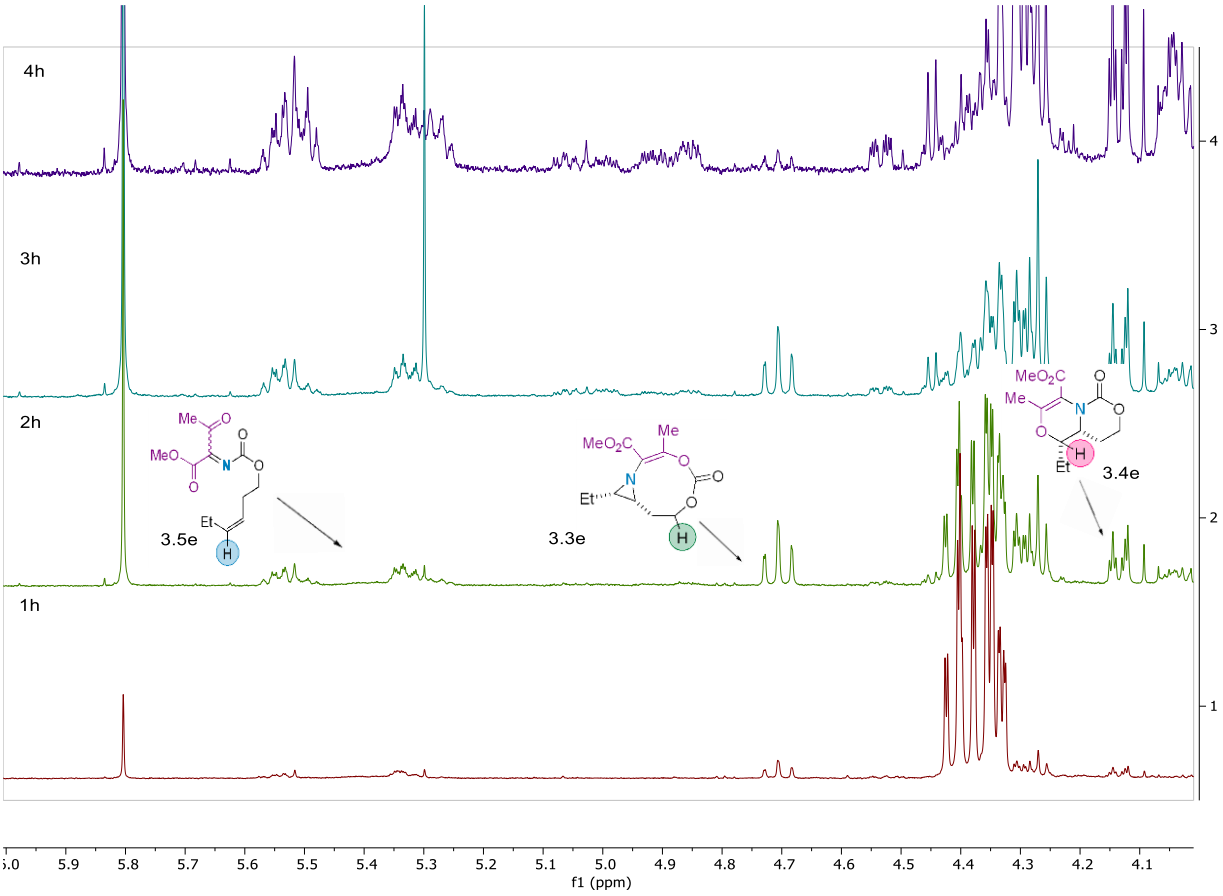


Figure 3.3 – ^{1}H NMR time course data for the reaction of **3.1** and **3.2e**.

2-4 h, at which time the cheletropic extrusion product **3.5e** was observed. The 2 h reaction aliquot was further analyzed by 1D TOCSY (see **Figure S-3.9** in the Supporting Information), which revealed a unique spin system corresponding to **3.3e**. These data are the first experimental evidence

supporting the conclusion that the reaction is under thermodynamic control (*see above*), where the [3,9]-aziridine **3.3e** gives rise to **3.5e**. This result is further supported by the computational data, which show that the formation of **3.3e** from **INT-6** is reversible in view of the low computed reaction and barrier energies (1.6 and 8.0 kcal/mol, respectively, see **Scheme 3.4d**).

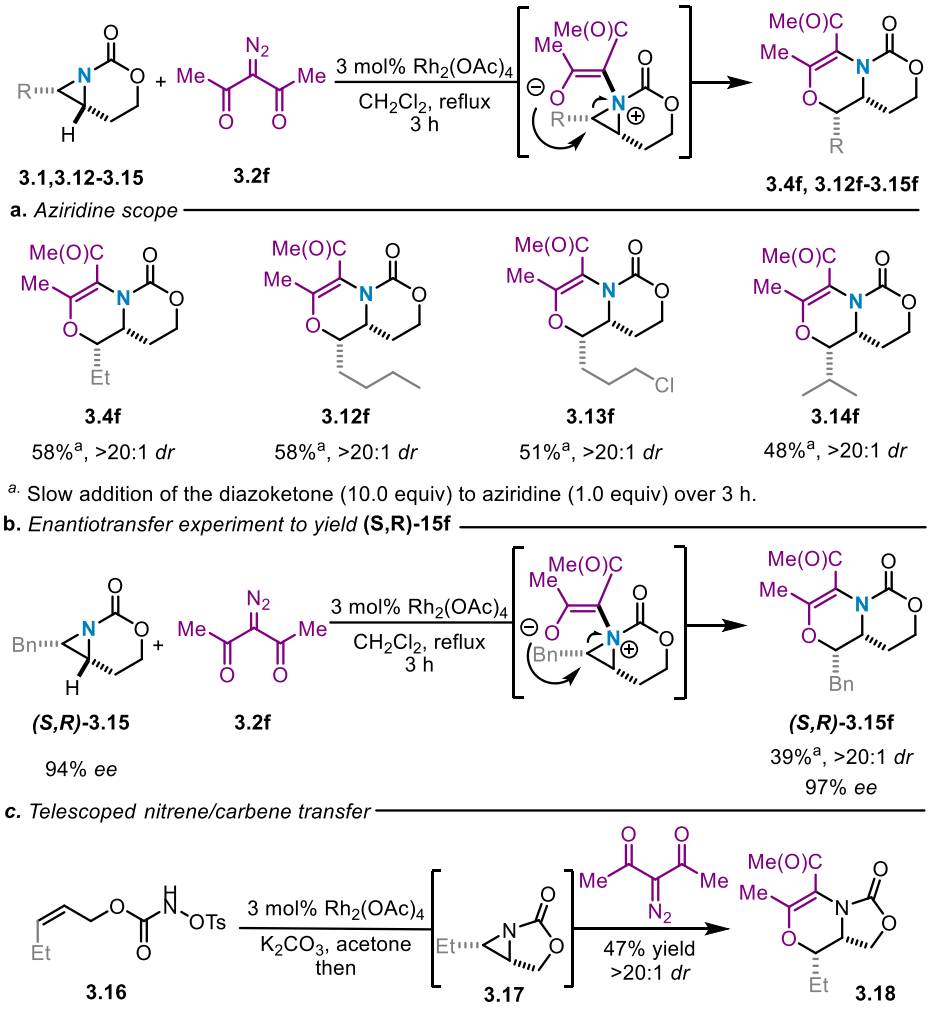
Our combined computational and experimental evidence suggests that divergent reactivity to give a ~1:1 mixture of **3.4e** and **3.5e** is due to the non-Curtin-Hammett kinetic formation of aziridinium ylide conformers **INT5** and **INT6** (**Scheme 3.4a**). **INT5** contains a *syn*-relationship between the enolate of the methyl ketone and the external aziridine C–N bond, which represents the correct geometry for dehydromorpholine formation. The other potential aziridinium ylide **INT6** does not display the correct orientation, and thus initially forms **3.3e**, which is ultimately converted to **3.5e**.

3.5 Application of Symmetric Diketone Carbene Precursors for the Formation of Dehydromorpholines

Our attempts to use non-symmetric acceptor-acceptor diazo carbene precursors to form dehydromorpholines highlighted the importance of steric effects, rotational barriers around the C–N bond of the aziridinium ylide, and NCIs in determining the reaction outcome. Symmetric diketone-containing carbene precursors, such as **3.2f** (**Scheme 3.5a**), mitigated these complications by yielding only a single ylide intermediate that engages in nucleophilic ring-opening of the aziridinium ylide to form the dehydromorpholine. A series of *cis*-substituted aziridines bearing linear alkyl chains, including a primary alkyl chloride, furnished **3.4f** and **3.12f-3.14f** as the sole products in moderate yields and high *dr* of >20:1. Isopropyl-substituted aziridine **3.14** was tolerated to furnish **3.14f**, albeit in moderate yield, indicating the sensitivity of the reaction to steric effects. Small amounts of cheletropic extrusion product (~8%) were also observed

in reactions of branched aziridines. Enantioenriched benzyl-substituted aziridine (*S*,*R*)-**3.15**, obtained in 94% *ee*, was subjected to the reaction conditions; the product **3.15f** was obtained in 39% yield and an excellent >20:1 *dr*. Importantly, the 97% *ee* of **3.15f** (**Scheme 3.5b**) highlighted our ability to effectively transfer stereochemical information from the aziridine into the products to furnish enantioenriched *N*-heterocycles.

Scheme 3.5 – Dehydromorpholine formation from symmetric carbene precursors.



This experimental result also excludes the possibility of a [4+2] hetero-Diels-Alder reaction being the operative mechanism that leads to the dehydromorpholine products **3.4f** and **3.12f-3.15f** (**Schemes 3.5ab**).

This chemistry was not restricted to aziridines bearing a 6-membered bicyclic tether; a [3,5]-bicyclic aziridine **3.17** was capable of yielding the substituted dehydromorpholine **3.18** (**Scheme 3.5c**). A nice feature of this chemistry was the ability to carry out the reaction in a telescoped fashion directly from the pre-oxidized nitrene precursor **3.16** to deliver **3.18** in 47% yield and >20:1 *dr* over both the aziridination and the ring expansion steps. Expansion of the telescoped reaction to more sterically demanding symmetric and unsymmetric carbene precursors with **3.1** proved challenging, highlighting the sensitivity of this transformation to sterics (see the Supporting Information for further details). Efforts are ongoing to address this limitation.

3.6 Conclusion

In conclusion, we have demonstrated a new method for the synthesis of highly substituted dehydromorpholines through the intermediacy of aziridinium ylides. The development of this chemistry has enabled the extension of aziridinium ylide chemistry to the concomitant formation of both a C–N and a C–O bond in a manner that preserves the stereochemical information embedded in the substrate aziridine. In addition, we have uncovered several key insights that describe the importance of steric effects, rotational barriers around the C–N bond of the aziridinium ylide, and NCIs on the ultimate reaction outcome. These critical insights will assist in the further development of this chemistry to generate novel and complex *N*-heterocycles that will further expand complex amine chemical space.

3.7 References

(1) (a) Dequina, H. J.; Schomaker, J. M. Aziridinium Ylides: Underused Intermediates for Complex Amine Synthesis. *Trends Chem.* **2020**, *2*, 874–887. (b) Ranjith, J.; Ha, H.-J. Synthetic Applications of Aziridinium Ions. *Molecules* **2021**, *26*, 1774.

(2) Schmid, S. C.; Guzei, I. A.; Schomaker, J. M. A Stereoselective [3+1] Ring Expansion for the Synthesis of Highly Substituted Methylene Azetidines. *Angew. Chem., Int. Ed.* **2017**, *56*, 12229–12233. (b) Schmid, S. C.; Guzei, I. A.; Fernández, I.; Schomaker, J. M. Ring Expansion of Bicyclic Methyleneaziridines via Concerted, Near-Barrierless [2,3]-Stevens Rearrangements of Aziridinium Ylides. *ACS Catal.* **2018**, *8*, 7907–7914.

(3) Eshon, J.; Nicastri, K. A.; Schmid, S. C.; Raskopf, W. T.; Guzei, I. A.; Fernández, I.; Schomaker, J. M. Intermolecular [3+3] Ring Expansion of Aziridines to Dehydropiperidines through the Intermediacy of Aziridinium Ylides. *Nat. Commun.* **2020**, *11*, 1273-1281.

(4) Rauk, A.; Allen, L. C.; Mislow, K. Pyramidal Inversion. *Angew. Chem., Int. Ed.* **1970**, *9*, 400–414.

(5) (a) Ju, M.; Weatherly, C. D.; Guzei, I. A.; Schomaker, J. M. Chemo- and Enantioselective Intramolecular Silver-Catalyzed Aziridinations. *Angew. Chem., Int. Ed.* **2017**, *56*, 9944–9948. (b) Rigoli, J. W.; Weatherly, C. D.; Alderson, J. M.; Vo, B. T.; Schomaker, J. M. Tunable, Chemoselective Amination via Silver Catalysis. *J. Am. Chem. Soc.* **2013**, *135*, 17238–17241. (c) Rigoli, J. W.; Weatherly, C. D.; Vo, B. T.; Neale, S.; Meis, A. R.; Schomaker, J. M. Chemoselective Allene Aziridination via Ag(I) Catalysis. *Org. Lett.* **2013**, *15*, 290–293.

(6) Clark, J. S.; Hodgson, P. B.; Goldsmith, M. D.; Blake, A. J.; Cooke, P. A.; Street, L. J. Rearrangement of Ammonium Ylides Produced by Intramolecular Reaction of Catalytically

Generated Metal Carbenoids. Part 2. Stereoselective Synthesis of Bicyclic Amines. *J. Chem. Soc., Perkin Trans. 1* **2001**, *24*, 3325–3337.

(7) Rowlands, G. J.; Kentish Barnes, W. Studies on the [2,3]-Stevens Rearrangement of Aziridinium Ions. *Tetrahedron Lett.* **2004**, *45*, 5347–5350.

(8) Hata, Y.; Watanabe, M. Fragmentation Reaction of Aziridinium Ylids. II. *Tetrahedron Lett*. **1972**, *13*, 4659–4660.

(9) L.; Liu, Q.-B.; Wang, D.-S.; Li, X.; Han, X.-W.; Xiao, W.-J.; Zhou, Y.-G. Tandem Ring-Opening/Closing Reactions of N-Ts Aziridines and Aryl Propargyl Alcohols Promoted by t-BuOK. *Org. Lett.* **2009**, *11*, 1119–1122.

(10) Zhang, S.; Shan, C.; Zhang, S.; Yuan, L.; Wang, J.; Tung, C.-H.; Xing, L.-B.; Xu, Z. Breaking Aziridines to Construct Morpholines with a Gold(i)-Catalyzed Tandem Ring-Opening and Cycloisomerization Reaction. *Org. Biomol. Chem.* **2016**, *14*, 10973–10980.

(11) Fang, S.; Zhao, Y.; Li, H.; Zheng, Y.; Lian, P.; Wan, X. [3+3]-Cycloaddition of α-Diazocarbonyl Compounds and N-Tosylaziridines: Synthesis of Polysubstituted 2H-1,4-Oxazines through Synergetic Catalysis of AgOTf/$Cu(OAc)_2$. *Org. Lett.* **2019**, *21*, 2356–2359.

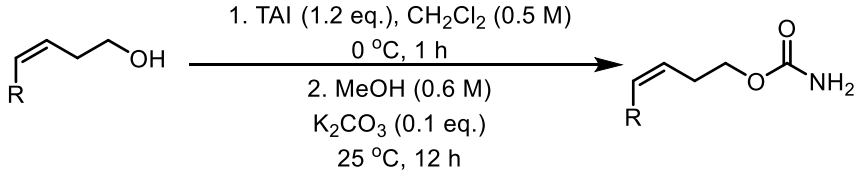
3.8. Experimental Details

Unless otherwise specified, all reactions were run under an inert atmosphere of N_2. Glassware was either oven-dried overnight at 130 °C or flame-dried under a stream of dry nitrogen prior to use. Unless otherwise specified, reagents were used as obtained from the vendor without further purification. Procedures for compounds requiring purification were obtained from "Purification of Laboratory Chemicals".[1a] All standard solvents (acetonitrile, dichloromethane, toluene) were obtained from a PureSolv MD5 5 column solvent purification system. All other solvents were also purified in accordance with methods reported in "Purification of Laboratory Chemicals".[1a] Analytical thin layer chromatography (TLC) was performed utilizing pre-coated silica gel 60 F_{254} plates containing a fluorescent indicator, while preparative chromatography was performed using SilicaFlash P60 silica gel (230-400 mesh) via Still's method.[1b] The mobile phases for column chromatography varied depending on the substrate; however, hexanes/ethyl acetate, or dichloromethane/ethyl acetate were commonly employed. Columns were typically run using a gradient method, beginning with 100% of the less polar eluent and gradually increasing the polarity with the other solvent. For reactions producing products without a UV signature, a potassium permanganate stain was employed to visualize the reaction products. ^{1}H NMR and ^{13}C NMR spectra were obtained using Bruker Avance-400, Bruker Avance-500 or Varian Inova-600 NMR spectrometers. For ^{1}H NMR, chemical shifts are reported relative to residual protiated solvent peaks (δ 7.26, 2.49, 7.15 and 4.80 ppm for $CDCl_3$, $(CD_3)_2SO$, C_6D_6 and CD_3OD respectively). ^{13}C NMR spectra were measured at either 125 MHz or 150 MHz on the same instruments noted above for recording ^{1}H NMR spectra. Chemical shifts were again reported in accordance to residual protiated solvent peaks (δ 77.1, 39.5, 128.0 and 49.0 ppm for $CDCl_3$, $(CD_3)_2SO$, C_6D_6, and CD_3OD, respectively). Accurate mass measurements were acquired at the University of Wisconsin, Madison using a Micromass LCT (electrospray ionization, time-of-flight analyzer or electron impact methods). Crystal structure data was collected on a Bruker D8 VENTURE Phot on II funded by NSF CHE-1919350. The Paul Bender Chemistry Instrumentation Center (NMR, mass spectrometry and X-ray crystallography) is funded

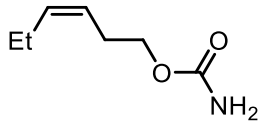
by the NSF (CHE-1048642), the NIH (1S10 OD020022-1), the Bender Fund, UW2020, and the University of Wisconsin-Madison.

3.8.1 Substrate synthesis

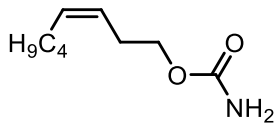
Preparation of carbamate aziridine precursors. All carbamates, if not explicitly mentioned in the subsequent sections, were synthesized according to reported literature procedures.[2]



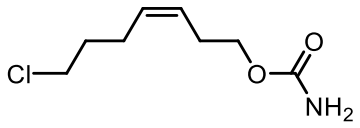
General procedure for carbamate formation. The homoallylic alcohol (1 eq.) was dissolved in CH_2Cl_2 (0.5 M) and cooled to 0 ˚C. Trichloroacetyl isocyanate (TAI) (1.2 eq.) was then added dropwise to the cooled solution. The reaction was stirred at 0 ˚C until TLC indicated complete consumption of the starting material (usually ~1 h). The solvent was then removed under reduced pressure and the crude reaction mixture was dissolved in MeOH (0.6 M). K_2CO_3 (0.1 eq.) was added in a single portion, and the mixture was stirred at room temperature until TLC indicated complete consumption of the starting material, generally overnight. Saturated aqueous NH_4Cl was added to quench the reaction and the mixture was extracted with three portions of CH_2Cl_2. The combined organic phases were washed with brine. The crude product was then diluted with CH_2Cl_2 (0.05 M) and 1 M aqueous NaOH solution (10 mL/mmol) was added. The biphasic solution was vigorously stirred for 30 min to remove the trichloroacetamide impurity. *Note: it is imperative that this step is done carefully. If not, it is likely that the aziridination will not proceed to completion.* The mixture was extracted with three portions of CH_2Cl_2. The combined organic phases were washed with brine, dried over Na_2SO_4 and concentrated under reduced pressure. The crude product was purified by silica gel column chromatography (generally, 40% EtOAc/ Hexanes).



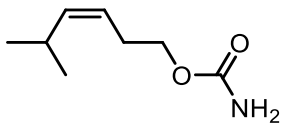
Carbamate precursor to Compound 3.1. Following the general procedure, the reaction to furnish the carbamate precursor to **3.1** was conducted on 22.1 mmol scale. The product was purified by silica gel flash column chromatography (0% to 50% EtOAc/Hex) to yield **3.1** as a white solid (2.92 g, 92% yield).[1]H NMR (500 MHz, $CDCl_3$) δ 5.50 (dtt, *J* = 10.5, 7.2, 1.6 Hz, 1H), 5.32 (dtt, *J* = 10.6, 7.3, 1.6 Hz, 1H), 4.68 (br s, 2H), 4.06 (t, *J* = 6.9 Hz, 2H), 2.37 (dt, *J* = 8.2, 6.3 Hz, 2H), 2.06 (m, 2H), 0.96 (t, *J* = 7.5 Hz, 3H). ^{13}C NMR (126 MHz, $CDCl_3$) δ 157.0, 134.6, 123.8, 64.7, 27.0, 20.6, 14.2. *m/z* matched already published data.[2]



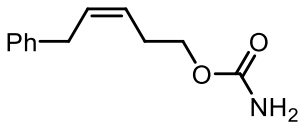
Carbamate precursor to Compound 3.12. Following the general procedure, the reaction to furnish the carbamate precursor to **3.12** was conducted on a 15.7 mmol scale. The product was purified by silica gel flash column chromatography (40% EtOAc/Hex) to yield **3.12** as a white solid (1.19 g, 44% yield). ^{1}H NMR (500 MHz, $CDCl_3$) δ 5.61 – 5.46 (m, 1H), 5.43 – 5.28 (m, 1H), 4.56 (bs, 2H), 4.06 (t, *J* = 6.9 Hz, 2H), 2.59 – 2.35 (m, 2H), 2.05 (m, 2H), 1.44 – 1.28 (m, 4H), 1.03 – 0.80 (m, 3H). ^{13}C NMR (126 MHz, $CDCl_3$) δ 157.0, 133.1, 124.5, 64.9, 31.9, 27.3, 27.2, 22.5, 14.1. HRMS (ESI) *m/z* calculated for $C_9H_{17}NO_2$ $[M+H]^+$ 172.1332; found, 172.1330.



Carbamate precursor to Compound 3.13. Following the general procedure, the reaction to furnish carbamate precursor to **3.13** was conducted on a 4.6 mmol scale. The product was purified by silica gel flash column chromatography (30% EtOAc/Hex) to yield **3.13** as a white solid (0.830 g, 95% yield). ^{1}H NMR (500 MHz, $CDCl_3$) δ 5.54 – 5.27 (m, 2H), 4.60 (br s, 2H), 4.08 (t, *J* = 6.8 Hz, 2H), 3.54 (t, *J* = 6.5 Hz, 2H), 2.51 – 2.33 (m, 2H), 2.33 – 2.17 (m, 2H), 1.93 – 1.74 (m, 2H). ^{13}C NMR (126 MHz, $CDCl_3$) δ 156.7, 130.5, 126.3, 64.5, 44.4, 32.2, 27.1, 24.4. HRMS (ESI) *m/z* calculated for $C_8H_{14}NO_2$ $[M+H]^+$ 192.0786; found, 192.0784.

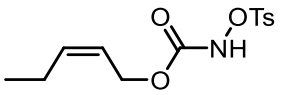


Carbamate precursor to Compound 3.14. Following the general procedure, the reaction to furnish carbamate precursor to **3.14** was conducted on a 6.02 mmol scale. The product was purified by silica gel flash column chromatography (40% EtOAc/Hex) to yield **3.14** as a white solid (0.690 g, 73% yield). ^{1}H NMR (500 MHz, $CDCl_3$) δ 5.34 (ddt, *J* = 11.0, 9.4, 1.5 Hz, 1H), 5.23 (dt, *J* = 10.7, 7.2 Hz, 1H), 4.53 (br s, 2H), 4.06 (t, *J* = 6.9 Hz, 2H), 2.60 (m, 1H), 2.39 (tdd, *J* = 7.0, 7.0, 1.5 Hz, 2H); (app qd, *J* = 7.0, 1.5 Hz, 2H), 0.96 (d, *J* = 6.6 Hz, 6H).^{13}C NMR (126 MHz, $CDCl_3$) δ 156.9, 140.4, 121.9, 64.8, 27.2, 26.6, 23.1. HRMS (ESI) *m/z* calculated for $C_8H_{15}NO_2$ $[M+H]^+$ 158.1176; found, 158.1175.



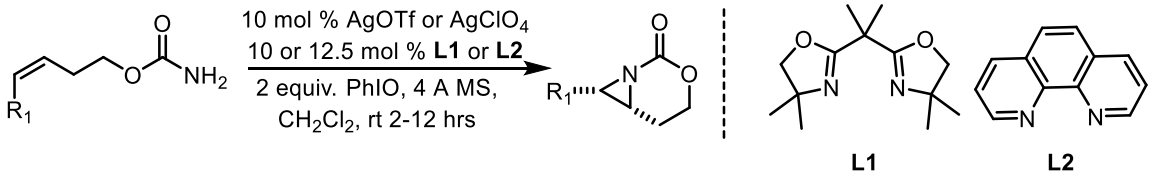
Carbamate precursor to Compound 3.15. Following the general procedure, the reaction to furnish the carbamate precursor to **3.15** was conducted on a 10 mmol scale. The product was purified by silica gel flash column chromatography (20% to 50% EtOAc/Hex) to yield **3.15** as a white solid (1.81g, 88% yield). ^{1}H NMR (500 MHz, $CDCl_3$) δ 7.31 – 7.27 (m, 2H), 7.22 – 7.17 (m, 3H), 5.72 (dtt, *J* = 10.8, 7.5, 1.6 Hz, 1H), 5.52 (dtt, *J* = 10.7, 7.3, 1.7 Hz, 1H), 4.55 (br s, 2H), 4.12 (t, *J* = 6.7 Hz, 2H), 3.43 (dd, *J* = 7.5, 1.5 Hz, 2H), 2.50 (tdd, *J* = 6.8, 6.8, 1.8 Hz); (app qd, *J* = 6.8, 1.8 Hz). ^{13}C NMR (126 MHz, $CDCl_3$) δ 156.9, 140.8,

131.1, 128.6, 128.5, 126.1, 125.8, 64.6, 33.6, 27.3. HRMS (ESI) *m/z* calculated for $C_{12}H_{15}NO_2$ $[M+H]^+$ 206.1176; found, 206.1173.



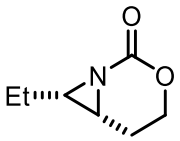
Carbamate precursor to Compound 3.18. The *N*-tosyl carbamate **3.18** was synthesized following Lebel's reported procedure.[3] ^{1}H NMR (500 MHz, $CDCl_3$) δ 7.89 – 7.86 (m, 2H), 7.77 (br s, 1H), 7.36 (d, *J* = 8.1 Hz, 2H), 5.62 (dtt, *J* = 10.3, 7.5, 1.4 Hz, 1H), 5.29 (dtt, *J* = 10.4, 7.0, 1.6 Hz, 1H), 4.56 (dd, *J* = 7.0, 1.2 Hz, 2H), 2.46 (s, 3H), 2.04 (qdd, *J* = 7.6 Hz, 7.6 Hz, 1.6 Hz); (app pd, *J* = 7.6, 1.6 Hz). , 0.96 (t, *J* = 7.5 Hz, 3H). ^{13}C NMR (126 MHz, $CDCl_3$) δ 155.5, 146.2, 138.2, 130.5, 129.9, 129.7, 121.5, 62.8, 21.9, 21.0, 14.1. δ HRMS (ESI) *m/z* calculated for $C_{13}H_{21}N_2O_5S$ $[M+NH_4]^+$ 317.1166; found, 317.1166.

Preparation of aziridine precursors. All aziridines, if not explicitly mentioned in the subsequent sections, were synthesized according to reported literature procedures.[2]

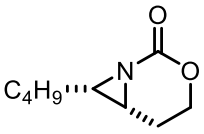


General procedure for silver-catalyzed aziridination of homoallylic carbamates. A cooled, flame-dried round bottom flask was charged with $AgClO_4$ or AgOTf (0.1 eq.) and dimethyl bisoxazoline **L1** or 1,10-phenanthroline ligand **L2** (0.1 eq.). Dry CH_2Cl_2 (0.05 M) was added to the round-bottom and the mixture was stirred vigorously for 15 minutes. *Note: Both **L1** and **L2** will furnish the aziridine product. **L2** may result in varying ratios of aziridine to C-H insertion product if the metal/ligand ratio is not carefully measured to be 1:1.*[2] ***L1** is the preferable ligand, as the ratio of metal/ligand is not as important to the aziridine/C-H insertion product ratio. However, **L2** is a good commercially available alternative if **L1** is unavailable.* After 15 minutes of pre-stirring, powdered 4Å molecular sieves (1g of sieves /mmol of substrate) were added. After 5 minutes, the carbamate ester

(1 eq.) and iodosobenzene (2 eq.) were added. The reaction was then capped, covered in aluminum foil (if AgOTf is used), and allowed to stir at room temperature for 2-12 h. After TLC indicated complete consumption of the starting material, the reaction mixture was filtered over celite and concentrated. The crude mixture was then purified by column chromatography – once with a gradient elution of 0-2.5% MeOH/CH_2Cl_2, followed by a second column with a gradient elution of 0-50% EtOAc/hexanes or 5% EtOAc/CH_2Cl_2. *Note*: *omitting the first plug with CH_2Cl_2 leaves silver byproducts in the mixture, which, upon concentration, can degrade the aziridine over time or cause decreased reactivity in the subsequent carbene transfer reaction.* The compounds were stored at -20 or -78 ˚C to prevent decomposition. All aziridines not described below were prepared according to published literature procedures.

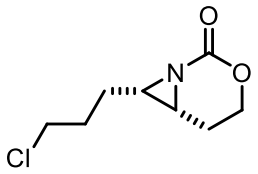


Compound 3.1. Following the general procedure, the aziridination reaction to furnish **3.1** was conducted on 6.98 mmol scale. The product was purified by silica gel flash column chromatography (0-2.5% MeOH/CH_2Cl_2, then 0 to 5% EtOAc/CH_2Cl_2) to yield **3.1** as a white solid (0.660 g, 67%). ^{1}H NMR (500 MHz, $CDCl_3$) δ 4.41 – 4.27 (m, 2H), 2.84 (ddd, *J* = 9.0, 6.9, 4.9 Hz, 1H), 2.57 (dt, *J* = 8.3, 5.2 Hz, 1H), 2.16 (dddd, *J* = 14.7, 7.0, 2.0, 2.0 Hz, 1H); (app ddt, *J* = 14.7, 7.0, 2.0 Hz, 1H), 1.83 (dqd, *J* = 14.4, 7.3, 5.3 Hz, 1H), 1.44 (dddd, *J* = 14.3, 12.1, 9.0, 4.9 Hz, 1H), 1.29 – 1.14 (m, 1H), 1.07 (t, *J* = 7.3 Hz, 3H). ^{13}C NMR (126 MHz, $CDCl_3$) δ 158.7, 68.0, 44.0, 37.3, 19.0 (d, *J* = 2.0 Hz), 10.9. HRMS (ESI) *m/z* matched already published data.[2]

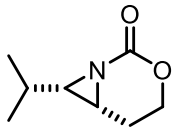


Compound 3.12. Following the general procedure, the aziridination reaction to furnish **3.12** was conducted on an 8.76 mmol scale. The product was purified by silica gel flash

column chromatography (2.5% MeOH/CH_2Cl_2 and 5% EtOAc/CH_2Cl_2) to yield **3.12** as a colorless oil (329.9 mg, 33%). ^{1}H NMR (500 MHz, $CDCl_3$) δ 4.48 – 4.29 (m, 2H), 2.87 (ddd, *J* = 8.9, 6.9, 4.9 Hz, 1H), 2.63 (dt, *J* = 9.4, 4.9 Hz, 1H), 2.18 (ddt, *J* = 14.6, 6.9, 2.0 Hz, 1H), 1.88 (ddt, *J* = 14.2, 9.6, 5.2 Hz, 1H), 1.63 – 1.32 (m, 5H), 1.16 (dtd, *J* = 14.6, 9.2, 5.2 Hz, 1H), 0.92 (t, *J* = 7.0 Hz, 3H). ^{13}C NMR (126 MHz, $CDCl_3$) δ 158.8, 68.0, 42.9, 37.5, 28.8, 25.2, 22.6, 19.3, 14.1. HRMS (ESI) *m/z* calculated for $C_9H_{16}NO_2$ $[M+H]^+$ 170.1176; found, 170.1174.

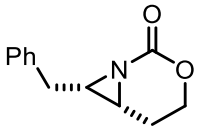


Compound 3.13. Following the general procedure, the aziridination reaction to furnish **3.13** was conducted on 0.42 mmol scale. The product was purified by silica gel flash column chromatography (2.5% MeOH/CH_2Cl_2 and then 0 to 50% EtOAc/Hex) to yield **3.13** as a colorless oil (49.7 mg, 62%). ^{1}H NMR (500 MHz, $CDCl_3$) δ 4.46 – 4.33 (m, 2H), 3.63 (ddd, *J* = 11.0, 6.8, 5.2 Hz, 1H), 3.55 (ddd, *J* = 11.0, 7.6, 5.2 Hz, 1H), 2.90 (ddd, *J* = 9.0, 6.9, 4.9 Hz, 1H), 2.65 (ddd, *J* = 7.5, 6.0, 4.9 Hz, 1H), 2.30 – 2.11 (m, 2H), 1.97 – 1.87 (m, 1H), 1.83 (dddd, *J* = 14.5, 9.6, 5.9, 4.8 Hz, 1H), 1.65 – 1.47 (m, 2H). ^{13}C NMR (126 MHz, $CDCl_3$) δ 158.6, 68.0, 44.3, 42.0, 37.4, 29.6, 23.2, 19.3 HRMS (ESI) *m/z* calculated for $C_8H_{12}ClNO_2[M+H]^+$ 190.0629; found, 190.0630.



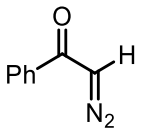
Compound 3.14. Following the general procedure, the aziridination reaction to furnish **3.14** was conducted on a 2.05 mmol scale. The product was purified by silica gel flash column chromatography (2.5% MeOH/CH_2Cl_2 and 5% EtOAc/CH_2Cl_2) to yield **3.14** as a white solid (0.316 g, 95%). ^{1}H NMR (500 MHz, $CDCl_3$) δ 4.45 – 4.22 (m, 2H), 2.81 (ddd, *J* = 9.1, 6.8, 5.0 Hz, 1H), 2.38 (dd, *J* = 9.9, 5.0 Hz, 1H), 2.19 (dddd, *J* = 14.6, 6.8, 2.0, 2.0

Hz, 1H); (app ddt, *J* = 14.6, 6.8, 2.0 Hz, 1H), 1.62 – 1.35 (m, 2H), 1.30 (d, *J* = 6.4 Hz, 3H), 1.01 (d, *J* = 6.7 Hz, 3H).^{13}C NMR (126 MHz, $CDCl_3$) δ 158.5, 67.7, 49.4, 36.9, 26.9, 20.1, 20.0, 19.6. HRMS-(ESI) *m/z* calculated for $C_8H_{13}NO_4$ $[M+Na]^+$ 156.1019; found, 156.1019.



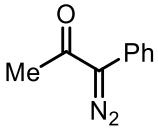
Compound 3.15. Following the general procedure, the aziridination reaction to furnish **3.15** was conducted on 0.48 mmol scale. The product was purified by silica gel flash column chromatography (0-2.5% MeOH/CH_2Cl_2, then 0 to 5% EtOAc/CH_2Cl_2) to yield **3.15** as a white solid (84.9 mg, 86%). ^{1}H NMR (500 MHz, $CDCl_3$ δ 7.34 (tt, *J* = 8.1, 1.5 Hz, 2H), 7.30 – 7.27 (m, 1H), 7.25 – 7.22 (m, 2H), 4.50 – 4.39 (m, 2H), 3.34 (dd, *J* = 15.4, 3.9 Hz, 1H), 2.98 (ddd, *J* = 8.9, 6.8, 4.8 Hz, 1H), 2.90 (ddd, *J* = 10.1, 4.8, 3.9 Hz, 1H), 2.41 (dd, *J* = 15.3, 10.1 Hz, 1H), 2.29 (dddd *J* = 14.6, 6.8, 1.9, 1.9 Hz, 1H);(app ddt, *J* = 14.6, 6.8, 1.9 Hz, 1H), 1.69 (dddd, *J* = 14.4, 12.1, 8.9, 4.7 Hz, 1H). ^{13}C NMR (126 MHz, $CDCl_3$) δ 158.6, 136.7, 129.0, 128.5, 127.2, 68.1, 42.8, 37.8, 31.1, 19.7. HRMS (ESI) *m/z* calculated for $C_{12}H_{13}NO_2[M+H]^+$ 204.1019; found, 204.1020.

Preparation of diazoketones. All diazoketone compounds, if not directly mentioned in the subsequent sections, were synthesized according to the reported literature procedures described therein. All spectroscopic data either matched that reported in the literature for the indicated compounds or new compounds were fully characterized in our facilities. When the data was not specifically obtained by us, a reference is provided so that the data may be easily located. [4-9] Frequently, the signal to noise ratio for the diazo-carbon is not intense enough to be seen on ^{13}C NMR as a result of quadrupolar broadening.

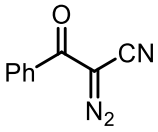


Compound 3.2a. The formation of **3.2a** was conducted on 1.5 mmol scale.[8] The product was used without further purification and was isolated as a red solid (0.220 g, 84%). ^{1}H

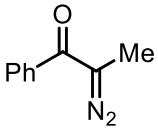
NMR (500 MHz, $CDCl_3$) δ 7.76 (dt, *J* = 7.1, 1.4 Hz, 2H), 7.67 – 7.52 (m, 1H), 7.45 (dd, *J* = 8.4, 7.0 Hz, 2H), 5.90 (s, 1H). ^{13}C NMR (126 MHz, $CDCl_3$) δ 186.4, 136.9, 132.9, 128.8, 126.9, 54.3. *m/z* matched already published data.[8]



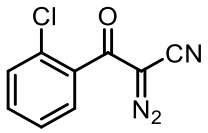
Compound 3.2b. The formation of **3.2b** was conducted on 14.2 mmol scale.[8] The product was used without further purification and **3.2b** was obtained as an orange solid (1.56 g, 69%). ^1H NMR (400 MHz, $CDCl_3$) δ 7.49 (d, *J* = 7.1 Hz, 2H), 7.46 – 7.37 (m, 2H), 7.26 (dt, *J* = 14.7, 1.3 Hz, 1H), 2.37 (s, 3H). ^{13}C NMR (126 MHz, $CDCl_3$) δ 189.9, 129.1, 127.03, 125.9, 125.6, 72.7, 27.0. *m/z* matched already published data.[8]



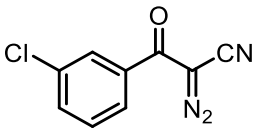
Compound 3.2c. The formation of **3.2c** was conducted on 4.0 mmol scale.[8] The product was used without the need for purification by column chromatography and yielded **3.2c** as a red solid (0.405 g, 59% yield). ^1H NMR (500 MHz, $CDCl_3$) δ 8.04 – 7.80 (m, 2H), 7.70 – 7.56 (m, 1H), 7.51 (t, *J* = 7.8 Hz, 2H). ^{13}C NMR (126 MHz, $CDCl_3$) δ 183.0, 134.8, 134.0, 129.0, 128.2, 109.3. *m/z* matched already published data.[8]



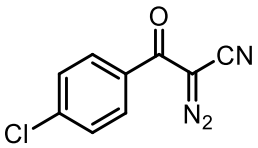
Compound 3.2d. The formation of **3.2d** was conducted on 1.5 mmol scale.[8] The product **3.2d** was used without further purification as an orange solid (121.8 mg, 51% yield). ^1H NMR (500 MHz, $CDCl_3$) δ 7.57 (dd, *J* = 7.0, 1.8 Hz, 2H), 7.53 – 7.45 (m, 1H), 7.43 (dd, *J* = 8.2, 6.5 Hz, 2H), 2.15 (s, 3H). ^{13}C NMR (126 MHz, $CDCl_3$) δ 190.3, 137.8, 131.5, 128.7, 127.3, 68.1, 25.8. *m/z* matched already published data.[8]



Diazoketone precursor to 3.6c. The formation of diazoketone precursor to **3.6c** was conducted on a 3.0 mmol scale according to the procedure reported by Krasavin.[8b] The product was additionally subjected to silica flash column chromatography (0% to 50% EtOAc/Hex) to yield the diazoketone precursor to **3.6c** as an orange solid (0.185 g, 30% yield).^{1}H NMR (500 MHz, $CDCl_3$) δ 7.50 – 7.47 (m, 2H), 7.46 – 7.43 (m, 1H), 7.39 (ddd, *J* = 7.7, 4.9, 3.5 Hz, 1H). ^{13}C NMR (126 MHz, $CDCl_3$) δ 183.8, 134.8, 133.1, 131.4, 130.8, 128.8, 127.3, 107.9. HRMS (ESI) *m/z* calculated for $C_9H_4ClNO_3$ [M+Na]+ 227.9935; found, 227.9933.

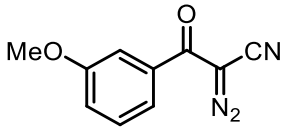


Diazoketone precursor to 3.7c. The formation of the diazoketone precursor to **3.7c** was conducted on a 4.0 mmol scale.[8] The product was pure and required no purification by column chromatography. The diazoketone precursor to **3.7c** was produced as an orange solid (0.400 g, 49% yield). ^{1}H NMR (500 MHz, $CDCl_3$) δ 7.85 (t, *J* = 2.0 Hz, 1H), 7.78 (dt, *J* = 7.7, 1.3 Hz, 1H), 7.60 (ddd, *J* = 8.1, 2.2, 1.0 Hz, 1H), 7.45 (t, *J* = 7.9 Hz, 1H). ^{13}C NMR (126 MHz, $CDCl_3$) δ 181.8, 136.1, 135.5, 134.0, 130.3, 128.3, 126.2, 108.9. *m/z* matched already published data.[8]

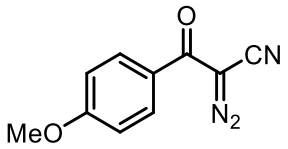


Diazoketone precursor to 3.8c. The formation of diazoketone precursor to **3.8c** was conducted on a 3.0 mmol scale according to the procedure reported by Krasavin.[8b] The product was additionally subjected to silica flash column chromatography (0% to 50% EtOAc/Hex) to yield the diazoketone precursor to **3.8c** as an orange solid (0.280 g, 47% yield). ^{1}H NMR (500 MHz, $CDCl_3$) 7.89 – 7.81 (m, 2H), 7.52 – 7.40 (m, 2H). δ ^{13}C NMR

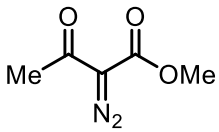
(126 MHz, $CDCl_3$) δ ^{13}C NMR (126 MHz, $CDCl_3$) δ 181.8, 140.6, 133.0, 129.7, 129.4, 109. HRMS (ASAP) $C_9H_4ClNO_3$ [M-N_2+H]+ 178.0054; found, 178.0055.



Diazoketone precursor to 3.10c. The formation of the diazoketone precursor to **3.10c** was conducted on a 4.0 mmol scale.[8] The product was used without further purification by chromatography to yield the diazoketone precursor to **3.10c** as a red solid (0.142 g, 46% yield). ^1H NMR (500 MHz, $CDCl_3$) δ 7.52 – 7.43 (m, 1H), 7.41 (t, *J* = 8.0 Hz, 1H), 7.37 (dd, *J* = 2.6, 1.7 Hz, 1H), 7.16 (ddd, *J* = 8.2, 2.7, 1.0 Hz, 1H), 3.86 (s, 3H). ^{13}C NMR (126 MHz, $CDCl_3$) δ 182.8, 160.0, 135.9, 130.1, 120.7, 120.6, 112.6, 109.3, 55.7. The *m/z* matched previously published data.[8]

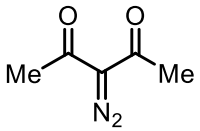


Diazoketone precursor to 3.11c. The formation of the diazoketone precursor to **3.11c** was conducted on a 3.0 mmol scale according to the procedure reported by Krasavin.[8b,9] The product was additionally subjected to silica flash column chromatography (0% to 50% EtOAc/Hex) to yield the diazoketone precursor to **3.11c** as a bright yellow solid (0.280 g, 46% yield). ^1H NMR (500 MHz, $CDCl_3$) δ 8.00 – 7.79 (m, 2H), 6.98 (d, *J* = 8.9 Hz, 2H), 3.89 (s, 3H). ^{13}C NMR (126 MHz, $CDCl_3$) δ 181.2, 164.3, 130.7, 127.5, 114.3, 109.9, 55.8. *m/z* matched already published data.[9]



Compound 3.2e. The formation of **3.2e** was conducted on a 21.5 mmol scale. The product was purified by trituration with pentane/diethyl ether (2:1 v/v) to yield **3.2e** as a yellow oil

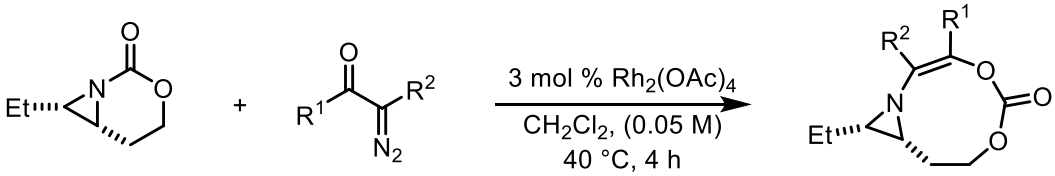
(2.50 g, 79% yield). ^{1}H NMR (400 MHz, $CDCl_3$) δ 3.84 (s, 3H), 2.48 (s, 3H). ^{13}C NMR (101 MHz, $CDCl_3$) δ 190.2, 162.0, 52.4, 28.4. *m/z* matched already published data.[4]



Compound 3.2f. The formation of **3.2f** was conducted on a 50 mmol scale. The product was purified by trituration with pentane/diethyl ether (2:1 v/v) to yield **3.2f** as a yellow oil (5.2 g, 82% yield). ^{1}H NMR (500 MHz, $CDCl_3$) δ 2.43 (s, 6H). ^{13}C NMR (126 MHz, $CDCl_3$) δ 188.4, 28.6 *m/z* matched already published data.[6]

2.8.2 General Procedures for Carbene Transfer.

General Procedure A:

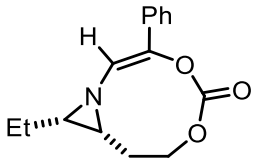


A flame-dried round bottom flask was placed under N_2 and charged with $Rh_2(OAc)_4$ (0.03 eq.), followed by a solution of the aziridine (0.1 M in dry CH_2Cl_2). The reaction setup was equipped with a reflux condenser and purged with N_2. *Note: Upon the addition of aziridine, a color change of green to purple will be observed. This does not signify catalyst death; rather, experiments show that if this color change is not observed, the reaction is less likely to proceed.* To this mixture was added a solution of the diazoketone compound (2.5 eq., brought to 0.1 M in CH_2Cl_2) dropwise over 3 h using a syringe pump. The conversion was checked by TLC and NMR after the addition was complete, and once all the starting material had been consumed, the crude material was concentrated *in vacuo* and subjected to flash column chromatography using silica-9, a basified silica gel with a pH of 9 in an aqueous solution (see below for procedure). *Note: Any exposure to standard silica gel or basic alumina led to extensive decomposition. On occasion, the [3,9]-aziridines generated via this method were unstable towards any purification media, including silica-9. Those*

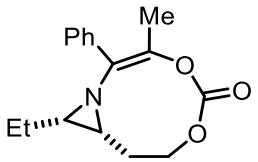
results are reported as NMR yields using 1,3,5-trimethoxybenzene as the internal standard. A gradient of 0% to 50% EtOAc/hexanes was used, with most compounds eluting around ~30% EtOAc/hexanes.

Procedure for generation of silica-9.

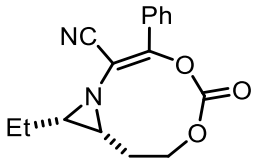
Silica-9 was prepared via a modified procedure described by both Deli[10a] and Yoon.[10b] Silica gel (200 g) was added to 2 L of saturated aqueous $NaHCO_3$. The resulting slurry was vigorously stirred for 2 h, at which point the mixture was diluted with 200 mL acetone and filtered. The silica gel was washed three times with a 1:1 H_2O/acetone mixture and once with acetone, and the filtrate was allowed to air dry overnight before use.



Compound 3.3a. Following the general procedure, the carbene transfer to furnish **3.3a** was conducted on 0.2 mmol scale. The product was purified by flash column chromatography using silica-9 (0% to 50% EtOAc/Hex) to yield **3.3a** as a white solid (40.0 mg, 78% yield, >20:1 *dr*). A crystal structure for this compound can be found in the crystallographic section. ^{1}H NMR (400 MHz, $CDCl_3$) δ 7.37 – 7.29 (m, 2H), 7.23 (t, *J* = 7.7 Hz, 2H), 7.19 – 7.12 (m, 1H), 6.48 (s, 1H), 4.77 – 4.68 (m, 1H), 4.38 (app d, *J* = 11.6 Hz, 1H), 2.05 (app q, *J* = 6.6 Hz, 1H), 1.98 (app dt, *J* = 14.6, 2.8 Hz, 1H), 1.85 (ddd, *J* = 11.2, 6.4, 1.8 Hz, 1H), 1.71 (dddd *J* = 14.5, 11.3, 11.3, 3.0 Hz); 1H (app dtd, *J* = 14.5, 11.3, 3.0 Hz, 1H), 1.51 (ddq, *J* = 14.7, 7.4, 7.4 Hz, 1H); (app dp, *J* = 14.7, 7.4 Hz, 1H), 1.45 – 1.30 (m, 1H), 0.95 (t, *J* = 7.5 Hz, 3H).^{13}C NMR (101 MHz, $CDCl_3$) δ 152.0, 143.7, 132.9, 128.7, 128.6, 127.7, 123.0, 69.7, 45.5, 28.5, 22.0, 11.7. HRMS (ESI) *m/z* calculated for $C_{15}H_{17}NO_3$ [M+Na]+ 282.1101; found, 382.1096.

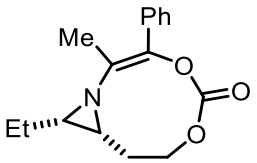


Compound 3.3b. Following the general procedure, the carbene transfer to furnish **3.3b** was conducted on a 0.3 mmol scale. The product was purified by flash column chromatography using silica-9 (0 to 50% EtOAc/Hex) to yield **3.3b** as a white solid (75.0 mg, 92% yield, >20:1 *dr*). ^{1}H NMR (500 MHz, $CDCl_3$) δ 7.37 – 7.33 (m, 2H), 7.33 – 7.26 (m, 3H), 4.74 (app t, *J* = 11.2 Hz, 1H), 4.42 (app d, *J* = 11.7 Hz, 1H), 2.04 (m, 4H), 1.99 (ddd, *J* = 11.1, 6.5, 1.9 Hz, 1H), 1.79 (m, 1H), 1.73 (app q, *J* = 6.6 Hz, 1H), 1.63 – 1.48 (m, 1H), 1.39 – 1.27 (m, 1H), 0.78 (t, *J* = 7.5 Hz, 3H). ^{13}C NMR (126 MHz, $CDCl_3$) δ 152.5, 140.0, 137.6, 134.7, 129.0, 128.3, 128.1, 69.34, 43.5, 29.0, 22.1, 17.1, 11.6. HRMS (ESI) *m/z* calculated for $C_{16}H_{19}NO_3$ [M+H]+ 274.1438; found, 274.1434.



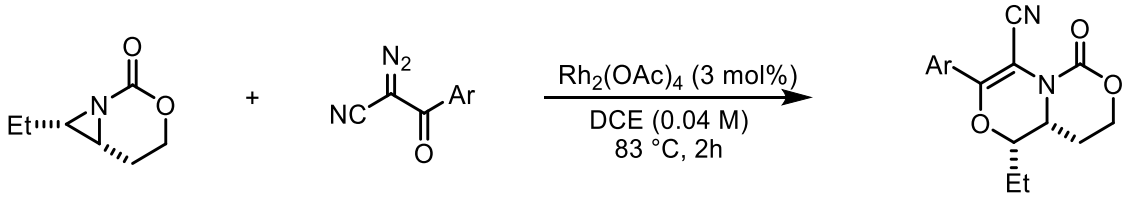
Compound 3.3c. Following the general procedure, the carbene transfer to furnish **3.3c** was conducted on a 0.2 mmol scale. Unfortunately, this compound was unstable to all forms of chromatography, including purification with silica-9. As a result, the yield reported below is an NMR yield using 1,3,5-trimethoxybenzene as an internal standard (68% yield, >20:1 *dr* 87% mass balance). ^{1}H NMR (500 MHz, $CDCl_3$) δ 7.80 – 7.66 (m, 2H), 7.50 – 7.40 (m, 3H), 4.66 (ddd, *J* = 11.6, 11.6, 23 Hz, 1H); (app td, *J* = 11.6, 2.3 Hz, 1H), 4.62 – 4.55 (jjjm, 1H), 2.56 (app q, *J* = 6.7 Hz, 1H), 2.10 (m, 2H), 1.92 (dddd *J* = 15.3, 11.3, 11.3, 4.0 Hz, 1H); (app dtd, *J* = 15.3, 11.3, 4.0 Hz, 1H), 1.59 (m, 2H), 1.09 (t, *J* = 7.5 Hz, 3H). ^{13}C NMR (126 MHz, $CDCl_3$) δ 154.5, 150.0, 130.9, 130.3, 128.9, 126.9, 123.4, 114.7, 69.5, 49.5, 46.4, 21.5, 11.5. HRMS (ESI) *m/z* calculated for $C_{16}H_{16}N_2O_3$ [M+H]+ 285.1234; found, 285.1230.

Given the overlapping peaks and complex nature of the NMR spectrum, an NMR key is provided below for both the ^{1}H NMR and ^{13}C NMR data:



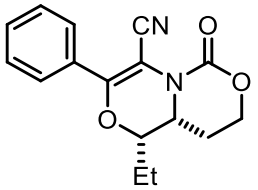
Compound 3.3d. Following the general procedure, the carbene transfer to furnish **3.3d** was conducted on a 0.3 mmol scale. The product was purified by flash column chromatography using silica-9 (0% to 50% EtOAc/Hex) to yield **3.3d** as a white solid (61.4 mg, 75% yield, >20:1 *dr*). ^{1}H NMR (500 MHz, $CDCl_3$) δ 7.51 – 7.39 (m, 2H), 7.39 – 7.32 (m, 2H), 7.25 – 7.22 (m, 1H), 4.81 (app t, *J* = 11.6 Hz, 1H), 4.35 (br d, 1H), 2.17 (app q, J= 6.3 Hz, 1H), 2.07 – 2.01 (m, 2H), 1.99 (s, 3H), 1.77 (dddd, *J* = 15.4, 12.4, 11.9, 3.3 Hz, 1H); (app dtd, *J* = 15.4, 12.4, 11.9, 3.3 Hz, 1H), 1.62 – 1.43 (m, 2H), 1.06 (t, *J* = 7.5 Hz, 3H). ^{13}C NMR (126 MHz, $CDCl_3$) δ 153.2, 137.7, 137.1, 133.9, 128.1, 127.6, 127.3, 69.3, 43.0, 28.9, 22.0, 15.5, 11.9. HRMS (ESI) *m/z* calculated for $C_{16}H_{19}NO_3$ [M+H]+ 274.1438; found, 274.1434.

General Procedure B:

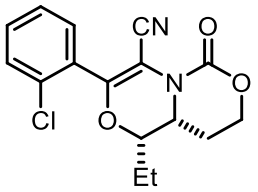


A flame-dried round bottom flask was placed under nitrogen and charged with $Rh_2(OAc)_4$ (0.03 eq.), followed by a solution of the aziridine (0.1 M in dry 1,2-dichloroethane). *Note: Unlike the previous experiments, addition of aziridine to 1,2-dichloroethane does not produce a color change of green to purple. These solutions remain green, and the reactions proceed as normal.* To this mixture was added a solution of the diazoketone (1.5 eq., brought to 0.1 M in 1,2-dichloroethane) dropwise over 2 h using a syringe pump. The conversion was checked by TLC and NMR after the addition was complete; once all the starting material had been consumed, the crude material was subjected to silica flash column chromatography using a Combiflash™ 12g gold resolution column with a 30 min method generated *via* the gradient optimizer, 0% to 100% EtOAc/He, with a hold at 52% EtOAc/Hex). *Note: The R_f differences between the aziridine and the morpholine product*

can be very small. Purification can be extremely challenging if the reaction does not go to completion.

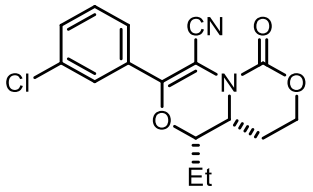


Compound 3.4c. Following the general procedure, the carbene transfer to furnish **3.4c** was conducted on 0.2 mmol scale. The product was purified by silica gel flash column chromatography using a Combiflash™ 12g gold resolution column with a 30 min method generated *via* the gradient optimizer (0% to 100% EtOAc/Hex, with a hold at 52% EtOAc/Hex) to yield **3.4c** as a light brown solid (26.6 mg, 47% yield, >19:1 *dr*).^{1}H NMR (500 MHz, $CDCl_3$) δ 7.78 – 7.68 (m, 2H), 7.50 – 7.37 (m, 3H), 4.42 (ddd, *J* = 10.2, 2.9, 2.9 Hz, 1H); (app dt, *J* = 10.2, 2.9 Hz, 1H), 4.40 – 4.30 (m, 2H), 4.02 (ddd, *J* = 10.4, 7.6, 2.4 Hz, 1H), 2.24 (ddt, *J* = 14.2, 7.5, 2.1 Hz, 1H), 2.08 – 1.96 (m, 1H), 1.76 – 1.54 (m, 2H), 1.13 (t, *J* = 7.4 Hz, 3H). ^{13}C NMR (126 MHz, $CDCl_3$) δ 154.6, 149.8, 131.5, 131.0, 128.6, 128.5, 114.4, 91.9, 79.5, 64.3, 54.0, 23.6, 19.9, 10.2. *m/z* calculated for $C_{16}H_{16}N_2O_3$ [M+H]+ 285.1234; found, 285.1230.

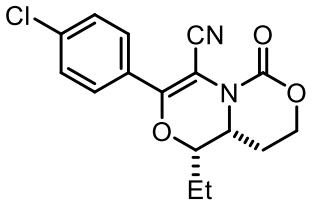


Compound 3.6c. Following the general procedure, the carbene transfer to furnish **3.6c** was conducted on 0.2 mmol scale. The product was purified by silica gel flash column chromatography using a Combiflash™ 12g gold resolution column with a 30 min method generated *via* the gradient optimizer (0% to 100% EtOAc/Hex with a hold at 52% EtOAc/Hex) to yield **3.6c** as a pale-yellow solid (21.1 mg, 33% yield, >20:1 *dr*). ^{1}H NMR (500 MHz, $CDCl_3$) δ 7.49 – 7.39 (m, 3H), 7.35 (td, *J* = 7.5, 1.3 Hz, 1H), 4.52 – 4.31 (m, 3H), 4.07 (ddd, *J* = 11.1, 7.3, 2.4 Hz, 1H), 2.24 (dddd, *J* = 14.3, 7.4, 2.2, 2.2 Hz, 1H); (app ddt, *J* = 14.3, 7.4, 2.2 Hz, 1H), 2.08 – 1.92 (m, 1H), 1.78 – 1.52 (m, 2H), 1.12 (t, *J* = 7.4 Hz, 3H).^{13}C NMR (126 MHz, $CDCl_3$) δ 152.8, 149.5, 134.0, 132.1, 131.7, 131.0, 130.3,

127.3, 113.0, 94.8, 80.2, 64.4, 54.1, 23.5, 20.0, 10.3. δ *m/z* calculated for $C_{16}H_{15}N_2O_3$ [M+H]+ 319.0844 ; found, 319.0836.

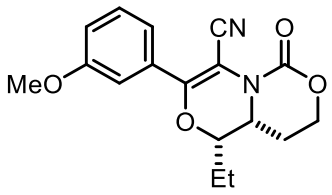


Compound 3.7c. Following the general procedure, the carbene transfer to furnish **3.7c** was conducted on 0.2 mmol scale. The product was purified by silica gel flash column chromatography using a Combiflash™ 12g gold resolution column with a 30 min method generated *via* the gradient optimizer (0% to 100% EtOAc/Hex, with a hold at 52% EtOAc/Hex) to yield **3.7c** as a brown solid (21.8 mg, 34% yield, >20:1 *dr*). ^{1}H NMR (500 MHz, $CDCl_3$) δ 7.68 – 7.63 (m, 2H), 7.43 (dt, *J* = 8.1, 1.4 Hz, 1H), 7.36 (t, *J* = 8.2 Hz, 1H), 4.42 (ddd, *J* = 10.7, 2.6, 2.6 Hz, 1H); (app dt, *J* = 10.7, 2.6 Hz, 1H), 4.40 – 4.29 (m, 2H), 4.01 (ddd, *J* = 10.9, 7.5, 2.4 Hz, 1H), 2.24 (dddd, *J* = 14.2, 7.5, 2.1, 2.1 Hz, 1H); (app ddt, *J* = 14.2, 7.5, 2.1 Hz, 1H), 1.97 (dddd, *J* = 14.2, 11.3, 11.3, 5.5 Hz, 1H); (app dtd, *J* = 14.2, 11.3, 5.5 Hz, 1H), 1.66 (m, 1H), 1.57 (m, 1H), 1.11 (t, *J* = 7.4 Hz, 3H). ^{13}C NMR (126 MHz, $CDCl_3$) δ 152.9, 149.7, 134.6, 133.3, 130.9, 129.9, 128.4, 126.7, 114.1 92.5, 79.6, 64.4, 54.0, 23.5, 20.0, 10.2. *m/z* calculated for $C_{16}H_{15}N_2O_3$ [M+H]+ 341.0663; found, 341.0659.

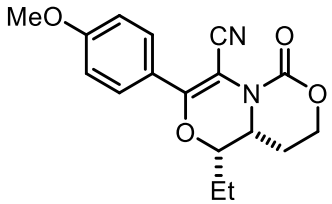


Compound 3.8c. Following the general procedure, the carbene transfer to furnish **3.8c** was conducted on 0.2 mmol scale. The product was purified by silica gel flash column chromatography using a Combiflash™ 12g gold resolution column with a 30 min method generated *via* the gradient optimizer (0% to 100% EtOAc/Hex, with a hold at 52% EtOAc/Hex) to yield **3.8c** as a beige solid (19.1 mg, 29% yield, >20:1 *dr*). ^{1}H NMR (500 MHz, $CDCl_3$) δ 7.73 – 7.59 (m, 2H), 7.48 – 7.34 (m, 2H), 4.42 (ddd, *J* = 10.6, 2.7, 2.7 Hz, 1H); (app dt, *J* = 10.6, 2.7 Hz, 1H), 4.40 – 4.31 (m, 2H), 4.01 (ddd, *J* = 11.0, 7.5, 2.4 Hz,

1H), 2.24 (dddd, *J* = 14.2, 7.6, 2.1, 2.1 Hz, 1H); (app ddt, *J* = 14.2, 7.6, 2.1 Hz, 1H), 2.08 – 1.86 (m, 1H), 1.63 (m, 2H), 1.12 (t, *J* = 7.4 Hz, 3H). ^{13}C NMR (126 MHz, $CDCl_3$) δ 153.2, 149.7, 137.1, 129.9, 129.8, 128.9, 114.2, 92.2, 79.6, 64.3, 54.0, 23.6, 20.0, 10.2. *m/z* calculated for $C_{16}H_{15}N_2O_3$ [M+NH_4]+ 336.1110 ; found, 336.1106.



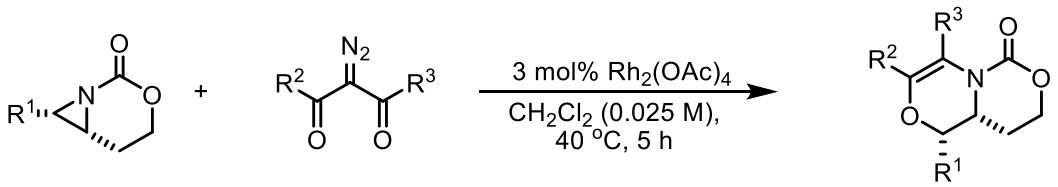
Compound 3.10c. Following the general procedure, the carbene transfer to furnish **3.10c** was conducted on a 0.2 mmol scale. The product was purified by silica gel flash column chromatography using a Combiflash™ 12g gold resolution column with a 30 min method generated *via* the gradient optimizer (0% to 100% EtOAc/Hex, with a hold at 52% EtOAc/Hex) to yield **3.10c** as a brown solid (21.5 mg, 43% yield, >20:1 *dr*).^{1}H NMR (500 MHz, $CDCl_3$) δ 7.36 – 7.28 (m, 2H), 7.28 – 7.21 (m, 1H), 6.99 (dt, *J* = 6.7, 2.7 Hz, 1H), 4.41 (ddd, *J* = 10.5, 2.7, 2.7 Hz, 1H); (app dt, *J* = 10.5, 2.7 Hz, 1H), 4.39 – 4.24 (m, 2H), 4.01 (ddd, *J* = 10.4, 7.7, 2.4 Hz, 1H), 3.82 (s, 3H), 2.23 (dddd, *J* = 14.2, 7.6, 2.1, 2.1 Hz, 1H); (app ddt, *J* = 14.2, 7.6, 2.1 Hz, 1H), 1.97 (dddd, *J* = 14.2, 11.4, 11.4, 5.3 Hz, 1H); (app dtd, *J* = 14.2, 11.4, 5.3 Hz, 1H), 1.72 – 1.54 (m, 2H), 1.11 (t, *J* = 7.4 Hz, 3H). ^{13}C NMR (126 MHz, $CDCl_3$) δ 159.5, 154.5, 149.8, 132.7, 129.7, 120.8, 117.0, 114.3, 113.6, 91.9, 79.5, 64.3, 55.6, 54.0, 23.6, 19.9, 10.2. *m/z* calculated for $C_{17}H_{18}NO_4$ [M+H]+ 315.1339; found, 315.1333.



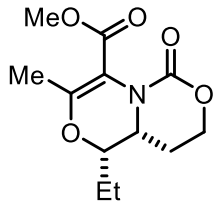
Compound 3.11c. Following the general procedure, the carbene transfer to furnish **3.11c** was conducted on a 0.2 mmol scale. The product was purified by silica gel flash column chromatography using a Combiflash™ 12g gold resolution column with a 30 min method

generated *via* the gradient optimizer (0% to 100% EtOAc/Hex, with a hold at 52% EtOAc/Hex) to yield **3.11c** as a beige solid (14.4 mg, 23% yield, >20:1 *dr*).^{1}H NMR (500 MHz, $CDCl_3$) 7.74 – 7.64 (m, 2H), 6.99 – 6.88 (m, 2H), 4.39 (ddd, *J* = 10.2, 3.5, 2.4 Hz, 1H), 4.37 – 4.27 (m, 2H), 4.00 (ddd, *J* = 10.5, 7.6, 2.4 Hz, 1H), 3.84 (s, 3H), 2.23 (dddd, *J* = 14.2, 7.6, 2.1, 2.1 Hz, 1H); (ddt, *J* = 14.2, 7.6, 2.1 Hz, 1H), 1.98 (dddd *J* = 14.1, 11.5, 11.5, 5.1 Hz, 1H); (app dtd, *J* = 14.1, 11.5, 5.1 Hz, 1H), 1.65 (m, 2H), 1.12 (t, *J* = 7.3 Hz, 3H). δ ^{13}C NMR (126 MHz, $CDCl_3$) δ 161.6, 154.4, 149.8, 130.0, 123.7, 114.8, 114.0, 90.9, 79.5, 64.2, 55.5, 54.0, 23.7, 19.9, 10.2. *m/z* calculated for $C_{17}H_{18}NO_4$ [M+H]+ 315.1339; found, 315.1332

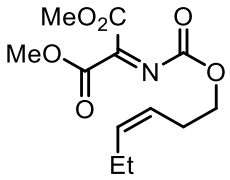
General Procedure C:



A flame-dried round bottom flask was placed under N_2 and charged with $Rh_2(OAc)_4$ (0.03 eq.), followed by a solution of the aziridine (0.1 M in dry CH_2Cl_2). The reaction setup was equipped with a reflux condenser and purged with N_2. *Note: Upon the addition of aziridine, a color change of green to purple will be observed. This does not signify catalyst death; rather, experiments show that if this color change is not observed, the reaction is less likely to proceed*. To this mixture was added a solution of the diazoketone compound (3.0 eq., brought to 0.1 M in CH_2Cl_2, unless otherwise noted) dropwise over 5 h using a syringe pump. The conversion was checked by TLC and NMR after the addition was complete; and once all the starting material had been consumed, the crude material was concentrated *in vacuo* and subjected to silica flash column chromatography using a Combiflash™ 12g gold resolution column with a 30 min method generated *via* the gradient optimizer (0% to 100% EtOAc/Hex, with a hold at 52% EtOAc/Hex). *Note: The R_f differences between the aziridine and the morpholine product can be very small. Purification can be extremely challenging if the reaction does not go to completion.*

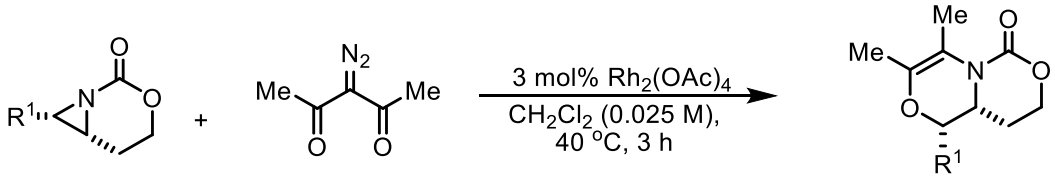


Compound 3.4e. Following the general procedure, the carbene transfer to furnish **3.4e** was conducted on 0.3 mmol scale. The product was purified by silica gel flash column chromatography using a Combiflash™ 12g gold resolution column with a 30 min method generated *via* the gradient optimizer (0% to 100% EtOAc/Hex), with a hold at 52% EtOAc/Hex) to yield **3.4e** as a white solid (27.1 mg, 38% yield, >20:1 *dr*). A crystal structure for this compound can be found below. ^{1}H NMR (500 MHz, $CDCl_3$) δ 4.41 – 4.22 (m, 2H), 4.13 (ddd, *J* = 10.4, 2.6, 2.6 Hz, 1H); (app dt, *J* = 10.4, 2.6 Hz, 1H), 3.85 (ddd, *J* = 13.6, 8.0, 3.9 Hz, 1H), 3.73 (s, 3H), 2.21 – 2.15 (m, 1H), 2.13 (s, 3H), 1.97 – 1.83 (m, 1H), 1.59 – 1.39 (m, 2H), 1.02 (t, *J* = 7.4 Hz, 3H). ^{13}C NMR (126 MHz, $CDCl_3$) δ 164.7, 152.0, 149.7, 107.8, 78.9, 64.0, 53.1, 52.0, 23.8, 19.7, 17.8, 10.2. HRMS (ESI) *m/z* calculated for $C_{12}H_{17}NO_5$ [M+Na]+ 278.0999; found, 278.0990.

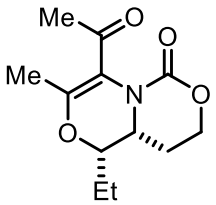


Compound SI-1. Following the general procedure, the carbene transfer to furnish **SI-1** was conducted on 0.1 mmol scale. This compound was unstable to all forms of chromatography; therefore, the NMR yield was determined using 10 μL of mesitylene as the internal standard. ^{1}H NMR (500 MHz, $CDCl_3$) δ 5.60 – 5.47 (m, 1H), 5.38 – 5.27 (m, 1H), 4.27 (t, *J* = 7.0 Hz, 2H), 3.84 (s, 6H) (over integrating as a result of excess diazoester), 2.53 – 2.43 (m, 2H), 2.06 (td, *J* = 7.6, 1.8 Hz, 2H), 0.97 (t, *J* = 7.5 Hz, 3H). ^{13}C NMR (126 MHz, $CDCl_3$) δ 166.1, 161.5, 159.7, 151.6, 135.2, 122.9, 67.2, 52.6, 26.6, 20.7, 14.2. HRMS (ESI) *m/z* calculated for $C_{12}H_{17}NO_6$[M+H]+ 272.1129; found, 272.1125.

General Procedure D:

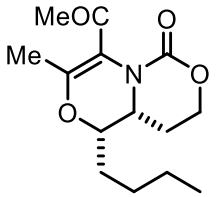


A flame-dried round bottom flask was placed under nitrogen and charged with $Rh_2(OAc)_4$ (0.03 eq.), followed by a solution of the aziridine (1.0 eq., 0.1 M in dry CH_2Cl_2). The reaction setup was equipped with a reflux condenser and purged with N_2. *Note: Upon the addition of aziridine, a color change of green to purple will be observed. This does not signify catalyst death; rather, experiments show that if this color change is not observed, the reaction is less likely to proceed*. To this mixture was added a solution of the diazoketone (10.0 eq., brought to 0.3 M in CH_2Cl_2) dropwise over 3 h using a syringe pump. *Note: the excess equivalents of the diazoketone coupling partner were necessary to achieve full conversion of the aziridine. If the equivalents are dropped, the unproductive dimerization process, along with other diazo-based side reactions, outcompetes the productive ylide-forming reaction and prevents full conversion of the starting material*. The conversion was checked by TLC and NMR after the addition was complete; once all the starting material had been consumed, the crude material was subjected to silica flash column chromatography using a Combiflash™ 12g gold resolution column with a 30 min method generated *via* the gradient optimizer (0% to 100% EtOAc/Hex, with a hold at 52% EtOAc/Hex). *Note: The R_f differences between the aziridine and the morpholine product can be very small dependent on the substrate. Purification can be extremely challenging if the reaction does not go to completion.*

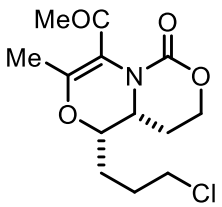


Compound 3.4f. Following the general procedure, the carbene transfer to furnish **3.4f** was conducted on a 0.2 mmol scale. The product was purified by silica gel flash column

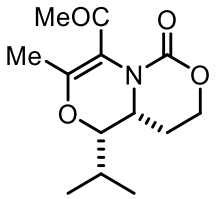
chromatography using a Combiflash™ 24g gold resolution column with a 30 min method generated *via* the gradient optimizer (0% to 100% EtOAc/Hex, with a hold at 52% EtOAc/Hex) to yield **3.4f** as a white solid (27.9 mg, 58% yield, >20:1 *dr*). ^{1}H NMR (500 MHz, $CDCl_3$) δ 4.40 – 4.27 (m, 2H), 4.14 (ddd, *J* = 10.7, 2.6, 2.6 Hz, 1H); (app dt, *J* = 10.7, 2.6 Hz, 1H), 3.92 (ddd, *J* = 10.6, 8.6, 2.5 Hz, 1H), 2.25 (dddd, *J* = 14.2, 8.5, 2.1, 2.1 Hz, 1H); (app ddt, *J* = 14.2, 8.5, 2.1 Hz, 1H), 2.14 (s, 3H), 2.11 (s, 3H), 2.04 – 1.93 (m, 1H), 1.55 (m, 1H), 1.51 – 1.41 (m, 1H), 1.03 (t, *J* = 7.3 Hz, 3H). ^{13}C NMR (126 MHz, $CDCl_3$) δ 195.1, 152.8, 148.9, 116.0, 78.7, 64.1, 53.0, 27.8, 23.7, 19.6, 18.0, 10.2. HRMS (ESI) *m/z* calculated for $C_{12}H_{17}NO_4$ [M+H]+ 240.1230; found, 240.1228.



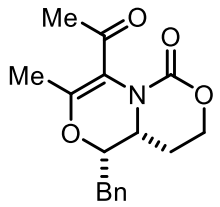
Compound 3.12f. Following the general procedure, the carbene transfer to furnish **3.12f** was conducted on a 0.3 mmol scale. The product was purified by silica gel flash column chromatography using a Combiflash™ 24g gold resolution column with a 30 min method generated *via* the gradient optimizer (0% to 100% EtOAc/Hex, with a hold at 52% EtOAc/Hex) to yield **3.12f** as a bluish-white solid (46.8 mg, 58% yield, >2:1 *dr*). ^{1}H NMR (500 MHz, $CDCl_3$ δ 4.43 – 4.26 (m, 2H), 4.19 (ddd, *J* = 7.6, 5.5, 2.5 Hz, 1H), 3.89 (ddd, *J* = 10.7, 8.6, 2.5 Hz, 1H), 2.22 (dddd, *J* = 14.2, 8.5, 2.0, 2.0 Hz, 1H); (app ddt, *J* = 14.2, 8.5, 2.0 Hz, 1H), 2.12 (s, 3H), 2.08 (s, 3H), 2.03 – 1.92 (m, 2H), 1.54 – 1.39 (m, 2H), 1.38 – 1.28 (m, 3H), 0.89 (t, *J* = 7.1 Hz, 3H). ^{13}C NMR (126 MHz, $CDCl_3$) 195.1, 152.7, 148.9, 116.0, 77.4, 64.1, 53.1, 27.9 (d, *J* = 16.4 Hz), 26.1, 23.8, 22.5, 18.0, 14.1. HRMS (ESI) *m/z* calculated for $C_{14}H_{21}NO_4$ [M+H]+ 268.1543; found, 268.1541.



Compound 3.13f. Following the general procedure, the carbene transfer to furnish **3.13f** was conducted on a 0.2 mmol scale. The product was purified by silica gel flash column chromatography using a Combiflash™ 12g gold resolution column with a 30 min method generated *via* the gradient optimizer (0% to 100% EtOAc/Hex with a hold at 52% EtOAc/Hex) to yield **3.13f** as a white solid (29.50 mg, 51% yield, >20:1 *dr*). ^{1}H NMR (500 MHz, $CDCl_3$) δ 4.42 – 4.28 (m, 2H), 4.26 (ddd, *J* = 11.1, 2.4, 2.4 Hz, 1H); (app dt, *J* = 11.1, 2.4 Hz, 1H), 3.95 (ddd, *J* = 10.8, 8.5, 2.5 Hz, 1H), 3.72 – 3.60 (m, 1H), 3.54 (ddd, *J* = 11.0, 7.5, 5.6 Hz, 1H), 2.27 (dddd, *J* = 14.4, 8.6, 2.1, 2.1 Hz, 1H); (app ddt, *J* = 14.4, 8.6, 2.1 Hz, 1H), 2.14 (s, 3H), 2.09 (s, 3H), 2.00 (m, 2H), 1.87 (m,1H), 1.78 (dddd, *J* = 15.8, 8.9, 6.2, 2.3 Hz, 1H), 1.52 (m, 1H). ^{13}C NMR (126 MHz, $CDCl_3$) δ 195.0, 152.6, 148.4, 116.1, 76.4, 64.1, 53.0, 44.3, 28.5, 27.9, 23.8, 23.5, 17.9. HRMS (ESI) *m/z* calculated for $C_{13}H_{18}ClNO_4$ [M+H]+ 288.0997; found, 288.0092.

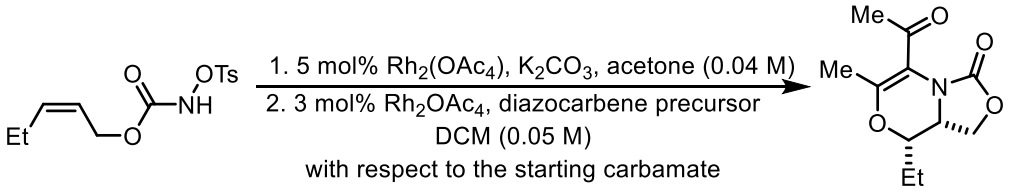


Compound 3.14f. Following the general procedure, the carbene transfer to furnish **3.14f** was conducted on a 0.2 mmol scale. The product was purified by silica gel flash column chromatography using a Combiflash™ 24g gold resolution column with a 30 min method generated *via* the gradient optimizer (0% to 100% EtOAc/Hex, with a hold at 52% EtOAc/Hex) to yield **3.14f** as a white solid (36.5 mg, 48% yield, >20:1 *dr*). This product coelutes with a minor NMR impurity that has two corresponding signals at 1.96 ppm and 1.92 ppm. These are likely a byproduct of the corresponding diazo precursor, but were inseparable from the dehydromorpholine compound in this case. ^{1}H NMR (500 MHz, $CDCl_3$) δ 4.37 (ddd, *J* = 10.8, 4.6, 2.3 Hz, 1H), 4.30 (ddd, *J* = 13.2, 11.0, 2.4 Hz, 1H), 4.08 (dd, *J* = 3.8, 3.8 Hz, 1H); (app t, *J* = 3.8 Hz, 1H), 3.96 (ddd, *J* = 11.2, 7.9, 3.5 Hz, 1H), 2.21 (ddt, *J* = 14.2, 7.9, 2.5 Hz, 1H), 2.17 – 2.12 (m, 1H), 2.11 (s, 3H), 2.10 (s, 3H), 2.01 (m, 1H), 1.09 (d, *J* = 6.8 Hz, 3H), 0.88 (d, *J* = 6.8 Hz, 3H).^{13}C NMR (126 MHz, $CDCl_3$) δ 194.8, 151.8, 150.6, 116.3, 81.0, 64.4, 53.1, 29.0, 27.9, 23.7, 22.7, 17.8, 17.0. HRMS (ESI) *m/z* calculated for $C_{13}H_{19}NO_4$ [M+Na]+ 276.1206; found, 276.1204.



Compound 3.15f. Following the general procedure, the carbene transfer to furnish **3.15f** was conducted on a 0.2 mmol scale. The product was purified by silica gel flash column chromatography using a Combiflash™ 24g gold resolution column with a 30 min method generated *via* the gradient optimizer (0% to 100% EtOAc/Hex, with a hold at 52% EtOAc/Hex) to yield **3.15f** as a white solid (21.6 mg, 36% yield, >20:1 *dr*). This product coelutes with a minor NMR impurity that has two corresponding signals at 1.96 ppm and 1.92 ppm. These are likely a byproduct of the corresponding diazo precursor, but were inseparable from the dehydromorpholine compound in this case. ^{1}H NMR (500 MHz, $CDCl_3$) δ 7.35 – 7.29 (m, 2H), 7.28 – 7.23 (m, 1H), 7.21 – 7.15 (m, 2H), 4.45 (ddd, *J* = 9.8, 3.3, 2.4 Hz, 1H), 4.43 – 4.33 (m, 2H), 4.00 (ddd, *J* = 10.7, 8.6, 2.4 Hz, 1H), 2.83 (dd, *J* = 14.4, 3.3 Hz, 1H), 2.74 (dd, *J* = 14.4, 9.8 Hz, 1H), 2.30 (dddd, J = 14.3, 8.6, 2.1, 2.1 Hz, 1H); (app ddt, *J* = 14.3, 8.6, 2.1 Hz, 1H), 2.18 (s, 3H), 2.16 – 2.03 (m, 4H).^{13}C NMR (126 MHz, $CDCl_3$) δ 194.9, 152.6, 148.4, 136.7, 129.4, 128.8, 127.0, 116.4, 78.0, 64.1, 53.3, 33.1, 28.0, 24.0, 18.0. HRMS (ESI) *m/z* calculated for $C_{17}H_{19}NO_4$ [M+H]+ 302.1387; found, 302.1384.

3.8.3 One-pot nitrene-carbene transfer reaction.

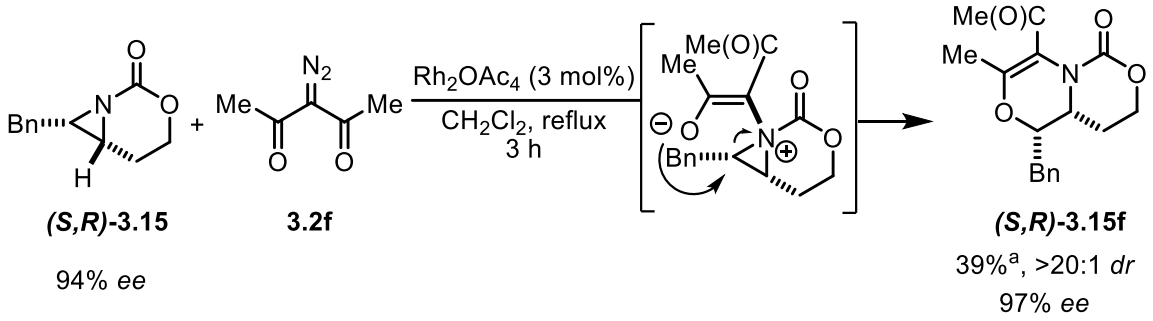


Preparation of Compound 3.18.

To a flame dried round bottom flask equipped with a stir bar was added K_2CO_3 (484.8 mg, 3.5 mmol, 7 eq.) and 5 mol % $Rh_2(OAc)_4$ (11.0 mg, 0.025 mmol, 0.05 eq.). This mixture was diluted with 8.0 mL of freshly distilled acetone and the *N*-tosyloxycarbamate precursor

to **3.18** (150.0 mg, 0.50 mmol, 1.0 eq.) was added in 4.0 mL of distilled acetone. This mixture was stirred vigorously for ~12 h (generally overnight). *Note: the reaction will start off as a deep green color, however, overnight, this color will change to a purple/gray*. The next morning CH_2Cl_2 was added to the reaction mixture and the combined organics were filtered through Celite using a fritted funnel *Note: generally coarse frits were used but medium were also acceptable*. The solution was concentrated *in vacuo* and transferred to a 50 mL flame dried round bottom flask. This flask was charged with 3 mol% of $Rh_2(OAc)_4$ (6.6 mg, 0.015 mmol, 0.03 eq.), and equipped with a reflux condenser. The combined crude aziridine and Rh catalyst were then diluted to 0.1 M with CH_2Cl_2 (5 mL). Separately, a solution 0.3 M solution of diazoketone (632.0 mg, 5.0 mmol, 10 eq.) in 15 mL of CH_2Cl_2 was prepared. This solution was added to the first solution *via* slow addition over 3 h. Once the addition of diazoketone was complete, the solution was concentrated *in vacuo* and purified by silica gel flash column chromatography using a Combiflash™ 24g gold resolution column with a 30 min method generated *via* the gradient optimizer (0% to 100% EtOAc/Hex, with a hold at 52% EtOAc/Hex) to yield **3.18** as an off-white solid (37.3 mg, 46% yield over two steps, >20:1 *dr*). *Note: Sometimes a residual tosyl acid impurity from the nitrene transfer step was identified in the final product. The residual acid was not always detected in the final purified compound. If tosyl acid is identified in the NMR after column chromatography, the best way to remove the impurity is by diluting the product in CH_2Cl_2 to 0.05 M and stirring with 10 mL of 1 M NaOH for 2 h. No product degradation has been observed when this purification technique has been applied after silica gel flash column chromatography*. ^{1}H NMR (500 MHz, $CDCl_3$) δ 4.64 (dd, *J* = 9.6, 8.2 Hz, 1H), 4.29 (dd, *J* = 9.6, 2.0 Hz, 1H), 4.24 – 4.15 (m, 1H), 3.88 (ddd, *J* = 8.1, 3.5, 1.9 Hz, 1H), 2.32 (s, 3H), 2.17 (s, 3H), 1.62 – 1.48 (m, 3H), 1.44 (m, 1H), 1.06 (t, *J* = 7.3 Hz, 3H). ^{13}C NMR (126 MHz, $CDCl_3$) δ 194.8, 156.3, 150.8, 114.0, 77.3, 64.0, 51.1, 28.3, 19.0, 18.0, 10.1. HRMS (ESI) *m/z* calculated for $C_{11}H_{15}NO_4$ [M+H]+ 226.1074; found 226.1072.

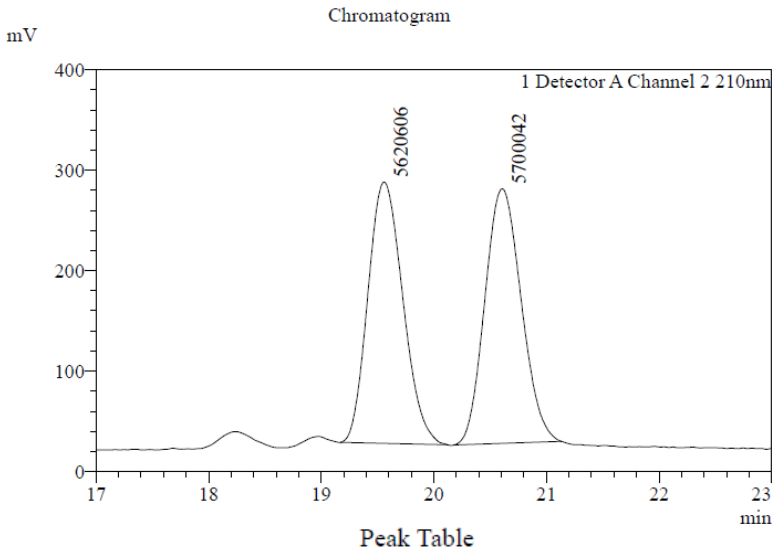
3.8.4 Transfer of chirality experiment.



Transfer of chirality experiment.

Enantioenriched bicyclic aziridine **3.15**: $AgClO_4$ (155.5 mg, 0.75 mmol, 0.20 eq.) and (***S***,***S***)-*t*BuBox (110.5 mg, 0.375 mmol, 0.10 eq.) were vigorously stirred in DCM (60 mL) for 15 min at room temperature. A charge of 4 Å MS (3.75 g; 1 g/mmol substrate) was added and the mixture was stirred for an additional 5 min. After cooling to -20 °C, a solution of the carbamate precursor to **3.15** (770 mg, 3.75 mmol, 1 eq.) in DCM (15 mL) was sequentially added along with iodosobenzene (1.651 g, 7.5 mmol, 2 eq.). The reaction was capped and stirred at -20 °C for 72 h. The reaction was filtered over Celite and concentrated, then passed through a short plug of silica gel, eluting with 5% EtOH/DCM to remove any silver salts. Purification by silica gel column chromatography (0-50% EtOAc/Hex) gave a white solid (313.6 mg, 41% yield, 87% *ee*). Recrystallization from 30% *i*PrOH/Hex gave the major enantiomer from the mother liquor (187.3 mg, 59% recovery, 94% *ee*).

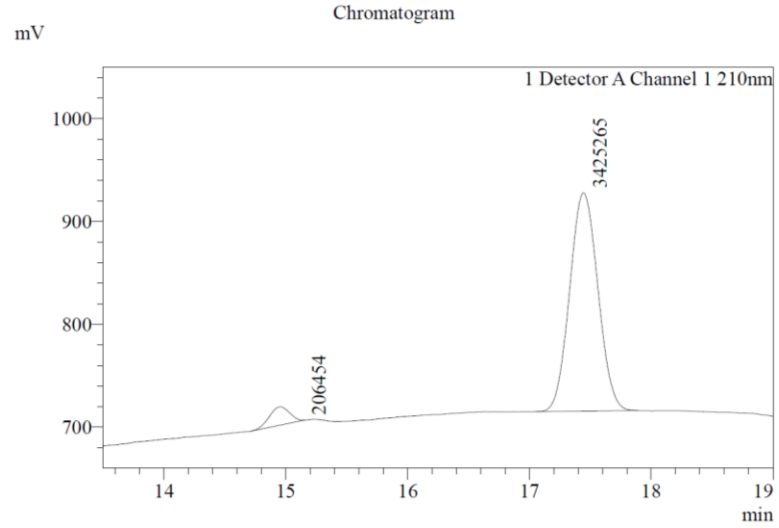
HPLC conditions: Shimadzu Prominence HPLC equipped with a 5 µm phase Chiralcel OJ-H column. Flow rate: 1 mL/min.; Oven temp: 40 °C; Solvent: 5% *i*PrOH/Hex, increased to 30% over 5 minutes, then to 35% over 10 minutes. The eluent was held at this solvent composition for 10 min to complete the analysis. The detector was set @ 210 nm.



Peak Table
Detector A Channel 2 210nm

Peak#	Ret. Time	Area	Area%
1	19.558	5620606	49.649
2	20.608	5700042	50.351
Total		11320647	100.000

Figure S-3.1. Racemic bicyclic aziridine **3.15** HPLC data.



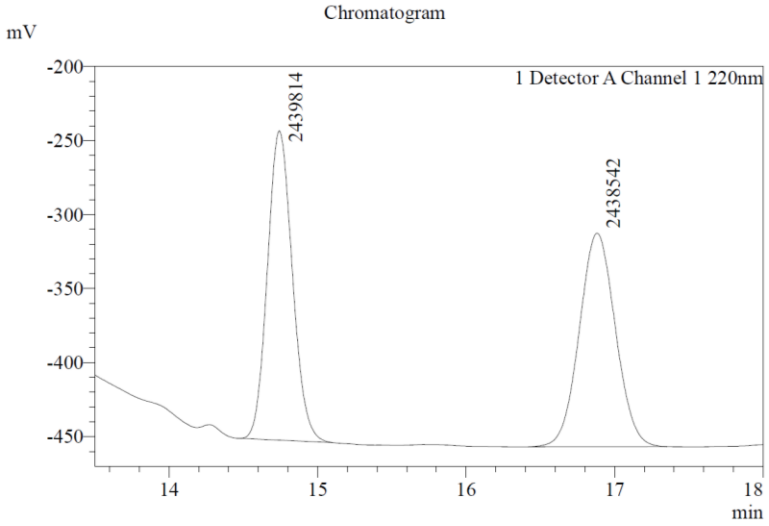
Peak Table
Detector A Channel 1 210nm

Peak#	Ret. Time	Area	Area%
1	15.138	206454	5.685
2	17.444	3425265	94.315
Total		3631719	100.000

Figure S-3.2. Enantioenriched bicyclic aziridine (*S*,*R*)-**3.15** HPLC data.

Enantioenriched morpholine **3.15f**. Following the General Procedure D, the carbene transfer reaction to furnish enantioenriched **3.15f** was conducted on a 0.2 mmol scale. The product was purified by silica gel flash column chromatography using a Combiflash™ 24g gold resolution column with a 30 min method generated *via* the gradient optimizer (0% to 100% EtOAc/Hex, with a hold at 52% EtOAc/Hex) to yield **3.15f** as a white solid (23.9 mg, 39% yield, >20:1 *dr*, 97% *ee*).

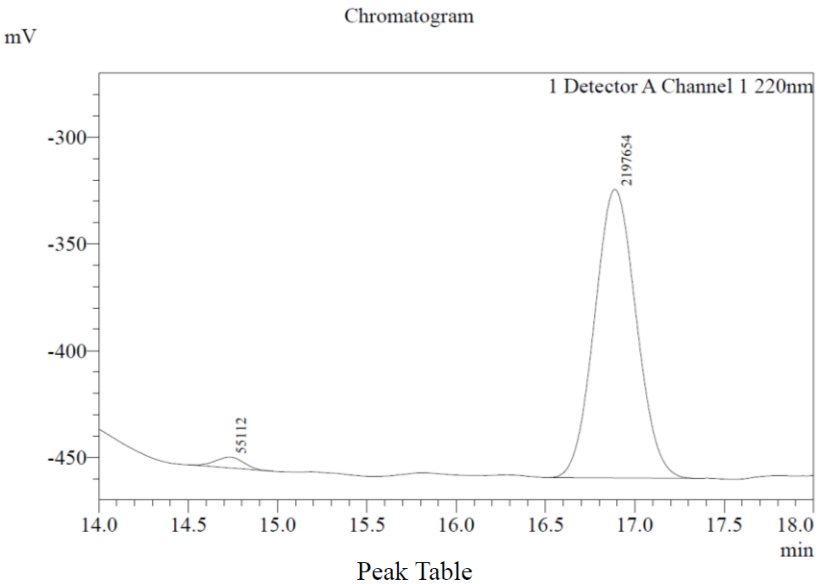
HPLC Conditions. Shimadzu Prominence HPLC equipped with a 5 µm phase Chiralpak IC column. Flow rate: 1 mL/min.; Oven temp: 40.0 °C; Solvent: 30% MeOH/H_2O (1% HCO_2H), increased to 80% over 10 minutes. The eluent was held at this composition for 15 minutes to complete analysis. Detector @ 220 nm.



Peak Table
Detector A Channel 1 220nm

Peak#	Ret. Time	Area	Area%
1	14.742	2439814	50.013
2	16.882	2438542	49.987
Total		4878356	100.000

Figure S-3.3. Racemic morpholine **3.15f** HPLC data.



Peak Table

Detector A Channel 1 220nm

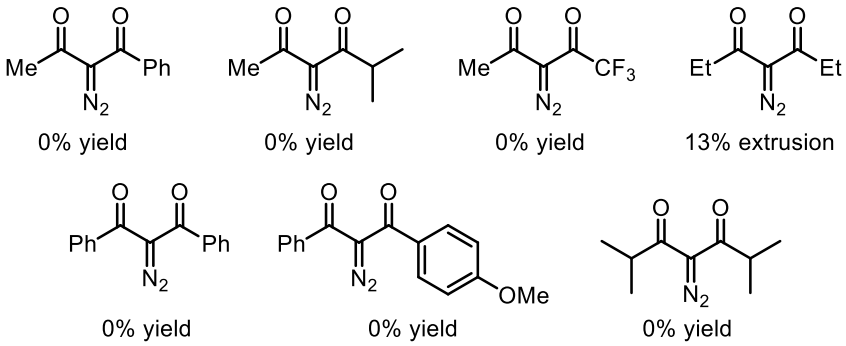
Peak#	Ret. Time	Area	Area%
1	14.730	55112	2.446
2	16.888	2197654	97.554
Total		2252766	100.000

Figure S-3.4. Enantioenriched morpholine (*S*,*R*)-**3.15f** HPLC data

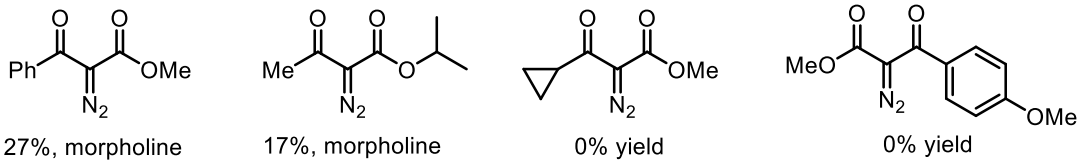
3.8.5 Limitations in substrate scope.

Diazoketones that failed under optimal reaction conditions

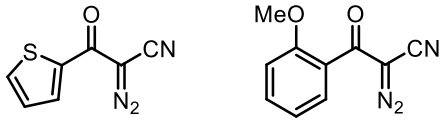
diketones:



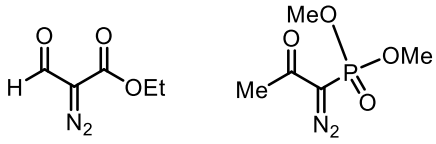
ester/ketone:



CN/ketone:



miscellaneous:



Aziridines that failed under optimal reaction conditions

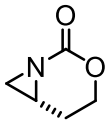
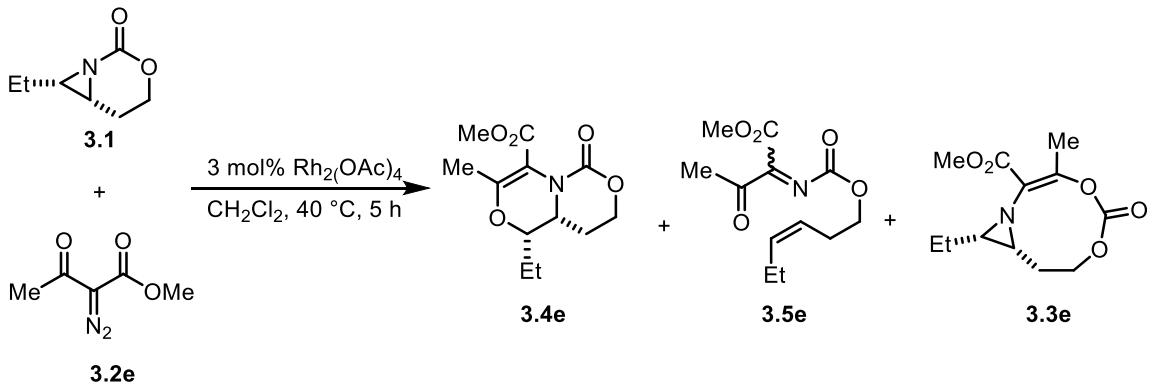


Figure S-3.5. Limitations of reaction scope.

3.8.6 NMR time course studies of the transformation of 3.1 and 3.2e to 3.3e, 3.4e and 3.5e.

A. Time course experiments to identify presence of additional products or intermediates.

The following reaction was run under standard reaction conditions reported in the General Procedure C:



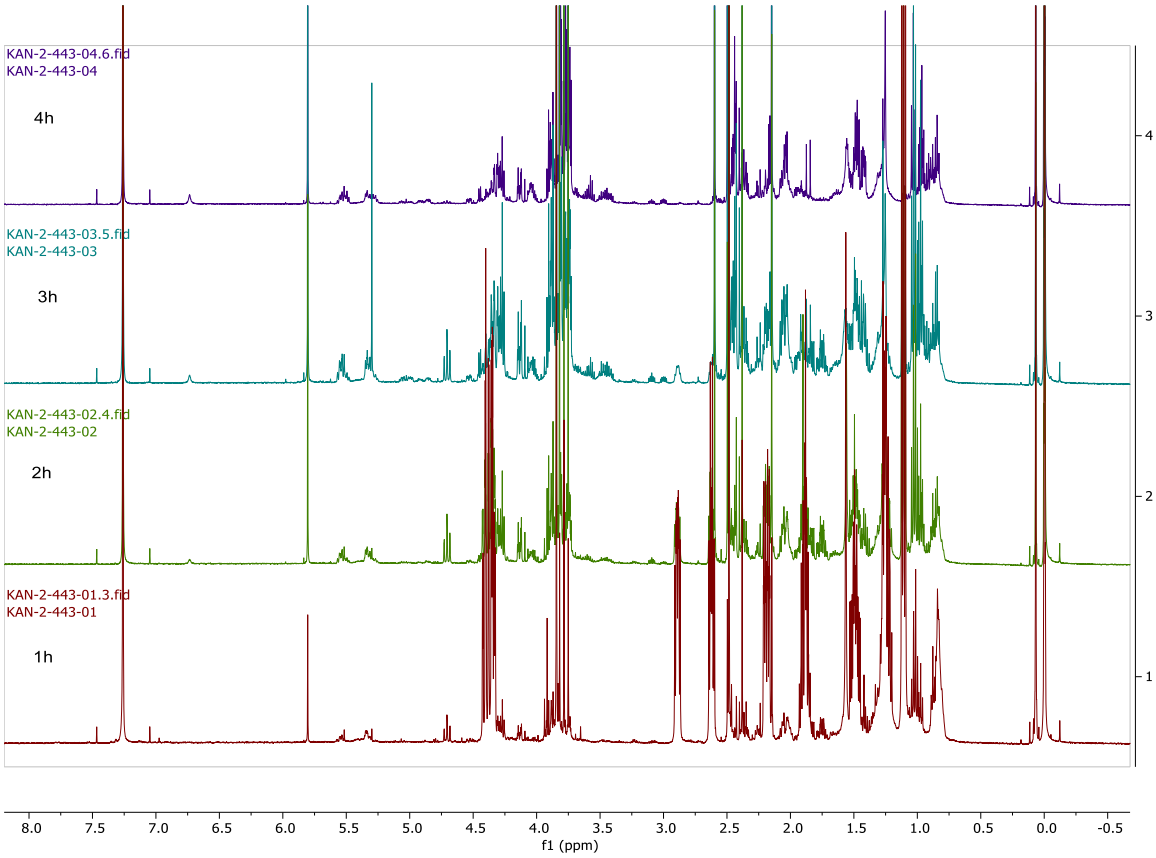


Figure S-3.6. Time course data was collected on a 500 MHz NMR, aliquots taken every hour to determine the presence of unique peaks that may provide insight into potential reaction intermediates or additional products.

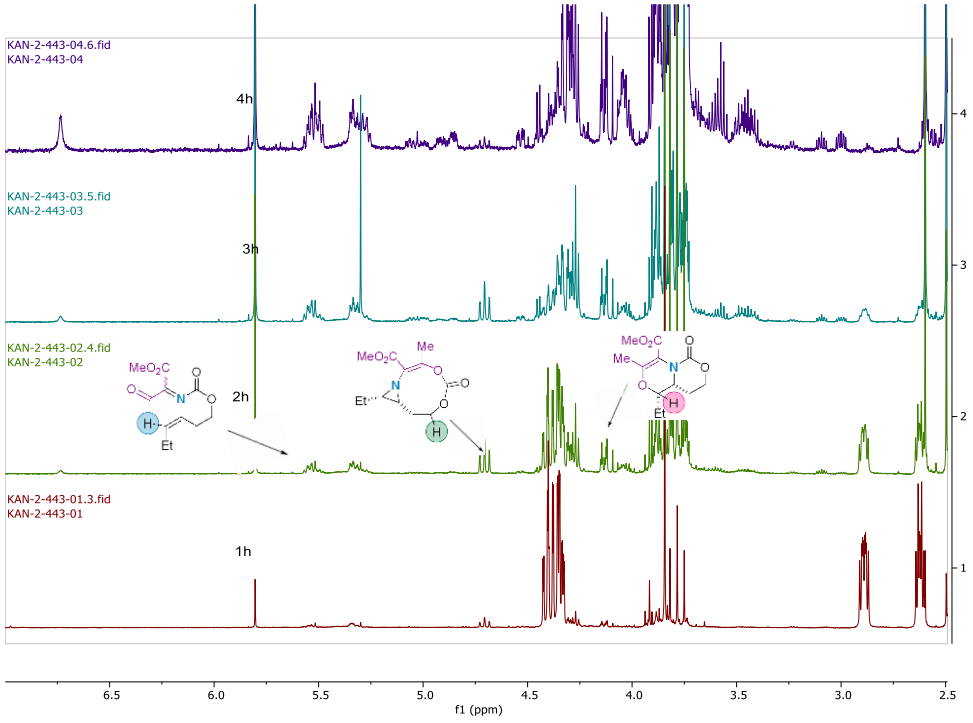


Figure S-3.7. Zoom-in of relevant peaks. As the reaction begins, after 1 h, little-to-no conversion is seen. After 2 h, conversion is seen primarily in the peaks corresponding to the morpholine **3.4e**, and [3,9]-aziridine **3.3e** with a small amount of cheletropic extrusion **3.5e.** The reaction appears to continue to consistently generate **3.4e** while **3.3e** grows in and disappears with a steady increase of **3.5e**, appearing as **3.3e** begins to disappear.

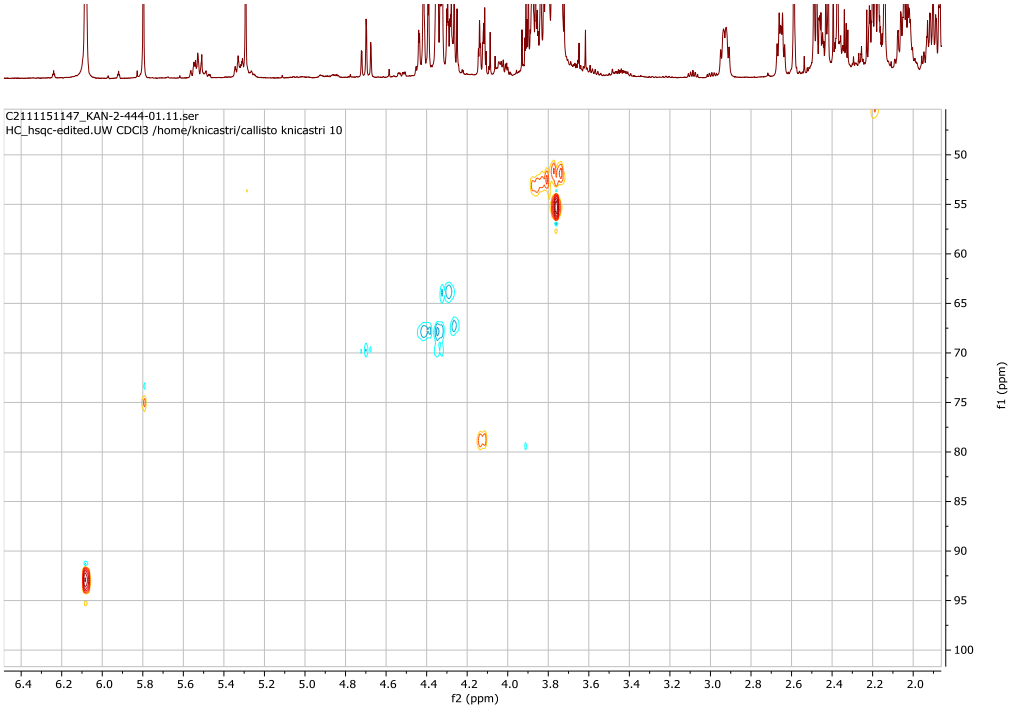


Figure S-3.8. HSQC spectrum of reaction aliquot that demonstrates the apparent t at 4.69 ppm corresponds to a CH_2 peak with a unique ^{13}CNMR shift at 69.9 ppm that matches known data for the [3,9]-aziridine.

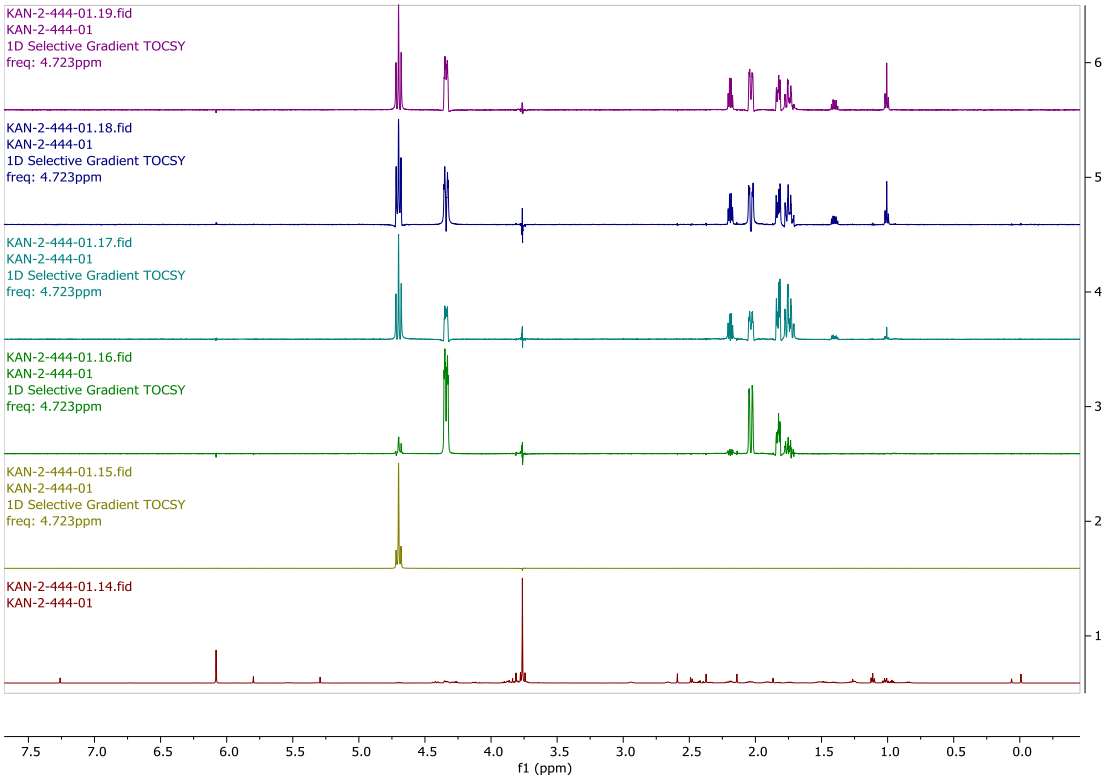


Figure S-3.9. 1D-TOCSY of an aliquot of **2h**. Irradiation of the apparent t at 4.69 ppm reveals the full chain for the unique compound proposed to be compound **3.3e**.

3.8.7 Crystallographic information for Compounds 3.3a and 3.4e.

Crystallographic Experimental Section

Data Collection for Compound 3.3a (CCDC Deposition Number 2124058).

A colorless crystal with approximate dimensions 0.40 x 0.09 x 0.09 mm^3 was selected under oil under ambient conditions and attached to the tip of a MiTeGen MicroMount©. The crystal was mounted in a stream of cold nitrogen at 100(1) K and centered in the X-ray beam by using a video camera.

The crystal evaluation and data collection were performed on a Bruker D8 VENTURE PhotonIII four-circle diffractometer with Cu Kα (λ = 1.54178 Å) radiation and the detector to crystal distance of 4.0 cm.[11]

The initial cell constants were obtained from a 180° φ scan conducted at a 2θ = 55° angle with the exposure time of 1 second per frame. The reflections were successfully indexed by an automated indexing routine built in the APEX3 program. The final cell constants were calculated from a set of 9321 strong reflections from the actual data collection.

The data were collected by using an automated data collection routine to survey the reciprocal space to the extent of a hemisphere to a resolution of 0.78 Å. A total of 26326 data were harvested by collecting 33 sets of frames with 0.8º scans in ω and φ with an exposure time 0.5–6 sec per frame. These highly redundant datasets were corrected for Lorentz and polarization effects. The absorption correction was based on fitting a function to the empirical transmission surface as sampled by multiple equivalent measurements.[12]

Structure Solution and Refinement

The systematic absences in the diffraction data were consistent for the space groups $P\bar{1}$ and *P*1. The *E*-statistics strongly suggested the centrosymmetric space group $P\bar{1}$ that yielded chemically reasonable and computationally stable results of refinement.[13-18]

A successful solution by the direct methods provided most non-hydrogen atoms from the *E*-map. The remaining non-hydrogen atoms were located in an alternating series of least-squares cycles and difference Fourier maps. All non-hydrogen atoms were refined with anisotropic displacement coefficients. All hydrogen atoms were included in the structure factor calculation at idealized positions and were allowed to ride on the neighboring atoms with relative isotropic displacement coefficients.

This compound crystallizes as a racemate with two symmetry-independent molecules in the asymmetric unit.

The final least-squares refinement of 345 parameters against 5590 data resulted in residuals *R* (based on F^2 for $I \geq 2\sigma$) and *wR* (based on F^2 for all data) of 0.0367 and 0.0889, respectively. The final difference Fourier map was featureless.

Summary

Crystal Data for $C_{15}H_{17}NO_3$ (*M* =259.29 g/mol): triclinic, space group $P\bar{1}$ (no. 2), *a* = 8.5412(8) Å, *b* = 11.6388(10) Å, *c* = 13.9486(14) Å, *α* = 75.092(6)°, *β* = 89.692(8)°, *γ* = 85.847(7)°, *V* = 1336.3(2) Å^3, *Z* = 4, *T* = 100.0 K, μ(Cu Kα) = 0.732 mm^{-1}, *Dcalc* =

1.289 g/cm^3, 26326 reflections measured (6.558° ≤ 2Θ ≤ 157.15°), 5590 unique (R_{int} = 0.0337, R_{sigma} = 0.0295) which were used in all calculations. The final R_1 was 0.0367 (I > 2σ(I)) and wR_2 was 0.0889 (all data).

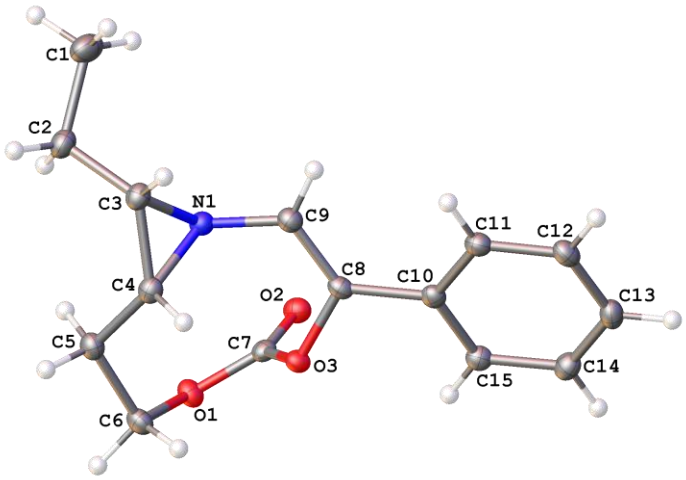


Figure S-3.10. A molecular drawing of the first symmetry-independent molecule in **3.3a** shown with 50% probability ellipsoids.

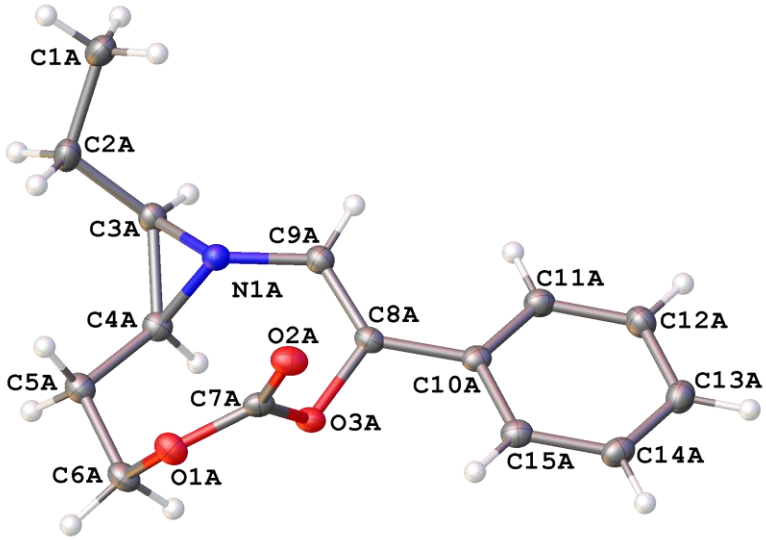


Figure S-3.11. A molecular drawing of the second symmetry-independent molecule in **3.3a** shown with 50% probability ellipsoids.

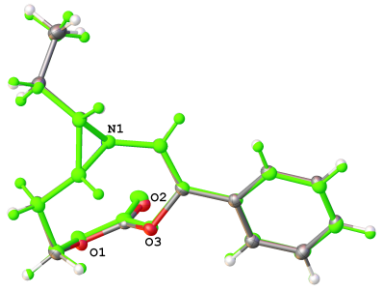


Figure S-3.12. An overlay of the two symmetry-independent molecules in **3.3a** shown with 50% probability ellipsoids. One of the enantiomers was inverted to demonstrate the conformation similarity.

Table S-1. Crystal data and structure refinement for **3.3a**.

Empirical formula	$C_{15}H_{17}NO_3$
Formula weight	259.29
Temperature/K	100.0
Crystal system	triclinic
Space group	$P\bar{1}$
a/Å	8.5412(8)
b/Å	11.6388(10)
c/Å	13.9486(14)
α/°	75.092(6)
β/°	89.692(8)
γ/°	85.847(7)
Volume/Å^3	1336.3(2)
Z	4
ρ_{calc}g/cm^3	1.289
μ/mm^{-1}	0.732
F(000)	552.0
Crystal size/mm^3	0.4 × 0.09 × 0.09
Radiation	Cu Kα (λ = 1.54178)
2Θ range for data collection/°	6.558 to 157.15
Index ranges	$-10 \leq h \leq 10$, $-14 \leq k \leq 14$, $-17 \leq l \leq 17$
Reflections collected	26326
Independent reflections	5590 [R_{int} = 0.0337, R_{sigma} = 0.0295]
Data/restraints/parameters	5590/0/345
Goodness-of-fit on F^2	1.066
Final R indexes [I>=2σ (I)]	R_1 = 0.0367, wR_2 = 0.0874
Final R indexes [all data]	R_1 = 0.0398, wR_2 = 0.0889
Largest diff. peak/hole / e Å^{-3}	0.26/-0.23

Table S-3.2. Fractional Atomic Coordinates ($\times 10^4$) and Equivalent Isotropic Displacement Parameters ($Å^2 \times 10^3$) for **3.3a**. U_{eq} is defined as 1/3 of the trace of the orthogonalised U_{IJ} tensor.

Atom	*x*	*y*	*z*	U(eq)
O1	8185.8(9)	6704.7(7)	4383.3(6)	18.02(17)
O2	9547.1(9)	5725.9(7)	5729.6(6)	18.05(17)
O3	7171.9(9)	5135.2(7)	5414.8(6)	15.18(16)
N1	6064.2(11)	6760.6(8)	6324.3(7)	15.99(19)
C1	4941.4(17)	8780.1(12)	7495.9(10)	28.4(3)
C2	4714.3(14)	8745.2(10)	6421.3(9)	21.2(2)
C3	4585.5(13)	7488.9(10)	6342.5(9)	17.7(2)
C4	5000.7(12)	7067.2(10)	5440.8(8)	16.6(2)
C5	5623.5(13)	7801.3(10)	4485.3(8)	18.1(2)
C6	6626.4(13)	7049.7(10)	3930.0(8)	18.6(2)
C7	8385.2(12)	5853.5(10)	5225.3(8)	14.9(2)
C8	6821.7(12)	4727.9(10)	6433.9(8)	15.0(2)
C9	6211.3(12)	5558.7(10)	6865.0(8)	16.4(2)
C10	7130.2(12)	3445.4(10)	6865.8(8)	15.2(2)
C11	6341.3(13)	2862.1(10)	7713.7(8)	17.5(2)
C12	6646.5(13)	1646.3(10)	8115.0(8)	19.4(2)
C13	7742.3(14)	993.3(10)	7682.1(9)	20.1(2)
C14	8520.9(13)	1569.2(10)	6837.9(9)	19.5(2)
C15	8216.5(13)	2785.3(10)	6425.6(8)	16.7(2)
O1A	3156.0(9)	6708.7(7)	9754.2(6)	19.20(17)
O2A	4575.9(9)	5647.5(8)	8910.7(6)	20.50(18)
O3A	2217.0(9)	5050.8(7)	9518.2(6)	15.82(16)
N1A	1144.8(11)	6521.4(8)	7839.9(7)	15.83(19)
C1A	472.3(15)	8395.0(11)	5708.7(9)	23.6(2)
C2A	0.2(15)	8475.0(10)	6748.5(9)	21.8(2)
C3A	-276.5(13)	7271.0(10)	7418.9(8)	17.5(2)
C4A	25.0(13)	6946.2(10)	8516.6(8)	17.0(2)
C5A	613.2(13)	7750.4(10)	9107.5(8)	18.6(2)
C6A	1576.0(13)	7068.4(11)	10020.8(8)	18.9(2)
C7A	3399.4(13)	5800.7(10)	9343.0(8)	15.9(2)
C8A	1880.7(12)	4533.1(10)	8733.7(8)	15.7(2)
C9A	1279.3(13)	5291.5(10)	7906.3(8)	16.5(2)
C10A	2166.4(12)	3232.6(10)	8965.3(8)	15.5(2)
C11A	1389.7(13)	2567.8(10)	8431.4(8)	18.3(2)
C12A	1660.4(14)	1333.7(11)	8663.9(9)	20.7(2)
C13A	2689.4(14)	742.6(10)	9433.8(9)	20.9(2)
C14A	3456.6(13)	1397.8(11)	9967.0(9)	19.6(2)

C15A	3203.1(13)	2633.4(10)	9739.0(8)	17.3(2)

Table S-3.3. Anisotropic Displacement Parameters ($Å^2 \times 10^3$) for **3.3a**. The Anisotropic displacement factor exponent takes the form: $-2\pi^2[h^2a^{*2}U_{11}+2hka^*b^*U_{12}+\ldots]$.

Atom	**U_{11}**	**U_{22}**	**U_{33}**	**U_{23}**	**U_{13}**	**U_{12}**
O1	15.5(4)	20.2(4)	16.1(4)	-0.5(3)	1.3(3)	-1.7(3)
O2	15.5(4)	21.0(4)	18.3(4)	-6.5(3)	-0.6(3)	-0.6(3)
O3	16.5(4)	16.3(4)	12.8(4)	-3.4(3)	1.4(3)	-3.1(3)
N1	16.0(4)	16.6(4)	15.7(4)	-5.0(4)	0.3(3)	0.0(3)
C1	37.1(7)	24.0(6)	27.4(7)	-11.4(5)	4.6(5)	-6.0(5)
C2	23.4(6)	16.3(5)	24.1(6)	-5.9(4)	1.9(4)	-0.3(4)
C3	16.1(5)	16.5(5)	20.4(6)	-5.0(4)	1.7(4)	-0.2(4)
C4	14.4(5)	16.4(5)	18.9(5)	-4.7(4)	-1.0(4)	-0.8(4)
C5	17.5(5)	17.5(5)	17.9(5)	-2.4(4)	-1.7(4)	-0.2(4)
C6	17.9(5)	21.7(5)	14.7(5)	-2.0(4)	-1.8(4)	-0.2(4)
C7	15.3(5)	15.1(5)	15.2(5)	-6.0(4)	3.0(4)	-0.5(4)
C8	14.0(5)	18.4(5)	12.1(5)	-2.7(4)	0.7(4)	-2.4(4)
C9	15.8(5)	17.9(5)	15.3(5)	-3.6(4)	0.5(4)	-1.7(4)
C10	14.4(5)	16.9(5)	14.5(5)	-4.3(4)	-2.4(4)	-1.6(4)
C11	17.3(5)	20.2(5)	15.2(5)	-5.3(4)	0.0(4)	-0.8(4)
C12	20.8(5)	20.9(5)	15.3(5)	-1.4(4)	-0.6(4)	-3.9(4)
C13	21.9(5)	15.7(5)	21.0(6)	-1.9(4)	-3.4(4)	-1.0(4)
C14	17.8(5)	18.6(5)	22.8(6)	-7.0(4)	-0.6(4)	0.7(4)
C15	15.2(5)	18.6(5)	16.6(5)	-4.6(4)	0.8(4)	-2.8(4)
O1A	15.2(4)	23.4(4)	21.4(4)	-9.7(3)	-0.2(3)	-3.0(3)
O2A	15.9(4)	28.3(4)	17.6(4)	-6.5(3)	1.1(3)	-0.9(3)
O3A	16.5(4)	18.5(4)	13.0(4)	-4.6(3)	0.5(3)	-2.9(3)
N1A	17.0(4)	16.2(4)	14.1(4)	-3.8(3)	-0.6(3)	-0.4(3)
C1A	30.7(6)	18.1(5)	20.0(6)	-1.9(4)	-3.8(5)	-0.1(5)
C2A	27.1(6)	15.2(5)	22.4(6)	-4.5(4)	-4.0(5)	1.7(4)
C3A	16.9(5)	17.2(5)	18.6(5)	-5.9(4)	-2.9(4)	1.3(4)
C4A	14.3(5)	18.6(5)	18.1(5)	-5.1(4)	0.4(4)	-0.8(4)
C5A	18.0(5)	19.8(5)	19.4(5)	-7.5(4)	1.3(4)	-1.4(4)
C6A	17.6(5)	23.1(6)	18.2(5)	-9.5(4)	2.5(4)	-1.4(4)
C7A	14.7(5)	19.8(5)	12.3(5)	-2.5(4)	-2.5(4)	-0.9(4)
C8A	15.0(5)	18.9(5)	14.6(5)	-6.3(4)	0.7(4)	-2.0(4)
C9A	16.5(5)	17.2(5)	16.4(5)	-5.2(4)	0.5(4)	-1.9(4)
C10A	14.1(5)	18.0(5)	13.8(5)	-3.1(4)	2.4(4)	-0.3(4)
C11A	18.1(5)	20.1(5)	16.1(5)	-4.4(4)	-1.1(4)	0.4(4)

C12A	22.9(6)	20.0(6)	20.6(6)	-7.7(4)	-1.1(4)	-1.3(4)
C13A	22.2(5)	16.9(5)	22.2(6)	-3.2(4)	1.7(4)	1.4(4)
C14A	16.6(5)	21.6(6)	18.0(5)	-1.3(4)	-0.6(4)	1.9(4)
C15A	14.6(5)	20.6(5)	16.2(5)	-4.0(4)	1.0(4)	-1.8(4)

Table S-3.4. Bond Lengths for **3.3a**.

Atom	**Atom**	**Length/Å**	**Atom**	**Atom**	**Length/Å**
O1	C6	1.4615(13)	O1A	C6A	1.4586(13)
O1	C7	1.3299(14)	O1A	C7A	1.3295(14)
O2	C7	1.1976(14)	O2A	C7A	1.1950(14)
O3	C7	1.3607(14)	O3A	C7A	1.3625(14)
O3	C8	1.4157(13)	O3A	C8A	1.4180(13)
N1	C3	1.4731(14)	N1A	C3A	1.4732(14)
N1	C4	1.4866(14)	N1A	C4A	1.4873(14)
N1	C9	1.4050(14)	N1A	C9A	1.4067(14)
C1	C2	1.5238(17)	C1A	C2A	1.5273(17)
C2	C3	1.5060(16)	C2A	C3A	1.5052(16)
C3	C4	1.4954(15)	C3A	C4A	1.4986(16)
C4	C5	1.5038(16)	C4A	C5A	1.5092(15)
C5	C6	1.5271(15)	C5A	C6A	1.5250(16)
C8	C9	1.3383(16)	C8A	C9A	1.3384(16)
C8	C10	1.4638(15)	C8A	C10A	1.4665(15)
C10	C11	1.3994(16)	C10A	C11A	1.4035(16)
C10	C15	1.4005(15)	C10A	C15A	1.4031(15)
C11	C12	1.3872(16)	C11A	C12A	1.3910(16)
C12	C13	1.3948(17)	C12A	C13A	1.3933(17)
C13	C14	1.3886(17)	C13A	C14A	1.3905(17)
C14	C15	1.3897(16)	C14A	C15A	1.3915(16)

Table S-3.5. Bond Angles for **3.3a**.

Atom	**Atom**	**Atom**	**Angle/°**	**Atom**	**Atom**	**Atom**	**Angle/°**
C7	O1	C6	120.74(9)	C7A	O1A	C6A	120.53(9)
C7	O3	C8	114.19(8)	C7A	O3A	C8A	115.25(8)
C3	N1	C4	60.69(7)	C3A	N1A	C4A	60.82(7)
C9	N1	C3	120.14(9)	C9A	N1A	C3A	121.20(9)
C9	N1	C4	116.73(9)	C9A	N1A	C4A	117.39(9)
C3	C2	C1	111.27(10)	C3A	C2A	C1A	111.86(10)
N1	C3	C2	117.05(10)	N1A	C3A	C2A	115.67(10)
N1	C3	C4	60.10(7)	N1A	C3A	C4A	60.06(7)
C4	C3	C2	124.35(10)	C4A	C3A	C2A	123.27(10)

Atom	Atom	Atom	Angle/°	Atom	Atom	Atom	Angle/°
N1	C4	C3	59.21(7)	N1A	C4A	C3A	59.12(7)
N1	C4	C5	117.47(9)	N1A	C4A	C5A	117.72(9)
C3	C4	C5	126.40(10)	C3A	C4A	C5A	126.18(10)
C4	C5	C6	112.57(9)	C4A	C5A	C6A	112.82(9)
O1	C6	C5	111.78(9)	O1A	C6A	C5A	111.41(9)
O1	C7	O3	112.75(9)	O1A	C7A	O3A	112.80(9)
O2	C7	O1	122.35(10)	O2A	C7A	O1A	122.34(11)
O2	C7	O3	124.85(10)	O2A	C7A	O3A	124.76(10)
O3	C8	C10	115.44(9)	O3A	C8A	C10A	115.13(9)
C9	C8	O3	115.80(10)	C9A	C8A	O3A	115.53(10)
C9	C8	C10	128.73(10)	C9A	C8A	C10A	129.26(10)
C8	C9	N1	119.76(10)	C8A	C9A	N1A	119.38(10)
C11	C10	C8	120.78(10)	C11A	C10A	C8A	120.71(10)
C11	C10	C15	119.21(10)	C15A	C10A	C8A	120.23(10)
C15	C10	C8	120.01(10)	C15A	C10A	C11A	119.05(10)
C12	C11	C10	120.13(10)	C12A	C11A	C10A	120.17(10)
C11	C12	C13	120.56(11)	C11A	C12A	C13A	120.56(11)
C14	C13	C12	119.40(11)	C14A	C13A	C12A	119.44(11)
C13	C14	C15	120.54(10)	C13A	C14A	C15A	120.61(11)
C14	C15	C10	120.16(10)	C14A	C15A	C10A	120.17(11)

Table S-3.6. Torsion Angles for **3.3a**.

A	B	C	D	Angle/°	A	B	C	D	Angle/°
O3	C8	C9	N1	-4.57(15)	O3A	C8A	C9A	N1A	5.04(15)
O3	C8	C10	C11	-156.30(10)	O3A	C8A	C10A	C11A	156.78(10)
O3	C8	C10	C15	23.18(14)	O3A	C8A	C10A	C15A	-22.06(14)
N1	C3	C4	C5	-103.17(12)	N1A	C3A	C4A	C5A	103.54(12)
N1	C4	C5	C6	82.16(12)	N1A	C4A	C5A	C6A	-79.59(12)
C1	C2	C3	N1	-83.30(13)	C1A	C2A	C3A	N1A	79.23(13)
C1	C2	C3	C4	-154.09(11)	C1A	C2A	C3A	C4A	148.93(11)
C2	C3	C4	N1	104.04(12)	C2A	C3A	C4A	N1A	-102.70(12)
C2	C3	C4	C5	0.86(17)	C2A	C3A	C4A	C5A	0.83(17)
C3	N1	C4	C5	117.95(11)	C3A	N1A	C4A	C5A	-117.57(11)
C3	N1	C9	C8	133.29(11)	C3A	N1A	C9A	C8A	-137.12(11)
C3	C4	C5	C6	152.68(10)	C3A	C4A	C5A	C6A	-150.08(10)
C4	N1	C3	C2	-115.92(12)	C4A	N1A	C3A	C2A	115.19(11)

C4	N1	C9	C8	63.25(13)	C4A	N1A	C9A	C8A	-66.28(13)
C4	C5	C6	O1	-76.04(12)	C4A	C5A	C6A	O1A	76.86(12)
C6	O1	C7	O2	-163.10(10)	C6A	O1A	C7A	O2A	162.38(10)
C6	O1	C7	O3	19.51(13)	C6A	O1A	C7A	O3A	-21.01(14)
C7	O1	C6	C5	75.10(12)	C7A	O1A	C6A	C5A	-75.69(13)
C7	O3	C8	C9	68.73(12)	C7A	O3A	C8A	C9A	-67.03(12)
C7	O3	C8	C10	-113.17(10)	C7A	O3A	C8A	C10A	116.01(10)
C8	O3	C7	O1	-145.12(9)	C8A	O3A	C7A	O1A	145.27(9)
C8	O3	C7	O2	37.57(14)	C8A	O3A	C7A	O2A	-38.22(15)
C8	C10	C11	C12	-179.96(10)	C8A	C10A	C11A	C12A	-179.44(10)
C8	C10	C15	C14	179.52(10)	C8A	C10A	C15A	C14A	179.11(10)
C9	N1	C3	C2	138.39(11)	C9A	N1A	C3A	C2A	-138.68(11)
C9	N1	C3	C4	-105.69(11)	C9A	N1A	C3A	C4A	106.13(11)
C9	N1	C4	C3	111.23(10)	C9A	N1A	C4A	C3A	-112.26(11)
C9	N1	C4	C5	-130.82(10)	C9A	N1A	C4A	C5A	130.16(11)
C9	C8	C10	C11	21.51(18)	C9A	C8A	C10A	C11A	-19.67(18)
C9	C8	C10	C15	-159.01(11)	C9A	C8A	C10A	C15A	161.49(11)
C10	C8	C9	N1	177.62(10)	C10A	C8A	C9A	N1A	-178.52(10)
C10	C11	C12	C13	0.19(17)	C10A	C11A	C12A	C13A	0.69(18)
C11	C10	C15	C14	-0.99(16)	C11A	C10A	C15A	C14A	0.25(16)
C11	C12	C13	C14	-0.50(17)	C11A	C12A	C13A	C14A	-0.44(18)
C12	C13	C14	C15	0.05(17)	C12A	C13A	C14A	C15A	0.10(17)
C13	C14	C15	C10	0.70(17)	C13A	C14A	C15A	C10A	-0.01(17)
C15	C10	C11	C12	0.55(16)	C15A	C10A	C11A	C12A	-0.59(16)

Table S-3.7. Hydrogen Atom Coordinates ($Å \times 10^4$) and Isotropic Displacement Parameters ($Å^2 \times 10^3$) for **3.3a**.

Atom	***x***	***y***	***Z***	**U(eq)**
H1A	4957.7	9610.13	7528.88	43
H1B	5937.68	8342.56	7755.79	43
H1C	4074.96	8410.09	7894.14	43
H2A	3749.34	9239.18	6143.7	25
H2B	5613.9	9087.38	6025.69	25
H3	3744.94	7056.46	6756.05	21
H4	4395.17	6392.6	5361.94	20
H5A	6261.93	8414.44	4631.08	22
H5B	4730.35	8217.92	4054.19	22
H6A	6092.17	6323.45	3927.59	22
H6B	6734.58	7510.16	3232.51	22
H9	5878.6	5336.63	7534.17	20
H11	5595.14	3299.64	8015.13	21
H12	6104.68	1255.17	8689.57	23
H13	7954.08	161.91	7962.25	24
H14	9267.7	1128.41	6539.88	23
H15	8746.57	3169.87	5843.74	20
H1AA	808.66	9166.53	5329.01	35
H1AB	-427.47	8185.33	5372.23	35
H1AC	1338.54	7781.86	5757.69	35
H2AA	839.75	8828.85	7039.25	26
H2AB	-969.69	9007.47	6702.47	26
H3A	-1118.39	6843.15	7192.52	21
H4A	-640.81	6319.44	8902.46	20
H5AA	-295.83	8197.54	9320.2	22
H5AB	1267.51	8336.64	8676.33	22
H6AA	1643.14	7578.3	10486.08	23
H6AB	1042.16	6351.36	10363.06	23
H9A	946.37	5001.88	7368.95	20
H11A	677.15	2961.65	7909.89	22
H12A	1139.41	890.07	8294.65	25
H13A	2865.32	-100.88	9593.12	25
H14A	4160.37	998.28	10491.78	24
H15A	3733.29	3072.25	10108.14	21

Data Collection for Compound 3.4e (CCDC Deposition Number 2124059).

A colorless crystal with approximate dimensions 0.09 x 0.06 x 0.06 mm^3 was selected under oil under ambient conditions selected under oil and attached to the tip of a MiTeGen MicroMount© . The crystal was mounted in a stream of cold nitrogen at 100(1) K and centered in the X-ray beam by using a video camera.

The crystal evaluation and data collection were performed on a Bruker D8 VENTURE PhotonIII four-circle diffractometer with Cu Kα (λ = 1.54178 Å) radiation and the detector to crystal distance of 4.0 cm.[11]

The initial cell constants were obtained from a 180° φ scan conducted at a 2θ = 50° angle with an exposure time of 1 second per frame. The reflections were successfully indexed by an automated indexing routine built into the APEX3 program. The final cell constants were calculated from a set of 9897 strong reflections from the actual data collection.

The data were collected by using a full sphere data collection routine to survey reciprocal space to the extent of a full sphere to a resolution of 0.79 Å. A total of 46757 data were harvested by collecting 33 sets of frames with 0.9º scans in ω and φ with exposure times of 2 - 25 sec per frame. These highly redundant datasets were corrected for Lorentz and polarization effects. The absorption correction was based on fitting a function to the empirical transmission surface as sampled by multiple equivalent measurements.[12]

Structure Solution and Refinement

The systematic absences in the diffraction data were consistent for the space groups *Pnma* and $Pna2_1$. The *E*-statistics strongly suggested the non-centrosymmetric space group $Pna2_1$ that yielded chemically reasonable and computationally stable results of refinement.[13-18]

A successful solution by direct methods provided most non-hydrogen atoms from the *E*-map. The remaining non-hydrogen atoms were located with an alternating series of least-squares cycles and difference Fourier maps. All non-hydrogen atoms were refined with anisotropic displacement coefficients. All hydrogen atoms were included in the structure factor calculation at idealized positions and were allowed to ride on the neighboring atoms with relative isotropic displacement coefficients.

The compound crystallizes as a racemate. The molecule shown in Figure S-13 with stereocenters C1 (*S*) and C7 (*R*) was chosen arbitrarily.

The compound crystallizes as an inversion twin, with a 43(9)% contribution from the minor component.

The final least-squares refinement of 167 parameters against 2554 data resulted in residuals *R* (based on F^2 for $I \geq 2\sigma$) and *wR* (based on F^2 for all data) of 0.0335 and 0.0856, respectively. The final difference Fourier map was featureless.

Summary.

Crystal Data for **3.4e.** $C_{12}H_{17}NO_5$ (*M* =255.26 g/mol): orthorhombic, space group *Pna*2$_1$ (no. 33), *a* = 11.2137(19) Å, *b* = 16.314(4) Å, *c* = 6.706(3) Å, *V* = 1226.8(6) Å^3, *Z* = 4, *T* = 100.0 K, μ(Cu Kα) = 0.907 mm^{-1}, *Dcalc* = 1.382 g/cm^3, 37289 reflections measured (9.57° ≤ 2Θ ≤ 157.854°), 2554 unique (R_{int} = 0.0576, R_{sigma} = 0.0215) which were used in all calculations. The final R_1 was 0.0335 (I > 2σ(I)) and wR_2 was 0.0856 (all data).

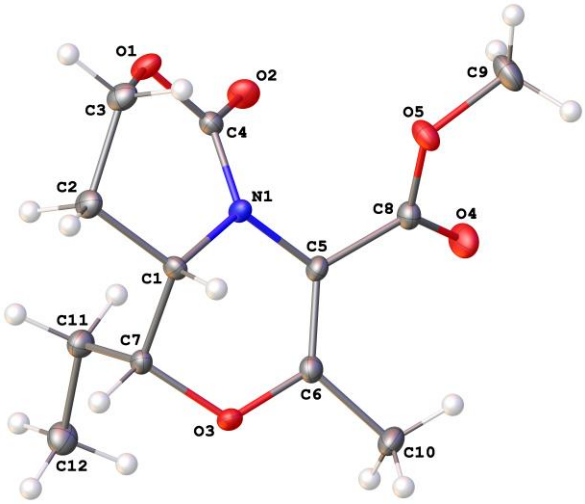


Figure S-3.13. A molecular drawing of **3.4e** shown with 50% probability ellipsoids.

Table S-3.8. Crystal data and structure refinement for **3.4e.**

Empirical formula	$C_{12}H_{17}NO_5$
Formula weight	255.26
Temperature/K	100.0
Crystal system	orthorhombic
Space group	*Pna*2$_1$

a/Å	11.2137(19)
b/Å	16.314(4)
c/Å	6.706(3)
α/°	90
β/°	90
γ/°	90
Volume/Å^3	1226.8(6)
Z	4
ρ_{calc}g/cm^3	1.382
μ/mm^{-1}	0.907
F(000)	544.0
Crystal size/mm^3	0.09 × 0.06 × 0.06
Radiation	Cu Kα (λ = 1.54178)
2Θ range for data collection/°	9.57 to 157.854
Index ranges	-14 ≤ h ≤ 14, -20 ≤ k ≤ 20, -8 ≤ l ≤ 7
Reflections collected	37289
Independent reflections	2554 [R_{int} = 0.0576, R_{sigma} = 0.0215]
Data/restraints/parameters	2554/1/167
Goodness-of-fit on F^2	1.086
Final R indexes [I>=2σ (I)]	R_1 = 0.0335, wR_2 = 0.0840
Final R indexes [all data]	R_1 = 0.0362, wR_2 = 0.0856
Largest diff. peak/hole / e Å^{-3}	0.30/-0.18
Flack parameter	0.43(9)

Table S-3.9. Fractional Atomic Coordinates (×10^4) and Equivalent Isotropic Displacement Parameters (Å^2×10^3) for **3.4e**. U_{eq} is defined as 1/3 of of the trace of the orthogonalised U_{IJ} tensor.

Atom	***x***	***y***	***z***	**U(eq)**
O1	8601.7(14)	5012.9(9)	4357(2)	16.9(3)
O2	7800.4(14)	4105.6(10)	2287(2)	17.9(4)
O3	6165.9(13)	3080.1(9)	8124(2)	13.9(3)
O4	7542.5(14)	1944.9(10)	2756(3)	21.7(4)
O5	9162.3(13)	2704.5(9)	3463(2)	17.5(4)
N1	7887.5(15)	3788.2(11)	5616(3)	11.3(4)
C1	7696.5(18)	4098.8(12)	7657(3)	11.9(4)
C2	8085(2)	4992.9(13)	7839(3)	15.7(4)
C3	9067(2)	5149.6(14)	6352(3)	16.6(5)
C4	8059.8(18)	4290.3(13)	3990(3)	12.4(4)
C5	7445.4(18)	2980.7(12)	5294(3)	12.2(4)
C6	6655.8(19)	2649.9(13)	6597(3)	13.6(4)
C7	6380.7(17)	3954.3(12)	8183(3)	12.3(4)
C8	8016.4(19)	2487.3(13)	3700(3)	14.3(4)

Atom	*x*	*y*	*z*	U(eq)
C9	9763(2)	2313.6(15)	1808(4)	22.9(5)
C10	6252(2)	1780.6(13)	6689(4)	18.6(5)
C11	5486.4(19)	4391.9(13)	6853(3)	16.2(4)
C12	4199.6(19)	4127.4(14)	7237(4)	19.7(5)

Table S-3.10. Anisotropic Displacement Parameters ($Å^2×10^3$) for **3.4e**. The Anisotropic displacement factor exponent takes the form: $2\pi^2[h^2a^{*2}U_{11}+2hka^*b^*U_{12}+\ldots]$.

Atom	U_{11}	U_{22}	U_{33}	U_{23}	U_{13}	U_{12}
O1	24.1(8)	12.3(7)	14.4(8)	1.6(5)	0.8(6)	-4.9(6)
O2	24.3(8)	19.1(8)	10.4(8)	1.1(6)	-0.4(6)	-0.9(6)
O3	17.0(7)	11.4(7)	13.2(7)	1.8(6)	4.0(6)	-0.8(5)
O4	22.6(8)	18.8(8)	23.9(9)	-9.4(6)	2.1(6)	-3.8(6)
O5	14.3(7)	20.3(8)	18.0(8)	-6.7(6)	3.3(6)	0.8(6)
N1	15.6(8)	9.4(8)	8.9(8)	-1.0(6)	1.2(7)	-1.4(6)
C1	13.7(9)	12.6(10)	9.3(10)	-1.4(7)	1.9(7)	0.1(7)
C2	19.6(11)	13.1(10)	14.4(11)	-2.9(7)	0.7(8)	-2.5(8)
C3	19.5(11)	14.5(10)	15.7(11)	-0.8(8)	-0.9(8)	-4.6(8)
C4	12.8(9)	12.4(9)	12.0(10)	-0.2(7)	1.8(7)	0.7(8)
C5	13.4(9)	9.0(9)	14.2(10)	-1.0(7)	0.3(8)	-0.6(7)
C6	12.6(10)	11.9(10)	16.3(10)	-0.8(7)	0.4(8)	1.4(8)
C7	14.6(9)	10.1(9)	12.3(10)	-0.5(7)	2.1(8)	0.9(7)
C8	15.9(9)	11.8(9)	15.3(10)	-2.1(8)	0.7(8)	0.6(8)
C9	19.2(11)	26.6(12)	22.8(12)	-9.7(9)	5.2(9)	3.5(9)
C10	18.2(10)	11.3(10)	26.2(12)	0.9(9)	2.9(9)	-1.0(8)
C11	15.7(10)	14.4(10)	18.3(11)	2.0(8)	0.6(8)	1.3(8)
C12	14.7(10)	19.4(11)	25.1(12)	0.0(9)	-1.8(9)	1.7(8)

Table S-3.11. Bond Lengths for **3.4e**.

Atom	Atom	Length/Å	Atom	Atom	Length/Å
O1	C3	1.453(3)	N1	C5	1.424(3)
O1	C4	1.349(3)	C1	C2	1.527(3)
O2	C4	1.216(3)	C1	C7	1.535(3)
O3	C6	1.358(3)	C2	C3	1.507(3)
O3	C7	1.447(2)	C5	C6	1.356(3)
O4	C8	1.211(3)	C5	C8	1.483(3)
O5	C8	1.342(3)	C6	C10	1.490(3)
O5	C9	1.446(3)	C7	C11	1.520(3)
N1	C1	1.476(3)	C11	C12	1.528(3)
N1	C4	1.377(3)			

Table S-3.12. Bond Angles for **3.4e**.

Atom	Atom	Atom	Angle/°	Atom	Atom	Atom	Angle/°
C4	O1	C3	117.65(17)	N1	C5	C8	117.45(18)
C6	O3	C7	117.56(16)	C6	C5	N1	119.85(19)
C8	O5	C9	114.88(17)	C6	C5	C8	122.02(18)
C4	N1	C1	123.41(17)	O3	C6	C10	109.73(18)
C4	N1	C5	118.62(17)	C5	C6	O3	123.00(19)
C5	N1	C1	114.07(17)	C5	C6	C10	127.2(2)
N1	C1	C2	111.13(17)	O3	C7	C1	107.76(16)
N1	C1	C7	107.44(16)	O3	C7	C11	109.70(16)
C2	C1	C7	113.72(17)	C11	C7	C1	115.30(17)
C3	C2	C1	108.52(18)	O4	C8	O5	123.44(19)
O1	C3	C2	108.71(18)	O4	C8	C5	125.71(19)
O1	C4	N1	116.00(18)	O5	C8	C5	110.82(17)
O2	C4	O1	119.72(19)	C7	C11	C12	113.05(18)
O2	C4	N1	124.21(19)				

Table S-3.13. Torsion Angles for **3.4e**.

A	B	C	D	Angle/°	A	B	C	D	Angle/°
O3	C7	C11	C12	49.5(2)	C4	N1	C1	C2	-17.3(3)
N1	C1	C2	C3	-28.7(2)	C4	N1	C1	C7	107.7(2)
N1	C1	C7	O3	61.7(2)	C4	N1	C5	C6	-142.0(2)
N1	C1	C7	C11	-61.2(2)	C4	N1	C5	C8	47.2(3)
N1	C5	C6	O3	6.5(3)	C5	N1	C1	C2	-174.64(16)
N1	C5	C6	C10	-169.4(2)	C5	N1	C1	C7	-49.6(2)
N1	C5	C8	O4	-152.5(2)	C5	N1	C4	O1	-172.94(17)
N1	C5	C8	O5	29.3(3)	C5	N1	C4	O2	4.0(3)
C1	N1	C4	O1	30.6(3)	C6	O3	C7	C1	-42.4(2)
C1	N1	C4	O2	-152.4(2)	C6	O3	C7	C11	83.9(2)
C1	N1	C5	C6	16.5(3)	C6	C5	C8	O4	37.0(3)
C1	N1	C5	C8	-154.22(18)	C6	C5	C8	O5	-141.2(2)
C1	C2	C3	O1	61.8(2)	C7	O3	C6	C5	8.5(3)
C1	C7	C11	C12	171.32(18)	C7	O3	C6	C10	-175.07(17)
C2	C1	C7	O3	-174.90(16)	C7	C1	C2	C3	-150.05(18)
C2	C1	C7	C11	62.2(2)	C8	C5	C6	O3	176.78(19)
C3	O1	C4	O2	-170.25(19)	C8	C5	C6	C10	1.0(3)
C3	O1	C4	N1	6.8(3)	C9	O5	C8	O4	7.6(3)
C4	O1	C3	C2	-53.0(2)	C9	O5	C8	C5	-174.19(18)

A	B	C	D	Angle/°	A	B	C	D	Angle/°

Table S-3.14. Hydrogen Atom Coordinates (Å×10^4) and Isotropic Displacement Parameters (Å^2×10^3) for **3.4e**.

Atom	*x*	*y*	*z*	U(eq)
H1	8195.65	3764.85	8588.63	14
H2A	7400.36	5359.74	7566.82	19
H2B	8374.85	5103.73	9206.54	19
H3A	9354.95	5720.83	6478.86	20
H3B	9744.49	4775.47	6608.48	20
H7	6250.35	4145.26	9582.9	15
H9A	9331.6	2431.11	569.94	34
H9B	9786.96	1719.91	2026.59	34
H9C	10579.19	2525.14	1705.9	34
H10A	6403.04	1560.94	8025.72	28
H10B	6690.25	1456.1	5702.08	28
H10C	5395.84	1752.99	6400.87	28
H11A	5687.69	4281.31	5440.98	19
H11B	5553.62	4990.17	7073.53	19
H12A	3659.22	4460.66	6423.7	30
H12B	4008.91	4203.65	8651.28	30
H12C	4105.28	3548.17	6883.13	30

3.8.8 Computational Methods.

Computational details

All the calculations reported in this paper were performed with the Gaussian 09 suite of programs.[19] Electron correlation was partially taken into account using the hybrid functional usually denoted as B3LYP[20] in conjunction with the D3 dispersion correction suggested by Grimme et al.[21] using the standard double-ζ quality def2-SVP[22] basis set for all atoms. The SMD continuum model was used to model the effects of the solvent. This level is denoted SMD(dichloromethane)-B3LYP-D3/def2-SVP. This DFT level has been selected to enable a direct comparison with our previous reports on the chemistry of strongly related systems.[23] Geometries were fully optimized in solution without any geometry or symmetry constraints. Reactants, intermediates, and products were characterized by frequency calculations[24], and have positive definite Hessian matrices. Transition structures (TS's) show only one negative eigenvalue in their diagonalized force

constant matrices, and their associated eigenvectors were confirmed to correspond to the motion along the reaction coordinate under consideration using the Intrinsic Reaction Coordinate (IRC) method.[25]

Donor-acceptor interactions were computed using the natural bond orbital (NBO6) method.[26] The energies associated with these two-electron interactions have been computed according to the following equation:

$$\Delta E^{(2)}_{\phi\phi^*} = -n_{\phi} \frac{\langle \phi^* | \hat{F} | \phi \rangle^2}{\varepsilon_{\phi^*} - \varepsilon_{\phi}}$$

where *F* is the DFT equivalent of the Fock operator and ϕ and ϕ^* are two filled and unfilled Natural Bond Orbitals having ε_{ϕ} and ε_{ϕ^*} energies, respectively; ; n_{ϕ} stands for the occupation number of the filled orbital. Noncovalent interactions were visualized with the help of the NCIPLOT method.[27]

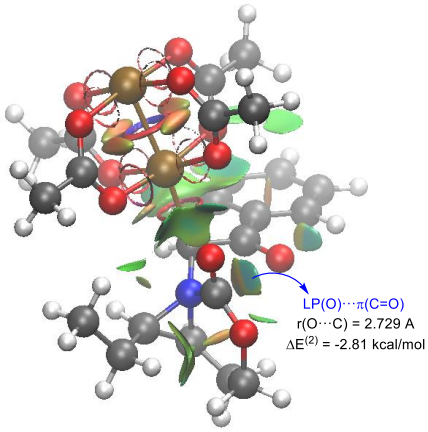


Figure S-3.14. Contour plots of the reduced density gradient isosurfaces (density cutoff of 0.04 a.u.) for intermediate **INT2-Rh** (the green surfaces indicate attractive noncovalent interactions) and associated SOPT-NBO stabilizing energy.

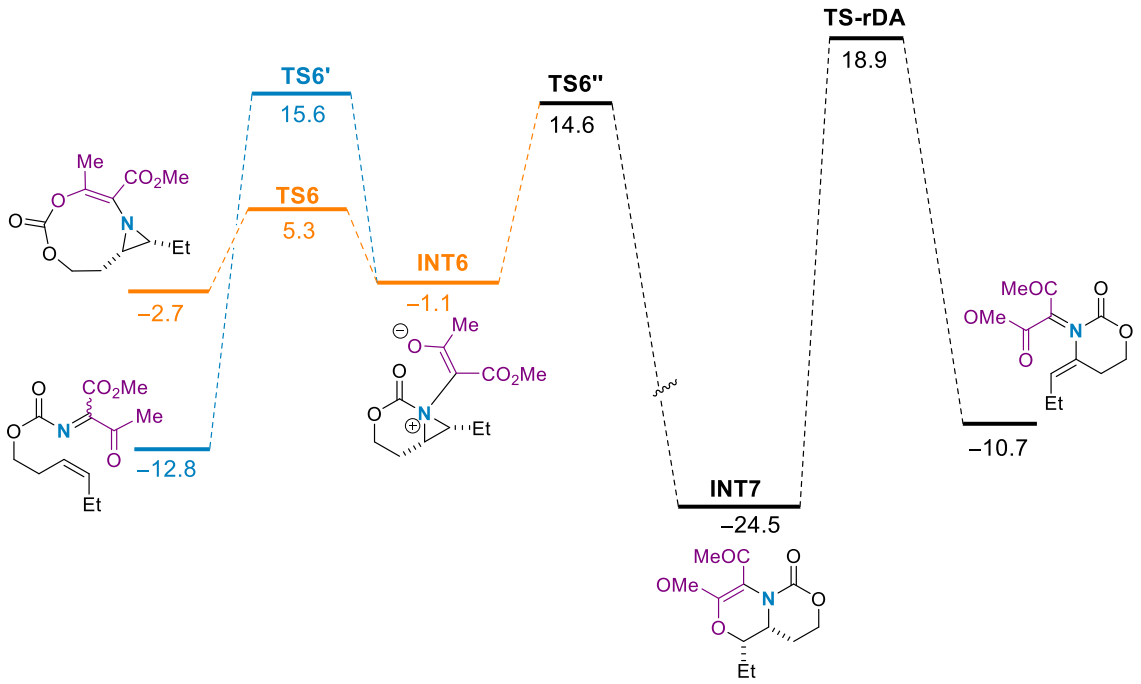


Figure S-3.15. Computed (SMD-B3LYP-D3/def2-SVP level) alternative pathways from ylide **INT6**. Relative free enrgies DG, at 298 K) are given in kcal/mol.

Cartesian coordinates (in Å) and energies (in free energies, in a.u.) of all the stationary points discussed in the text. All calculations have been performed at the SMD(dichloromethane)-B3LYP-D3/def2-SVP level.

INT1-Rh, G = -1995.875237

Rh	0.376539000	-0.244547000	-0.055558000
C	-1.515318000	0.981021000	-0.185397000
N	-2.895546000	0.367058000	-0.036059000
C	-4.049881000	1.258977000	0.374702000
C	-3.669328000	0.139435000	1.268128000
H	-3.671727000	2.220585000	0.723952000
C	-5.194607000	1.404484000	-0.594344000
C	-5.431739000	0.184028000	-1.459129000

O	-4.185686000	-0.423613000	-1.891671000
C	-3.182188000	-0.679891000	-1.063813000
O	-2.500994000	-1.649938000	-1.136004000
H	-6.013977000	-0.593447000	-0.943647000
H	-5.956788000	0.443726000	-2.386035000
H	-6.115305000	1.648765000	-0.041497000
H	-4.959439000	2.269297000	-1.233478000
Rh	2.476966000	-1.524128000	-0.064946000
O	3.340391000	0.061020000	-1.067220000
C	2.639071000	1.078334000	-1.341479000
O	1.410514000	1.227247000	-1.060848000
O	1.854823000	-2.348704000	-1.854228000
C	0.790454000	-1.927738000	-2.397917000
O	0.012715000	-1.048239000	-1.920938000
O	2.945611000	-0.605713000	1.725985000
C	2.119665000	0.201491000	2.245157000
O	0.982362000	0.504588000	1.771884000
O	1.475650000	-3.007464000	0.951704000
C	0.255424000	-2.850371000	1.253414000
O	-0.453629000	-1.837003000	0.972187000
C	-0.422682000	-3.974007000	2.001087000
H	-1.174381000	-4.440169000	1.344528000
H	0.308420000	-4.731713000	2.310701000
H	-0.950952000	-3.576370000	2.879605000
C	2.526734000	0.900101000	3.519088000
H	3.300926000	0.329864000	4.049702000
H	2.938286000	1.888536000	3.254212000
H	1.652008000	1.060053000	4.164595000
C	0.401311000	-2.507356000	-3.736199000
H	1.080114000	-3.317914000	-4.031090000
H	-0.633587000	-2.878742000	-3.684188000

H	0.427547000	-1.709942000	-4.496341000
C	3.305123000	2.231693000	-2.049786000
H	2.718177000	2.509811000	-2.937987000
H	3.312053000	3.103989000	-1.377447000
H	4.333030000	1.978087000	-2.338851000
H	-3.044034000	0.460517000	2.103463000
C	-4.429451000	-1.144521000	1.492693000
H	-4.945604000	-1.490262000	0.585272000
H	-5.229737000	-0.882387000	2.206556000
C	-1.211898000	2.034845000	0.781193000
O	-1.612912000	2.034614000	1.952788000
H	-1.460063000	1.287167000	-1.234755000
C	-0.305624000	3.153118000	0.340788000
C	0.577014000	3.689297000	1.292507000
C	-0.341888000	3.708873000	-0.946159000
C	1.422603000	4.747399000	0.958081000
C	0.486664000	4.785589000	-1.276079000
C	1.376871000	5.301718000	-0.328550000
H	0.595456000	3.246303000	2.289034000
H	-1.023944000	3.306757000	-1.698029000
H	2.119704000	5.145428000	1.700666000
H	0.442911000	5.217841000	-2.279351000
H	2.033947000	6.135512000	-0.590688000
C	-3.548005000	-2.258516000	2.051647000
H	-4.140877000	-3.167972000	2.235341000
H	-2.737284000	-2.492639000	1.350948000
H	-3.084497000	-1.952107000	3.003025000

INT2-Rh, G = -1995.884377

Rh	-0.500375000	-0.186460000	0.008702000

C	1.603120000	0.459144000	-0.381425000
N	2.796774000	-0.456619000	-0.263513000
C	4.013288000	0.005974000	-1.034951000
C	3.304252000	-1.217633000	-1.479781000
H	3.762042000	0.898274000	-1.613209000
C	5.293258000	0.157653000	-0.260124000
C	5.466369000	-0.878832000	0.827433000
O	4.237246000	-1.160901000	1.535087000
C	3.005539000	-1.126248000	1.054097000
O	2.087103000	-1.640951000	1.605971000
H	5.840351000	-1.833755000	0.431671000
H	6.167226000	-0.533924000	1.598021000
H	6.150609000	0.111978000	-0.949822000
H	5.274781000	1.164416000	0.182148000
Rh	-2.876957000	-0.812315000	0.140860000
O	-3.305317000	1.152974000	0.596734000
C	-2.353166000	1.983667000	0.669743000
O	-1.125508000	1.715471000	0.498652000
O	-2.569285000	-1.214818000	2.136692000
C	-1.434347000	-0.973872000	2.651014000
O	-0.415868000	-0.539797000	2.036391000
O	-3.001590000	-0.343730000	-1.876307000
C	-1.976606000	0.053224000	-2.499798000
O	-0.812890000	0.190390000	-2.001438000
O	-2.315104000	-2.731924000	-0.330183000
C	-1.093829000	-2.997364000	-0.536577000
O	-0.132487000	-2.169507000	-0.475915000
C	-0.748804000	-4.427437000	-0.879992000
H	-0.097712000	-4.845168000	-0.096526000
H	-1.658088000	-5.036129000	-0.963251000
H	-0.189595000	-4.460245000	-1.826539000

C	-2.128017000	0.426317000	-3.954051000
H	-3.095116000	0.090601000	-4.349939000
H	-2.061596000	1.523162000	-4.044671000
H	-1.304091000	-0.005245000	-4.541533000
C	-1.272794000	-1.204734000	4.134210000
H	-2.138663000	-1.737177000	4.548669000
H	-0.348386000	-1.770775000	4.322413000
H	-1.171478000	-0.228744000	4.636547000
C	-2.688793000	3.428407000	0.943452000
H	-1.939502000	3.871662000	1.614445000
H	-2.645803000	3.979809000	-0.010524000
H	-3.696694000	3.525803000	1.367855000
H	2.616971000	-1.056180000	-2.316118000
C	3.776886000	-2.648089000	-1.370365000
H	4.326178000	-2.831231000	-0.437850000
H	4.510368000	-2.777765000	-2.184704000
H	1.472376000	0.631216000	-1.452188000
C	2.634030000	-3.650812000	-1.500493000
H	3.015614000	-4.682117000	-1.448541000
H	1.900292000	-3.500901000	-0.698493000
H	2.107187000	-3.527928000	-2.460243000
C	1.924355000	1.655404000	0.406964000
O	2.659699000	1.558895000	1.399084000
C	1.404188000	2.999587000	-0.013997000
C	1.701957000	4.103912000	0.801995000
C	0.672284000	3.206410000	-1.197324000
C	1.276003000	5.386561000	0.451210000
C	0.251838000	4.489694000	-1.551722000
C	0.550509000	5.583340000	-0.729542000
H	2.269779000	3.934169000	1.718953000
H	0.393657000	2.363351000	-1.830235000

H	1.509770000	6.235721000	1.099094000
H	-0.321115000	4.637373000	-2.471146000
H	0.216045000	6.586454000	-1.007990000

$Rh_2(OAc)_4$, G = -1134.513729

Rh	0.000007000	0.000031000	-1.194774000
Rh	-0.000069000	-0.000011000	1.196480000
O	1.414789000	-1.487532000	1.125943000
C	1.868866000	-1.864363000	0.001673000
O	1.489053000	-1.413770000	-1.123393000
O	-1.485550000	-1.417053000	1.125754000
C	-1.864709000	-1.868590000	0.001136000
O	-1.410985000	-1.491602000	-1.123525000
O	1.485447000	1.417024000	1.125711000
C	1.864749000	1.868518000	0.001150000
O	1.411037000	1.491625000	-1.123569000
O	-1.414836000	1.487571000	1.125928000
C	-1.868846000	1.864464000	0.001644000
O	-1.489076000	1.413803000	-1.123414000
C	-2.961820000	2.898234000	-0.001356000
H	-3.928550000	2.381473000	-0.122943000
H	-2.975850000	3.454233000	0.945071000
H	-2.835914000	3.582924000	-0.851769000
C	2.958274000	2.901675000	-0.003731000
H	2.981276000	3.448276000	0.948314000
H	3.923560000	2.384023000	-0.133926000
H	2.827088000	3.594314000	-0.846410000
C	-2.958018000	-2.901981000	-0.003882000
H	-2.981661000	-3.447976000	0.948496000
H	-3.923309000	-2.384689000	-0.135365000

H	-2.825877000	-3.595166000	-0.845974000
C	2.961904000	-2.898076000	-0.001324000
H	2.835722000	-3.583133000	-0.851397000
H	3.928542000	-2.381292000	-0.123544000
H	2.976341000	-3.453667000	0.945338000

INT1, G = -861.359966

O	2.720223000	-1.579524000	-1.123459000
O	1.642274000	0.107764000	-2.078118000
O	-0.789480000	1.660716000	-0.136667000
N	1.271854000	-0.250165000	0.205452000
C	2.116750000	-0.470615000	1.445978000
H	1.490112000	-0.865237000	2.249176000
C	3.401094000	-1.228569000	1.184552000
H	4.221833000	-0.570556000	0.863663000
H	3.718632000	-1.741420000	2.103292000
C	3.116168000	-2.254741000	0.101193000
H	4.006092000	-2.834730000	-0.172354000
H	2.312149000	-2.948695000	0.394638000
C	1.900245000	-0.539226000	-1.107653000
C	-0.141716000	-0.575785000	0.223203000
C	-1.075226000	0.445042000	0.013025000
C	1.825531000	0.916358000	1.014080000
H	0.998158000	1.409443000	1.526501000
H	-0.345953000	-1.623465000	0.426586000
C	2.820746000	1.855110000	0.381987000
H	3.545739000	1.303862000	-0.237661000
H	3.403112000	2.282446000	1.217210000
C	2.160911000	2.967027000	-0.434095000
H	2.928059000	3.628267000	-0.867458000
H	1.495467000	3.576297000	0.196579000

H	1.548315000	2.544793000	-1.241606000
C	-2.542563000	0.045937000	0.030175000
C	-3.492221000	1.064468000	0.218737000
C	-3.004361000	-1.270085000	-0.154965000
C	-4.859845000	0.779151000	0.245893000
C	-4.372263000	-1.558570000	-0.132635000
C	-5.306407000	-0.536093000	0.072117000
H	-3.124886000	2.086096000	0.337893000
H	-2.295478000	-2.079660000	-0.341160000
H	-5.582316000	1.586066000	0.399387000
H	-4.711163000	-2.587409000	-0.284600000
H	-6.376036000	-0.763038000	0.088151000

INT2, G = -861.366629

O	-2.223382000	-1.600002000	0.859470000
O	-1.328220000	0.038756000	2.059530000
O	0.657391000	-1.456892000	0.249297000
N	-1.230734000	0.279421000	-0.262485000
C	-3.404761000	2.494357000	1.004007000
H	-4.346490000	2.663070000	1.548674000
H	-2.630061000	2.221467000	1.736329000
H	-3.109450000	3.445814000	0.532565000
C	-3.578483000	1.391990000	-0.042744000
H	-4.354695000	1.674402000	-0.774342000
H	-3.930131000	0.462169000	0.430065000
C	-2.318186000	1.152017000	-0.837792000
H	-1.877038000	2.058718000	-1.262023000
C	-1.973090000	-0.110974000	-1.536154000
H	-1.292481000	-0.015470000	-2.384568000
C	-2.807814000	-1.374650000	-1.477282000
H	-3.863509000	-1.154937000	-1.259735000

H	-2.765160000	-1.878517000	-2.453270000
C	-2.237020000	-2.292743000	-0.413255000
H	-1.201964000	-2.588317000	-0.636938000
H	-2.862822000	-3.178418000	-0.248739000
C	-1.549181000	-0.476093000	1.005484000
C	1.056183000	-0.287992000	-0.058745000
C	0.150825000	0.723148000	-0.343572000
H	0.310922000	1.794245000	-0.417839000
C	2.533540000	0.002777000	-0.071298000
C	3.092684000	1.141264000	-0.680336000
H	2.448781000	1.857608000	-1.195831000
C	4.473111000	1.357034000	-0.655677000
H	4.892253000	2.245029000	-1.137293000
C	5.320346000	0.436909000	-0.025176000
H	6.400450000	0.606538000	-0.008265000
C	4.775207000	-0.703553000	0.575514000
H	5.429904000	-1.429094000	1.066780000
C	3.394722000	-0.918443000	0.548567000
H	2.951814000	-1.805455000	1.006204000

TS1, G = -861.349113 (i = -128 cm-1)

O	-3.144244000	-0.887472000	1.067987000
O	-1.262252000	-0.491887000	2.185555000
O	0.642663000	1.274518000	0.575153000
N	-1.151764000	-0.713959000	-0.118458000
C	-1.980497000	-0.487504000	-1.393282000
H	-1.376806000	-0.869638000	-2.221529000
C	-3.388101000	-1.087430000	-1.346825000
H	-4.137275000	-0.302938000	-1.525645000
H	-3.503809000	-1.840852000	-2.138927000

C	-3.620179000	-1.741571000	0.002917000
H	-4.685753000	-1.905102000	0.207770000
H	-3.097110000	-2.709236000	0.073170000
C	-1.815340000	-0.670485000	1.137719000
C	0.226885000	-0.898171000	-0.198366000
C	1.078109000	0.165727000	0.186754000
C	-1.785448000	0.934806000	-1.116679000
H	-0.822962000	1.359500000	-1.408757000
H	0.547013000	-1.681210000	-0.889075000
C	-2.772690000	1.854066000	-0.505274000
H	-3.492078000	1.301350000	0.119107000
H	-3.378202000	2.238000000	-1.356500000
C	-2.148448000	3.018115000	0.265321000
H	-2.931285000	3.677079000	0.671559000
H	-1.498284000	3.621899000	-0.388010000
H	-1.526732000	2.641423000	1.089291000
C	2.568549000	-0.027184000	0.035010000
C	3.384390000	1.115834000	-0.026645000
C	3.178073000	-1.293070000	-0.025744000
C	4.768910000	1.001391000	-0.169746000
C	4.564604000	-1.409946000	-0.164756000
C	5.364845000	-0.263883000	-0.241063000
H	2.904138000	2.094245000	0.043230000
H	2.568713000	-2.195640000	0.060827000
H	5.387918000	1.901605000	-0.222057000
H	5.024345000	-2.401486000	-0.203420000
H	6.449209000	-0.356738000	-0.347439000

TS2, G = -861.364226 (i = -101 cm-1)

O	-2.053699000	-1.658586000	0.759171000

O	-1.257045000	0.017788000	1.990797000
O	0.518365000	-1.214714000	0.463904000
N	-1.225967000	0.338729000	-0.354482000
C	-3.457757000	2.337944000	1.192177000
H	-4.370758000	2.408198000	1.803996000
H	-2.614919000	2.101315000	1.858018000
H	-3.276896000	3.327698000	0.741319000
C	-3.611551000	1.261837000	0.116198000
H	-4.462513000	1.499374000	-0.545562000
H	-3.838213000	0.287787000	0.573919000
C	-2.398622000	1.160088000	-0.777738000
H	-2.067771000	2.117824000	-1.192188000
C	-2.035593000	-0.041866000	-1.579469000
H	-1.448509000	0.147709000	-2.481280000
C	-2.771150000	-1.367103000	-1.525256000
H	-3.823464000	-1.230885000	-1.233654000
H	-2.758620000	-1.826444000	-2.523996000
C	-2.081410000	-2.289970000	-0.531646000
H	-1.048338000	-2.519887000	-0.833855000
H	-2.639006000	-3.225192000	-0.390785000
C	-1.336368000	-0.542347000	0.932731000
C	1.013669000	-0.132137000	-0.047192000
C	0.131745000	0.813595000	-0.506041000
H	0.291162000	1.826249000	-0.862320000
C	2.491878000	0.056127000	-0.060240000
C	3.122969000	1.028343000	-0.858319000
H	2.526910000	1.667499000	-1.514044000
C	4.512001000	1.171003000	-0.836528000
H	4.989274000	1.928645000	-1.464171000
C	5.294086000	0.341875000	-0.021830000
H	6.381704000	0.453210000	-0.008677000

C	4.675600000	-0.632963000	0.768885000
H	5.279463000	-1.285340000	1.405835000
C	3.285810000	-0.776341000	0.747578000
H	2.789439000	-1.533272000	1.357983000

TS_{rot}(INT1-INT2), G = -861.354625 (i = -59 cm-1)

O	-2.900357000	-1.786518000	0.451535000
O	-1.869959000	-0.724704000	2.099030000
O	0.945273000	1.665586000	-0.832350000
N	-1.238234000	-0.167594000	-0.073001000
C	-2.653959000	2.466738000	1.529422000
H	-3.547723000	2.874912000	2.026336000
H	-2.138954000	1.803768000	2.240701000
H	-1.978688000	3.305898000	1.297470000
C	-3.042439000	1.709966000	0.258111000
H	-3.556372000	2.386190000	-0.447483000
H	-3.766209000	0.910871000	0.487797000
C	-1.844388000	1.183460000	-0.487979000
H	-1.011094000	1.877363000	-0.642066000
C	-1.863419000	0.055824000	-1.447869000
H	-1.068611000	0.070365000	-2.197859000
C	-3.078577000	-0.792886000	-1.758820000
H	-4.016111000	-0.273359000	-1.510848000
H	-3.097799000	-1.025553000	-2.833001000
C	-2.980307000	-2.084028000	-0.971614000
H	-2.091028000	-2.670925000	-1.250659000
H	-3.873380000	-2.711526000	-1.075531000
C	-2.031472000	-0.918726000	0.932188000
C	1.159268000	0.539369000	-0.291050000
C	0.198816000	-0.385500000	0.104434000

H	0.417329000	-1.396084000	0.437960000
C	2.609126000	0.130710000	-0.082140000
C	3.033386000	-0.845756000	0.837915000
H	2.304535000	-1.354614000	1.472585000
C	4.389599000	-1.155791000	0.978501000
H	4.699291000	-1.912757000	1.704757000
C	5.350409000	-0.493430000	0.204938000
H	6.410800000	-0.735914000	0.317152000
C	4.941972000	0.489244000	-0.704057000
H	5.684661000	1.019000000	-1.307809000
C	3.586232000	0.799968000	-0.839150000
H	3.251852000	1.575638000	-1.531201000

3a, G = -861.397067

O	1.179366000	2.609991000	0.491485000
O	-0.182079000	1.614930000	1.935073000
O	-0.347531000	1.167003000	-0.284431000
N	1.540785000	-0.667583000	0.049771000
C	3.781952000	-2.826638000	1.013395000
H	4.713549000	-3.014100000	1.571140000
H	2.968962000	-2.700067000	1.747933000
H	3.559007000	-3.728820000	0.418709000
C	3.905563000	-1.589321000	0.122834000
H	4.730131000	-1.721685000	-0.599450000
H	4.155663000	-0.710439000	0.737419000
C	2.633825000	-1.322511000	-0.650742000
H	2.335601000	-2.141482000	-1.322042000
C	2.154211000	0.034028000	-1.080170000
H	1.546327000	0.023494000	-1.995341000
C	2.844815000	1.357049000	-0.841650000

H	3.446144000	1.333024000	0.079637000
H	3.535913000	1.548452000	-1.680436000
C	1.881395000	2.541928000	-0.773790000
H	1.159127000	2.527469000	-1.603516000
H	2.438823000	3.487411000	-0.812306000
C	0.199280000	1.770971000	0.808173000
C	-0.780898000	-0.160279000	-0.121104000
C	0.212229000	-1.071611000	0.017952000
H	0.001606000	-2.128596000	0.194376000
C	-2.229296000	-0.377136000	-0.128846000
C	-2.786212000	-1.668177000	-0.262948000
H	-2.134290000	-2.535005000	-0.391059000
C	-4.168114000	-1.852671000	-0.248777000
H	-4.576896000	-2.861490000	-0.352148000
C	-5.031512000	-0.756799000	-0.116025000
H	-6.114393000	-0.905063000	-0.111102000
C	-4.492112000	0.527701000	0.003307000
H	-5.153291000	1.392542000	0.105494000
C	-3.108004000	0.718087000	-0.003280000
H	-2.698254000	1.724315000	0.097305000

3.4a, G = -861.448979

O	-3.747147000	-1.362999000	0.207390000
O	-2.126082000	-2.509193000	1.189004000
O	0.450321000	1.173300000	-0.763720000
N	-1.531011000	-0.693969000	-0.066199000
C	-1.868679000	0.515944000	-0.834891000
H	-1.688786000	0.295257000	-1.901943000
C	-3.337364000	0.861900000	-0.646674000
H	-3.522682000	1.284760000	0.352493000

H	-3.645992000	1.605592000	-1.396107000
C	-4.143088000	-0.410145000	-0.795219000
H	-5.216795000	-0.243888000	-0.635263000
H	-4.003882000	-0.861850000	-1.793038000
C	-2.445617000	-1.574010000	0.483817000
C	-0.163613000	-0.961552000	0.085138000
C	0.784640000	-0.068426000	-0.285975000
C	-0.872564000	1.626464000	-0.448493000
H	-1.041014000	2.480588000	-1.122443000
H	0.080282000	-1.924870000	0.523551000
C	-0.962832000	2.101082000	1.005414000
H	-0.943714000	1.230026000	1.681035000
H	-1.943832000	2.582982000	1.142784000
C	0.149448000	3.078025000	1.382742000
H	0.017741000	3.440683000	2.414612000
H	0.157128000	3.956591000	0.715398000
H	1.139073000	2.601109000	1.316286000
C	2.238748000	-0.305908000	-0.211122000
C	3.132323000	0.767937000	-0.400551000
C	2.779539000	-1.584991000	0.041955000
C	4.514408000	0.572289000	-0.324435000
C	4.158619000	-1.773729000	0.123257000
C	5.036711000	-0.696809000	-0.059253000
H	2.732243000	1.761165000	-0.606801000
H	2.119338000	-2.445266000	0.168304000
H	5.186908000	1.421519000	-0.473637000
H	4.552862000	-2.773874000	0.322729000
H	6.117395000	-0.850026000	-0.000217000

INT3, G = -953.555890

O	-2.947871000	-0.858063000	1.435091000
O	-1.514697000	0.733063000	2.013132000
O	0.709187000	1.757389000	-0.143142000
N	-1.306305000	-0.151470000	-0.139106000
C	-2.168458000	-0.630992000	-1.304037000
H	-1.558585000	-1.231037000	-1.982816000
C	-3.500341000	-1.230274000	-0.902479000
H	-4.301112000	-0.477532000	-0.876808000
H	-3.784153000	-2.000677000	-1.632872000
C	-3.347962000	-1.868625000	0.464328000
H	-4.293568000	-2.266964000	0.850120000
H	-2.588542000	-2.665928000	0.466568000
C	-1.936246000	-0.043126000	1.213232000
C	0.111332000	-0.506431000	-0.103756000
C	1.058673000	0.566420000	-0.112345000
C	-1.830581000	0.804589000	-1.216013000
H	-0.998279000	1.140913000	-1.835901000
C	-2.802832000	1.886342000	-0.820864000
H	-3.547050000	1.505309000	-0.103666000
H	-3.369853000	2.116679000	-1.740045000
C	-2.132380000	3.147453000	-0.276977000
H	-2.893849000	3.907295000	-0.041377000
H	-1.434410000	3.572704000	-1.014057000
H	-1.553907000	2.925660000	0.629516000
C	2.533436000	0.244461000	-0.079416000
C	3.371670000	1.138510000	0.610095000
C	3.110521000	-0.848977000	-0.746608000
C	4.750225000	0.926823000	0.661392000
C	4.493897000	-1.053248000	-0.706843000
C	5.316079000	-0.172123000	0.002729000
H	2.921047000	2.002228000	1.103628000

H	2.486635000	-1.536969000	-1.319578000
H	5.388015000	1.622779000	1.213211000
H	4.930765000	-1.903143000	-1.238102000
H	6.396428000	-0.336922000	0.037170000
C	0.338065000	-1.879845000	0.072782000
N	0.454431000	-3.036994000	0.212396000

INT4, G = -953.561464

O	-2.285963000	-1.824999000	0.814172000
O	-1.396594000	-0.244454000	2.096188000
O	0.631010000	-1.658860000	0.105181000
N	-1.273786000	0.092469000	-0.206210000
C	-3.546085000	2.213982000	1.033625000
H	-4.520021000	2.361954000	1.524591000
H	-2.817560000	1.916838000	1.803073000
H	-3.221941000	3.180856000	0.616834000
C	-3.655762000	1.150812000	-0.061408000
H	-4.400813000	1.451819000	-0.817478000
H	-4.013758000	0.197171000	0.355395000
C	-2.362028000	0.965593000	-0.813346000
H	-1.924329000	1.898868000	-1.178541000
C	-1.948275000	-0.261884000	-1.529052000
H	-1.234031000	-0.125957000	-2.343781000
C	-2.775313000	-1.532542000	-1.547557000
H	-3.841519000	-1.314944000	-1.388268000
H	-2.673955000	-2.011519000	-2.531575000
C	-2.272495000	-2.484516000	-0.481378000
H	-1.241245000	-2.809798000	-0.672677000
H	-2.930052000	-3.353133000	-0.358798000
C	-1.629684000	-0.705640000	1.021569000
C	1.048908000	-0.489452000	-0.056429000

C	0.109995000	0.569524000	-0.199774000
C	2.527308000	-0.229183000	-0.054919000
C	3.128102000	0.836264000	-0.747483000
H	2.518561000	1.532035000	-1.326215000
C	4.515883000	1.003015000	-0.721316000
H	4.971577000	1.832374000	-1.268687000
C	5.319439000	0.110030000	-0.004376000
H	6.404195000	0.245133000	0.017680000
C	4.729914000	-0.960973000	0.678682000
H	5.353373000	-1.664549000	1.236995000
C	3.345440000	-1.133189000	0.646143000
H	2.873018000	-1.970024000	1.164352000
C	0.303379000	1.951426000	-0.078132000
N	0.427860000	3.113211000	-0.003265000

TS3, G = -953.542486 (i = -145 cm-1)

O	-3.180028000	-0.596186000	1.282207000
O	-1.216361000	-0.306254000	2.292434000
O	0.432285000	1.417973000	0.317804000
N	-1.247969000	-0.660192000	0.008592000
C	-2.082987000	-0.374830000	-1.234096000
H	-1.559985000	-0.844989000	-2.072507000
C	-3.536150000	-0.854976000	-1.112213000
H	-4.228264000	-0.021395000	-1.295995000
H	-3.737667000	-1.623191000	-1.871936000
C	-3.771105000	-1.441036000	0.268651000
H	-4.838544000	-1.500227000	0.515639000
H	-3.333160000	-2.448278000	0.356550000
C	-1.836317000	-0.495601000	1.282332000
C	0.146426000	-0.847123000	-0.092561000

C	0.967461000	0.304204000	0.138420000
C	-1.794869000	1.064220000	-1.125985000
H	-0.884211000	1.423226000	-1.609064000
C	-2.674566000	2.061904000	-0.505067000
H	-3.336176000	1.601576000	0.245998000
H	-3.361508000	2.318133000	-1.348164000
C	-1.994901000	3.323611000	0.019555000
H	-2.751013000	4.056111000	0.339502000
H	-1.367930000	3.790291000	-0.756253000
H	-1.347552000	3.077429000	0.871468000
C	2.465353000	0.210678000	0.094997000
C	3.185290000	1.350154000	-0.306990000
C	3.172969000	-0.941474000	0.478436000
C	4.579571000	1.328688000	-0.357796000
C	4.570395000	-0.958980000	0.435503000
C	5.276861000	0.171448000	0.011519000
H	2.630025000	2.250563000	-0.577665000
H	2.637680000	-1.823708000	0.833130000
H	5.126903000	2.217944000	-0.682056000
H	5.109378000	-1.859344000	0.742031000
H	6.369541000	0.154227000	-0.023297000
C	0.553355000	-2.049454000	-0.707701000
N	0.851484000	-3.054267000	-1.227016000

TS4, G = -953.553095 (i = -183 cm-1)

O	-1.964182000	-2.054571000	0.166313000
O	-1.246310000	-0.847252000	1.901467000
O	0.399146000	-1.394692000	0.173252000
N	-1.277031000	0.279765000	-0.240096000
C	-3.528798000	1.483918000	1.966798000

H	-4.412207000	1.279357000	2.591975000
H	-2.640975000	1.101546000	2.491054000
H	-3.431903000	2.577632000	1.866560000
C	-3.670861000	0.812901000	0.600154000
H	-4.569775000	1.187331000	0.080654000
H	-3.803450000	-0.272271000	0.715876000
C	-2.505698000	1.111736000	-0.314003000
H	-2.263373000	2.177423000	-0.392802000
C	-2.114670000	0.287801000	-1.493905000
H	-1.605401000	0.824504000	-2.299405000
C	-2.766774000	-1.030239000	-1.871593000
H	-3.812912000	-1.062659000	-1.532378000
H	-2.769277000	-1.129116000	-2.966590000
C	-1.999661000	-2.195716000	-1.261357000
H	-0.971699000	-2.254859000	-1.652615000
H	-2.505716000	-3.151326000	-1.452330000
C	-1.227723000	-1.068676000	0.718365000
C	0.961287000	-0.243645000	-0.037674000
C	0.071608000	0.804202000	-0.235456000
C	2.434545000	-0.160838000	0.006412000
C	3.155086000	0.842350000	-0.668263000
H	2.634121000	1.587725000	-1.270776000
C	4.548503000	0.878081000	-0.589613000
H	5.099443000	1.658719000	-1.120141000
C	5.237492000	-0.084419000	0.157294000
H	6.328532000	-0.052097000	0.217494000
C	4.527541000	-1.091937000	0.821278000
H	5.062144000	-1.846841000	1.403431000
C	3.135421000	-1.135374000	0.742620000
H	2.572625000	-1.916970000	1.255711000
C	0.301454000	2.183048000	-0.356342000

N	0.452469000	3.335215000	-0.470226000

TS4‘, G = -953.535200 (i = -408 cm-1)

C	0.128266000	0.607671000	0.046521000
N	-1.171117000	0.372329000	0.271940000
C	-2.218118000	-0.574623000	-1.640281000
C	-2.391972000	0.699760000	-1.081923000
H	-1.332317000	-0.733768000	-2.262091000
C	-3.032853000	-1.762741000	-1.280410000
C	-2.483661000	-2.358330000	0.017509000
O	-2.532189000	-1.399368000	1.097006000
C	-1.586709000	-0.478733000	1.326552000
O	-1.208375000	-0.249199000	2.446836000
H	-3.108642000	-3.195829000	0.358136000
H	-1.446085000	-2.695723000	-0.107481000
H	-4.095577000	-1.509170000	-1.141580000
H	-2.957649000	-2.536260000	-2.061326000
H	-1.823792000	1.504532000	-1.560009000
C	-3.658827000	1.181771000	-0.418764000
H	-4.094256000	0.388640000	0.206088000
H	-4.377535000	1.361678000	-1.238925000
C	1.086109000	-0.514582000	0.102910000
O	0.643453000	-1.660657000	0.200391000
C	-3.471456000	2.461730000	0.395997000
H	-4.438645000	2.817958000	0.783279000
H	-2.803545000	2.294754000	1.255097000
H	-3.034840000	3.267049000	-0.217452000
C	0.463069000	1.896901000	-0.456581000
N	0.688732000	2.947501000	-0.907763000
C	2.557788000	-0.271843000	0.026471000

C	3.170080000	0.884182000	0.542472000
C	3.359551000	-1.280589000	-0.540271000
C	4.558248000	1.031891000	0.477057000
C	4.742593000	-1.122498000	-0.619072000
C	5.344938000	0.035533000	-0.110059000
H	2.573147000	1.661576000	1.022024000
H	2.878665000	-2.184587000	-0.919750000
H	5.026574000	1.928098000	0.891624000
H	5.355902000	-1.904759000	-1.073705000
H	6.429894000	0.157784000	-0.165794000

TS_{rot}(INT3-INT4), G = -953.541306 (i = -55 cm-1)

O	-2.718808000	-0.757866000	1.768866000
O	-2.346679000	1.405088000	1.458604000
O	0.869444000	-1.374593000	-1.468023000
N	-1.326636000	-0.078627000	-0.034630000
C	-2.879144000	2.534266000	-1.560007000
H	-3.802914000	3.111380000	-1.719406000
H	-2.438599000	2.850038000	-0.602871000
H	-2.172884000	2.794194000	-2.365203000
C	-3.176787000	1.034270000	-1.557020000
H	-3.621907000	0.730670000	-2.520864000
H	-3.924845000	0.783680000	-0.788968000
C	-1.935132000	0.193838000	-1.411488000
H	-1.124780000	0.459212000	-2.097425000
C	-1.864031000	-1.203611000	-0.918889000
H	-1.022134000	-1.774811000	-1.312918000
C	-2.992272000	-1.990104000	-0.290688000
H	-3.974365000	-1.518452000	-0.444194000
H	-3.021240000	-2.994816000	-0.735288000

C	-2.708624000	-2.097659000	1.196195000
H	-1.731680000	-2.560934000	1.404577000
H	-3.491055000	-2.639309000	1.740591000
C	-2.189425000	0.266881000	1.139791000
C	1.112002000	-0.547429000	-0.564134000
C	0.126483000	0.103298000	0.237742000
C	2.567015000	-0.236832000	-0.294571000
C	3.074822000	1.069249000	-0.210484000
H	2.400834000	1.924165000	-0.290502000
C	4.446572000	1.284891000	-0.041610000
H	4.830686000	2.306961000	0.013515000
C	5.323726000	0.199724000	0.052623000
H	6.394738000	0.370239000	0.191447000
C	4.825871000	-1.106096000	-0.040386000
H	5.507404000	-1.958494000	0.026665000
C	3.459139000	-1.321200000	-0.226331000
H	3.066672000	-2.336053000	-0.323652000
C	0.448544000	0.981841000	1.286714000
N	0.735472000	1.689962000	2.172370000

3c, G = -953.572534

O	-1.225062000	-2.802994000	0.481993000
O	0.053158000	-1.767567000	1.976089000
O	0.363654000	-1.392395000	-0.241126000
N	-1.551629000	0.395483000	0.029493000
C	-3.824306000	2.527065000	0.969747000
H	-4.771366000	2.701730000	1.504852000
H	-3.030296000	2.389971000	1.722363000
H	-3.585650000	3.439319000	0.397683000
C	-3.922237000	1.305267000	0.054757000

H	-4.728769000	1.446456000	-0.685719000
H	-4.180621000	0.413222000	0.646145000
C	-2.631750000	1.064312000	-0.693432000
H	-2.316667000	1.908349000	-1.323319000
C	-2.125633000	-0.266752000	-1.153829000
H	-1.488350000	-0.222875000	-2.047210000
C	-2.814477000	-1.598683000	-0.970183000
H	-3.486522000	-1.584383000	-0.099354000
H	-3.434598000	-1.794182000	-1.861494000
C	-1.846374000	-2.770445000	-0.829230000
H	-1.072040000	-2.759998000	-1.610192000
H	-2.387603000	-3.723935000	-0.883844000
C	-0.272102000	-1.961000000	0.839753000
C	0.794027000	-0.080766000	-0.116335000
C	-0.215890000	0.833852000	0.012022000
C	2.244219000	0.119376000	-0.155731000
C	2.828339000	1.292385000	-0.676011000
H	2.200734000	2.077809000	-1.099606000
C	4.215002000	1.447548000	-0.679727000
H	4.653413000	2.361242000	-1.088969000
C	5.041820000	0.434263000	-0.181013000
H	6.127755000	0.558093000	-0.189662000
C	4.472039000	-0.742246000	0.319553000
H	5.111053000	-1.539391000	0.707974000
C	3.086707000	-0.903248000	0.329004000
H	2.646472000	-1.816518000	0.732280000
C	0.008234000	2.223710000	0.259039000
N	0.120678000	3.361791000	0.466524000

3.4c, G = -953.620596

O	-3.727374000	-1.105931000	0.266971000
O	-2.164520000	-1.800104000	1.681544000
O	0.409390000	1.377127000	-0.641417000
N	-1.507822000	-0.619966000	-0.172520000
C	-1.795837000	0.513872000	-1.067398000
H	-1.389988000	0.249765000	-2.058018000
C	-3.298873000	0.752994000	-1.191172000
H	-3.666935000	1.432950000	-0.409150000
H	-3.521003000	1.211147000	-2.165559000
C	-4.011581000	-0.573133000	-1.039927000
H	-5.103118000	-0.467872000	-1.087153000
H	-3.691866000	-1.299503000	-1.806941000
C	-2.446284000	-1.202609000	0.666724000
C	-0.119986000	-0.839799000	0.045772000
C	0.791076000	0.142516000	-0.263126000
C	-0.990515000	1.721870000	-0.558045000
H	-1.109262000	2.554107000	-1.268375000
C	-1.325312000	2.189558000	0.858794000
H	-1.177868000	1.352412000	1.561201000
H	-2.395959000	2.443654000	0.894314000
C	-0.496302000	3.395864000	1.297418000
H	-0.778861000	3.714369000	2.313071000
H	-0.648163000	4.253210000	0.620469000
H	0.579412000	3.162023000	1.306075000
C	2.263411000	-0.001211000	-0.234557000
C	3.034916000	1.068014000	0.262023000
C	2.918004000	-1.147567000	-0.720193000
C	4.426568000	0.976446000	0.301186000
C	4.311603000	-1.232653000	-0.681331000
C	5.069504000	-0.175493000	-0.167149000
H	2.534370000	1.966560000	0.626670000

H	2.341787000	-1.968116000	-1.149246000
H	5.012782000	1.808308000	0.700011000
H	4.807075000	-2.127621000	-1.066030000
H	6.160015000	-0.245512000	-0.137988000
C	0.298850000	-2.128878000	0.492339000
N	0.669559000	-3.175369000	0.838479000

3.5c, G = -953.576426

C	0.575864000	0.674007000	-0.381319000
N	-0.638312000	0.542169000	-0.028645000
C	-3.727146000	0.706938000	-1.174442000
C	-4.372483000	1.067534000	-0.054160000
H	-3.220683000	1.492537000	-1.748992000
C	-3.562019000	-0.688498000	-1.714907000
C	-2.161201000	-1.248748000	-1.483045000
O	-1.924666000	-1.399766000	-0.064278000
C	-1.136594000	-0.600615000	0.635062000
O	-0.949682000	-0.751708000	1.817933000
H	-2.065035000	-2.260760000	-1.901430000
H	-1.387303000	-0.617886000	-1.942310000
H	-4.290881000	-1.384254000	-1.272483000
H	-3.730329000	-0.695661000	-2.806188000
H	-4.364873000	2.134035000	0.209115000
C	-5.092326000	0.185147000	0.929182000
H	-5.125764000	-0.857682000	0.577212000
H	-6.142568000	0.524494000	1.004792000
C	1.584506000	-0.495633000	-0.352646000
O	1.123118000	-1.587044000	-0.627238000
C	-4.460202000	0.234341000	2.328096000
H	-5.042070000	-0.368015000	3.045175000

H	-3.429646000	-0.154787000	2.316635000
H	-4.422877000	1.267657000	2.713341000
C	0.973290000	1.943008000	-0.958716000
N	1.302753000	2.940273000	-1.449307000
C	3.002114000	-0.259825000	-0.011416000
C	3.429765000	0.892580000	0.675859000
C	3.935501000	-1.264463000	-0.338583000
C	4.773672000	1.037728000	1.023349000
C	5.277133000	-1.106517000	-0.003043000
C	5.696819000	0.044476000	0.679098000
H	2.719558000	1.668652000	0.967322000
H	3.589741000	-2.158428000	-0.861443000
H	5.100323000	1.927852000	1.565842000
H	6.000992000	-1.880712000	-0.268264000
H	6.750017000	0.165257000	0.945792000

INT5, G = -897.496004

O	-1.042416000	-1.828351000	1.262548000
O	-0.707213000	0.179231000	2.130960000
O	-0.491398000	2.747576000	-0.034884000
N	-0.349141000	-0.033884000	-0.157677000
C	-0.700915000	-0.869954000	-1.383952000
H	0.081147000	-0.747838000	-2.134810000
C	-1.191057000	-2.283965000	-1.138185000
H	-2.286940000	-2.332136000	-1.210084000
H	-0.780638000	-2.945667000	-1.913924000
C	-0.732464000	-2.787741000	0.215344000
H	-1.261927000	-3.700794000	0.512395000
H	0.348951000	-2.967265000	0.239277000
C	-0.706085000	-0.554642000	1.190574000

C	0.840581000	0.816500000	-0.186661000
C	0.637454000	2.233009000	-0.088343000
C	-1.522756000	0.319675000	-1.087693000
H	-1.282559000	1.229699000	-1.636739000
C	-2.931000000	0.263038000	-0.551625000
H	-3.082091000	-0.633078000	0.070164000
H	-3.573853000	0.120886000	-1.438300000
C	-3.351361000	1.517847000	0.213980000
H	-4.396724000	1.423592000	0.547844000
H	-3.264430000	2.415331000	-0.415818000
H	-2.709992000	1.677328000	1.091350000
C	1.864458000	3.132795000	-0.068502000
H	1.520578000	4.176538000	-0.036140000
H	2.497202000	2.918254000	0.806551000
H	2.500798000	2.968423000	-0.950691000
C	2.098525000	0.132408000	-0.126411000
O	3.220415000	0.619471000	-0.149564000
O	1.930805000	-1.233915000	-0.025585000
C	3.123685000	-2.011783000	0.015615000
H	3.733568000	-1.765903000	0.899493000
H	2.808544000	-3.063273000	0.066297000
H	3.736442000	-1.852130000	-0.885770000

INT6, G = -953.572534

O	-1.225062000	-2.802994000	0.481993000
O	0.053158000	-1.767567000	1.976089000
O	0.363654000	-1.392395000	-0.241126000
N	-1.551629000	0.395483000	0.029493000
C	-3.824306000	2.527065000	0.969747000
H	-4.771366000	2.701730000	1.504852000

H	-3.030296000	2.389971000	1.722363000
H	-3.585650000	3.439319000	0.397683000
C	-3.922237000	1.305267000	0.054757000
H	-4.728769000	1.446456000	-0.685719000
H	-4.180621000	0.413222000	0.646145000
C	-2.631750000	1.064312000	-0.693432000
H	-2.316667000	1.908349000	-1.323319000
C	-2.125633000	-0.266752000	-1.153829000
H	-1.488350000	-0.222875000	-2.047210000
C	-2.814477000	-1.598683000	-0.970183000
H	-3.486522000	-1.584383000	-0.099354000
H	-3.434598000	-1.794182000	-1.861494000
C	-1.846374000	-2.770445000	-0.829230000
H	-1.072040000	-2.759998000	-1.610192000
H	-2.387603000	-3.723935000	-0.883844000
C	-0.272102000	-1.961000000	0.839753000
C	0.794027000	-0.080766000	-0.116335000
C	-0.215890000	0.833852000	0.012022000
C	2.244219000	0.119376000	-0.155731000
C	2.828339000	1.292385000	-0.676011000
H	2.200734000	2.077809000	-1.099606000
C	4.215002000	1.447548000	-0.679727000
H	4.653413000	2.361242000	-1.088969000
C	5.041820000	0.434263000	-0.181013000
H	6.127755000	0.558093000	-0.189662000
C	4.472039000	-0.742246000	0.319553000
H	5.111053000	-1.539391000	0.707974000
C	3.086707000	-0.903248000	0.329004000
H	2.646472000	-1.816518000	0.732280000
C	0.008234000	2.223710000	0.259039000
N	0.120678000	3.361791000	0.466524000

TS5, G = -897.478147 (i = -196 cm-1)

O	-1.332595000	-1.808971000	1.320667000
O	-0.600074000	0.022706000	2.355315000
O	-0.731822000	2.333507000	0.056230000
N	-0.091140000	-0.269021000	0.122611000
C	-0.649249000	-0.818767000	-1.166119000
H	0.143212000	-0.715728000	-1.912530000
C	-1.151290000	-2.266774000	-1.052184000
H	-2.226632000	-2.327953000	-1.270486000
H	-0.629712000	-2.899462000	-1.784317000
C	-0.874407000	-2.775439000	0.349253000
H	-1.416264000	-3.703914000	0.569996000
H	0.203583000	-2.943703000	0.502297000
C	-0.678096000	-0.627463000	1.346711000
C	0.925976000	0.709606000	0.091739000
C	0.490849000	2.065480000	0.100994000
C	-1.632665000	0.280681000	-1.230891000
H	-1.356326000	1.172812000	-1.793826000
C	-3.006149000	0.202083000	-0.712056000
H	-3.092333000	-0.553232000	0.085214000
H	-3.550848000	-0.250196000	-1.575667000
C	-3.656937000	1.525088000	-0.318559000
H	-4.718647000	1.367344000	-0.075770000
H	-3.594783000	2.260671000	-1.135812000
H	-3.145164000	1.950602000	0.554415000
C	1.496818000	3.198249000	0.102825000
H	0.957420000	4.152656000	0.181530000
H	2.209963000	3.094388000	0.933679000
H	2.098378000	3.184374000	-0.819334000

C	2.278677000	0.255182000	-0.120426000
O	3.287929000	0.943030000	-0.193746000
O	2.342342000	-1.110415000	-0.241034000
C	3.640828000	-1.661923000	-0.432960000
H	4.307291000	-1.424029000	0.412129000
H	3.507625000	-2.750342000	-0.501654000
H	4.108843000	-1.286011000	-1.357562000

TS6, G = -897.487520 (i = -160 cm-1)

O	2.507014000	-1.018156000	0.071406000
O	1.477982000	-0.633205000	-1.869883000
O	0.393976000	-2.330404000	-0.351907000
N	0.325775000	0.085423000	0.092000000
C	1.573096000	2.584566000	-1.903761000
H	2.468387000	3.043164000	-2.352643000
H	1.276867000	1.728107000	-2.526203000
H	0.762519000	3.331675000	-1.929229000
C	1.859625000	2.132390000	-0.471590000
H	2.153164000	2.998860000	0.146972000
H	2.706978000	1.433870000	-0.444765000
C	0.642763000	1.550021000	0.209147000
H	-0.258975000	2.152361000	0.105590000
C	0.685776000	0.692945000	1.425734000
H	-0.201324000	0.747940000	2.061758000
C	1.962365000	0.199056000	2.082442000
H	2.779220000	0.922830000	1.939389000
H	1.796377000	0.091418000	3.163942000
C	2.365212000	-1.145295000	1.493907000
H	1.622366000	-1.927136000	1.717079000
H	3.346372000	-1.471833000	1.863025000

C	1.412928000	-0.794727000	-0.680215000
C	-0.811077000	-1.896916000	-0.332211000
C	-0.983719000	-0.524948000	-0.134817000
C	-1.926873000	-2.880112000	-0.531881000
H	-2.453757000	-2.670092000	-1.475568000
H	-1.507216000	-3.894982000	-0.563740000
H	-2.678591000	-2.799153000	0.265995000
C	-2.266705000	0.123713000	0.001404000
O	-3.341992000	-0.408017000	-0.227576000
O	-2.196363000	1.406258000	0.454138000
C	-3.440546000	2.086638000	0.630675000
H	-4.071962000	1.570011000	1.370085000
H	-3.188671000	3.092909000	0.990498000
H	-3.994199000	2.156282000	-0.318612000

TS6‘, G = -897.471166 (i = -411 cm-1)

C	0.920243000	-0.689280000	0.049112000
N	-0.186361000	0.033291000	0.281067000
C	-1.453650000	0.343112000	-1.687291000
C	-0.749452000	1.287961000	-0.924558000
H	-0.870902000	-0.292383000	-2.360385000
C	-2.885149000	0.004063000	-1.486503000
C	-2.994426000	-0.980017000	-0.320078000
O	-2.457373000	-0.417994000	0.894318000
C	-1.155813000	-0.405052000	1.219697000
O	-0.815754000	-0.588216000	2.361730000
H	-4.047783000	-1.193223000	-0.087713000
H	-2.464829000	-1.916381000	-0.539890000
H	-3.495575000	0.894516000	-1.266966000
H	-3.298410000	-0.488622000	-2.380952000

H	0.241870000	1.555823000	-1.295196000
C	-1.410897000	2.401237000	-0.145395000
H	-2.288475000	2.020319000	0.396514000
H	-1.801256000	3.109592000	-0.898909000
C	2.205197000	-0.001274000	-0.158841000
O	3.258628000	-0.538779000	-0.451643000
C	0.774383000	-2.154838000	-0.042872000
O	-0.355117000	-2.643856000	0.029955000
C	1.979279000	-3.048346000	-0.201173000
H	2.717850000	-2.855055000	0.591128000
H	1.646208000	-4.094800000	-0.166367000
H	2.493881000	-2.842631000	-1.151763000
O	2.109166000	1.334961000	0.019575000
C	3.310098000	2.088216000	-0.155207000
H	3.702840000	1.978956000	-1.178570000
H	3.043960000	3.135980000	0.034933000
H	4.084755000	1.763228000	0.556593000
C	-0.471012000	3.130861000	0.813944000
H	-1.008763000	3.936463000	1.338438000
H	-0.058522000	2.444047000	1.567587000
H	0.378467000	3.582340000	0.277572000

TS_{rot}(INT5-INT6), G = -897.464750 (i = -38 cm-1)

O	0.970042000	0.307910000	-2.153821000
O	1.271164000	1.885927000	-0.616406000
O	-0.737437000	-2.701798000	1.010189000
N	0.459004000	-0.237898000	0.079674000
C	1.877509000	1.636917000	2.501783000
H	2.669759000	2.326336000	2.832871000
H	1.147570000	2.208648000	1.910139000

H	1.366538000	1.251580000	3.399438000
C	2.464189000	0.494662000	1.672367000
H	3.176855000	-0.090309000	2.280643000
H	3.032279000	0.879601000	0.814522000
C	1.418307000	-0.499044000	1.238730000
H	0.834295000	-0.924731000	2.060208000
C	1.469404000	-1.402755000	0.064865000
H	0.935663000	-2.340262000	0.218311000
C	2.386714000	-1.362112000	-1.132593000
H	3.188980000	-0.612922000	-1.046237000
H	2.854122000	-2.348068000	-1.266436000
C	1.504087000	-1.039981000	-2.334277000
H	0.665190000	-1.746521000	-2.430424000
H	2.062881000	-1.005325000	-3.278090000
C	0.925188000	0.789330000	-0.921275000
C	-1.479183000	-1.796250000	0.571852000
C	-1.012760000	-0.514982000	0.118499000
C	-2.974720000	-2.089246000	0.559012000
H	-3.409800000	-1.971130000	-0.443103000
H	-3.100295000	-3.123550000	0.910014000
H	-3.530513000	-1.403240000	1.215227000
C	-1.925007000	0.587981000	-0.100357000
O	-3.135505000	0.510897000	-0.264696000
O	-1.308597000	1.800891000	-0.100062000
C	-2.102908000	2.933144000	-0.434684000
H	-2.884290000	3.110837000	0.321523000
H	-1.415612000	3.789415000	-0.465898000
H	-2.588893000	2.808327000	-1.415592000

3.4e, G = -897.558269

O	0.052377000	-2.760382000	0.540028000
O	1.080085000	-1.200596000	1.741203000
O	-1.535162000	1.661709000	-0.766058000
N	0.042020000	-0.574363000	-0.209840000
C	-1.179615000	-0.711963000	-1.016534000
H	-0.901784000	-0.476011000	-2.057243000
C	-1.721594000	-2.140077000	-0.954462000
H	-2.434839000	-2.267255000	-0.127176000
H	-2.246341000	-2.383389000	-1.889585000
C	-0.559185000	-3.082725000	-0.721126000
H	-0.881065000	-4.129250000	-0.639284000
H	0.195779000	-3.005738000	-1.523345000
C	0.424126000	-1.483295000	0.761133000
C	0.577514000	0.741045000	-0.170383000
C	-0.221259000	1.803397000	-0.481385000
C	-2.162375000	0.380692000	-0.554231000
H	-3.034675000	0.385889000	-1.226490000
C	-2.629306000	0.271716000	0.898767000
H	-1.747909000	0.234967000	1.560558000
H	-3.158973000	-0.685953000	1.022607000
C	-3.545051000	1.422209000	1.314318000
H	-3.871878000	1.303996000	2.359521000
H	-4.447986000	1.464847000	0.681865000
H	-3.030731000	2.391566000	1.227258000
C	0.199257000	3.231058000	-0.621462000
H	-0.261683000	3.652105000	-1.529198000
H	-0.181291000	3.810760000	0.236869000
H	1.286048000	3.350354000	-0.658173000
C	2.036288000	0.883204000	0.054477000
O	2.587100000	1.847091000	0.547149000
O	2.708298000	-0.195309000	-0.387180000

C	4.100062000	-0.250318000	-0.072571000
H	4.252875000	-0.233608000	1.018183000
H	4.470865000	-1.197272000	-0.485995000
H	4.644688000	0.594783000	-0.521885000

3.3e, G = -897.500278

O	2.762020000	-0.631617000	0.304281000
O	1.998916000	-0.863016000	-1.772766000
O	1.003619000	-2.020899000	-0.095210000
N	0.151457000	0.400535000	0.145947000
C	0.842953000	2.387628000	-2.266745000
H	1.595482000	2.894376000	-2.892689000
H	0.807757000	1.330024000	-2.572195000
H	-0.137602000	2.843523000	-2.486132000
C	1.192683000	2.497338000	-0.781511000
H	1.281408000	3.557633000	-0.484385000
H	2.171676000	2.027087000	-0.601802000
C	0.142519000	1.842773000	0.090226000
H	-0.843292000	2.320137000	0.053139000
C	0.436769000	1.119867000	1.381738000
H	-0.388173000	1.140546000	2.104885000
C	1.828984000	0.917230000	1.969551000
H	2.537500000	1.671584000	1.592330000
H	1.784141000	1.045596000	3.062963000
C	2.414872000	-0.468843000	1.699009000
H	1.730157000	-1.270916000	2.011623000
H	3.363980000	-0.594156000	2.238376000
C	1.881824000	-1.057347000	-0.596265000
C	-0.348479000	-1.843992000	-0.195108000
C	-0.843131000	-0.578502000	-0.062400000

C	-1.066974000	-3.136880000	-0.352615000
H	-0.900277000	-3.520565000	-1.374316000
H	-0.641159000	-3.877009000	0.344123000
H	-2.143528000	-3.033775000	-0.188950000
C	-2.298419000	-0.297427000	-0.067628000
O	-3.165972000	-1.000190000	-0.545822000
O	-2.572615000	0.864569000	0.559165000
C	-3.950020000	1.250371000	0.621782000
H	-4.369429000	1.374283000	-0.388722000
H	-4.543414000	0.497373000	1.163033000
H	-3.974659000	2.206445000	1.159700000

3.5e, G = -897.516431

C	1.572981000	-0.206047000	0.191744000
N	0.321382000	-0.139382000	0.382979000
C	-2.157768000	1.091930000	-1.255687000
C	-2.934045000	1.446261000	-0.219777000
H	-1.325773000	1.755717000	-1.522140000
C	-2.253964000	-0.174309000	-2.064048000
C	-1.166917000	-1.188190000	-1.710055000
O	-1.318850000	-1.626037000	-0.344005000
C	-0.541855000	-1.212041000	0.651280000
O	-0.685030000	-1.622139000	1.779111000
H	-1.269091000	-2.097979000	-2.319156000
H	-0.160509000	-0.781155000	-1.881168000
H	-3.234122000	-0.659311000	-1.940481000
H	-2.139923000	0.051540000	-3.138966000
H	-2.697941000	2.392631000	0.285621000
C	-4.085475000	0.686024000	0.379824000
H	-4.305599000	-0.223018000	-0.201055000

H	-4.992184000	1.318082000	0.328981000
C	2.341586000	1.084899000	-0.016255000
O	3.426110000	1.120309000	-0.553498000
C	2.298404000	-1.559491000	0.067293000
O	1.621228000	-2.510700000	-0.262086000
C	3.757883000	-1.653222000	0.388364000
H	3.988086000	-1.108308000	1.318114000
H	4.043112000	-2.709950000	0.476151000
H	4.336793000	-1.167150000	-0.412204000
O	1.674742000	2.144814000	0.417514000
C	2.296585000	3.424319000	0.213420000
H	2.466404000	3.604926000	-0.858923000
H	1.598661000	4.166666000	0.619002000
H	3.259009000	3.474762000	0.745044000
C	-3.835024000	0.306491000	1.847069000
H	-4.716676000	-0.194836000	2.279695000
H	-2.975452000	-0.375790000	1.944722000
H	-3.624430000	1.199126000	2.460591000

3.9 References

(1) (a)Armarego, W. L. F. *Purification of Laboratory Chemicals*, 6th ed.; Chai, C. L. L., Series Ed.; Boston: Elsevier/Butterworth-Heinemann, 2009. (b) Still, W. C.; Kahn, M.; Mitra, A. Rapid Chromatographic Technique for Preparative Separations with Moderate Resolution. *J. Org. Chem.* **1978**, *43*, 2923–2925.

(2) Ju, M.; Weatherly, C. D.; Guzei, I. A.; Schomaker, J. M. Chemo- and Enantioselective Intramolecular Silver-Catalyzed Aziridinations. *Angew. Chem. Int. Ed.* **2017**, *56*, 9944–9948.

(3) (a) Lebel, H.; Lectard, S.; Parmentier, M. Copper-Catalyzed Alkene Aziridination with N-Tosyloxycarbamates. *Org. Lett.* **2007**, *9*, 4797–4800. (b) Lebel, H.; Huard, K.; Lectard, S. N-Tosyloxycarbamates as a Source of Metal Nitrenes: Rhodium-Catalyzed C−H Insertion and Aziridination Reactions. *J. Am. Chem. Soc.* **2005**, *127*, 14198–14199.

(4) Schwartz, B. D.; Denton, J. R.; Lian, Y.; Davies, H. M. L.; Williams, C. M. Asymmetric [4 + 3] Cycloadditions between Vinylcarbenoids and Dienes: Application to the Total Synthesis of the Natural Product (−)-5-Epi-Vibsanin E. *J. Am. Chem. Soc.* **2009**, *131*, 8329–8332.

(5) Dias, R. M. P.; de Oliveira, G. P.; Burtoloso, A. C. B. One-Pot Synthesis of β-O-4 Lignin Models via the Insertion of Stable 2-Diazo-1,3-Dicarbonyls into O–H Bonds. *Org. Biomol. Chem.* **2020**, *18*, 4815–4823.

(6) Muthyala, M. K.; Choudhary, S.; Kumar, A. Synthesis of Ionic Liquid-Supported Sulfonyl Azide and Its Application in Diazotransfer Reaction. *J. Org. Chem.* **2012**, *77*, 8787–8791.

(7) Meng, L.; Wu, P.; Fang, J.; Xiao, Y.; Xiao, X.; Tu, G.; Ma, X.; Teng, S.; Zeng, J.; Wan, Q. Glycosylation Enabled by Successive Rhodium (II) and Brønsted Acid Catalysis. *J. Am. Chem. Soc.* **2019**, *141* (30), 11775–11780. https://doi.org/10.1021/jacs.9b04619.

(8) (a) Dar'in, D.; Kantin, G.; Krasavin, M. A 'Sulfonyl-Azide-Free' (SAFE) Aqueous-Phase Diazo Transfer Reaction for Parallel and Diversity-Oriented Synthesis. *Chem. Commun.* **2019**, *55*, 5239–5242.(b) Dar'in, D.; Kantin, G.; Krasavin, M. Practical Application of the Aqueous 'Sulfonyl-Azide-Free' (SAFE) Diazo Transfer Protocol to Less α-C–H Acidic Ketones and Esters. *Synthesis* **2019**, *51*, 4284–4290.

(9) Lindsay, V. N. G.; Nicolas, C.; Charette, A. B. Asymmetric Rh(II)-Catalyzed Cyclopropanation of Alkenes with Diacceptor Diazo Compounds: P-Methoxyphenyl Ketone as a General Stereoselectivity Controlling Group. *J. Am. Chem. Soc.* **2011**, *133*, 8972–8981.

(10) (a) Nagy, V.; Agócs, A.; Turcsi, E.; Deli, J. Isolation and Purification of Acid-Labile Carotenoid 5,6-Epoxides on Modified Silica Gels. *Phytochem. Ana1*. **2009**, *20*, 143–148. (b) Scholz, S. O.; Farney, E. P.; Kim, S.; Bates, D. M.; Yoon, T. P. Spin-Selective Generation of Triplet Nitrenes: Olefin Aziridination through Visible-Light Photosensitization of Azidoformates. *Angew. Chem. Int. Ed.* **2016**, *55*, 2239–2242.

(11) Bruker-AXS (2018). *APEX3.* Version 2018.1-0. Madison, Wisconsin, USA.

(12) Krause, L.; Herbst-Irmer, R.; Sheldrick, G. M.; Stalke, D. Comparison of Silver and Molybdenum Microfocus X-Ray Sources for Single-Crystal Structure Determination. *J. Appl. Crystallogr.* **2015**, *48*, 3–10.

(13) Sheldrick, G. M. (2013b). *XPREP*. Version 2013/1. Georg-August-Universität Göttingen, Göttingen, Germany.

(14) The *SHELX* homepage, https://shelx.uni-goettingen.de (accessed 2021-12-18).

(15) Sheldrick, G. M. It SHELXT – Integrated Space-Group and Crystal-Structure Determination. *Acta Crystallogr. A* **2015**, *71* , 3–8.

(16) Sheldrick, G. M. Crystal Structure Refinement with It SHELXL. *Acta Crystallogr. C* **2015**, *71*, 3–8.

(17) Dolomanov, O. V.; Bourhis, L. J.; Gildea, R. J.; Howard, J. A. K.; Puschmann, H. It OLEX2: A Complete Structure Solution, Refinement and Analysis Program. *J. Appl. Crystallogr.* **2009**, *42* (2), 339–341. https://doi.org/10.1107/S0021889808042726.

(18) Programs *Gn*. University of Wisconsin-Madison; Guzei, I. A. (2007-2020).Madison, Wisconsin, USA.

(19) Gaussian 09, Revision D.01, Frisch, M. J.; Trucks, G. W.; Schlegel, H. B.; Scuseria, G. E.; Robb, M. A.; Cheeseman, J. R.; Scalmani, G.; Barone, V.; Mennucci, B.; Petersson, G. A.; Nakatsuji, H.; Caricato, M.; Li, X.; Hratchian, H. P.; Izmaylov, A. F.; Bloino, J.; Zheng, G.; Sonnenberg, J. L.; Hada, M.; Ehara, M.; Toyota, K.; Fukuda, R.; Hasegawa, J.; Ishida, M.; Nakajima, T.; Honda, Y.; Kitao, O.; Nakai, H.; Vreven, T.; Montgomery, J. A., Jr.; Peralta, J. E.; Ogliaro, F.; Bearpark, M.; Heyd, J. J.; Brothers, E.; Kudin, K. N.; Staroverov, V. N.; Kobayashi, R.; Normand, J.; Raghavachari, K.; Rendell, A.; Burant, J. C.; Iyengar, S. S.; Tomasi, J.; Cossi, M.; Rega, N.; Millam, J. M.; Klene, M.; Knox, J. E.; Cross, J. B.; Bakken, V.; Adamo, C.; Jaramillo, J.; Gomperts, R.; Stratmann, R. E.; Yazyev, O.; Austin, A. J.; Cammi, R.; Pomelli, C.; Ochterski, J. W.; Martin, R. L.; Morokuma, K.; Zakrzewski, V. G.; Voth, G. A.; Salvador, P.; Dannenberg, J. J.; Dapprich, S.; Daniels, A. D.; Farkas, Ö.; Foresman, J. B.; Ortiz, J. V.; Cioslowski, J.; Fox, D. J. Gaussian, Inc., Wallingford CT, 2009.

(20) (a) Becke, A. D. Density-functional Thermochemistry. III. The Role of Exact Exchange. *J. Chem. Phys.* **1993**, *98*, 5648–5652. b) Lee, C.; Yang, W.; Parr, R. G. Development of the Colle-Salvetti Correlation-Energy Formula into a Functional of the Electron Density. *Phys. Rev. B* **1988**, *37*, 785–789. (c) Vosko, S. H.; Wilk, L.; Nusair, M. Accurate Spin-Dependent Electron Liquid Correlation Energies for Local Spin Density Calculations: A Critical Analysis. *Can. J. Phys.* **1980**, *58*, 1200–1211.

(21) Grimme, S.; Antony, J.; Ehrlich, S.; Krieg, H. A Consistent and Accurate Ab Initio Parametrization of Density Functional Dispersion Correction (DFT-D) for the 94 Elements H-Pu. *J. Chem. Phys.* **2010**, *132*, 154104.

(22) Weigend, F.; Ahlrichs, R. Balanced Basis Sets of Split Valence, Triple Zeta Valence and Quadruple Zeta Valence Quality for H to Rn: Design and Assessment of Accuracy. *Phys. Chem. Chem. Phys.* **2005**, *7*, 3297–3305.

(23) (a) Schmid, S. C.; Guzei, I. A.; Fernández, I.; Schomaker, J. M. Ring Expansion of Bicyclic Methyleneaziridines via Concerted, Near-Barrierless [2,3]-Stevens Rearrangements of Aziridinium Ylides. *ACS Catal.* **2018**, *8*, 7907–7914. (b) Eshon, J.; Nicastri, K. A.; Schmid, S. C.; Raskopf, W. T.; Guzei, I. A.; Fernández, I.; Schomaker, J. M. Intermolecular [3+3] Ring Expansion of Aziridines to Dehydropiperidines through the Intermediacy of Aziridinium Ylides. *Nat. Commun.* **2020**, *11*, 1273.

(24) McIver, J. W.; Komornicki, A. Structure of Transition States in Organic Reactions. General Theory and an Application to the Cyclobutene-Butadiene Isomerization Using a Semiempirical Molecular Orbital Method. *J. Am. Chem. Soc.* **1972**, *94*, 2625–2633.

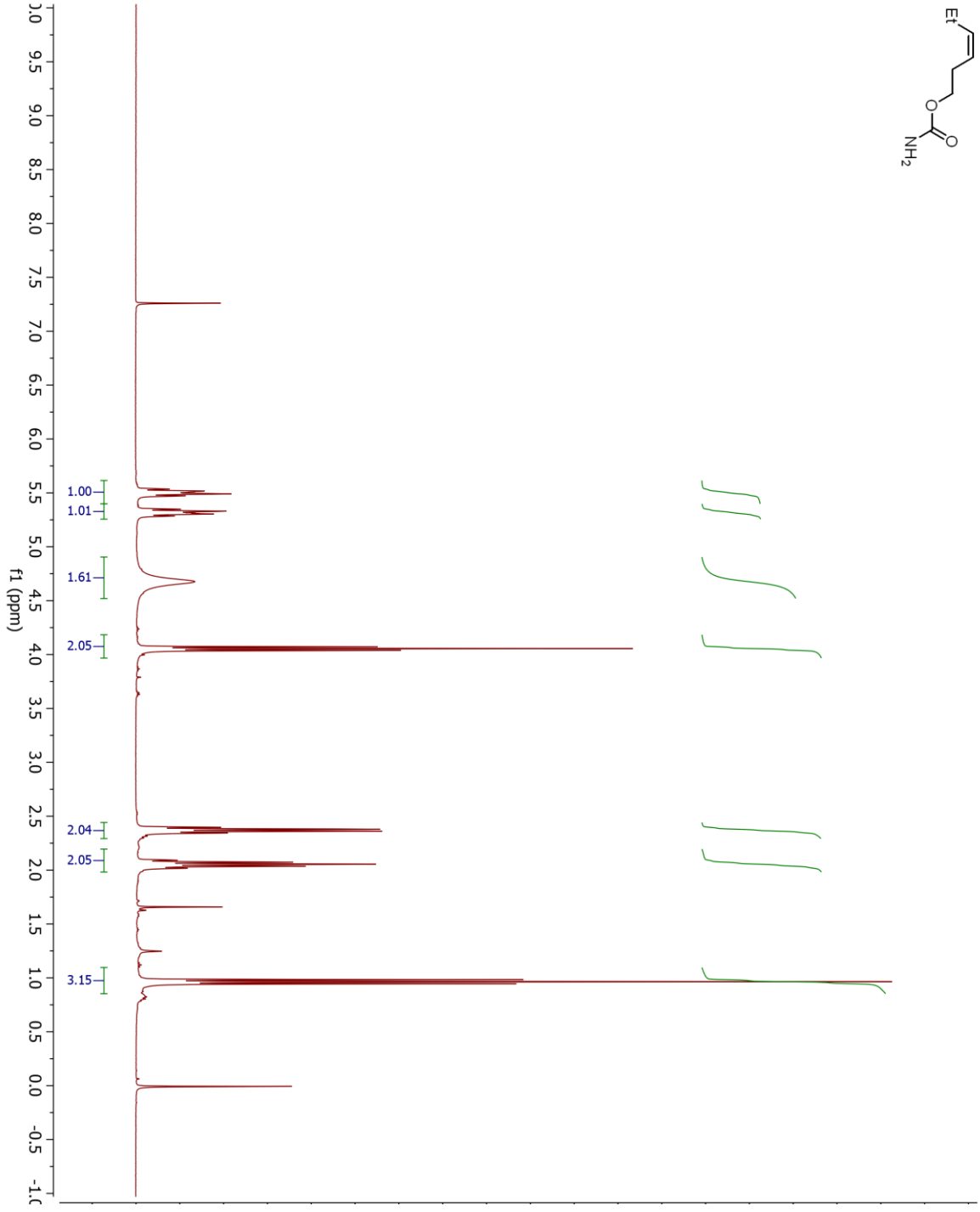
(25) Gonzalez, C.; Schlegel, H. B. Reaction Path Following in Mass-Weighted Internal Coordinates. *J. Phys. Chem.* **1990**, *94*, 5523–5527.

(26) (a) Foster, a) J.; Weinhold, F. Natural Hybrid Orbitals. *J. Am. Chem. Soc.* **1980**, *102*, 7211–7218. (b) Reed, A. E.; Weinhold, F. Natural Localized Molecular Orbitals. *J. Chem. Phys.* **1985**, *83*, 1736–1740. (c) Reed, A. E.; Weinstock, R. B.; Weinhold, F. Natural Population Analysis. *J. Chem. Phys.* **1985**, *83*, 735–746. (d) Reed, A. E.; Curtiss, L. A.; Weinhold, F. Intermolecular Interactions from a Natural Bond Orbital, Donor-Acceptor Viewpoint. *Chem. Rev.* **1988**, *88*, 899–926.

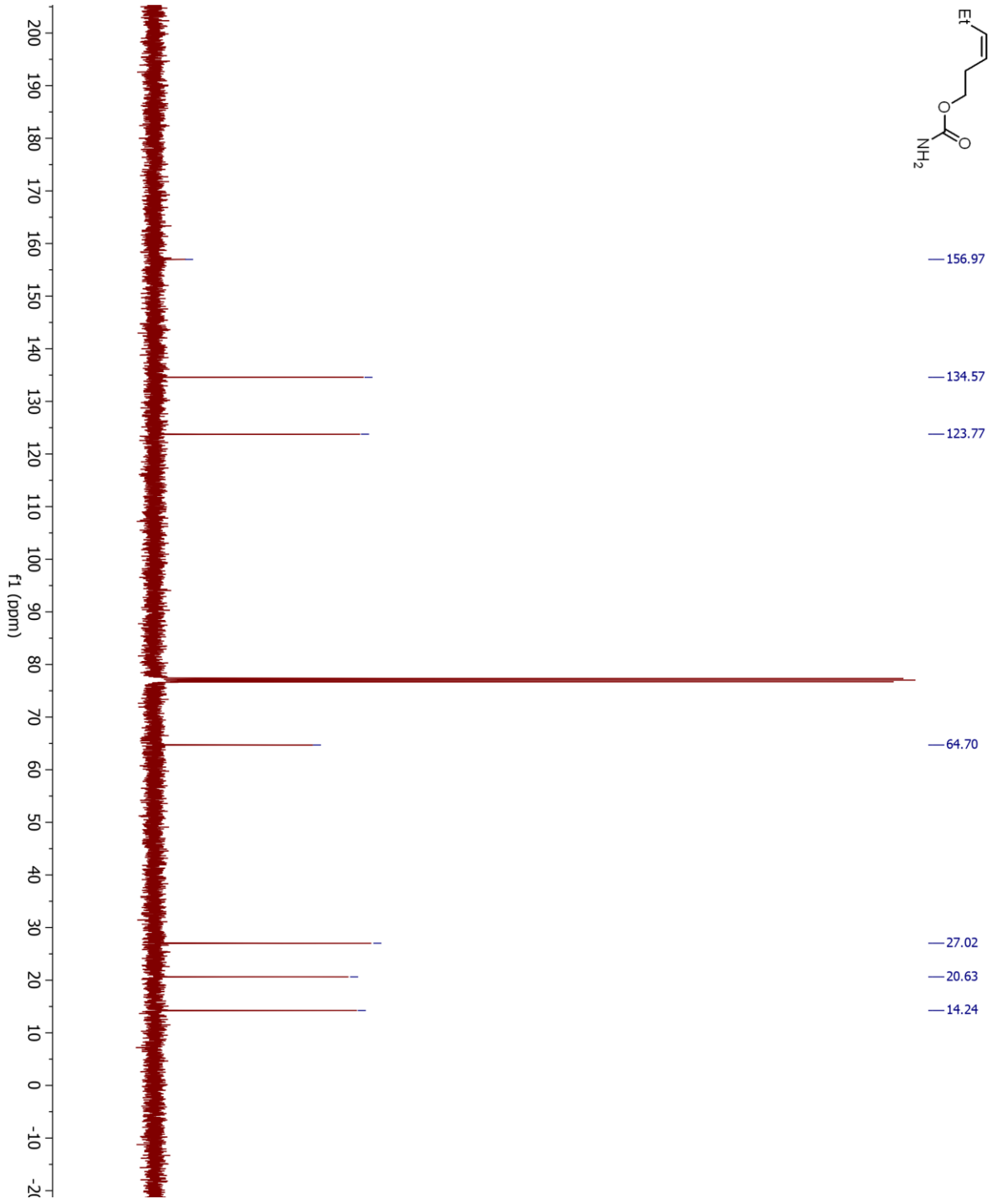
(27) Johnson, E. R.; Keinan, S.; Mori-Sánchez, P.; Contreras-García, J.; Cohen, A. J.; Yang, W. Revealing Noncovalent Interactions. *J. Am. Chem. Soc.* **2010**, *132*, 6498–6506.

3.10 NMR Spectra

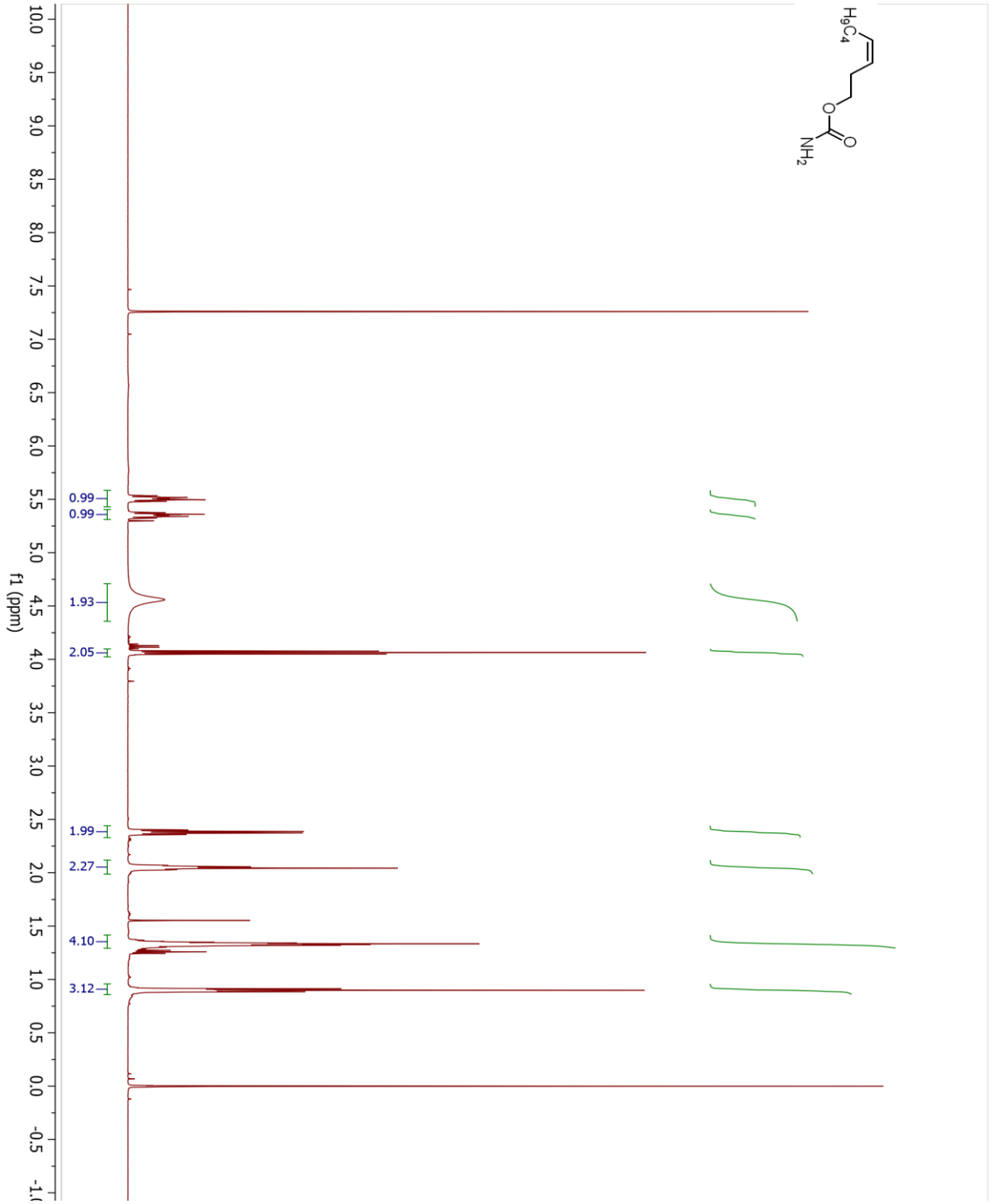
Precursor to compound **3.1.** ^{1}H NMR (500 MHz, $CDCl_3$)



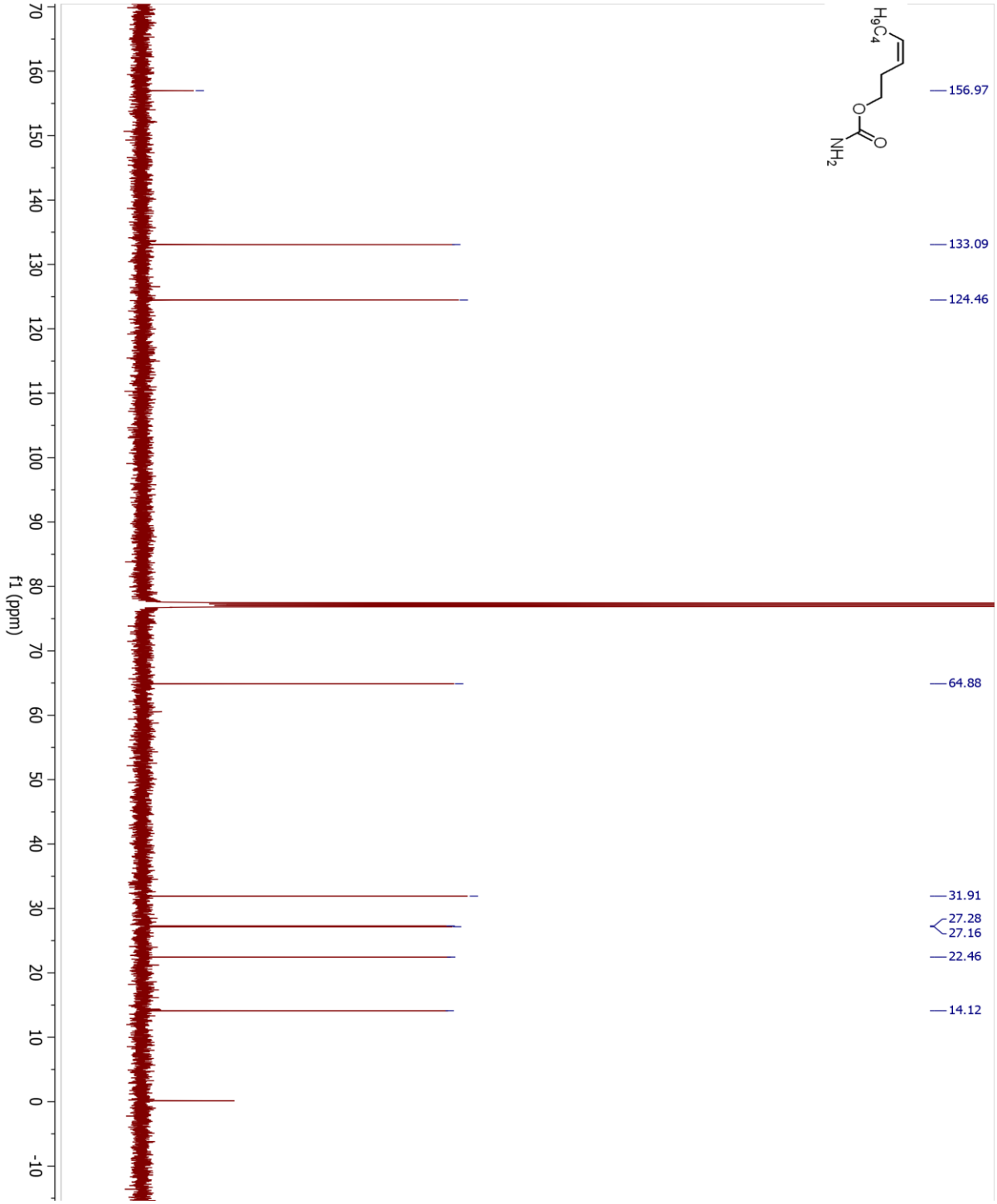
Precursor to compound **3.1.** ^{13}C NMR (126 MHz, $CDCl_3$)



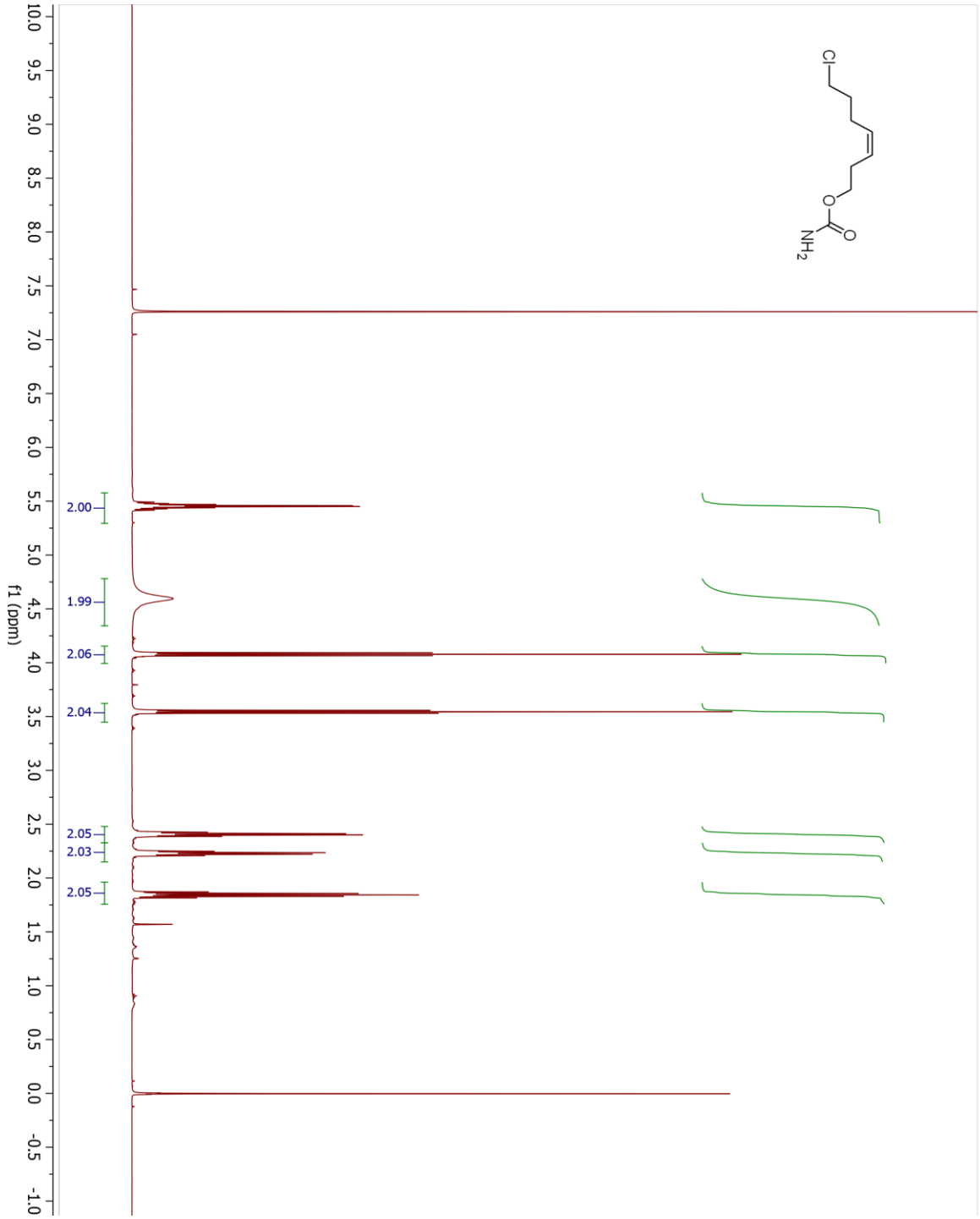
Precursor to compound **3.12.** ^{1}H NMR (500 MHz, $CDCl_3$)



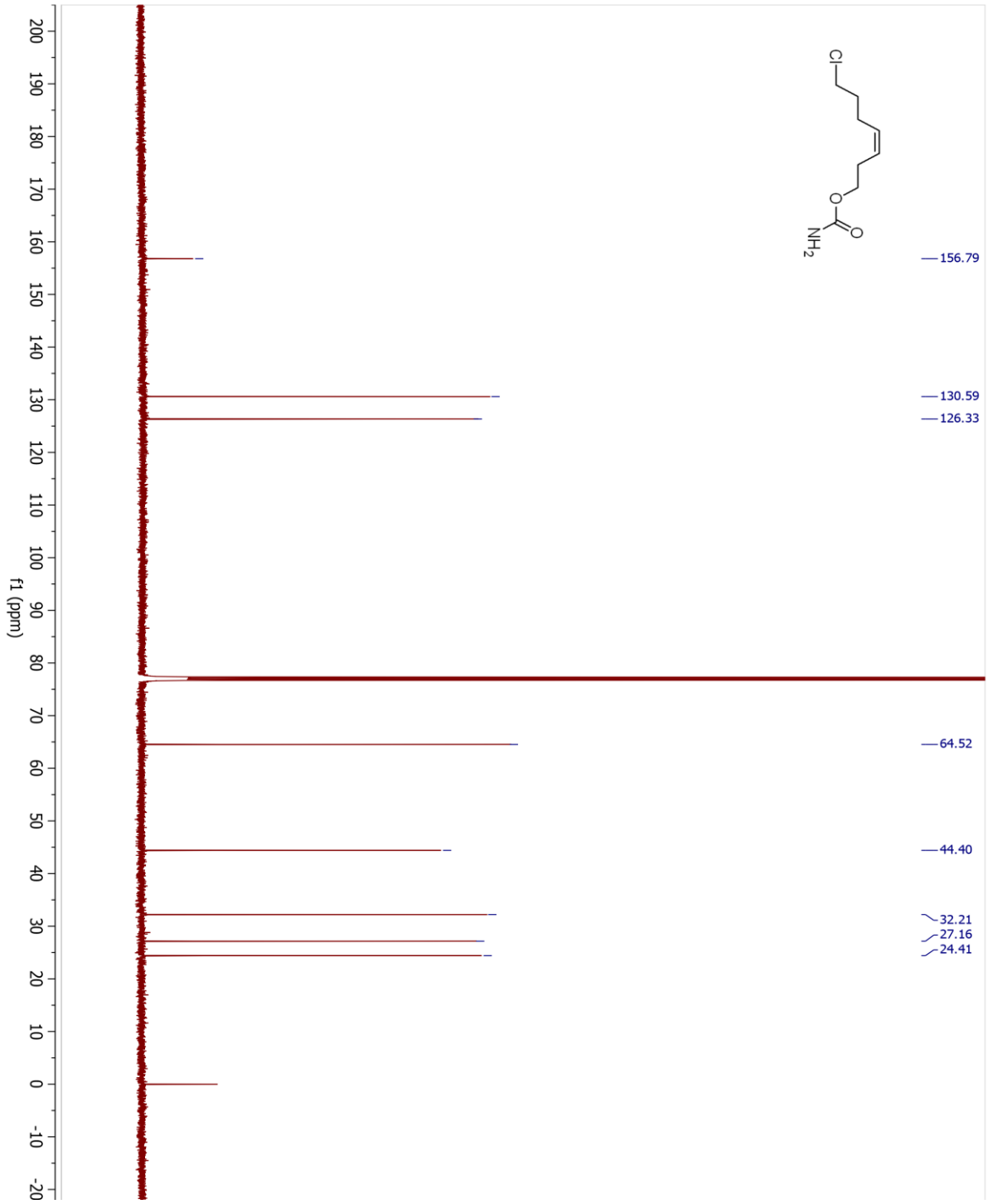
Precursor to compound **12.** ^{13}C NMR (126 MHz, $CDCl_3$)



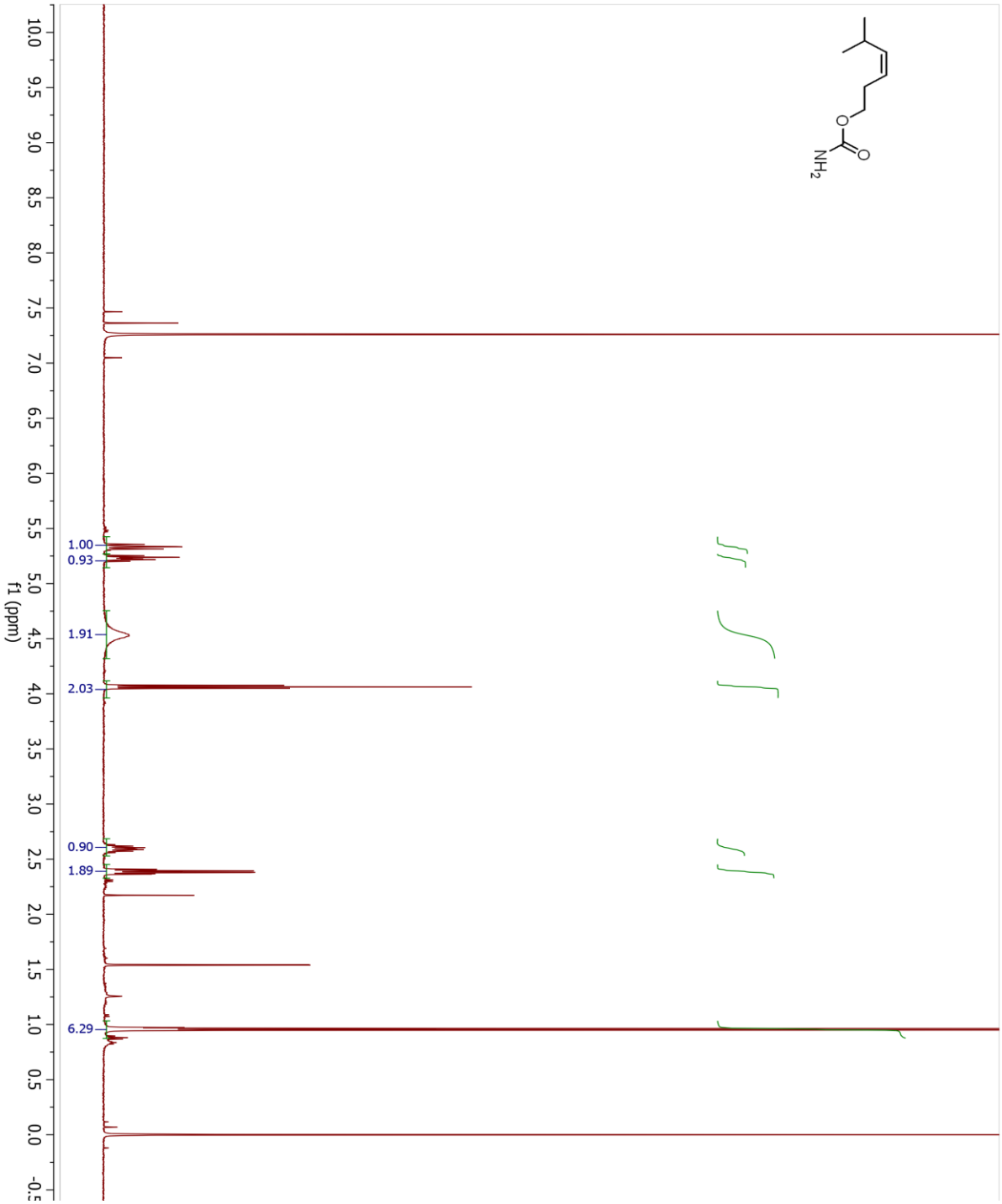
Precursor to compound **3.13.** ^{1}H NMR (500 MHz, $CDCl_3$)



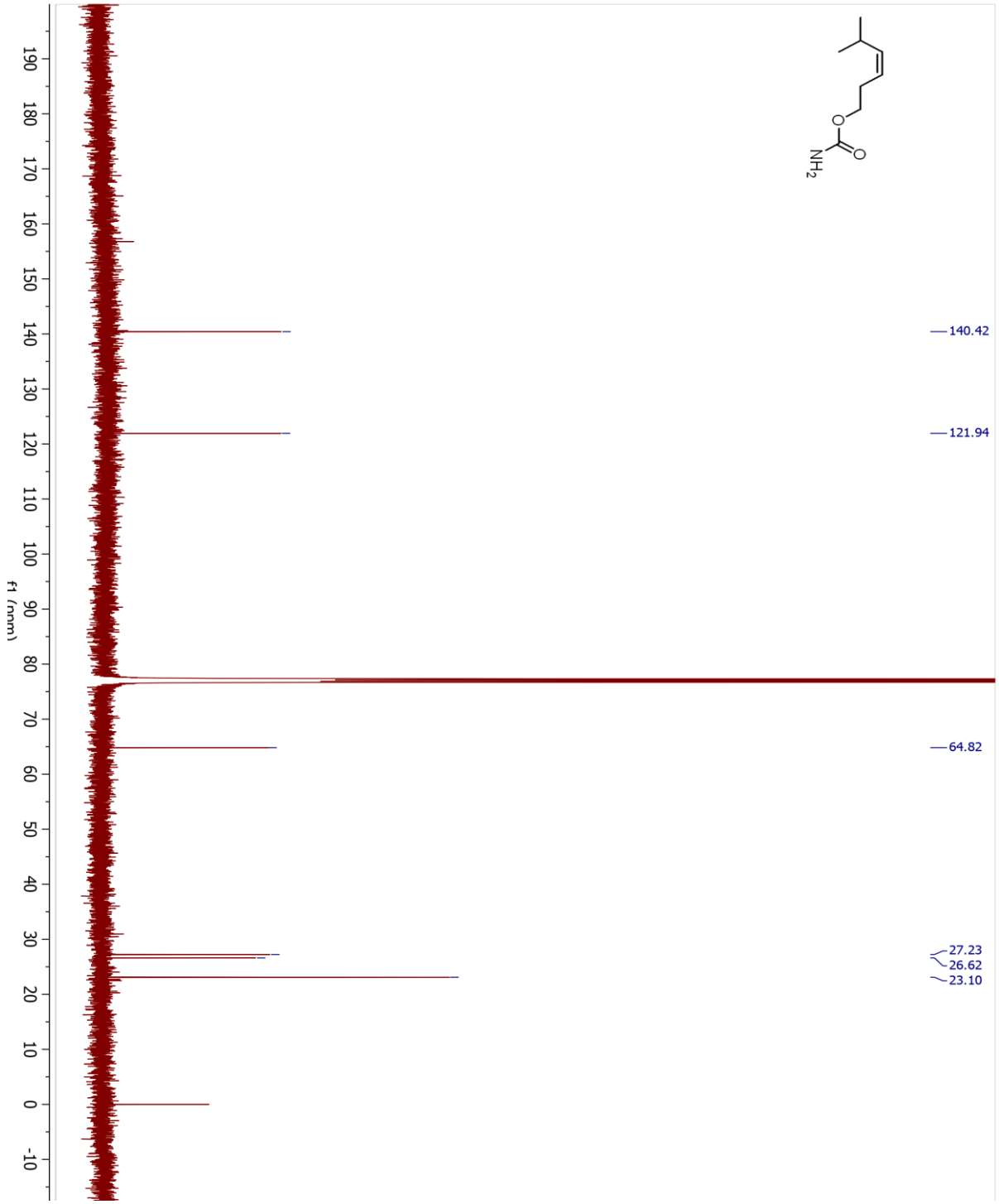
Precursor to compound **3.14** ^{13}C NMR (126 MHz, $CDCl_3$)



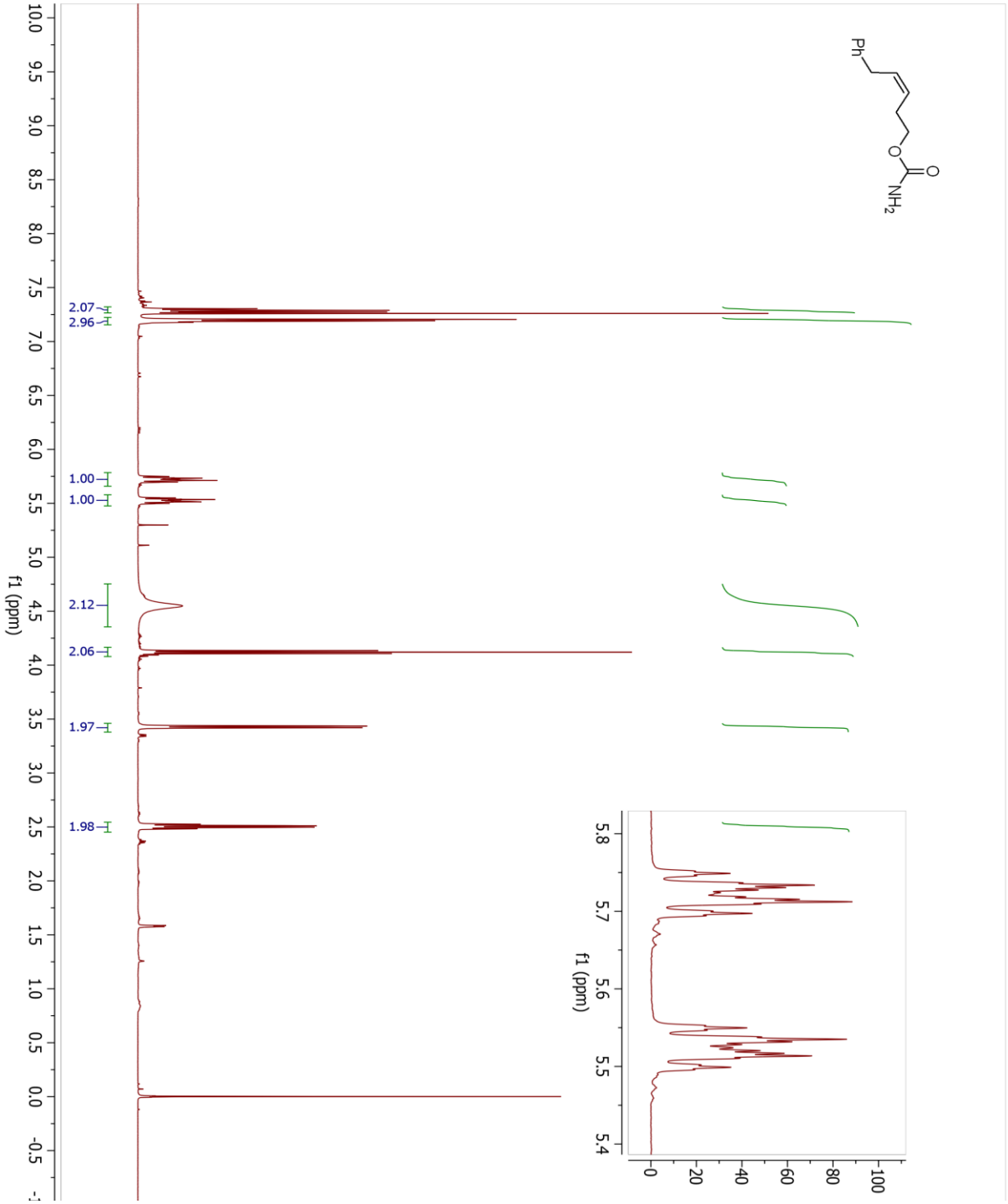
Precursor to compound **3.14.** ^{1}H NMR (500 MHz, $CDCl_3$)



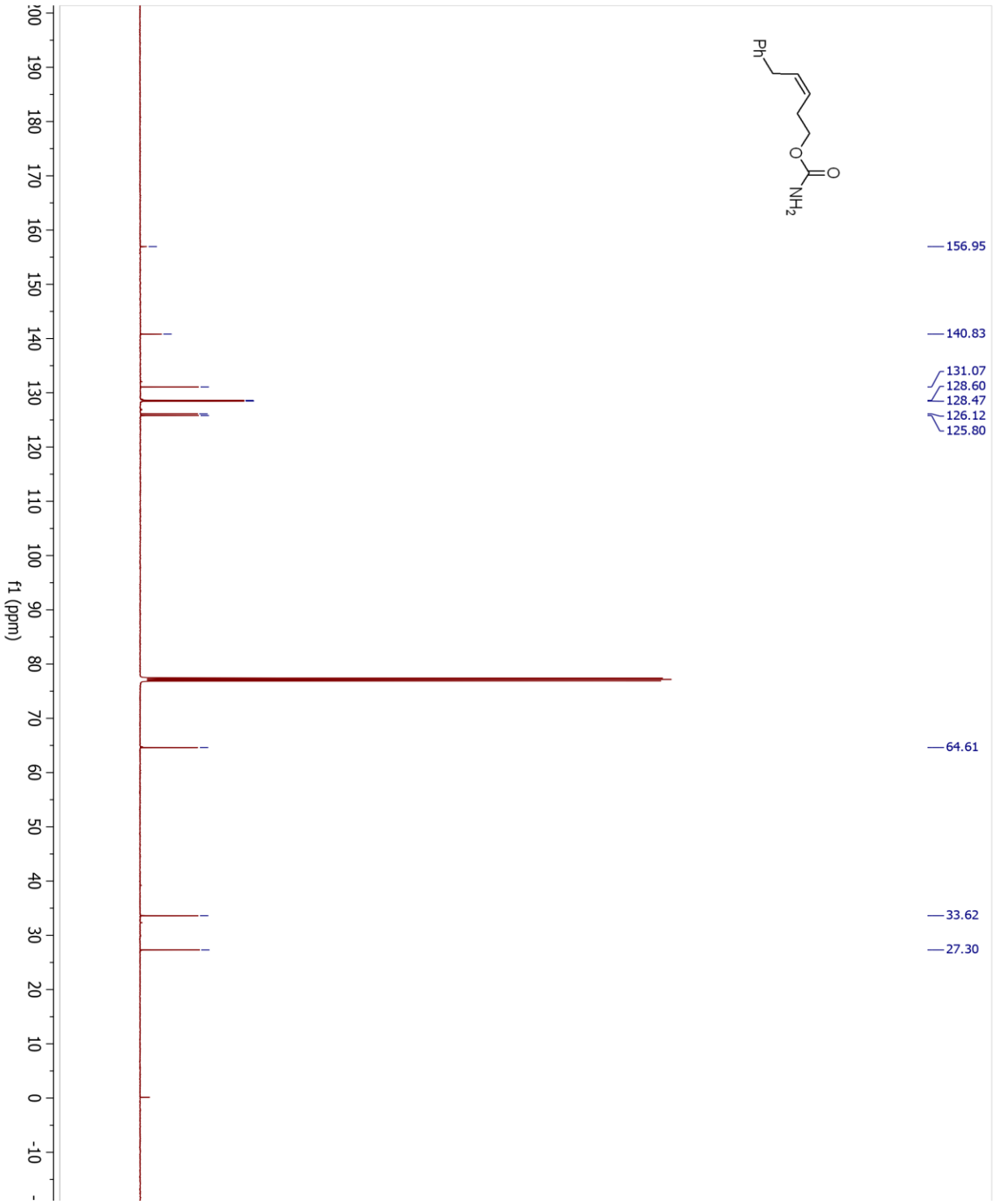
Precursor to compound **3.14.** ^{13}C NMR (126 MHz, $CDCl_3$)



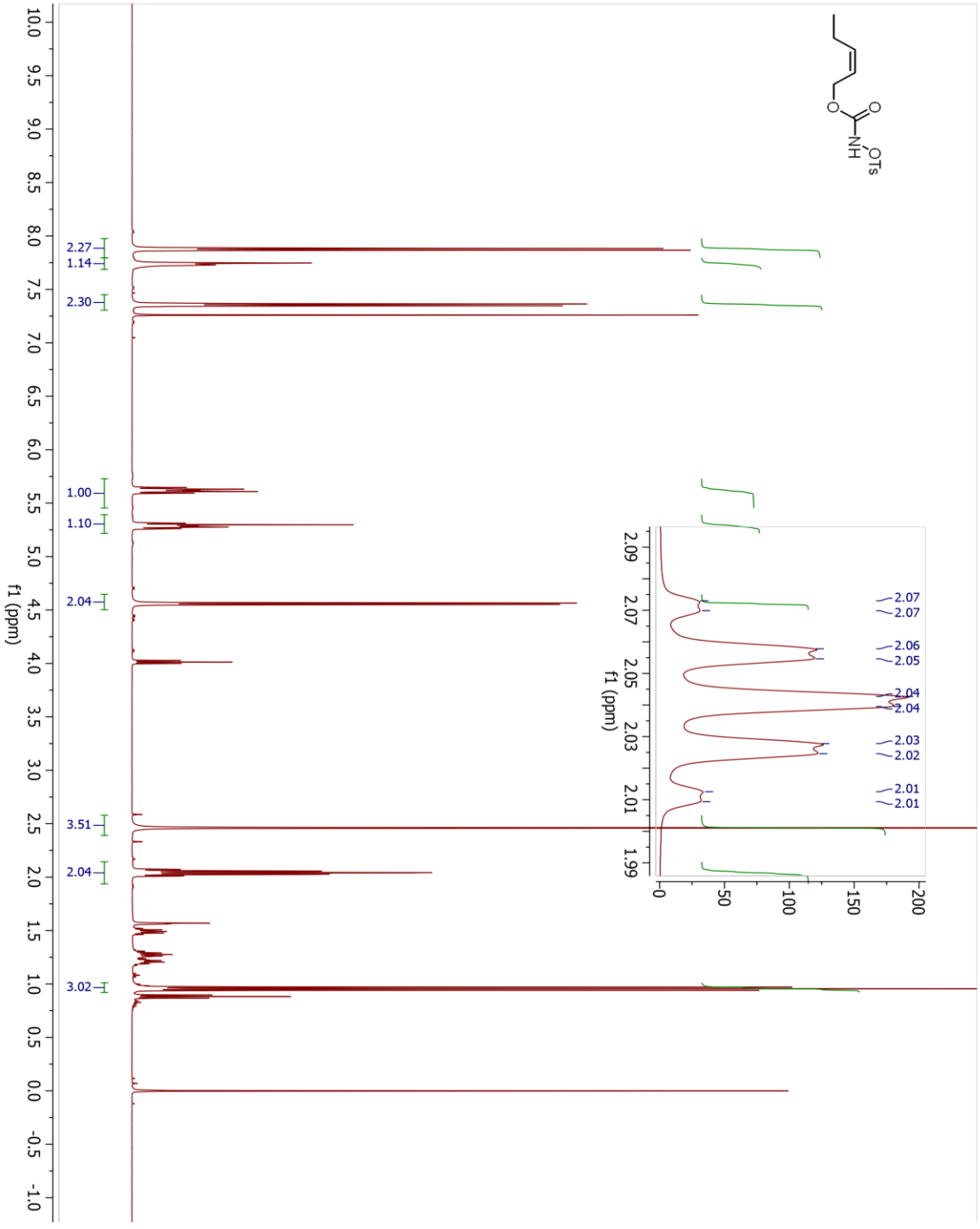
Precursor to compound **3.15.** ^{1}H NMR (500 MHz, $CDCl_3$)



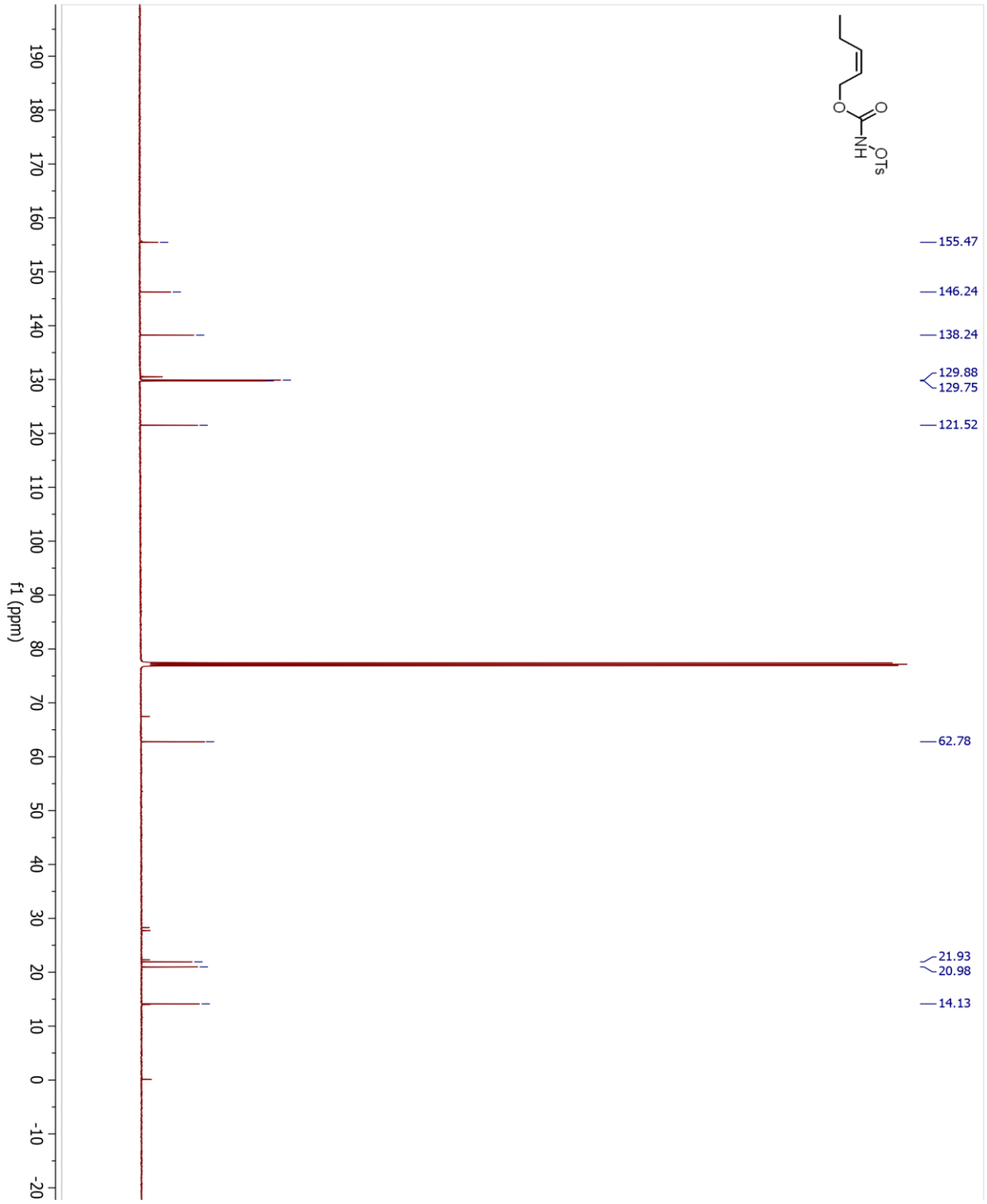
Precursor to compound **3.15.** ^{13}C NMR (126 MHz, $CDCl_3$)



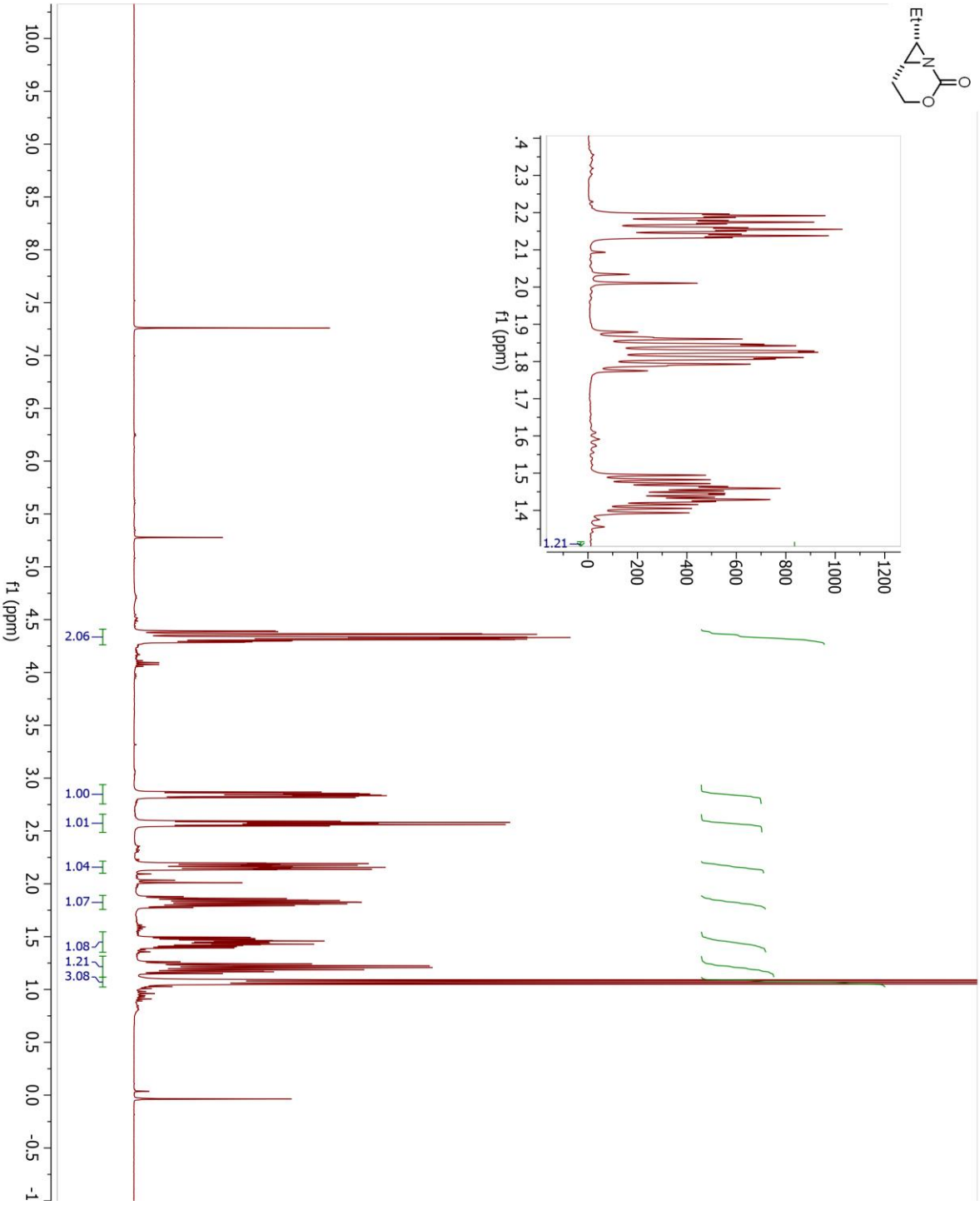
Compound **3.16** ^{1}H NMR (500 MHz, $CDCl_3$)



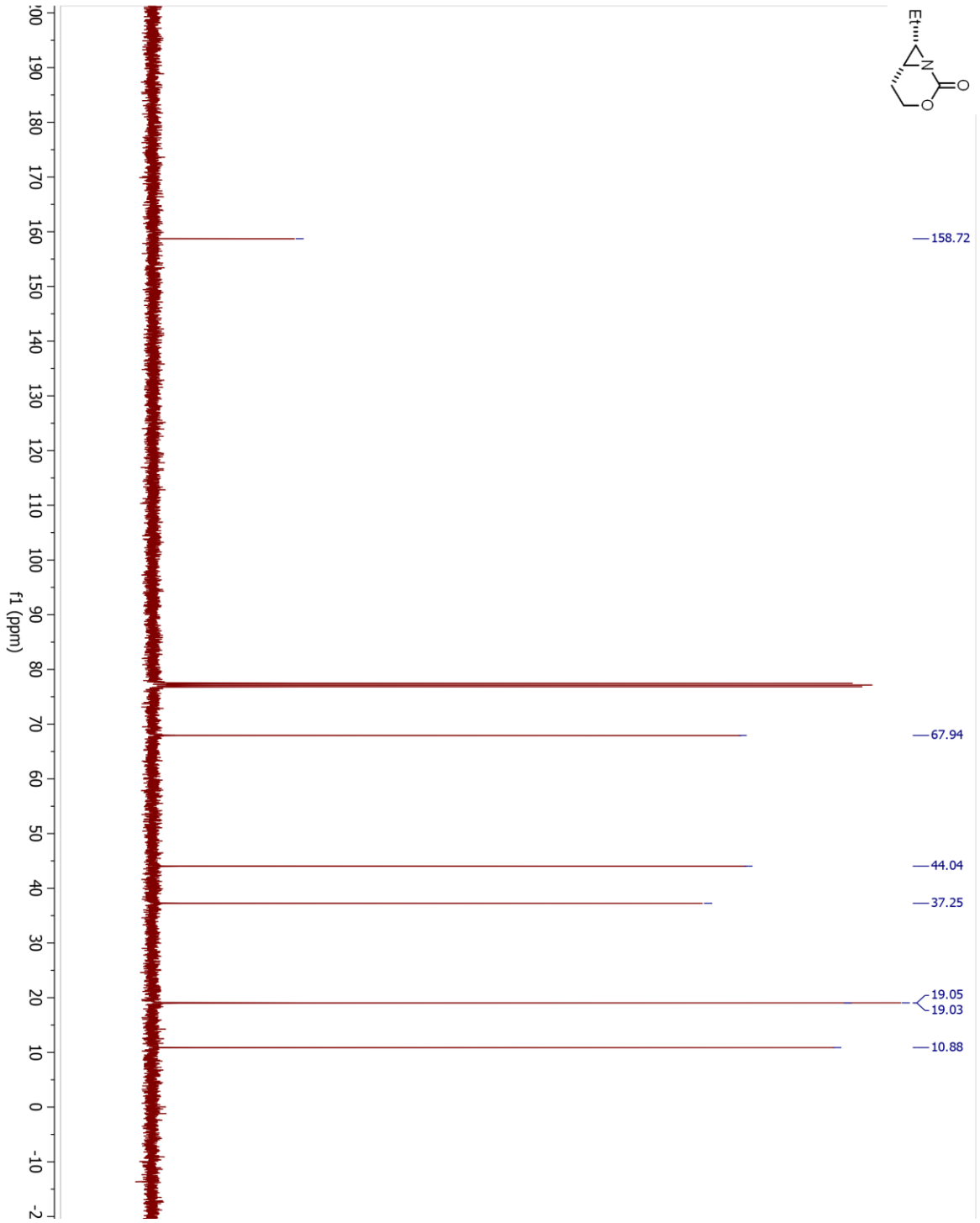
Precursor to compound **3.16.** ^{13}C NMR (126 MHz, $CDCl_3$)



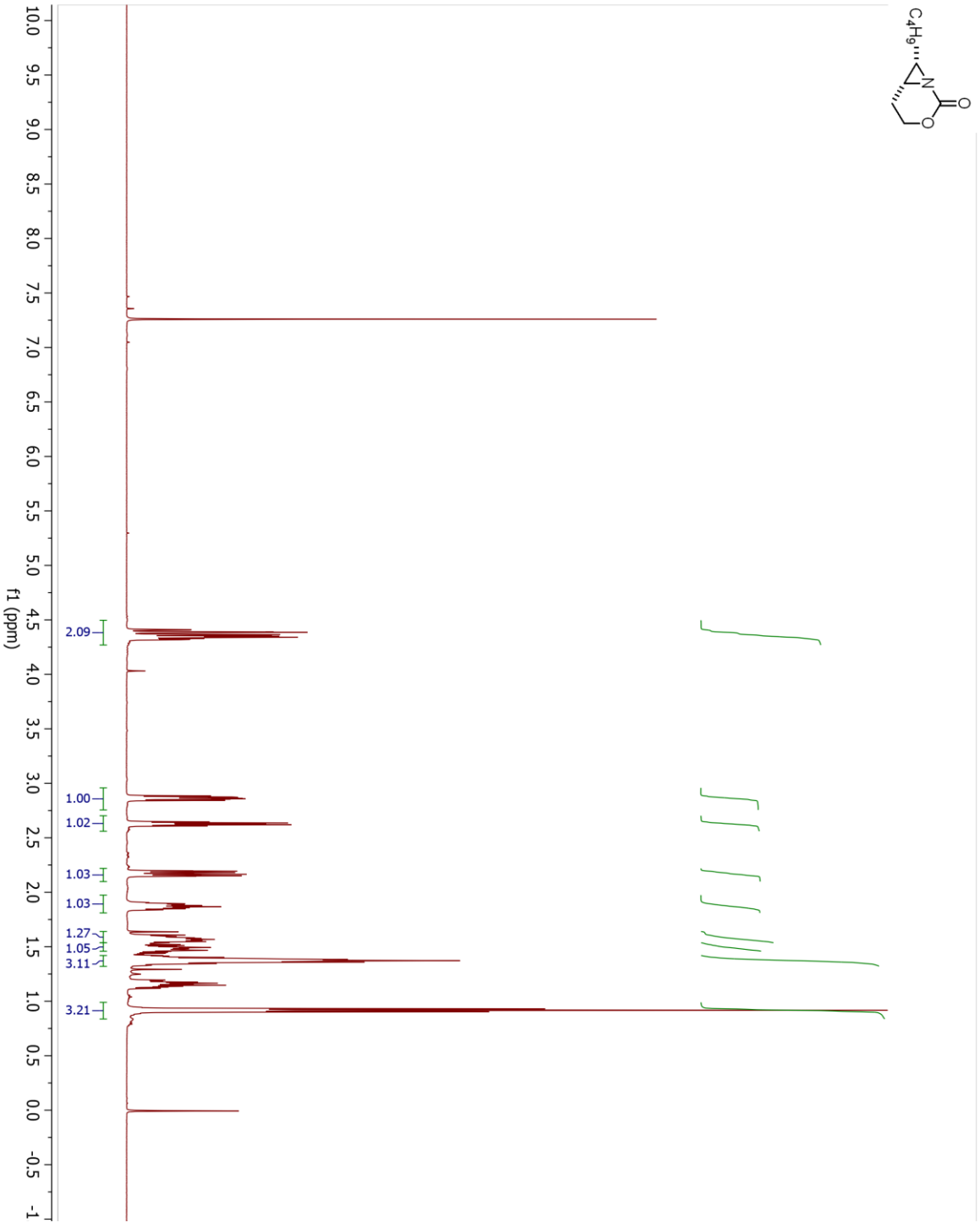
Compound **3.1.** ^{1}H NMR (500 MHz, $CDCl_3$)



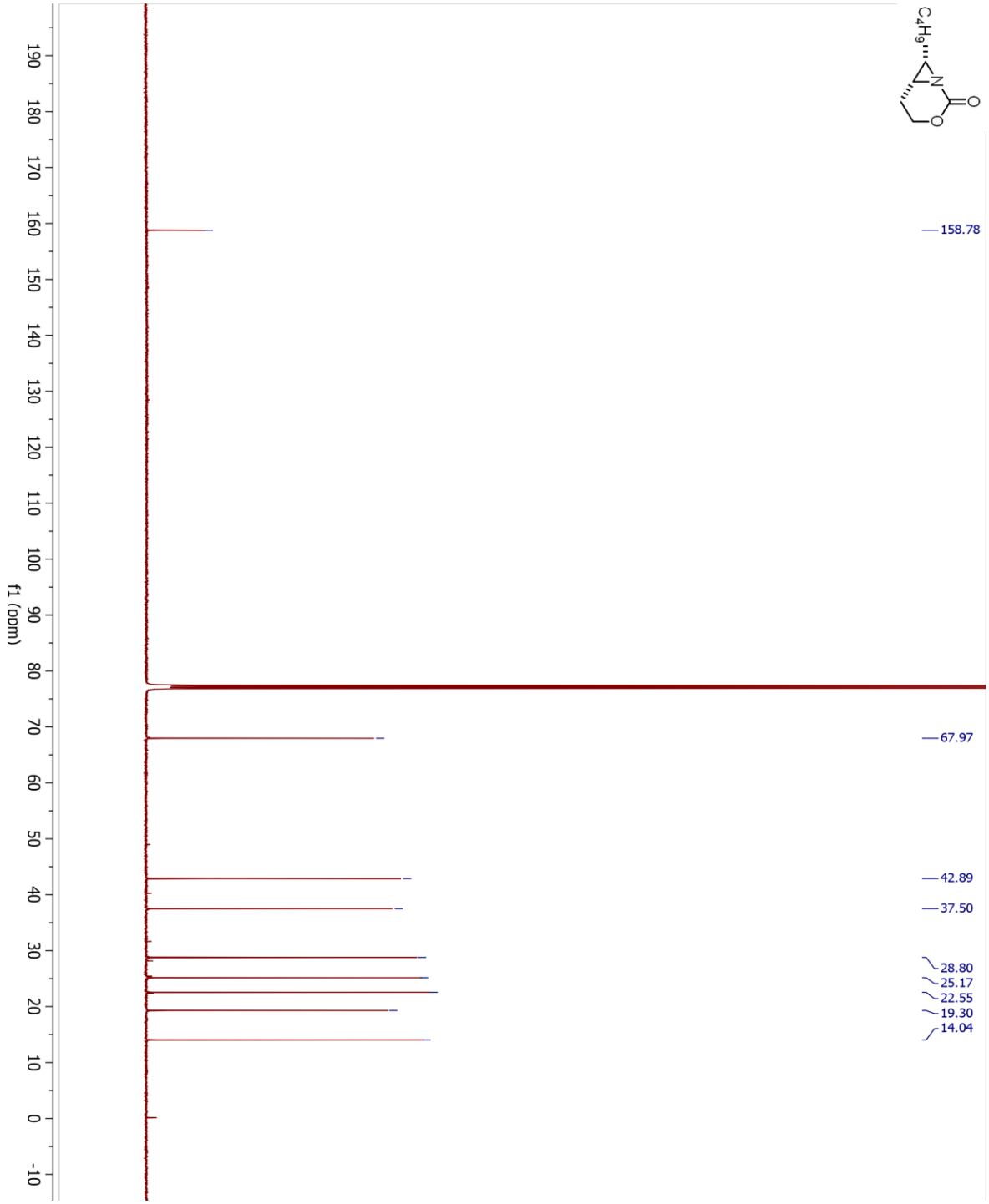
Compound **1.** ^{13}C NMR (126 MHz, $CDCl_3$)



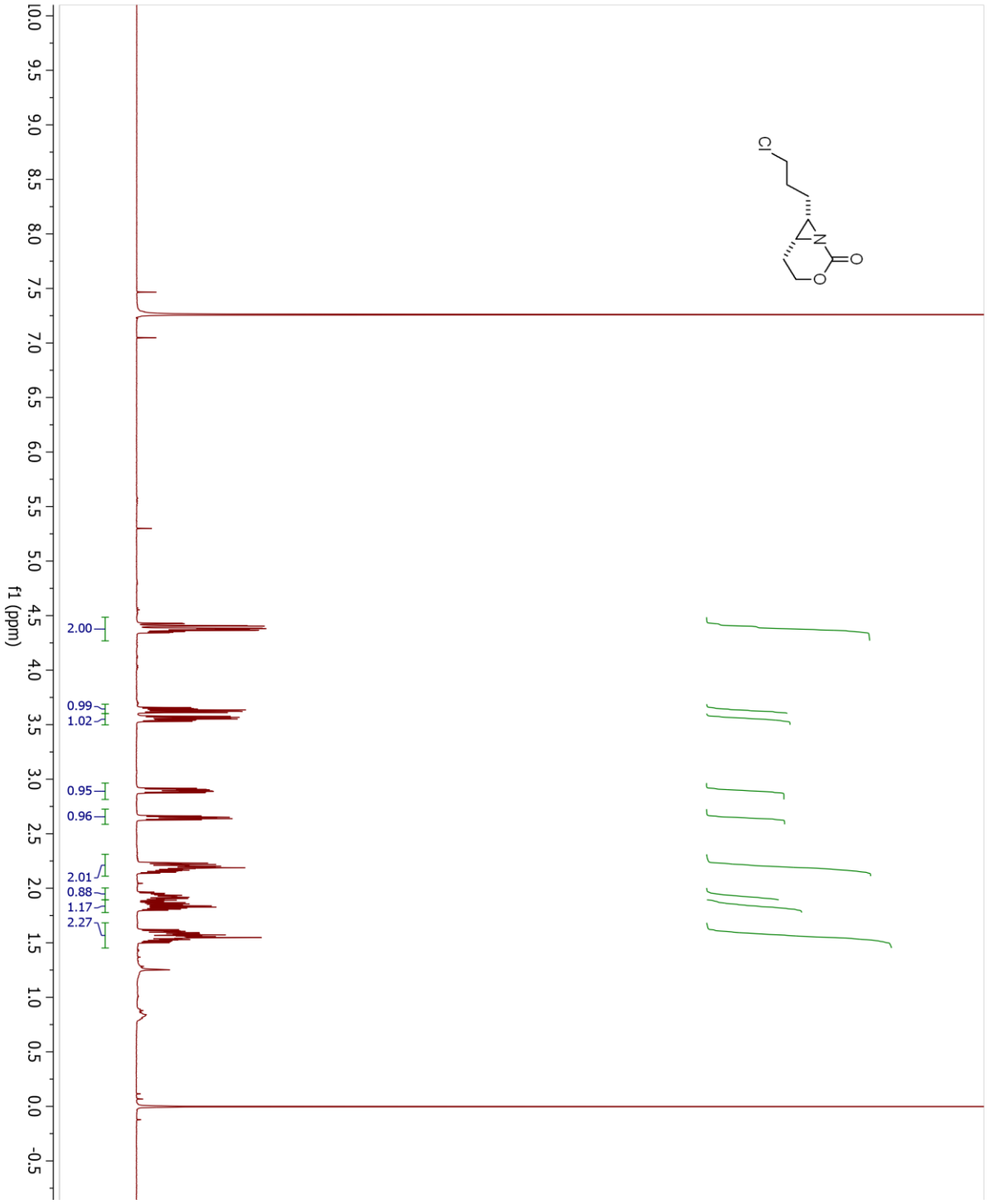
Compound **3.12.** ^{1}H NMR (500 MHz, $CDCl_3$)



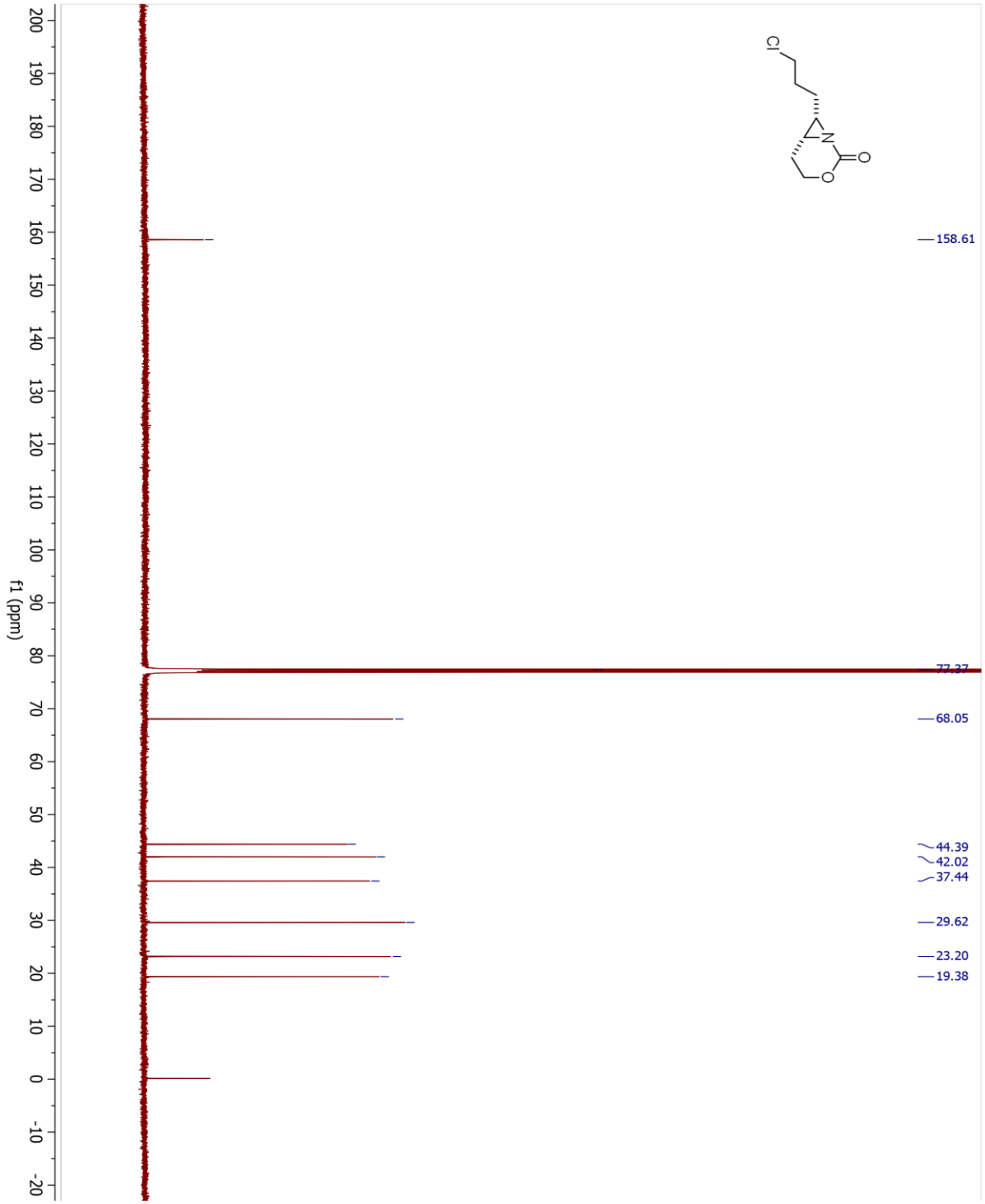
Compound **3.12.** ^{13}C NMR (126 MHz, $CDCl_3$)



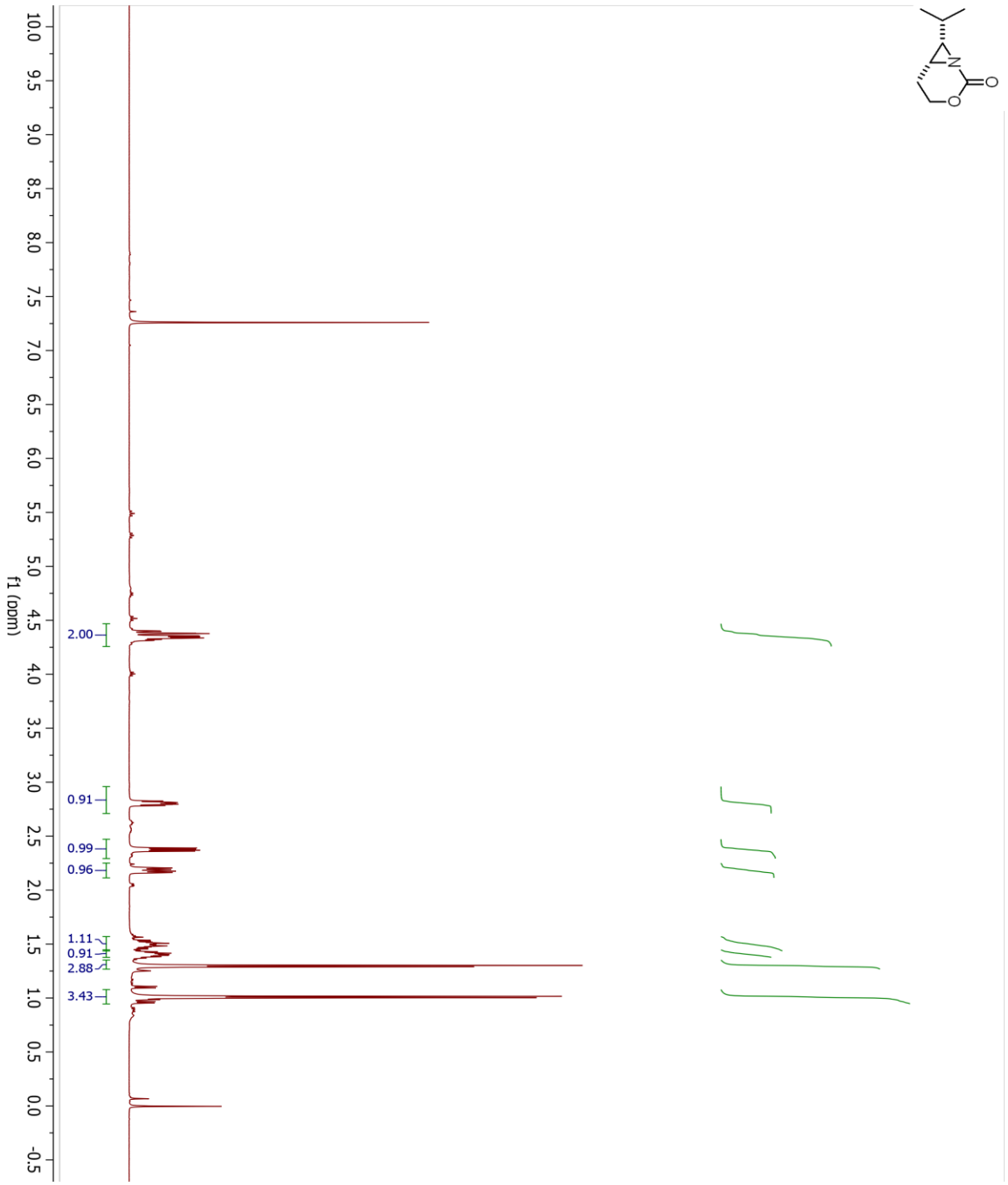
Compound **3.13.** ^{1}H NMR (500 MHz, $CDCl_3$)



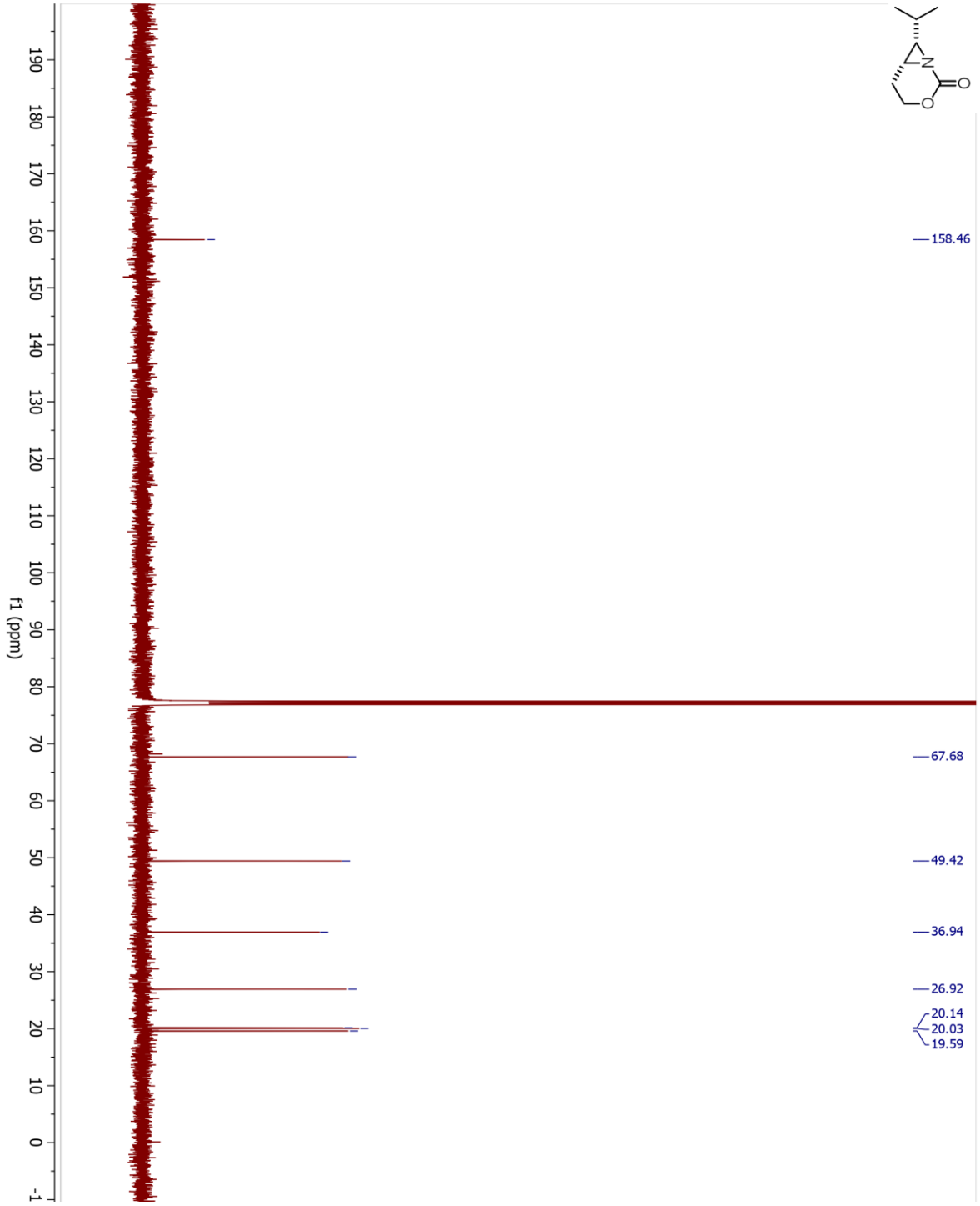
Compound **3.13.** ^{13}C NMR (126 MHz, $CDCl_3$)



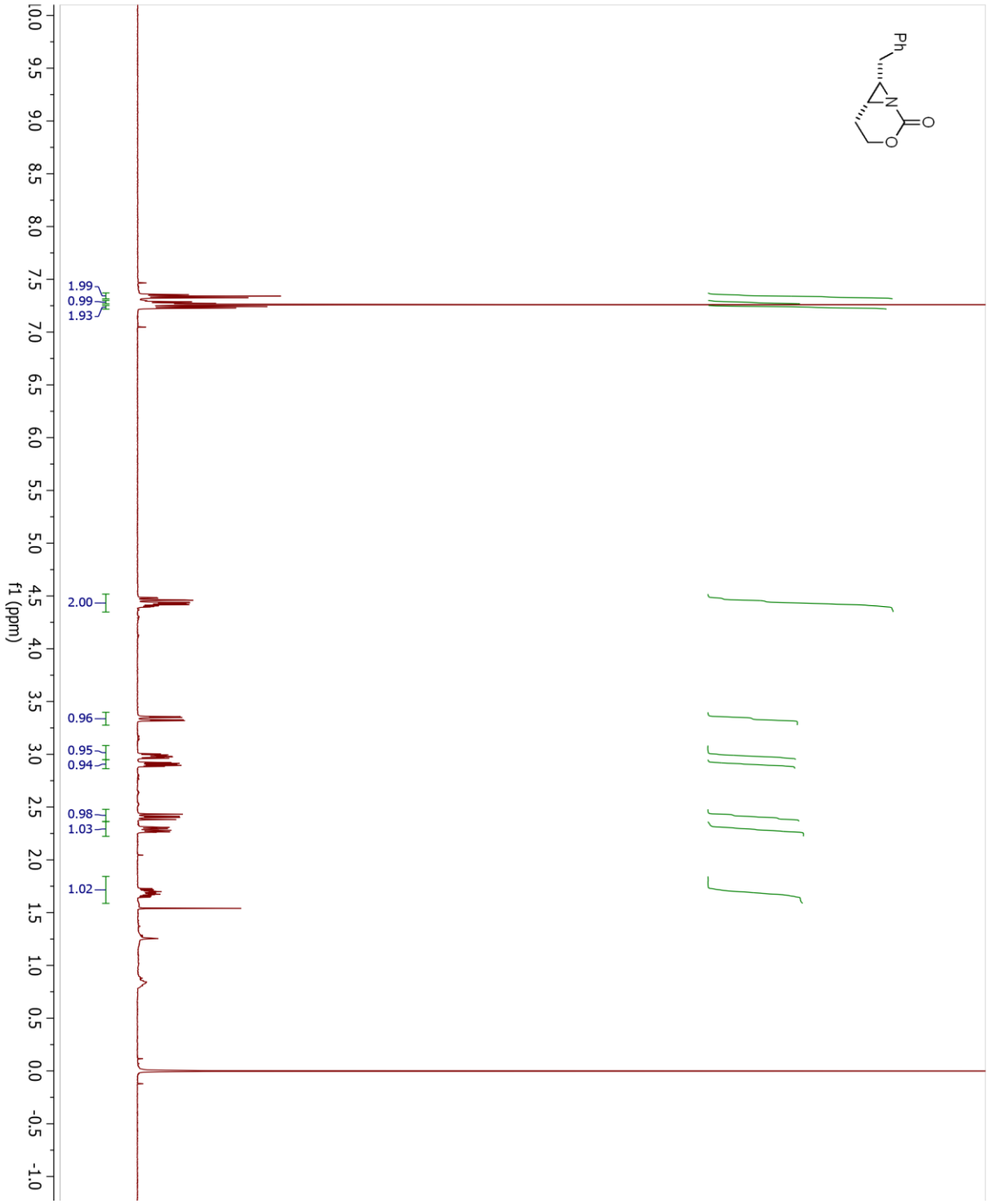
Compound **3.14.** ^{1}H NMR (500 MHz, $CDCl_3$)



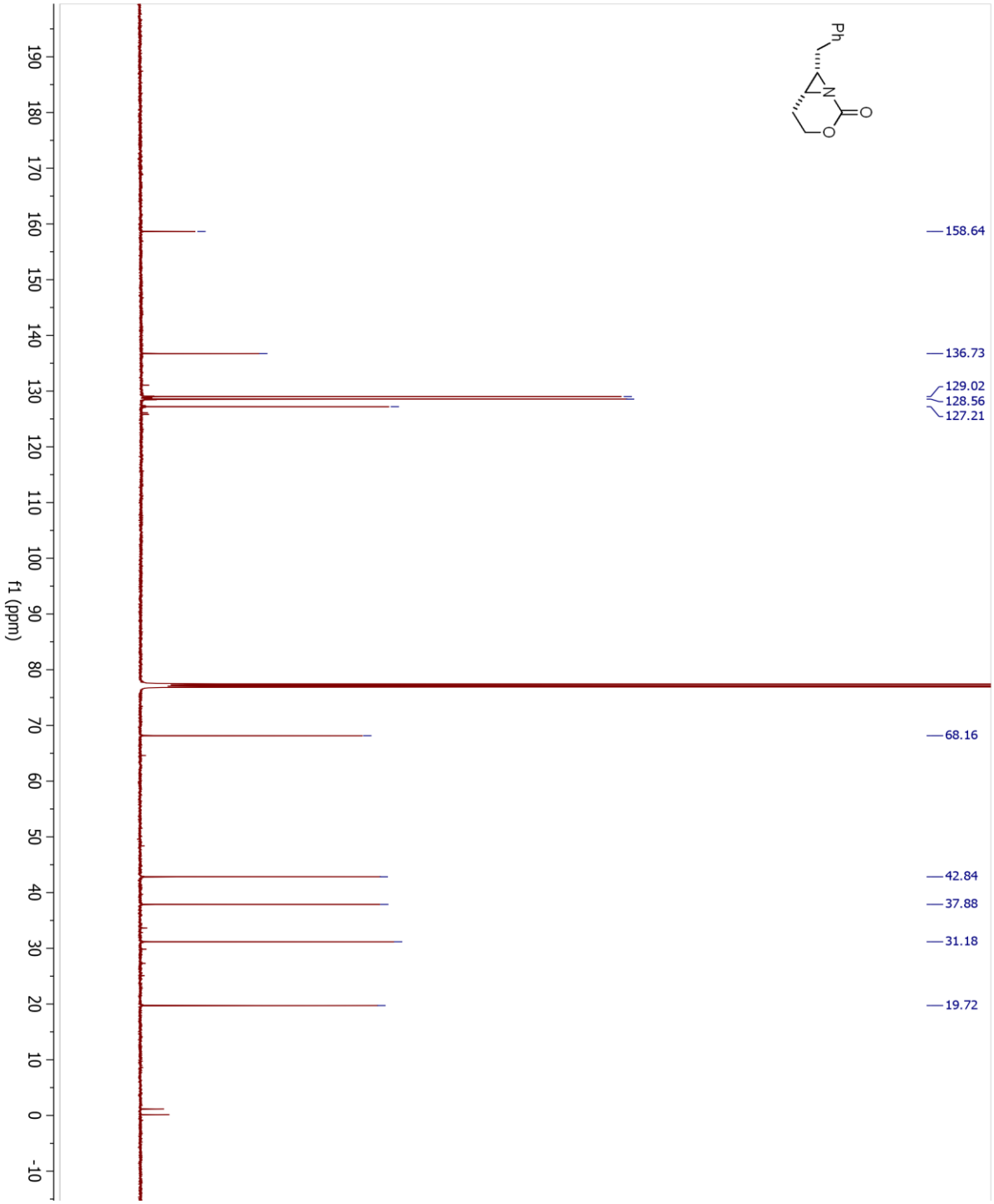
Compound **3.14.** ^{13}C NMR (126 MHz, $CDCl_3$)



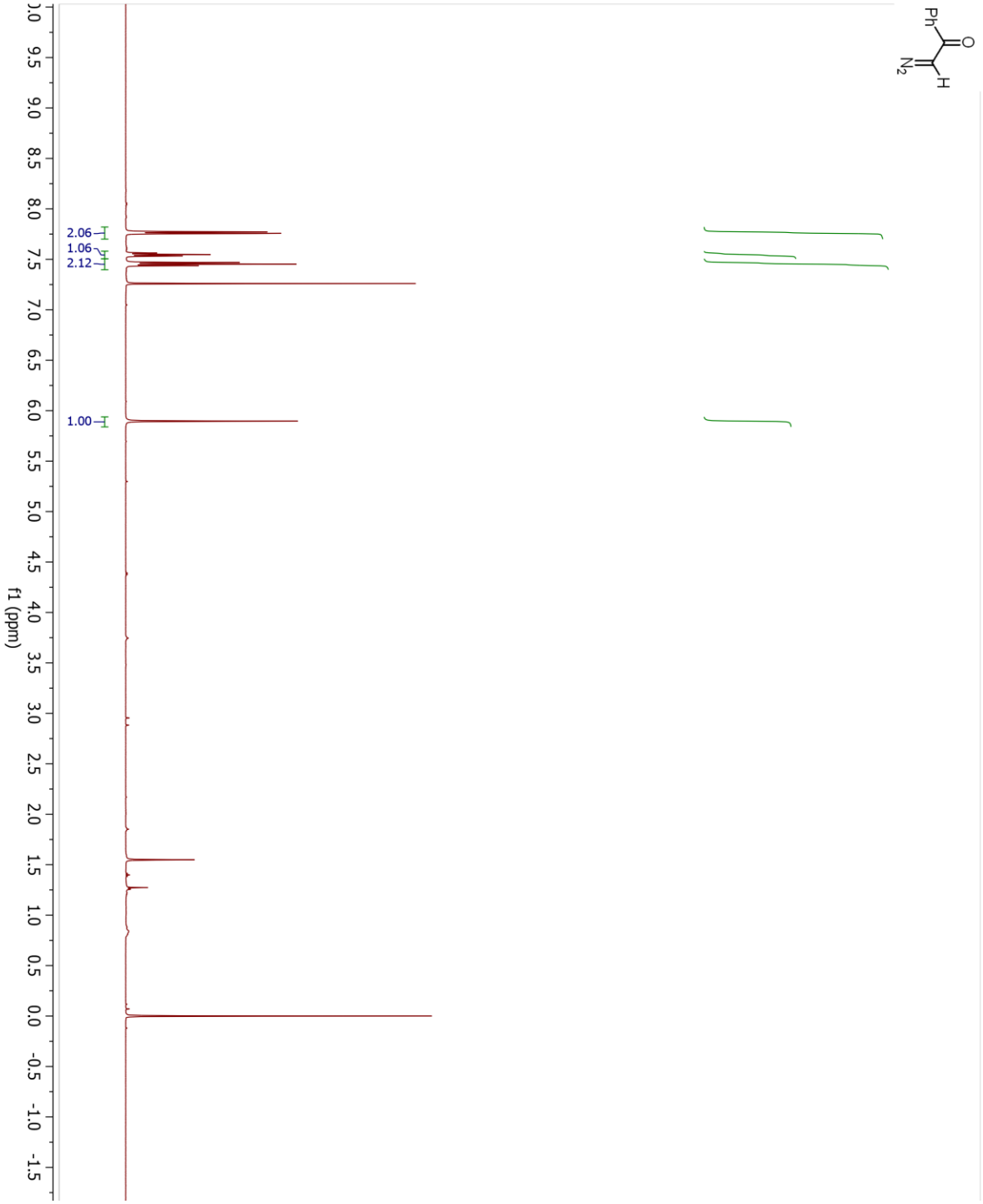
Compound **3.15.** ^{1}H NMR (500 MHz, $CDCl_3$)



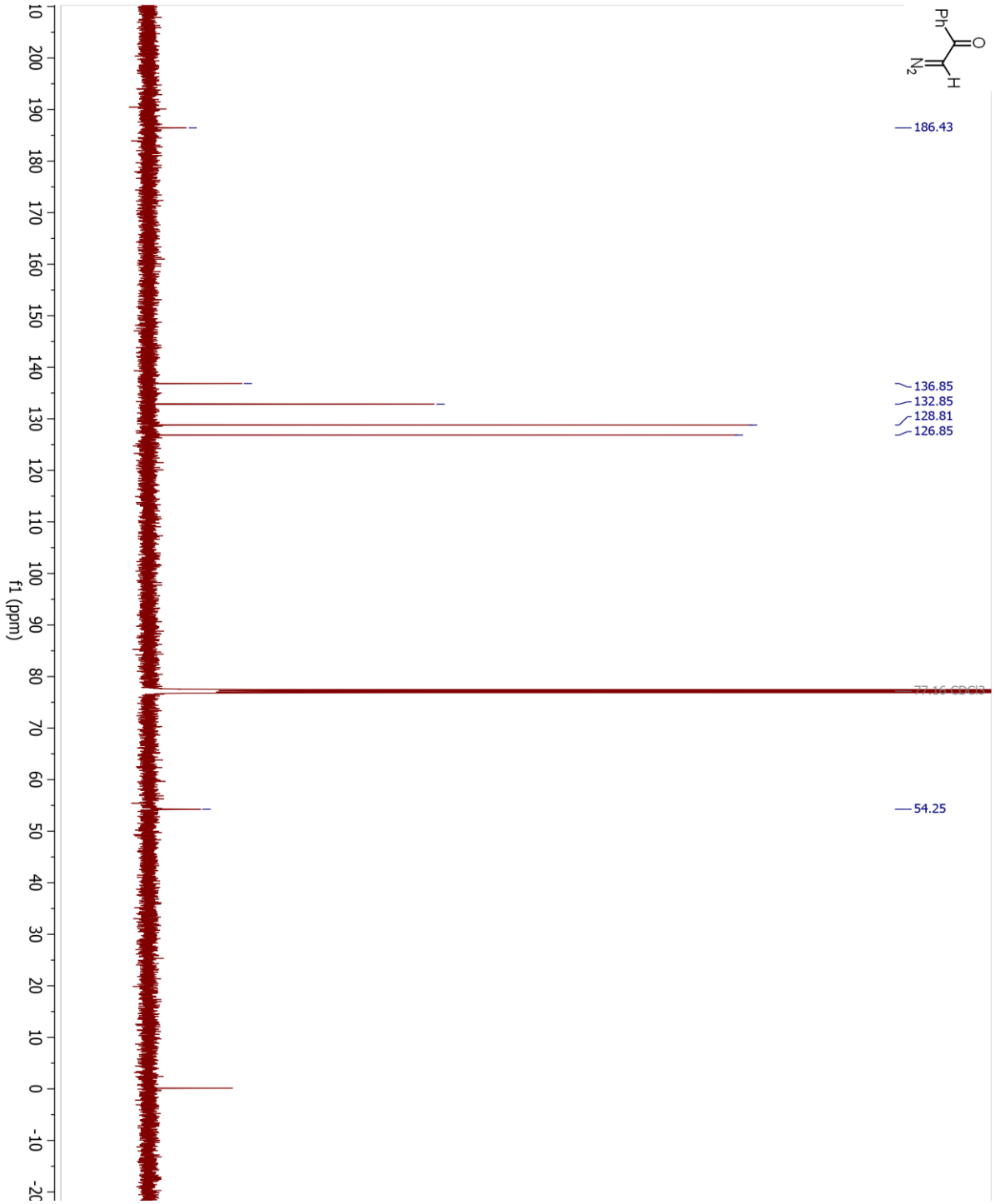
Compound **3.15.** ^{13}C NMR (126 MHz, $CDCl_3$)



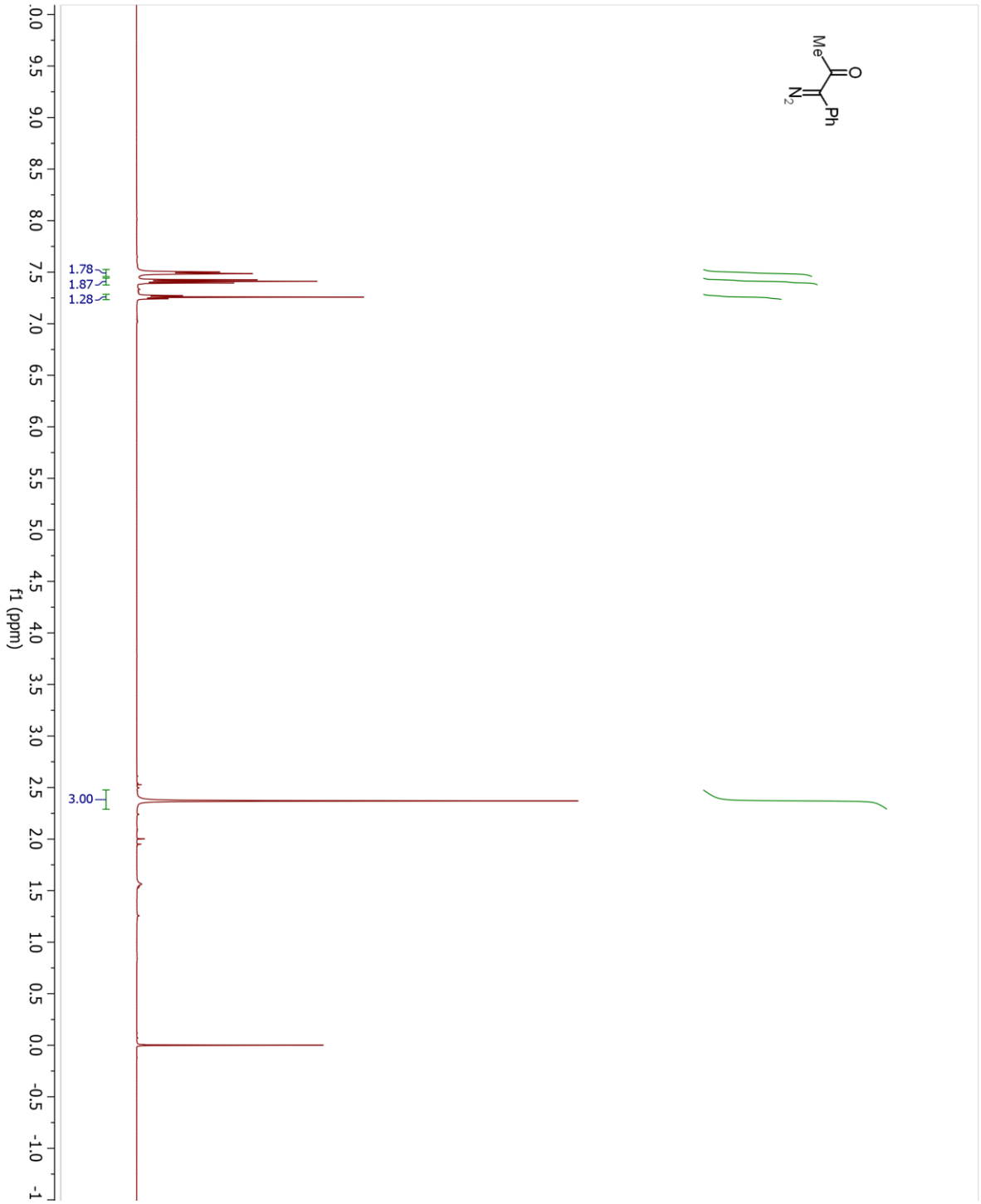
Compound **3.2a.** ^{1}H NMR (500 MHz, $CDCl_3$)



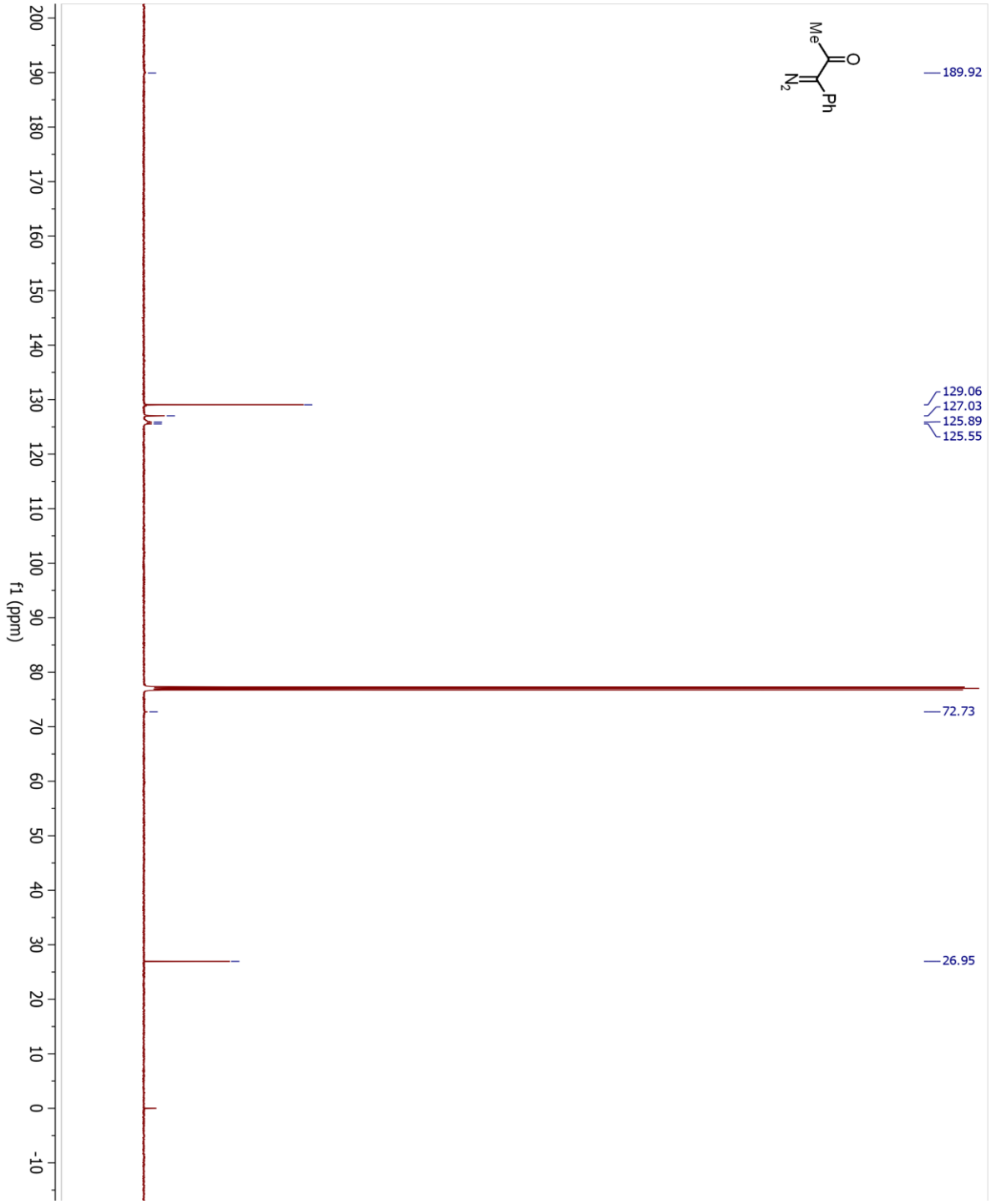
Compound **3.2a.** ^{13}C NMR (126 MHz, $CDCl_3$)



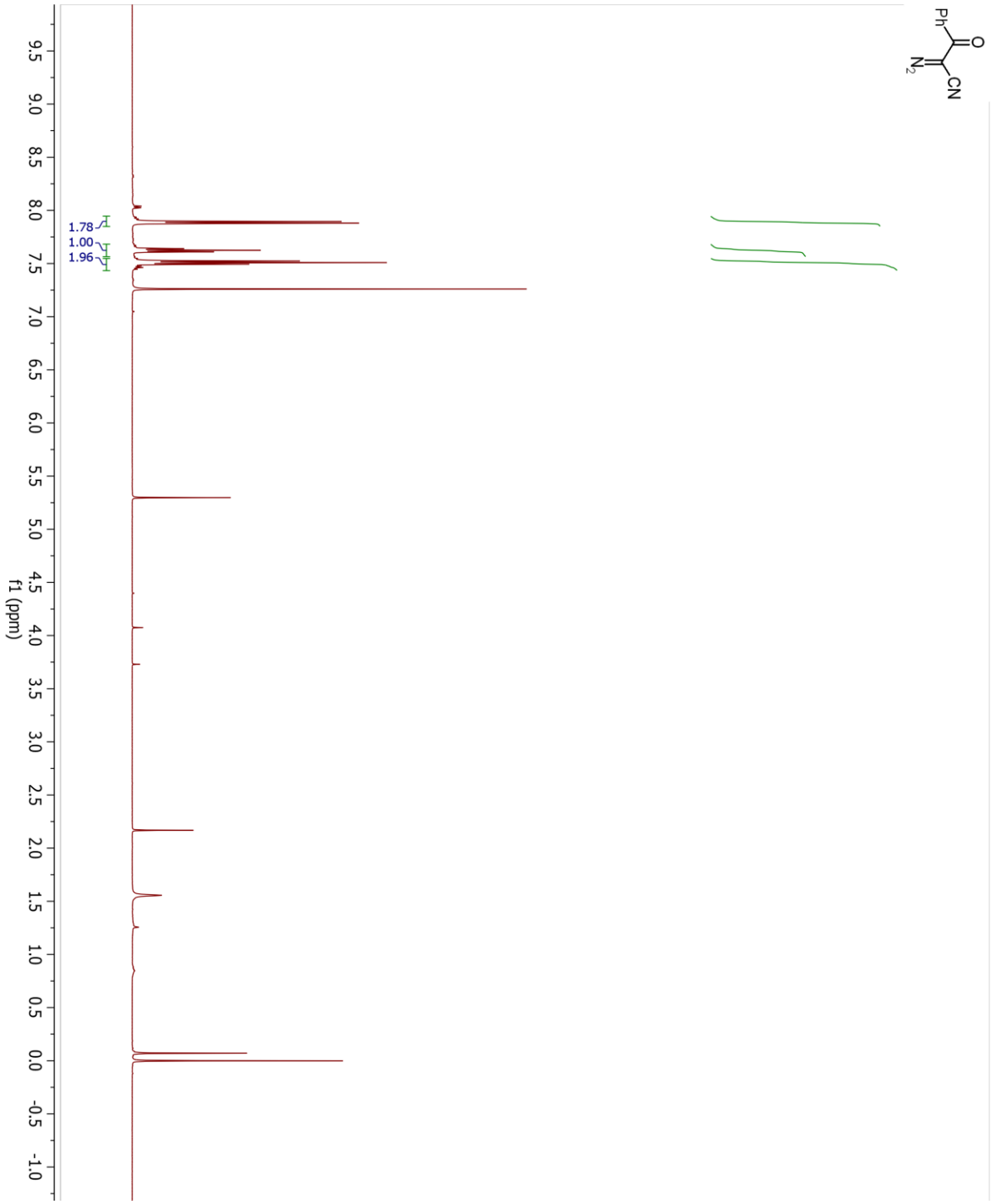
Compound **3.2b.** ^{1}H NMR (500 MHz, $CDCl_3$)



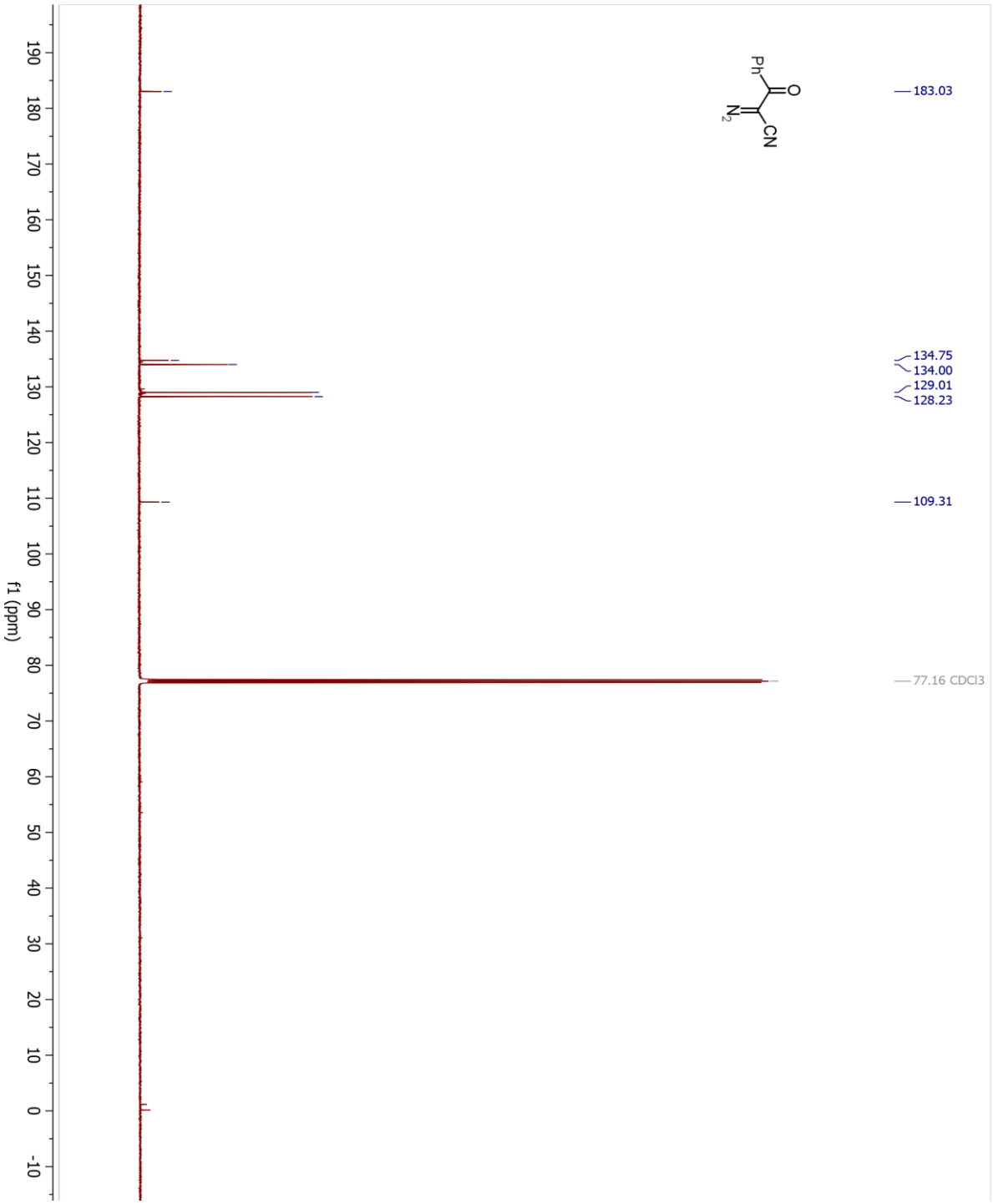
Compound **3.2b.** ^{13}C NMR (126 MHz, $CDCl_3$)



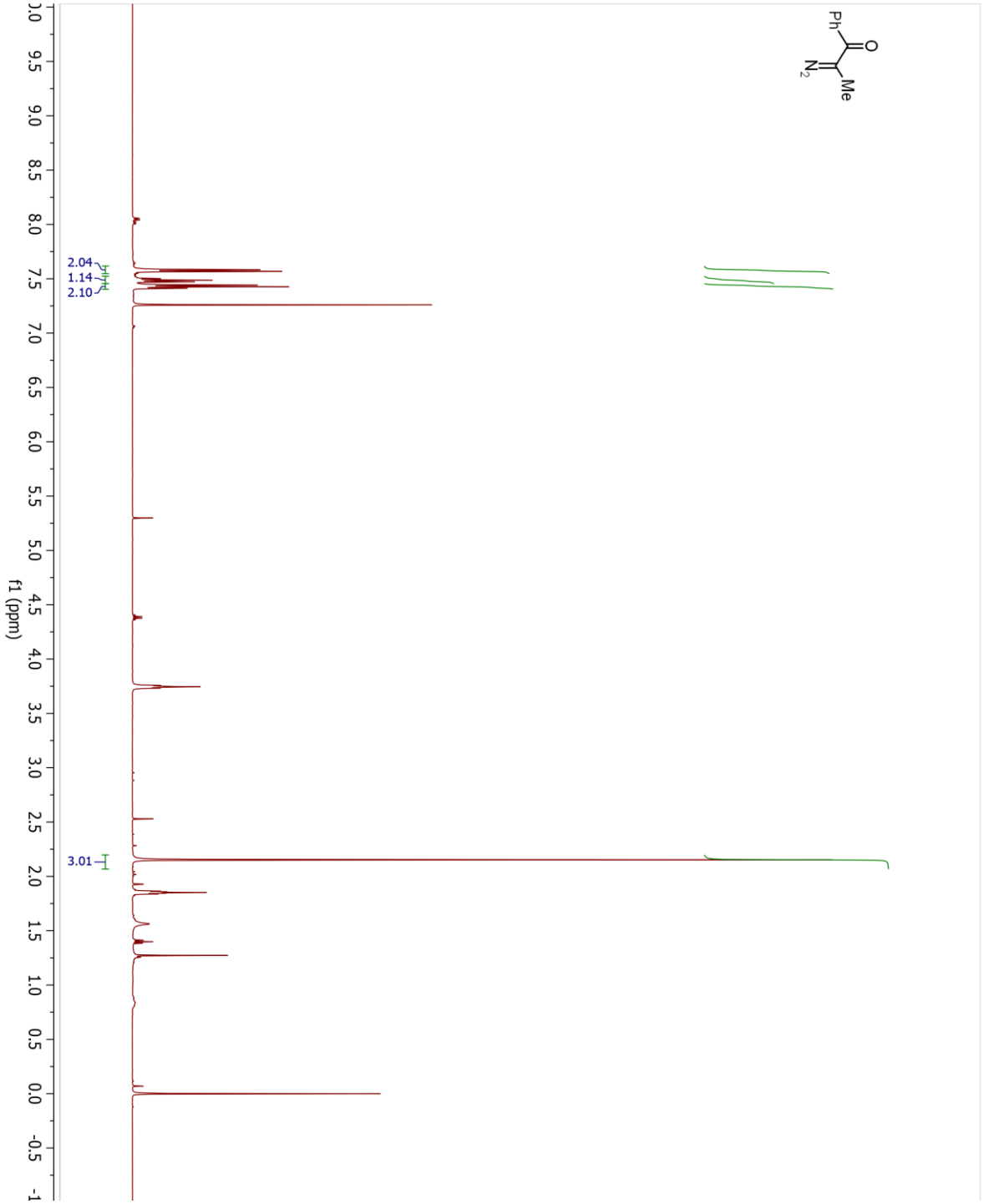
Compound **3.2c.** ^{1}H NMR (500 MHz, $CDCl_3$)



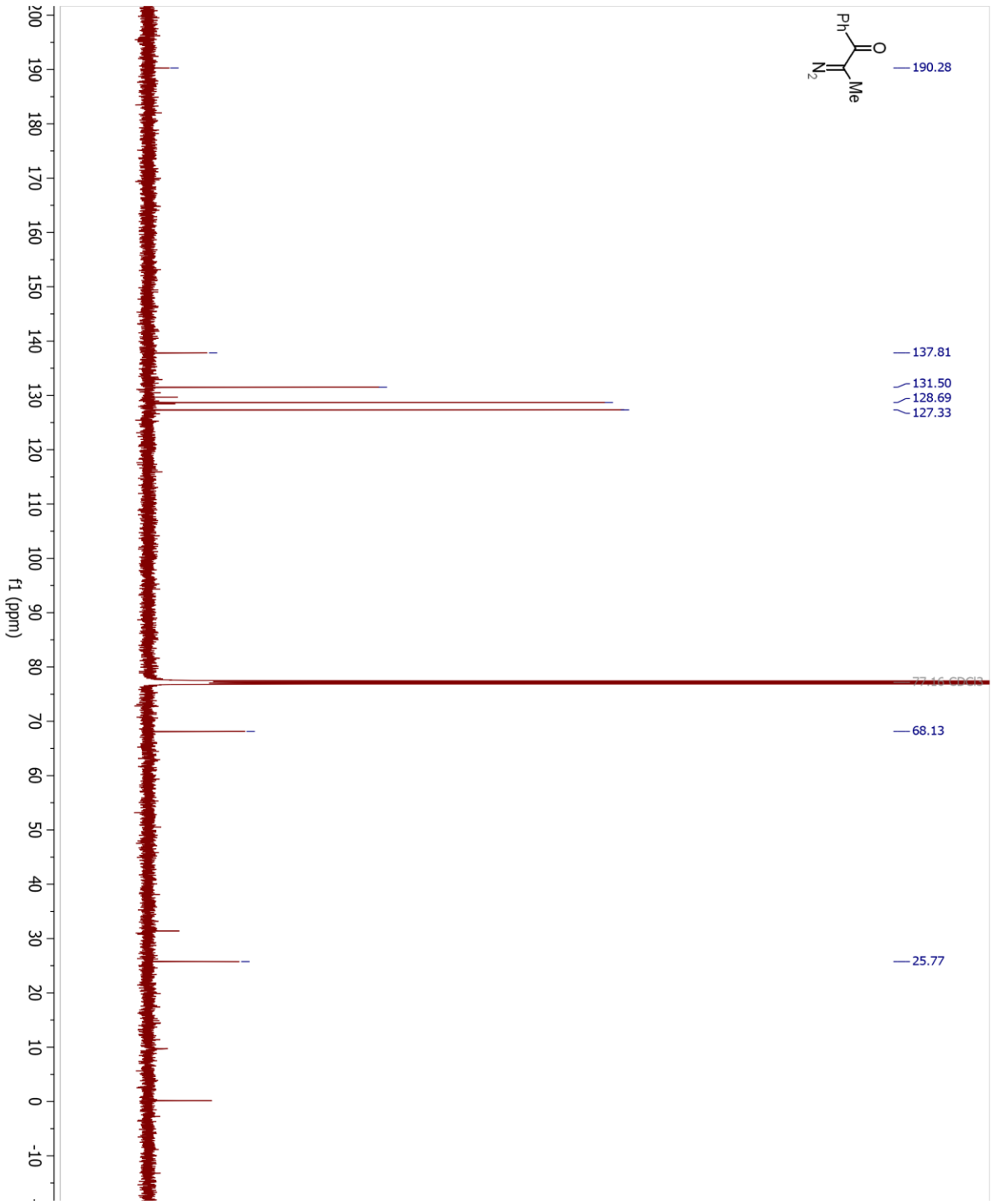
Compound **3.2c.** ^{13}C NMR (126 MHz, $CDCl_3$)



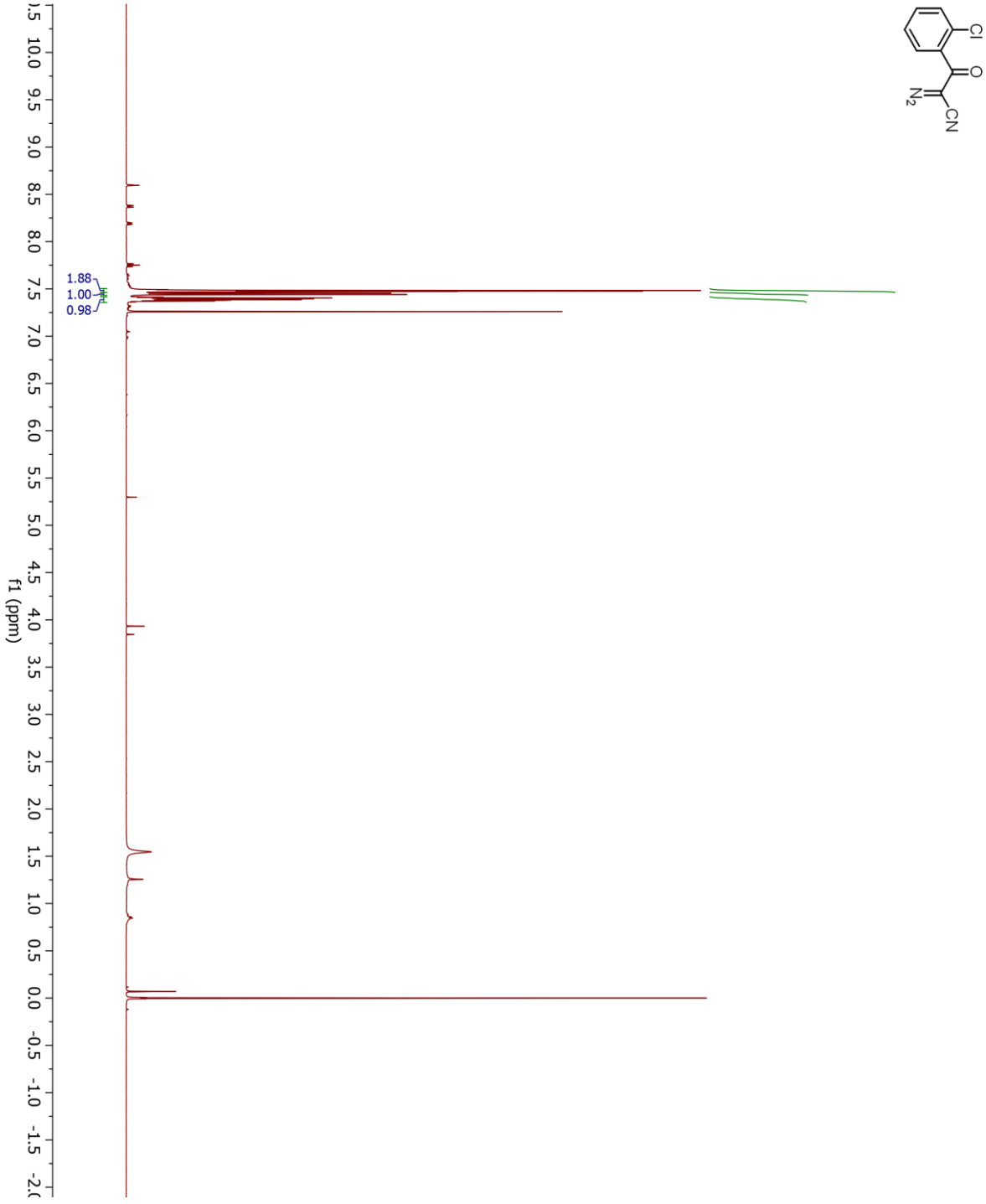
Compound **3.2d.** ^{1}H NMR (500 MHz, $CDCl_3$)



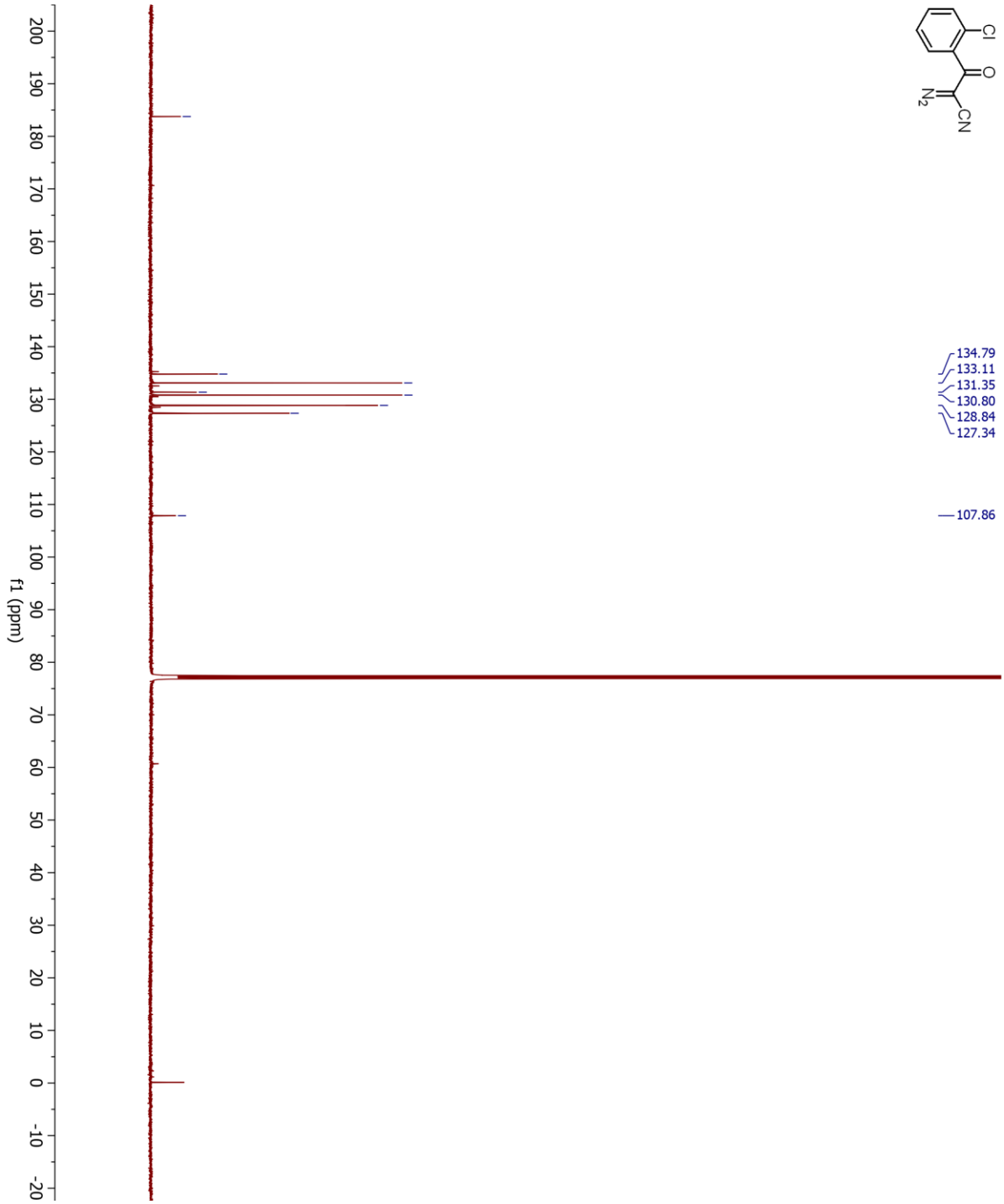
Compound **3.2d.** ^{13}C NMR (126 MHz, $CDCl_3$)



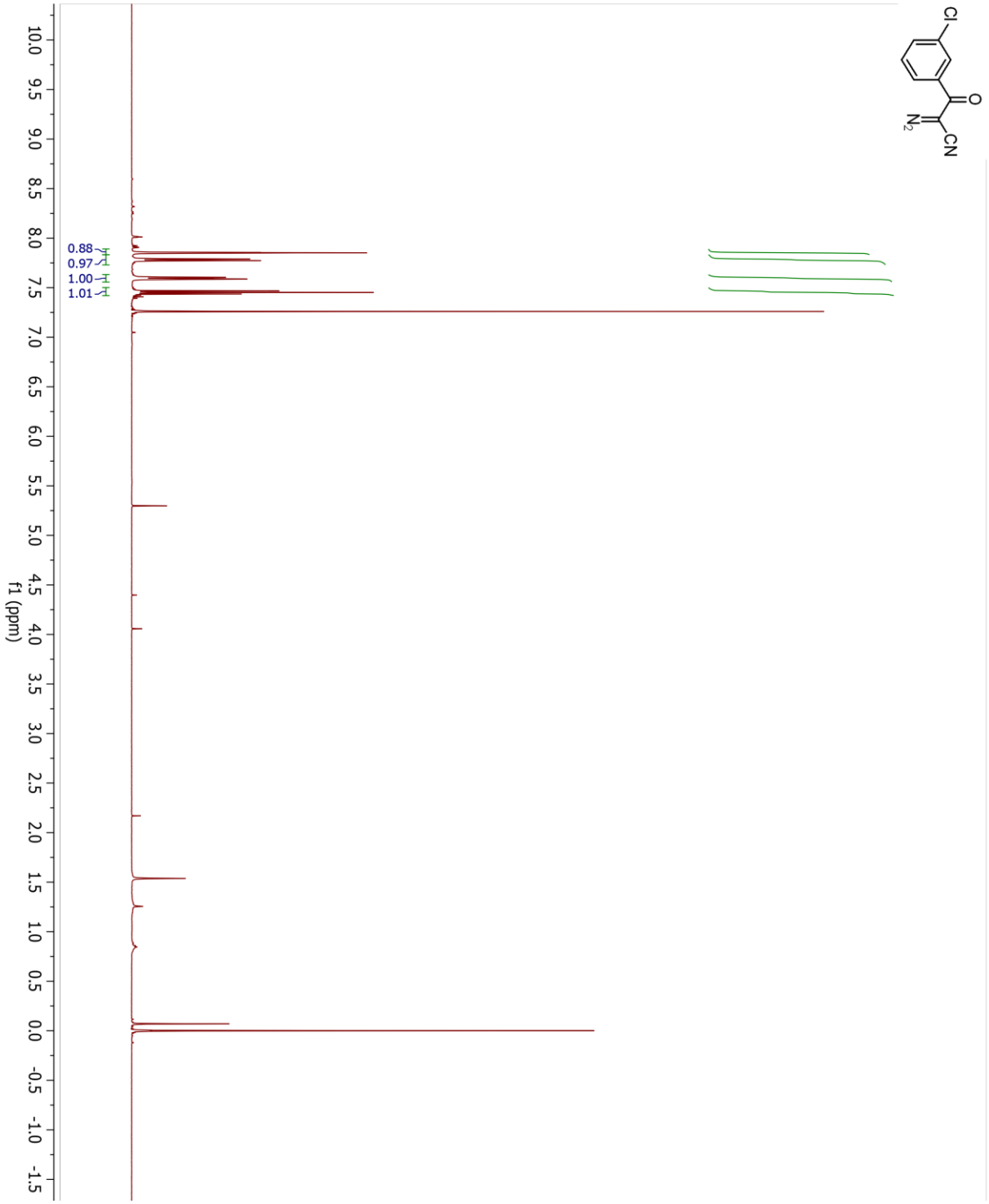
Precursor to **3.6c.** ^{1}H NMR (500 MHz, $CDCl_3$)



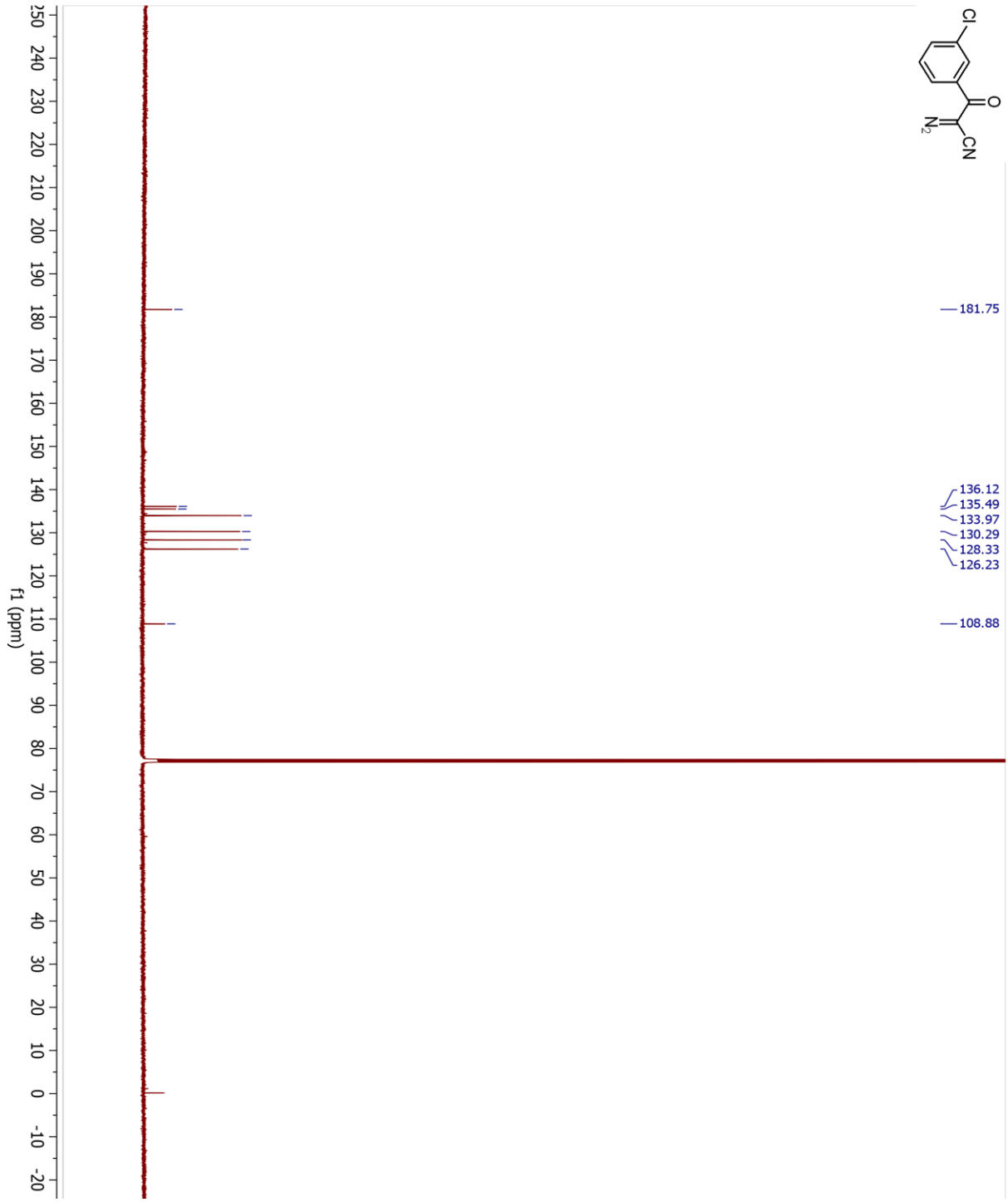
Precursor to **3.6c.** ^{13}C NMR (126 MHz, $CDCl_3$)



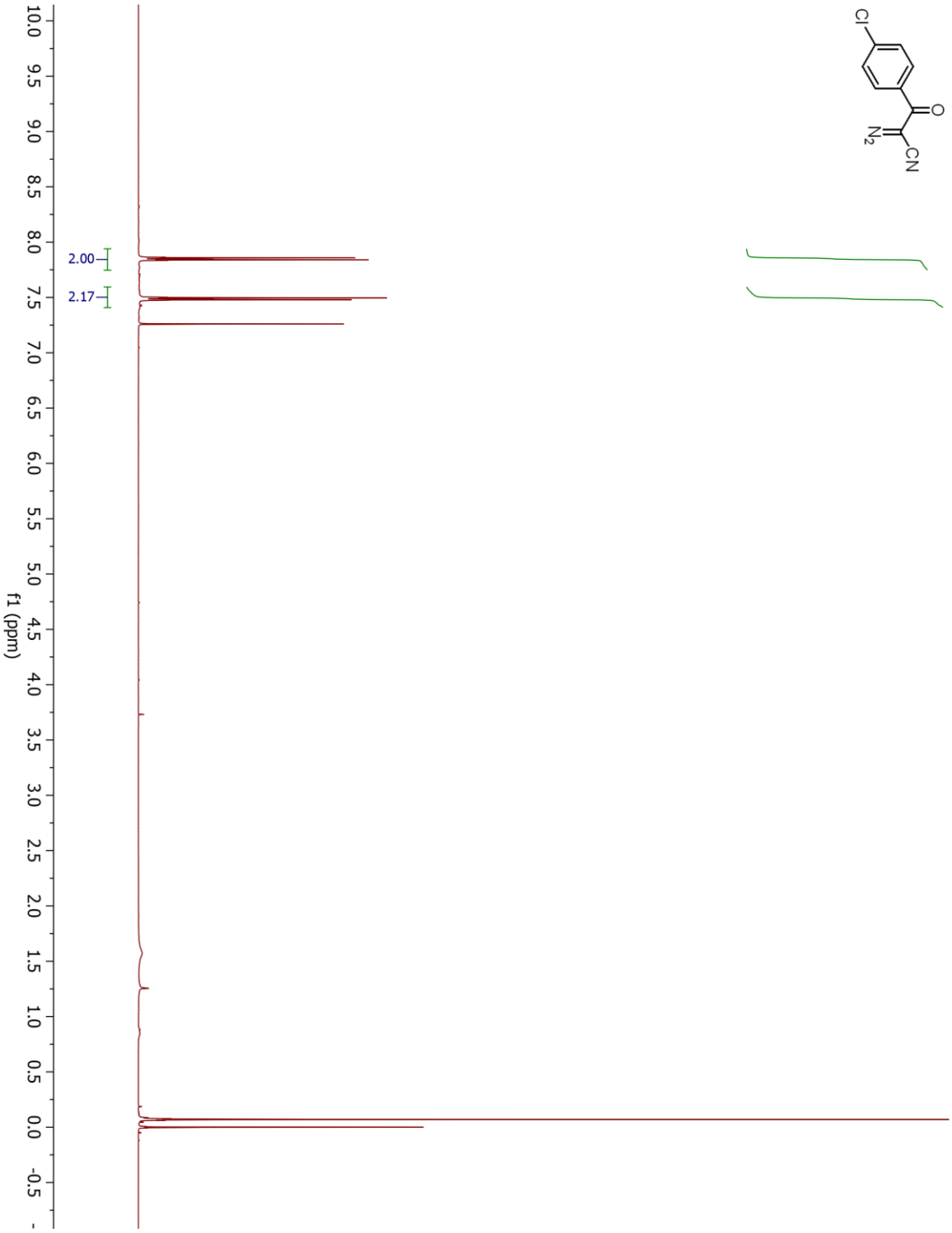
Precursor to **3.7c.** ^{1}H NMR (500 MHz, $CDCl_3$)



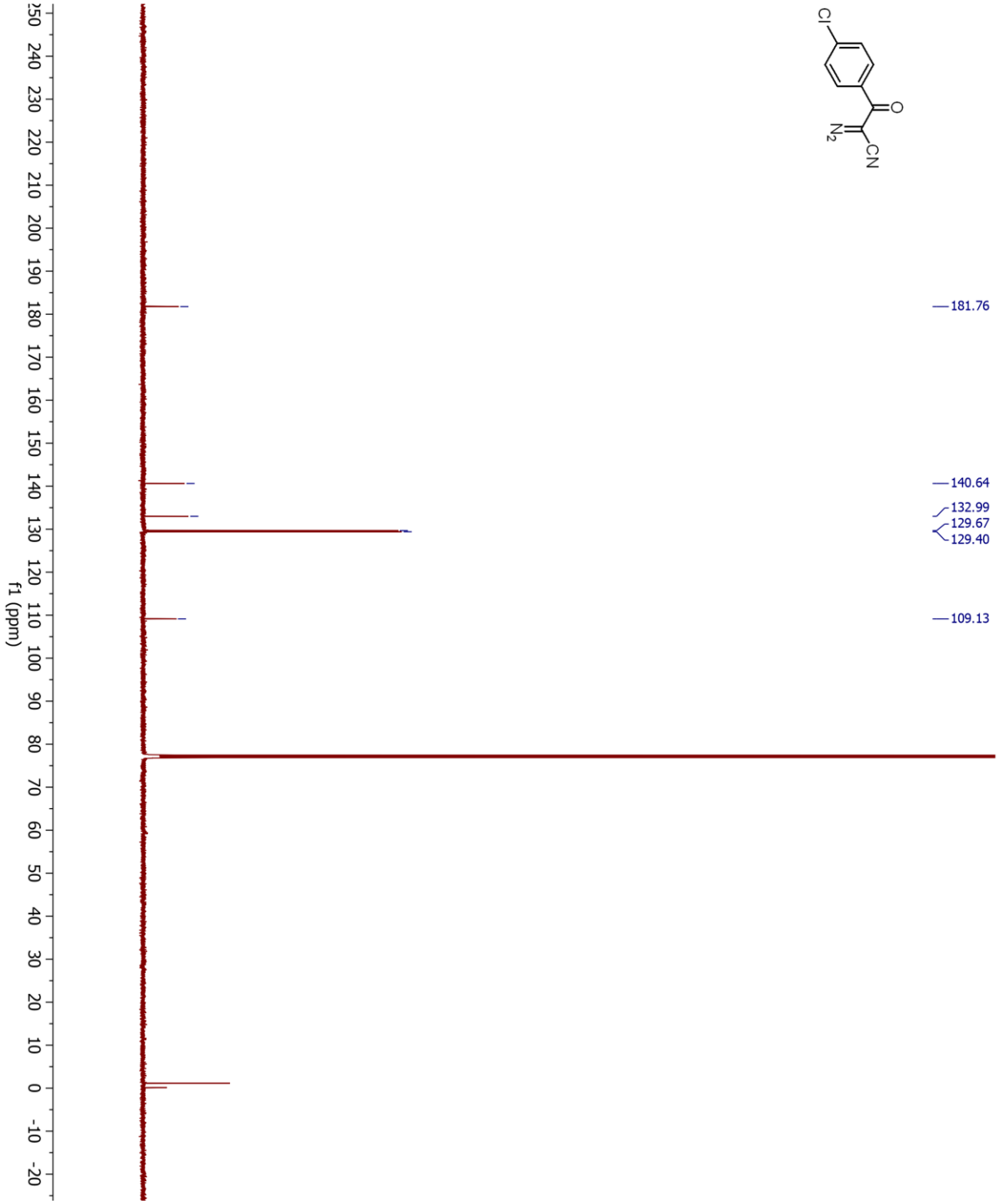
Precursor to **3.7c.** ^{13}C NMR (126 MHz, $CDCl_3$)



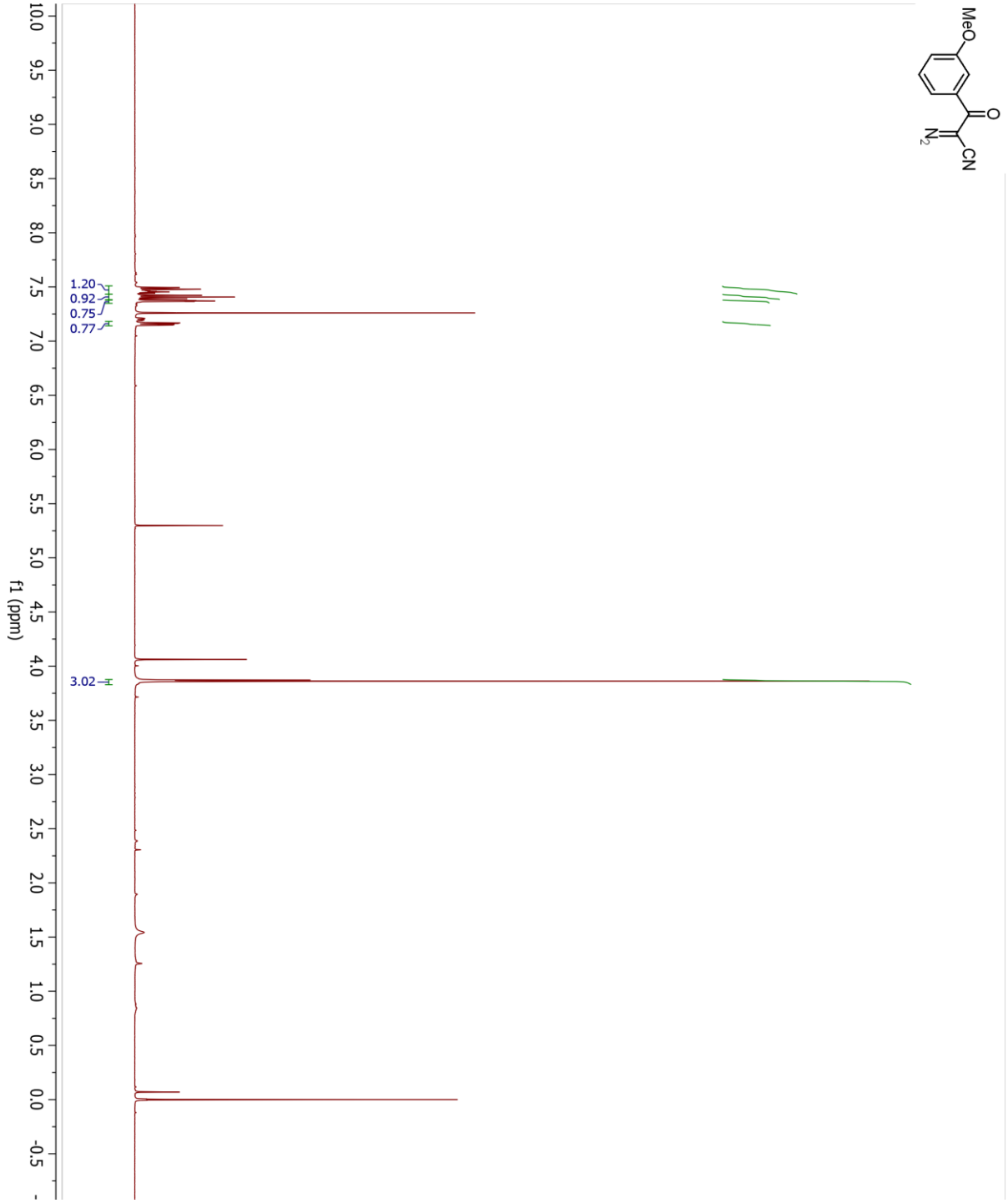
Precursor to **3.8c.** ^{1}H NMR (500 MHz, $CDCl_3$)



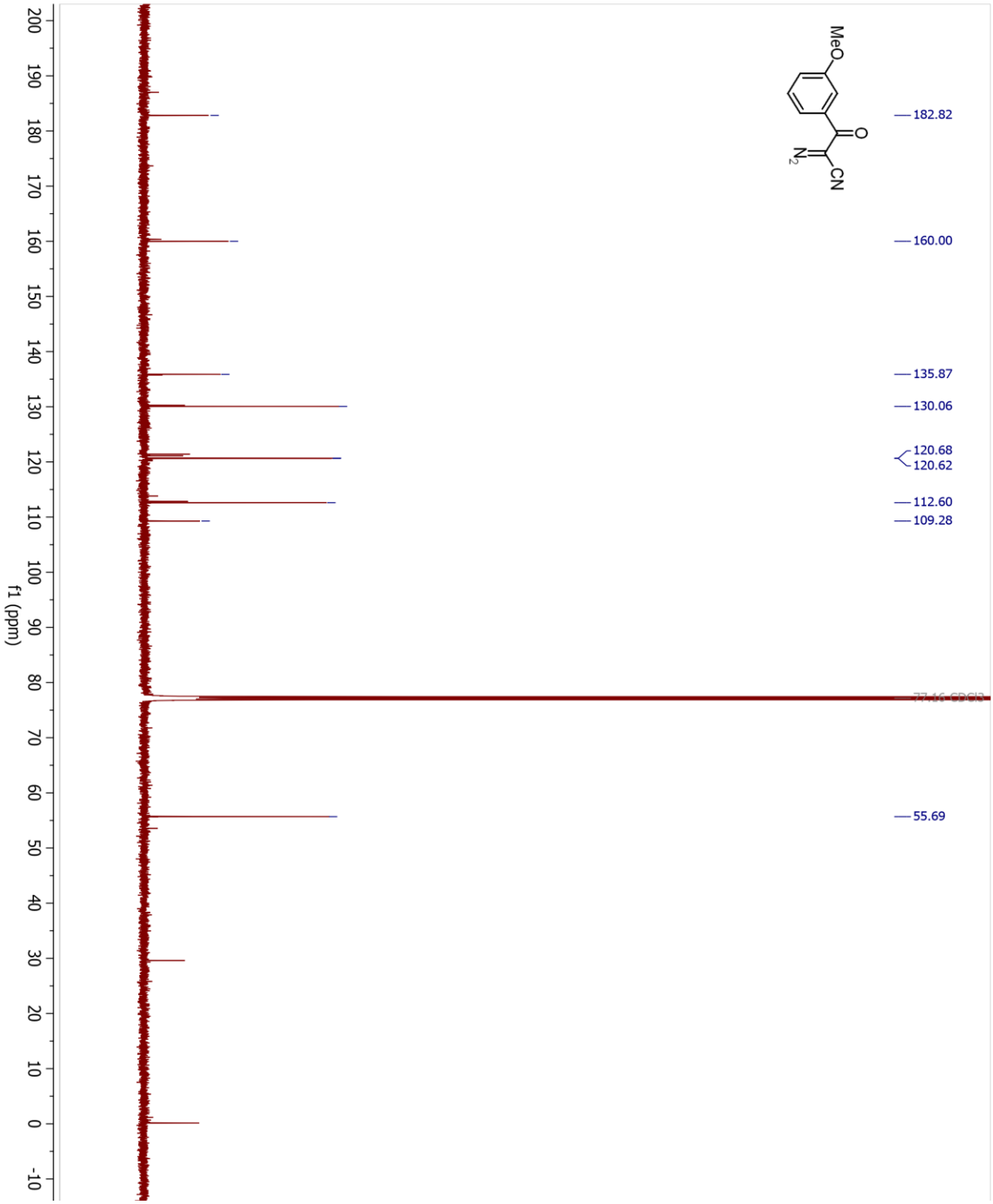
Precursor to **3.8c.** ^{13}C NMR (500 MHz, $CDCl_3$)



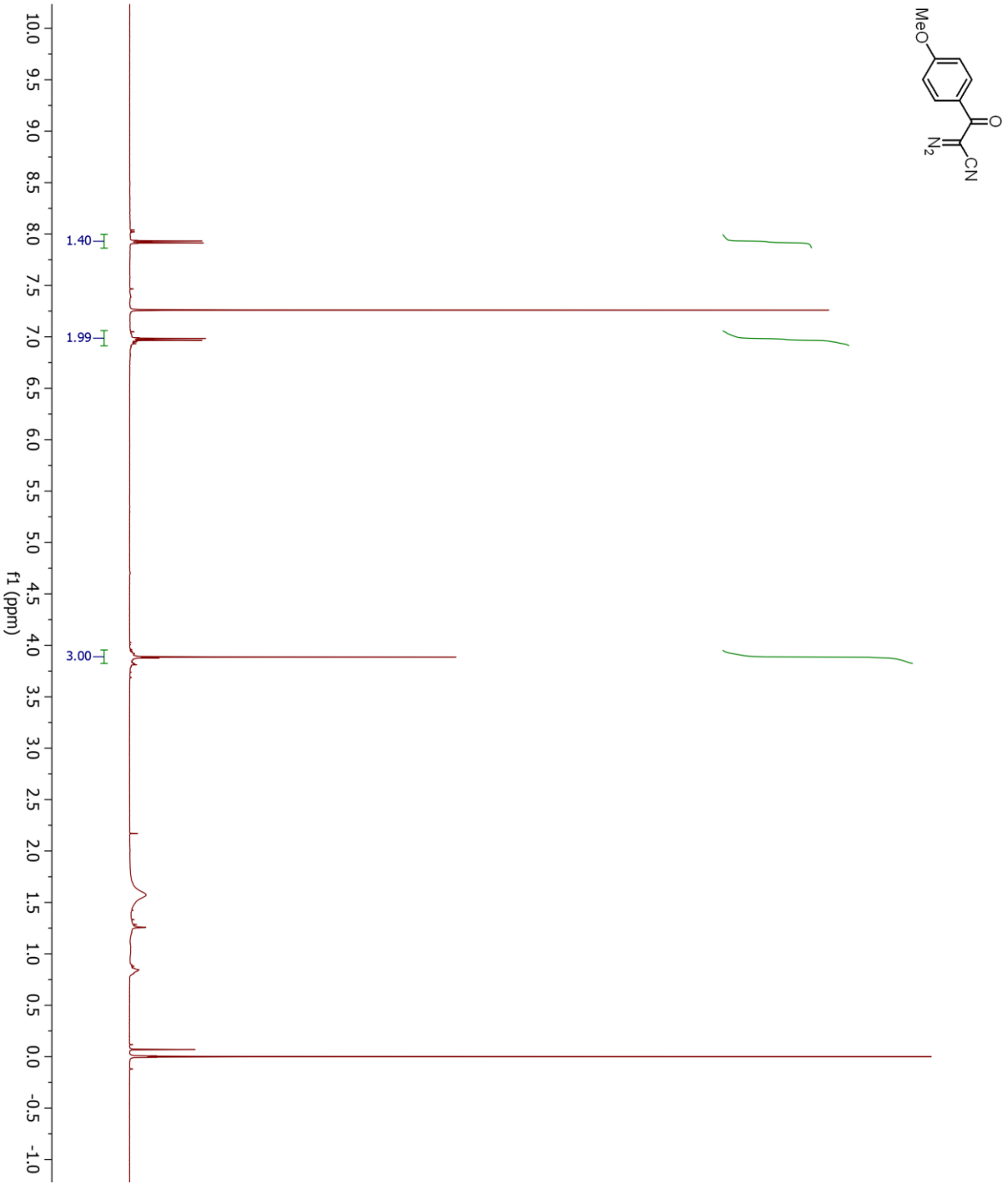
Precursor to **3.10c.** ^{1}H NMR (500 MHz, $CDCl_3$)



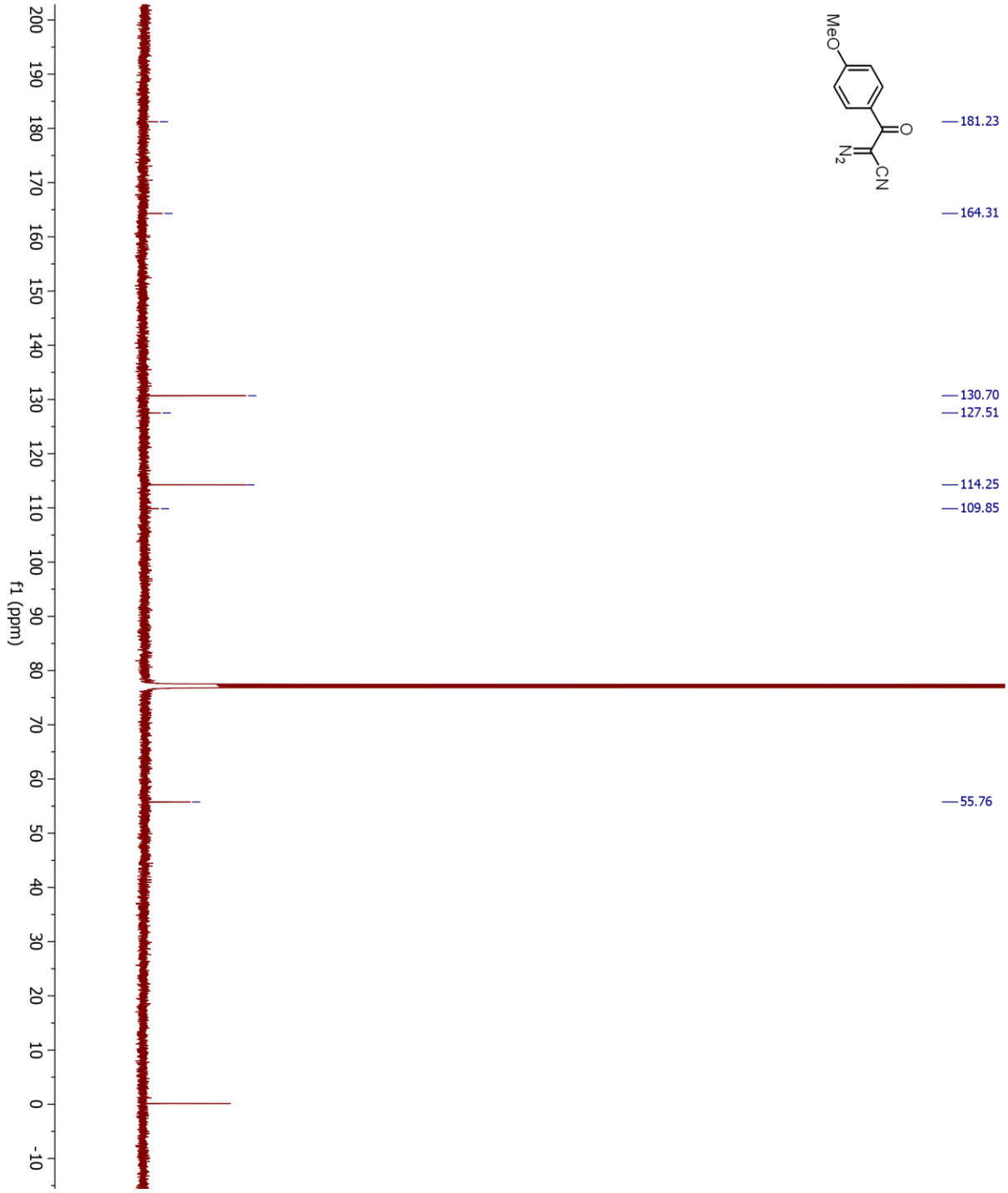
Precursor to **3.10c.** ^{13}C NMR (126 MHz, $CDCl_3$)



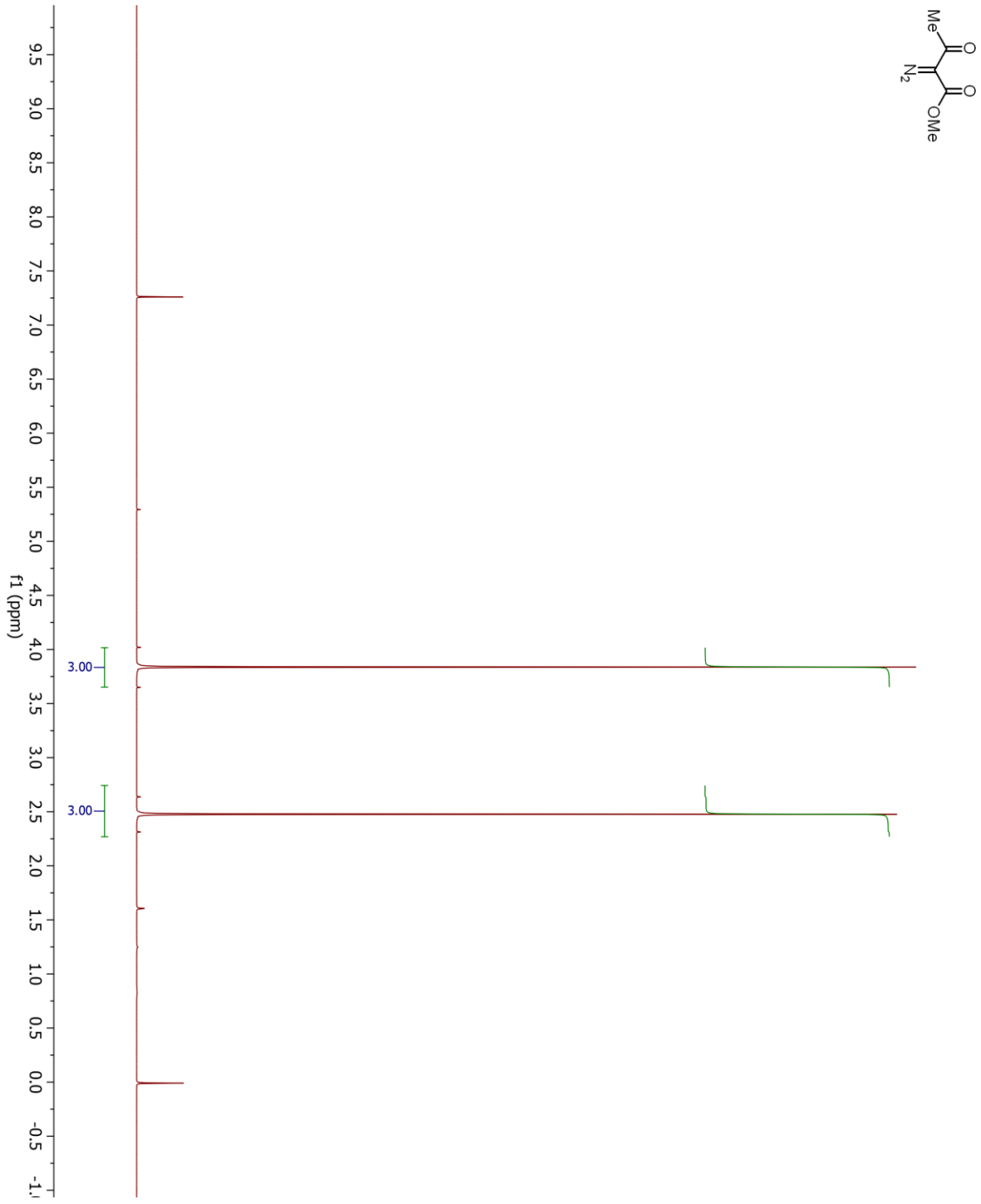
Precursor to **3.11c.** ^{1}H NMR (500 MHz, $CDCl_3$)



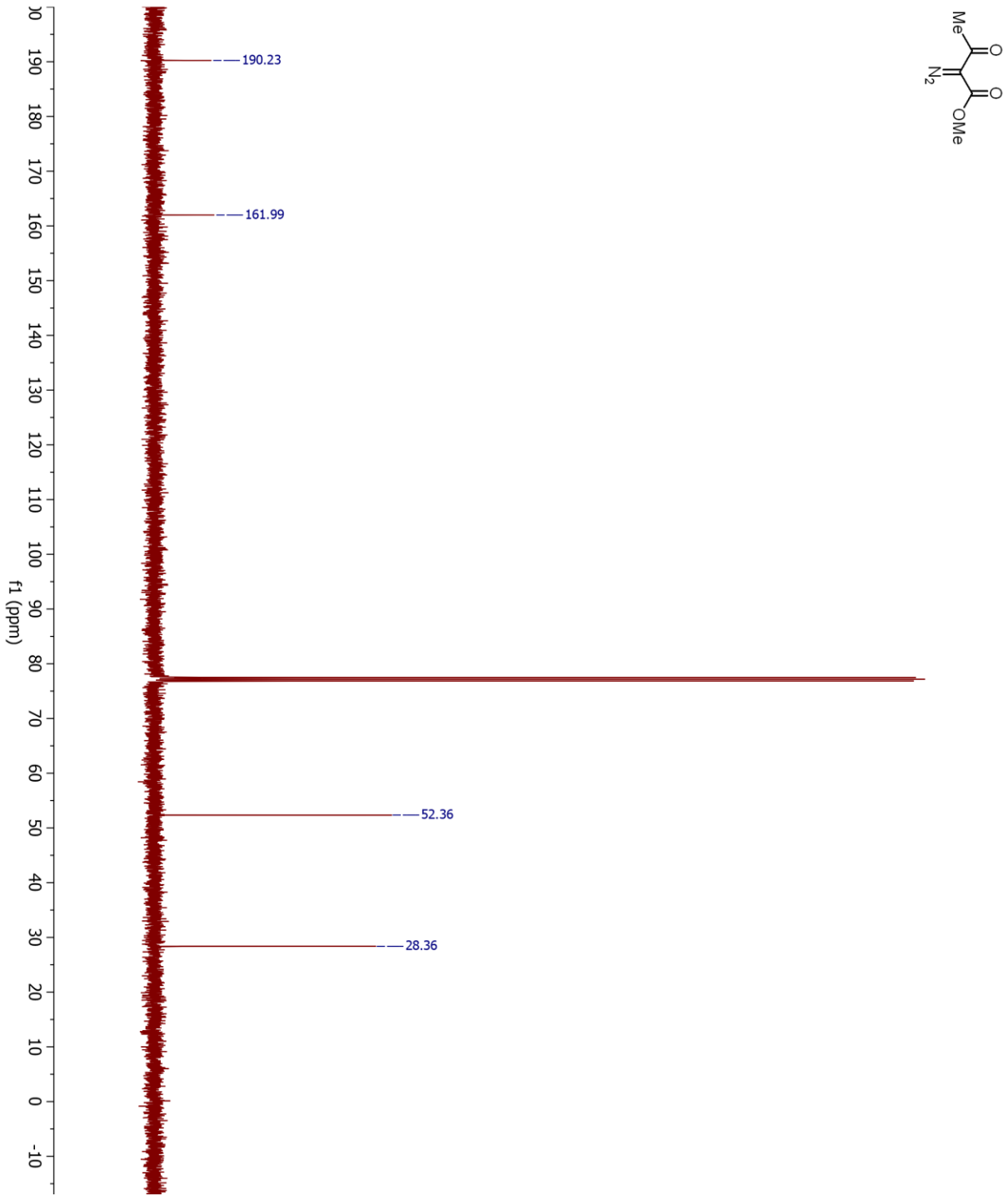
Precursor to **3.11c.** ^{13}C NMR (126 MHz, $CDCl_3$)



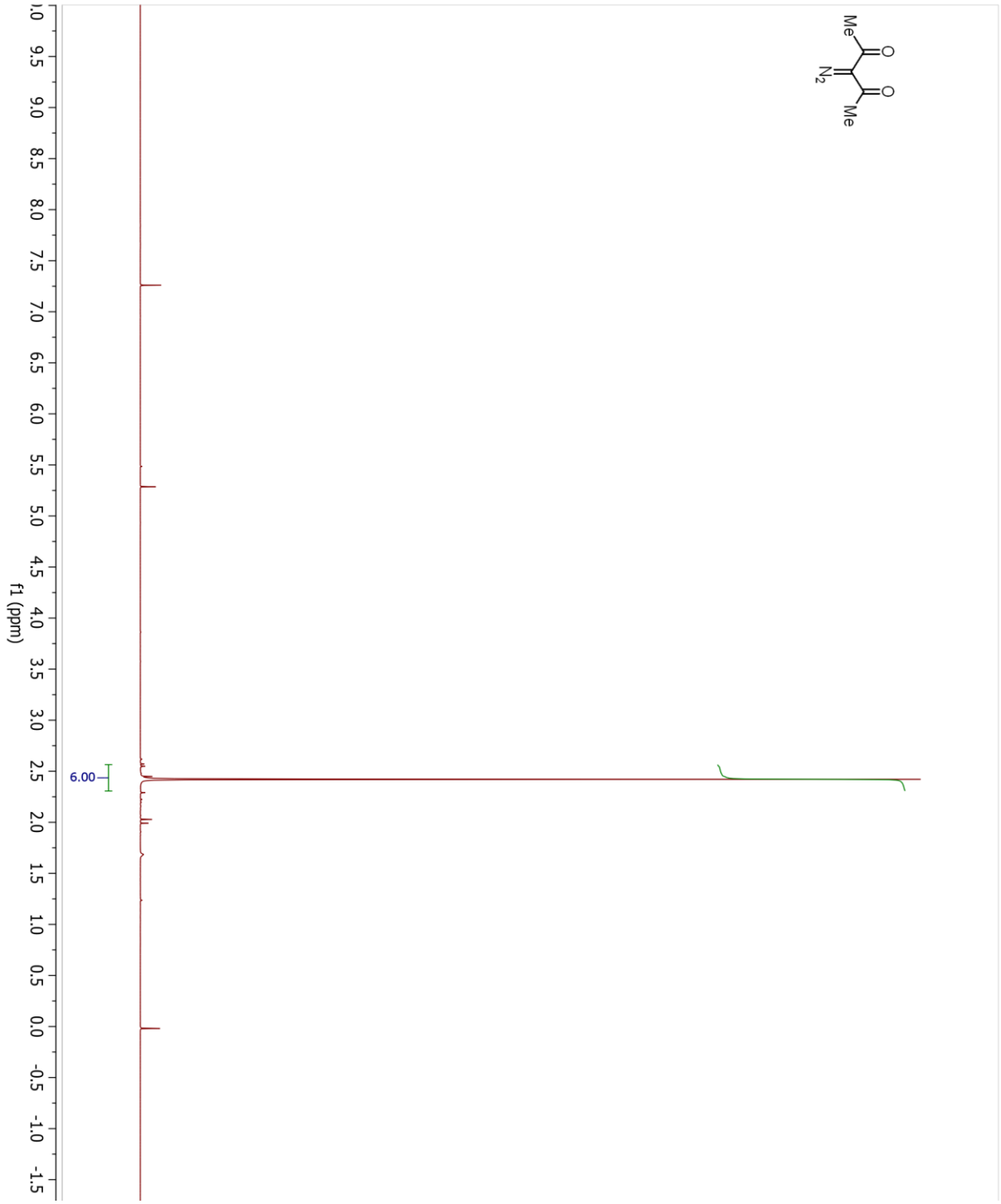
Compound **3.2e.** ^{1}H NMR (500 MHz, $CDCl_3$)



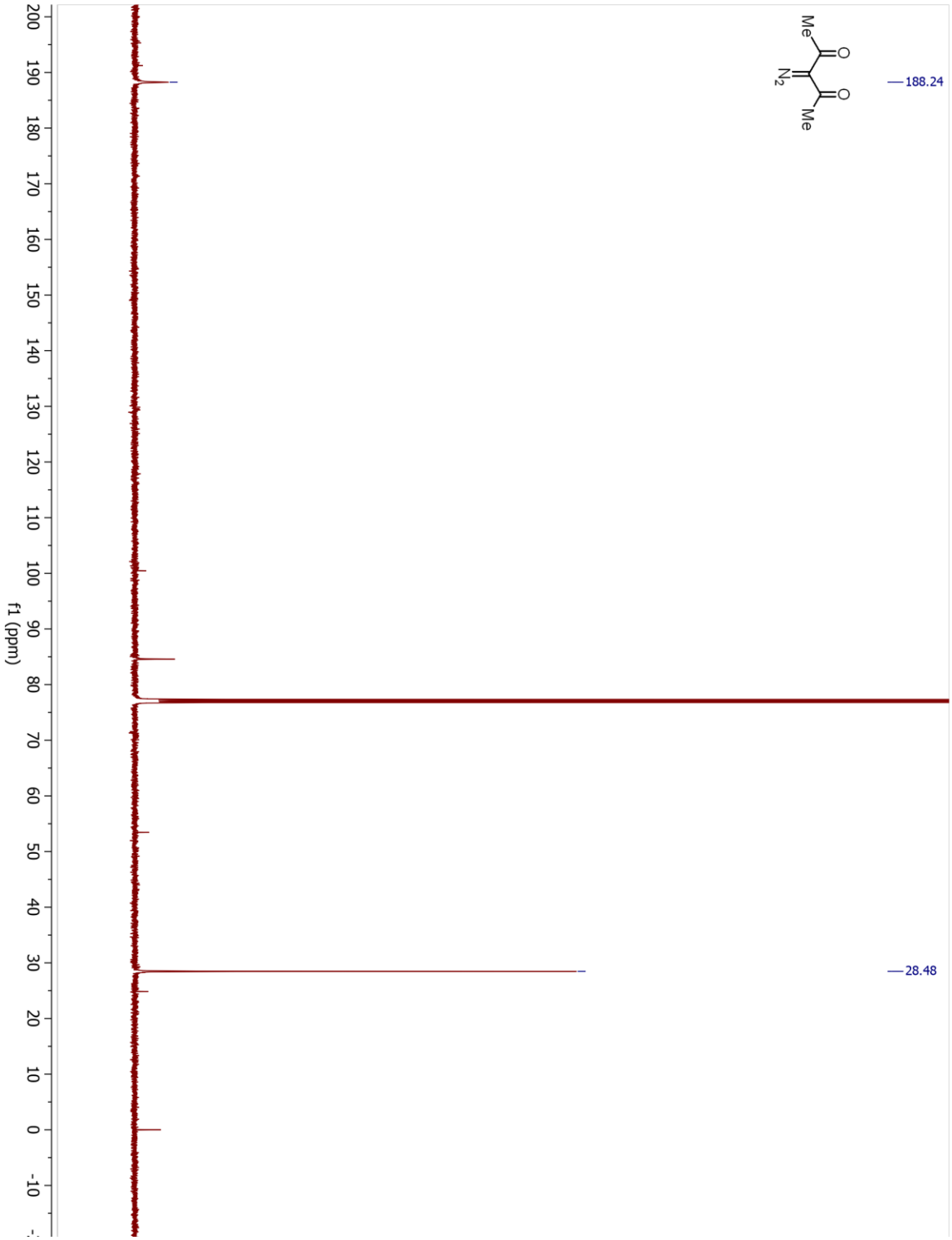
Compound **3.2e.** ^{13}C NMR (126 MHz, $CDCl_3$)



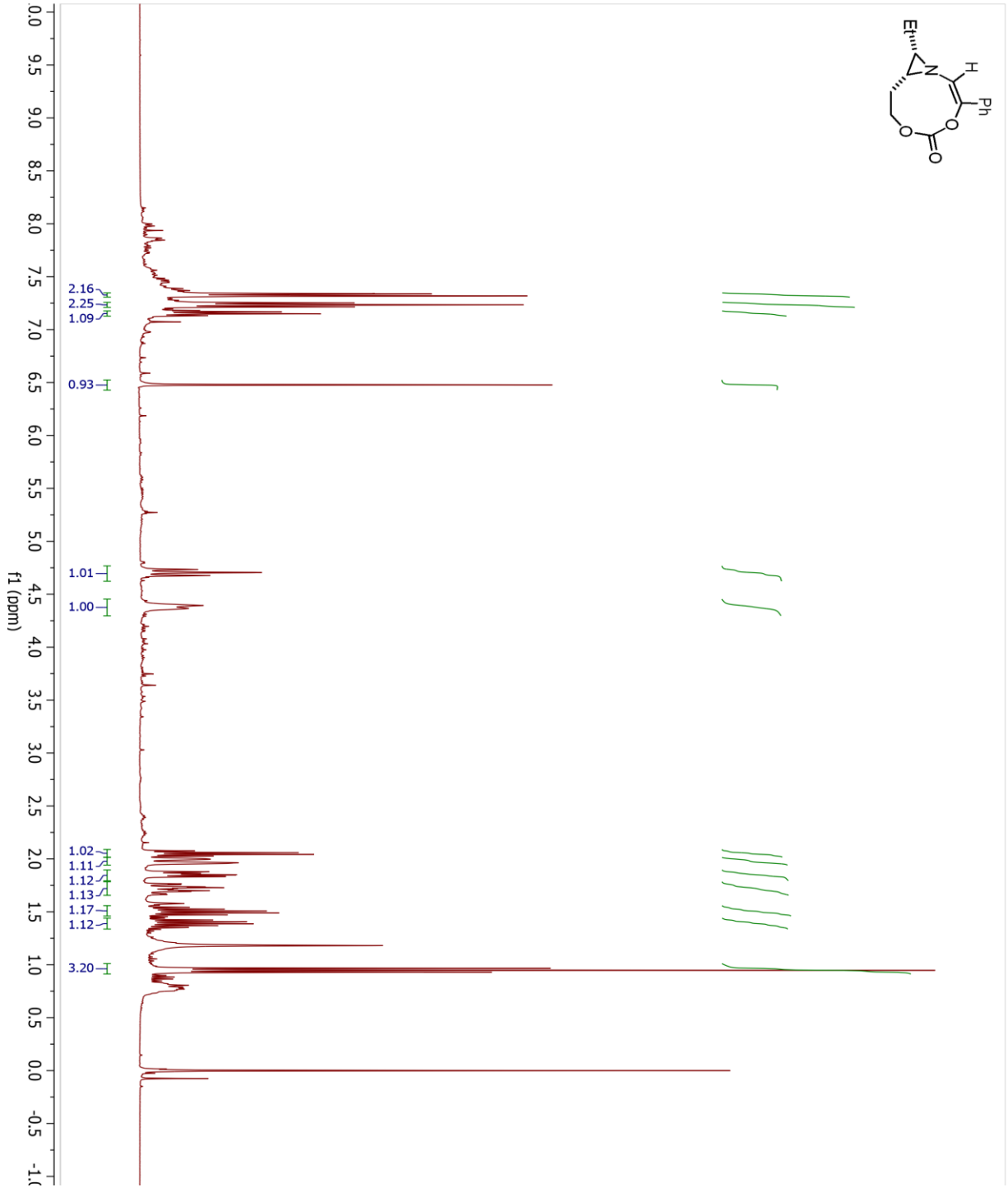
Compound **3.2f.** ^{1}H NMR (500 MHz, $CDCl_3$)



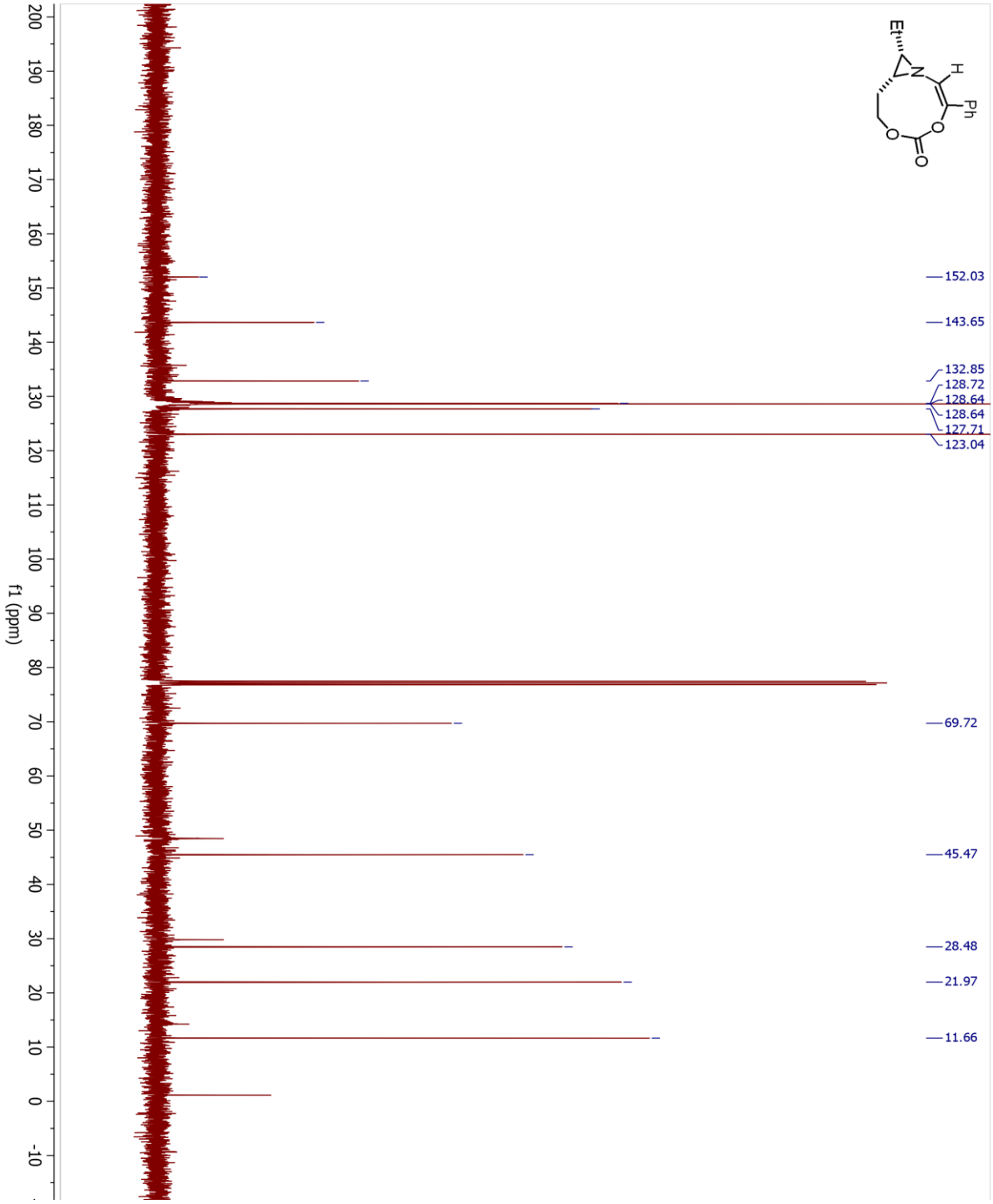
Compound **3.2f.** ^{13}C NMR (126 MHz, $CDCl_3$)



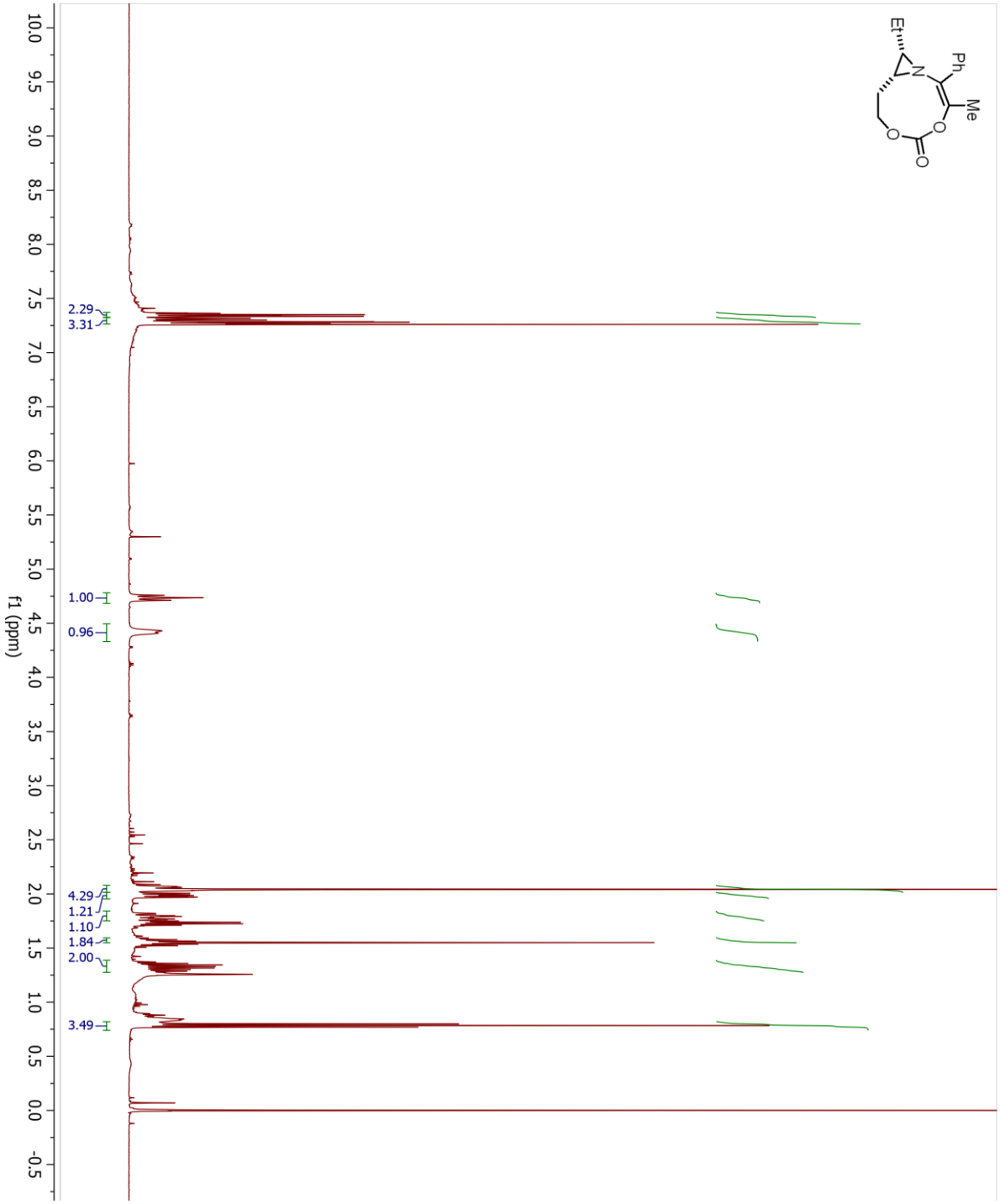
Compound **3.3a.** ^{1}H NMR (400 MHz, $CDCl_3$)



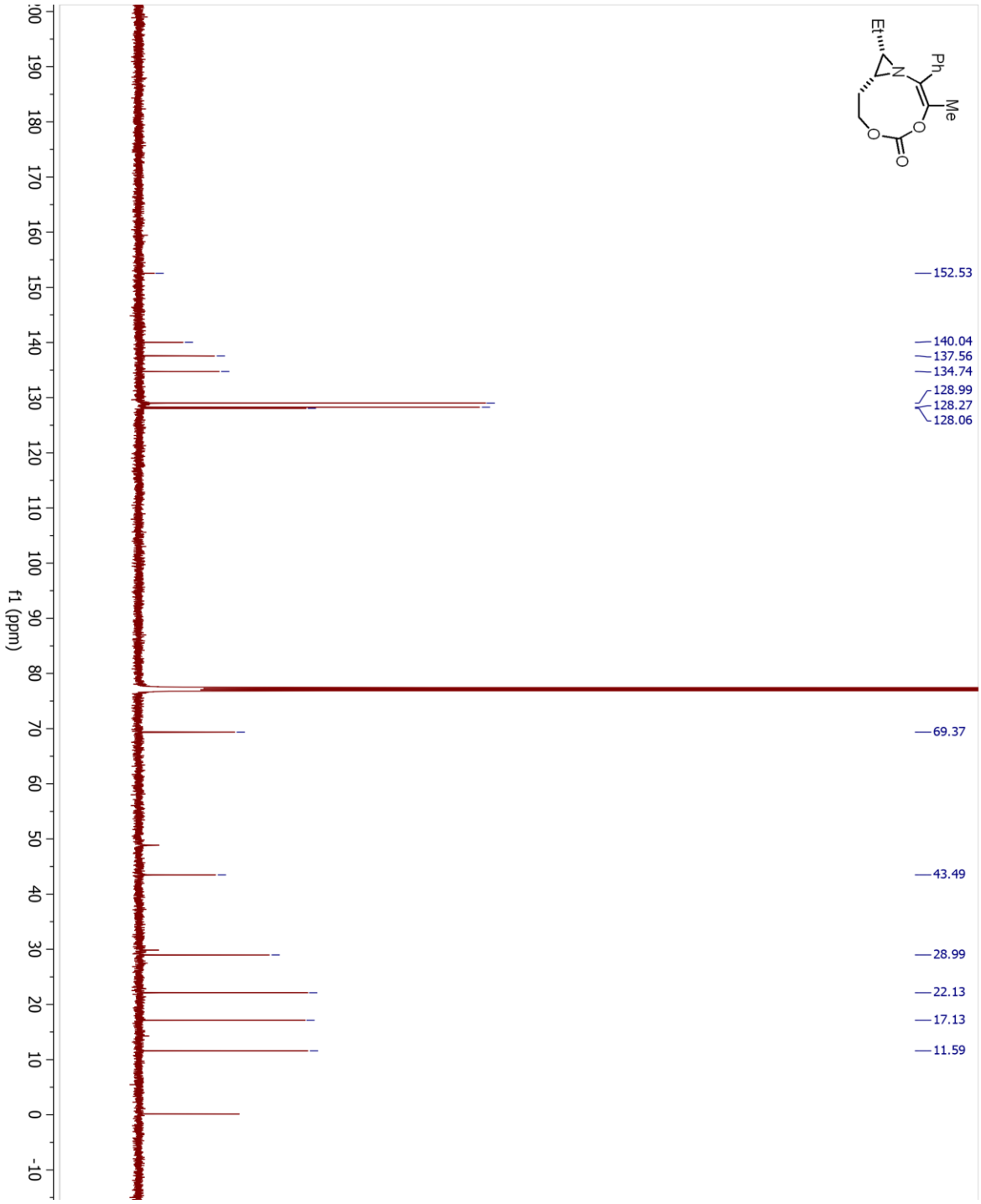
Compound **3.3a.** ^{13}C NMR (101 MHz, $CDCl_3$)



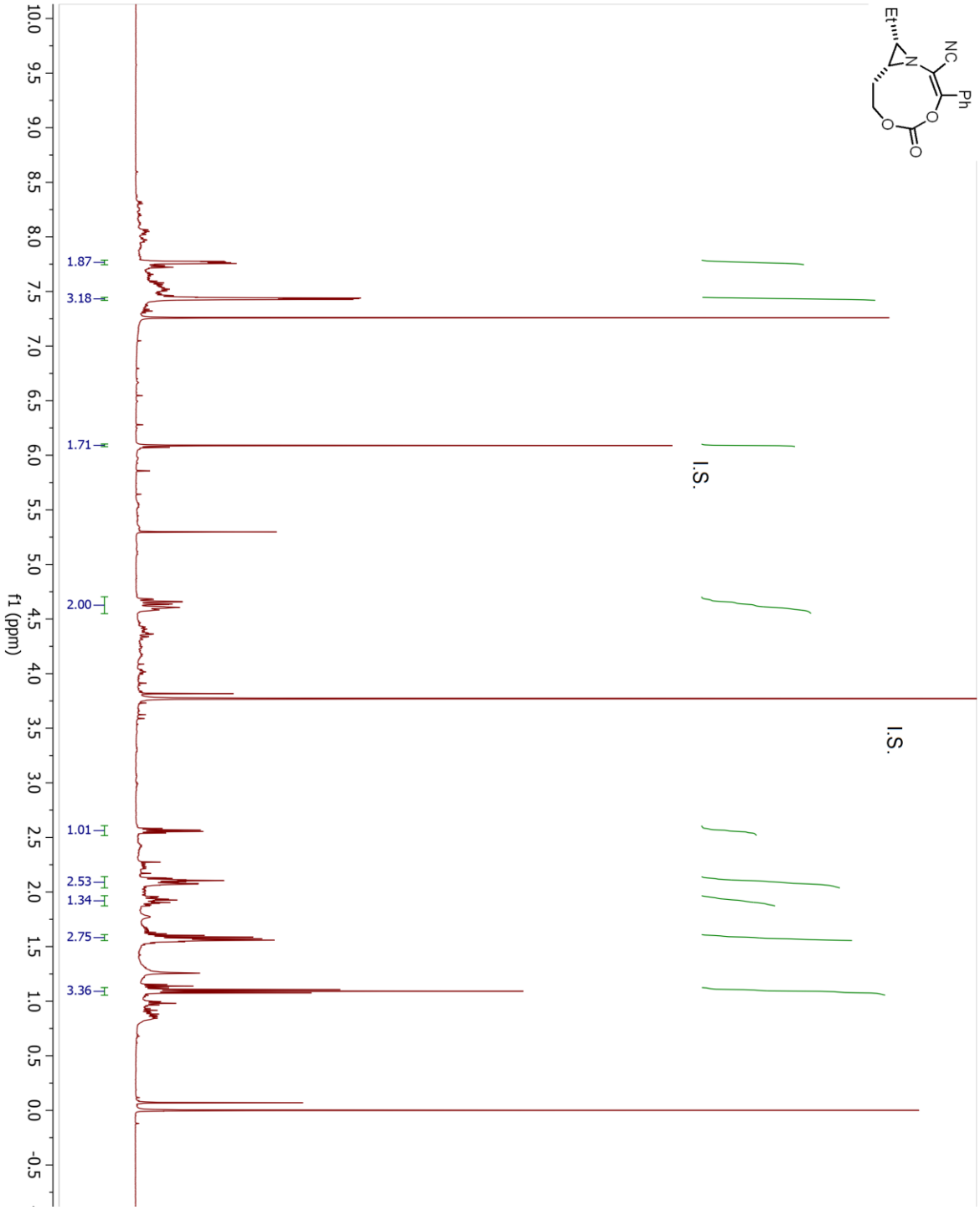
Compound **3.3b.** ^{1}H NMR (500 MHz, $CDCl_3$)



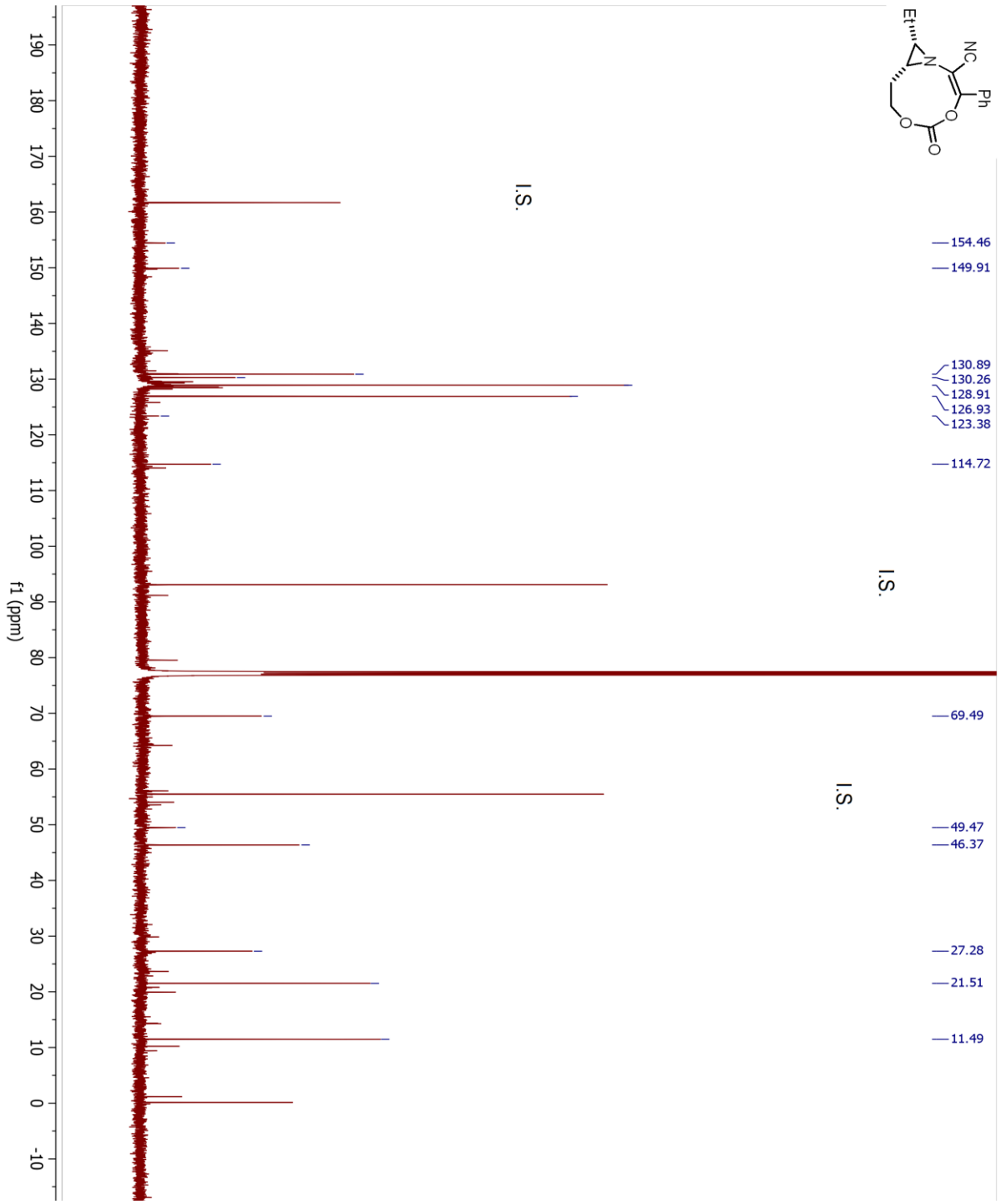
Compound **3.3b.** ^{13}C NMR (126 MHz, $CDCl_3$)



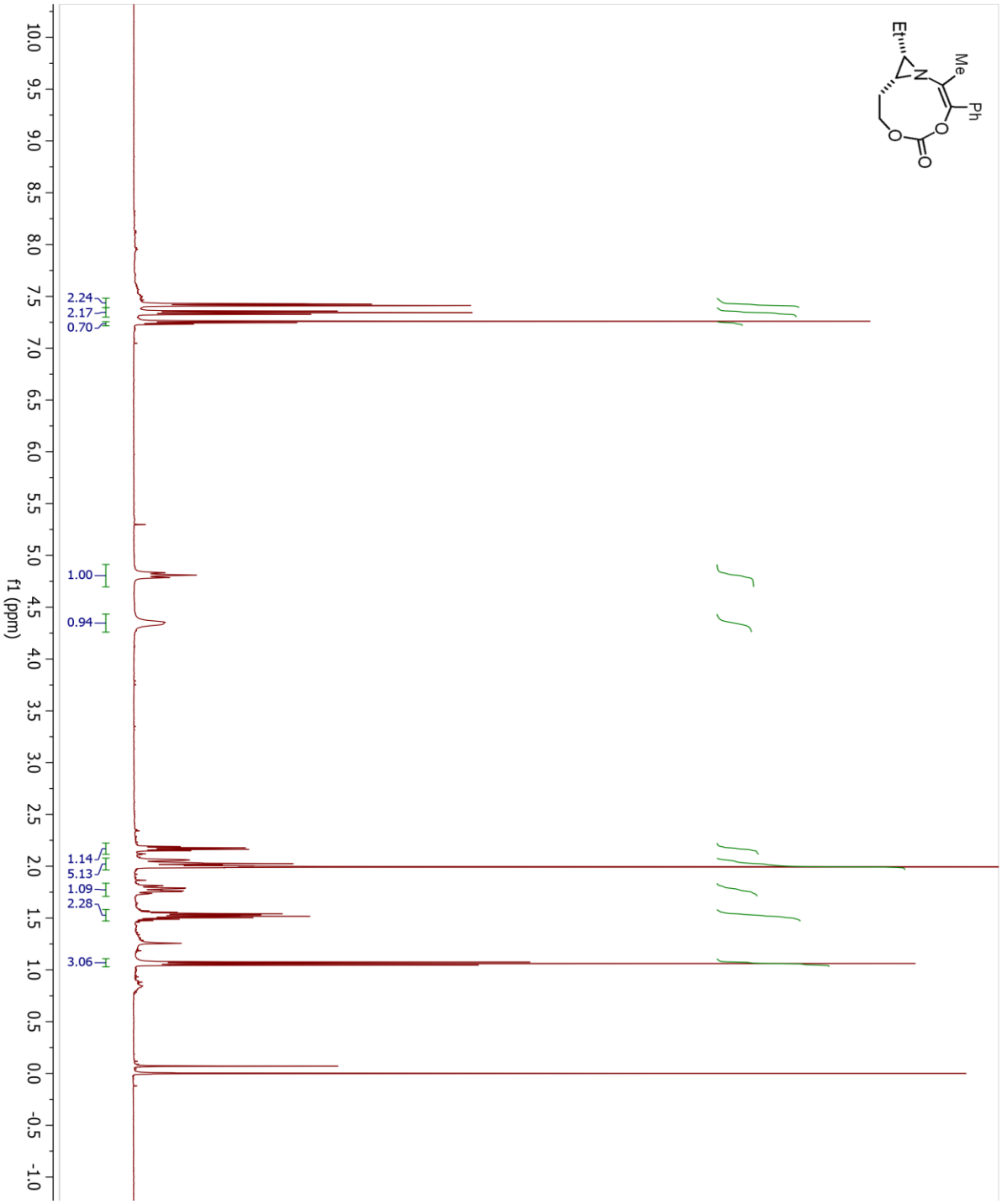
Compound **3.3c.** ^{1}H NMR (500 MHz, $CDCl_3$)



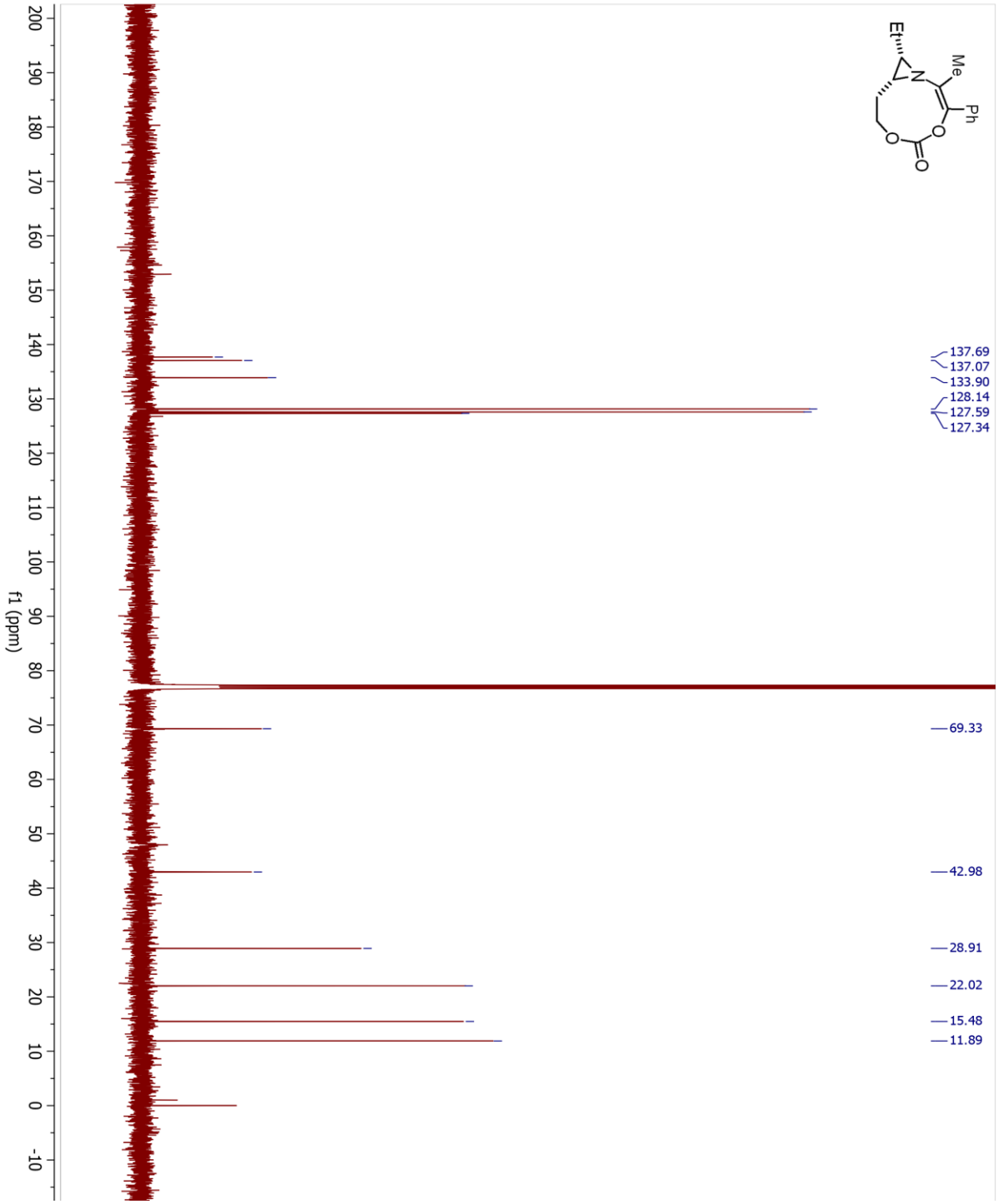
Compound **3.3c.** ^{13}C NMR (126 MHz, $CDCl_3$)



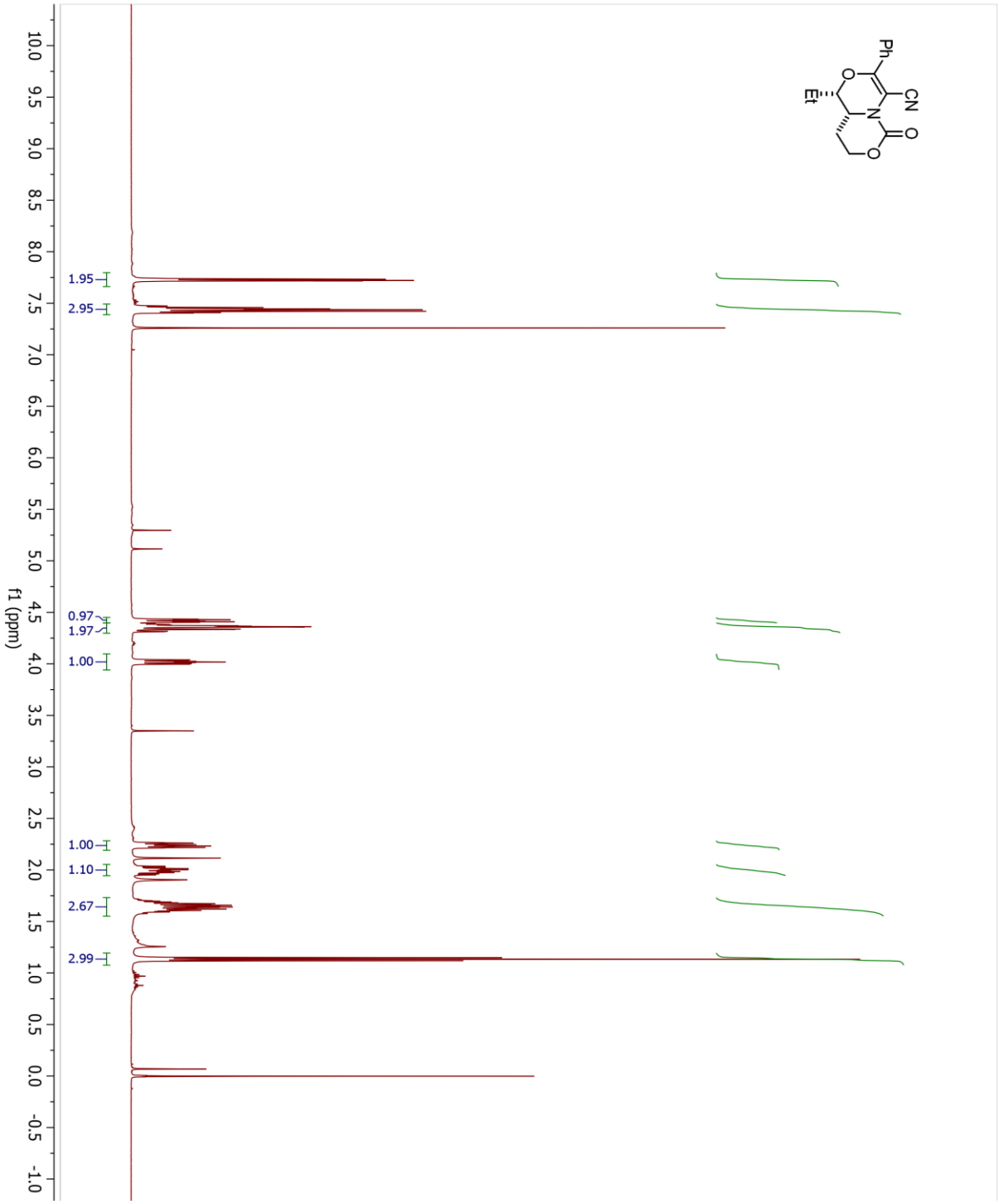
Compound **3.3d.** ^{1}H NMR (500 MHz, $CDCl_3$)



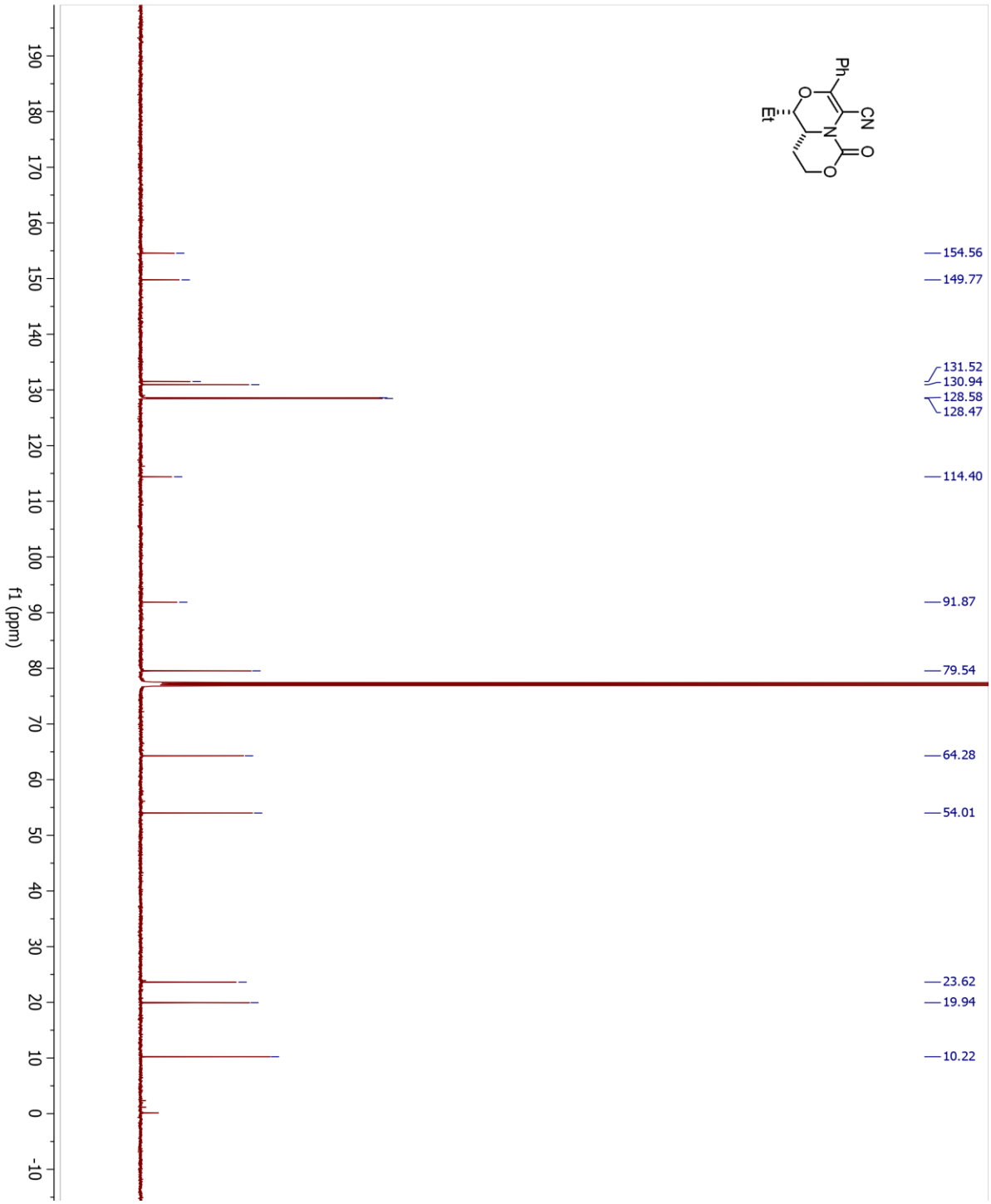
Compound **3.3d.** ^{13}C NMR (126 MHz, $CDCl_3$)



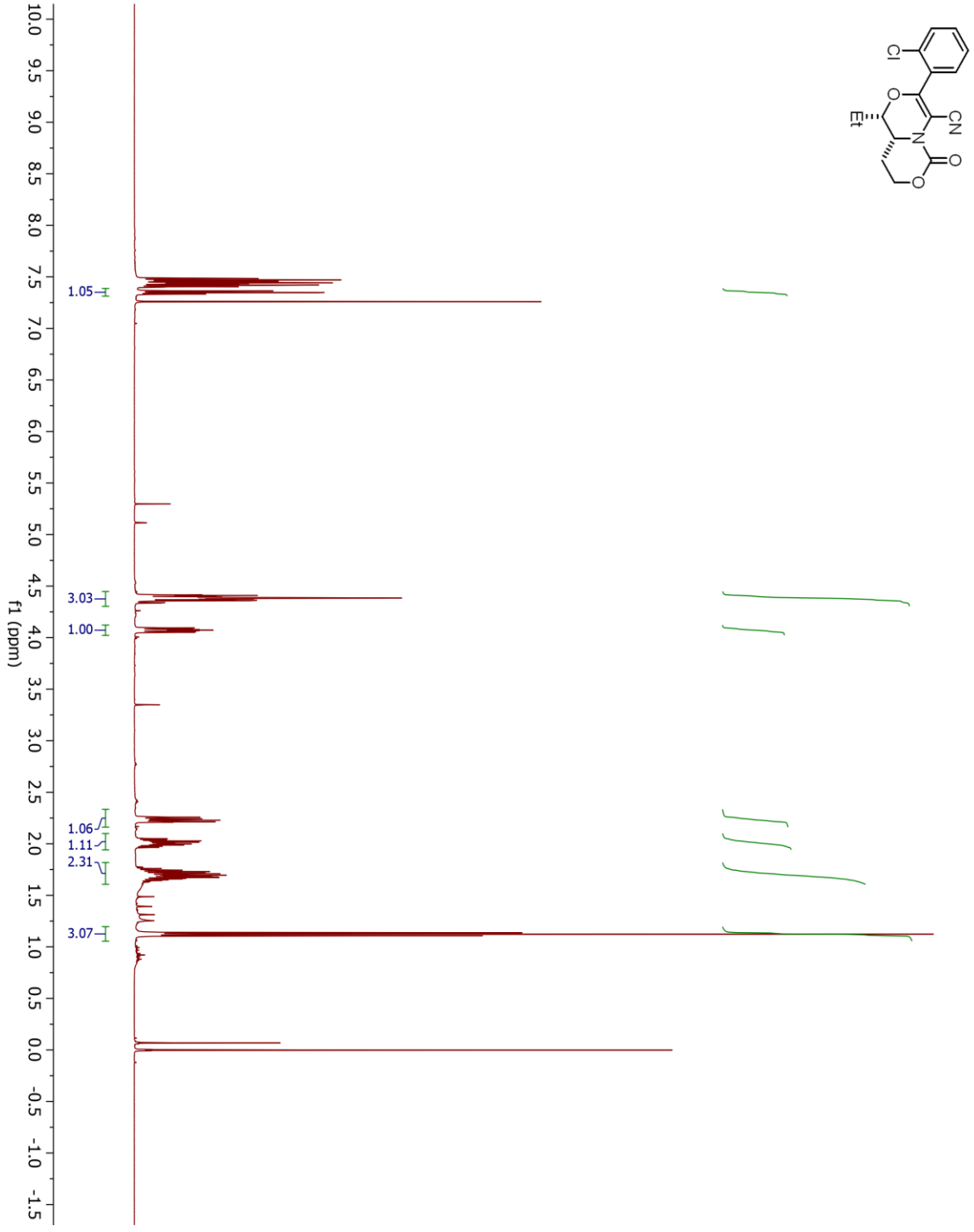
Compound **3.4c**. ^{1}H NMR (500 MHz, $CDCl_3$)



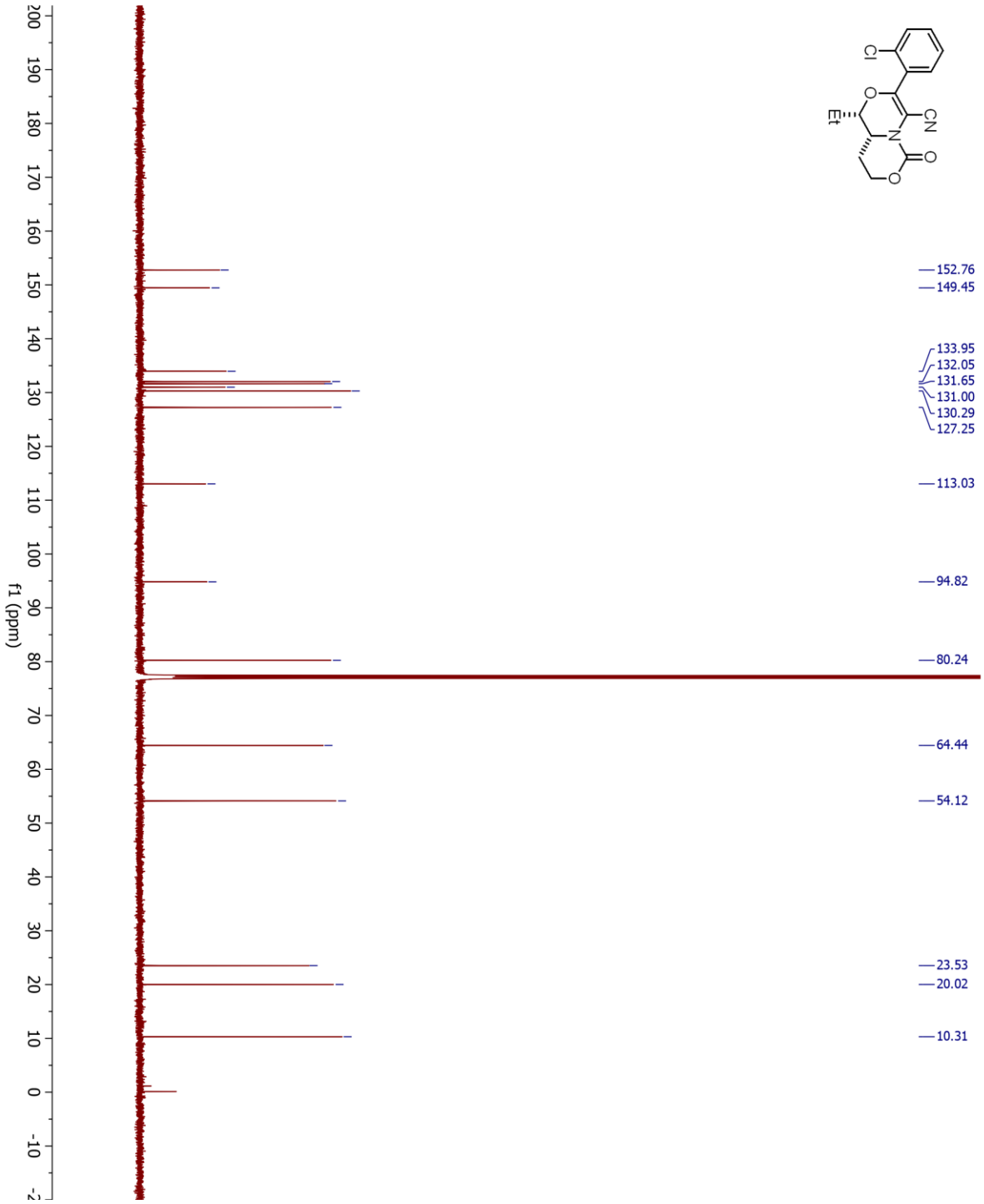
Compound **3.4c**. ^{13}C NMR (126 MHz, $CDCl_3$)



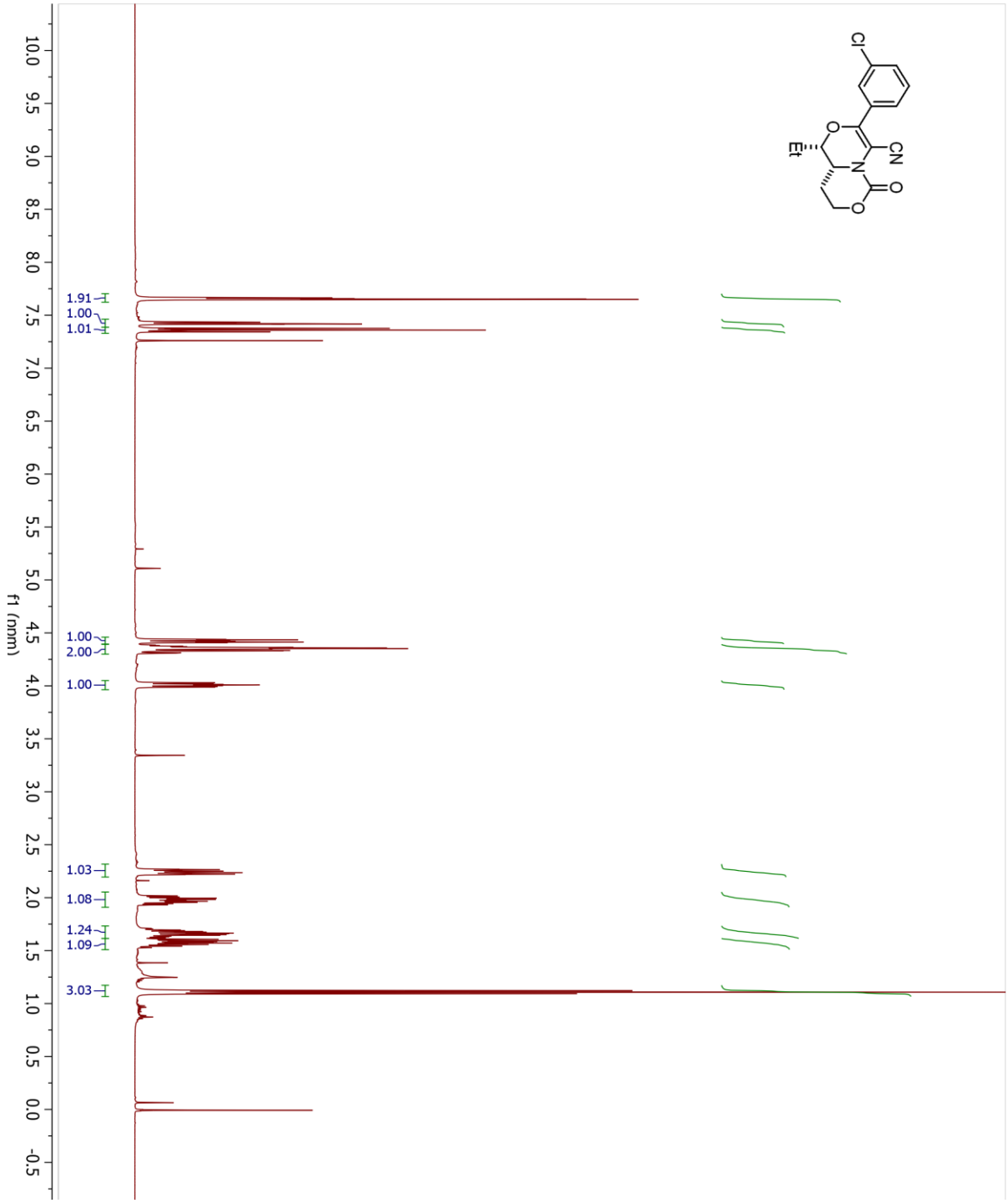
Compound **3.6c.** ^{1}H NMR (500 MHz, $CDCl_3$)



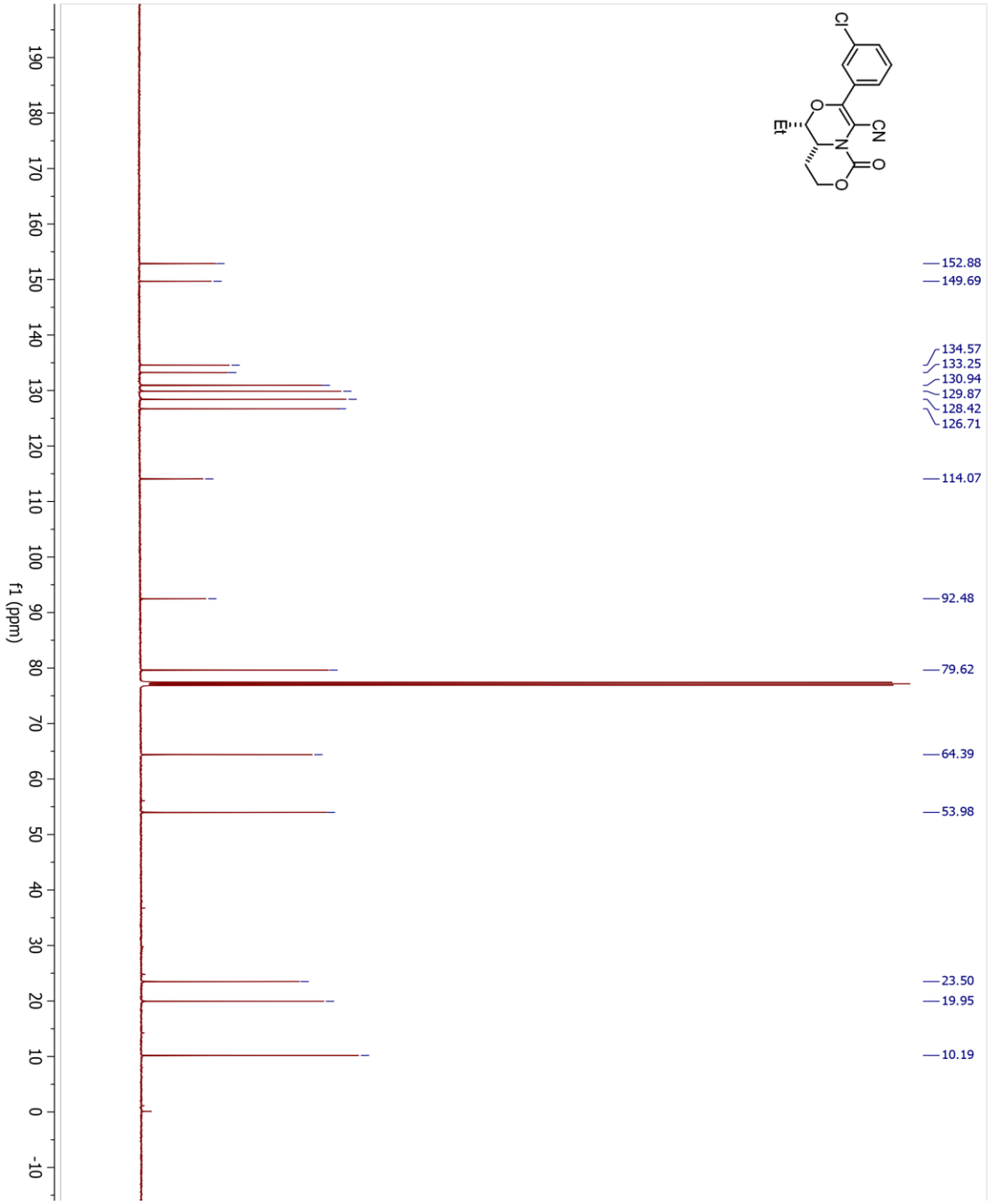
Compound **3.6c.** ^{13}C NMR (126 MHz, $CDCl_3$)



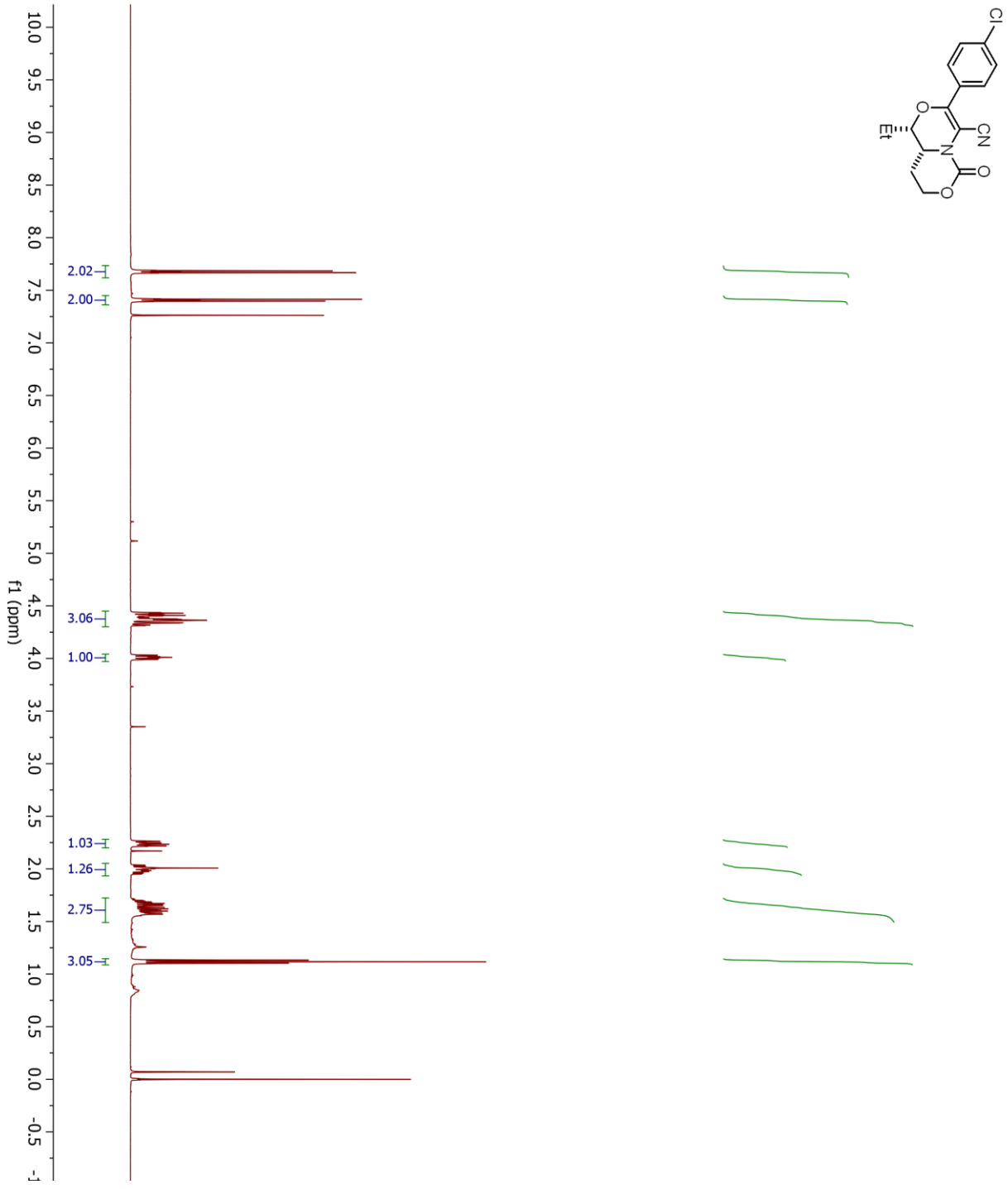
Compound **3.7c.** ^{1}H NMR (500 MHz, $CDCl_3$)



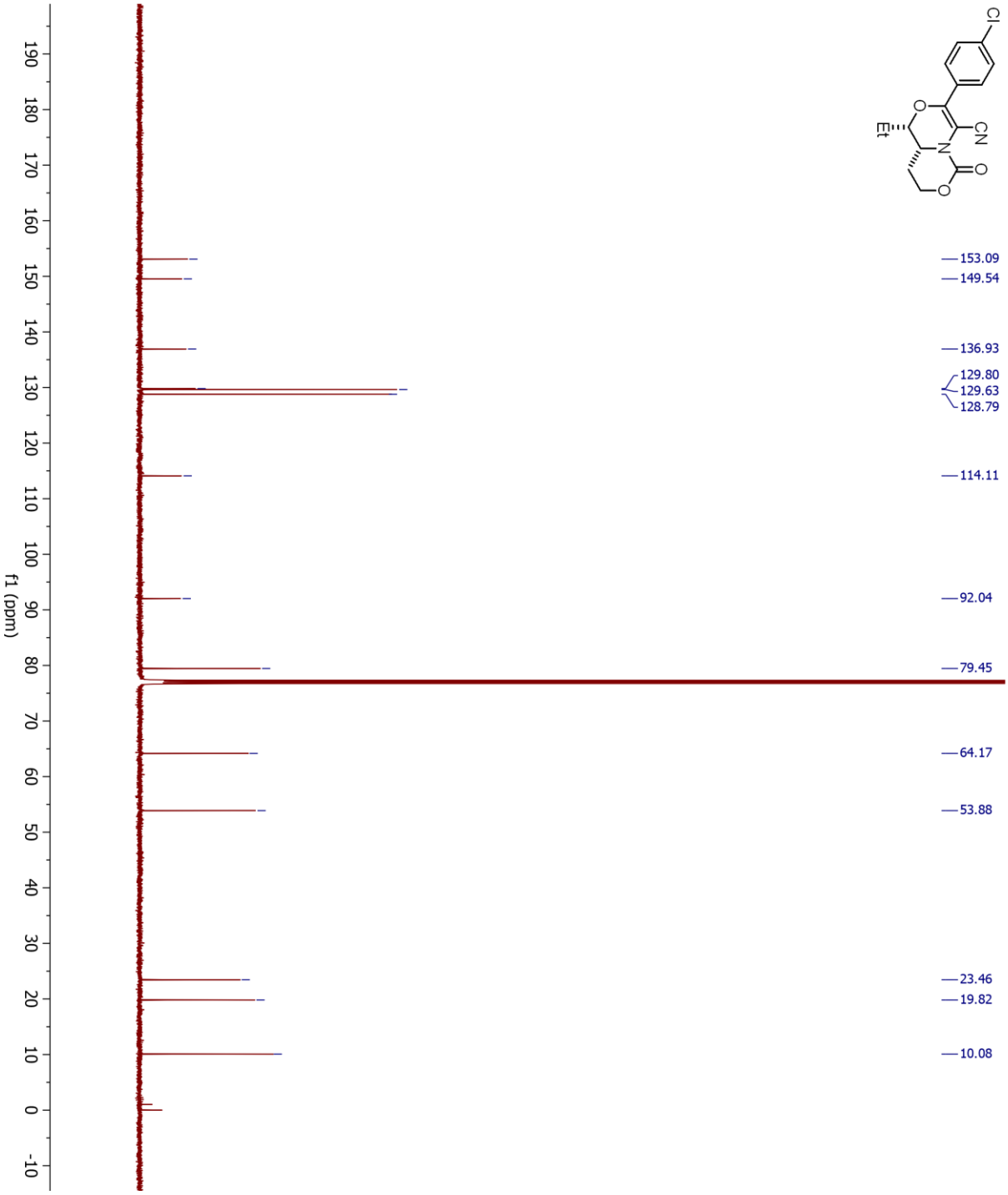
Compound **3.7c.** ^{13}C NMR (126 MHz, $CDCl_3$)



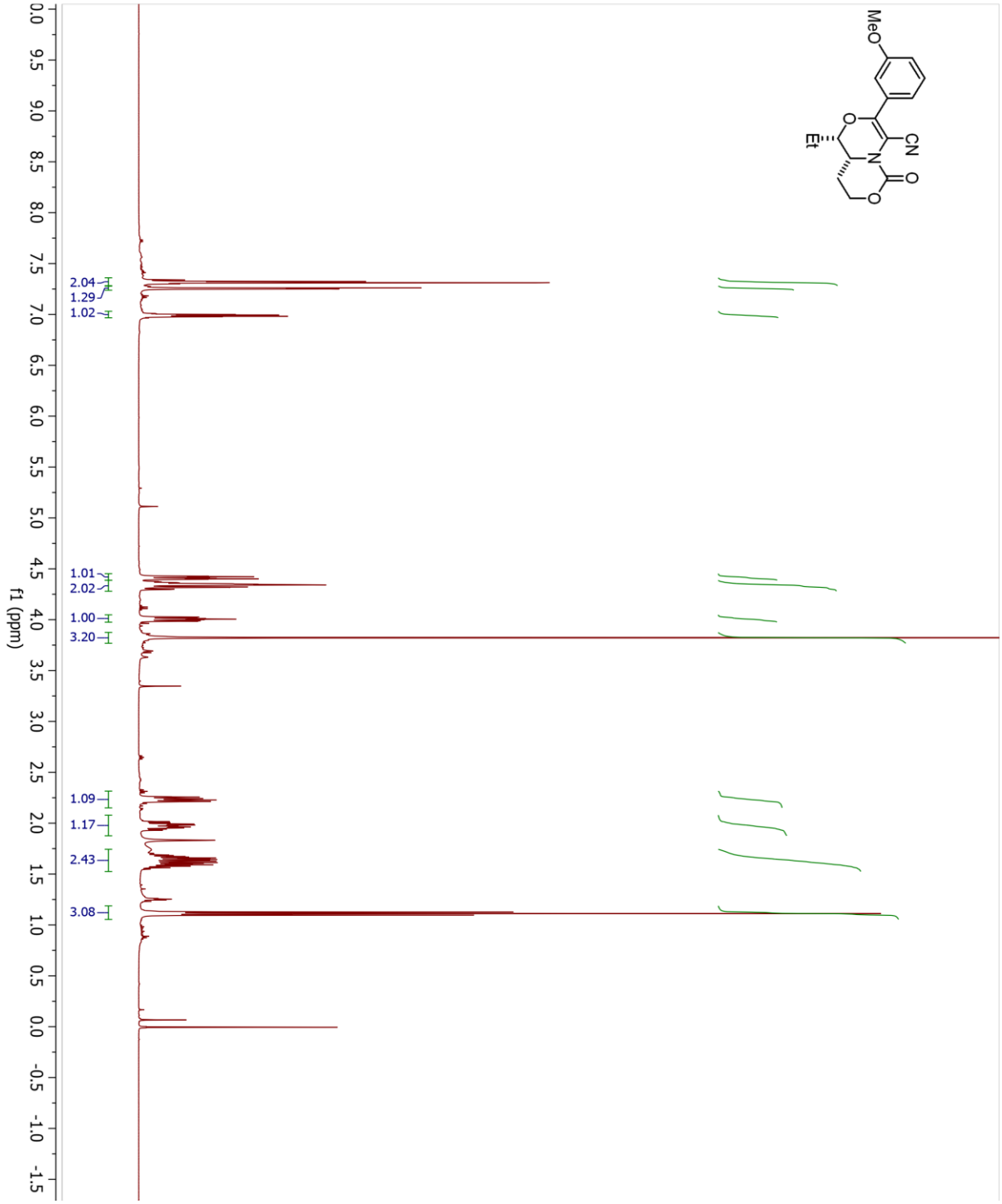
Compound **3.8c.** ^{1}H NMR (500 MHz, $CDCl_3$)



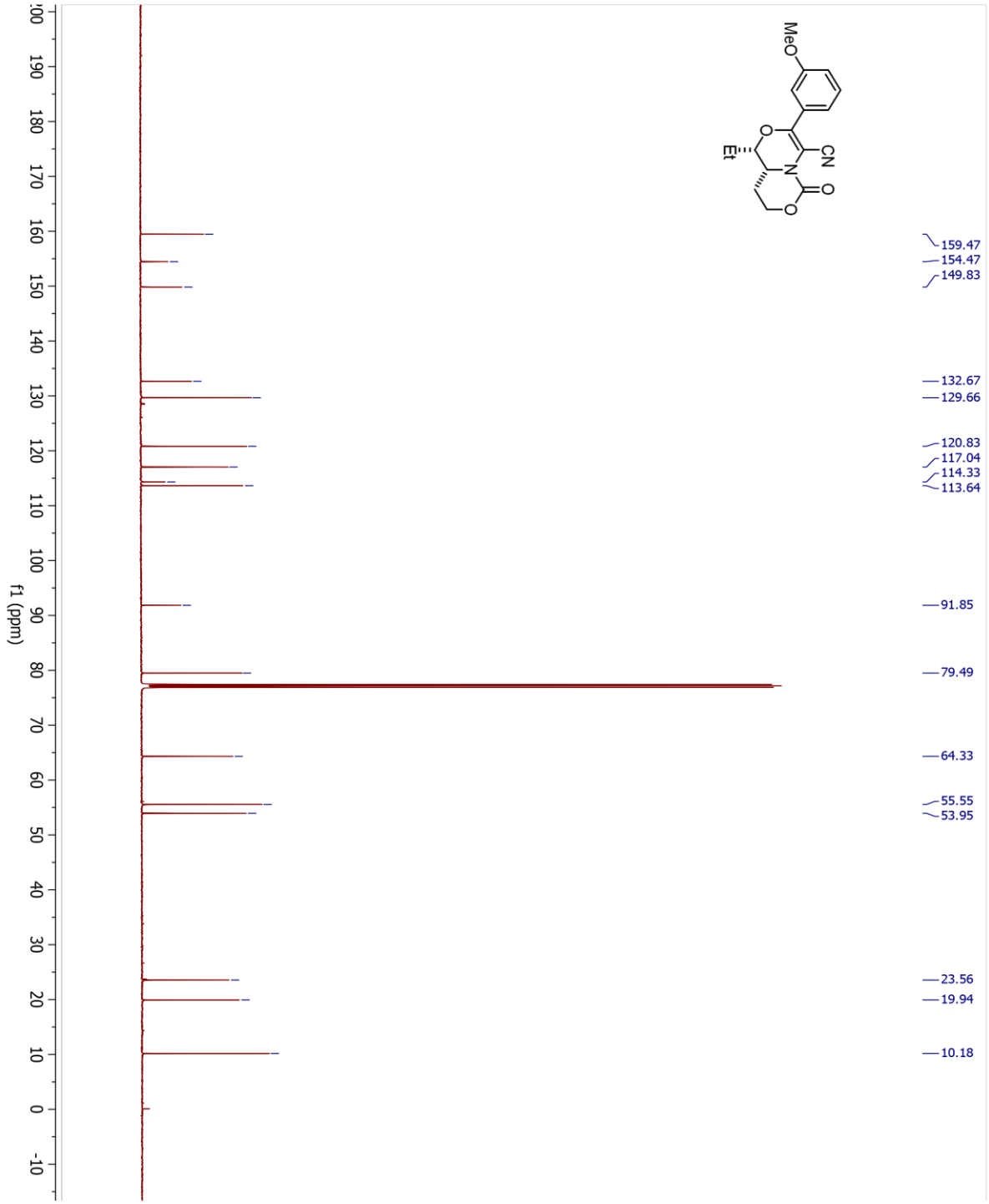
Compound **3.8c.** ^{13}C NMR (126 MHz, $CDCl_3$)



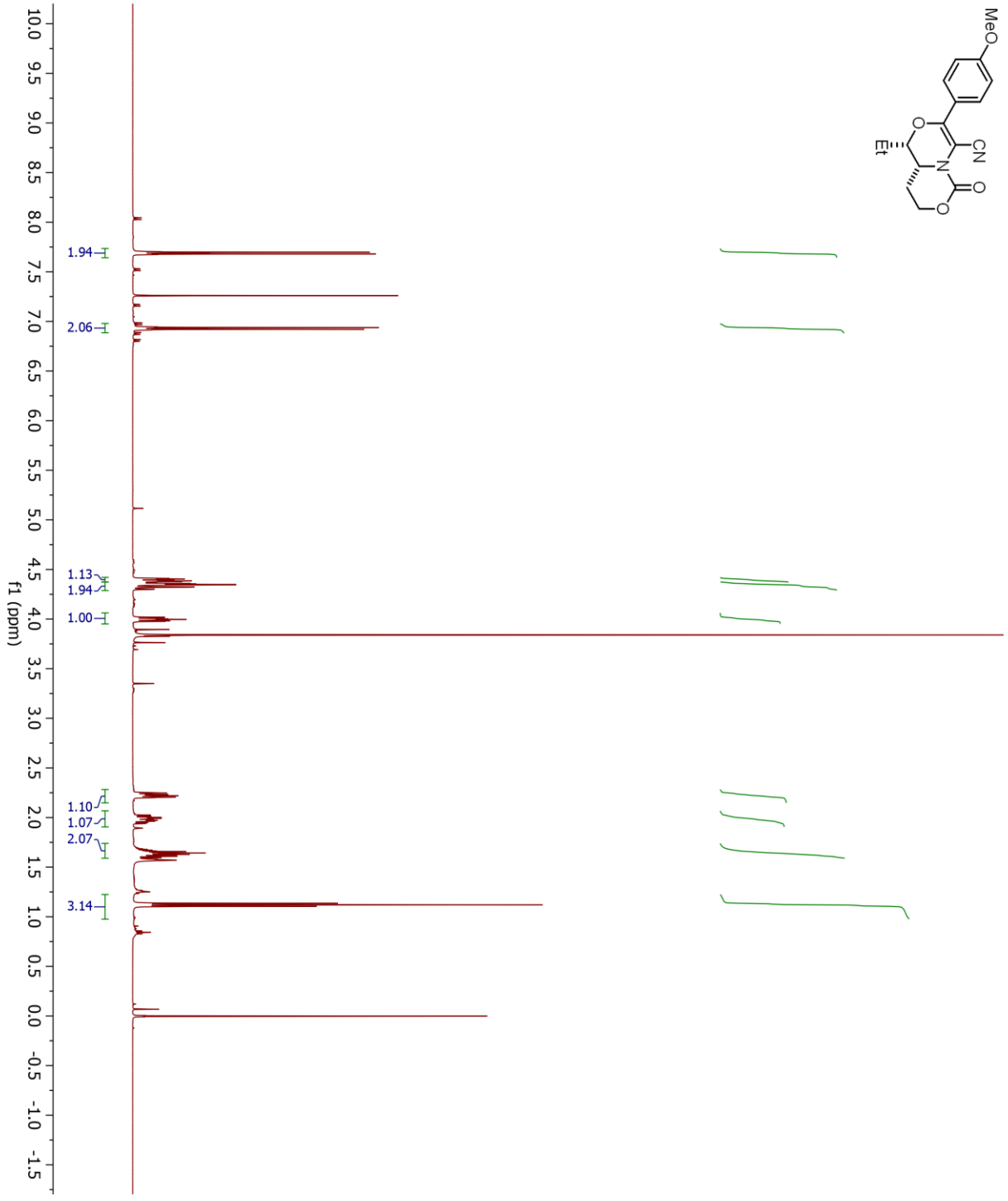
Compound **3.10c.** ^{1}H NMR (500 MHz, $CDCl_3$)



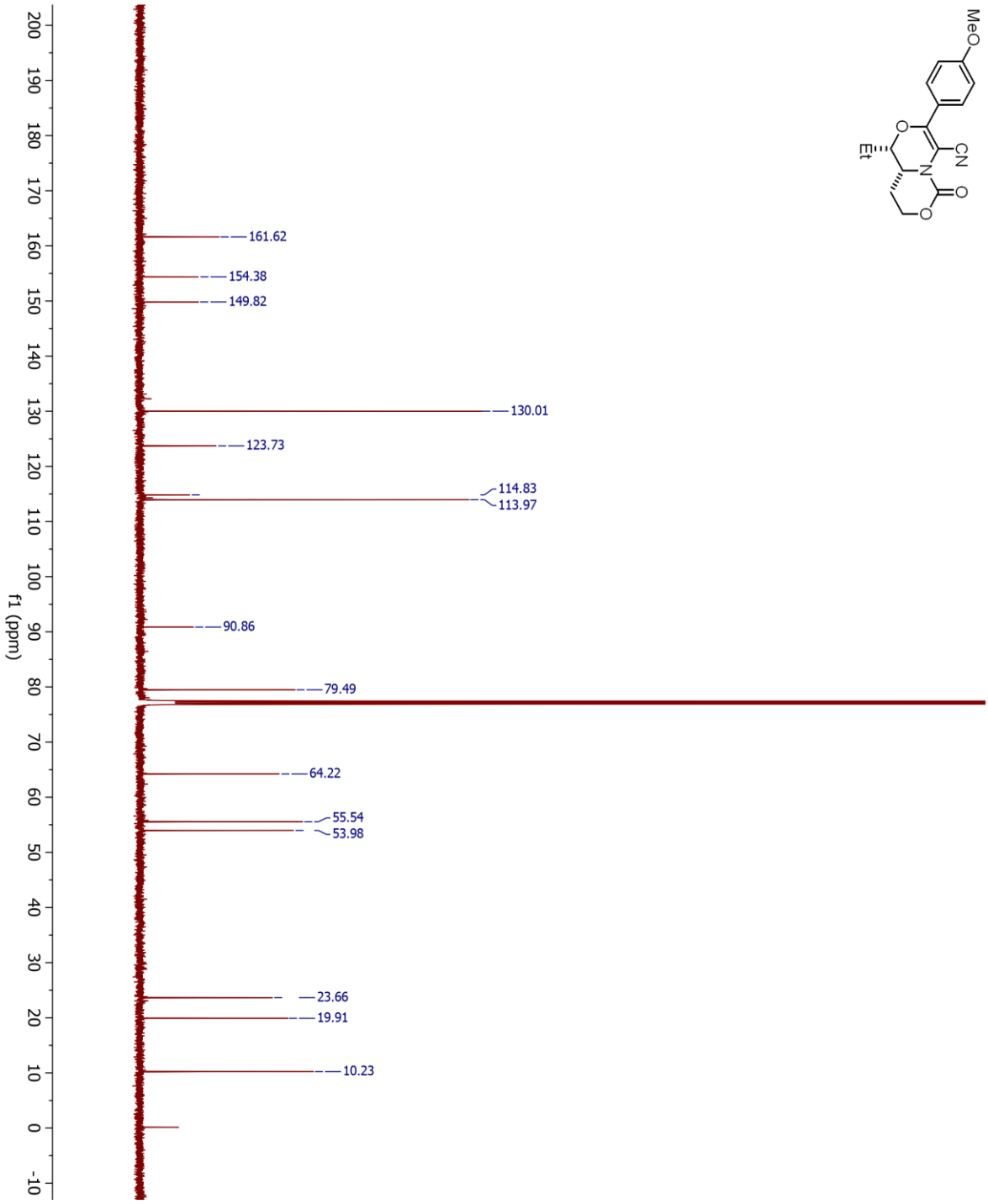
Compound **3.10c.** ^{13}C NMR (126 MHz, $CDCl_3$)



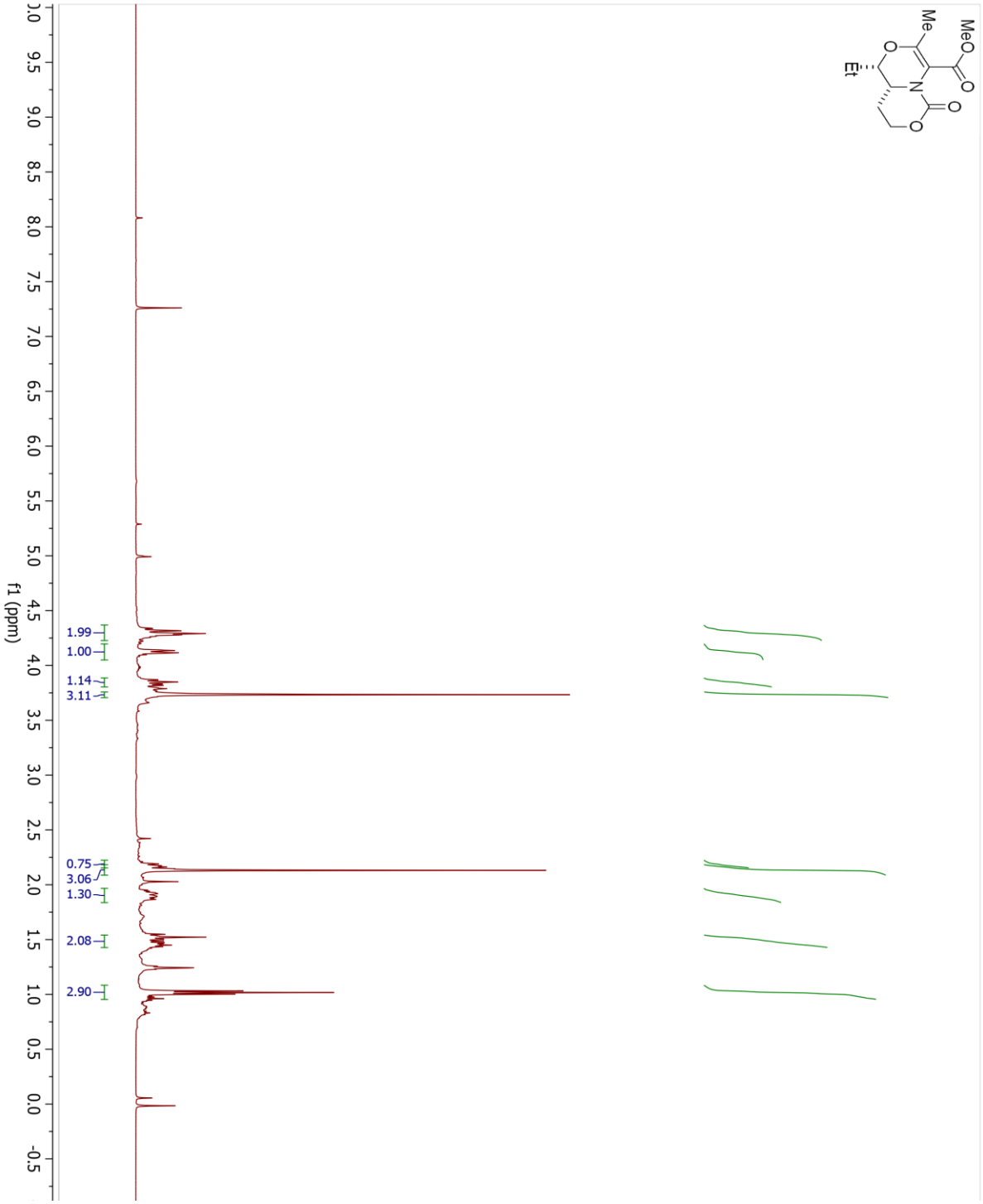
Compound **3.11c.** ^{1}H NMR (500 MHz, $CDCl_3$)



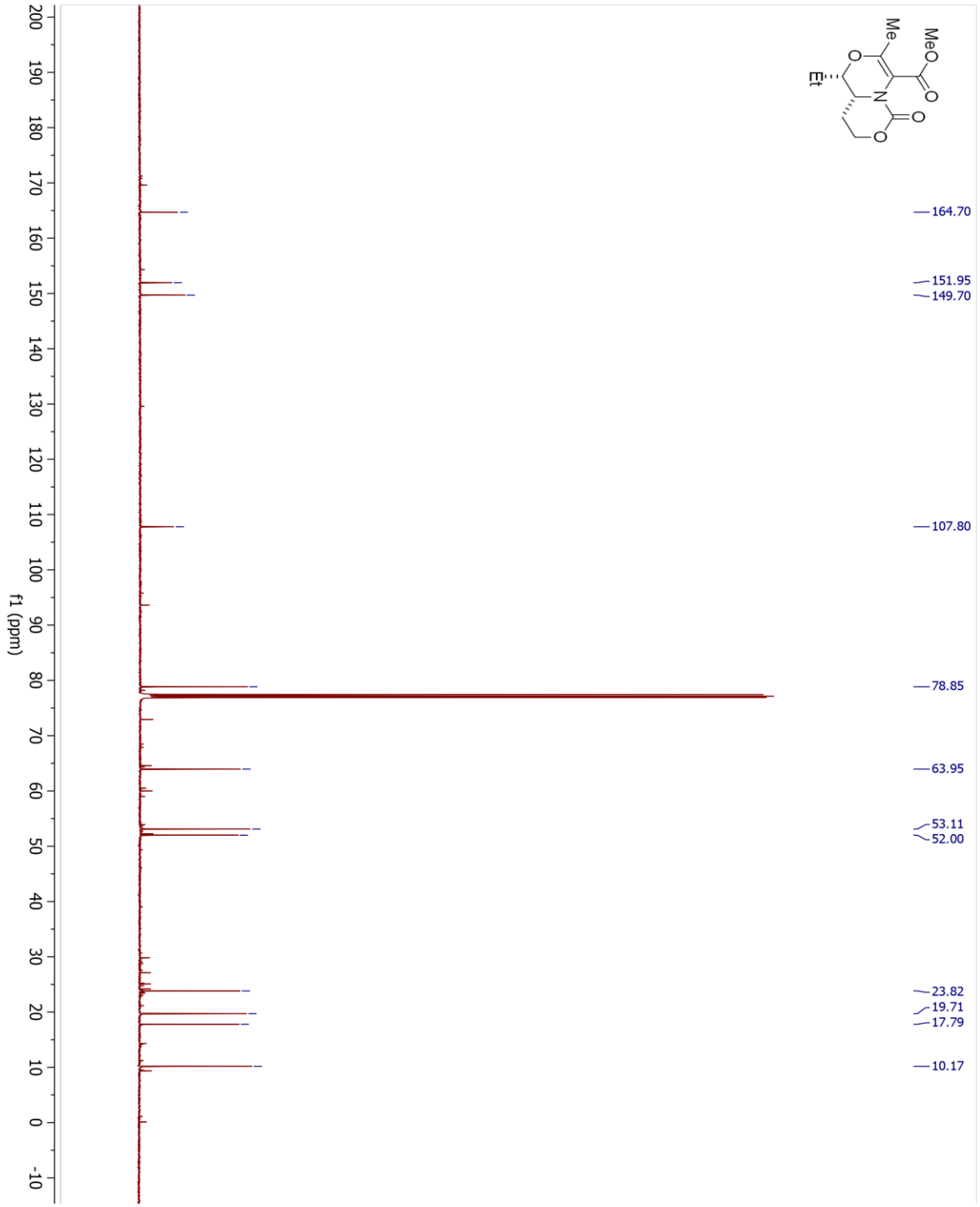
Compound **3.11c.** ^{13}C NMR (126 MHz, $CDCl_3$)



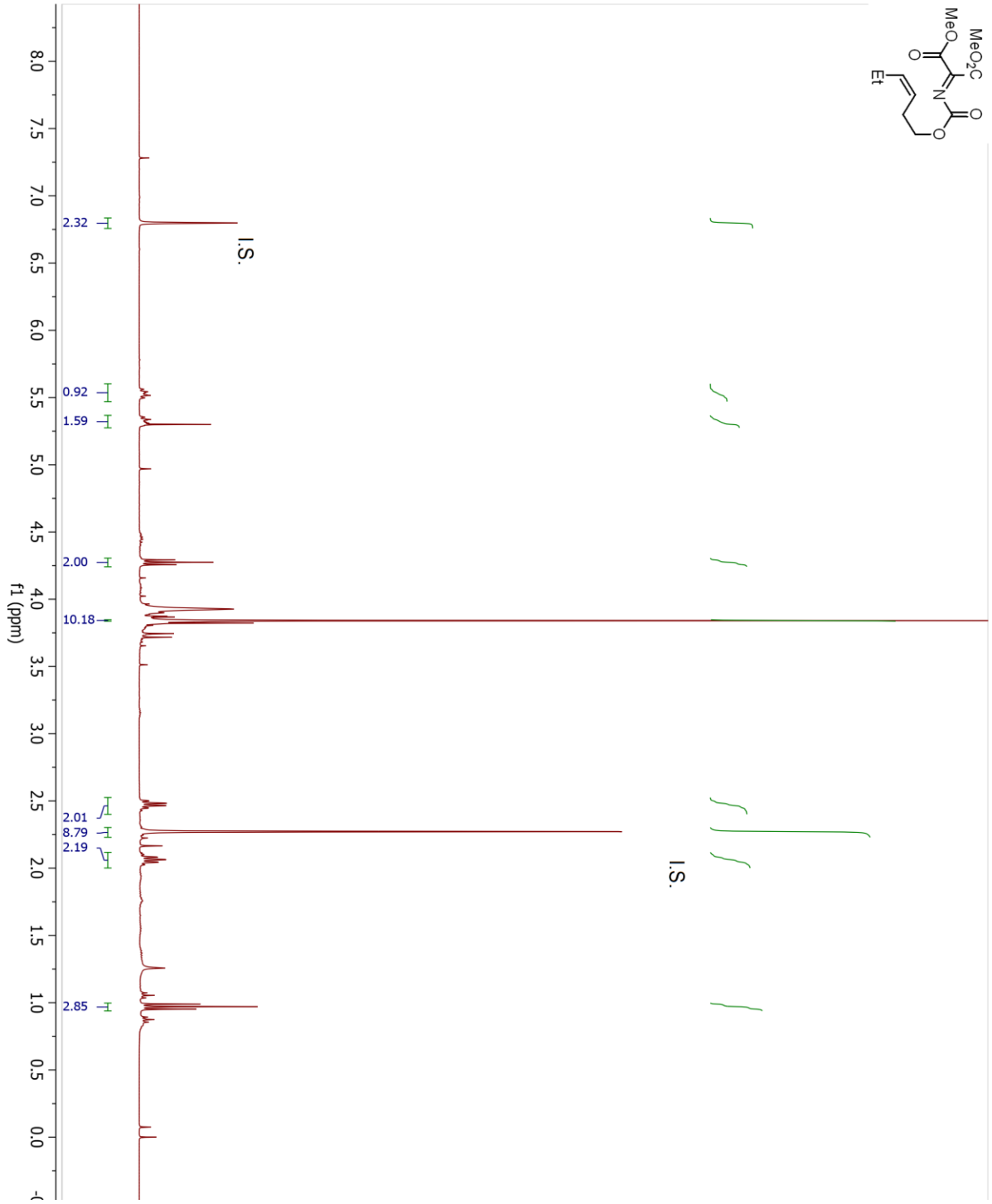
Compound **3.4e.** ^{1}H NMR (500 MHz, $CDCl_3$)



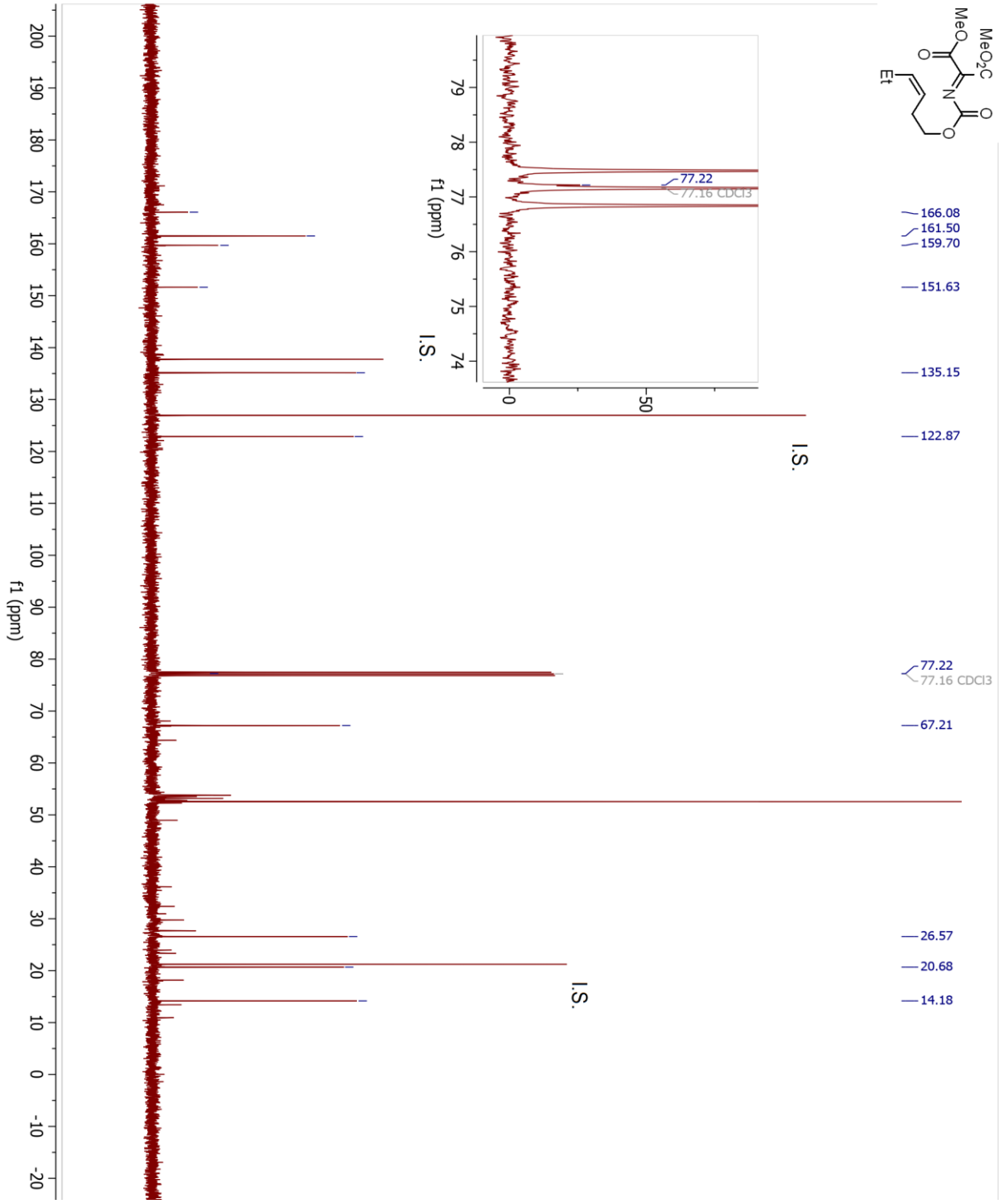
Compound **3.4e.** ^{13}C NMR (126 MHz, $CDCl_3$)



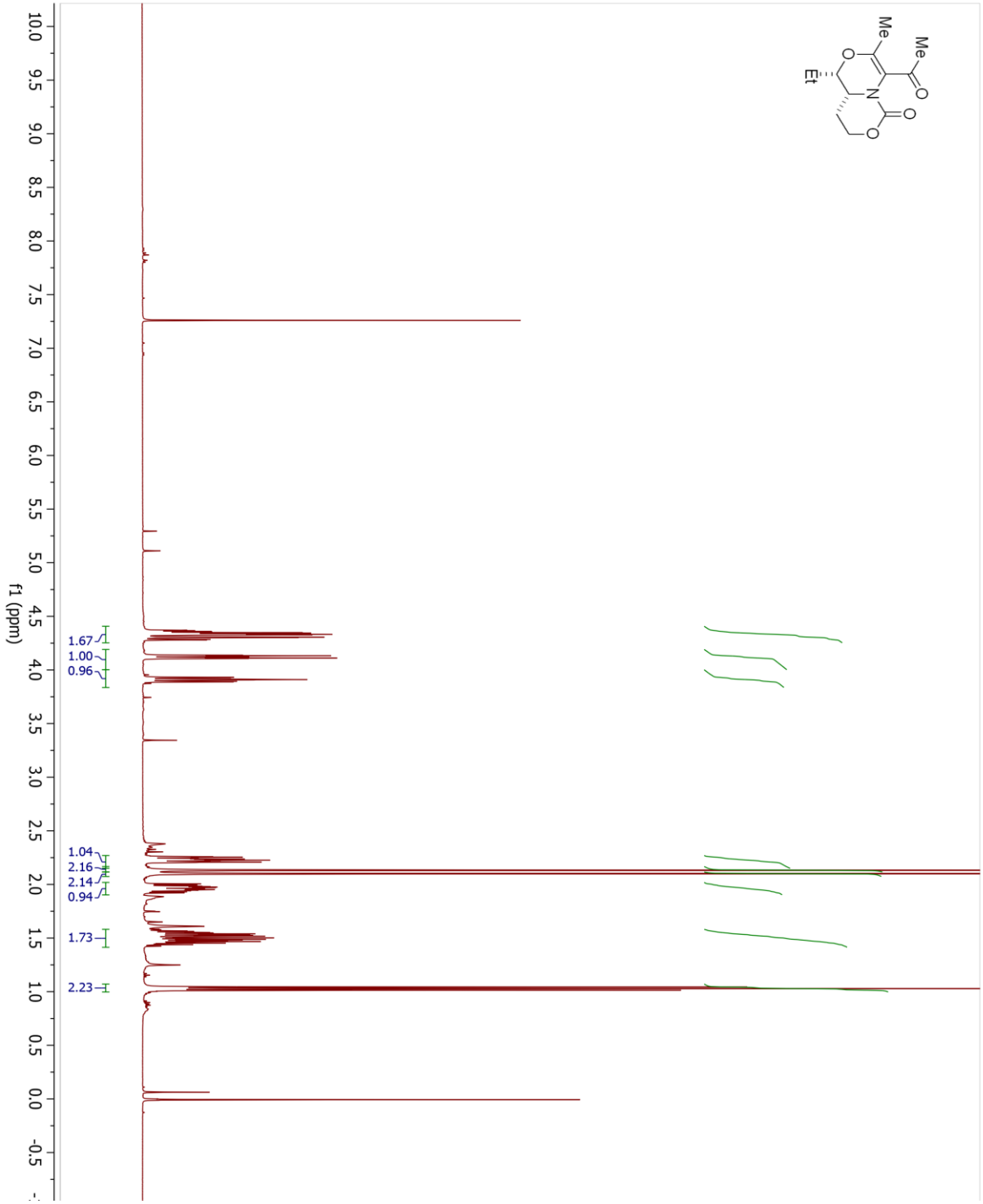
Compound **SI-1.** ^{1}H NMR (400 MHz, $CDCl_3$)



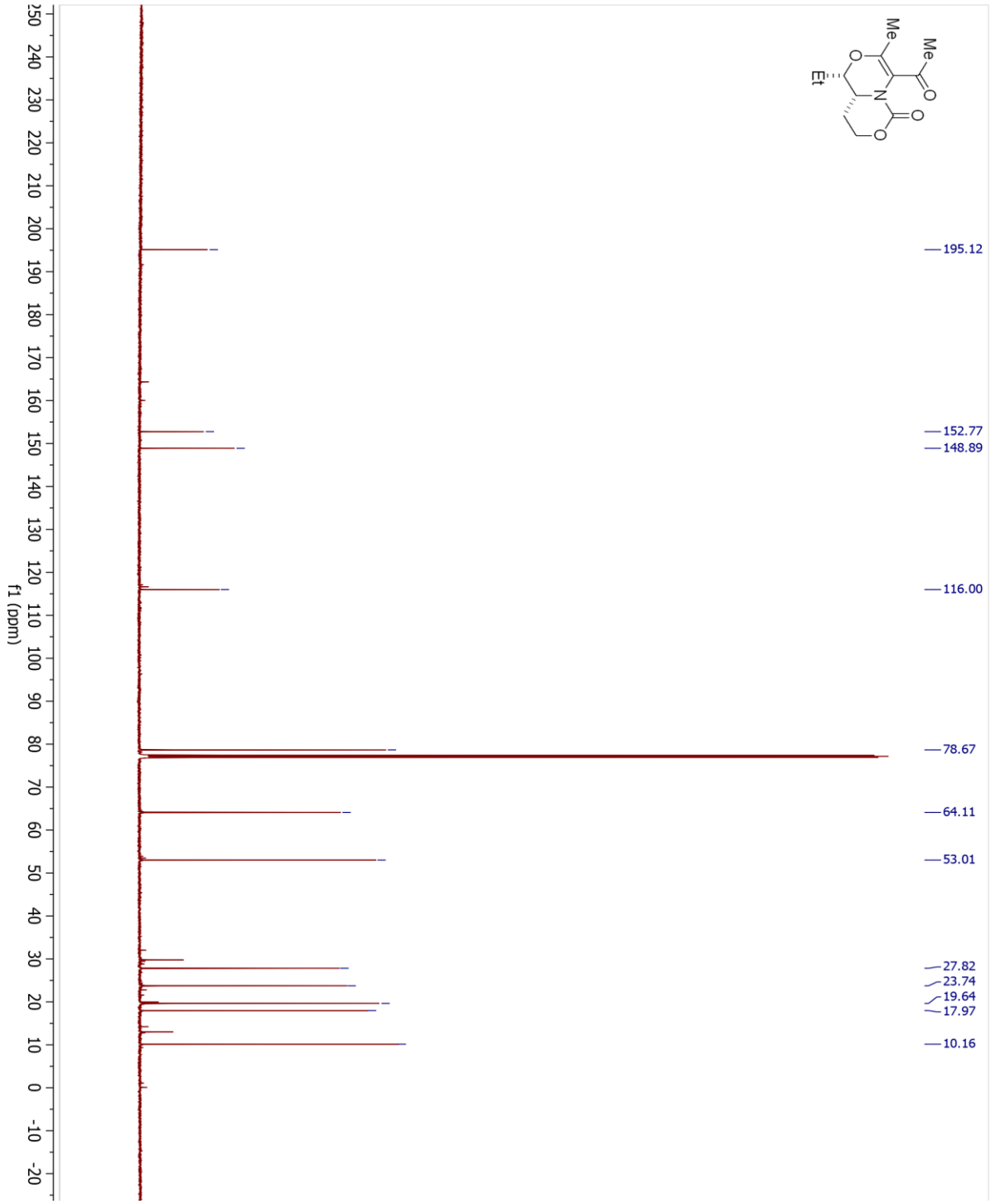
Compound **SI-1.** ^{13}C NMR (101 MHz, $CDCl_3$)



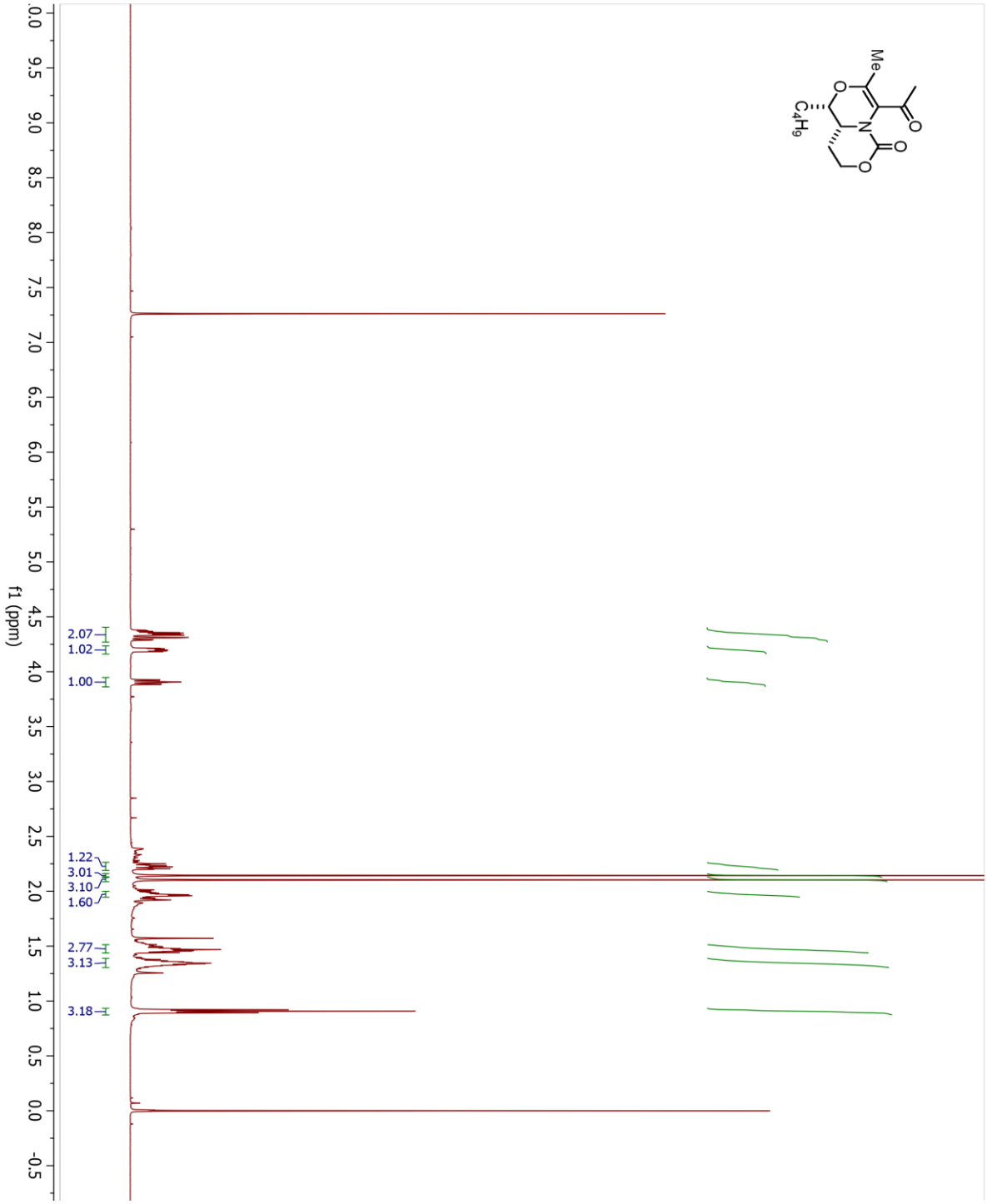
Compound **3.4f.** ^{1}H NMR (500 MHz, $CDCl_3$)



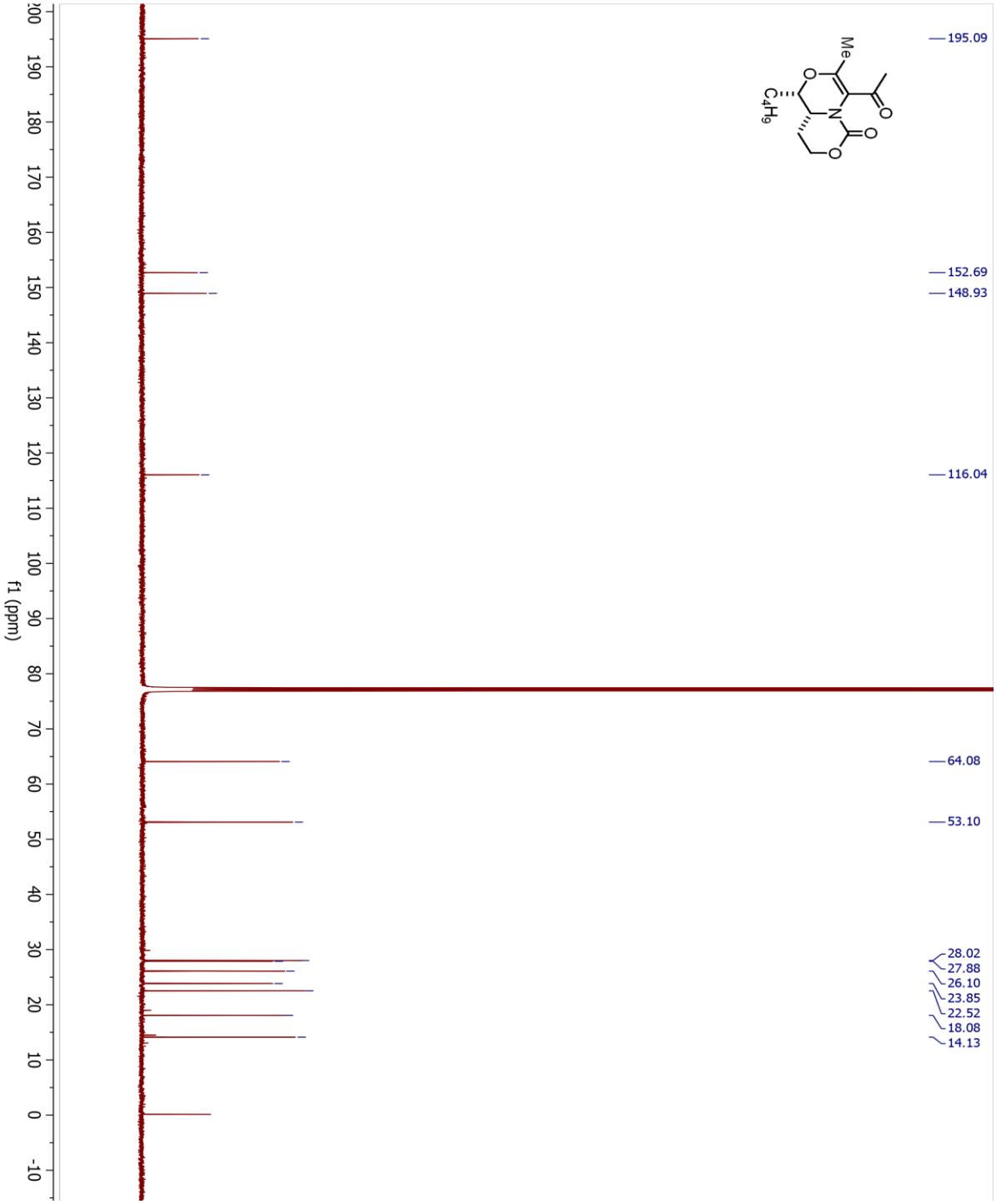
Compound **3.4f.** ^{13}C NMR (126 MHz, $CDCl_3$)



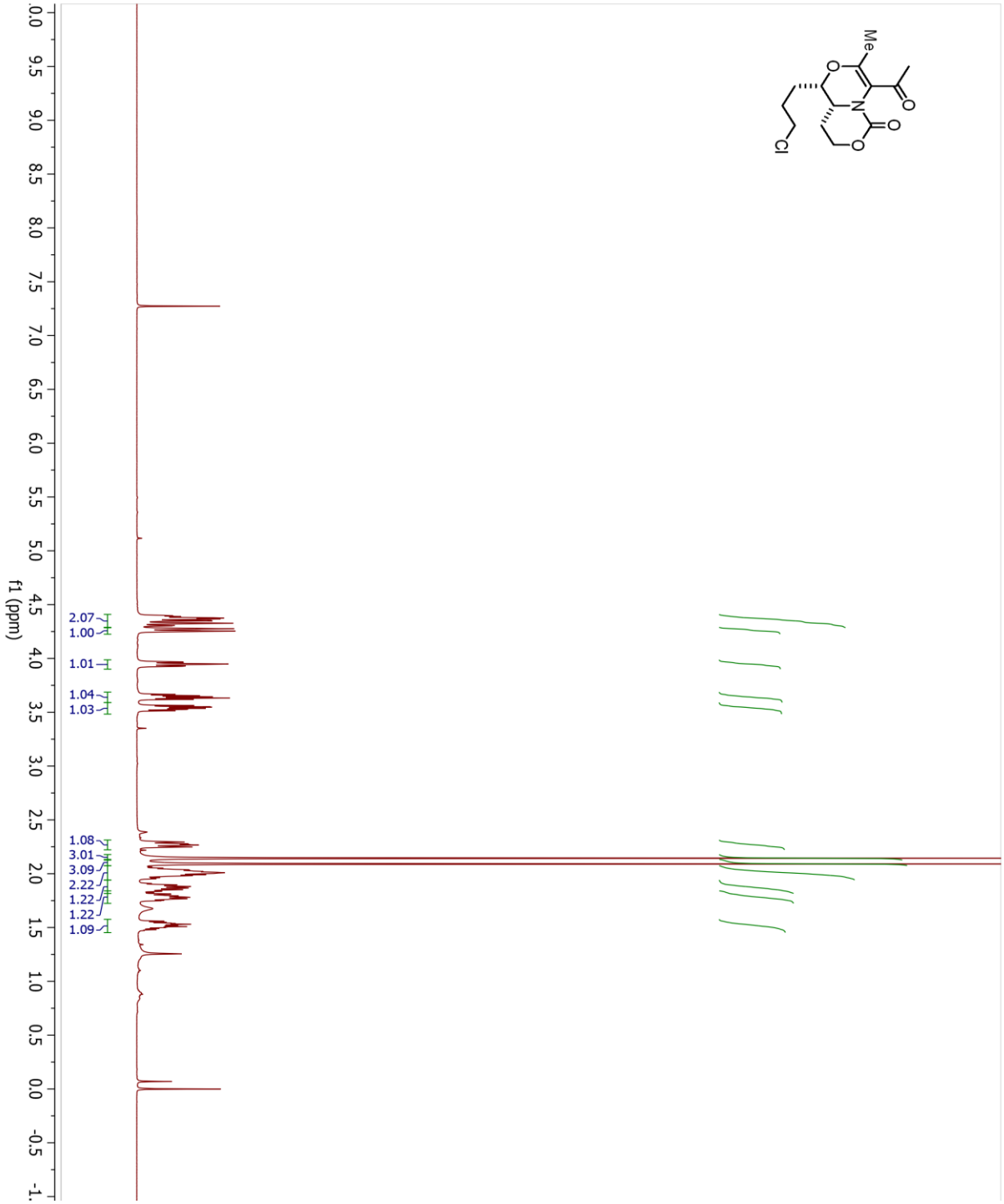
Compound **3.12f.** ^{1}H NMR (500 MHz, $CDCl_3$)



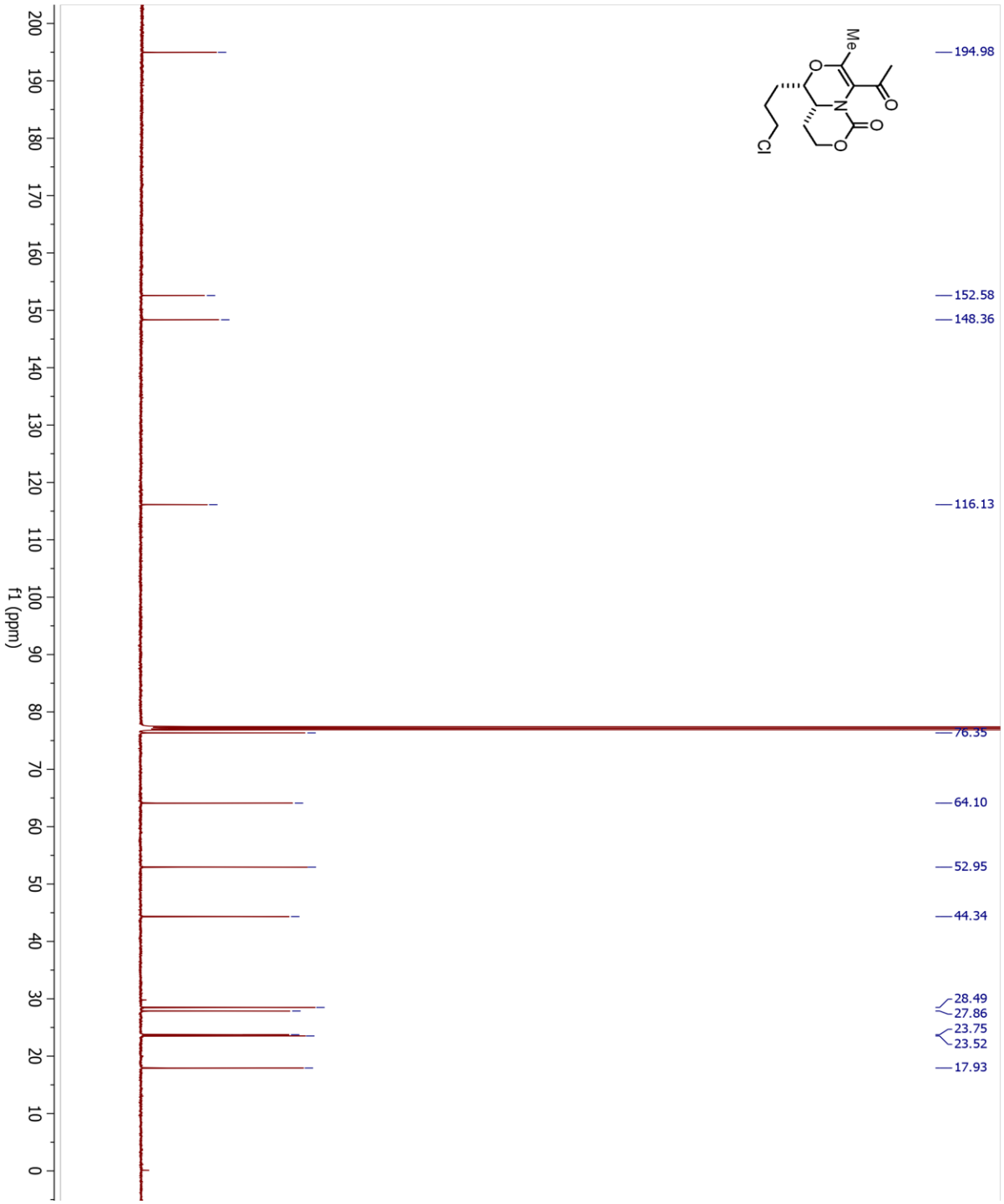
Compound **3.12f.** ^{13}C NMR (126 MHz, $CDCl_3$)



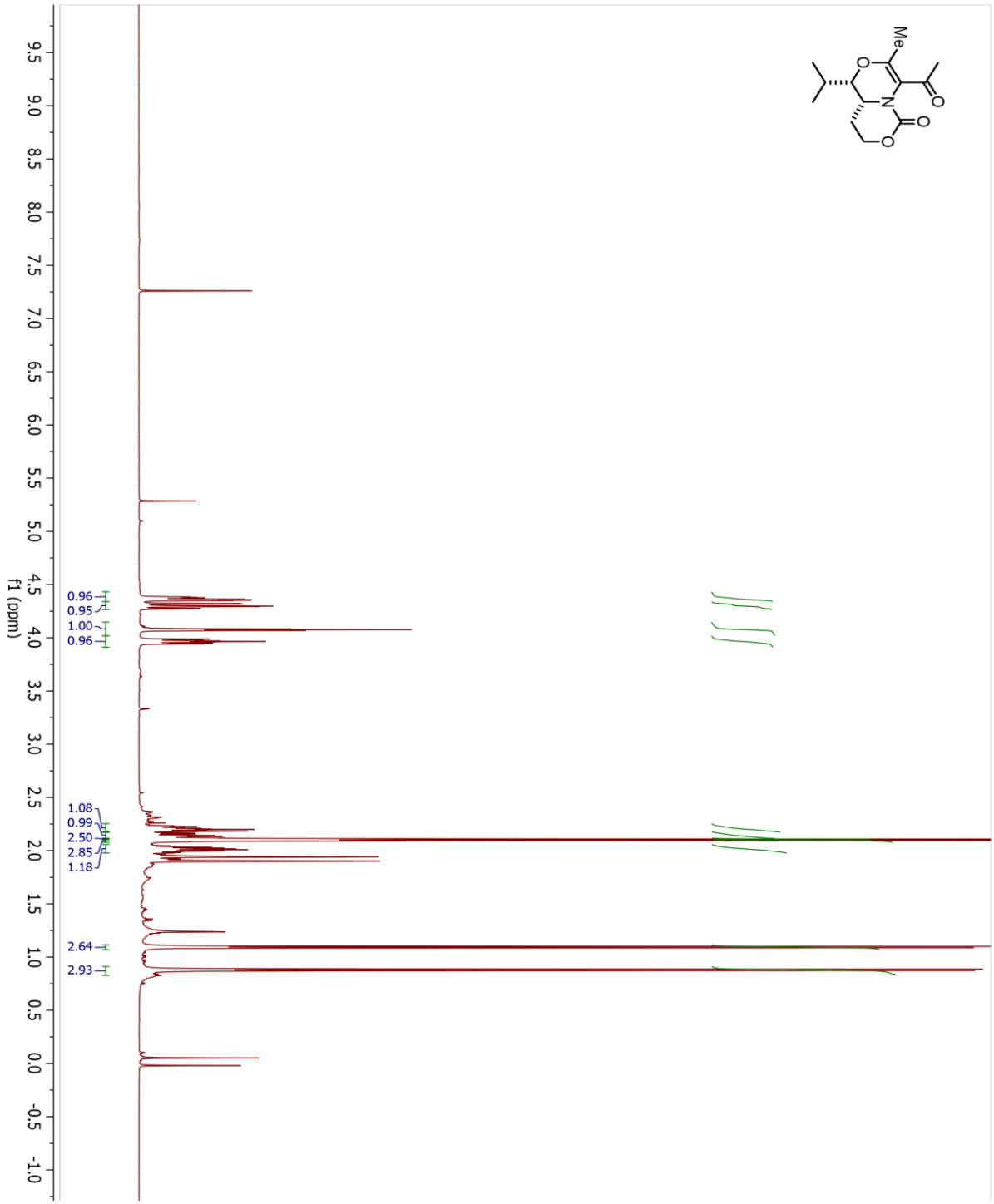
Compound **3.13f.** ^{1}H NMR (500 MHz, $CDCl_3$)



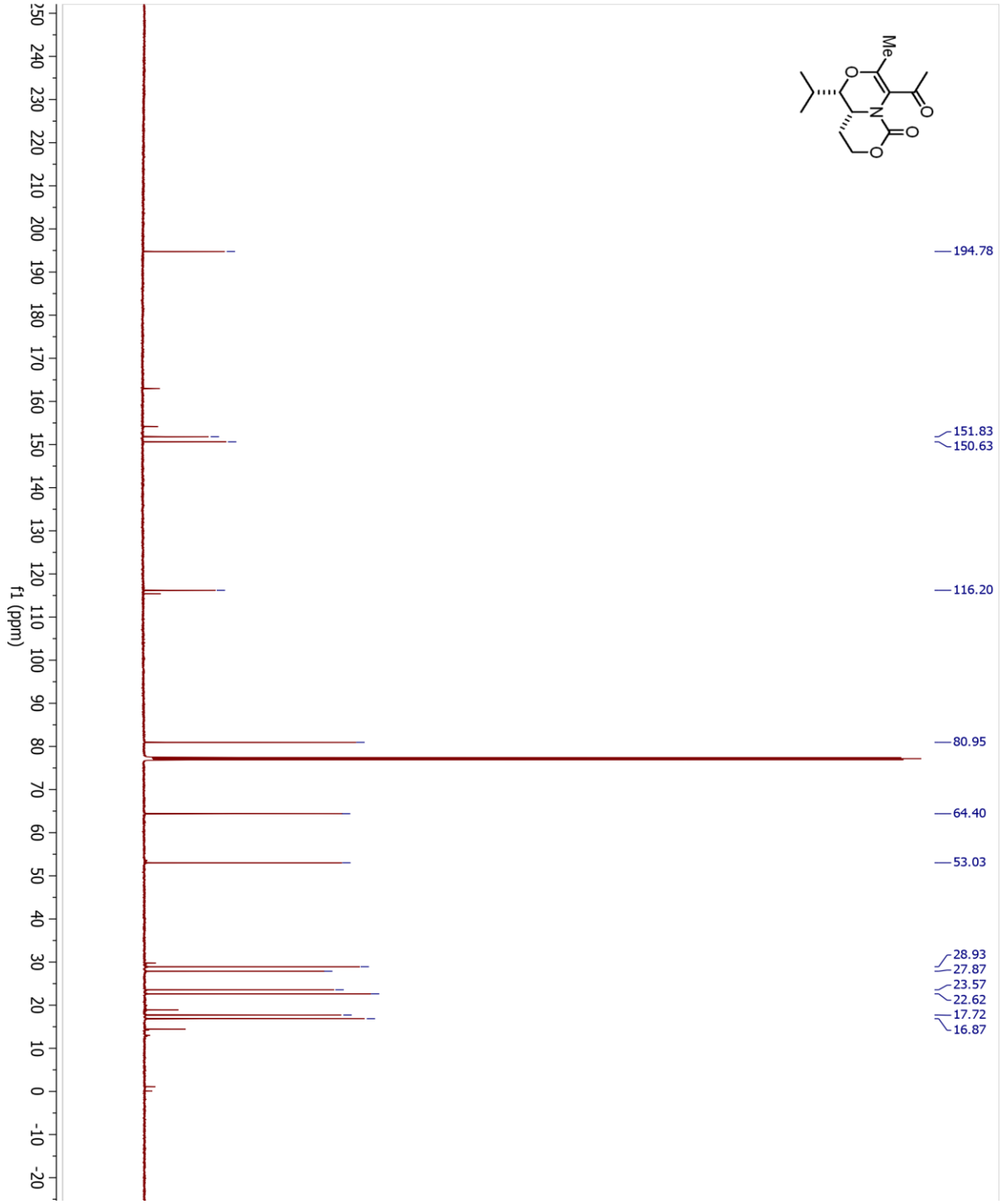
Compound **3.13f** · ^{13}C NMR (126 MHz, $CDCl_3$)



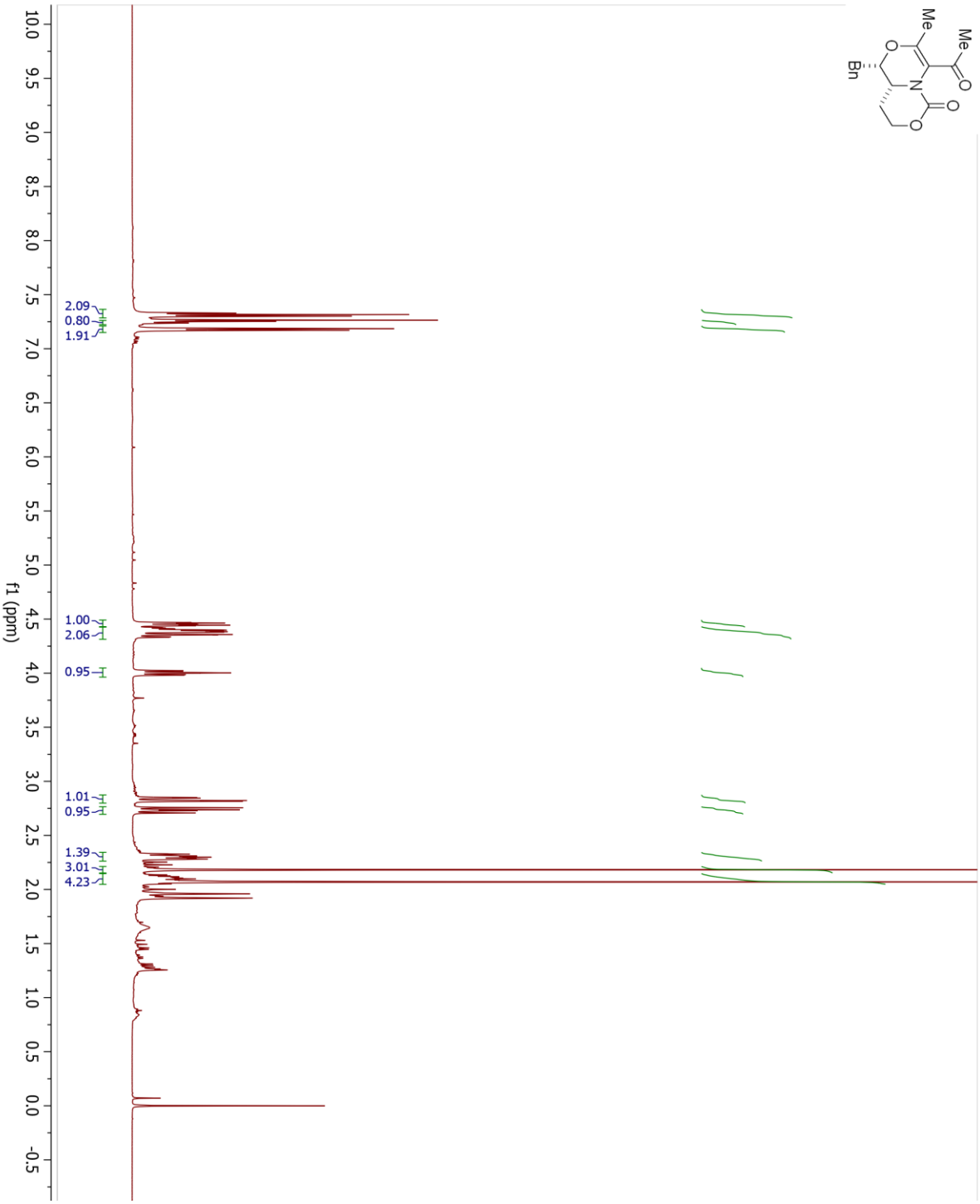
Compound **3.14f.** ^{1}H NMR (500 MHz, $CDCl_3$)



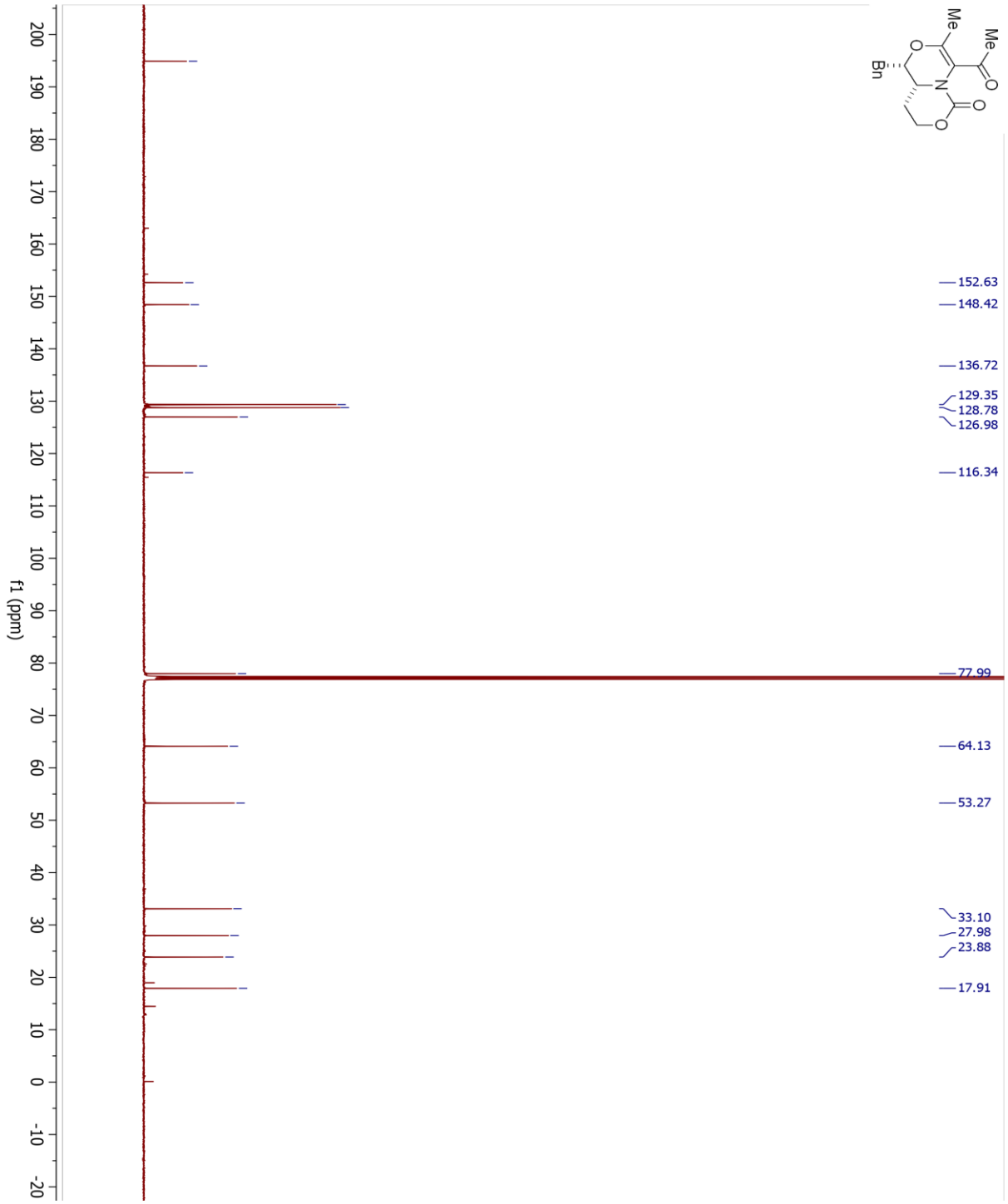
Compound **3.14f.** ^{13}C NMR (126 MHz, $CDCl_3$)



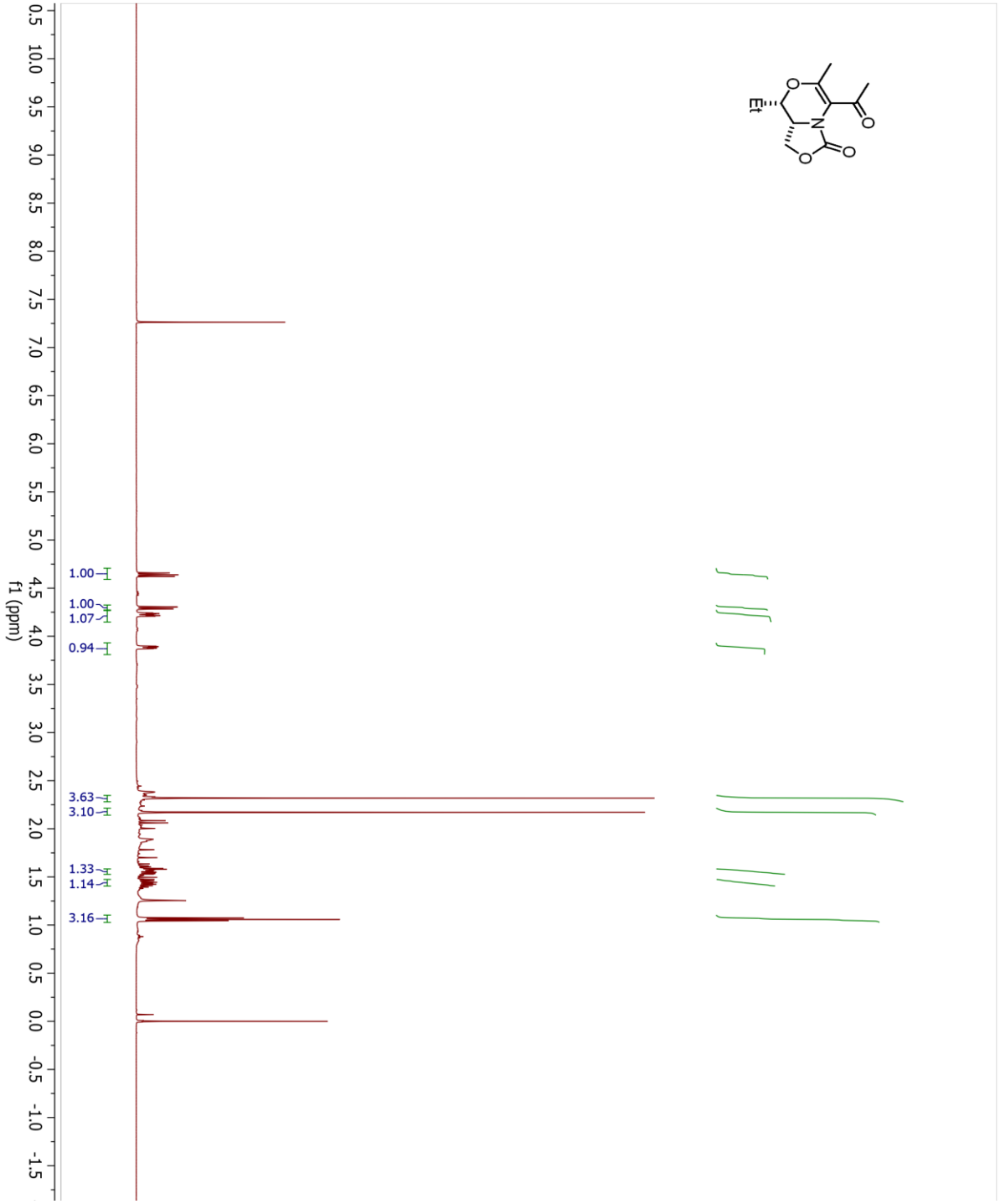
Compound **3.15f.** ^{1}H NMR (500 MHz, $CDCl_3$)



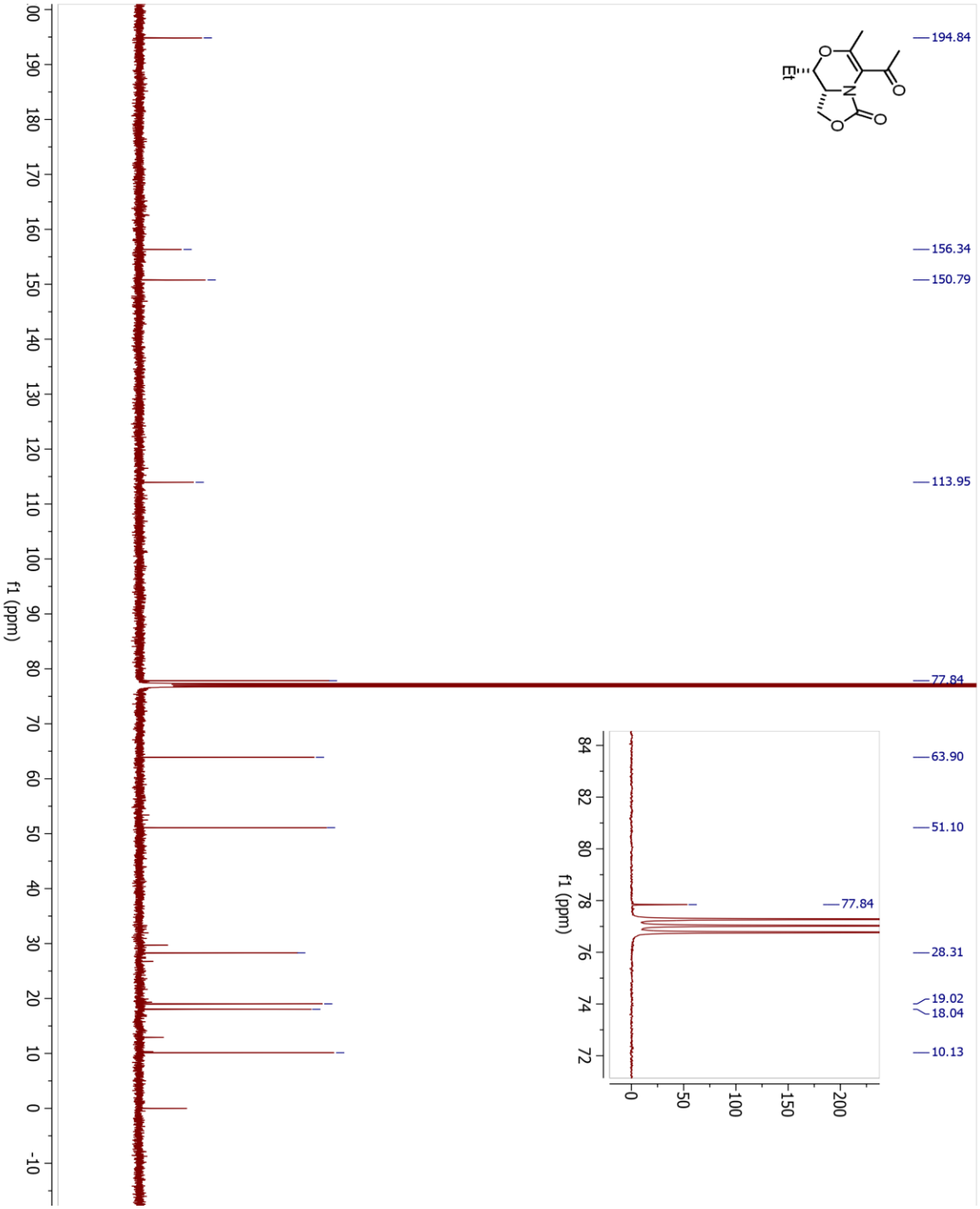
Compound **3.15f.** ^{13}C NMR (126 MHz, $CDCl_3$)



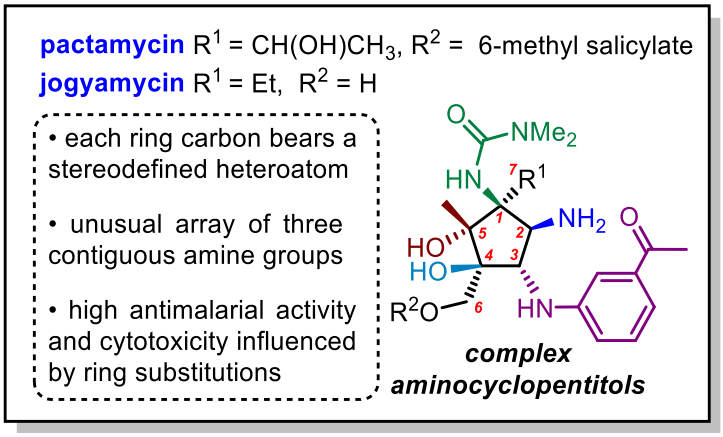
Compound **3.18.** ^{1}H NMR (500 MHz, $CDCl_3$)



Compound **3.18.** ^{13}C NMR (126 MHz, $CDCl_3$)



Chapter 4. Strategies for the Syntheses of Pactamycin and Jogyamycin



Parts of this chapter have been reprinted with permission from:

Gerstner, N. C.*; **Nicastri, K. A.***; Schomaker, J. M. Strategies for the Syntheses of Pactamycin and Jogyamycin. *Angew. Chem., Int. Ed.* **2021**, *60*, 14252–14271. *Indicates co-first authorship.

Copyright © 2021 John Wiley & Sons, Inc.

4.1 Introduction to Aminocyclopentitols

Natural products continue to capture the attention of synthetic chemists for their distinctive and complex molecular architectures. The aminocyclopentitol class of natural products, pactamycin **4.1**, pactamycin **4.2**, cranomycin **4.3** (**Figure 4.1**) represent a unique subgroup of natural products that have a dense network of functional groups that lead to a high degree of molecular complexity. In the aminocyclopentitol family, each cyclopentane core carbon bears one stereodefined heteroatom and three contiguous stereocenters that each possess an amine functionality. In fact, one paper expressed the opinion that this class of natural products was likely "inaccessible to synthesis!"[1] Their formidable structures, coupled with their high degree of antimalarial, antibacterial, and cytotoxic properties, make the aminocyclopentitols interesting targets for total synthesis.

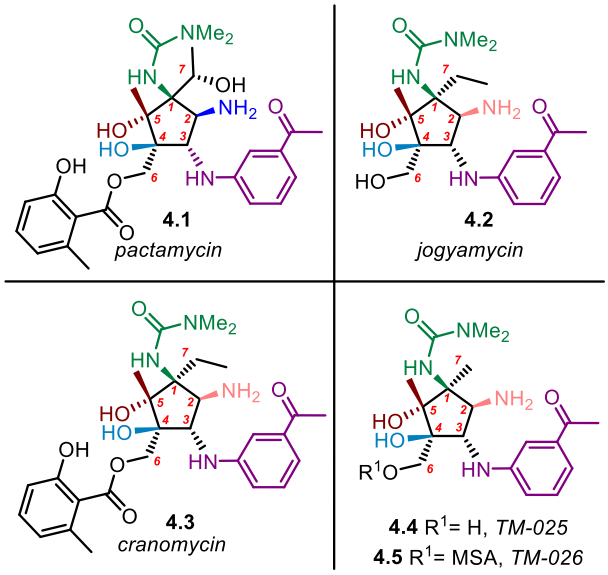
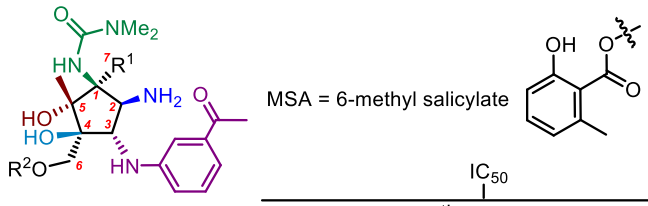
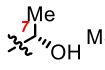


Figure 4.1 – The aminocyclopentitol family of natural products and genetically engineered analogues.

Pactamycin **4.1 (Figure 4.1)** is the most well-known natural product of this class and was first isolated from *Streptomyces pactum* in 1961.[2] Its structure was not assigned until 1972 when

Duchamp solved its single-crystal x-ray structure.[3] Cranomycin **4.3** (**Figure 4.1**), otherwise known as 7-deoxypactamycin, was isolated in 1964 from a culture broth of *Streptomyces SE-801*, and later found to be present in two other species of *Streptomyces*.[4a-d] One of the more recently discovered aminocyclopentitols is jogyamycin **4.2**, which was also isolated from a strain of *Streptomyces* in 2012 by Otogura, Omura and co-workers. [5] This natural product was named after the city of Jogjakarta, Indonesia where this particular strain of *Streptomyces* was first discovered. In addition to aminocyclitols isolated from natural sources, the Mahmud group has made great strides in identifying the gene cluster responsible for the biosynthesis of these molecules. This has enabled them to leverage their discoveries into producing genetically engineered analogues, including TM-025 and -026 (**4.4**, **4.5**). [6a-c]



				IC$_{50}$			
				antibacterial	anti-malarial	*T.b.b.*	cytotoxicity
R^1	R^2			*Staphylococcus*	*P. f.* [a,b]	*GUTat 3.1*[c]	*MRC-5*
	MSA	Pactamycin	**4.1**	10 μM	14.2 nM	7.4 nM	7 nM
Et	H	Jogyamycin	**4.2**	---	1.5 nM	12.3 nM	4 nM
Et	MSA	Cranomycin	**4.3**	50 μM	0.4 nM	0.9 nM	74 nM
Me	H	TM-025	**4.4**	> 1 mM	25-30 nM	---	>1000 nM[d]
Me	MSA	TM-026	**4.5**	> 1 mM	25-30 nM	---	>1000 nM[d]

[a] *Plasmodium falciparum* K1 (resistant). [c] *Trypanosoma brucei brucei.*
[b] *Plasmodium falciparum* Dd2 (resistant). [d] Evaluated using HCT116.

Figure 4.2 – Biological activity of the aminocyclopentitol family and genetically engineered analogues.

Pactamycin **4.1**, jogyamycin **4.2**, and their analogues all boast impressive biological activity (**Figure 4.2**). All of these molecules exhibit nanomolar levels of potency against strains of drug-resistant malaria.[5,6,7] However, the bioactivity is non-selective, with natural products **4.1-4.3**

all demonstrating nanomolar levels of cytotoxicity against MRC-5 cells which inhibits their therapeutic potential. Interestingly, genetically engineered analogues TM-025 **4.4** and TM-026 **4.5** have reduced mammalian cell cytotoxicity.[6c] The structural modifications that give rise to this change in biological activity are minor (methyl group at C1 and presence or absence of salicylate moiety on C7). Although these findings are encouraging, not all analogues are accessible through genetic engineering; as a result, new and modular approaches towards this class of natural products are need that are also capable of accessing key analogues.

As mentioned above, these aminocyclopentitols are well-known for their dense functionality. Each compound in **Figure 4.2** possesses three contiguous stereocenters, where each C1 bears a urea moiety, C2 bears a free amine, and C3 bears an aniline derivative. The C1/C4/C5 carbons of the core are contiguous quaternary centers that possess either an O- or N-containing substituent. Differentiation of these functional groups and preventing cross-reactivity are key in any proposed synthesis of the aminocyclopentitols. The stereochemistry also represents a unique challenge in this class of molecules, including the *syn*-relationship between the C1 urea and the C2 amine and the *trans*-relationship between the C4-C5 tertiary alcohols, which may cause unwanted cross reactivity. Unlike **4.2**-**4.5**, **4.1** bears an exocyclic secondary alcohol. Although the C7 alcohol appears to increase the complexity of the molecule, this stereocenter frequently serves as an effective lynchpin in synthetic strategies toward **4.1** by enabling the remaining stereocenters to be set through diastereoselective reactions. In contrast, jogyamycin **4.2** does not have this additional functional group, and as a result, any successful strategy toward **4.2** needs to be reimagined.

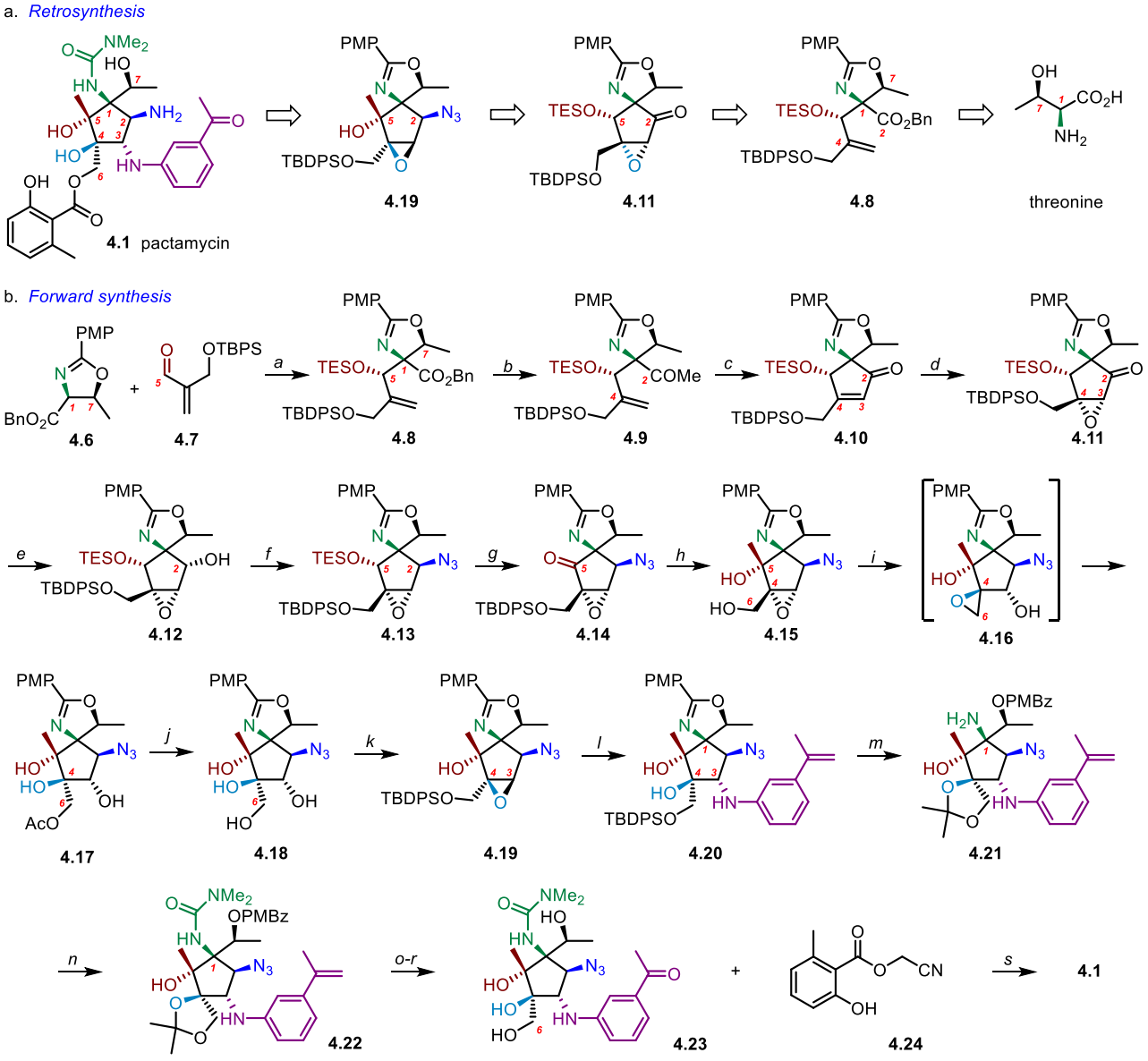
4.2 Syntheses of Pactamycin

4.2.1 Hanessian's Total Synthesis of Pactamycin

More than 50 years after it was isolated, Hanessian and co-workers achieved a considerable milestone in 2011 by reporting the first and asymmetric total synthesis of **4.1.** [8] Key to their success was establishing the *trans* stereochemistry between the C4 alcohol and the C3 aniline *via* a late-stage ring-opening of epoxide **4.19** by the aniline (**Scheme 4.1a**). The urea was generated through hydrolysis of a C1/C7 cyclic oxazolidinone in **4.19**, while the C2 amine was masked as an azide. The C2 azide originated from carbonyl functionalization and the C5 3° alcohol from a 2° alcohol in **4.11**. The 2° alcohol of **4.8** was to be formed by a reliable aldol reaction employing a key intermediate obtained from threonine.

The forward synthesis commenced with oxazolidinone **4.6**, available in three steps from threonine. Aldol reaction of **4.6** with **4.7** afforded **4.8** in good yield after protection (**Scheme 4.1b**). This key transformation established the correct C1 stereochemistry, as dictated by the C7 stereocenter; while the C5 stereocenter is temporary, it plays a critical role in contributing to the overall sterics that likely impact the *dr* of several subsequent steps. Conversion of **4.8** to cyclopentenone **4.10** involved alkene ozonolysis and a two-step aldol condensation. Nucleophilic epoxidation of **4.10** with $NaOH/H_2O_2$ gave **4.11**. While the C3/C4 stereochemistry in **4.11** is the opposite orientation than initially predicted, this was corrected later in the synthesis. The inability to predict the correct stereochemistry of the epoxidation reaction further underscores the difficulty in predicting stereochemical outcomes of these highly functionalized cyclopentene intermediates.

Scheme 4.1 – a. Retrosynthetic analysis of Hanessian's route to pactamycin **4.1** b. Forward route to pactamycin **4.1.**



a) i) LiHMDS, **4.7**, THF, ii) TESOTf, 2,6-lutidine, CH_2Cl_2, 67%; b) i) DIBAL-H, CH_2Cl_2, -78 °C, ii) MeMgBr, Et_2O, 0 °C, iii) $(COCl)_2$, DMSO, NEt_3 CH_2Cl_2, -78 °C, 67%; c) i) O_3, CH_2Cl_2, then Me_2S, ii) *i*-Pr_2NEt, $TiCl_4$, TMSCl, CH_2Cl_2, iii) Cl_3CCOCl, pyr., CH_2Cl_2, 64%; d) H_2O_2, NaOH, MeOH, CH_2Cl_2, 75%; e) $NaBH_4$, $CeCl_3$-$7H_2O$, MeOH, CH_2Cl_2, 92%; f) Tf_2O, pyr., -78 °C to 0 °C, then *n*Bu_4NN_3, PhMe, 87%; g) i) TFA, MeCN, H_2O, ii) DMP, CH_2Cl_2, 89%; h) MeMgBr, THF, then TBAF, THF, 86%; i) $Zn(OTf)_2$, AcOH; j) K_2CO_3, MeOH, 87% from **4.15**; k) TBDPSCl, Et_3N, DMAP, then Tf_2O, pyr., 94%; l) aniline, $Yb(OTf)_3$, PhMe, 81%; m) 2 M HCl, THF, then TASF, DMF, then 2,2-dimethyoxypropane, CSA, CH_2Cl_2, 68%; n) diphosgene, Et_3N, activated charcoal, THF, then Me_2NH, 86%; o) DIBAL, CH_2Cl_2; p) cat. OsO_4, NMO, THF, acetone, H_2O; q) $NaIO_4$, THF, H_2O, r) TFA, MeCN, H_2O, 61% from **4.22**; s) **4.24**, K_2CO_3, DMA, then Zn, NH_4Cl, EtOH, H_2O, 85%.

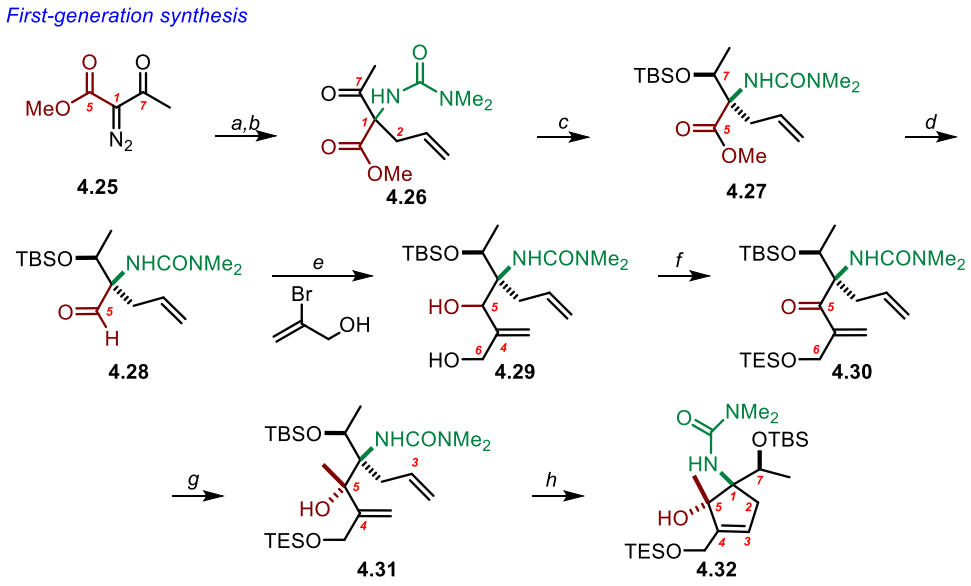
Conversion of the C2 ketone of **4.11** into the azide in **4.13** was achieved *via* Luche reduction to give **4.12** as a single diastereomer. Hanessian comments that reduction of **4.11** showed high stereoselectivity utilizing a variety of reduction methods, suggesting greater steric accessibility and thus a substrate preference for reduction from the top face of **4.11**. Activation of the alcohol with Tf_2O and displacement with Bu_4NN_3 gave **4.13** in excellent yield. At this point, Hanessian converted the C5 2° alcohol in **4.13** to the 3° alcohol of **4.15** in four steps. Organometallic addition to the ketone **4.14** proceeded smoothly, even though the C5 ketone is flanked by fully substituted carbons at C1 and C4. This step fails in the Trost route (**Scheme 4.5,** *vide infra*) when a C4 alcohol is present, Hanessian's use of an epoxide may alter the puckering in the cyclopentane ring, making the ketone more accessible. Next, the C4 stereochemistry in **4.15** was inverted *via* a Payne rearrangement to **4.16**, where the epoxide was opened with acetic acid at the less substituted carbon. Cleavage of the acetate ester gave **4.18** in good yield.

The final sequence of steps required protection of the C6 alcohol and reformation of the epoxide in **4.19** with the correct stereochemistry required for $Yb(OTf)_3$-catalyzed aniline ring-opening to set the final stereocenter in **4.20**. Attempts to transform the oxazolidinone into the urea via hydrolysis under acidic conditions and subsequent reaction of the sterically hindered 1° amine proved problematic, as the C4 alcohol engages the intermediate to form a cyclic carbamate. A workaround solution involved desilylation of **4.20** and formation of acetal **4.21** to tie up the C4 alcohol. Isocyanate formation and trapping with Me_2NH gave urea **4.22**; cleavage of C7 ester, unmasking of the aniline carbonyl and deprotection of the C4/C6 diol yielded **4.23**. Acylation of the C6 alcohol with **4.24** and reduction of the C2 azide furnished **4.1** in 32 steps from threonine, marking a landmark achievement in the syntheses of aminocyclopentitol natural products.

4.2.2 Johnson’s Total Synthesis of Pactamycin

In 2012, the Johnson group published a racemic route to the core of **4.1** (**Scheme 4.2**) that informed their future efforts that culminated in a successful total synthesis.[9] Instead of delaying installation of the urea, Johnson chose to introduce it early in the synthesis. Rh-catalyzed insertion of **4.25** into the N-H urea bond was followed by Pd-catalyzed Tsuji-Trost alkylation to furnish the C-alkylated **4.26**. Diastereoselective ketone reduction with L-Selectride gave the desired *syn* C1-C7 relationship in **4.27** after TBS protection. The ester of **4.27** was converted to enone **4.30** in five steps. Chelation-controlled addition of MeMgBr to **4.30** gave **4.31** in >20:1 *dr*. The final cyclopentene **4.32** was formed *via* ring-closing metathesis. Although this route appeared promising, the authors eventually encountered challenges in their efforts to install both the C3 and C4 nitrogen functional groups. Efforts toward allylic amination or oxidation of the C3/C4 methylene were unsuccessful. Ultimately, these issues were avoided by the early installation of the C2 amine.

Scheme 4.2 – Johnson's partial route to pactamycin.



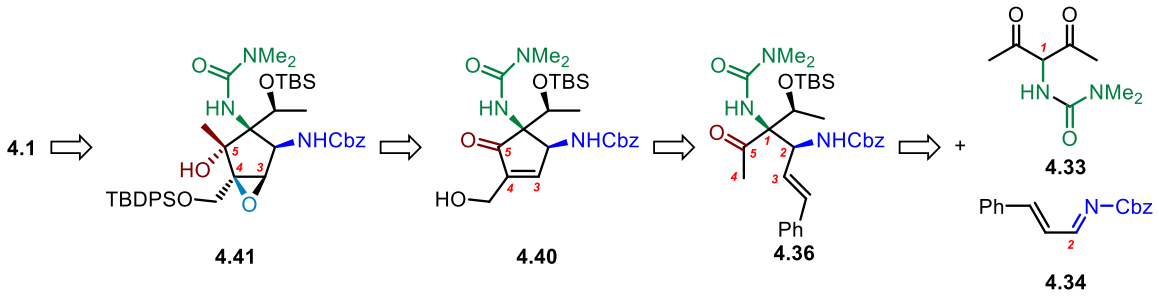
a) cat. $Rh_2(oct)_4$, Me_2NCONH_2, 1,2-DCE/PhMe, 80 °C, 79%; b) cat. [allylPdCl]$_2$]BINAP, allyl acetate, KO*t*Bu, PhMe, 77%; c) L-Selectride, -78 °C, THF, then TBSOTf, 2,6-lutidine, 0 °C to rt, CH_2Cl_2, 68%; d) DIBAL, CH_2Cl_2, 0 °C, then DMP, CH_2Cl_2, 89%; e) MeMgBr, *t*BuLi, Et_2O, -78 °C to rt, 62%; f) TESCl, DMAP, Et_3N, CH_2Cl_2, then DMP, CH_2Cl_2, 73%; g) MeMgBr, $CeCl_3$, THF, -78 °C, 88%, >20:1 *dr*; h) cat. Grubbs II, CH_2Cl_2, 85%.

In their second-generation asymmetric route, published in 2013, Johnson envisaged an endgame similar to Hanessian's (**Scheme 4.1,** *vide supra)* where the C3/C4 epoxide of **4.41** would be opened by an aniline (**Scheme 4.3a**). A key difference is that Johnson did not utilize a C2 azide or mask the C1 urea as an oxazolidinone. The C5 alcohol in **4.41** resulted from organometallic attack on a ketone, while the epoxide was derived from enone **4.40**, which in turn arose from **4.36** obtained by an asymmetric Mannich/desymmetrization of urea **4.33** and imine **4.34**.[10]

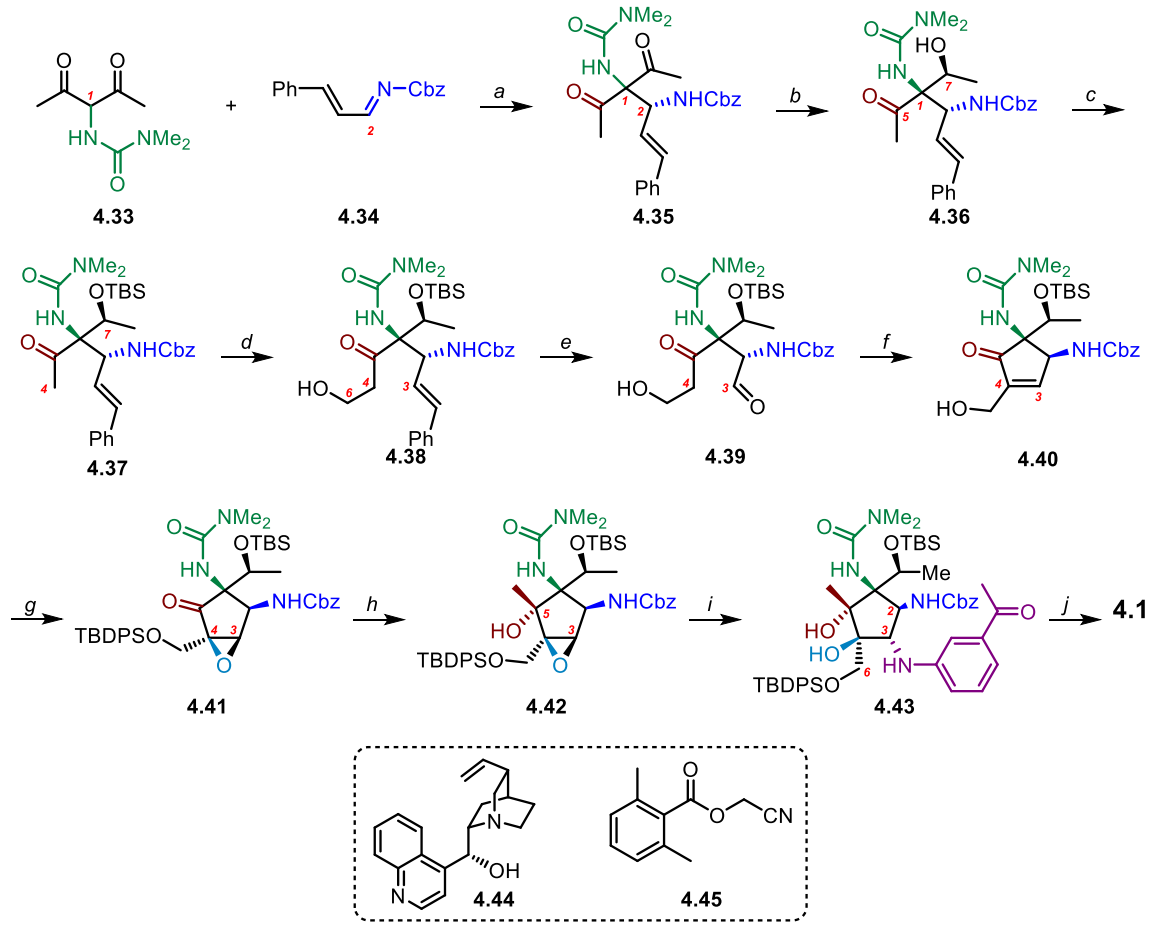
In the forward synthesis, asymmetric Mannich reaction of **4.33** and **4.34** catalyzed by Cinchona alkaloid **4.44** (**Scheme 4.3b**) gave **4.35** in 98:2 *er* after a single recrystallization. Although the C2 amine stereochemistry is incorrect in **4.35** this error serves as a way to control the installation of additional stereocenters and was ultimately corrected later in the synthesis. Desymmetrization of **4.35** with $LiAlH(O\textit{t}\text{-}Bu)_3$ established the C7 and C1 stereochemistry of **4.36** in one powerful step. Formation of the cyclopentene involved silylation of the C7 alcohol of **4.36**, followed by an aldol between **4.37** and formaldehyde to form the C4/C6 bond in **4.38**. Ozonolysis and aldol condensation gave enone **4.40**, where epimerization corrects the C2 stereocenter. Directed epoxidation of **4.40** from the same face of the Cbz protected C2 amine, followed by TBDPS protection of the C6 alcohol resulted in **4.41**. Addition of MeMgBr to **4.41** proceeded cleanly to furnish **4.42** in >10:1 *dr*; interestingly, the nucleophile approaches from the same face as the epoxide, in contrast to Hanessian's work. The authors hypothesize that the concave trajectory of the nucleophile may be in part directed from the adjacent urea functionality. This stereochemical outcome underscores the difficulty in predicting facial selectivity in nucleophilic addition to sterically congested cyclopentanones. The epoxide of **4.42** was opened with *m*-acetylaniline to furnish **4.43**. A global desilylation, esterification of the C6 alcohol, and deprotection of the C2 amine gave the desired target **4.1**.

Scheme 4.3 – Retrosynthetic analysis of Johnson's successful route to pactamycin **4.1** b. Forward route of Johnson's successful synthesis of pactamycin **4.1.**

a. *Retrosynthesis*



b. *Second-generation synthesis*



a) cat. **4.44**, CH_2Cl_2, -65 °C, 70%, 98:2 *er*; b) $LiAl(O^tBu)_3H$, THF, -40 °C, 72%, >10:1 *dr*; c) TBSOTf, 2,6-lutidine, CH_2Cl_2, -78 °C, 88%; d) LDA, $H_2CO_{(g)}$, THF, -78 °C to -45 °C 70%; e) O_3, CH_2Cl_2, -78 °C then Me_2S, -78 °C to rt; f) NaOMe, THF, MeOH, 0 °C, 50% over 2 steps; g) *i*) H_2O_2, NaOH, CH_2Cl_2, MeOH, 0 °C, *ii*) TBDPSCl, Et_3N, DMAP, CH_2Cl_2, 0 °C to rt, 62%; h) MeMgBr, THF, 0 °C, 75%; i) 3-acetyl-aniline, $Sc(OTf)_3$, PhMe, 60 °C, 66%; j) *i*) TBAF, THF, 0 °C, *ii*) **4.45**, K_2CO_3, DMA, *iii*) H_2, $[Pd(OH)_2/C]$, 59%.

4.2.3 Concluding Thoughts

Johnson's overall synthesis is only 14 steps from commercially available starting materials, a step count less than half of the Hanessian synthesis, despite thematic similarities between the two approaches. Both groups employ an aldol-type reaction to form the new C1 bond, where the C7 stereocenter dictates the C1 stereochemistry. In both approaches, the cyclopentane ring is formed *via* aldol condensation. The C5 stereocenter is set in a Grignard addition to a ketone and both employed a diastereoselective nucleophilic C3/C4 enone epoxidation. The end games are the same, relying on nucleophilic opening of an epoxide to establish the C3 aniline. The difference in step count is largely due to Johnson's focus on adding the functional groups to the cyclopentane core in their final form and in the correct orientation, particularly in the case of the urea. Hanessian required two steps to mask the C1 urea as an oxazolidinone and four steps to cleave it and form the urea, manipulations not needed in the Johnson route. Hanessian also needed six steps to transform the carboxylic acid of threonine into the C2 azide, whereas Johnson introduced it in a single step. Finally, Johnson obtained the C3/C4 epoxide with the correct stereochemistry, whereas Hanessian is forced to install the epoxide from the opposite face and then invert the stereochemistry. Thus, Johnson's approach represents an elegantly streamlined version of the Hanessian synthesis.

Successful application of Johnson's work to the synthesis of 7-deoxy analogues is unlikely, as setting the C1/C7 stereocenters is key to the success of this synthesis; utilizing the same Mannich reaction for the synthesis of **4.2** would require removal of the C7 alcohol. Indeed, Johnson explored this possibility in 2015, but reported “reduction of the C7 hydroxyl to its corresponding methylene was also probed. Unfortunately, all conditions explored (from a number of different

intermediates in our route) failed to deliver the desired C7 methylene." [11] This offers a compelling argument for a new strategy to access **4.2.**

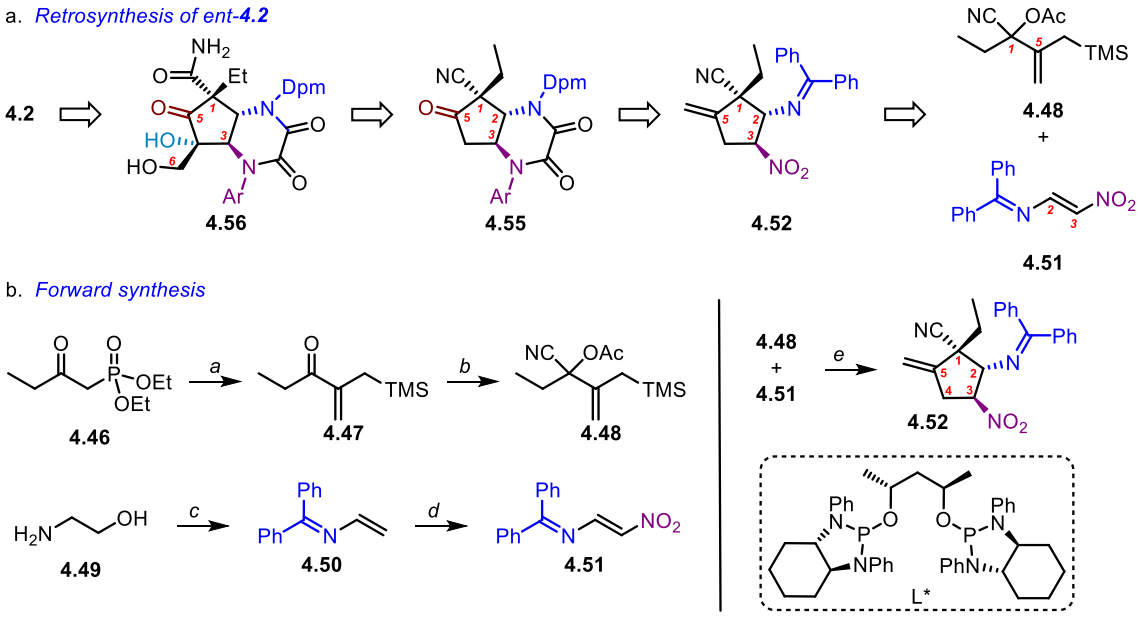
4.3 Syntheses of the Core of Jogyamycin

Although a successful total synthesis of **4.2** has not yet been achieved, approaches to the core of **4.2** have been reported. The following section will detail accounts of these attempts, the issues surrounding them, and the ways these challenges may be surmounted in the future.

4.3.1 Trost's Progress Toward the Synthesis of Jogyamycin

In 2018, Trost and co-workers reported an asymmetric route to the core of **4.2**. [12] The C1 urea was incorporated *via* a late-stage Hofmann rearrangement of an amide in **4.56** (**Scheme 4.4a**), with the C5 3° alcohol formed from an organometallic addition, and oxidation at C4 and C6 achieved through alkene dihydroxylation. The C3 aniline and C2 amine were protected in **4.55** as an oxalamide, while the amide in **4.56** was to be formed from nitrile hydrolysis. The C5 ketone and C4 alkene resulted from ozonolysis of **4.52**, followed by aldol condensation. The C2 imine of **4.52** was formed by a Pd-catalyzed trimethylene methane (TMM) [3+2]-cycloaddition of **4.48** and **4.51**. This clever synthetic plan proposed the formation of chemically differentiated amines at the beginning of the synthesis, leaving the installation of more robust oxygenated functionality until the endgame.

Scheme 4.4 – a. Retrosynthetic analysis of Trost's partial synthesis of jogyamycin **4.2** b. Forward synthesis of Trost's partial synthesis of jogyamycin **4.2.**



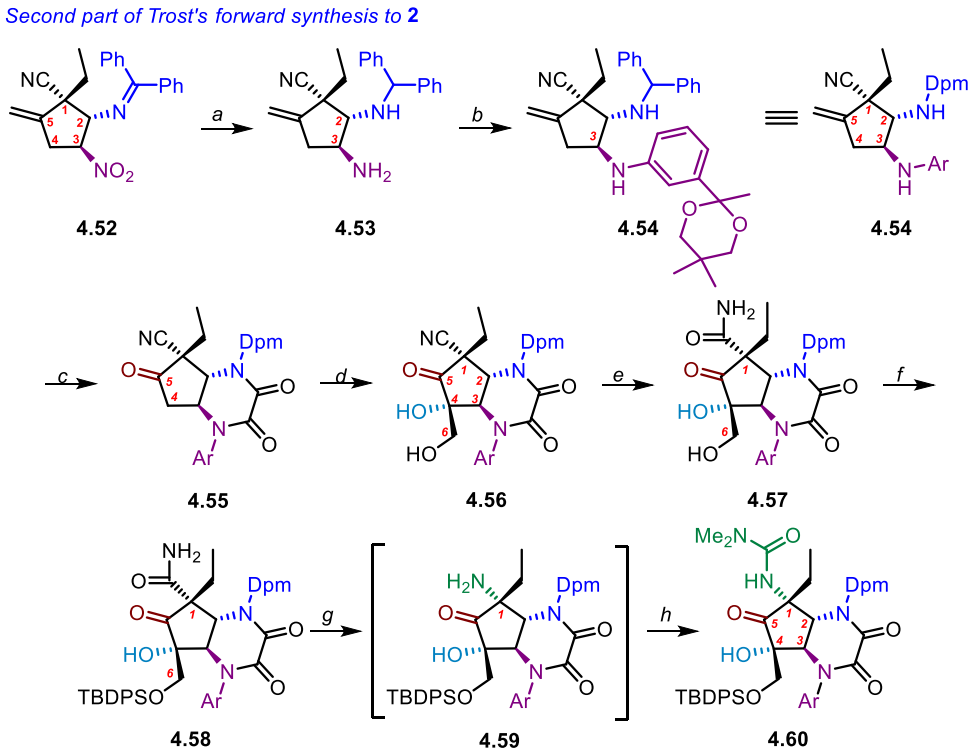
a) ICH_2TMS, Cs_2CO_3, DME, 60 °C, then CH_2O, K_2CO_3, rt, 67%; b) *i*) cat. ZnI_2, TMSCN, 0 °C; *ii*) cat. TMSOTf, Ac_2O, MeCN, 0 °C, 71%; c) *i*) Ph_2CO, cat. AcOH, benzene, 120 °C; *ii*) MsCl, Et_3N, CH_2Cl_2, 0 °C; *iii*) KO*t*Bu, THF, 0 °C, 76%; d) $AgNO_2$, cat. TEMPO, 4A MS, 1,2-DCE, 70 °C, 64%; e) cat. [Pd(allyl)Cp]/L*, $B(OEt)_3$, Et_2BOMe, dioxane, 60 °C, 95%, 13:1 *dr*, 89% *ee*.

The forward synthesis required routes to the precursors for the TMM cycloaddition (**Scheme 4.4b**). Cyanoacetate **4.48** was available in three steps from **4.46** using standard chemistry. A scalable route to **4.51** was achieved in four steps from 2-ethanolamine **4.49**. Conditions for the TMM reaction use a combination of $B(OEt)_3$ and Et_2BOMe and a diamidophosphite ligand which gave **4.52** in 13:1 *dr* and 89% *ee*. For reasons not discussed, the authors used the (*S,S,R,R,S,S*) version of the ligand, which is predicted to give the opposite enantiomer of **4.2**.[13] No crystal structure was obtained to confirm the absolute stereochemistry of the cycloadduct; presumably, the remainder of the synthesis was conducted using the unnatural enantiomer.

Advancement of **4.52** involved reduction of both the nitro group and the benzophenone imine with SmI_2 to furnish **4.53** (**Scheme 4.5**). The C3 aniline was formed *via* a Buchwald-Hartwig

coupling, which delivered the protected aniline **4.54** in 86% yield. Problematic protection of the C2/C3 diamine was solved using oxalyl chloride to force the C2 amine in close proximity to the acyl chloride to form oxalamide.

Scheme 4.5 – Second half of Trost's partial synthesis of jogyamycin **4.2.**



a) SmI_2, THF/H_2O, 85%; b) cat. XPhos-Pd-GII/XPhos, Ar-Br, Cs_2CO_3, dioxane, 100 °C, 86%; c) *i*) $(COCl)_2$, Et_3N, *ii*) O_3, CH_2Cl_2, -78 °C, then Me_2S, 73%; d) *i*) Ac_2O, $(Me_2N)_2CH_2$, dioxane, 0 °C; *ii*) OsO_4, $(DHQ)_2PHAL$, THF, -78 °C, 75%; e) cat. $Pt(Me_6P_3OH_3)$, EtOH, H_2O, 45 °C, 92%; f) TBDPSCl, imidazole, CH_2Cl_2, reflux, 90%; g) PhINTs, CH_2Cl_2, 0 °C, then h) triphosgene, pyr., CH_2Cl_2, -78 °C, then Me_2NH, 84%.

Ozonolysis of the C4 alkene delivered **4.55** and serves as an inflection point in the synthesis, where the focus turned to functionalization of C1, C4, and C5. C4 α-methylenation of ketone **4.56** failed with basic conditions; fortunately, Ac_2O and $(Me_2N)_2CH_2$ proved fruitful. The resulting exocyclic enone was sensitive to polymerization; thus, it was quickly subjected to stoichiometric OsO_4 and $(DHQ)_2PHAL$ to give the correct diastereomer of **4.56**. Attempts to run the dihydroxylation reaction with the pseudo enantiomer, $(DHQD)_2PHAL$, led to poor conversion

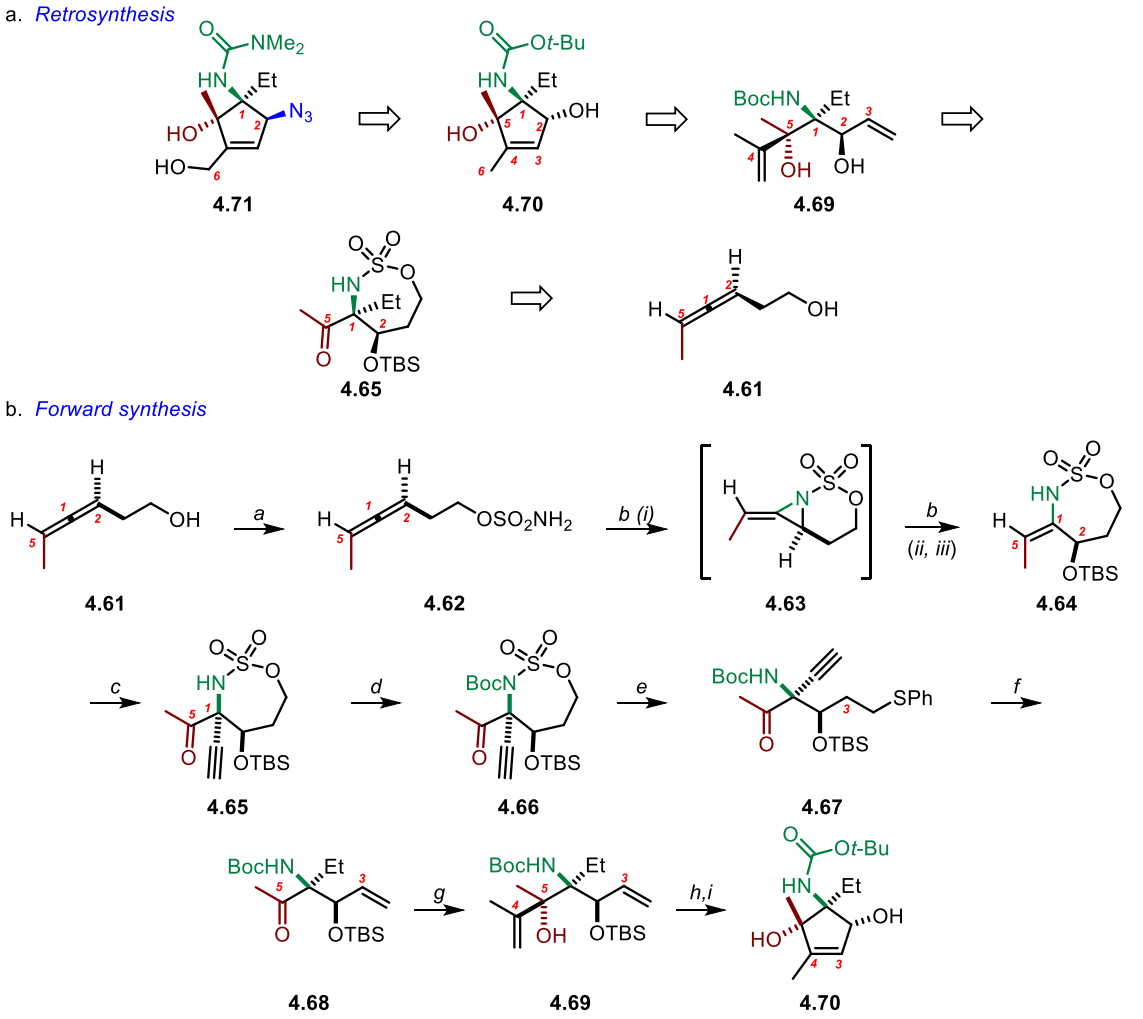
and mismatched diastereoselectivity. The next sequence of steps transformed **4.56** to a precursor suitable for the Hoffman rearrangement through nitrile hydrolysis with the Parkins-Ghaffar catalyst to yield **4.57**. Protection of the 1° alcohol, followed by PhINTs-mediated amide isomerization gave an unstable isocyanate that rapidly hydrolyzed to the amine **4.59**. Ultimately, **4.59** was converted to a carbamoyl chloride with triphosgene and quenched with Me_2NH to furnish **4.60**. The only remaining steps involved addition of a methyl group to **4.60** to form a C5 3° alcohol, followed by final deprotection. Unfortunately, the ketone proved resistant towards nucleophilic attack by Grignard reagents, MeLi, or $AlMe_3$. Addition of $CeCl_3$ did not help and the only product resulted from cleavage of the oxalamide. The failure of this creative route to **4.2** highlights how even very robust reactions, such as the addition of organometallic reagents to ketones, can be challenging in this complex and congested system. The steric hindrance posed by the flanking C1 and C4 fully substituted stereocenters likely plays a role in the failure of this reaction to occur. Careful consideration of the endgame of any synthesis within this family of molecules is critical, as many seemingly reliable reactions have met with unexpected failures. Despite this unfortunate setback, the Trost route accesses four of the stereocenters on the ring without requiring oxygenation at C7. It also successfully differentiated the C1, C2, and C3 amines, a noteworthy accomplishment.

4.3.2. Schomaker Group Allene Aziridination Approach

Before Trost's report in 2018**,** the Schomaker group was the first to report a strategy to construct the core of jogyamycin **4.2** (**Scheme 4.6**), by an approach that would enable access to unusual C7-deoxy analogues unavailable through bioengineering.[14] The retrosynthesis (**Scheme 4.6a**) employs the Hanessian end game, where the C3 C-N bond forms by opening an epoxide obtained via directed epoxidation of **4.71**. Intended late-stage introduction of the C6 alcohol by allylic oxidation

of **4.70** simplified the synthesis, allowing for greater flexibility in forming the key C4/C5 bond. The C2 allylic amine rose from manipulation of the C2 alcohol, **4.70**. Ring-closing metathesis of **4.69** installed the C3/C4 alkene, while the C4/C5 accessible from allene **4.61** using chemistry developed by the Schomaker group. [15a-c]

Scheme 4.6 – a. Retrosynthetic analysis to Schomaker's allene aziridination strategy to the ore of Jjogyamycin **4.2** b. Forward route to the core of jogyamycin **4.2.**



a) $ClSO_2NCO$, HO_2CH, MeCN, DMA, 0 °C, 90%; b) *i*) 1 mol% $Rh_2(OAc)_4$, PhIO, CH_2Cl_2, rt, *ii*) H_2O/MeCN, rt, *iii*) TBSOTf, lutidine, CH_2Cl_2, 0 °C, 50%, 3 steps; c) DMDO, CH_2Cl_2, rt, then HCCMgBr, THF, 0 °C, then DMP, 68%, 11.5:1 *dr*; d) Boc_2O, DMAP, Et_3N, THF, 91%; e) PhSH, K_2CO_3, MeCN, rt, 15 h, 98%; f) *i*) 30% H_2O_2, thiophenol, rt, *ii*) 750 psi H_2, 5% Pd/C, EtOAc, *iii*) $NaHCO_3$, xylene, 130 °C, 68% over 3 steps; g) isopropenylMgBr, $CeCl_3$•2LiCl, THF, -40 °C, 61%, >20:1 dr; h) TBAF, THF, 60%; i) 5 mol % Grubbs II, PhMe, 91%.

The forward synthesis toward the racemic core of **4.2** commenced with homoallenic alcohol **4.61**, prepared in two steps from commercially available material (**Scheme 4.6b**). Sulfamate **4.62** was subjected to an oxidative aziridination/ring-opening/silylation sequence to furnish **4.64** in >20:1 *E:Z*, a process that forms both the C2 alcohol stereocenter and the C1 amine in a single step. Oxidation of the enesulfamate **4.64** with DMDO, followed by addition of a pre-cooled solution of ethynylmagnesium bromide at 0 °C to the intermediate imine, delivered **4.65** in good yield and 11.5: 1 *dr*. The *dr* of the Grignard addition to the imine is rationalized by its preference to approach opposite the bulky C2 silyl ether, as smaller C2 protecting groups gave lower *dr*. Attempts to install the urea in **4.65** using dimethylcarbamoyl chloride or methyl isocyanate failed, perhaps due to steric congestion. Instead, the nitrogen of **4.65** was protected with Boc_2O to afford **4.66** in excellent yield. Direct hydrolysis of the sulfamate of **4.66** proved intractable; thus, **4.66** was ring-opened with PhSH to give **4.67**. Alkyne reduction was sluggish in the presence of the thioether; thus, it was oxidized to a sulfoxide with H_2O_2. The less Lewis basic sulfoxide enabled hydrogenation to proceed smoothly; sulfoxide elimination in hot xylenes formed alkene **4.68** over a three-step sequence from **4.67**. Introduction of a second alkene into **4.68** was achieved by addition of isopropenylmagnesium bromide to the C5 ketone mediated by $CeCl_3 \cdot 2LiCl$ to deliver **4.69**, where the high *dr*, >20:1, likely results from chelation control. To prepare **4.69** for the RCM, the TBS group was removed; treating the product with catalytic Grubbs II gave cyclopentenediol **4.70** in excellent yield. The diol stereochemistry was confirmed *via* NOESY experiments.

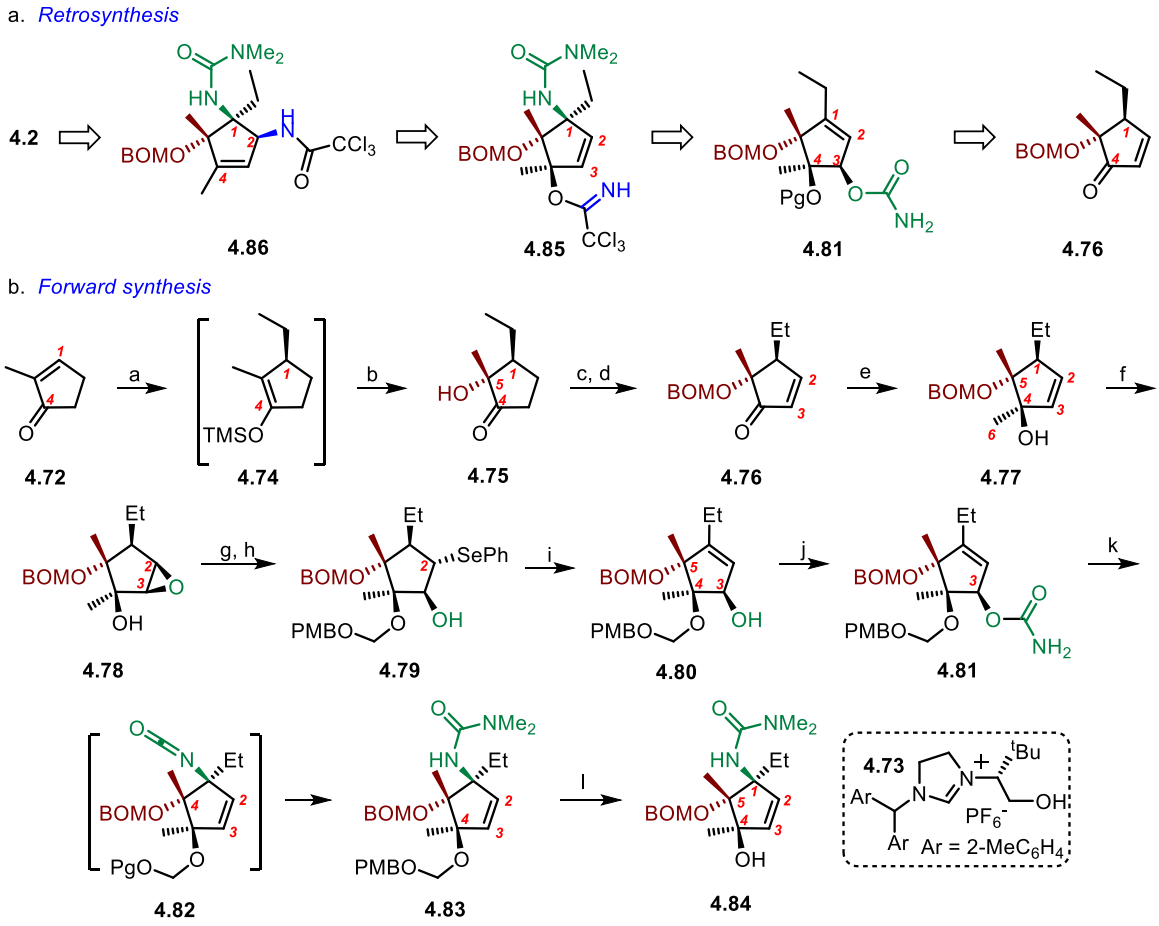
Overall, diol **4.70** was synthesized in 15 steps from **4.61**. Unfortunately, the inability to establish the C1 stereocenter by direct addition of EtMgBr to the imine, due to undesired hydride reduction, adds three steps to the sequence. In addition, unsuccessful formation of the urea in **4.65**

forced Schomaker into the situation faced by Hanessian, where a late-stage installation significantly increases step count. Finally, concern over the efficiency of transforming the C2 alcohol to an amine prompted the Schomaker group to consider an alternative approach (**Scheme 4.7**). Nonetheless, the flexibility afforded in the oxidative aziridination sequence, where diverse nucleophiles are able to open the aziridine or add to the imine, makes this approach ideal for preparing analogues not easily obtained with other routes.

4.3.2. Schomaker Group Overman/Ichikawa Approach

To address concerns in the 1st-generation approach, especially in forming the C2 amine, the Schomaker group envisaged a sequential Ichikawa/Overman rearrangement strategy which was reported in 2019 (**Scheme 4.7a**).[16] The C2 amine was to be generated from Overman rearrangement of **4.85**, itself formed from Ichikawa rearrangement of carbamate **4.81**. The viability of this disconnection was strengthened by the potential to form the C2 amine via a second Ichikawa rearrangement, alleviating some risk if the Overman were to fail. The *cis* C3/C4 diol in **4.79** was to rise from manipulations of enone **4.76**, accessible in a few steps from 2-methyl-2-cyclopenten-1-one.

Scheme 4.7 – a. Retrosynthetic analysis of Schomaker's Ichikawa/Overman rearrangement strategy to jogyamycin **4.2** b. Forward route to the core of jogyamycin **4.2.**

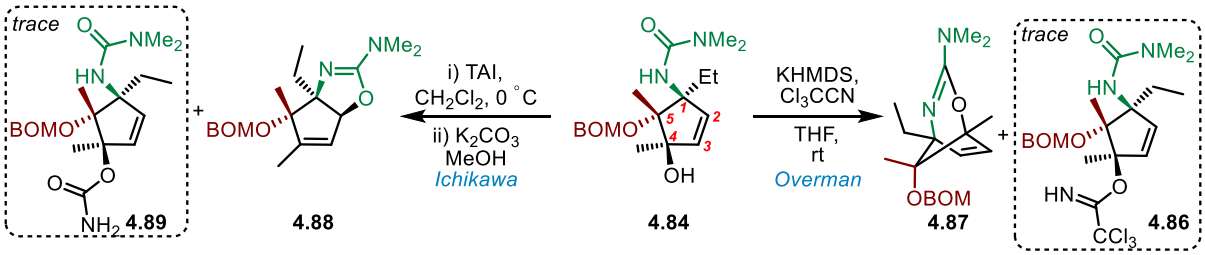


a) *i*) 0.75 mol% $Cu(OTf)_2$, 1 mol% **4.73**, EtMgBr, Et_2O, -30 °C, *ii*) HMPA, TMSCl, Et_3N, *iii*) silica filter; b) i) DMDO, acetone, CH_2Cl_2, -78 °C, *ii*) NH_4F, MeOH, -78 °C to rt, 52%, 1.4:1 *dr*; c) BOMCl, *i*Pr_2NEt, CH_2Cl_2, 78%; d) *i*) NaHMDS, TMSCl, THF, -45 °C, *ii*) IBX, DMSO, 4-MeO-pyridine oxide, CH_2Cl_2, overnight, 58%, 73% brsm; e) MeMgBr, $CeCl_3$•2LiCl, THF, -78 Â°C, then f) $VO(acac)_2$, *t*BuOOH, CH_2Cl_2, 0 °C to rt, 78%, >20:1 *dr*; g) $PMBOCH_2Cl$, *i*Pr_2NEt, CH_2Cl_2, 40 °C, 81%; h) *i*) Ph_2Se_2, NaH, DMSO, 50 °C, *ii*) 100 °C, 58%; i) H_2O_2, pyr., THF, rt, 78%; j) *i*) TAI, CH_2Cl_2, *ii*) K_2CO_3, MeOH, 90%; k) *i*) PPh_3, CBr_4, Et_3N, CH_2Cl_2, 0 °C to rt, *ii*) Me_2NH, THF, 50%; l) DDQ, pH 7 buffer, CH_2Cl_2, *t*BuOH, 64%.

The forward route was rendered asymmetric *via* an enantioselective cuprate addition to **4.72** using $Cu(OTf)_2$ and ligand **4.73** (**Scheme 4.7b**). The intermediate magnesium enolate was trapped as silyl enol ether **4.74** in 57% crude yield. Oxidation of **4.74** with DMDO gave a mixture of α-hydroxy ketones, with **4.75** as the major product. The stereochemistry of **4.75** was confirmed *via* NOESY analysis of a later intermediate. Conversion of **4.75** to an enone involved initial

protection of the C5 alcohol as a BOM ether, followed by silyl enol ether formation and oxidation to **4.76** with IBX and 4-methoxypyridine oxide; recovered **4.75** was easily separated from **4.76** and could be re-subjected to the reaction conditions to improve the overall efficiency of the chemistry. With enone **4.76** in hand, the C4/C6 bond was formed by chemoselective 1,2-addition of MeMgBr to the ketone in the presence of $CeCl_3 \cdot 2LiCl$; omitting the additive resulted in a 3:1 mixture of 1,2- and 1,4-addition products. Even though organometallic addition to **4.76** occurs adjacent to a quaternary carbon bearing two sterically similar groups, chelation between the adjacent ether and the carbonyl group gave >20:1 *dr*. Directed epoxidation was carried out on crude **4.77** to furnish **4.78** in >20:1 *dr*. To prime **4.78** for the key Ichikawa rearrangement, the epoxide needed to be transformed to allylic alcohol **4.80**; however, the *cis* relationship of the C1 Et and C2 epoxide precluded a concerted, base-mediated elimination. As a result, the 3° C4 alcohol was protected with an orthogonal $PMBOCH_2$ group, and the epoxide opened with PhSeNa to afford alcohol **4.79** as one regioisomer. Selenide oxidation with H_2O_2 furnished **4.80** via elimination of the selenoxide. Carbamate **4.81** was formed in 90% yield from **4.80** to give the Ichikawa precursor, which was successfully converted to isocyanate **4.82** using $CBr_4/PPh_3/Et_3N$ which was then trapped with Me_2NH to afford the C1 urea of **4.83.** The $PMBOCH_2$ group was cleaved with DDQ to unmask the C4 alcohol in **4.84**.

Scheme 4.8 – Failed Overman and Ichikawa reactions.



Unfortunately, attempts to carry out Overman rearrangement on to furnish desired **4.86** (**Scheme 4.8**) failed. Attempts to convert the alcohol to an allylic trichloroacetimidate gave only oxazoline **4.87**, likely due to the nucleophilicity of the urea oxygen in this sterically congested ring. Attempts to form a C4 carbamate such as **4.89** to initiate a second Ichikawa rearrangement, resulted in an undesired S_N2' attack of the urea oxygen ultimately displacing the C4 leaving group to give **4.88**. These studies highlight two issues with the sequential Ichikawa/Overman rearrangement strategy. The first is the potential for the C4 alkoxide to react with the urea, while the second is the propensity for the urea oxygen to displace even mediocre leaving groups at C4. Successful rearrangement requires the C4 group be non-nucleophilic and not easily displaced by the urea oxygen.

4.3.3. Introduction to the Ichikawa/Winstein Approach

A potential solution to these challenges involves incorporating a sigmatropic rearrangement of an allylic azide as the second step of the sequence. Ichikawa reaction on a C4 azido carbamate version of **4.84** would furnish a disubstituted alkene adjacent to a 3° azide. The non-nucleophilic azide is not expected to react with the C1 isocyanate produced in the Ichikawa; in addition, Hanessian was able to form the C1 urea via an isocyanate in the presence of a C2 azide. [8] As the 180° dihedral angle in the isocyanate does not permit a C-O bond to form between

this oxygen and the C2 carbon, the azide should be able to undergo [3,3]-sigmatropic rearrangement to form the thermodynamically favored trisubstituted alkene. Quenching with Me_2NH would generate the urea and provide an excellent way to generate analogues. Progress and challenges of this synthetic strategy will be discussed in **Chapter 5**.

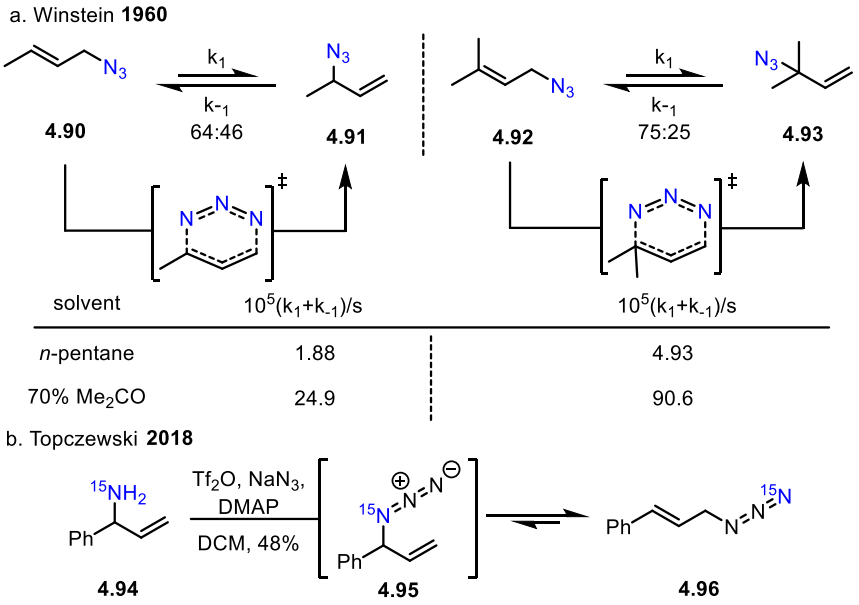
4.4.1 The Winstein Rearrangement

The equilibrating rearrangement of allylic azides was termed the "Winstein rearrangement" after its discovery by Young and Winstein in 1960.[17] This reaction, similar to the well-known Cope rearrangement, results in an equilibrium distribution of products.[18] In contrast to other well-known sigmatropic rearrangements, the Winstein rearrangement is unique in that it occurs at or even below room temperature. [17] Although seldom applied in total synthesis, the 21st century has brought significant advancements in both the mechanism and synthetic application of the Winstein rearrangement. [19a,b]

In the initial discovery, Winstein and coworkers found that both crotyl **4.90** and prenyl azides **4.92** spontaneously equilibrate to form their corresponding azide isomers **4.91** and **4.93** (**Scheme 4.9a**).[17] To examine the origin of the observed azide mixtures further, the azides were separated and stored at -80 ˚C to prevent isomerization. Winstein found upon warming up the samples to 25 ˚C enabled monitoring of the equilibration to the same mixture of isomers initially observed, which ruled out a potential S_N2 or $S_N2`$ substitution mechanism. To better understand the mechanism of the equilibration, the authors also examined the rate of isomerization in a variety of solvents. The rearrangement rate had only a minor solvent dependence with only a 10-fold increase when measured in 70% aqueous acetone. This minor rate increase in polar media corresponds to rate increases similar to those reported for Diels-Alder cycloadditions.[20] With this

information in hand, Winstein proposed that this rearrangement proceeds via a concerted mechanism.

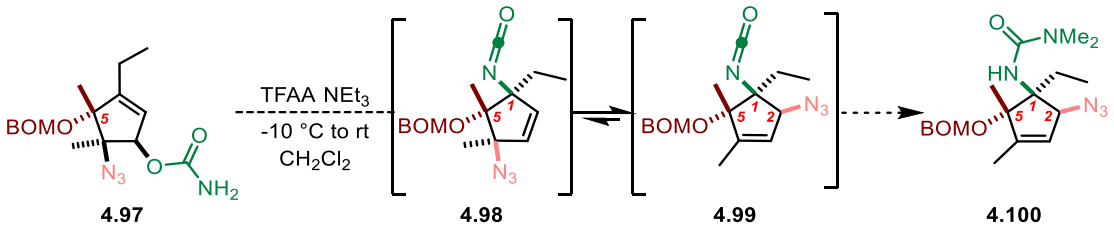
Scheme 4.9 – a. The Winstein rearrangement b. ^{15}N labeling experiment to unambiguously identify the [3,3]-sigmatropic mechanism of the Winstein rearrangement.



Other mechanistic investigations have been undertaken, including extensive computational studies.[21a,b,22] Topczewski reported the first direct evidence for the [3,3]-sigmatropic mechanism utilizing ^{15}N labeling studies (**Scheme 4.9b**).[22] In this experiment, ^{15}N-**4.94** was used to generate a ^{15}N labeled azide **4.95**. Azide **4.95** spontaneously rearranged to afford ^{15}N-cinnamyl azide **4.96**, which was isolated as a single isomer. In this case, conjugation drives the equilibrium to favor **4.96**. The migration of the ^{15}N-label to the terminus of the azide unambiguously supports a [3,3]-sigmatropic rearrangement and rules out a [1,3]-sigmatropic rearrangement or an ionic mechanism. In contrast, Topczewski and coworkers also found other pathways, including an ionic pathway, may be operable under specific conditions that include use of high temperature or Lewis acids.[22]

The equilibrium of the Winstein rearrangement can be influenced by several factors including conjugation, *syn*-pentane interactions, stereoelectronic effects, and alkene substitution.[19a,b] In the Schomaker application of the Winstein rearrangement, it is proposed that the thermodynamic favorability of forming tri-substituted isomer **4.99** (**Scheme 4.10**) will drive the reaction towards the desired product. In addition to the thermodynamic favorability of **4.99**, the formation of **4.99** relieves steric strain as **4.98** contains three contiguous quaternary centers whereas **4.99** only contains two. By replacing the troublesome Overman rearrangement with this reaction, it was hypothesized that off-target reactivity could be avoided between the urea oxygen and the C4 alcohol (**See above, Scheme 4.7**)

Scheme 4.10 – Schomaker's tandem Ichikawa/Winstein rearrangement strategy to set C1 and C2 simultaneously.



4.97 **4.98** **4.99** **4.100**

It is important to highlight that in both instances where the sequential rearrangements fail (**Scheme 4.7**) it is directly related to the presence of the urea. Given that the Winstein rearrangement happens spontaneously at room temperature, we hypothesized we could circumvent this off-target reactivity by performing both rearrangements in the same pot prior to quenching the intermediate isocyanate **4.99** with dimethylamine to yield **4.100** (**Scheme 4.10**). If this strategy proves successful, formation of the urea could be avoided until the C2 stereocenter is installed.

4.5 Conclusion

In conclusion, a number of different routes have been developed to synthesize the core of pactamycin **4.1** and jogyamycin **4.2**. Two routes developed by Johnson and Hanessian have resulted in the successful enantioselective synthesis of pactamycin **4.1**. Both routes rely on the exocyclic C7 alcohol stereocenter as a key functional group in the synthesis, making it unlikely that any of these routes could easily be adapted to the synthesis of jogyamycin **4.2**. The only routes designed to access jogyamycin **4.2** have failed at a late stage of synthesis. To explore the 7-deoxy series of pactamycin **4.1**, a new, modular route to this scaffold needs to be developed. One of the key challenges to accessing jogyamycin **4.2** has been identified as the formation of the adjacent C1 and C2 stereocenters; we have proposed a tandem Ichikawa-Winstein rearrangement to circumvent these issues. The following chapter will cover the progress we have made thus far toward the completion of **4.2** via the tandem Ichikawa-Winstein rearrangement route.

4.6 References

(1) Lu, W.; Roongsawang, N.; Mahmud, T. Biosynthetic Studies and Genetic Engineering of Pactamycin Analogues with Improved Selectivity toward Malarial Parasites. *Chem. Biol.* **2011**, *18*, 425–431.

(2) Bhuyan, B. K. Pactamycin Production by Streptomyces Pactum. *Appl. Environ. Microb.* **1962**, *10*, 302–304.

(3) Wiley, P. F.; Jahnke, H. K.; MacKellar, F. A.; Kelly, R. B.; Argoudelis, A. D. Structure of Pactamycin. *J. Org. Chem.* **1970**, *35*, 1420–1425.

(4) (a) Kondo, T.; Sezaki, M.; Sato, K.; Hara, T.; Niida, K.; Noguchi, T.; Kohmoto, K. A New Antibiotic, Cranomycin. *J. Antibiot.* **1964**, *17*, 266. (b) Kazuyuki, D.; Isshiki, K.; Sawa, T.; Obata, T.; Hamada, M.; Naganawa, H.; Takita, T.; Takeuchi, T.; Umezawa, H.; Hongsheng, B.; Baoquan, Z.; Tong, C.; Xu, W. 8'-Hydroxypactamycin and 7-Deoxypactamycin, New Members of the

Pactamycin Group. *J. Antibiot.* **1986**, *39*, 1779–1783. (c) Hurley, T. R.; Smitka, J. H.; Wilton, R. H.; Bunge, G. C.; Hokanson, J. C.; French, P. D. New Pactamycin Analogues. *J. Antibiot.* **1986**, *39*, 1086–1091. (d) Elshahawi, S. I.; Shaaban, K. A.; Kharel, M. K.; Thorson, J. S. A Comprehensive Review of Glycosylated Bacterial Natural Products. *Chem. Soc. Rev.* **2015**, *44*, 7591–7697.

(5) Iwatsuki, M.; Nishihara-Tsukashima, A.; Ishiyama, A.; Namatame, M.; Watanabe, Y.; Handasah, S.; Pranamuda, H.; Marwoto, B.; Matsumoto, A.; Takahashi, Y.; Otoguro, K.; Ōmura, S. Jogyamycin, a New Antiprotozoal Aminocyclopentitol Antibiotic, Produced by Streptomyces Sp. a-WM-JG-16.2. *J. Antibiot.* **2012**, *65*, 169–171.

(6) (a) Ito, T.; Roongsawang, N.; Shirasaka, N.; Lu, W.; Flatt, P. M.; Kasanah, N.; Miranda, C.; Mahmud, T. Deciphering Pactamycin Biosynthesis and Engineered Production of New Pactamycin Analogues. *ChemBioChem.* **2009**, *10*, 2253–2265. (b) Lu, W.; Roongsawang, N.; Mahmud, T. Biosynthetic Studies and Genetic Engineering of Pactamycin Analogues with Improved Selectivity toward Malarial Parasites. *Chem. Biol* **2011**, *18*, 425–431. (c) Guha, G.; Lu, W.; Li, S.; Liang, X.; Kulesz-Martin, M. F.; Mahmud, T. Novel Pactamycin Analogues Induce P53 Dependent Cell-Cycle Arrest at S-Phase in Human Head and Neck Squamous Cell Carcinoma (HNSCC) Cells. *PLoS One* **2015**, *10*, 1–25.

(7) Otoguro, K.; Iwatsuki, M.; Ishiyama, A.; Namatame, M.; Nishihara-Tukashima, A.; Shibahara, S.; Kondo, S.; Yamada, H.; Ōmura, S. Promising Lead Compounds for Novel Antiprotozoals. *J. Antibiot.* **2010**, *63*, 381–384.

(8) Hanessian, S.; Vakiti, R. R.; Dorich, S.; Banerjee, S.; Lecomte, F.; DelValle, J. R.; Zhang, J.; Deschênes-Simard, B. Total Synthesis of Pactamycin. *Angew. Chem., Int. Ed.* **2011**, *50*, 3497–3500.

(9) Malinowski, J. T.; McCarver, S. J.; Johnson, J. S. Diastereocontrolled Construction of Pactamycin's Complex Ureido Triol Functional Array. *Org. Lett.* **2012**, *14*, 2878–2881.

(10) Malinowski, J.T.; Sharpe, R. J.; Johnson, J.S. Enantioselective Synthesis of Pactamycin, a Complex Antitumor Antibiotic. *Science* **2013**, *340*, 180–182.

(11) Sharpe, R. J.; Malinowski, J. T.; Sorana, F.; Luft, J. C.; Bowerman, C. J.; DeSimone, J. M.; Johnson, J. S. Preparation and Biological Evaluation of Synthetic and Polymer-Encapsulated Congeners of the Antitumor Agent Pactamycin: Insight into Functional Group Effects and Biological Activity. *Bioorg. Med. Chem.* **2015**, *23*, 1849–1857.

(12) Trost, B. M.; Zhang, L.; Lam, T. M. Synthesis of the Aminocyclitol Core of Jogyamycin via an Enantioselective Pd-Catalyzed Trimethylenemethane (TMM) Cycloaddition. *Org. Lett.* **2018**, *20*, 3938–3942.

(13) Trost, B. M.; Lam, T. M.; Herbage, M. A. Regio- and Enantioselective Synthesis of Pyrrolidines Bearing a Quaternary Center by Palladium-Catalyzed Asymmetric [3 + 2] Cycloaddition of Trimethylenemethanes. *J. Am. Chem. Soc.* **2013**, *135*, 2459–2461.

(14) Gerstner, N. C.; Adams, C. S.; Grigg, R. D.; Tretbar, M.; Rigoli, J. W.; Schomaker, J. M. Diastereoselective Synthesis of the Aminocyclitol Core of Jogyamycin via an Allene Aziridination Strategy. *Org. Lett.* **2016**, *18*, 284–287.

(15) for selected references using allene aziridination see: (a) Boralsky, L. A.; Marston, D.; Grigg, R. D.; Hershberger, J. C.; Schomaker, J. M. Allene Functionalization via Bicyclic Methylene Aziridines. *Org. Lett.* **2011**, *13*, 1924–1927. (b) Adams, C. S.; Boralsky, L. A.; Guzei, I. A.; Schomaker, J. M. Modular Functionalization of Allenes to Aminated Stereotriads. *J. Am. Chem. Soc.* **2012**, *134*, 10807–10810. (c) Adams, C. S.; Grigg, R. D.; Schomaker, J. M. Complete

Stereodivergence in the Synthesis of 2-Amino-1,3-Diols from Allenes. *Chem. Sci.* **2014**, *5*, 3046–3056.

(16) Gerstner, N. C.; Schomaker, J. M. Stereocontrolled Synthesis of the Aminocyclopentitol Core of Jogyamycin via an Ichikawa Rearrangement Reaction. *J. Org. Chem.* **2019**, *84*, 14092–14100.

(17) Gagneux, A.; Winstein, S.; Young, W. G. Rearrangement of Allylic Azides. *J. Am. Chem. Soc.* **1960**, *82*, 5956–5957.

(18) von E. Doering, W.; Roth, W. R. Thermal Rearrangements. *Angew. Chem., Int. Ed.* **1963**, *2*, 115–122.

(19) (a) Carlson, A. S.; Topczewski, J. J. Allylic Azides: Synthesis, Reactivity, and the Winstein Rearrangement. *Org. Biomol. Chem.* **2019**, *17*, 4406–4429. (b) Ott, A. A.; Topczewski, J. J. On the Winstein Rearrangement: Equilibrium and Mechanism. *ARKIVOC* **2019**, 1–17.

(20) Breslow, R..; Guo, T. Diels-Alder Reactions in Nonaqueous Polar Solvents. Kinetic Effects of Chaotropic and Antichaotropic Agents and of β-Cyclodextrin. *J. Am. Chem. Soc.* **1988**, *110*, 5613–5617.

(21) (a) Kang, H.-Y.; Kang, Y. K. Allylic Azide Rearrangements Investigated by Density Functional Theory Calculations. *Bull. Korean Chem. Soc.* **2017**, *38*, 1419–1426. (b.) Porta, E. O. J.; Vallejos, M. M.; Bracca, A. B. J.; Labadie, G. R. Experimental and Theoretical Studies of the [3,3]-Sigmatropic Rearrangement of Prenyl Azides. *RSC Adv.* **2017**, *7*, 47527–47538.

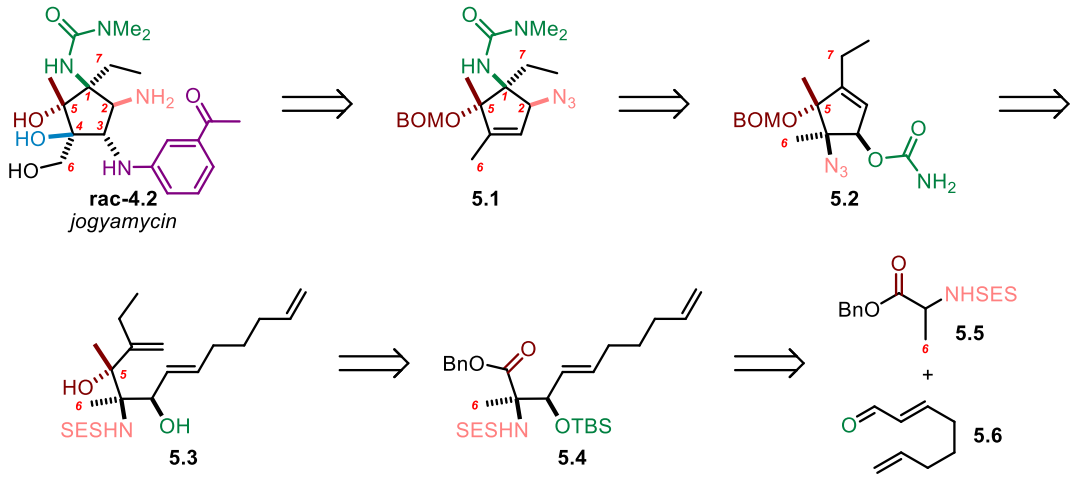
(22) Ott, A. A.; Packard, M. H.; Ortuño, M. A.; Johnson, A.; Suding, V. P.; Cramer, C. J.; Topczewski, J. J. Evidence for a Sigmatropic and an Ionic Pathway in the Winstein Rearrangement. *J. Org. Chem.* **2018**, *83*, 8214–8224.

Chapter 5. Progress Toward the Total Synthesis of Jogyamycin

5.1 Ichikawa/Winstein Rearrangement Retrosynthetic Analysis

The challenges encountered during the Overman/Ichikawa route required a novel strategy to set the C1 and C2 amine stereocenters simultaneously and avoid intramolecular reactivity at the C1 and C2 amines. Toward this goal, it was envisioned that the conversion of **5.1** to *rac*-**5.2** (**Scheme 5.1**) would involve a selenium-catalyzed allylic oxidation, followed by an epoxidation/nucleophilic ring-opening sequence similar to that employed by both Hanessian[1] and Johnson[2] in their total syntheses of pactamycin **4.1**. Urea **5.1** can be directly traced back to cyclopentene **5.2**, where both the C1 urea and C2 amine stereocenters are formed via a key tandem Ichikawa/Winstein rearrangement. Cyclopentene **5.2** is formed from a relay ring closing metathesis (RRCM) of **5.3** which can be traced back to ester **5.4** via carbonyl functionalization. Ester **5.4** is a clear aldol synthon and can be traced back to amino acid derivative **5.5** and conjugated aldehyde **5.6**.

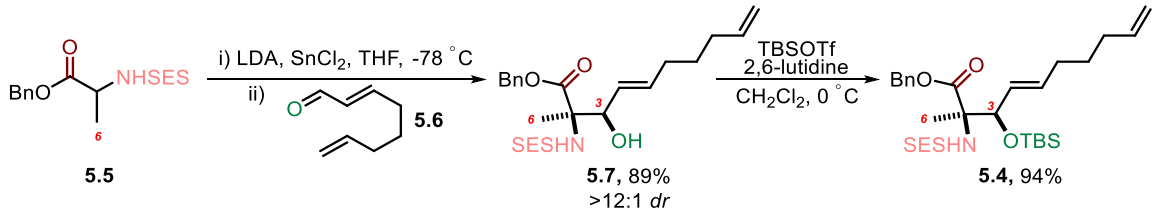
Scheme 5.1 – Retrosynthetic analysis of the Ichikawa/Winstein rearrangement route.



5.2 Progress on the Ichikawa/Winstein Rearrangement Route to Intermediate 5.1

The tandem Ichikawa/Winstein route commenced from readily available racemic alanine. In two known steps, the amino acid was converted to the benzyl ester, and the amine protected as the SES sulfonamide **5.5** (further analysis of the protecting group choice will be discussed later).[3,4] Amino acid derivative **5.5** was converted to aldol adduct **5.4** via reaction with aldehyde **5.6** and $SnCl_2$ in 12:1 *dr* and 89% yield (**Scheme 5.2**). This procedure, first developed by Kazameir, was hypothesized to furnish high diastereoselectivity based on the greater coordinating ability of tin chelated enolates compared to the corresponding lithium enolates.[5] Aldehyde **5.6** was chosen as the coupling partner for ease of synthesis as well as its ability to serve as a substrate for a later RRCM type reaction (*vide infra*). With **5.7** in hand, the newly formed secondary alcohol was protected as the TBS ether **5.4** to prevent retro-aldol reaction and set up for the next set of organometallic additions to establish the C5 stereocenter (**Scheme 5.2**).

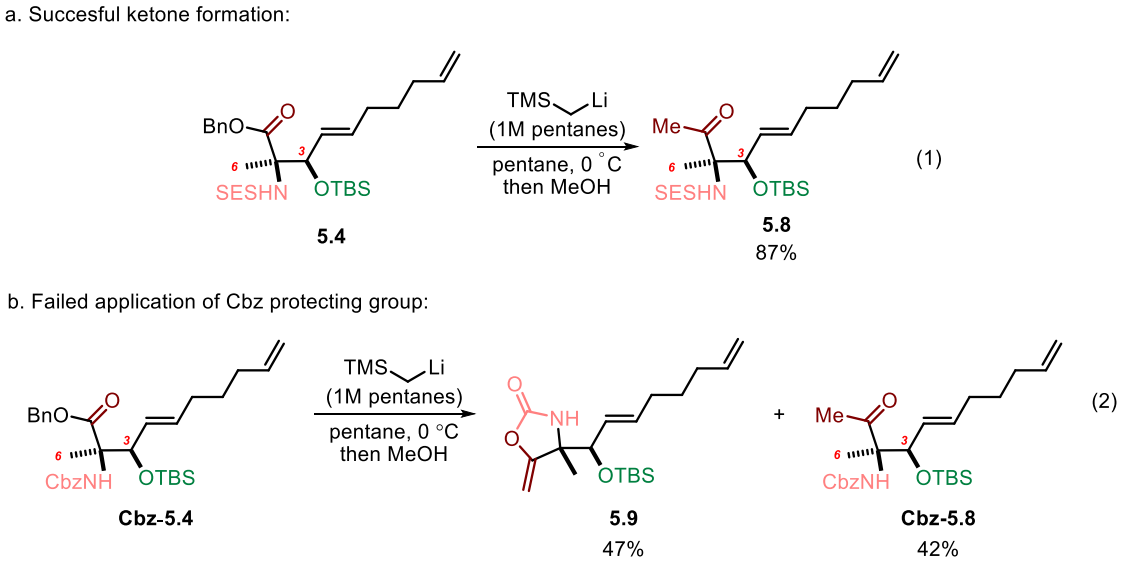
Scheme 5.2 – Aldol condensation and protection to form conjugated ester **5.4.**



First, the Bn ester **5.4** was converted to the silyl ketone **5.8** using $TMSCH_2Li$. A methanolic work-up removed the TMS group to reveal the methyl ketone. This strategy was first employed by Johnson in his partial synthesis of pactamycin **4.1** to access a sterically encumbered ketone.[6] In

their work, Johnson and coworkers found that a sterically encumbered ester was unreactive to traditional methods (MeMgBr, MeLi, Cp_2TiMe_2) due to the adjacent quaternary center. However, $TMSCH_2Li$ proved particularly nucleophilic. $TMSCH_2Li$ was applied to ester **5.7** and it was found that the nucleophilic addition proceeded smoothly to yield **5.4** in 87% yield (**Scheme 5.3**, **eq. 1**). It should be noted that early route scouting efforts using a Cbz protecting group performed similarly to the SES-protected amine in the aldol condensation and silyl ether formation reactions. However, when **Cbz-5.4** was exposed to $TMSCH_2Li$, the Cbz group reacted preferentially with the ester to form the cyclic carbamate **5.9** (**Scheme 5.3**, **eq. 2**).

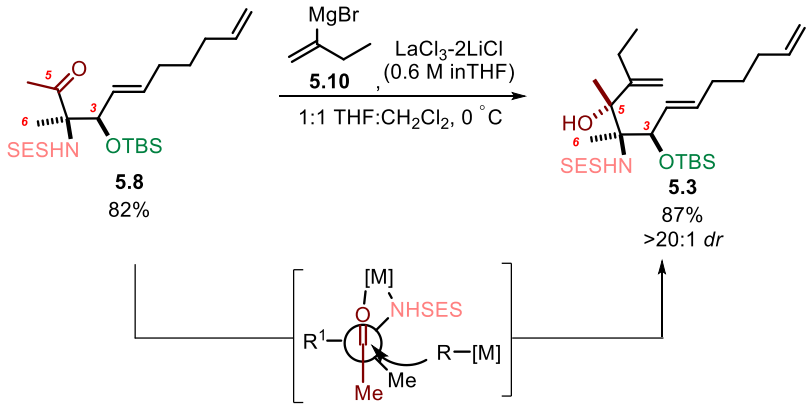
Scheme 5.3 – Organometallic addition for the synthesis of methyl ketones.



The next goal was to set the C5 quaternary center by the addition of Grignard reagent **5.10** to the methyl ketone. To generate the C5 stereocenter in high yield and *dr*, Castles' work on the diastereoselective synthesis of vicinal tertiary diols was utilized.[7] The authors found that the construction of vicinal tertiary diols in extremely hindered systems could be accomplished more efficiently using $LaCl_3$-2LiCl as compared to traditional $CeCl_3$. Furthermore, the authors

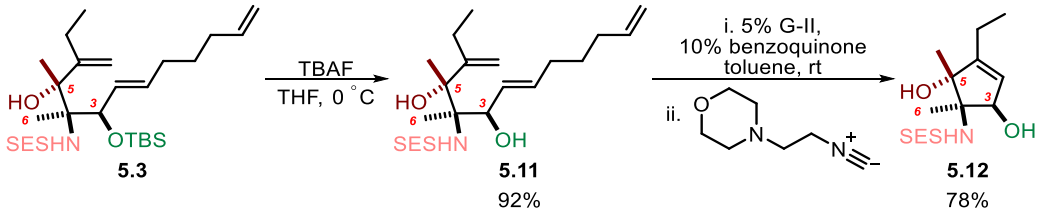
discovered that a mixed 1:1 solvent system of CH_2Cl_2: THF was essential to achieving good diastereocontrol in the reaction, as reductions run in solely THF furnished lower *dr*. To our delight, conversion of **5.8** to **5.3** proceeded smoothly, presumably through chelation control, to furnish the C5 stereocenter as a single diastereomer **5.3** in 87% yield (**Scheme 5.4**).

Scheme 5.4 – Organometallic addition to ketone **5.8** for the formation of the C5 stereocenter.



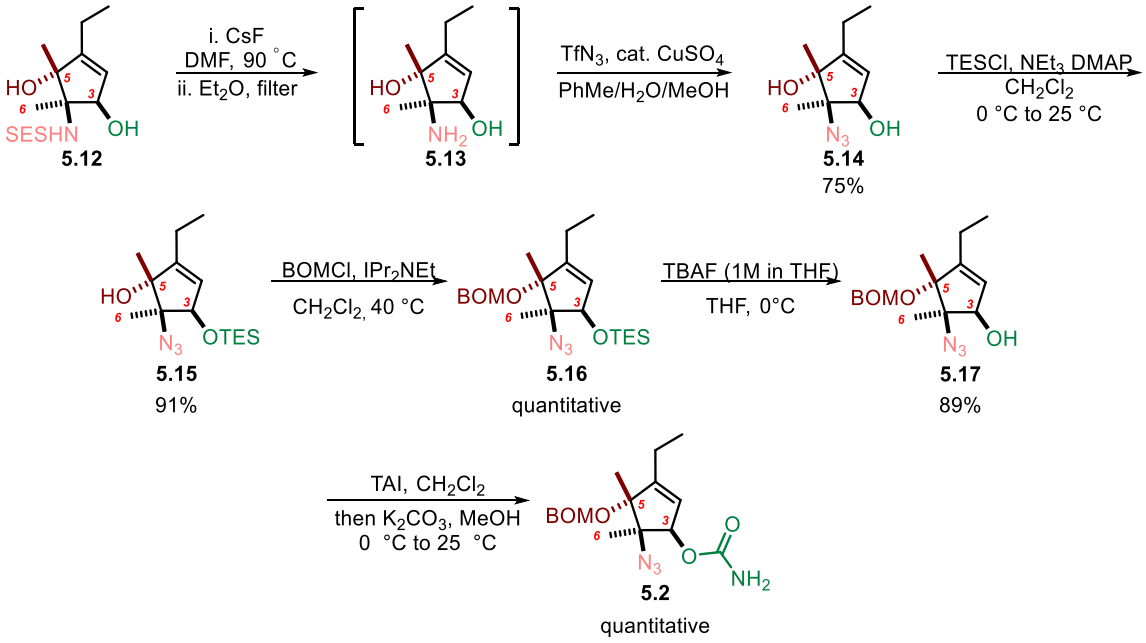
With the C5 stereocenter set and the other functional groups poised for later transformations, the stage was set for formation of the core of jogyamycin *rac*-**4.2**. A RRCM furnished cyclopentene **5.12** and released cyclopentene as an inert byproduct (**Scheme 5.5**). [8] Initially, the RRCM was explored in the presence of the TBS protecting group to obviate the need for later tedious protection/deprotection steps. Unfortunately, this was unsuccessful, likely due to steric encumbrance of the -OTBS group imposed on the internal alkene. Deprotection of the C3 protecting group was followed by smooth RRCM at room temperature to furnish the cyclic core of jogyamycin **4.2** in 78% yield.

Scheme 5.5 – RRCM of **5.11** for formation of the core of jogyamycin **4.2.**



To explore the key Ichikawa/Winstein step, the SES protected amine needed to be converted into the corresponding tertiary azide. To do this, the SES protecting group was deprotected with CsF and directly subjected to azide transfer conditions with triflic azide to furnish azide **5.14** in 75% yield (**Scheme 5.6**). Best yields were obtained using a solution of TfN_3 in toluene instead of DCM; this also avoids formation of explosive byproducts such as diazidomethane and azido-chloromethane. [9] The need to deprotect the TBS ether prior to RRCM required a series of steps to protect the tertiary alcohol before carbamate formation of the secondary alcohol. To accomplish this, the C3 secondary alcohol was first protected as TES ether **5.15** in 91% yield (**Scheme 5.6**). Next, the C5 tertiary alcohol was protected as the BOM ether to generate **5.16** in quantitative yield (**Scheme 5.6**). Though high yielding, this reaction was sluggish and took up to 4 days to complete on larger scale. The TES ether **5.16** was then deprotected to reveal secondary alcohol **5.17**, which was subsequently functionalized using TAI to furnish carbamate **5.2** in quantitative yield (**Scheme 5.6**). Finally, with **5.2** in hand, we were ready to test the key Ichikawa/Winstein rearrangement.

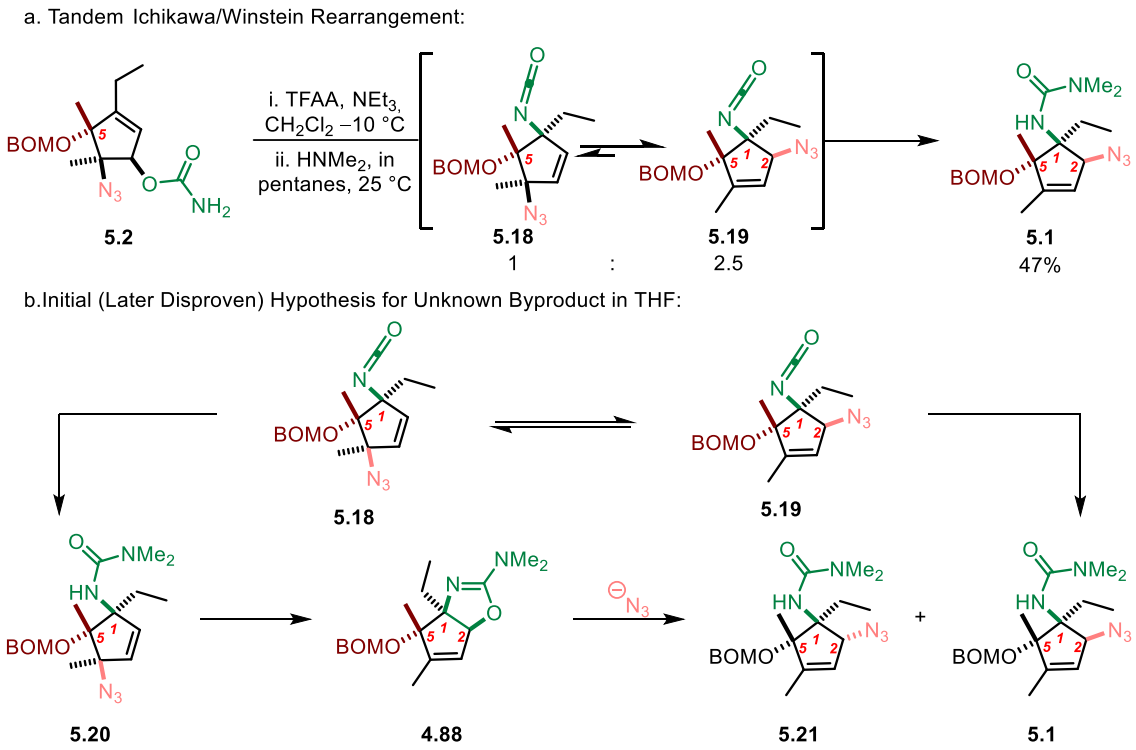
Scheme 5.6 – Azidation and protecting group manipulation for the formation of Ichikawa precursor **5.2.**



Upon exposure of carbamate **5.2** to azide-friendly Ichikawa conditions,[10] it was found that dehydration to the allyl cyanate and rearrangement to the C1 isocyanate happen almost immediately. In the same pot at -10 ˚C, simultaneous rearrangement of the tertiary azide to the secondary azide can also be observed in a 1:2.5 ratio of **5.19**:**5.18** (**Scheme 5.7a**). We observed this reactivity using VT-NMR spectroscopy and found the reaction was nearly complete by the time NMR data could be collected. Unfortunately, upon direct quench with a dimethyl amine solution in THF, an unidentified byproduct of the same molecular weight as **5.1** was observed. This byproduct was initially assigned as the incorrect C2-diastereomer, **5.21** (**Scheme 5.7b**). Given our prior experience with oxazoline formation at C2,[11] it was proposed that quenching the isocyanate with dimethyl amine in a polar solvent like THF initiated a S_N2' reaction similar to that observed in the Overman/Ichikawa route (**Chapter 4, Scheme 4.8**). The displaced azide anion could then undergo a nucleophilic attack to open the oxazoline and deliver **5.21** with the wrong

configuration at C2. With this hypothesis in mind, the intermediate isocyanates **5.19** and **5.18** were isolated and the residue redissolved in a dilute solution of pentanes and treated with freshly condensed $HNMe_2$. Pentanes were chosen to discourage the formation of charged intermediates and prevent S_N2' type reactivity while hopefully not altering the desired pathway. This alteration in reaction conditions furnished the desired product **5.1** in 47% yield over two steps. Although the reaction was successfully modified, later data suggested that the byproduct may not be the result of an S_N2' type reaction. Efforts are ongoing to grow a crystal and unambiguously establish the structure of the unknown byproduct.

Scheme 5.7 – Tandem Ichikawa/Winstein rearrangement and hypothesized by-product formation.

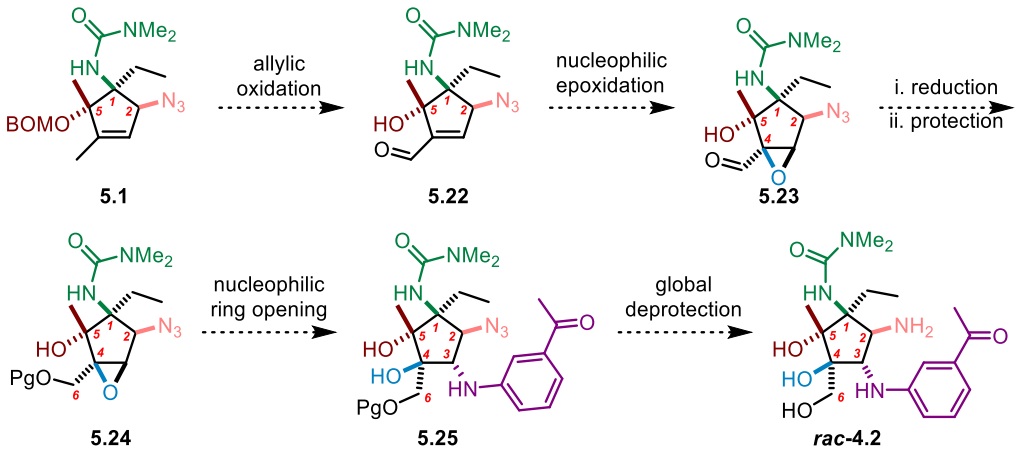


Overall, the success of this transformation reinforces that a group capable of undergoing simultaneous [3,3]-sigmatropic rearrangement prior to the formation of the urea at C1 is the best strategy to avoid intramolecular cross-reactivity at the C2 and C4 positions. Additionally, any off-target reactivity can be reliably controlled using solvent effects. This is the first time the adjacent C1 and C2 stereocenters have been set successfully and the first known tandem Ichikawa/Winstein rearrangement.

5.3 Attempts at Allylic Functionalization of Intermediate 5.1

With the entire northern hemisphere of the molecule successfully installed (C5, C1, and C2), efforts turned towards elaboration of the southern half of jogyamycin *rac*-**4.2.** As mentioned earlier, the initial endgame strategy was an allylic oxidation to furnish **5.22** and a subsequent epoxidation/ring opening sequence. A global protecting group removal would furnish *rac*-**4.2** (**Scheme 5.8**).

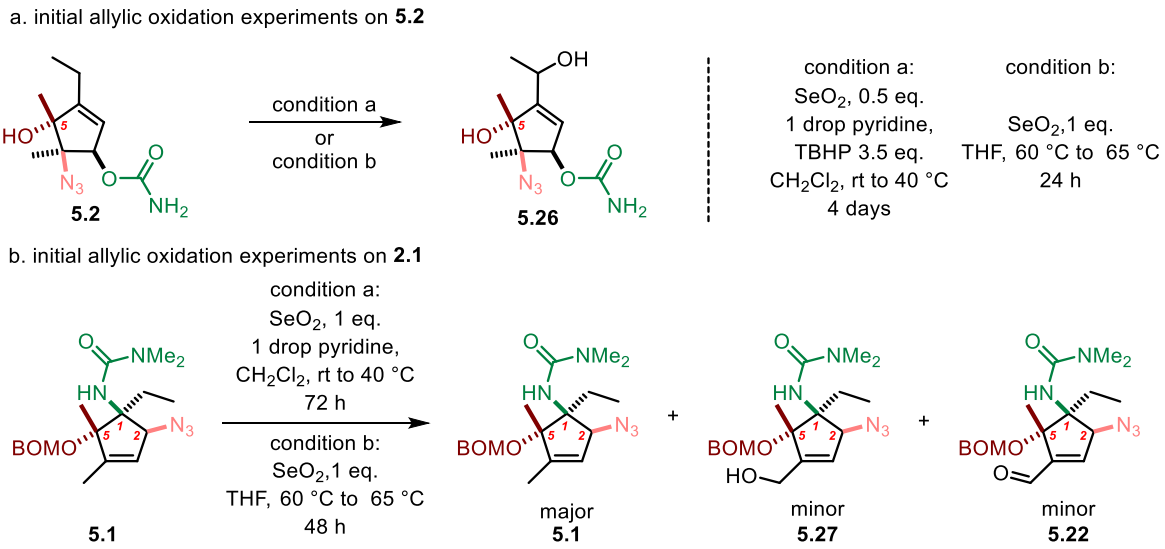
Scheme 5.8 – End game strategy via allylic functionalization of the C4 methyl group.



This end game strategy was first initiated by pursuing allylic oxidation on carbamate **5.2** while simultaneously optimizing the tandem Ichikawa/Winstein rearrangement. Oxidation of the

allylic C7 site of **5.2** enabled exploration of this route's applicability to the synthesis of pactamycin **4.1** and would confirm the functional group compatibility of the C4 and C5 stereocenters. Two sets of conditions were successful for the conversion of **5.2** to **5.26** (**Scheme 5.9a**). Unfortunately, when these conditions were applied to trisubstituted alkene **5.1** using THF as the solvent, only minimal progress was noted after 24 h and full decomposition after 48 h. When CH_2Cl_2 was utilized, a similar outcome was observed with minimal progress identified after 28 h and full decomposition after 72 h (**Scheme 5.9b**). Although both the alcohol and aldehyde were detected via mass spectroscopy in trace amounts after 24 h and 28 h, the majority of the mass balance was starting material.

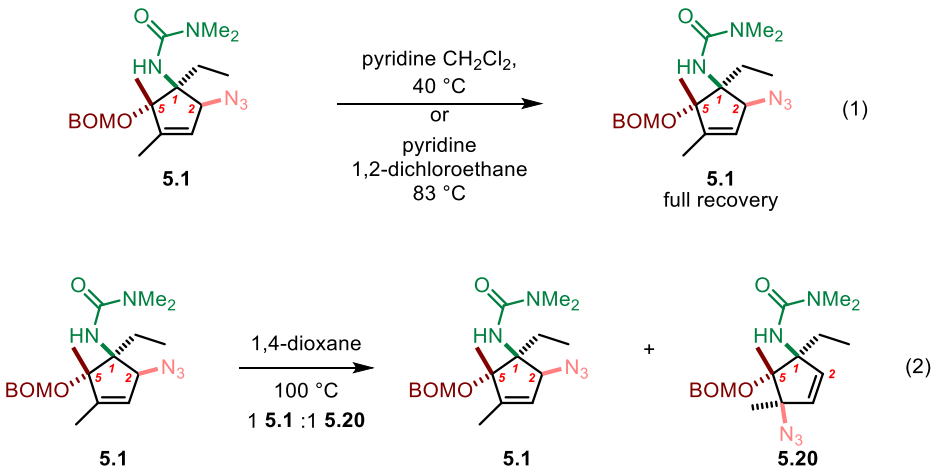
Scheme 5.9 – Attempted allylic oxidation of **5.1** and **5.2.**



The lack of success in allylic oxidation under standard conditions suggested a need for harsher oxidation conditions. A series of stability studies were conducted to explore functional group tolerance; **5.1** was found to be stable to refluxing CH_2Cl_2 and 1,2-dichloroethane (**Scheme 5.10, eq 1**). Importantly, we found that refluxing **5.1** in 1,4-dioxane reestablished the Winstein

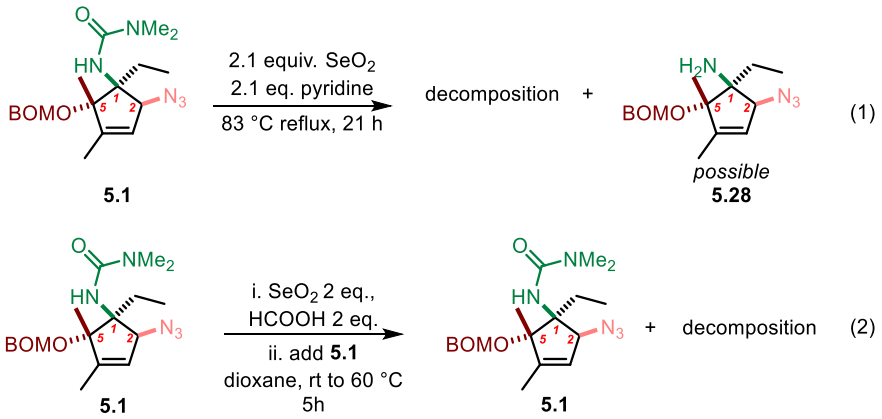
equilibrium, setting an upper temperature bound that would be feasible for SeO_2 oxidation (**Scheme 5.10, eq 2**).

Scheme 5.10 – Temperature and base stability studies of **5.1.**



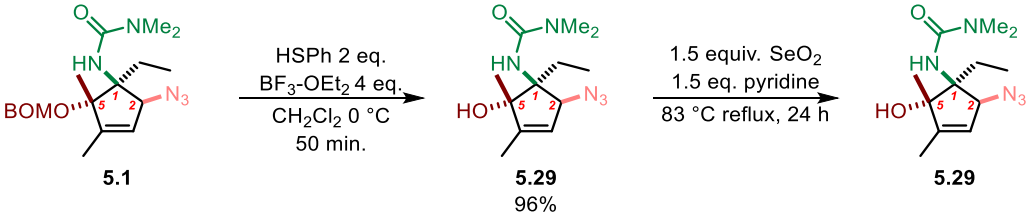
With this information in hand, stoichiometric SeO_2 and pyridine in 1,2-dichloroethane at elevated temperatures were tested. These reaction conditions only furnished decomposition and possibly free amine **5.28** (**Scheme 5.11, eq. 1)**. It was noted in the literature that premixing formic acid and SeO_2 at elevated temperatures can generate a more active oxidizing species.[12] Although confident an excess of formic acid would cause functional group compatibility issues; it was hypothesized that careful equivalence and a long enough pre-stir before introduction of the substrate may mitigate these concerns. Unfortunately, these conditions gave a mixture of recovered starting material and decomposition (**Scheme 5.11, eq. 2**).

Scheme 5.11 – Harsher allylic oxidation conditions applied to **5.1.**



It was hypothesized that the lack of reactivity at the allylic methyl group may stem from steric crowding by the adjacent C5 stereocenter.[13] To explore this possibility, the C5 BOM alcohol was deprotected using BF_3-Et_2O and HSPh to furnish free alcohol **5.29** in 96% yield. Under stoichiometric SeO_2, pyridine in 1,2-dichloroethane, only recovered starting material was observed (**Scheme 5.12**).

Scheme 5.12 – Attempted allylic oxidation on C5-BOM deprotected **5.29.**

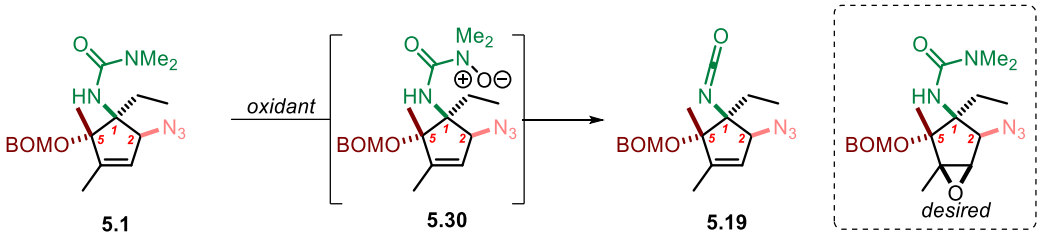


Other types of allylic functionalizations were also attempted, including visible light and thermal-mediated bromination, both of which furnished decomposition.[14] Tambar's allylic amination chemistry[15] was also attempted and resulted in only recovered starting material.

5.4 Attempts at Epoxidation of 5.1

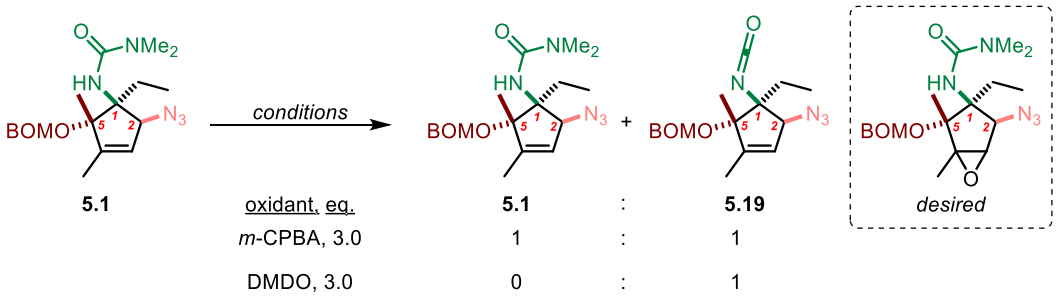
The difficulties in oxidizing the C6 methyl group led to exploration of other alkene functionalizations to reroute the endgame strategy. Epoxidation was considered for its robustness and the multitude of possible reaction conditions. If achieved, epoxidation of the C4/C5 olefin would enable a reimagining of the endgame strategy via epoxide elimination or rearrangement. Unfortunately, Trost experienced significant challenges in utilizing *m*-CPBA in the presence of the C1 urea, where the C1 urea was preferentially oxidized over the alkene of interest.[16] A hypothesized mechanism for this decomposition can be found in **Scheme 5.13**.

Scheme 5.13 – Potential mechanism of urea decomposition *via* oxidants.



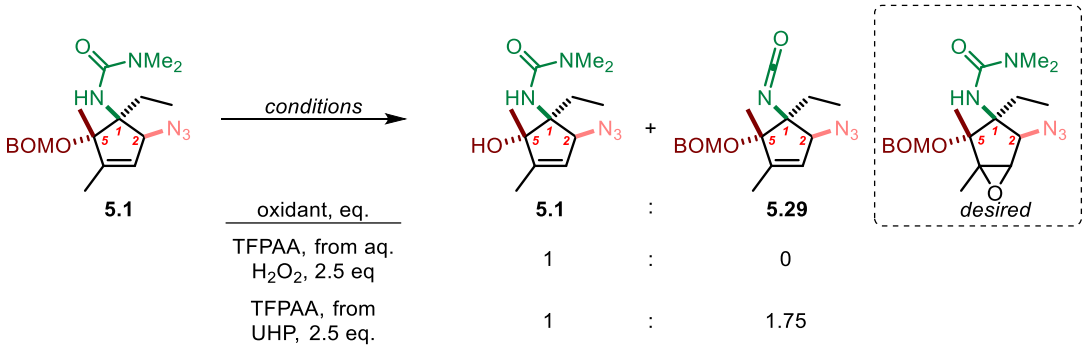
Given Trost's system was hindered, it was hypothesized the desired epoxidation reaction may proceed prior to urea oxidation or undergo a double oxidative event (by which the urea could be reestablished by a dimethyl amine quench of the intermediate isocyanate), however, it was acknowledged that the potential for the reactivity shown in **Scheme 5.13** may be the dominant path. Exposing the azide to *m*-CPBA furnished a 1:1 mixture of recovered starting material and oxidation of the urea back to the isocyanate (**Scheme 5.14**). The isocyanate could be trapped with dimethylamine and recovered without significant loss of material. Similarly, treatment of **5.1** with DMDO furnished only isocyanate **5.19**.

Scheme 5.14 – Attempts at olefin oxidation of intermediate **5.1.**



It was hypothesized that exposing **5.1** to a more potent oxidizing agent might accomplish a double oxidation of both the C3/C4 olefin and the C1 urea. Attempted oxidation with TFPAA generated *in situ* from H_2O_2 furnished only C5 BOM deprotection (**Scheme 5.15**). Attempting these conditions with anhydrous TFPAA synthesized from urea-hydrogen peroxide (UHP), to avoid acid generated BOM-deprotection, gave full conversion of the starting material to a 1.75:1 mixture of isocyanate **5.19** and C5 BOM deprotection product **5.29**, but no productive C3/C4 olefin oxidation.

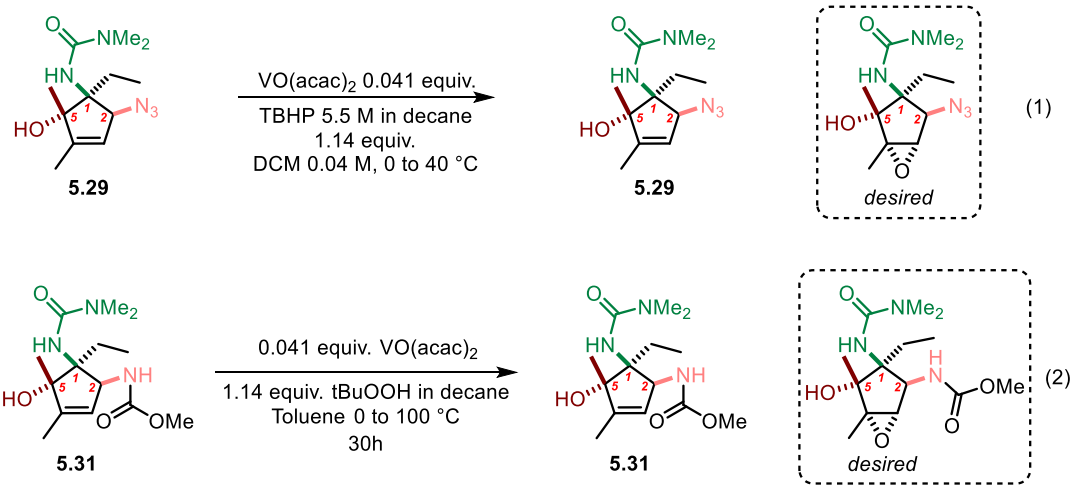
Scheme 5.15 – Exposure of **5.1** to TFPAA for C3/C4 olefin oxidation.



As traditional oxidants were incompatible with the urea, metal-directed epoxidation was attempted to avoid this off target reactivity. Unfortunately, $VO(acac)_2$-catalyzed epoxidation of BOM-deprotected tertiary alcohol **5.29** only furnished recovered starting material (**Scheme 5.16,**

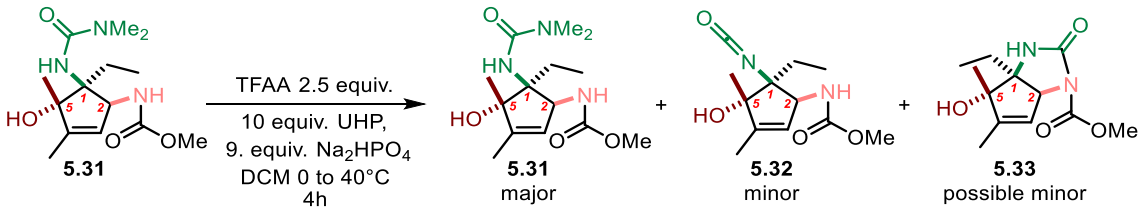
eq. 1). Reduction of the azide to the Cbz amine **5.31** was carried out in the hope that a more electron-rich olefin would be more prone to undergo epoxidation. Unfortunately, only recovered starting material was obtained (**Scheme 5.16, eq. 2**).

Scheme 5.16 – Attempts at Metal-Catalyzed Epoxidation Reactions of **5.1.**



Finally, protected amine **5.31** was exposed to the harshest epoxidation conditions possible (TFPAA derived from UHP) as a proof of concept that the alkene could be epoxidized despite the understanding that there would likely be significant cyclic urea formation. Unfortunately, the major product was recovered starting material, along with oxidation to the isocyanate **5.32** and subsequent cyclic urea formation **5.33** with no epoxidation of the alkene observed (**Scheme 5.17**).

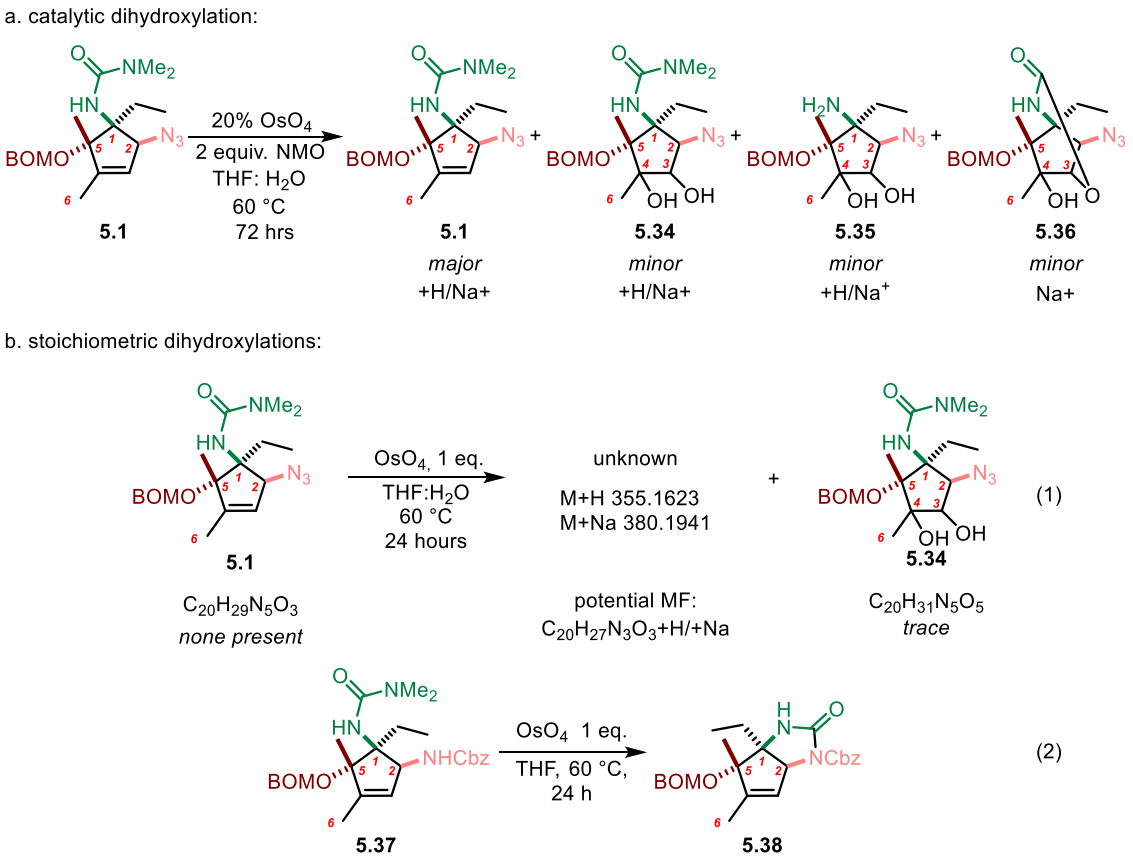
Scheme 5.17 – Attempts at olefin oxidation of amine **5.32** with TFPAA.



5.4 Attempts at Dihydroxylation of Compound 5.1

Due to a lack of success using traditional oxidation reactions, dihydroxylation of the C3/C4 olefin was examined as it proceeds through a cycloaddition mechanism which would not impact the urea in the same way as the epoxidizing reagents. OsO_4-catalyzed dihydroxylation of **5.1** furnished mainly recovered starting material, along with a minor amount of diol, urea oxidation and cyclization (**Scheme 5.18a**). The use of stoichiometric OsO_4 led to decomposition (**Scheme 5.18b, eq. 1**) of the azide of **5.1**.

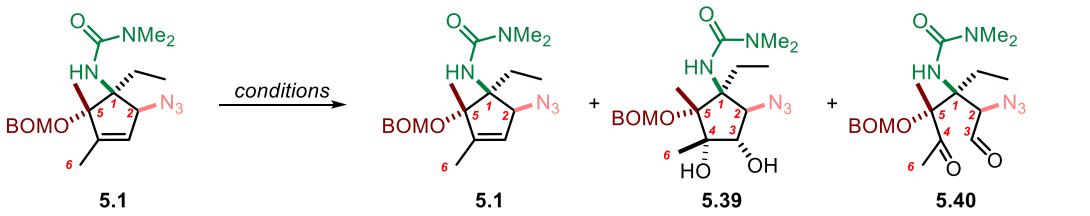
Scheme 5.18 – Attempts at olefin oxidation with OsO_4.



To circumvent this issue, the reaction was performed on protected amine **5.37**; however, only the cyclic carbamate **5.38** was formed, suggesting that OsO_4 prefers to oxidize the urea to the isocyanate, as opposed to the desired alkene functionalization (**Scheme 5.18b, eq. 2**).

RuO_4 is known for its remarkably high reactivity; in fact, reactions of RuO_4 and alkenes are often termed "flash dihydroxylations."[17] To our delight, dihydroxylation with 10% $RuCl_3$-xH_2O, 2.8 eq. $NaIO_4$, and a MeCN:H_2O mixed solvent system furnished dihydroxylated product **5.39** as a single diastereomer (confirmed by nOe) in 35% yield, along with 39% recovered **5.1** and a small amount of scission product **5.40** (**Scheme 5.19, eq. 1**).

Scheme 5.19 – Olefin dihydroxylation with RuO_4.



10% $RuCl_3$ 2.8 equiv. $NaIO_4$ H_2O/MeCN, 25 °C 22 min.	39%	35%	17%	(1)
7% $RuCl_3$ 1.5 equiv. $NaIO_4$ H_2O/MeCN/EtOAc, 0 °C 20 min.	27%	42%	14%	(2)

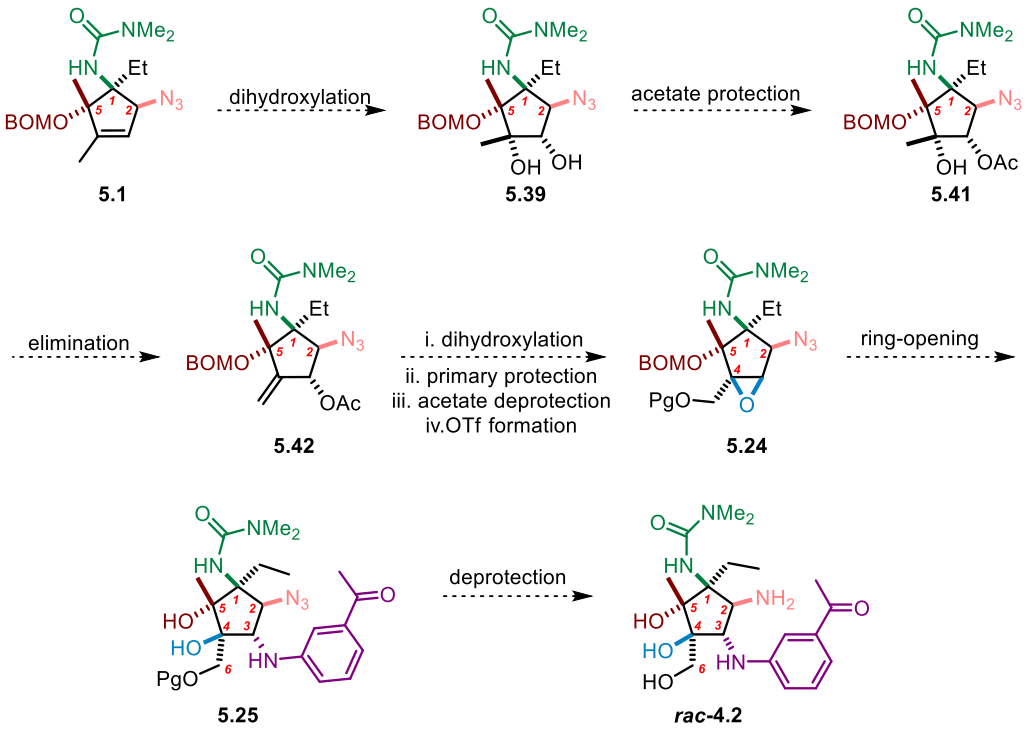
Optimization studies revealed that the solvent mixture, temperature, and number of equivalents are all important to maximizing yield.[18a-c] Ideal conditions were a mixed EtOAc:H_2O:MeCN solvent system to deliver **5.39** in 42% yield as a single diastereomer with a small amount of scission product **5.40** (**Scheme 5.19, eq. 2**). While MeCN is needed for catalytic

turnover, an immiscible solvent such as EtOAc helps to sequester the product and prevent competing diol scission. [18b]

5.5 Revised Dihydroxylation End Game Strategy

With **5.39** in hand, a new end game was needed to successfully complete the total synthesis of jogyamycin. Diol **5.39** possesses the correct C5/C1/C2 functional groups in the correct orientation, however, the oxygen at C4 has been introduced with the wrong stereochemistry and the C6 methyl group remains unoxidized.

Scheme 5.20 – New dihydroxylation end game strategy.

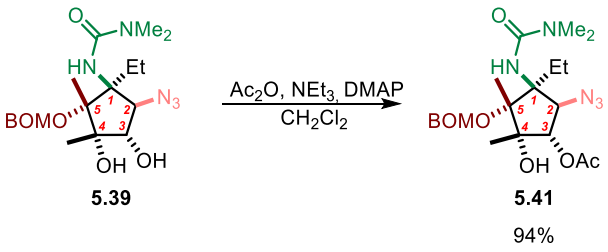


To reset the stereochemistry at C4 and introduce an alcohol at C6, the most direct route involves an elimination of the C4 tertiary alcohol after protection of the C3 secondary alcohol (**Scheme**

4.20). A multitude of elimination conditions (thionyl chloride, Burgess reagent, Martin's sulfurane) were envisaged to have potential to furnish the 1,1-disubstituted alkene. A subsequent dihydroxylation, alcohol protection, and epoxidation sequence would furnish **5.24**. The original end game could then be executed, where nucleophilic addition of the aniline derivative to give **5.25** could be followed by a global deprotection to furnish jogyamycin ***rac*-4.2**.

Progress on this endgame strategy hinged on successful elimination to furnish **5.42**. Research efforts toward this goal commenced with acetate protection of **5.39** to furnish **5.41** in 94% yield (**Scheme 5.21**).

Scheme 5.21 – Acetate protection of diol **5.39.**

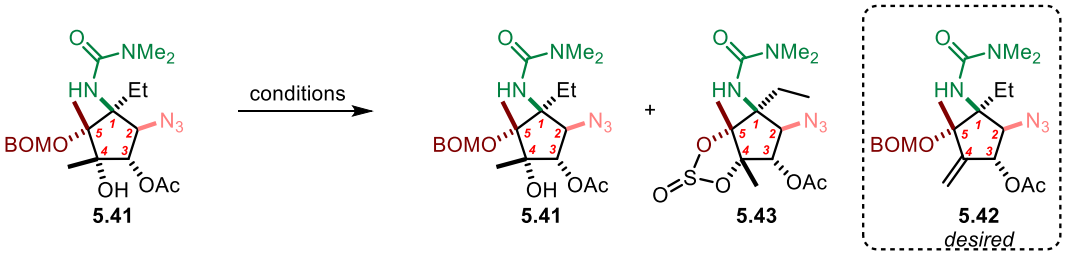


5.39 **5.41**

94%

Attempted Burgess elimination[14] of **5.41** (**Scheme 22, eq. 1**) gave complete decomposition. Reaction with thionyl chloride, followed by proposed elimination using an excess of pyridine to inhibit BOM deprotection, was explored next. Reaction did not occur until excess $SOCl_2$ was added, with complete reaction after the addition of 5.1 eq. (6 eq. of pyridine were added at the outset of the reaction to maintain neutral reaction conditions) (**Scheme 5.22, eq. 3**). Unfortunately, the 1,1-disubstituted alkene **5.42** was not observed; the cyclic sulfite **5.43** was formed instead, presumably aided by acid-mediated BOM deprotection.

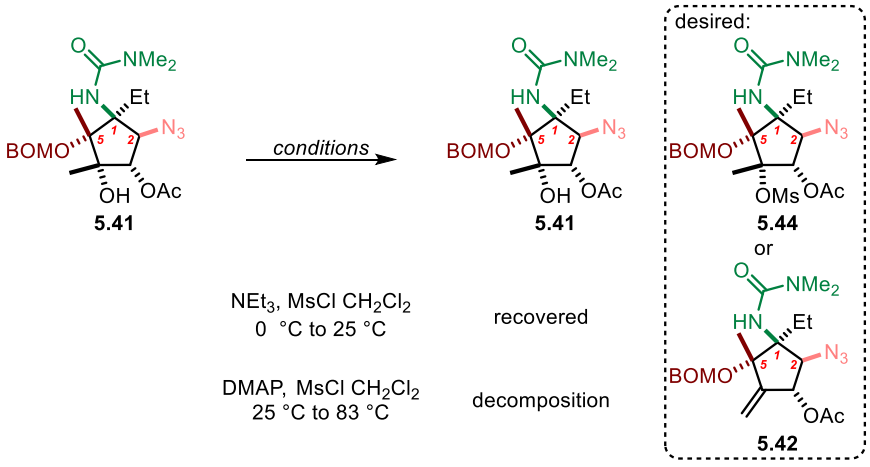
Scheme 5.22 – Attempts at elimination of the C4 tertiary alcohol of **5.41.**



Burgess reagent 4 eq. toluene, 25 °C to 70 °C	-		-	(1)
1.2 eq. $SOCl_2$ 6 eq. pyridine CH_2Cl_2, 0 °C	recovered		-	(2)
5.1 eq. $SOCl_2$ 6 eq. pyridine CH_2Cl_2, 0 °C	1	:	2.5	(3)
20 eq. $SOCl_2$ pyridine, 0 °C	-		-	(4)

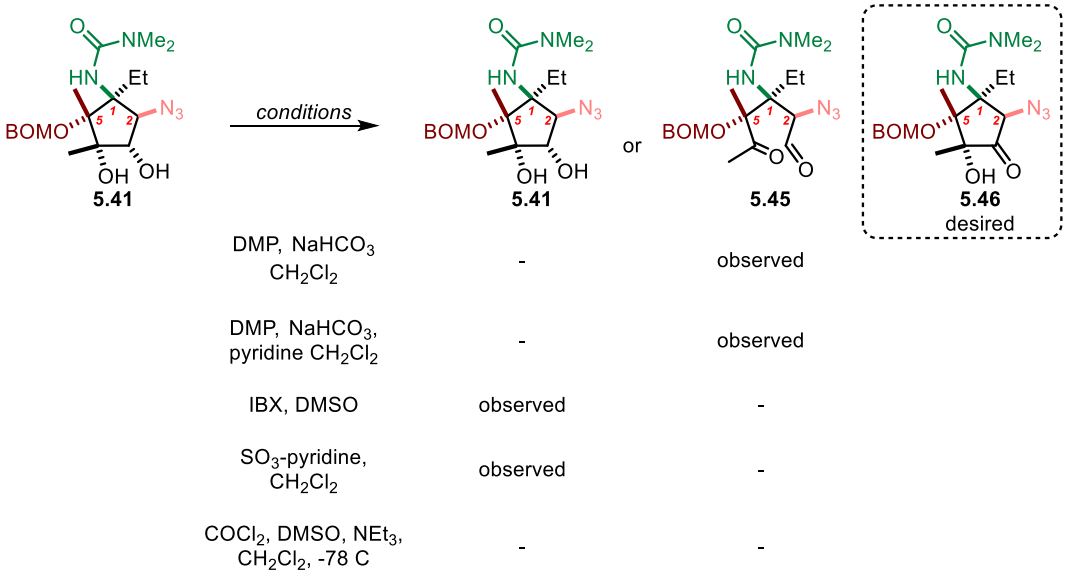
An attempt to eliminate the cyclic sulfite with KHMDS was unsuccessful. Conducting the reaction in pyridine as the solvent gave only decomposition (**Scheme 5.22, eq. 4.**). Next, we explored formation of the mesyl tertiary alcohol for a direct elimination. Unfortunately, mild conditions furnished no reaction and forcing conditions led to decomposition (**Scheme 5.23**).

Scheme 5.23 – Attempts at C4 tertiary alcohol elimination of **5.41** *via* mesylate formation**.**



Given the studies described above, it appeared that the tertiary alcohol was too hindered for successful elimination. With this in mind, a strategy to alter the pucker of the cyclopentane via secondary alcohol oxidation was developed to gain better access to the tertiary alcohol for elimination and facilitate the correction of the C2 stereocenter at a later time. Exposure to DMP furnished exclusive 1,2-diol scission (**Scheme 5.24, eq. 1**). Pyridine has been shown in certain cases to avoid cleavage of *syn*-1,2 diols with DMP,[19] but this was not effective in our system (**Scheme 5.24, eq. 2**). Oxidation with IBX to avoid the iodinane-mediated scission gave only recovered starting material (**Scheme 5.24, eq. 3**).[20] SO_3-pyridine also returned starting material **(Scheme 5.24, eq. 4)**. Swern oxidation, though challenging on small scale, was also attempted after demonstration on a test substrate. Despite a similar Swern oxidation reported by Johnson,[6] **5.41** underwent exclusive decomposition under these reaction conditions (**Scheme 5.24, eq. 5)**.

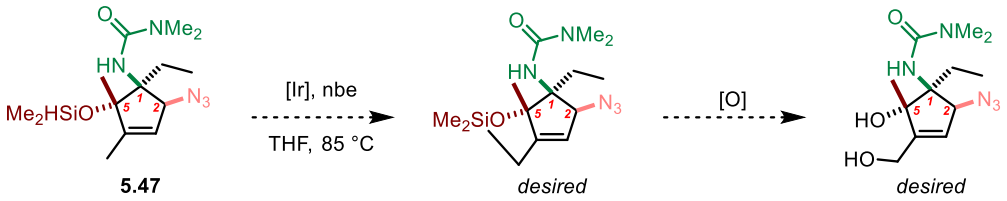
Scheme 5.24 – Attempts to access the C4 tertiary alcohol by oxidation of the C2 alcohol in **5.41.**



5.6 Investigation of Late-Stage C-H activation chemistry

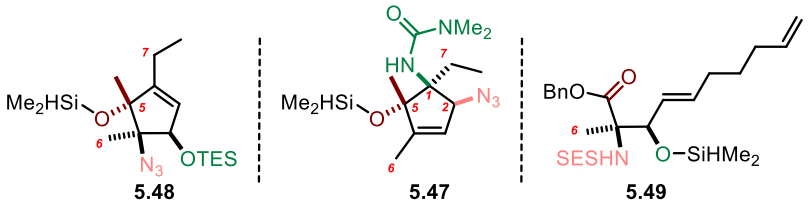
At this point, oxidizing the C6 methyl and/or pursuing an end-game strategy with diol **5.41** was proving challenging. Another end-game strategy considered at the outset was employing Hartwig's catalytic functionalization of unactivated primary C–H bonds directed by an alcohol to generate a hydridosilyl ether that could be easily cleaved to the primary alcohol using a Fleming-Tamao oxidation reaction.[21]

Scheme 5.25 – Possible alternative late-stage oxidation strategy, Hartwig unactivated C–H oxidation conditions.



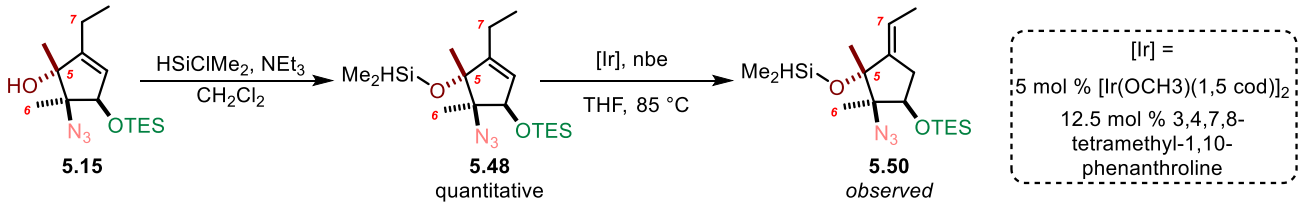
This reaction has been applied in a few total synthesis efforts including Sarpong's total synthesis of (+)-phomactin A[22] and Herzon's development of (+)-plueromutilin analogues.[23] Although elegant examples of this reaction in complex molecules, these reports do not demonstrate the level of amine tolerance required for application in a molecule such as jogyamycin **4.2**, which is why this effort remained a later resort. It was hypothesized that this reaction would have the best chances of working at three different stages of the synthesis: adjacent quaternary alcohol/azide **5.48**, rearrangement product **5.47**, and aldol product **5.49**.

Scheme 5.26 – Suggested substrates for Hartwig's C–H activation chemistry.



The first molecule examined was compound **5.48** as it was hypothesized it may demonstrate functional group compatibility with the azide but avoid dealing with the troublesome urea. If this reaction were to work, the newly generated C6 alcohol could be protected along with the C5 tertiary alcohol in a single di-protection step that would avoid the need for the BOM protection step prior to rearrangement and further streamline the synthesis. This reaction was performed using modified Herzon/Sarpong conditions and was found to deliver undesired alkene isomerization product **5.50**.

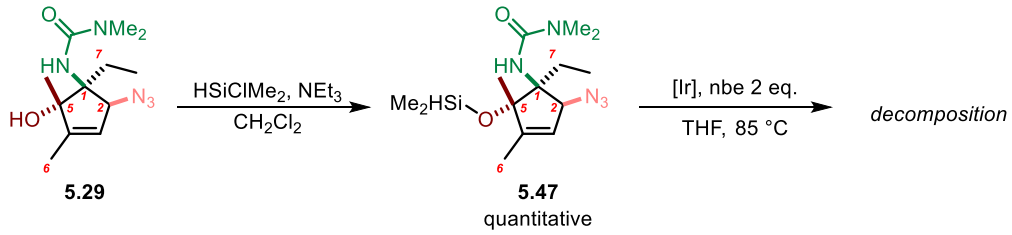
Scheme 5.27 – Hartwig C-H activation chemistry on tertiary azide **5.48.**



The lack of C–H activation of the desired methyl group led to the hypothesis that the adjacent quaternary centers were too hindered to be engaged by the iridium catalyst, and as a result, the iridium catalyst participated in an alkene isomerization to deliver **5.50**. Importantly, it appeared as though the azide group was tolerated under the reaction conditions, suggesting that the reaction may be more tolerant of amine functionality than was initially expected. With this information in hand, **5.47** was next examined as there was greater hope that the urea in **5.47** would be stable under the reaction conditions. In addition, the steric challenge associated with **5.48** would be alleviated,

as the adjacent quaternary center now resides at the C1 position. In contrast to **5.48**, the alkene isomerization was also hypothesized to not be likely as the isomerization would be contra thermodynamic, isomerizing from a trisubstituted to a disubstituted alkene. This reaction was run after preparation of **5.47** in quantitative yield. Unfortunately, exposure to the Hartwig C–H activation chemistry yielded extensive decomposition likely due to the urea functionality.

Scheme 5.28 – Hartwig C–H activation chemistry on urea **5.47.**

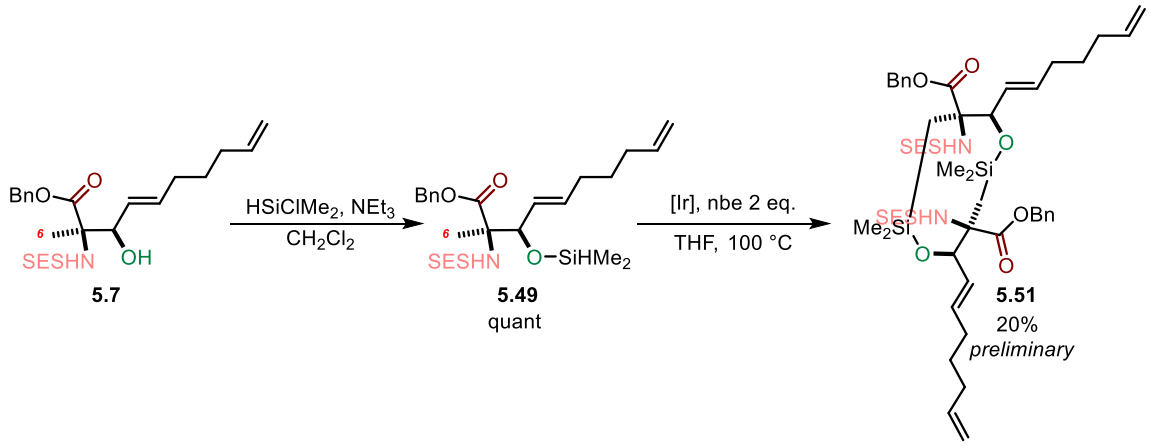


5.29 **5.47** quantitative

Finally, the reaction was tested on early aldol substrate **5.49.** The initial formation of silyl ether **5.49** proceeded well, though the NMR spectrum revealed possible rotomers. Although the initial TBS protected ether **5.4** did not demonstrate such behavior, here it is hypothesized that there may be an intramolecular H-bonding interaction between the newly installed protecting group and the adjacent protected nitrogen. The possibility that **5.7** underwent a diprotection event was considered, however, 2D-NMR ruled out a silyl protection of the nitrogen. Next, Hartwig C–H activation chemistry was explored, yielding a product with the molecular formula $C_{50}H_{82}N_2O_{10}S_2Si_4$. This unusual mass suggests the formation of a C–H insertion dimer where two molecules have undergone a double C–H activation event to form a unique 10-member ring (**Scheme 5.29**, **5.51**). Although it could be hypothesized that this reaction is happening on the mass-spectrometer, the lack of any monomer (single C–H activation event) suggests otherwise. The 1D-NMR data is unique in that the ^{1}H-NMR spectrum appears to contain symmetry (see supporting information) while the ^{13}C-NMR shows doubling and unexpected splitting of peaks.

2D-NMR and VT-NMR studies are currently underway to confirm this possibility. This preliminarily assigned compound will be subjected to Fleming-Tamao reaction to further prove a potential intermolecular C–H activation event. Despite running this reaction relatively concentrated (0.4 M), Hartwig never demonstrates an intermolecular C–H activation which further reinforces the need for better supporting data.

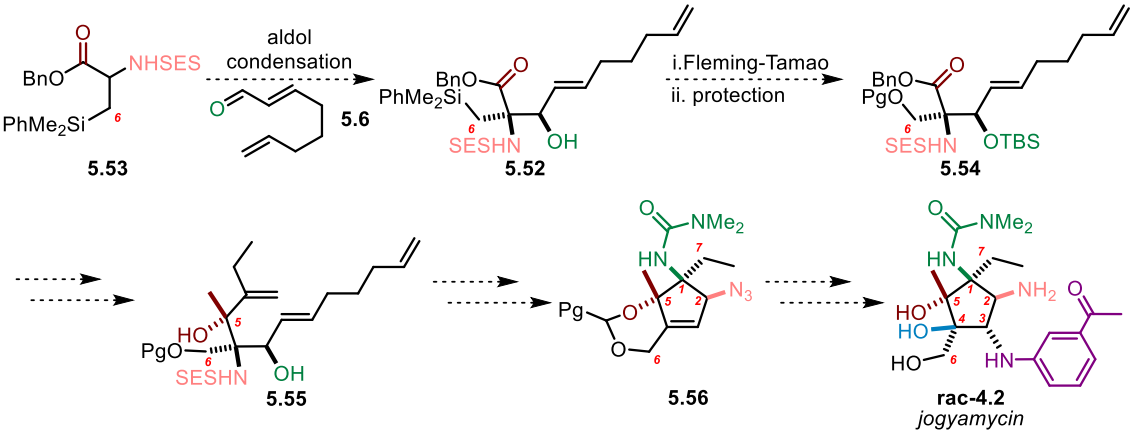
Scheme 5.29 – Hartwig C–H activation chemistry on aldol compound **5.49.**



5.7 Incorporation of C6 primary alcohol at outset

Another way the molecule could be rerouted to furnish jogyamycin (rac-**4.2**) would be to incorporate the C6 primary alcohol at the outset. The most direct method of incorporating this functionality would be to modify the starting amino acid from alanine to serine, however, even a protected alcohol at this position would likely lead to competing elimination in the early aldol reaction. A way to avoid this undesired reactivity would be to mask the alcohol as a dimethylphenyl group which could be later exposed to modified Fleming-Tamao conditions to reveal the C6 alcohol (**Scheme 5.30**). In this reimagined route, the conversion of **5.52** would still follow the same strategy as Hanessian and Johnson but avoid the troublesome allylic oxidation (**Scheme 5.30**).

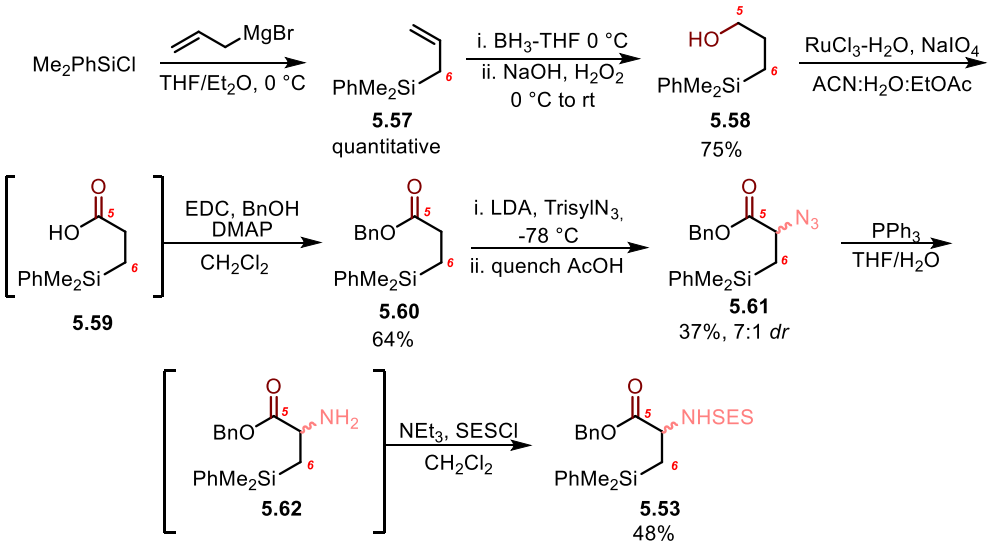
Scheme 5.30 – Incorporation of the C6 alcohol at the outset, proposed application of the Fleming-Tamao reaction.



To explore this goal a synthesis of **5.53** was required (**Scheme 5.31**). This route began with a simple Grignard addition to dimethylphenylsilylchloride which proceeded in quantitative yield. Hydroboration oxidation of **5.57** generated alcohol **5.58** in 75% yield. Ruthenium mediated oxidation yielded carboxylic acid **5.59** which could be immediately converted to benzyl ester **5.60** using EDC mediated esterification in 64% yield over two steps. $RuCl_3$-xH2O was utilized as the oxidant due to supply chain issues that precluded the procurement of PDC. Next, an azide needed to be introduced in the alpha position. This was done using an electrophilic source of azide, trisyl azide, to yield compound **5.61**in 37%, (**Scheme 5.31**) Interestingly, Evan's found that similar reactions are extremely sensitive toward base, counter cation, quenching reagent, and identity of sulfonyl azide,[24] which may account for the low observed yield. For substrate **5.60**, the most consistent data were obtained utilizing LDA and HOAc as the quenching reagent with a long stir time to account for the slow formation of LiOAc. SES protection of amine **5.62** yielded SES-protected amine **5.53** which was then ready to be examined in the aldol condensation reaction.

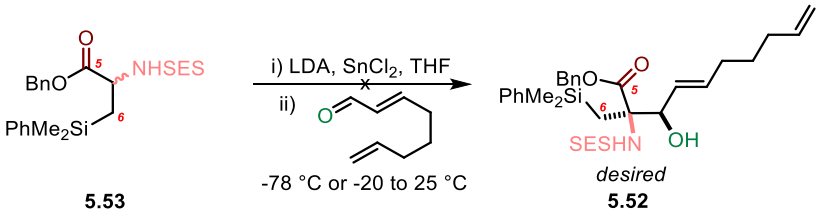
was enough to move on to the desired aldol condensation after reduction and protection as the SES amine **5.53**.

Scheme 5.31 – Synthesis of the Fleming-Tamao substrate.



Application in the aldol condensation yielded no conversion at -78 C. (**Scheme 5.32**). No homoaldol was observed, supporting a successful deprotonation. It was hypothesized that the additional bulk at C6 may be causing reactivity challenges at -78 ˚C so the temperature was raised, unfortunately, this too did not lead to any conversion of the aldol condensation product (**Scheme 5.32**).

Scheme 5.32– Attempted aldol reaction with **5.53**.



There are many other ways this reaction could be optimized and should be looked into at a later time. Unfortunately, time constraints led us to move on. It is possible that deprotonation is not occurring, and a smaller strong base could be applied to circumvent these issues.

5.8 Overall thoughts/Conclusions

Jogyamycin is a formidable molecule. Although not completed, this body of work demonstrates the possibility of setting three of jogyamycin's adjacent stereocenters (C5, C1, C2). The route reported herein also demonstrates the first known Ichikawa/Winstein rearrangement, which could be further pursued for the installation of various adjacent 1,2 diamines in complex molecules and natural products. Ultimately, there are several avenues that can be exploited to utilize the tandem Ichikawa/Winstein rearrangement route to finish this molecule. It is possible that the Hartwig C–H activation chemistry will prove fruitful after exploration of potential dimer **5.51**. Furthermore, Sanford's C–H acetoxylation chemistry[25] should be examined on substrate **5.8** to determine if this is a viable method of C6-oxidation. Finally, there is more exploration to be done on the aldol reroute proposed in section **5.7**.

5.9 References

(1) Hanessian, S.; Vakiti, R. R.; Dorich, S.; Banerjee, S.; Lecomte, F.; DelValle, J. R.; Zhang, J.; Deschênes-Simard, B. Total Synthesis of Pactamycin. *Angew.Chem., Int. Ed.* **2011**, *50*, 3497–3500.

(2) Malinowski Justin T.; Sharpe Robert J.; Johnson Jeffrey S. Enantioselective Synthesis of Pactamycin, a Complex Antitumor Antibiotic. *Science* **2013**, *340*, 180–182.

(3) Hale, K. J.; Domostoj, M. M.; Tocher, D. A.; Irving, E.; Scheinmann, F. Enantiospecific Formal Total Synthesis of the Tumor and GSK-3β Inhibiting Alkaloid, (−)-Agelastatin A. *Org. Lett.* **2003**, *5*, 2927–2930.

(4) Huang, J.; Widlanski, T. S. Facile Synthesis of Sulfonyl Chlorides. *Tet. Lett.* **1992**, *33*, 2657–2660.

(5) Grandel, R.; Kazmaier, U. Diastereoselective Synthesis of β-Substituted α-Methylserines via Chelated Alanine Ester Enolates. *Eur. J. Org. Chem.* **1998**, 409–417.

(6) Malinowski, J. T.; McCarver, S. J.; Johnson, J. S. Diastereocontrolled Construction of Pactamycin's Complex Ureido Triol Functional Array. *Org. Lett.* **2012**, *14*, 2878–2881.

(7) Loertscher, B. M.; Young, P. R.; Evans, P. R.; Castle, S. L. Diastereoselective Synthesis of Vicinal Tertiary Diols. *Org. Lett.* **2013**, *15*, 1930–1933.

(8) Hoye, T. R.; Jeffrey, C. S.; Tennakoon, M. A.; Wang, J.; Zhao, H. Relay Ring-Closing Metathesis (RRCM): A Strategy for Directing Metal Movement Throughout Olefin Metathesis Sequences. *J. Am. Chem. Soc.* **2004**, *126*, 10210–10211.

(9) Titz, A.; Radic, Z.; Schwardt, O.; Ernst, B. A Safe and Convenient Method for the Preparation of Triflyl Azide, and Its Use in Diazo Transfer Reactions to Primary Amines. *Tet. Lett.* **2006**, *47*, 2383–2385.

(10) Toma, T.; Kita, Y.; Fukuyama, T. Total Synthesis of (+)-Manzamine A. *J. Am. Chem. Soc.* **2010**, *132*, 10233–10235.

(11) Gerstner, N. C.; Schomaker, J. M. Stereocontrolled Synthesis of the Aminocyclopentitol Core of Jogyamycin via an Ichikawa Rearrangement Reaction. *J. Org. Chem.* **2019**, *84*, 14092–14100.

(12) Shibuya, K. A Novel Allylic Oxidation Using a Combination of Formic Acid and Selenium Dioxide. *Synth. Commun.* **1994**, *24*, 2923–2941.

(13) This was actually suggested in one of my job interviews by folks on a team that study RNA nucleotides. They have found in their work that steric congestion can sometimes be a surprising culprit for reactions on elaborated cyclopentanes. Unfortunately it didn't seem to be a smoking gun. (a).

(14) Kanda, Y.; Nakamura, H.; Umemiya, S.; Puthukanoori, R. K.; Murthy Appala, V. R.; Gaddamanugu, G. K.; Paraselli, B. R.; Baran, P. S. Two-Phase Synthesis of Taxol. *J. Am. Chem. Soc.* **2020**, *142*, 10526–10533.

(15) Bao, H.; Tambar, U. K. Catalytic Enantioselective Allylic Amination of Unactivated Terminal Olefins via an Ene Reaction/[2,3]-Rearrangement. *J. Am. Chem. Soc.* **2012**, *134*, 18495–18498.

(16) Trost, B. M.; Zhang, L.; Lam, T. M. Synthesis of the Aminocyclitol Core of Jogyamycin via an Enantioselective Pd-Catalyzed Trimethylenemethane (TMM) Cycloaddition. *Org. Lett.* **2018**, *20*, 3938–3942.

(17) Bataille, C. J. R.; Donohoe, T. J. Osmium-Free Direct Syn-Dihydroxylation of Alkenes. *Chem. Soc. Rev.* **2011**, *40*, 114–128.

(18a) Shing, T. K. M.; Tai, V. W.-F.; Tam, E. K. W. Practical and Rapid Vicinal Hydroxylation of Alkenes by Catalytic Ruthenium Tetraoxide. *Angew. Chem., Int. Ed.* **1994**, *33*, 2312–2313. (18b) Shing, T. K. M.; Tam, E. K. W.; Tai, V. W.-F.; Chung, I. H. F.; Jiang, Q. Ruthenium-Catalyzed Cis-Dihydroxylation of Alkenes: Scope and Limitations. *Chem. Eur. J.* **1996**, *2*, 50–57. (18c) Shing, T. K. M.; Tam, E. K. W. Solvent Effect on Ruthenium Catalyzed Dihydroxylation. *Tet. Lett.***1999**, *40*, 2179–2180.

(19) Paquette, L. A.; Edmondson, S. D.; Monck, N.; Rogers, R. D. Studies Directed toward the Synthesis of the Unusual Antileukemic Diterpene Jatrophatrione. 2. Functionalization of Advanced Polycyclic Precursors to the 9-Epi and 8,9-Dehydro Congeners. *J. Org. Chem.* **1999**, *64*, 3255–3265.

(20) Frigerio, M.; Santagostino, M. A Mild Oxidizing Reagent for Alcohols and 1,2-Diols: O-Iodoxybenzoic Acid (IBX) in DMSO. *Tet. Lett.* **1994**, *35*, 8019–8022.

(21) Simmons, E. M.; Hartwig, J. F. Catalytic Functionalization of Unactivated Primary C–H Bonds Directed by an Alcohol. *Nature* **2012**, *483*, 70–73.

(22) Leger, P. R.; Kuroda, Y.; Chang, S.; Jurczyk, J.; Sarpong, R. C–C Bond Cleavage Approach to Complex Terpenoids: Development of a Unified Total Synthesis of the Phomactins. *J. Am. Chem. Soc.* **2020**, *142*, 15536–15547.

(23) Ma, X.; Kucera, R.; Goethe, O. F.; Murphy, S. K.; Herzon, S. B. Directed C–H Bond Oxidation of (+)-Pleuromutilin. *J. Org. Chem.* **2018**, *83*, 6843–6892.

(24) Evans, D. A.; Britton, T. C.; Ellman, J. A.; Dorow, R. L. The Asymmetric Synthesis of .Alpha.-Amino Acids. Electrophilic Azidation of Chiral Imide Enolates, a Practical Approach to the Synthesis of (R)- and (S)-.Alpha.-Azido Carboxylic Acids. *J. Am. Chem. Soc.* **1990**, *112*, 4011–4030.

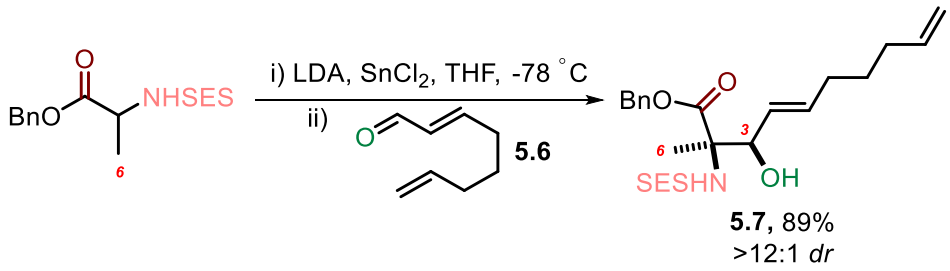
(25) Desai, L. V.; Hull, K. L.; Sanford, M. S. Palladium-Catalyzed Oxygenation of Unactivated Sp3 C−H Bonds. *J. Am. Chem. Soc.* **2004**, *126*, 9542–9543.

5.10 General Information

All glassware was either oven dried overnight, or flame dried under vacuum three times and purged with nitrogen before use. All glassware was allowed to cool under vacuum and placed under nitrogen after reaching room temperature. Unless otherwise specified, reagents were used as obtained from the vendor without further purification. Tetrahydrofuran was passed through an alumina column before use or freshly distilled from a Na/benzophenone ketyl. Dichloromethane was freshly distilled from calcium hydride or passed through an alumina column before use. Toluene, dimethylformamide, pentane, and hexanes were all freshly distilled from calcium hydride before use. Other solvents, if mentioned, were purified using accepted procedures from the sixth edition of "Purification of Laboratory Chemicals".[1] Air- and moisture- sensitive reactions were performed using standard Schlenk Techniques under nitrogen atmosphere. Analytical thin layer chromatography (TLC) was performed using pre-coated silica gel 60 F_{24} plates containing a fluorescent indicator. Either $KMnO_4$ or UV-lamp were used to visualize the reaction products. Preparative chromatography for most compounds, unless otherwise specified, was performed using SilicaFlash P60 silica gel (230-400 mesh) via Still's method,[2] Or purified via Combiflash™ Column chromatography. If a prepacked Combiflash™ column was used size will be specified along with the eluent program utilized. Unless stated otherwise, columns were typically run using a gradient method with EtOAc/hexanes. ^{1}H NMR and ^{13}C NMR spectra were obtained using Bruker Avance-500 spectrometers. For ^{1}H NMR, chemical shifts are reported relative to the tetramethylsilane peak (δ 0.00 ppm). ^{13}C NMR spectra were measured at 125 MHz on the same instruments noted above for recording ^{1}H NMR spectra, chemical shifts are reported relative to the solvent peaks (δ 77.16 ppm for $CDCl_3$). Accurate mass measurements were acquired at the University of Wisconsin, Madison using a Micromass LCT (electrospray ionization or electron

impact methods). The NMR and Mass Spectrometry facilities are funded by the NSF (CHE-1048642), the NIH (S10 OD012245, 1S10 OD020022-1), the Bender Fund, UW2020, and the University of Wisconsin-Madison.

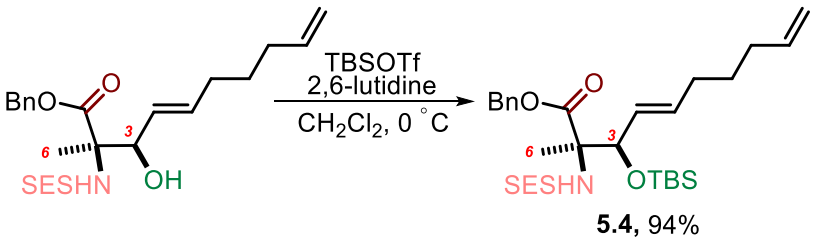
5.10.1 Synthesis of all previously unreported compounds



Compound 5.7. The following procedure was adapted from a method published by Kazmaier.[2] Three flasks, a 500 mL, 100 mL, and 50 mL were flame dried under vacuum twice. The largest flask was charged with $SnCl_2$ (4.12 g, 21.75 mmol, 2.5 eq.), vacuum cycled, and the SES protected amino acid derivative **5.5** (3.0g, 8.7 mmol, 1.0 eq.) added. To this mixture was added THF (0.2 M with respect to **5.5**). The flask was cooled to -78 ˚C in an acetone/dry ice bath. Next, the medium flask was charged with DIPA (3.17 mL, 22. 6 mmol, 1.6 eq.) and 38 mL of THF (0.6 M with respect to DIPA). The flask was then cooled to -78 ˚C in an acetone/dry ice bath. After 5 minutes of cooling *n*Buli (2.6 M in hexanes, 8.7 mL, 21.8 mmol, 2.5 eq.) is added dropwise. Once *n*BuLi addition is complete, the medium flask was warmed to 0 ˚C in a water/ice bath for 15 minutes to ensure LDA formation. During this 15-minute interval the third, smallest flask, is charged with the **5.6** and 28 mL of THF (0.4 M with respect to **5.6**) and cooled to -78 ˚C. The flask containing DIPA is then re-cooled to -78 ˚C in an acetone/dry ice bath for 15 minutes. After this period the LDA is cannula transferred into the largest flask containing **5.5** and $SnCl_2$, followed by a subsequent THF rinse (also at -78 ˚C). This is allowed to stir for 5 minutes at -78 ˚C before addition of the **5.6**. The aldehyde **5.6** (0.4 M in THF at -78 ˚C) is cannula transferred into the enolate followed by a

subsequent THF rinse (also at -78 ˚C). Once both the LDA and aldehyde are cannula transferred into the reaction flask the reaction mixture is allowed to stir at -78 ˚C until TLC indicates completion, usually around 70 minutes. *Note: This reaction is sensitive to scale. All reactions performed above 9 mmol result in loss of dr and conversion. If kept below 9 mmol, most frequently we ran these reactions at 8.7 mmol (3.0 g), the dr is consistently >12:1*. Once TLC indicates completion, (*Note: It can be difficult to differentiate product from starting material in the TLC a 95:5 CH_2Cl_2:EtOAc is recommended for reaction monitoring*) the reaction is quenched with 0.1 M pH 7 phosphate buffer, diluted with Et_2O and warmed to room temperature. Once warmed to room temperature the reaction mixture is filtered through a fritted funnel containing a pad of celite to remove solids. *Note: This mixture was filtered through a fritted funnel using a thick layer of celite with a sand layer on top. If a sand layer is not used the solids tend to clog up the celite.* The recollected mixture is then diluted with water and extracted three times with Et_2O. The combined organic layers were washed with brine, dried with Na_2SO_4, and concentrated *in vacuo*. The crude material was subjected to silica flash column chromatography using a Combiflash™ 80g gold resolution column with a method generated *via* the gradient optimizer, 0 to 40% EtOAc in Hexanes, yielding **Compound 5.7** as a thick yellow oil (3.64 g, 89% yield) with a *dr* >12:1 *Note: There is a small CH_2Cl_2 impurity in the ^{1}HNMR spectrum. This oil is extremely viscous; removing all residual solvent was nearly impossible.* ^{1}H NMR (500 MHz, $CDCl_3$) δ 7.37 (m, 5H), 5.77 (ddd, *J* = 16.9, 10.2, 6.6 Hz, 1H), 5.68 (dt, *J* = 14.3, 6.8 Hz, 1H), 5.36 (s, 1H), 5.33 – 5.25 (m, 1H), 5.20 (app d, *J* = 2.9 Hz, 2H), 5.09 – 4.90 (m, 2H), 4.13 (dd, *J* = 7.9 Hz, 1H); (app t, *J* = 7.9 Hz, 1H), 2.99 (m, 2H), 2.65 (d, *J* = 8.6 Hz, 1H), 2.12 – 1.82 (m, 4H), 1.61 (s, 3H), 1.41 (q, *J* = 7.4 Hz, 2H), 1.10 – 0.95 (m, 2H), 0.04 (s, 9H). ^{13}C NMR (125 MHz, $CDCl_3$) δ 172.4, 138.5, 136.6, 135.1, 128.8,

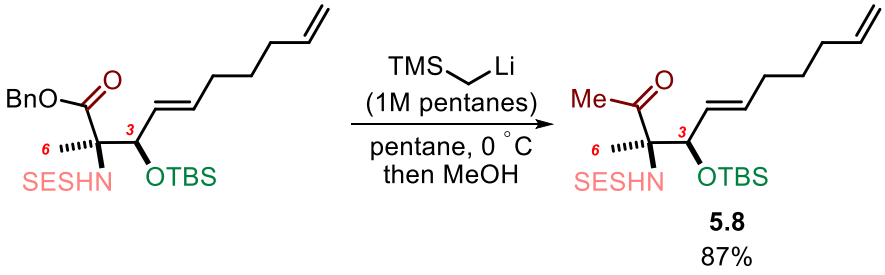
128.8, 128.7, 126.1, 115.0, 77.7, 68.0, 65.3, 52.5, 33.3, 31.8, 28.2, 19.9, 10.8, -1.9. HRMS (ESI) *m/z* calculated for $C_{23}H_{37}NO_5SSi$ $[M+NH_4]^+$ 485.2500, found 485.2499.



5.4, 94%

Compound 5.4. To a 250 mL flame dried round bottom flask charged with stir bar was added **5.7** (13.6 g, 29.2 mmol, 1 eq.), and 146 mL of CH_2Cl_2 (0.2 M with respect to **5.7**). The flask is cooled to 0 ˚C and to it is added 2,6-lutidine (10.2 mL, 87.6 mmol, 3 eq.). This was allowed to stir for 5 minutes at 0 ˚C. After 5 minutes, TBSOTf was added dropwise (13.4 mL, 58.4 mmol, 2 eq.). The reaction was allowed to stir until TLC indicated completion, usually around 40 minutes. Once TLC indicated completion the reaction was poured in a separatory funnel and washed once with 1M HCl, sat. $NaHCO_3$ and sat. NaCl. The organic layer was then dried with Na_2SO_4 concentrated *in vacuo* and subjected to silica flash column chromatography using a CombiFlash™ 120g gold resolution column with a method generated *via* the gradient optimizer, 0 to 30% EtOAc in Hexanes, yielding **Compound 5.4** as a light-yellow oil (15.9g, 94% yield). *The minor residual NMR impurity is silyl in nature, although unable to be removed by column chromatography, it was easily separated after the subsequent reaction.* ^{1}H NMR (500 MHz, $CDCl_3$) δ 7.43 – 7.30 (m, 5H), 5.77 (ddt, *J* = 17.0, 10.2, 6.7 Hz, 1H), 5.60 (dt, *J* = 15.3, 6.7 Hz, 1H), 5.31 (ddt, *J* = 15.3, 8.2, 1.4 Hz, 1H), 5.15 (s, 2H), 5.05 – 4.94 (m, 2H), 4.89 (s, 1H), 4.14 (d, *J* = 8.4 Hz, 1H), 3.13 – 2.88 (m, 2H), 2.12 – 1.91 (m, 4H), 1.60 (s, 3H), 1.51 – 1.35 (m, 2H), 1.14 – 1.02 (m, 2H), 0.85 (s, 9H), 0.05 (s, 3H), 0.03 (s, 9H), -0.03 (s, 3H).^{13}C NMR (125 MHz, $CDCl_3$) δ 171.7, 138.4, 136.1, 135.5, 128.7, 128.6, 128.5, 127.9, 115.0, 78.0, 67.6, 66.3, 52.4, 33.4, 31.7, 28.2, 25.9, 25.8, 20.0, 18.2,

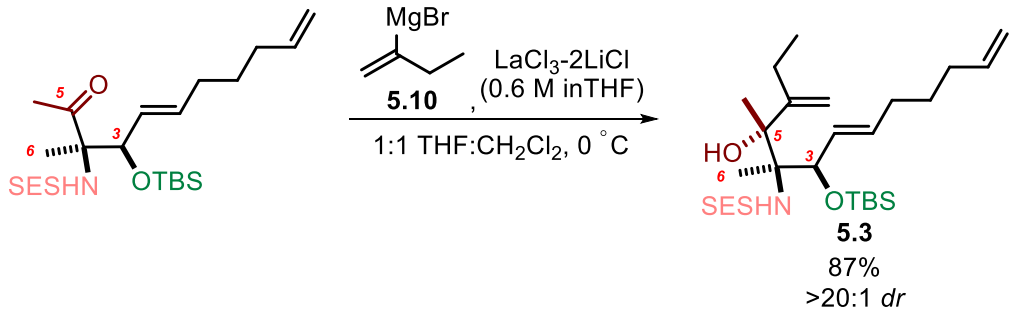
10.8, -1.8, -3.4, -3.7, -4.9. HRMS (ESI) *m/z* calculated for $C_{29}H_{51}NO_5SSi_2$ $[M+NH_4]^+$ 599.3365, found 599.3364.



5.8
87%

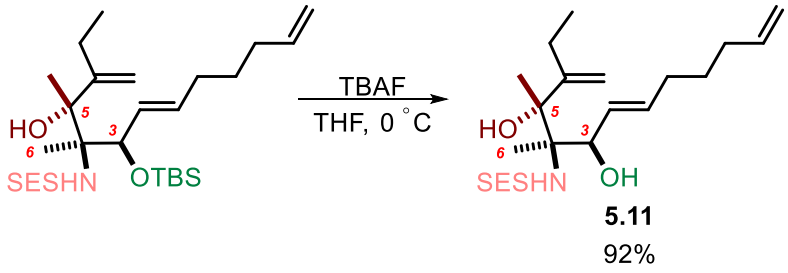
Compound 5.8. The following procedure was adapted from a method reported by Johnson.[3] To a flame dried 250 mL round bottom flask charged with a stir bar was added **5.4** (2.8 g, 4.9 mmol, 1 eq.) in pentanes. *Note: Compound **5.4** is extremely thick so diluting the viscous oil with a portion of pentanes will assist in charging the flask with the compound*. The remainder of pentanes was then added to equal 0.2 M of **5.4** in pentanes. The mixture was cooled to 0 ˚C for 10 minutes and after that period $TMSCH_2Li$ (1 M in pentanes, 14.7 mL, 3 eq.) was added dropwise. This was allowed to stir until the TLC indicated completion, approximately 3-4 hours. *Note: This reaction is very sensitive to scale. Reactions that exceed 5.5 mmol do not go to completion. Due to the length of reaction and already large excess of organometallic reagent, adding additional $TMSCH_2Li$ does not further reaction progress. If the reaction does not go to completion, it should be noted that the starting material and product can be separated via silica flash column chromatography using a CH_2Cl_2/EtOAc solvent system, although not the ideal solvent system for purification if the reaction goes to completion. Further it should be noted that recollected starting material can be re-exposed to the reaction conditions and furnish product without issue.* After TLC indicated completion, MeOH was added (0.6 M in **5.4**, 8.2 mL) and this was allowed to stir for 1 h at room temperature. After 1h, H_2O was added to quench the reaction and the mixture poured into a separatory funnel. The aqueous layer was extracted with Et_2O three times, the

combined organics washed with sat. NaCl, dried with Na_2SO_4, and concentrated *in vacuo*. The product was purified *via* CombiFlash™ and subjected to silica flash column chromatography using a CombiFlash™ 80g gold resolution column with a method generated *via* the gradient optimizer, 0 to 100% EtOAc in Hexanes, with a hold at 5% EtOAc:Hexanes, yielding **Compound 5.8** as a viscous clear oil (1.90 g , 82% yield) ^{1}H NMR (500 MHz, $CDCl_3$) δ ^{1}H NMR (500 MHz, Chloroform-*d*) δ 5.78 (ddt, *J* = 17.0, 10.1, 6.7 Hz, 1H), 5.67 (dt, *J* = 15.5, 6.7 Hz, 1H), 5.35 – 5.25 (m, 1H), 5.07 – 4.92 (m, 3H), 4.05 (d, *J* = 8.3 Hz, 1H), 3.19 – 2.84 (m, 2H), 2.33 (s, 3H), 2.12 – 2.01 (m, 4H), 1.51 (s, 3H), 1.48 (m, 2H), 1.04 (m, 2H), 0.90 (s, 9H), 0.07 (s, 3H), 0.06 (s, 9H), 0.02 (s, 3H).^{13}C NMR (125 MHz, $CDCl_3$) δ 210.8, 140.2, 138.5, 129.2, 117.0, 81.98, 71.1, 54.4, 35.3, 33.6, 30.3, 30.1, 27.8, 21.0, 20.1, 12.7, 2.0, -1.8, -3.0. HRMS (ESI) *m/z* calculated for $C_{23}H_{47}NO_4SSi_2$ $[M+NH_4]^+$ 507.3103, found 507.3104.



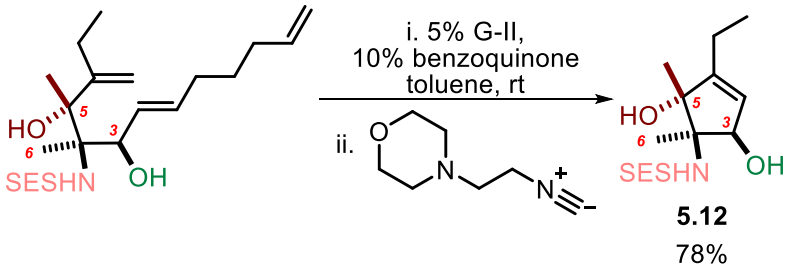
Compound 5.3. To a 250 mL flame dried round bottom flask charged with a stir bar was added **5.8** *via* syringe (1.90 g, 3.96 mmol, 1 eq.). **5.8** was then diluted with 63 mL CH_2Cl_2. The reaction vessel was placed in an ice bath and stirred for 5 minutes. After this period, $LaCl_3$·2 LiCl (0.6 M solution in THF, 32.6 mL, 19.8 mmol, 5 eq.) was added. *Note: the mixture will turn cloudy during the addition of $LaCl_3$·2LiCl but will clear after full addition of the reagent.* This mixture was allowed to stir at 0 ˚C for 10 minutes. After this period Grignard reagent **5.10** (0.4 M in THF, 29.7 mL, 11.9 mmol, 3 equiv.) was added rapidly. The total volume of THF (from both the Grignard

reagent and $LaCl_3 \cdot 2LiCl$) was 63 mL. The total concentration of the substrate in the 1:1 mixture of CH_2Cl_2 to THF should be 0.03 M. *Note: The Grignard reagent must be added rapidly, or the reaction will stall. Adding additional Grignard will not force the reaction to go to completion after it has stalled. It is worth noting that we explored the possibility of whether we were seeing competing enolization of the methyl ketone, however, quenching this reaction with D_2O offered no deuterium incorporation. It is also worth noting that cerium based organometallic reagents such as $CeCl_3$ or $CeCl_3 \cdot LiCl$ did not effect this transformation.* The reaction was monitored by TLC until it indicated completion, generally around 25 minutes. Once complete, it was quenched with 10 mL of AcOH and poured into a separatory funnel containing H_2O. The organic layer was extracted three times with EtOAc and the combined organics were washed with saturated $NaHCO_3$ three times, and once with brine. The combined organics were dried with Na_2SO_4, filtered, concentrated *in vacuo* and subjected to silica flash column chromatography using a CombiFlash™ 40 g gold resolution column with a method generated *via* the gradient optimizer, 0 to 40% EtOAc in Hexanes, yielding **Compound 5.3** as a thick light yellow oil (1.86 g , 87% yield) ^{1}H NMR (500 MHz, $CDCl_3$) δ 5.79 (ddt, *J* = 16.9, 10.1, 6.7 Hz, 1H), 5.64 (m, 2H), 5.38 (br s, 1H), 5.13 (app s, 1H), 5.06 (app s, 1H), 5.04 – 4.91 (m, 2H), 4.86 (s, 1H), 4.82 (dd, *J* = 5.5, 2.5 Hz, 1H), 3.05 – 2.73 (m, 2H), 2.33 – 2.09 (m, 2H), 2.06 (m, 3H), 1.52 (s, 3H), 1.51 – 1.42 (m, 2H), 1.27 (s, 3H), 1.05 (m, 5H), 0.92 (s, 9H), 0.22 (s, 3H), 0.09 (s, 3H), 0.02 (s, 9H).^{13}C NMR (126 MHz, $CDCl_3$) δ 154.2, 138.5, 136.2, 130.2, 115.0, 112.7, 85.8, 81.4, 65.5, 53.1, 33.5, 32.0, 28.3, 26.2, 26.1, 26.0, 18.1, 13.6, 11.0, -1.9, -3.7, -4.6. HRMS (ESI) *m*/*z* calculated for $C_{27}H_{55}NO_4SSi_2$ $[M+Na]^+$ 568.3283, found 568.3274.

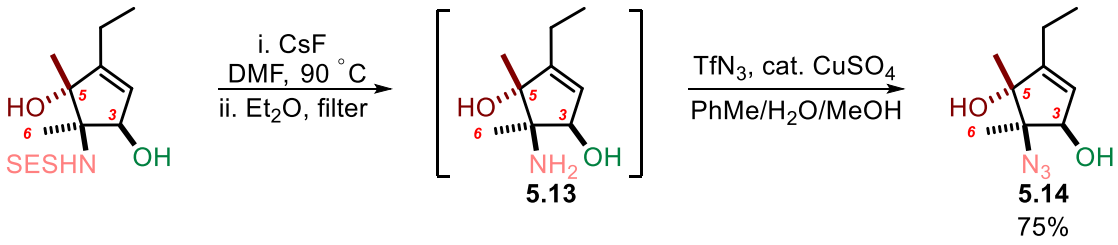


5.11
92%

Compound 5.11. To a 250 mL flame dried round bottom flask charged with a stir bar was added (5.89 g, 10.8 mmol, 1 eq.) *via* syringe. To the reaction vessel was added 108 mL of THF (0.1 M in **5.3**). This mixture was cooled to 0 ˚C. After stirring at this temperature for 15 minutes, TBAF (1M in THF, 12.9 mL, 1.2 eq.) was added dropwise. The reaction was stirred until TLC indicated completion, usually around 15 minutes. The reaction mixture was diluted with Et_2O and poured into a separatory funnel containing H_2O. The layers were separated, and the organic layer washed twice with NH_4Cl^+, and then once with brine. The organics were then dried with Na_2SO_4, filtered, concentrated *in vacuo* and subjected to silica flash column chromatography using a CombiFlash™ 120 g gold resolution column with a method generated *via* the gradient optimizer, 0 to 40% Acetone in Hexanes, yielding **Compound 5.11** as clear oil which solidifies at -20 ˚C (4.27g , 92% yield) ^{1}H NMR (500 MHz, $CDCl_3$) δ 5.94 – 5.63 (m, 3H), 5.18 (d, *J* = 1.7 Hz); (app s, 1H), 5.13 (d, *J* = 1.7 Hz, 1H), 5.03 – 4.91 (m, 2H), 4.86 (br s, 1H), 4.26 (dd, *J* = 6.9, 4.9 Hz, 1H), 3.40 (s, 1H), 3.32 (d, *J* = 4.9 Hz, 1H), 2.92 (ddd, *J* = 12.1, 5.2, 1.4 Hz, 2H), 2.27 (dq, *J* = 15.4, 7.2 Hz, 1H), 2.18 (dq, *J* = 15.4, 7.2 Hz, 1H), 2.08 (ddd, *J* = 14.7, 12.6, 7.0 Hz, 4H), 1.51 (s, 3H), 1.49 (m, 3H), 1.46 (s, 3H), 1.08 (t, *J* = 7.3 Hz, 5H), 0.04 (s, 9H).^{13}C NMR (125 MHz, $CDCl_3$) δ 154.6, 138.4, 135.7, 129.3, 115.1, 113.0, 81.6, 79.1, 65.6, 53.1, 33.5, 32.1, 28.3, 26.2, 25.8, 25.7, 13.7, 10.8, -1.9 HRMS (ESI) *m/z* calculated for $C_{21}H_{41}NO_4SSi$ $[M+NH_4]^+$ 449.2864, found 449.2858.



Compound 5.12. To a flame dried 500 mL round bottom flask charged with a stir bar was added Grubbs II catalyst (233 mg, 0.275 mmol, 0.05 eq.) and 1,4-benzoquinone (60.0 mg, 0.55 mmol. 0.1 eq.). The reaction vessel was vacuum cycled and then diluted with 250 mL of toluene. The remainder of the toluene, 25 mL was used to dissolve **5.11** (2.37 g, 5.5 mmol, 1 eq.) and the solution was syringed into the reaction vessel. This makes the final concentration of **5.11** in toluene (0.02 M). *Note: The low concentration is essential to promote the intramolecular ring closing metathesis reaction. If the concentration is raised by a factor of 10 the reaction will terminate early and not undergo the second ring closing metathesis of the RRCM. If this occurs the interrupted product can be re-exposed to the catalyst to achieve the cyclopentane.* Once the reaction is complete by TLC, usually in about 2 h, the catalyst is quenched the isocyanate (0.1 mL,1.21 mmol, 0.22 eq.), and allowed to stir for 5 minutes. After this period the reaction is concentrated *in vacuo* and subjected to silica flash column chromatography using a CombiFlash™ 120 g gold resolution column with a method generated *via* the gradient optimizer, 0% to 70% EtOAc in Hexanes, with the product eluting around 32% EtOAc in hexanes. **Compound 5.12** was isolated as a white solid (1.44 g , 78% yield) ^{1}H NMR (500 MHz, $CDCl_3$) δ 5.50 (d, *J* = 2.7 Hz, 1H), 5.34 (br s, 1H), 4.17 (dd, *J* = 6.8, 3.0 Hz, 1H), 3.15 – 2.96 (m, 3H), 2.29 – 2.03 (m, 2H), 1.47 (s, 3H), 1.34 (s, 3H), 1.19 – 1.01 (m, 5H), 0.07 (s, 9H).^{13}C NMR (125 MHz, $CDCl_3$) δ 159.4, 119.7, 83.6, 80.1, 67.3, 52.9, 28.4, 21.0, 19.7, 11.4, 11.0, -1.8. HRMS (ESI) *m/z* calculated for $C_{14}H_{29}NO_4SSi$ $[M\text{-}OH]^+$ 318.1554, found 318.1554

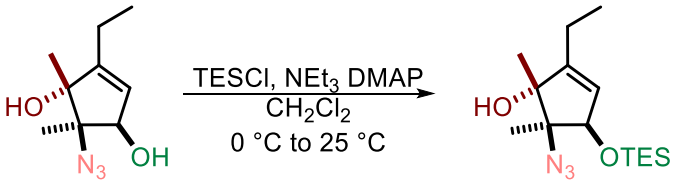


Compound 5.14. A flame dried 25 mL round bottom flask charged with a stir bar was added CsF (203.7 mg, 1.3 mmol, 3.0 eq.) and **5.12** (150.0 mg, 0.45 mmol, 1 eq.). The flask was vacuum cycled, charged with 4.5 mL DMF (0.1 M in **5.12**) and heated to 95 ˚C. The reaction was allowed to stir until TLC indicated completion, usually about 18 h. After TLC indicates completion 4.5 mL MeOH (0.1 M in **5.12**) is added, and this mixture is stirred for 30 min. The reaction was transferred to a new round bottom flask with EtOAc and added to it 4.5 g of celite and the solvent removed *in vacuo*, and then placed under vacuum. After vacuumed to dryness, the compound dry-loaded onto celite was transferred to a fritted funnel and washed with three portions of Et_2O. The combined Et_2O washes were collected in a round bottom flask and the solvent removed *in vacuo*. The residue is transferred to a 65 mL flask, solvent removed, flask charged with a stir bar, and then placed under vacuum while fresh TfN_3 solution is prepared as indicated below:

The following procedure for TfN3 formation was adapted from a report by Ernst.[4] To a 25 mL round bottom flask with a stir bar was added NaN_3 (2.107 g, 32.4 mmol, 72.5 eq.) and 5.4 mL of H_2O. This mixture was cooled in an ice bath open to air for five minutes. Next, 3.0 mL of toluene was added and with vigorous stirring Tf_2O (1.36 mL, 8.09 mmol, 18.1 eq.) was added dropwise. The reaction was allowed to stir for 3 h at 0 ˚C and at which point 3.0 mL of $NaHCO_3$ was added. The mixture is then transferred to a separatory funnel and the organic layer separated. The aqueous layer is extracted twice with 3.0 mL of toluene. The combined extracts were dried with Na_2SO_4.

This solution was stored over Na_2SO_4 and used quickly and left-over reagent was quenched with PPh_3 at 0 ˚C. *Note: TfN_3 is explosive. Handle this reagent with care, it must be maintained in solution, not made on large scale, and not allowed to evaporate to dryness.*

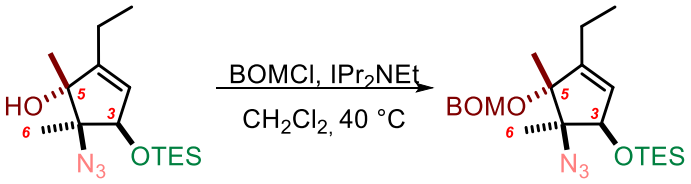
To the 65 mL flask containing the intermediate free amine, K_2CO_3 (185.3 mg, 1.34 mmol, 3.0 eq.), $CuSO_4 \cdot 5H_2O$ (5.6 mg, 0.02 mmol, 0.05 eq.) is added. To this mixture was added 7.6 mL MeOH (0.06 M in **5.12**) and 5.4 mL H_2O (0.08 M in **5.12**). Subsequently, the solution TfN_3 in toluene (1.94 mL) was added dropwise. This mixture was capped and allowed to stir overnight. After stirring for ~12 h the reaction was worked up by concentration *in vacuo with a blast shield in front of the rotovap*. Once concentrated the mixture was placed on hi-vac. Once dry, the crude material was redissolved in EtOAc and filtered through celite. The recollected EtOAc was removed, and the crude material subjected to silica flash column chromatography using a CombiFlash™ 12 g gold resolution column with a method generated via the gradient optimizer, 0 to 60% Acetone in Hexanes, yielding Compound **5.14** as a yellow oil (65.9 mg, 75 % yield). ^{1}H NMR (500 MHz, $CDCl_3$) δ 5.52 (dt, *J* = 2.0, 2.0 Hz, 1H); (app q, *J* = 2.0 Hz, 1H), 4.48 (dt, *J* = 2.1, 2.1 Hz, 1H); (app q, *J* = 2.1 Hz, 1H), 2.10 (qdd, *J* = 7.4, 2.0, 2.0 Hz, 2H); (app qt, *J* = 7.4, 2.0 Hz, 2H), 1.50 (s, 3H), 1.41 (s, 3H), 1.12 (t, *J* = 7.3 Hz, 4H). ^{13}C NMR (125 MHz, $CDCl_3$) δ 153.1, 125.9, 85.0, 79.9, 74.7, 22.4, 19.5, 16.1, 11.6. HRMS (ESI) *m*/*z* was not calculable for these intermediate, later intermediates were more amenable to characterization by HRMS (ESI)



5.15

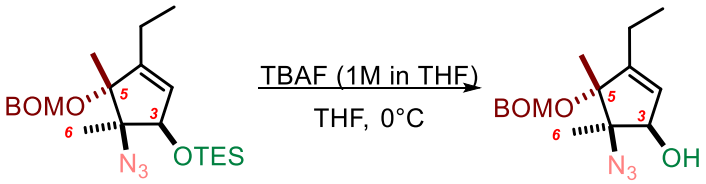
91%

Compound 5.15. A flame dried 25 mL round bottom flask charged with a stir bar was added DMAP (5.5 mg, 0.05 mmol, 0.1 eq.) and vacuum cycled. To this was added **5.14** (106.3 mg, 0.54 mmol, 1 eq.) and CH_2Cl_2 (5.3 mL, 0.1 M). The flask was cooled to 0 ˚C and NEt_3 was added dropwise (0.18 mL, 1.0 mmol, 2 eq.). After this stirred for 5 minutes, TESCl was added dropwise (0.1 mL, 0.59 mmol, 1.1 eq.) and the mixture was allowed to warm to room temperature. The reaction was stirred until TLC indicated completion, usually in about 70 minutes. The reaction was then poured into water, extracted with EtOAc (x3), the combined organics washed with brine, dried with Na_2SO_4, filtered, concentrated *in vacuo* and subjected to silica flash column chromatography using a CombiFlash™ 4 g gold resolution column with a method generated *via* the gradient optimizer, 0 to 60% Acetone in Hexanes, yielding **Compound 5.15** as clear oil which (153.0 mg, 91% yield) ^{1}H NMR (500 MHz, $CDCl_3$) δ 5.46 (dt, *J* = 1.9, 1.9 Hz, 1H); (app q, *J* = 1.9 Hz, 1H), 4.73 (dt, *J* = 2.1, 2.1 Hz, 1H); (app q, *J* = 2.1 Hz, 1H), 2.08 (m, 2H), 1.42 (s, 3H), 1.32 (s, 3H), 1.11 (t, *J* = 7.3 Hz,3H), 1.00 (t, *J* = 8.0 Hz, 9H), 0.67 (q, *J* = 7.9 Hz, 6H).^{13}C NMR (125 MHz, $CDCl_3$) δ 150.8, 127.4, 84.0, 81.2, 74.6, 21.1, 19.4, 15.8, 11.5, 6.8, 4.8 HRMS (ESI) *m*/*z* was not calculable for this intermediate, later intermediates were more amenable to characterization by HRMS (ESI)



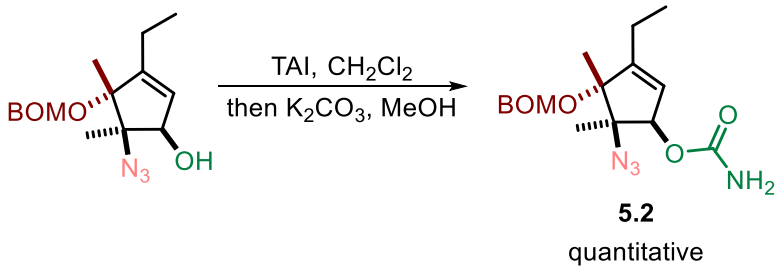
5.16
quantitative

Compound 5.16. To A flame dried 10 mL round bottom flask charged with a stir bar and equipped with a reflux condenser was added **5.15** (40.0 mg, 0.13 mmol, 1 eq.) in CH_2Cl_2 (2.6 mL, 0.05 M in **5.15**). iPr_2NEt (0.11 mL, 0.64 mmol, 5 eq.) was added dropwise at room temperature, followed by BOMCl (0.05 mL, 0.39 mmol, 3 eq.). The reaction was heated to reflux, and allowed to stir until the TLC indicated completion, generally around 48 h, on larger scales up to 72 h. Once the TLC indicated completion, the reaction mixture was cooled to room temperature, and diluted with Et_2O and quenched with NH_4Cl^+. This mixture was transferred to a separatory funnel and the aqueous layer was extracted with Et_2O three times. The combined organics were then were washed with H_2O and brine, dried with Na_2SO_4, filtered, concentrated *in vacuo* and subjected to silica flash column chromatography using a CombiFlash™ 4 g gold resolution column with a method generated *via* the gradient optimizer, 0 to 60% Acetone in Hexanes, with a hold at 5% Acetone in Hexanes, yielding **Compound 5.16** as a clear oil (56.1 mg, quantitative yield) ^{1}H NMR (500 MHz, $CDCl_3$) δ 7.39 – 7.28 (m, 5H), 5.55 (d, J = 1.9 Hz, 1H), 4.81 – 4.70 (m, 2H), 4.68 (d, J = 7.4 Hz, 1H), 4.57 (ABq, Δδ J_{AB} = 11.8 Hz, 2H), 2.08 (dqd, J = 15.5, 10.1, 7.4 Hz, 2H), 1.39 (s, 3H), 1.38 (s, 3H), 1.08 (t, J = 7.3 Hz, 3H), 0.99 (t, J = 7.9 Hz, 9H), 0.66 (q, J = 7.9 Hz, 6H).^{13}C NMR (125 MHz, $CDCl_3$) δ 149.5, 137.9, 129.2, 128.4, 127.7, 127.6, 89.9, 89.2, 81.4, 76.4, 69.6, 20.5, 18.1, 15.8, 11.3, 6.8, 4.8. HRMS (ESI) *m/z* calculated for $C_{23}H_{37}N_3O_3Si$ $[M+NH_4]^+$ 449.2942, found 449.2944.



5.17
89%

Compound 5.17. To a flame dried 5 mL round bottom flask charged with a stir bar was added Compound **5.16** (25.0 mg, 0.58 mmol, 1 eq.). **5.16** was diluted with THF (1.1 mL 0.05 M) and cooled to 0 ˚C. After stirring at 0 ˚C for 5 minutes TBAF (1M in THF, 0.07 mL, 1.2 eq.) was added dropwise. The reaction was allowed to stir at 0 ˚C until the TLC indicated completion, usually around 20 minutes. Once TLC indicated completion, the reaction was poured into Et_2O in a separatory funnel, washed twice with NH_4Cl^+, once with brine, and the organic layer was dried over Na_2SO_4. The volatiles were concentrated *in vacuo* and subjected to silica flash column chromatography using a CombiFlash™ 4 g gold resolution column with a method generated *via* the gradient optimizer, 0 to 60% Acetone in Hexanes, with a hold at 10% Acetone in Hexanes, yielding **Compound 5.17** as a clear oil (16.4 mg , 89% yield) ^{1}H NMR (500 MHz, $CDCl_3$) δ 7.41 – 7.27 (m, 5H), 5.60 (dt, J = 1.9, 1.9 Hz, 1H); (app q, J = 1.9 Hz, 1H), 4.73 (ABq, Δδ J_{AB} = 7.43 Hz, 2H), 4.58 (app s, 2H), 4.57 – 4.54 (m, 1H), 2.21 – 2.04 (m, 2H), 1.49 (s, 3H), 1.45 (s, 3H), 1.08 (t, J = 7.3 Hz, 3H).^{13}C NMR (125 MHz, $CDCl_3$) δ 151.1, 137.9, 128.6, 128.3, 127.9, 127.8, 90.1, 90.0, 80.4, 76.9, 69.8, 20.6, 18.8, 15.6, 11.4 HRMS (ESI) *m*/*z* calculated for $C_{17}H_{23}N_3O_3$ $[M+NH_4]^+$ 335.2078, found 335.2073.

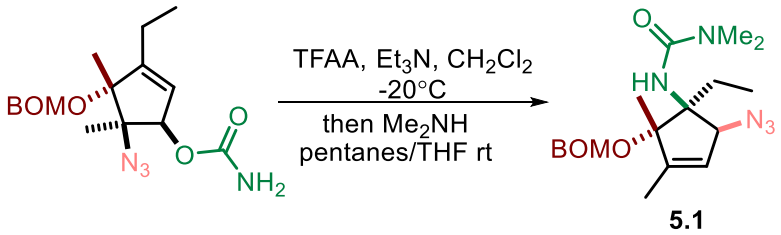


5.2

quantitative

Compound 5.2. To a flame dried 5 mL round bottom flask was added **5.17** (32.4 mg, 0.10 mmol, 1 eq.) which was diluted with 0.6 mL of CH_2Cl_2 (0.17 M in **5.17**). The reaction flask was cooled to 0 ˚C, and this was allowed to stir for 5 minutes. After this period, trichloroacetyl isocyanate was added (15 µL, 0.12 mmol, 1.2 eq.). Once the TLC indicated completion, usually in about 1 h, the solvent was removed *in vacuo*, and methanol (0.3 mL, 0.33 M in **5.17**) was added to the reaction vessel along with K_2CO_3 (8.4 mg, 0.6 mmol, 0.6 eq.). This reaction was allowed to stir overnight and in the morning the solvent removed *in vacuo*, re-dissolved in Et_2O, and transferred to a separatory funnel. H_2O was added and the aqueous layer extracted three times with Et_2O. The combined organics were then washed with brine, dried with Na_2SO_4 and the volatiles concentrated *in vacuo*. The crude mixture was subjected to silica flash column chromatography using a CombiFlash™ 4 g gold resolution column with a method generated *via* the gradient optimizer, 0 to 40% Acetone in Hexanes, yielding **Compound 5.2** as a white solid (35.9 mg, quantitative yield). *Note: There may be a residual trichloroacetamide impurity which may make the purified product appear to be greater than 100% yield. Generally, this can be removed by column chromatography, but if not a wash with 1M NaOH will remove it fully. It is also worth noting that carrying this impurity forward to the next step will not harm the following reaction and will be removed via the subsequent column* ^{1}H NMR (500 MHz, $CDCl_3$) δ 7.42 – 7.28 (m, 5H), 5.62 (dt, J = 2.0, 2.0 Hz, 1H); (app q, J = 2.0 Hz, 1H), 5.58 (dt, J = 2.1, 2.1 Hz, 1H); (app q, J = 2.1 Hz, 1H), 4.78 (ABq, Δδ J_{AB} = 7.4 Hz, 2H), 4.71 (br s, 2H), 4.60 (ABq, Δδ J_{AB} = 11.9 Hz, 2H), 2.20 (m, 1H), 2.14 –

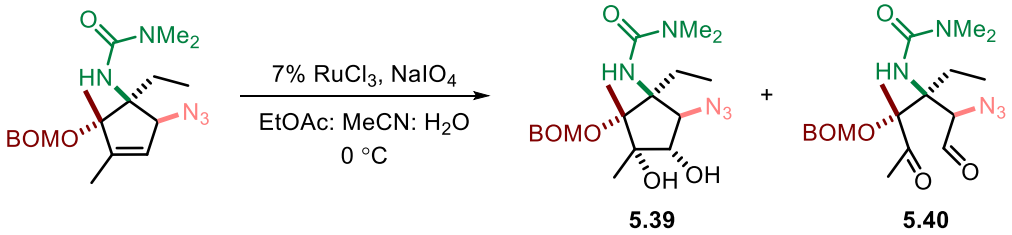
2.02 (m, 1H), 1.46 (s, 3H), 1.42 (s, 3H), 1.09 (t, J = 7.3 Hz, 3H).^{13}C NMR (125 MHz, $CDCl_3$) δ 156.3, 154.4, 137.9, 128.6, 127.9, 127.8, 123.6, 90.0, 89.3, 82.6, 74.9, 69.8, 20.6, 18.9, 17.2, 11.4. HRMS (ESI) *m*/*z* calculated for $C_{18}H_{24}N_4O_4$ $[M+Na]^+$ 383.1690, found 383.2693.



5.1

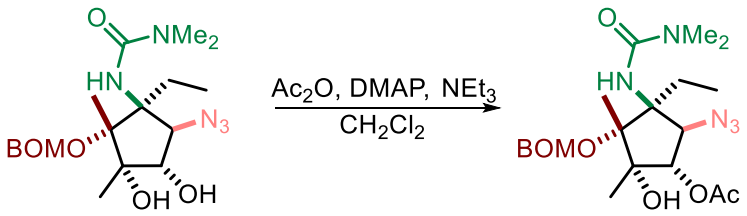
Compound 5.1. To a 5 mL flame dried round bottom flask charged with a stir bar was added compound **5.2** (10.0 mg, 0.028 mmol, 1 eq.) which was diluted with 1.4 mL of CH_2Cl_2 (0.02 M in **5.2**) and charged with NEt_3 (0.03 mL, 0.19 mmol, 6.7 eq.). The reaction vessel was then cooled to -20 ˚C and allowed to stir for 10 minutes. After this period TFAA was added dropwise (13.5 µL, 0.09 mmol, 3.5 eq.). When the TLC indicated completion, generally in about 30 minutes, the reaction was quenched with saturated $NaHCO_3$ transferred to a vial and extracted twice with EtOAc. The combined organics were then washed with brine, dried with Na_2SO_4, filtered and concentrated *in vacuo*. Once concentrated, the sample is placed under vacuum for approximately 15 minutes. The intermediate isocyanate was then re-dissolved in pentane and transferred to a flame dried 10 mL round bottom flask charged with a stir bar and diluted to 0.005 M. *Note: it is extremely important that the reaction be dilute. If not, there are competing byproduct forming reactions that will impact the overall yield.* Once diluted, to the reaction is added a solution of dimethyl amine (0.17 mL, 0.08 mmol, 3 eq.) in a solution of pentanes made freshly from condensation of $NHMe_2$ (g). This is allowed to stir for 1 h and after this period the volatiles are concentrated *in vacuo* and the crude compound subjected to silica flash column chromatography using a CombiFlash™ 4 g gold resolution column with a method generated *via* the gradient

optimizer, 0 to 50% Acetone in Hexanes, yielding **Compound 5.1** as a clear oil (4.4 mg , 41 % yield) ^{1}H NMR (500 MHz, $CDCl_3$) δ 7.38 – 7.32 (m, 4H), 7.29 – 7.23 (m, 1H), 5.51 (dq, *J* = 3.0, 1.5 Hz, 1H), 5.17 (s, 1H), 5.13 (ABq, Δδ J_{AB} = 8.1 Hz), 4.67 (ABq, Δδ J_{AB} = 11.8 Hz, 2H), 4.30 (dd, *J* = 2.7, 1.3 Hz, 1H), 2.89 (s, 6H), 2.58 (dq, *J* = 14.7, 7.4 Hz, 1H), 1.84 (t, *J* = 1.3 Hz, 3H), 1.37 (s, 3H), 0.80 (t, *J* = 7.3 Hz, 3H). ^{13}C NMR (125 MHz, $CDCl_3$) δ 157.2, 154.1, 138.5, 128.5, 127.9, 127.6, 118.7, 91.1, 91.0, 70.8, 70.0, 68.5, 36.5, 24.8, 20.1, 13.5, 9.4. (ESI) *m/z* calculated for C20H29N5O3 $[M+H]^+$ 388.2343, found 388.2338.



Compounds 5.39, 5.40. To a vigorously stirred solution of the **5.1** (11.1 mg, .0286 mmol, 1 eq.) in EtOAc (0.3 mL), CH_3CN (0.3 mL) at 0°C was added 0.1 mL of $RuCl_3$·(H_2O) in distilled water (0.4 mg/0.1 mL, 0.07 eq.) and sodium periodate (9.2 mg, 0.043 mmol, 1.5 eq.) were added. The two-phase mixture was stirred vigorously for 5 minutes and quenched with a saturated aqueous solution of $Na_2S_2O_3$ (0.5 mL). The reaction mixture was extracted with EtOAc (x3) and the combined organics dried with sodium sulfate. The organics were concentrated and the crude compound subjected to silica gel flash column chromatography using a pipette column using a Hexane:Acetone solvent system 0 to 80 % in 5% increments with the desired product eluting around 20% **Compound 5.39** as a white solid (5.1 mg, 42 % yield) and **Compound 5.40** as a clear oil (5.0 mg, 42% yield) NMR reported for desired product **Compound 5.39** ^{1}H NMR (500 MHz, $CDCl_3$) δ 7.34 (d, *J* = 4.4 Hz, 4H), 5.30 (ABq, Δδ J_{AB} = 7.7 Hz, 2H), 5.16 (s, 1H), 4.67

(ABq, Δδ J_{AB} = 11.9 Hz, 2H), 3.79 (d, J = 8.9 Hz, 1H), 3.58 (t, J = 9.7 Hz, 1H), 3.27 (d, J = 1.0 Hz, 1H), 2.91 (s, 6H), 2.62 (dq, J = 14.8, 7.4 Hz, 1H), 2.37 (d, J = 10.8 Hz, 1H), 1.46 – 1.35 (m, 1H), 1.29 (s, 3H), 1.19 (s, 3H), 0.78 (t, J = 7.4 Hz, 3H).^{13}C NMR (125 MHz, $CDCl_3$) δ 157.6, 138.2, 128.6, 127.8,90.9, 87.8, 79.7, 79.6, 74.9, 70.4, 66.4, 36.5, 27.8, 20.3, 19.1, 8.1. HRMS (ESI) *m/z* calculated for $C_{20}H_{31}N_5O_5$ $[M+NH_4]^+$ 444.2217, found 444.2212.

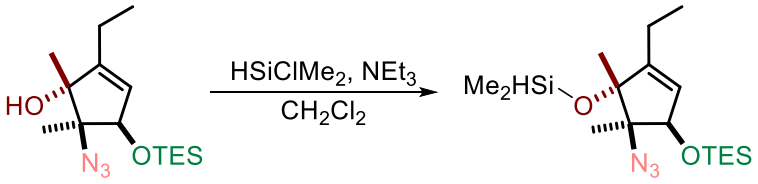


5.41

94%

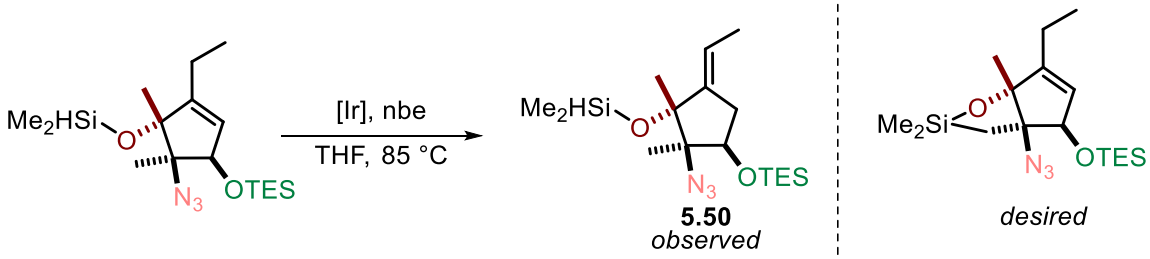
Compound 5.41. DMAP (90 µg, 0.00074 mmol, 0.1 eq.) in CH_2Cl_2 was added to a solution of diol (3.1 mg, 0.0074 mmol, 1.0 eq.), triethylamine (2.5 µL, 0.018 mmol, 2.4 eq.), and Ac_2O (1.7 µL, 0.018 mmol, 2.4 eq.) in CH_2Cl_2 (0.05 M) at room temperature (for ease of reaction set-up all reagents can be made as solutions in dry CH_2Cl_2, but the total volume should be 0.05 M in **5.39**). The reaction was monitored by TLC and after the TLC indicated completion, the reaction mixture was quenched by saturated aqueous NH_4Cl. The resulting mixture was extracted with DCM (x2). The combined organic extracts were washed with brine, dried over Na_2SO_4 and concentrated. The crude compound subjected to silica flash column chromatography using a pipette column using a Hexane:Acetone solvent system 0 to 40 % Acetone:Hexanes in 5% increments with the desired product eluting around 15% **Compound 5.41** as a clear oil (3.2 mg , 94 % yield) ^{1}H NMR (500 MHz, $CDCl_3$) δ 7.44 – 7.30 (m, 5H), 5.72 (d, J = 7.7 Hz, 1H), 5.15 (s, 1H), 4.93 (d, J = 7.7 Hz, 1H), 4.66 (ABq, Δδ J_{AB} = 11.9 Hz, 2H), 4.62 (ABq, Δδ J_{AB} = 9.8 Hz, 2H), 3.31 (s, 1H), 2.92 (s,

6H), 2.73 – 2.57 (m, 1H), 2.21 (s, 3H), 2.06 – 1.94 (m, 1H), 1.37 (s, 3H), 1.12 (s, 3H), 0.80 (t, *J* = 7.4 Hz, 3H). HRMS (ESI) *m*/*z* calculated for $C_{22}H_{33}N_5O_6$ $[M+Na]^+$ 486.2323, found 486.2317.

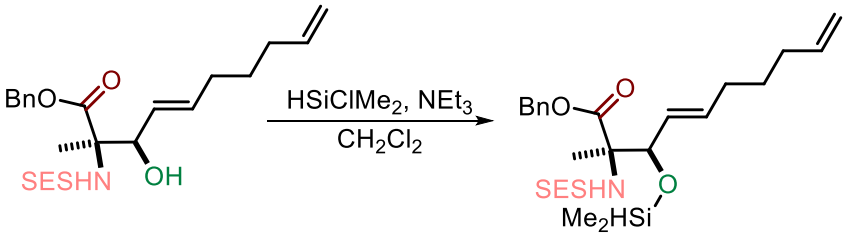


5.48

Compound 5.48. Dimethyl chlorosilane (.07 mL, 0.642 mmol, 2.0 eq.) was added dropwise via syringe to a solution of **5.15** (100.0 mg, 0.32 mmol, 1.0 eq.) and NEt_3 (0.18 mL, 0.642 mmol, 4.0 eq.) in CH_2Cl_2 (0.2 M) at 0 ˚C. The reaction was stirred until TLC indicated completion. Once complete, the reaction mixture was diluted with pentane and quenched with a pH 7 buffer. This biphasic solution was extracted with CH_2Cl_2 three times, and the combined organics dried with Na_2SO_4 and concentrated in vacuo. The crude mixture was passed through a silica filter to yield **Compound 5.48** as a yellow oil (118.2 mg, quantitative yield) ^{1}H NMR (600 MHz, $CDCl_3$) δ 5.42 (dt, *J* = 1.9, 1.9 Hz, 1H); (app q, *J* = 1.9 Hz, 1H), 4.67 (m, 2H), 2.13 – 1.89 (m, 2H), 1.34 (s, 3H), 1.33 (s, 3H), 1.10 (t, *J* = 7.3 Hz, 3H), 1.00 (t, *J* = 7.9 Hz, 9H), 0.66 (q, *J* = 7.9 Hz, 6H), 0.17 (d, *J* = 2.8 Hz, 3H), 0.14 (d, *J* = 2.8 Hz, 3H). ^{13}C NMR (151 MHz, $CDCl_3$) δ 151.1, 127.1, 86.8, 81.5, 75.7, 21.1, 20.0, 16.3, 11.2, 6.9, 5.0, 0.7, 0.5. HRMS (ESI) *m*/*z* was not calculable for this intermediate.

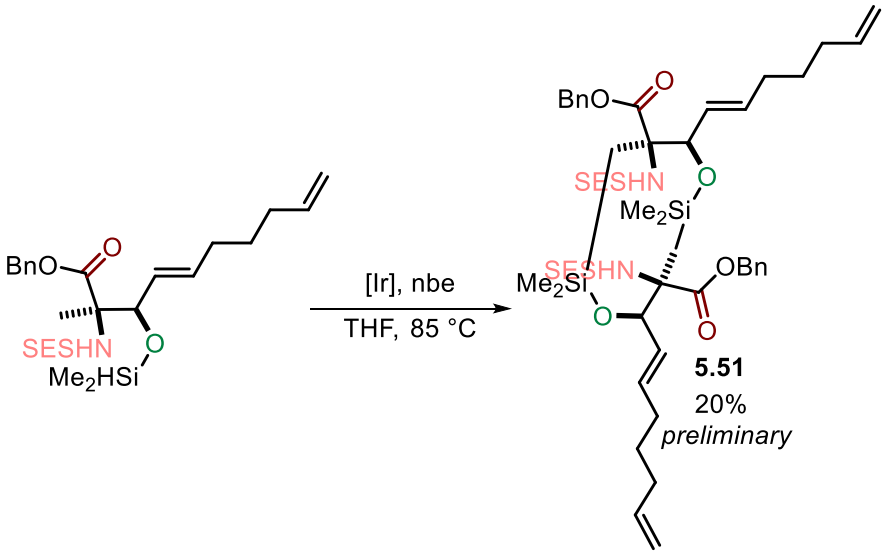


Compound 5.50. This experiment was adapted from the work of Hartwig and co-workers.[6,7,8] A 5mL vial was charged with **Compound 5.50** and a stir bar and brought into a glove box. The vial was then charged with 3,4,7,8-tetramethyl-1,10-phenanthroline (9.4 mg, 0.040 mmol, 12.5 mol%) and norbornene (60.0 mg, 0.642 mmol, 2 eq.). Next, a solution of Methoxy(cyclooctadiene)iridium(I) dimer was generated (10.6 mg, .016 mmol, 5 mol%) in 2 mL of THF which was added directly to the reaction vial. The vial was sealed and stirred for 2h in the glovebox to ensure catalyst formation. After this period, the reaction was brought out of the glove box and heated at 85 ˚C for 18 h. Once complete, the reaction was concentrated and observed without further purification. ^{1}H NMR (500 MHz, $CDCl_3$) δ 5.60 (qt, *J* = 6.7, 2.7 Hz, 1H), 4.48 (p, *J* = 2.8 Hz, 1H), 4.33 (t, *J* = 8.4 Hz, 1H), 2.59 – 2.49 (m, 1H), 2.31 – 2.21 (m, 1H), 1.62 (dt, *J* = 6.8, 1.6 Hz, 3H), 1.36 (s, 3H), 1.25 (s, 3H), 1.00 (t, *J* = 7.9 Hz, 9H), 0.64 (q, *J* = 8.1 Hz, 6H), 0.10 (d, *J* = 2.9 Hz, 3H), 0.04 (d, *J* = 2.8 Hz, 3H). ^{13}C NMR (126 MHz, $CDCl_3$) δ 142.1, 120.0, 82.2, 77.6, 74.7, 68.1, 35.0, 18.9, 14.3, 13.3, 6.9, 5.0, 0.3, 0.2. HRMS (ESI) *m/z* was not calculable for this intermediate.

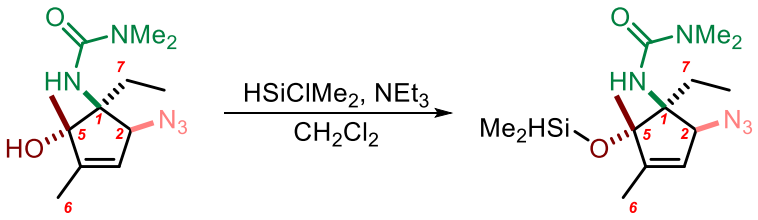


5.49

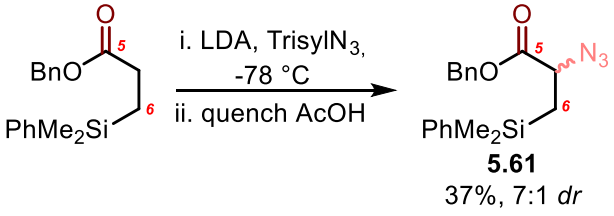
Compound 5.49. Dimethyl chlorosilane (0.1 mL, 0.863mmol, 2.0 eq.) was added dropwise via syringe to a solution of **5.7** (201.5 mg, 0.43 mmol, 1 eq.) and NEt_3 (0.24 mL, 1.72 mmol, 4.0 eq.) in CH_2Cl_2 (0.2 M) at 0 ˚C. The reaction was stirred until TLC indicated completion. Once complete, the reaction mixture was diluted with pentane and quenched with a pH 7 buffer. This biphasic solution was extracted with CH_2Cl_2 three times, and the combined organics dried with Na_2SO_4 and concentrated in vacuo. This compound was not stable to silica gel and was not put through a silica filter and instead pulled directly into the next step. **Compound 5.49**. *This compound revealed serious rotamers in the NMR. Initial evaluation pointed to possible double protection of the nitrogen to yield a mixture of compounds that were mono and deprotected, however, this was ruled out by mass spectrometry and 2D-NMR spectroscopy. Current data supports formation of the desired compound and a possible H-bonding effect between the nitrogen and silicon protecting group which may be causing the rotamers*. ^{1}H NMR (500 MHz, $CDCl_3$) δ ^{1}H NMR (500 MHz, Chloroform-*d*) δ 7.40 – 7.35 (m, 5H), 5.82 – 5.72 (m, 1H), 5.67 – 5.55 (m, 1H), 5.34 (dddd, *J* = 15.3, 8.0, 3.4, 1.9 Hz, 1H), 5.22 – 5.12 (m, 2H), 5.05 – 4.93 (m, 2H), 4.88 (br s, 1H), 4.57 (hept, *J* = 2.9 Hz, 1H), 4.14 (d, *J* = 8.0 Hz, 1H), 3.16 – 3.04 (m, 1H), 3.04 – 2.92 (m, 1H), 2.09 – 1.94 (m, 4H), 1.62 (s, 3H), 1.47 – 1.39 (m, 2H), 1.08 – 1.02 (m, 2H), 0.17 (d, *J* = 3.0 Hz, 3H), 0.14 (d, *J* = 2.8 Hz, 3H), 0.03 (s, 9H). ^{13}C NMR (126 MHz, $CDCl_3$) δ 171.5, 138.4, 136.5, 135.5, 128.7, 128.5, 128.4, 126.9, 115.0, 80.8, 67.6, 66.3, 52.3, 33.3, 31.7, 28.2, 20.4, 10.8, -1.8. HRMS (ESI) *m*/*z* $[C_{25}H_{43}NO_5SSi_2+NH_4]^+$ 543.2739, found 543.2737.



Compound 5.51. This experiment was adapted from the work of Hartwig and co-workers.[6,7,8] A 5mL vial was charged with **Compound 5.49** and a stir bar and brought into a glove box. The vial was then charged with 3,4,7,8-tetramethyl-1,10-phenanthroline (9.4 mg, 0.040 mmol, 12.5 mol%) and norbornene (60.0 mg, 0.642 mmol, 2 eq.). Next, a solution of Methoxy(cyclooctadiene)iridium(I) dimer was generated (10.6 mg, .016 mmol, 5 mol%) in 2 mL of THF which was added directly to the reaction vial. The vial was sealed and stirred for 2h in the glovebox to ensure catalyst formation. After this period, the reaction was brought out of the glove box and heated at 85 ˚C for 18 h. Once complete, the reaction was concentrated and columned 0% to 50% EtOAc:Hex to yield **Compound 5.51** as a clear oil (50.0 mg, 20% yield). This compound is still being evaluated and as such the NMR data will be included in the final submission. *m/z* calculated for $C_{50}H_{82}N_2O_{10}S_2Si_4$ $[M+NH_4+H_2O]^+$ 1082.4932, found 1082.4946.

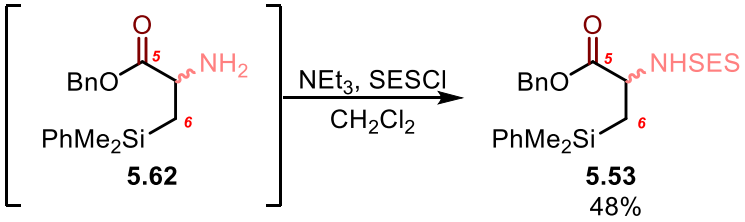


Compound 5.47. Dimethyl chlorosilane (0.07 mL, 0.642 mmol, 2.0 eq.) was added dropwise via syringe to a solution of **5.15** (100.0 mg, 0.32 mmol, 1 eq.) and NEt_3 (0.18 mL, 0.642 mmol, 4.0 eq.) in CH_2Cl_2 (0.2 M) at 0 ˚C. The reaction was stirred until TLC indicated completion. Once complete, the reaction mixture was diluted with pentane and quenched with a pH 7 buffer. This biphasic solution was extracted with CH_2Cl_2 three times, and the combined organics dried with Na_2SO_4 and concentrated in vacuo. The crude mixture was passed through a silica filter to yield **Compound 5.47** as a yellow oil which was carried directly into the next step. ^{1}H NMR (500 MHz, $CDCl_3$) δ 5.45 (dq, *J* = 3.1, 1.6 Hz, 1H), 4.95 (s, 1H), 4.84 (p, *J* = 2.8 Hz, 1H), 4.33 (dq, *J* = 2.1, 1.0 Hz, 1H), 2.93 (s, 6H), 2.63 (dq, *J* = 14.9, 7.5 Hz, 1H), 1.74 (t, *J* = 1.3 Hz, 3H), 1.42 (m, 1H), 1.36 (s, 3H), 0.78 (t, *J* = 7.4 Hz, 3H), 0.26 (d, *J* = 2.7 Hz, 3H), 0.21 (d, *J* = 2.8 Hz, 3H). ^{13}C NMR (126 MHz, $CDCl_3$) δ 157.4, 153.8, 118.7, 88.0, 70.1, 68.8, 36.6, 29.9, 25.3, 23.6, 13.0, 9.7, 1.3, 0.7.



Compound 5.61. The following procedure was adapted from a report by Evans.[5] To a flame dried round bottom flask equipped with a solid addition funnel was added solution of diisopropyl amine

(0.1 mL, 0.737 mmol, 1.1 eq.) in 2.0 mL of THF. The solution was cooled to -78 ˚C and *n*BuLi (0.437 mL, 1.1 eq, 1.68 M) was added dropwise. This mixture was allowed to stir at -78 ˚C for 5 minutes and warmed to 0 ˚C for 15 minutes to ensure LDA formation. The solution of LDA was cooled back to -78 ˚C and to it was added a solution of **Compound 5.60** in 2 mL of THF at -78 ˚C via cannula transfer. The flask was rinsed with 1 mL of THF to ensure quantitative transfer of **5.60**. This mixture was stirred at -78 ˚C for 30 min. Trisyl azide was rapidly added as a solid (249.0 mg, 0.804 mmol, 1.2 eq.) After 2 min the reaction was quenched with 0.1 mL (2.0 mmol, 3.0 eq.) of glacial acetic acid. The cooling bath was removed, and the reaction was stirred at 25 °C for 12 h. After this period the reaction was quenched with pH 7 aqueous phosphate buffer and extracted with three portions of CH_2C1_2. The organic extracts were combined, dried (Na_2SO_4), and evaporated *in vacuo*. The crude material was flash chromatographed on 24 g of silica gel 0 to 20% EtOAc in Hexanes to yield **5.61** as a light-yellow oil (85.0 mg, 37% yield). ^{1}H NMR (500 MHz, $CDCl_3$) δ 7.57 – 7.51 (m, 2H), 7.35 (m, 6H), 7.31 (m, 2H), 5.07 (d, *J* = 12.2 Hz, 1H), 4.95 (d, *J* = 12.2 Hz, 1H), 3.53 (dd, *J* = 9.3, 5.7 Hz, 1H), 1.34 (dd, *J* = 14.7, 5.7 Hz, 1H), 1.11 (dd, *J* = 14.7, 9.2 Hz, 1H), 0.35 (s, 4H), 0.34 (s, 3H). ^{13}C NMR (126 MHz, $CDCl_3$) δ 177.2, 138.9, 135.9, 133.8, 129.2, 128.7, 128.4, 128.4, 128.0, 66.7, 52.1, 22.6. HRMS (ESI) *m/z* was not calculable for these intermediate, later intermediates were more amenable to characterization by HRMS (ESI)

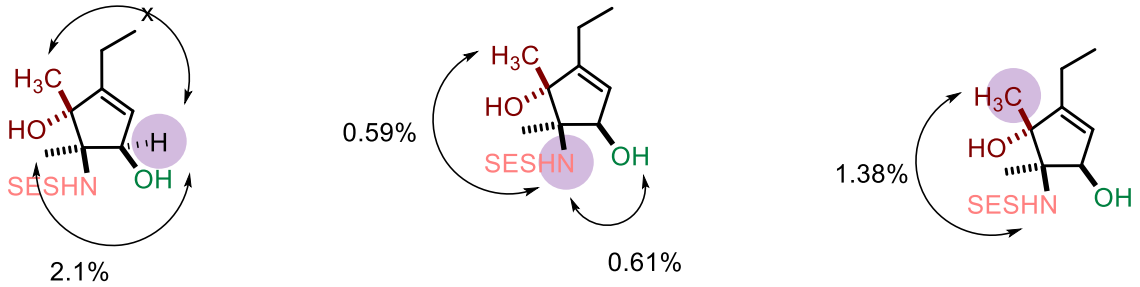


Compound 5.53. SESCl (.07 mL, 0.371 mmol, 1.2 eq.) was added dropwise to precooled solution of **Compound 5.62** (97.0 mg, 0.309 mmol, 1.0 eq.) and NEt_3 (0.08 mL, 0.619 mmol, 2 eq.) in

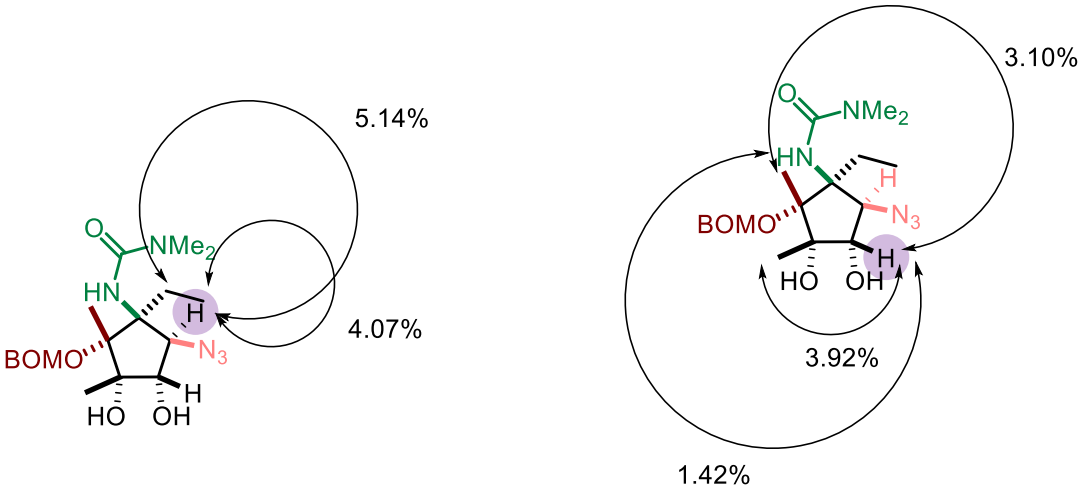
CH_2Cl_2 (0.7 mL, 0.4 M) at 0 ˚C. This reaction was allowed to stir until TLC indicated completion. Once the reaction was complete the mixture was washed with brine, dried with Na_2SO_4 and concentrated. The crude mixture was purified via flash column chromatography using a gradient solvent system (Hex:EtOAc) 0 to 50% to yield **Compound 5.53** as a yellow oil (71.4 mg, 48% yield). ^{1}H NMR (500 MHz, $CDCl_3$) δ 7.58 – 7.42 (m, 2H), 7.40 – 7.32 (m, 6H), 7.29 (m, 2H), 5.08 (d, *J* = 12.2 Hz, 1H), 4.91 (d, *J* = 12.2 Hz, 1H), 4.55 (d, *J* = 9.5 Hz, 1H), 2.85 – 2.69 (m, 2H), 1.40 (dd, *J* = 14.9, 6.1 Hz, 1H), 1.00 – 0.90 (m, 1H), 0.38 (s, 3H), 0.37 (s, 3H), -0.01 (s, 9H). ^{13}C NMR (126 MHz, $CDCl_3$) δ 175.3, 139.6, 137.0, 135.6, 131.5, 130.7, 130.6, 130.4, 130.1, 69.4, 55.7, 51.9, 23.8, 12.2, 2.0, 0.0. *m/z* calculated for $C_{23}H_{35}NO_4SSi_2$ $[M+NH_4]^+$ 495.2164, found 495.2163.

5.11 nOe Data for Select Intermediates

Compound 5.12



Compound 5.39



5.12 References

(1) Armarego, W. L. F.; Chai, C. L. L. Chapter 4 - Purification of Organic Chemicals. In *Purification of Laboratory Chemicals (Sixth Edition)*; Armarego, W. L. F., Chai, C. L. L., Eds.; Butterworth-Heinemann: Oxford, 2009; pp 88–444.

(2) Grandel, R.; Kazmaier, U. Diastereoselective Synthesis of β-Substituted α-Methylserines via Chelated Alanine Ester Enolates. *Eur. J. Org. Chem.* **1998**, *1998*, 409–417.

(3) Malinowski, J. T.; McCarver, S. J.; Johnson, J. S. Diastereocontrolled Construction of Pactamycin's Complex Ureido Triol Functional Array. *Org. Lett.* **2012**, *14*, 2878–2881.

(4) Titz, A.; Radic, Z.; Schwardt, O.; Ernst, B. A Safe and Convenient Method for the Preparation of Triflyl Azide, and Its Use in Diazo Transfer Reactions to Primary Amines. *Tetrahedron Lett.* **2006**, *47*, 2383–2385.

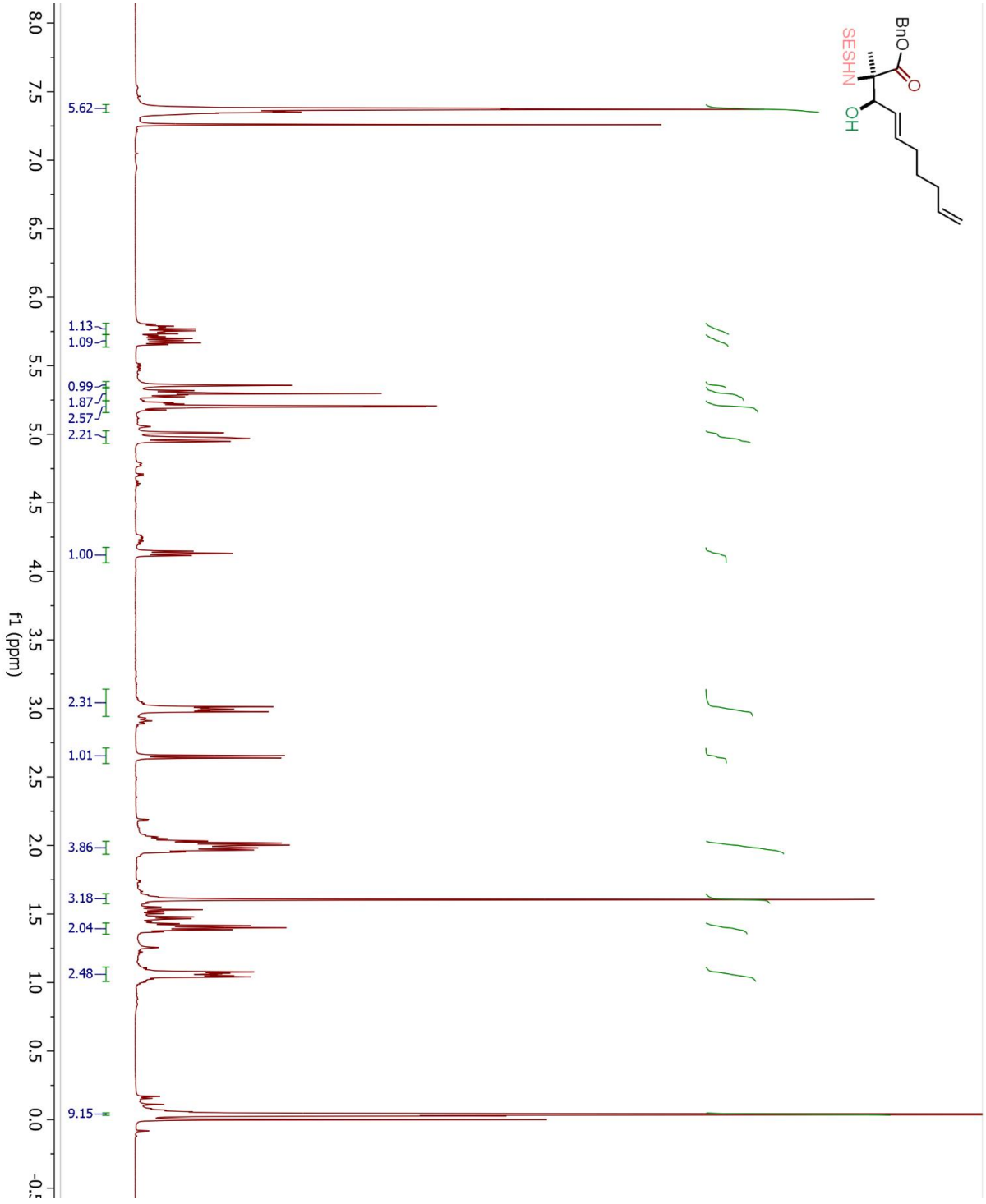
(5) Simmons, E. M.; Hartwig, J. F. Catalytic Functionalization of Unactivated Primary C–H Bonds Directed by an Alcohol. *Nature* **2012**, *483*, 70–73.

(6) Leger, P. R.; Kuroda, Y.; Chang, S.; Jurczyk, J.; Sarpong, R. C–C Bond Cleavage Approach to Complex Terpenoids: Development of a Unified Total Synthesis of the Phomactins. *J. Am. Chem. Soc.* **2020**, *142*, 15536–15547.

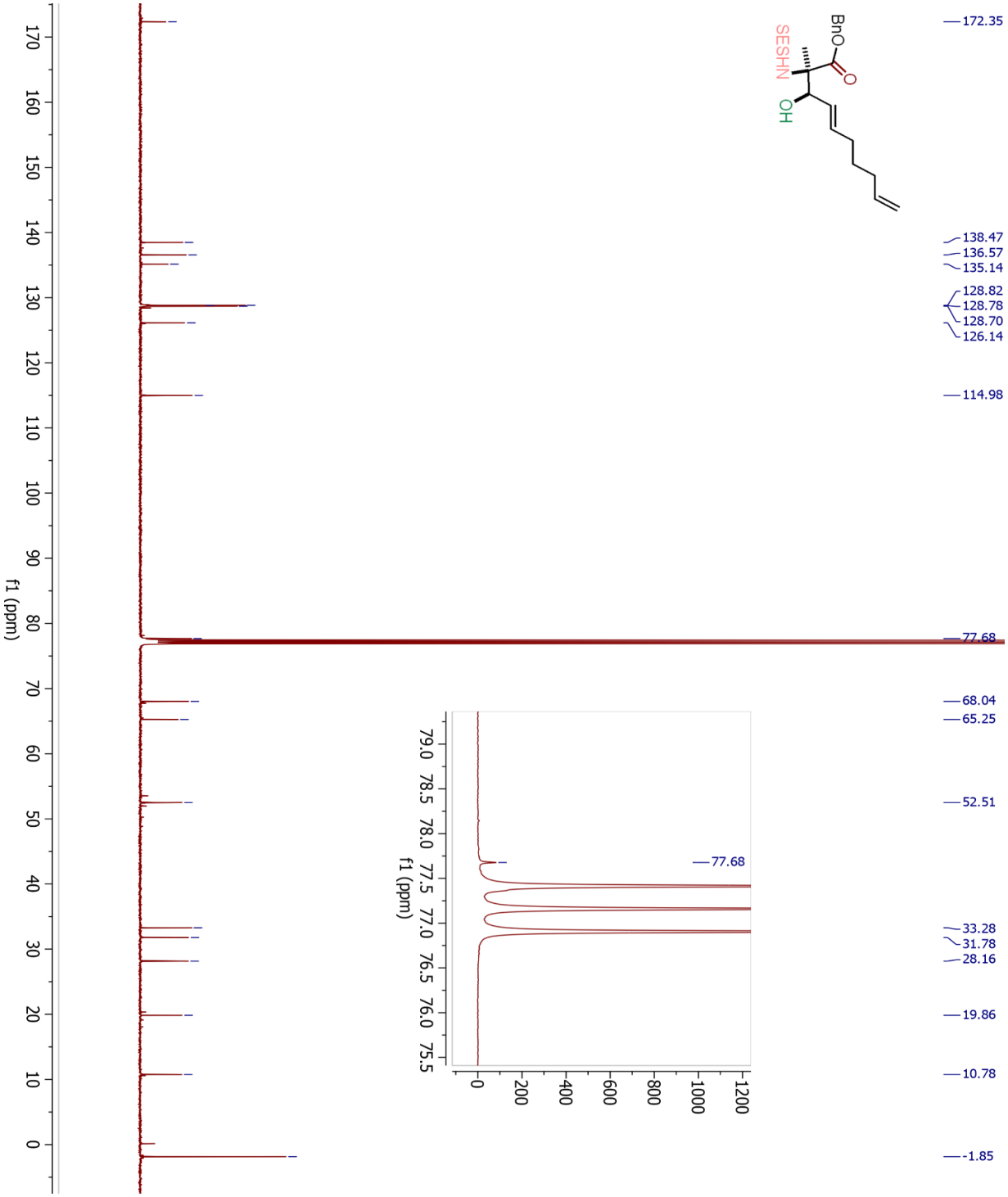
(7) Ma, X.; Kucera, R.; Goethe, O. F.; Murphy, S. K.; Herzon, S. B. Directed C–H Bond Oxidation of (+)-Pleuromutilin. *J. Org. Chem.* **2018**, *83*, 6843–6892.

5.12 NMR Spectra

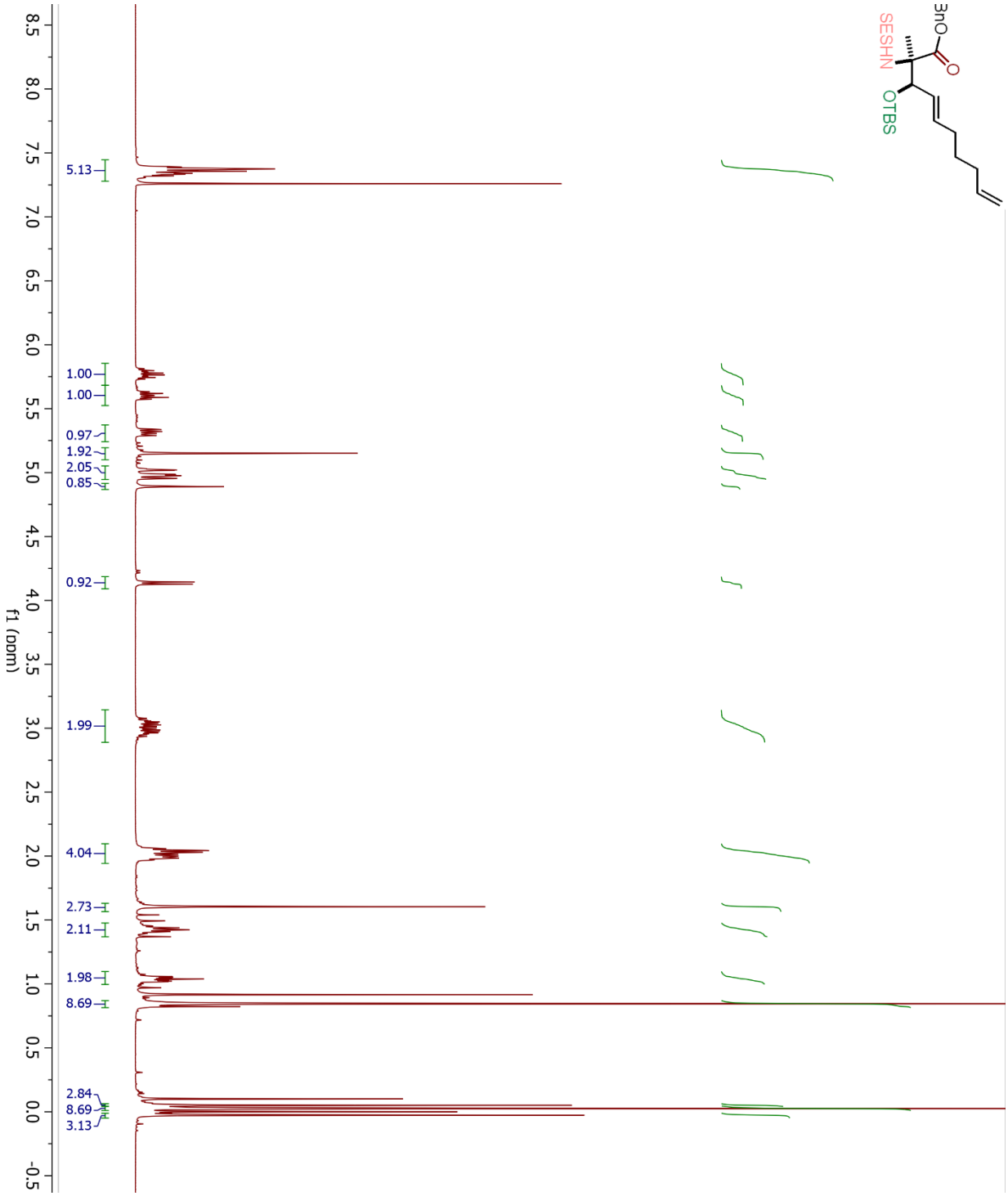
^{1}H NMR (500 MHz, $CDCl_3$) for compound **5.7**



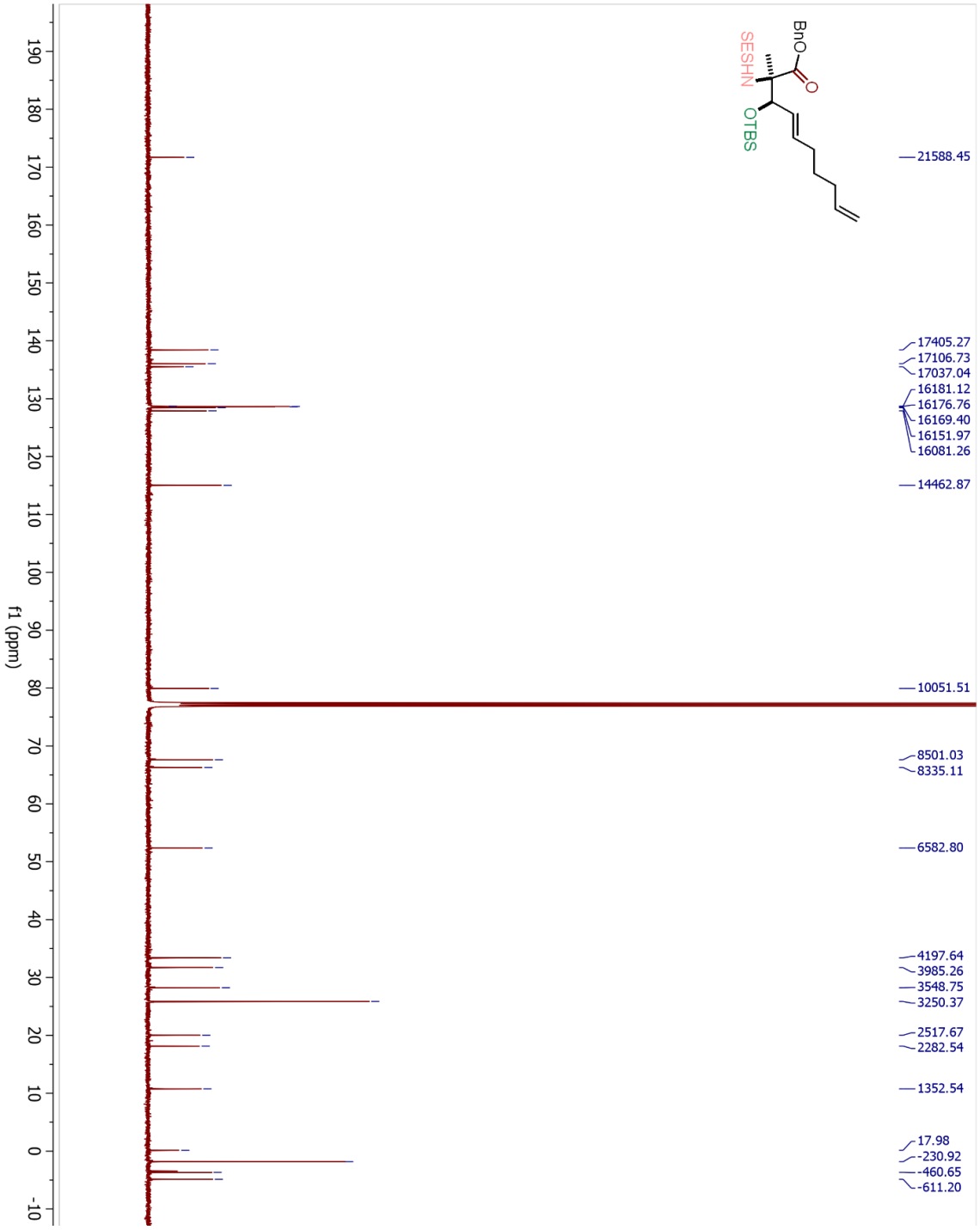
^{13}C NMR (126 MHz, $CDCl_3$) for compound **5.7**



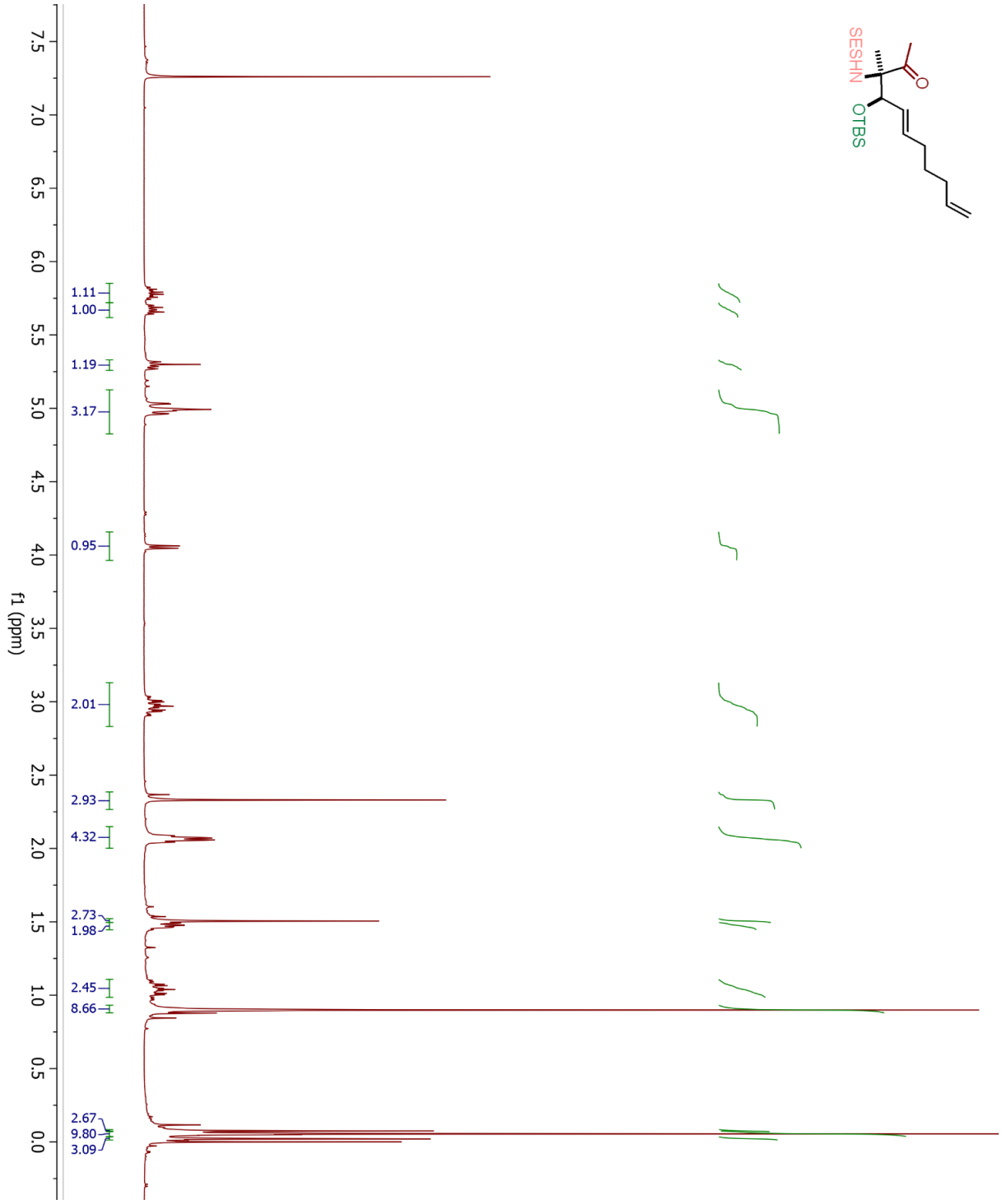
^{1}H NMR (500 MHz, $CDCl_3$) for compound **5.4**



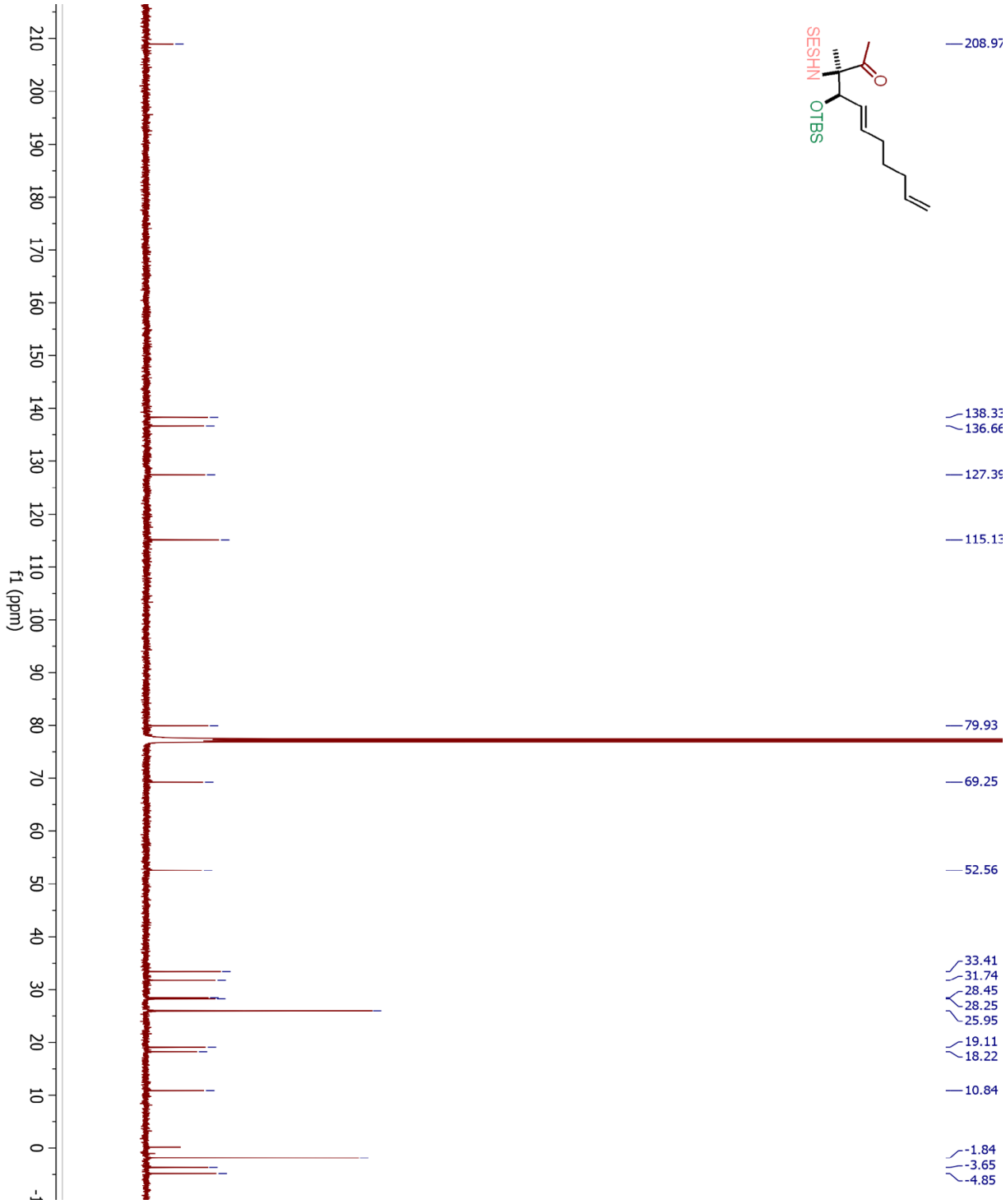
^{13}C NMR (126 MHz, $CDCl_3$) for compound **5.4**



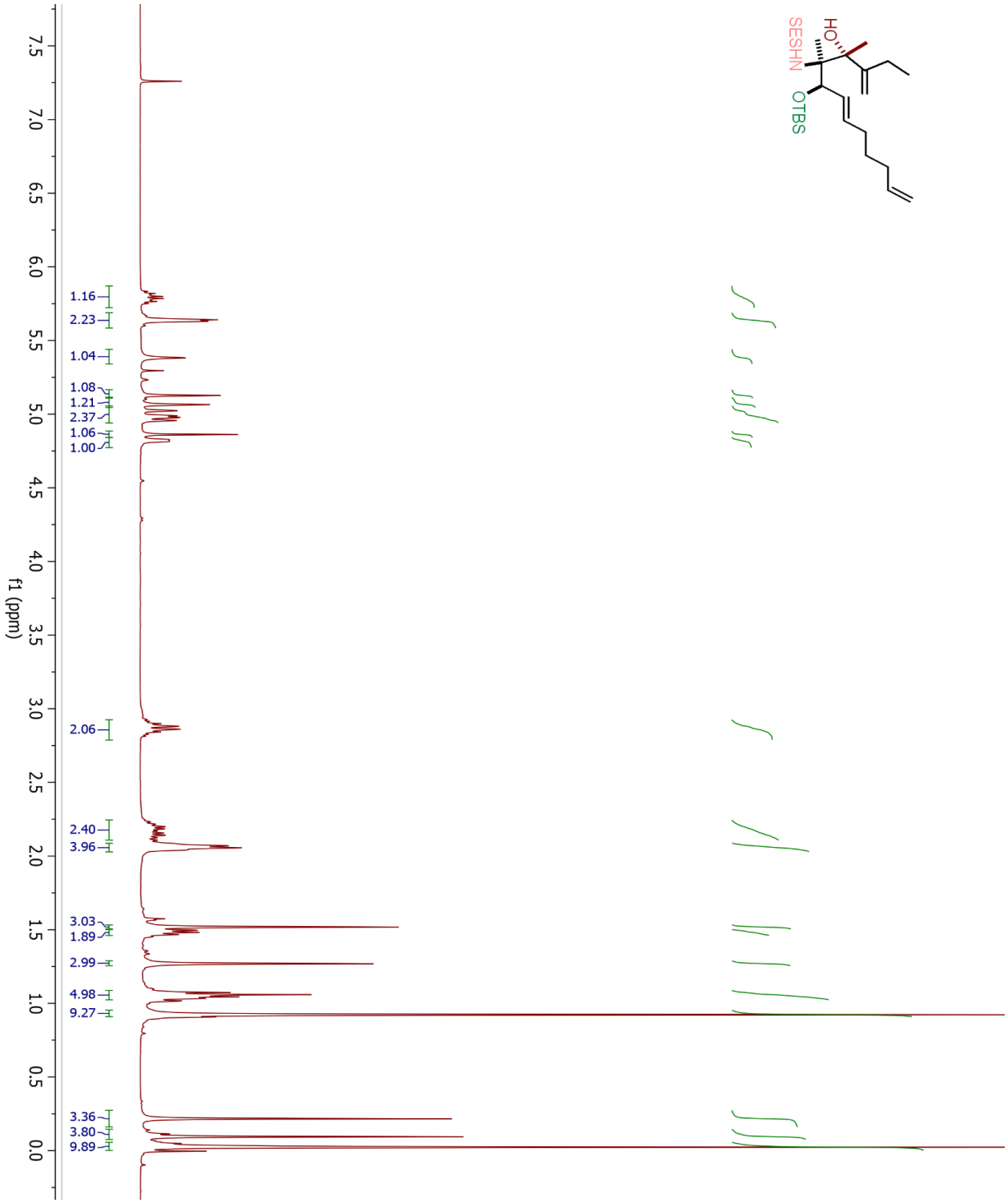
^{1}H NMR (500 MHz, $CDCl_3$) for compound **5.8**



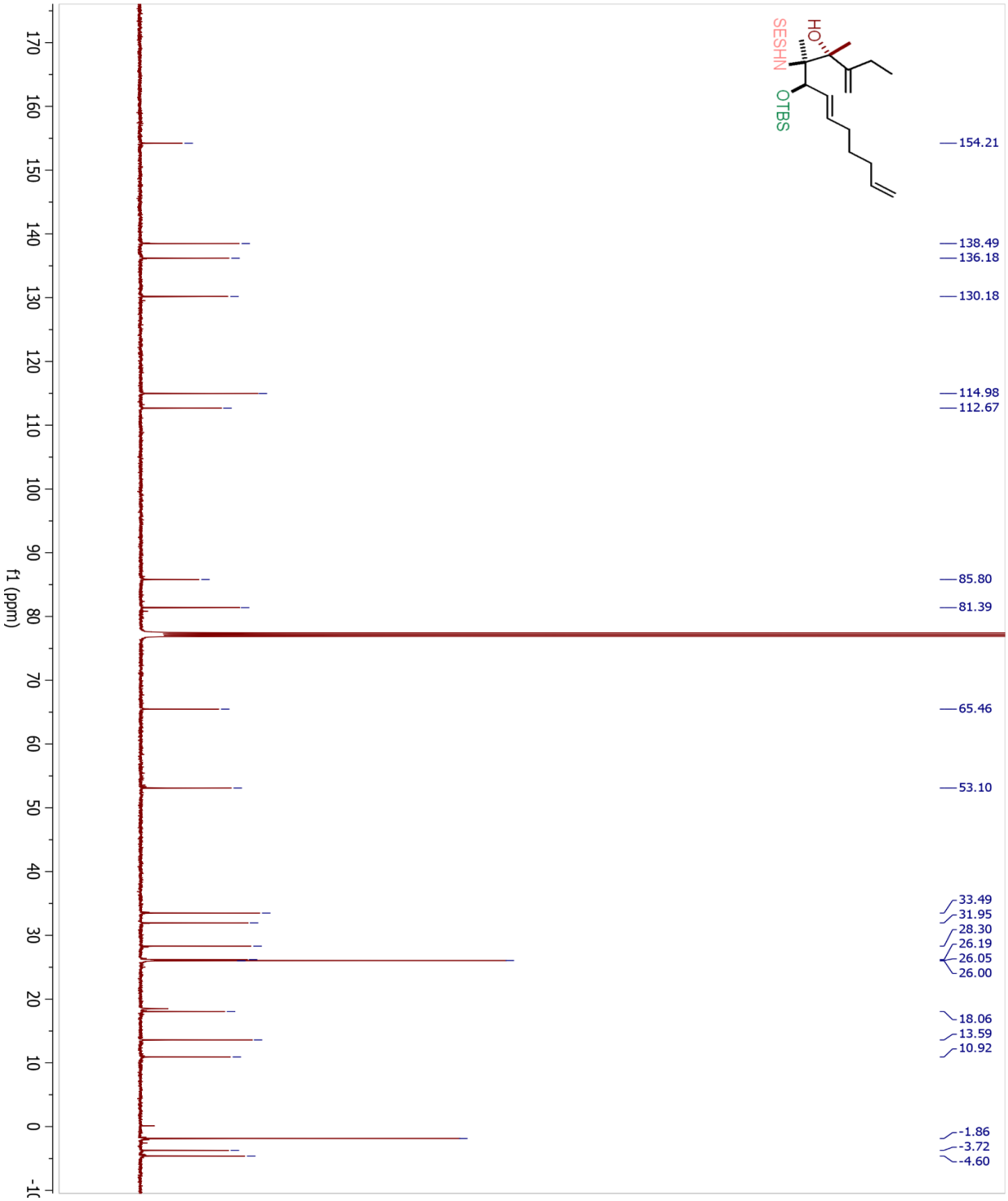
^{13}C NMR (126 MHz, $CDCl_3$) for compound **5.8**



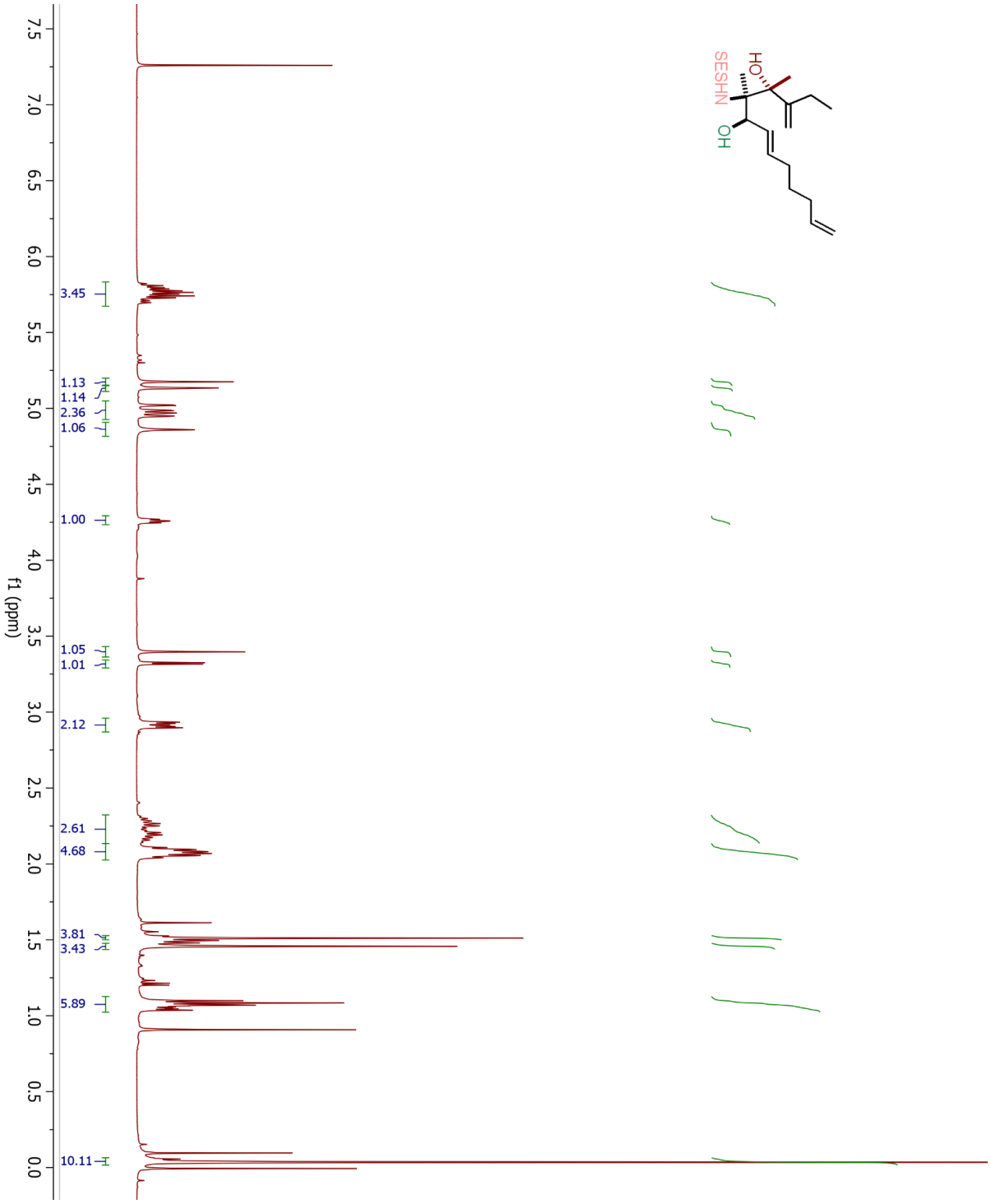
^{1}H NMR (500 MHz, $CDCl_3$) for compound **5.3**



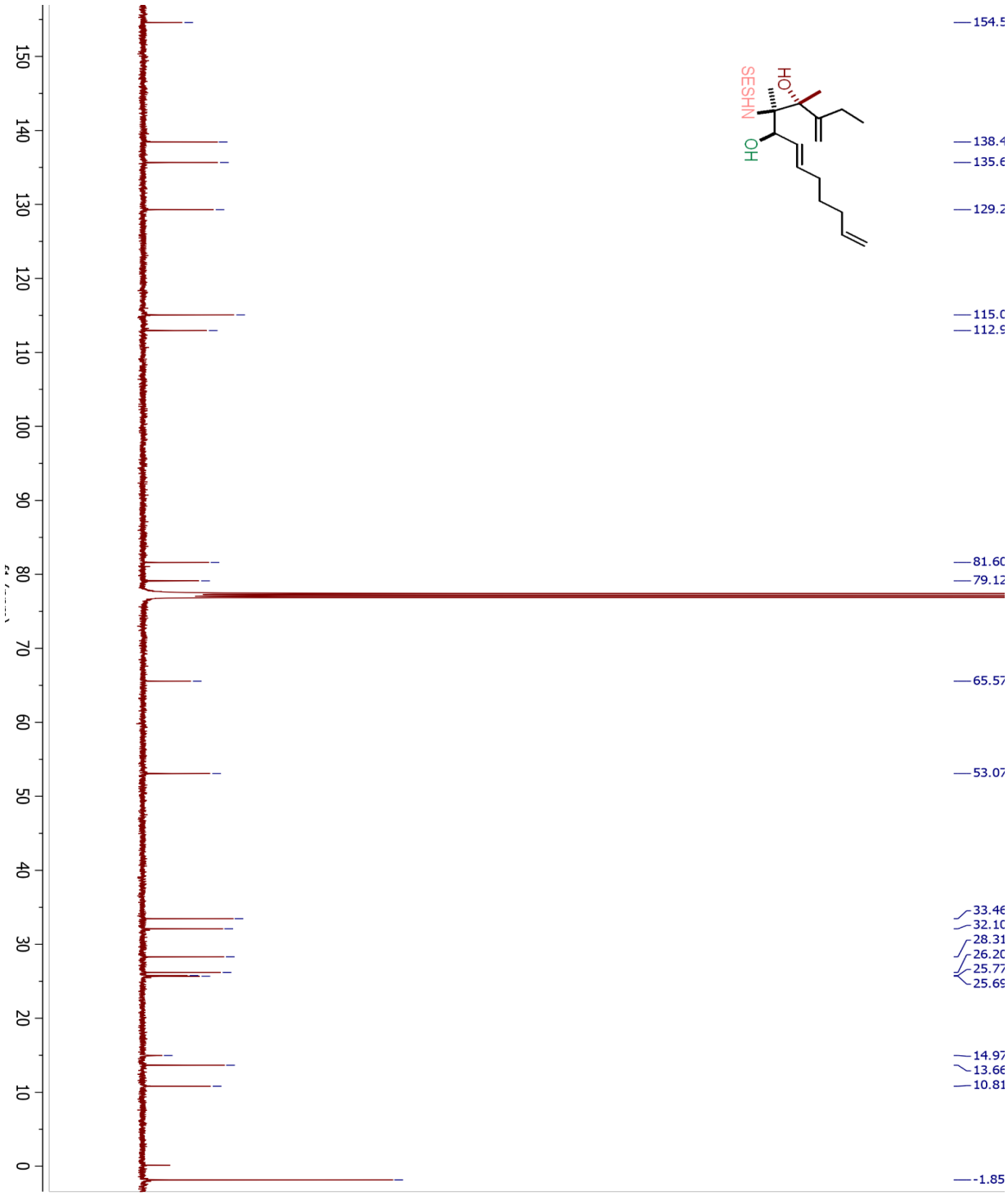
^{13}C NMR (126 MHz, $CDCl_3$) for compound **5.3**



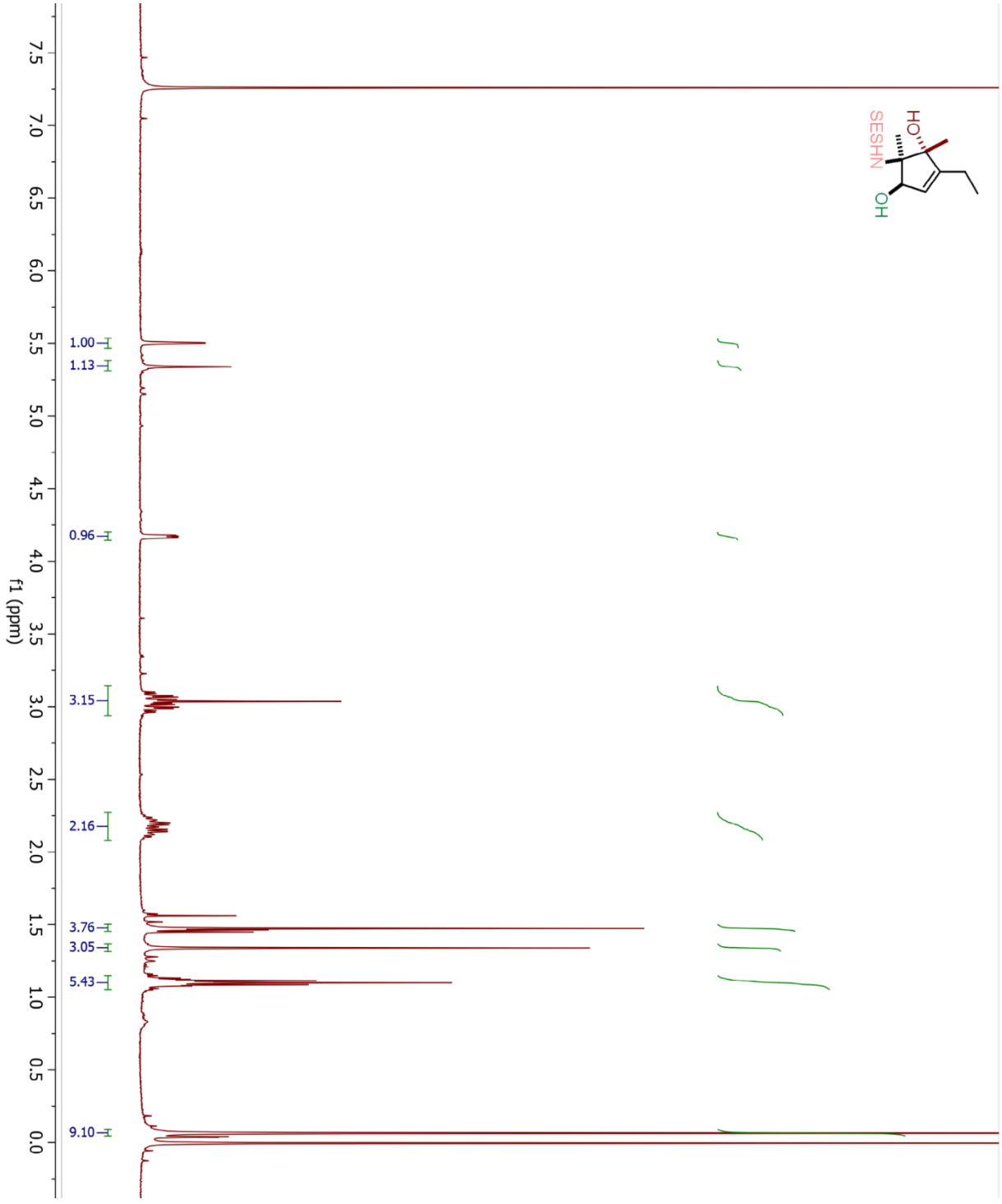
^{1}H NMR (500 MHz, $CDCl_3$) for compound **5.11**



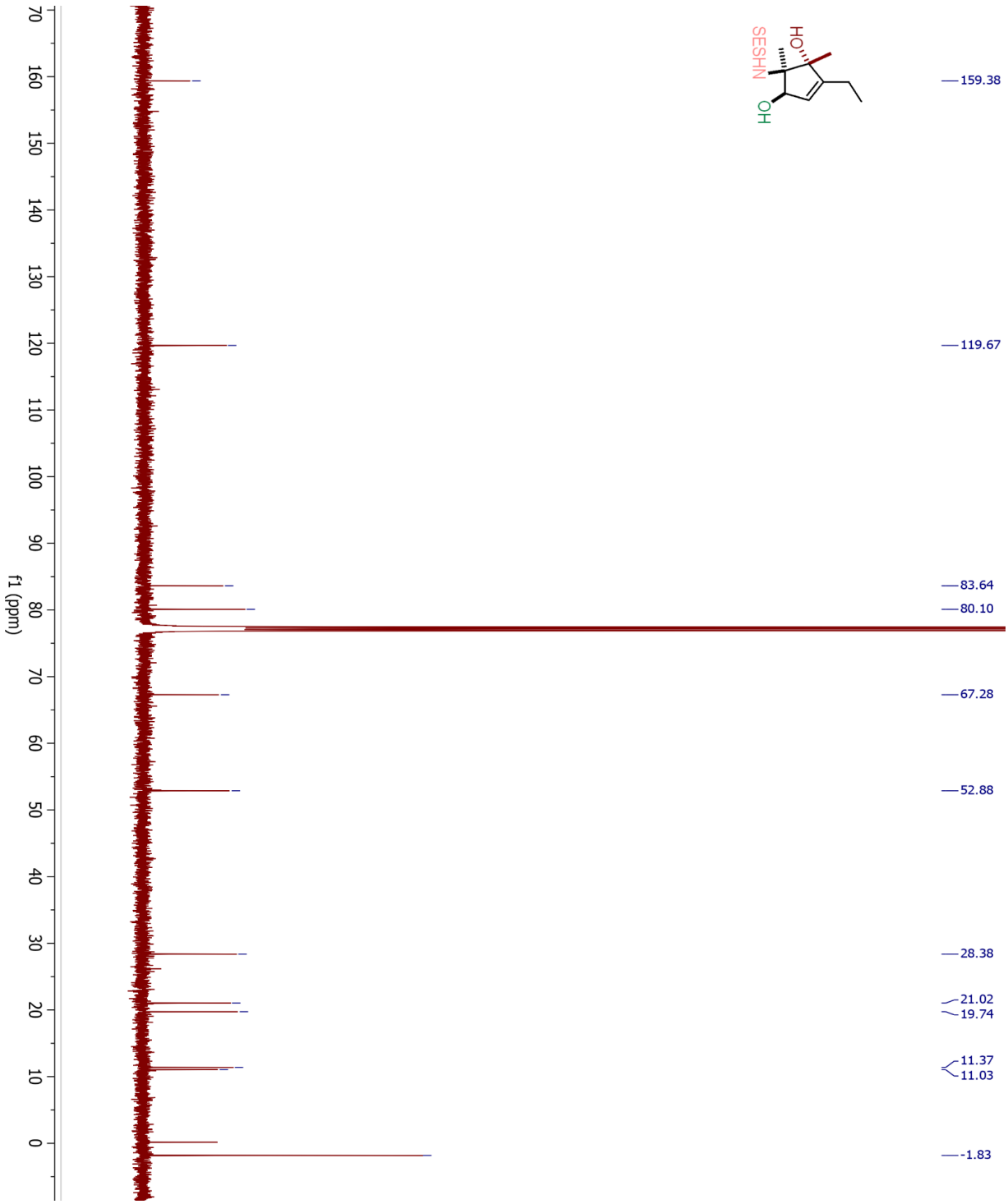
^{13}C NMR (126 MHz, $CDCl_3$) for compound **5.11**



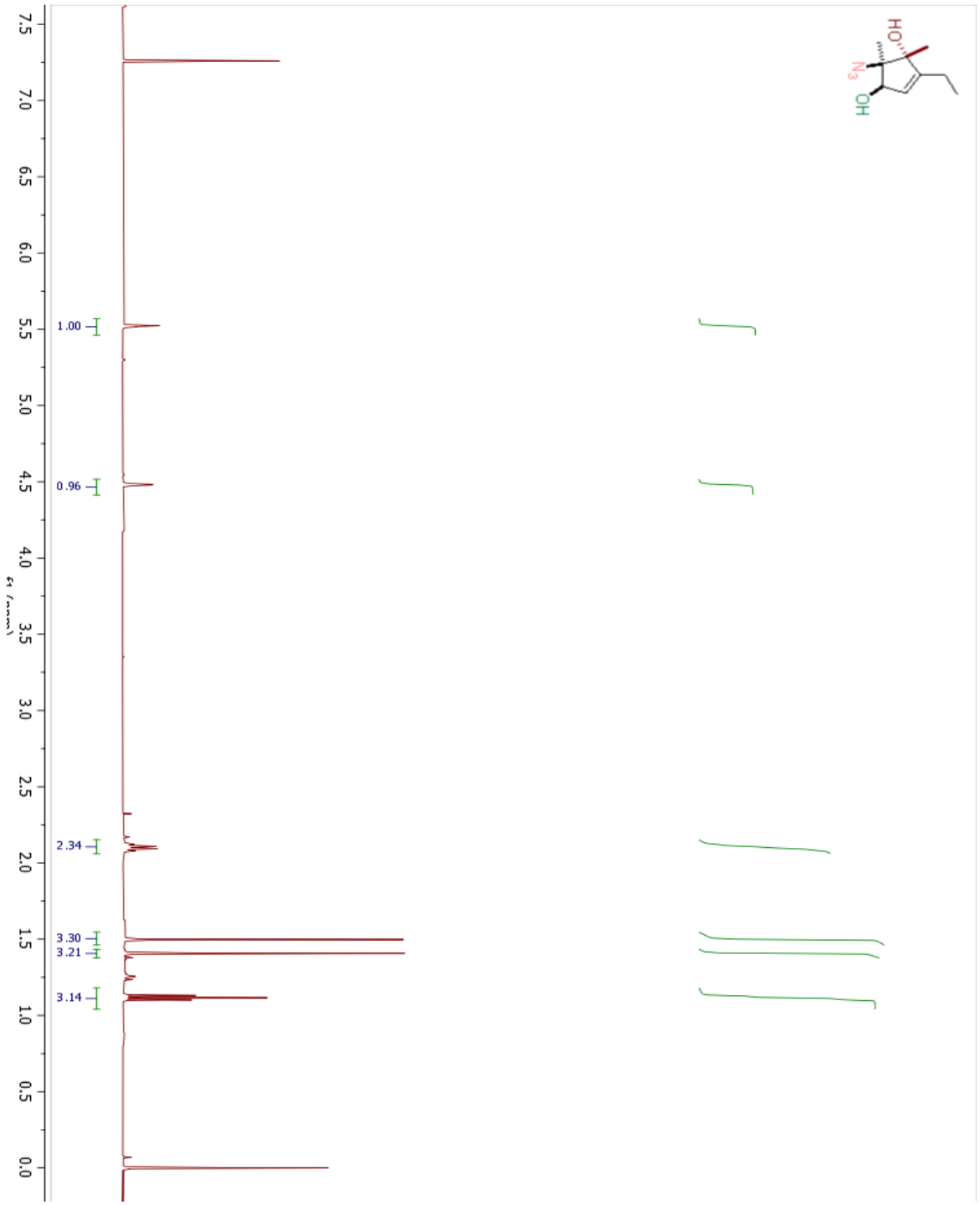
^{1}H NMR (500 MHz, $CDCl_3$) for compound **5.12**



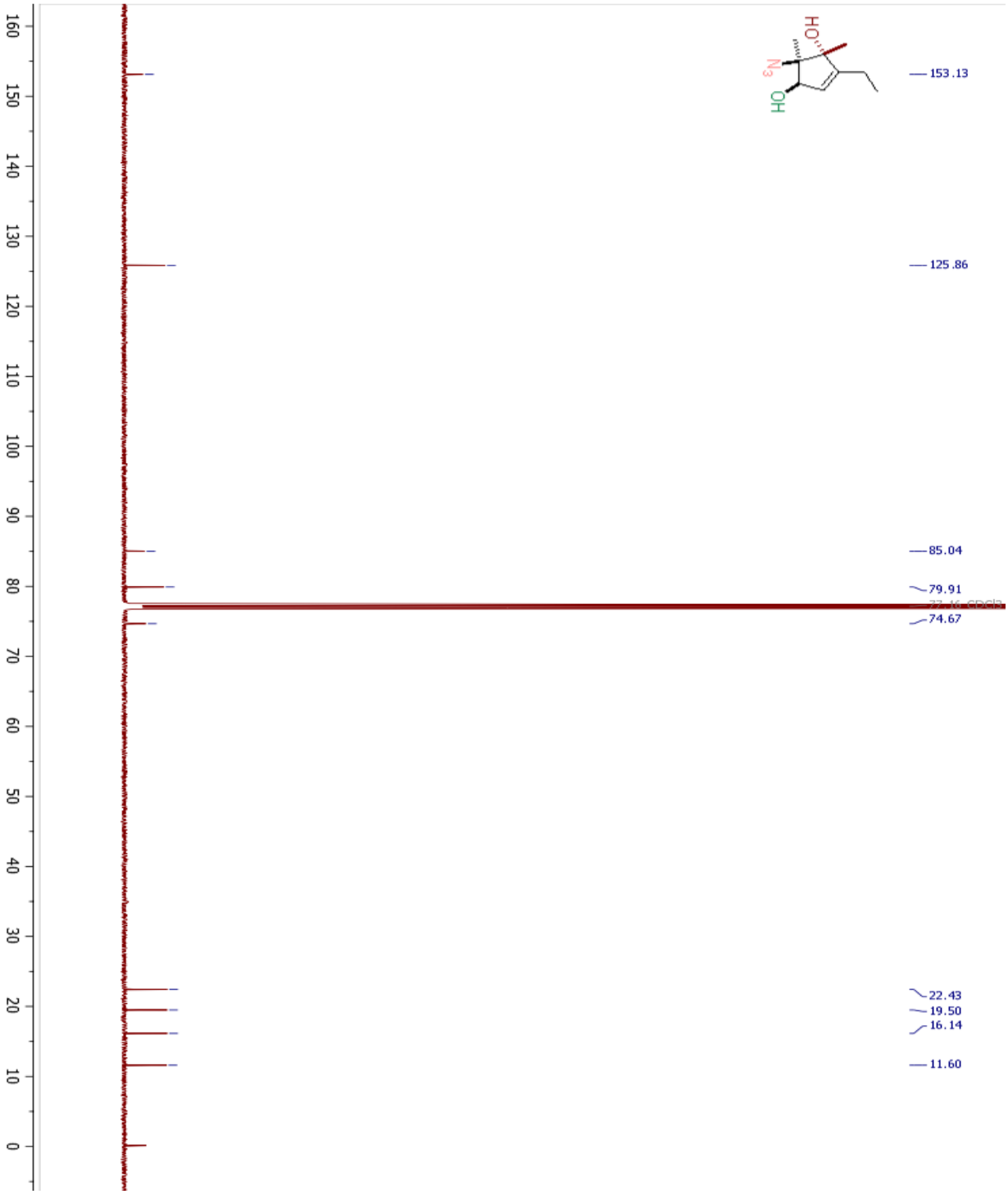
^{13}C NMR (126 MHz, $CDCl_3$) for compound **5.12**



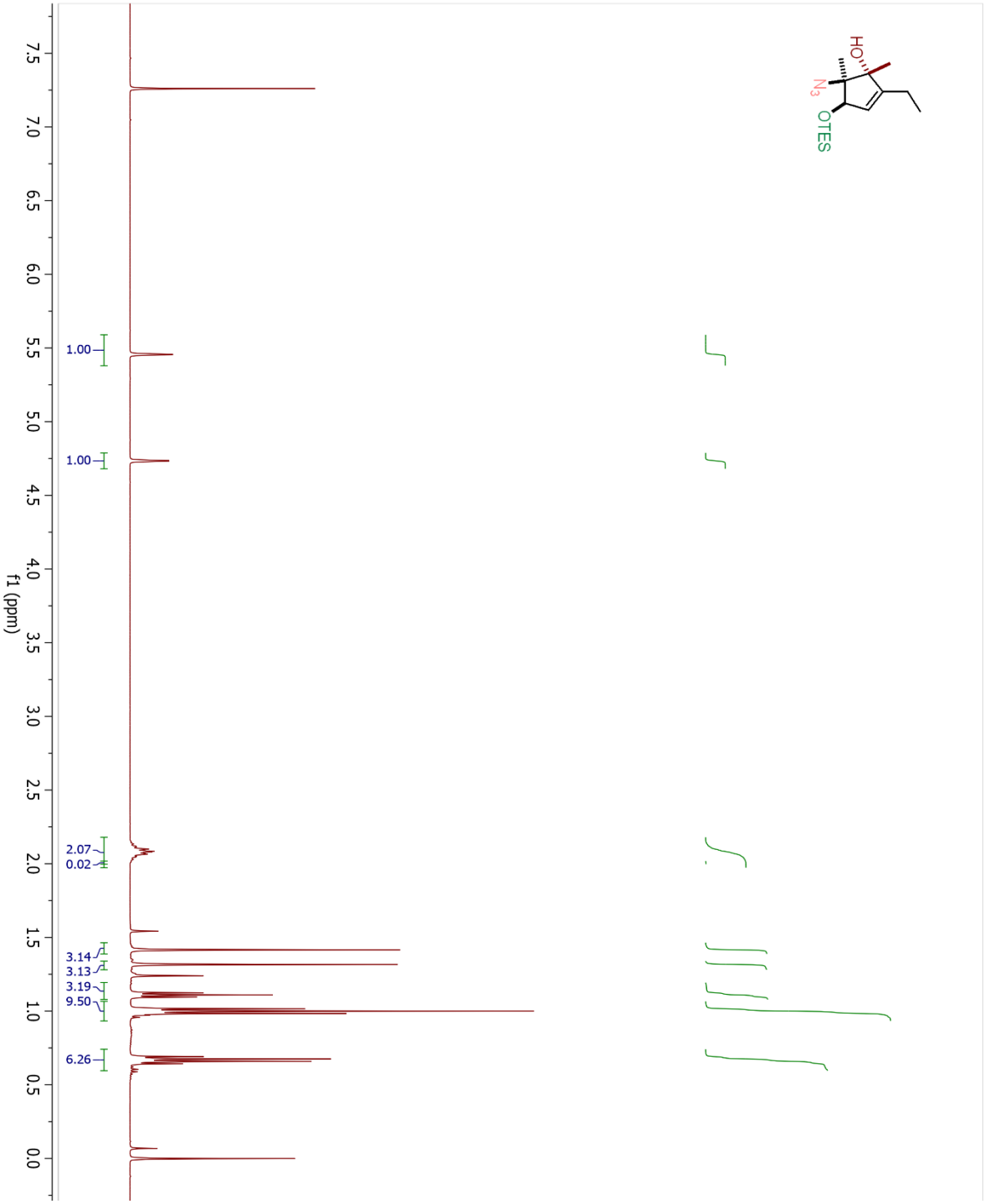
^{1}H NMR (500 MHz, $CDCl_3$) for compound **5.14**



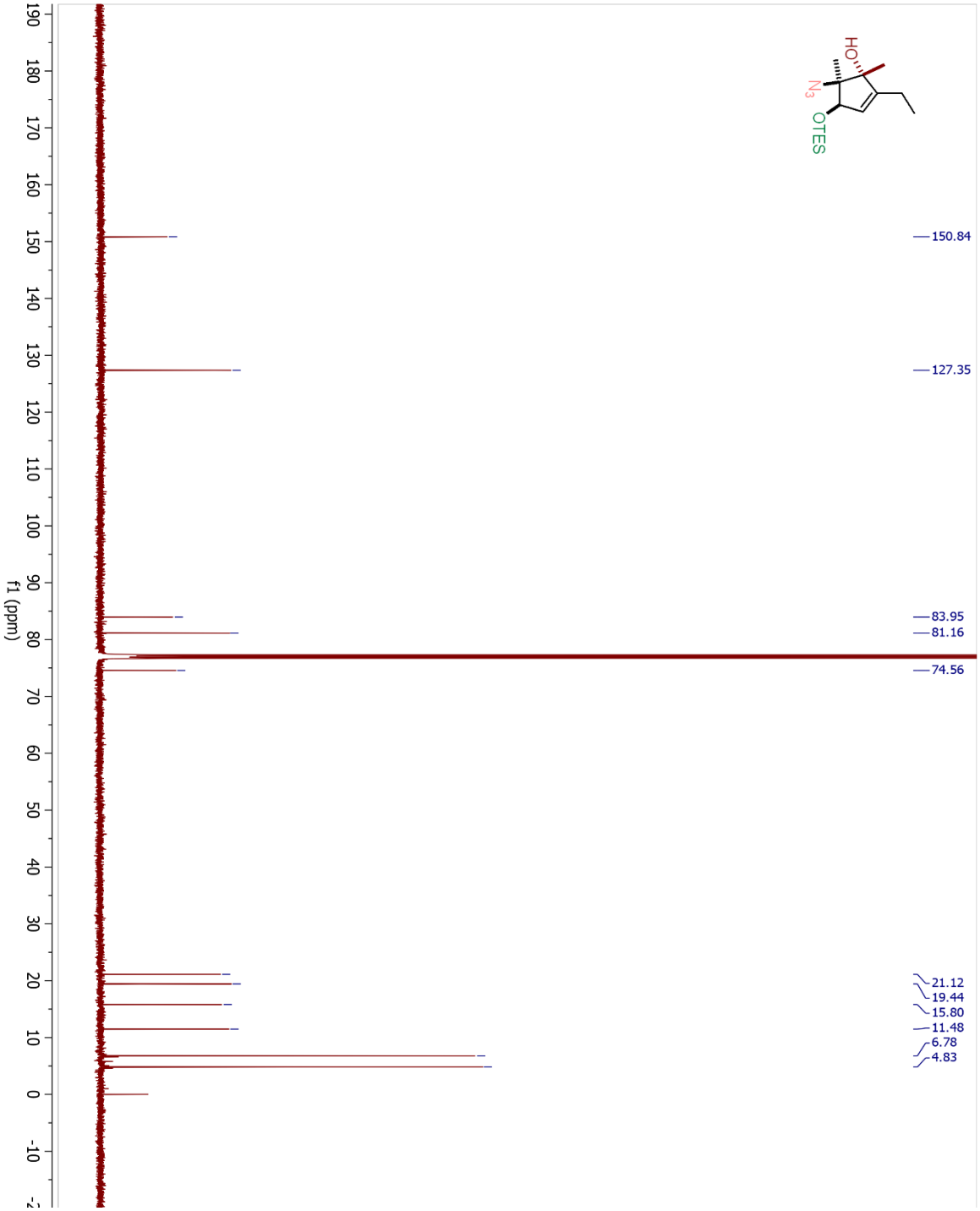
^{13}C NMR (126 MHz, $CDCl_3$) for compound **5.14**



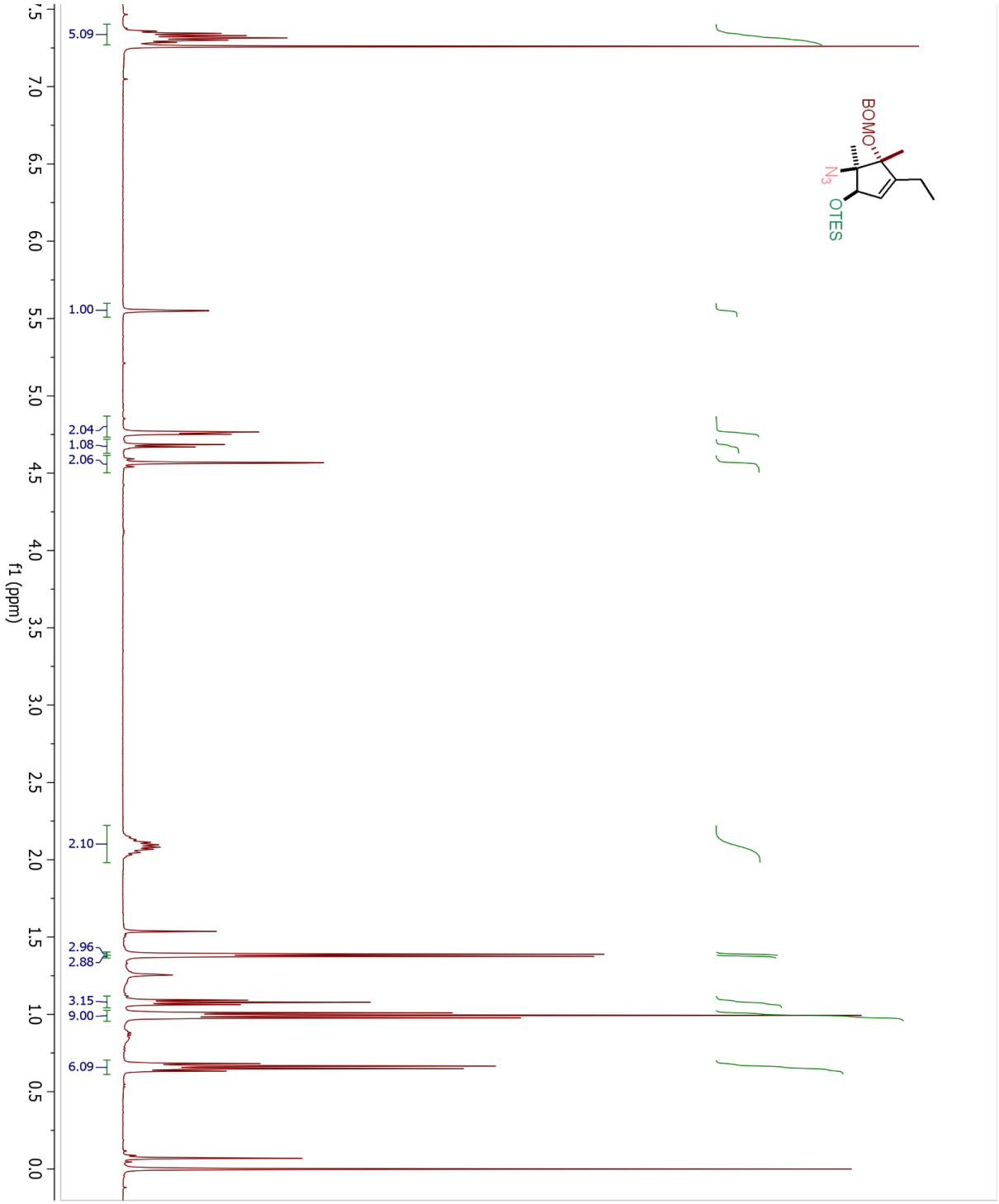
^{1}H NMR (500 MHz, $CDCl_3$) for compound **5.15**



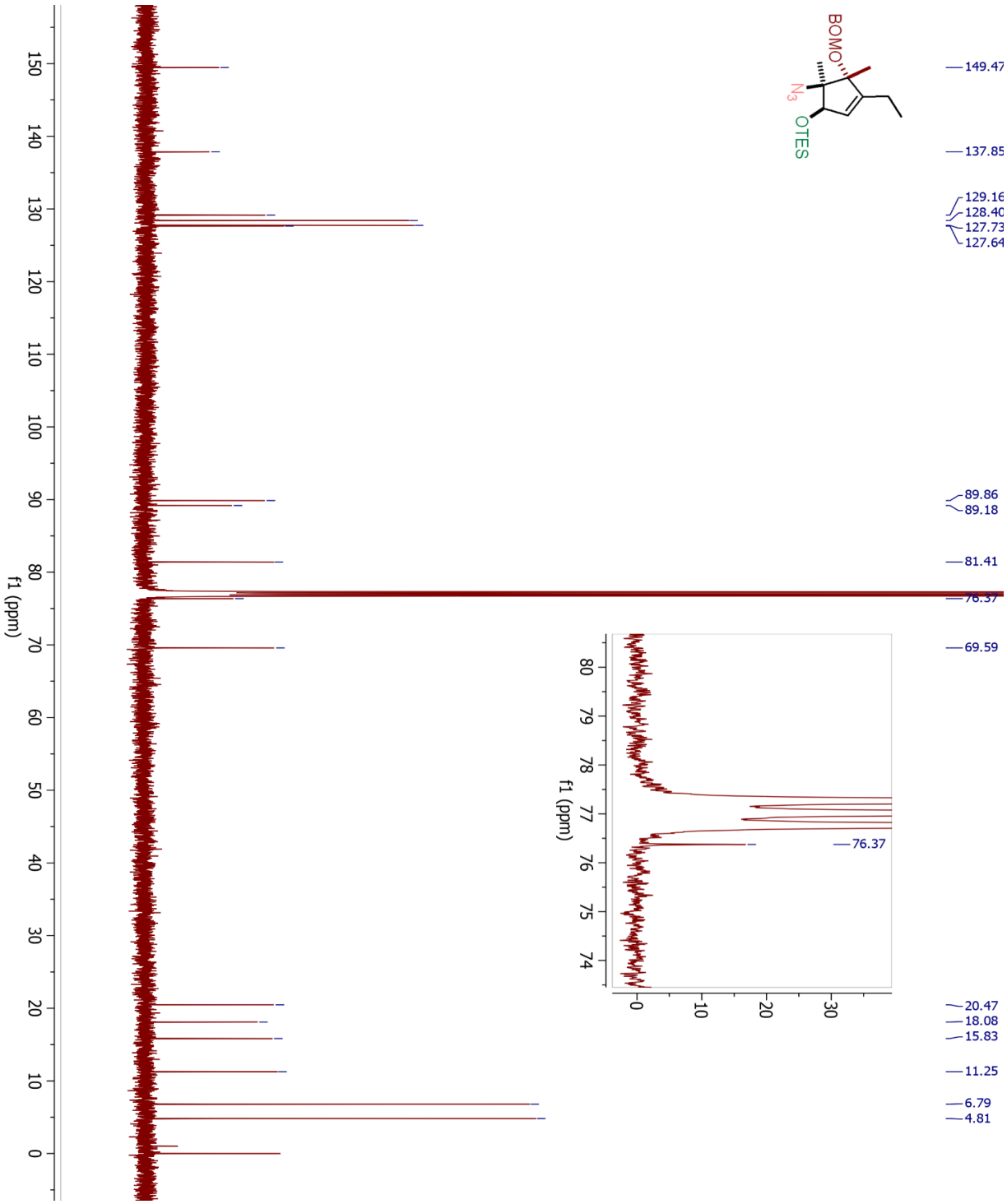
^{13}C NMR (126 MHz, $CDCl_3$) for compound **5.15**



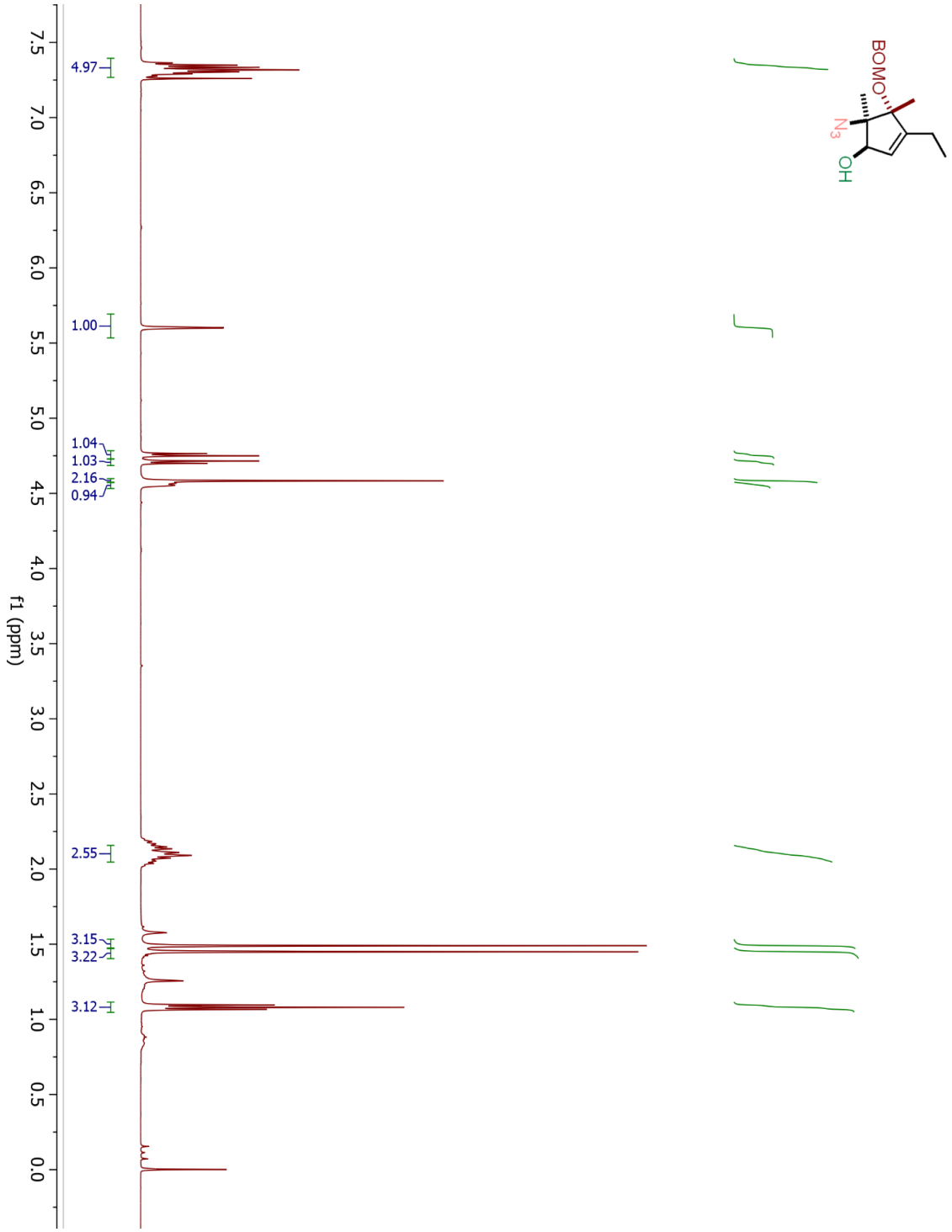
^{1}H NMR (500 MHz, $CDCl_3$) for compound **5.16**



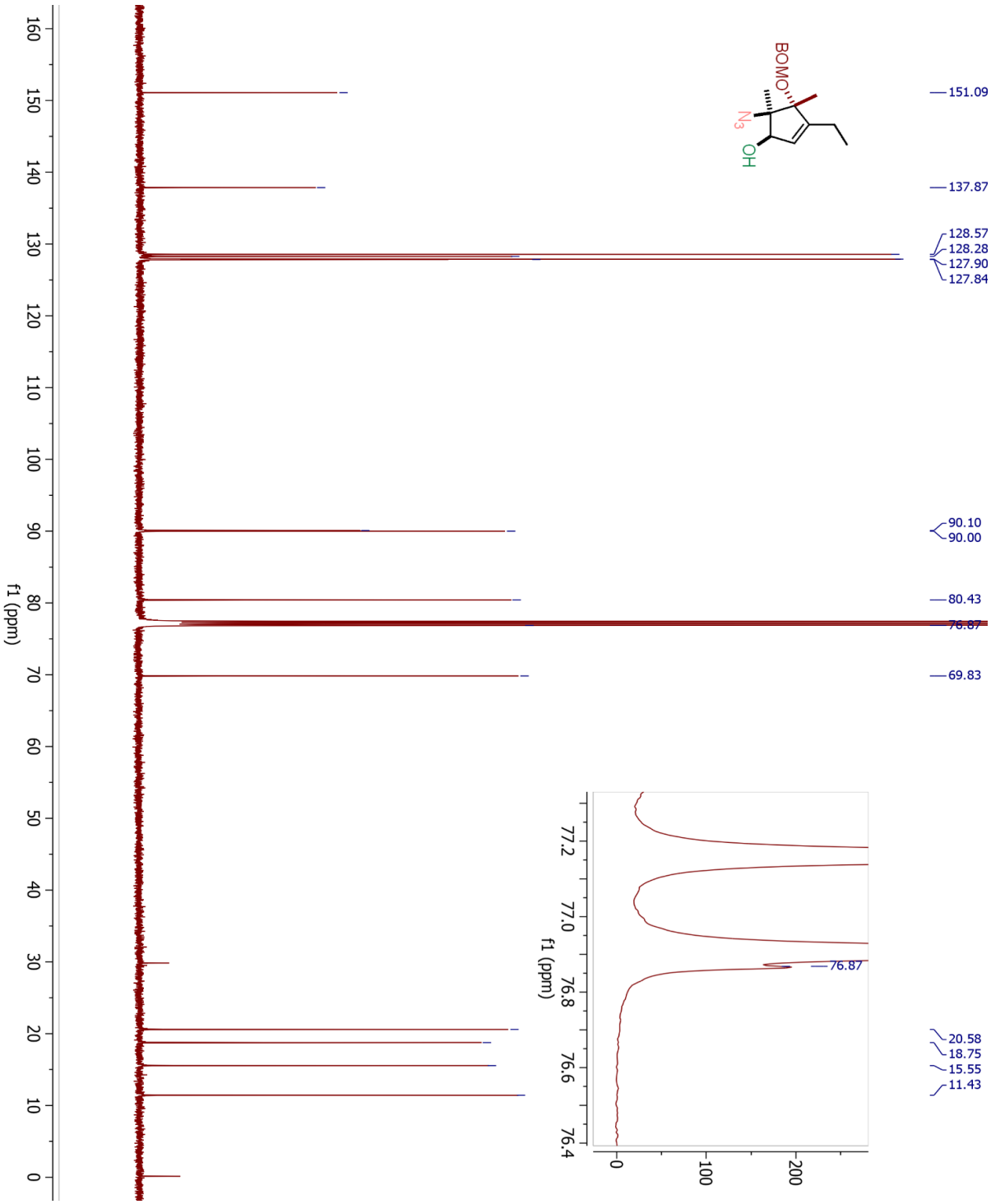
^{13}C NMR (126 MHz, $CDCl_3$) for compound **5.16**



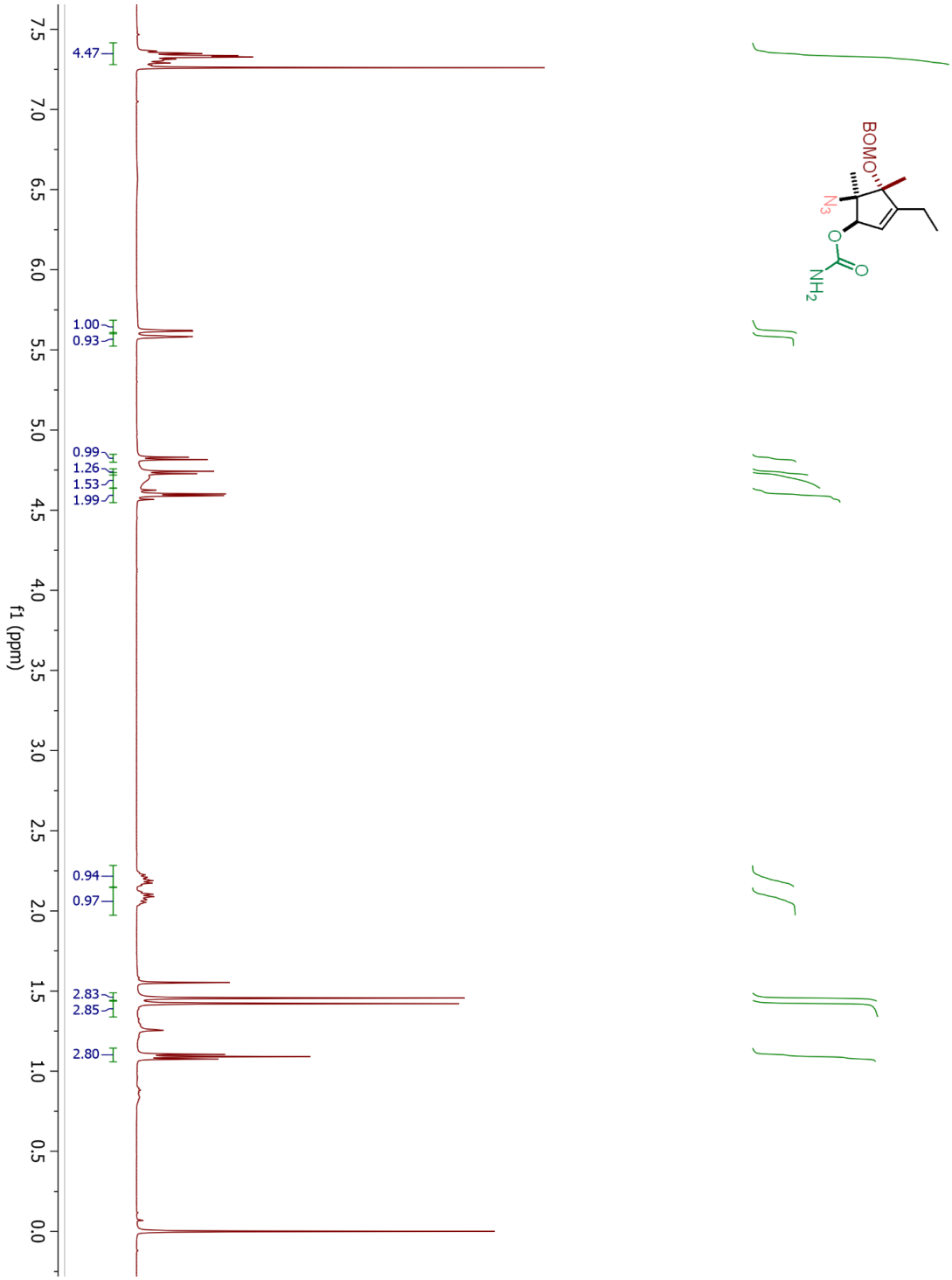
^{1}H NMR (500 MHz, $CDCl_3$) for compound **5.17**



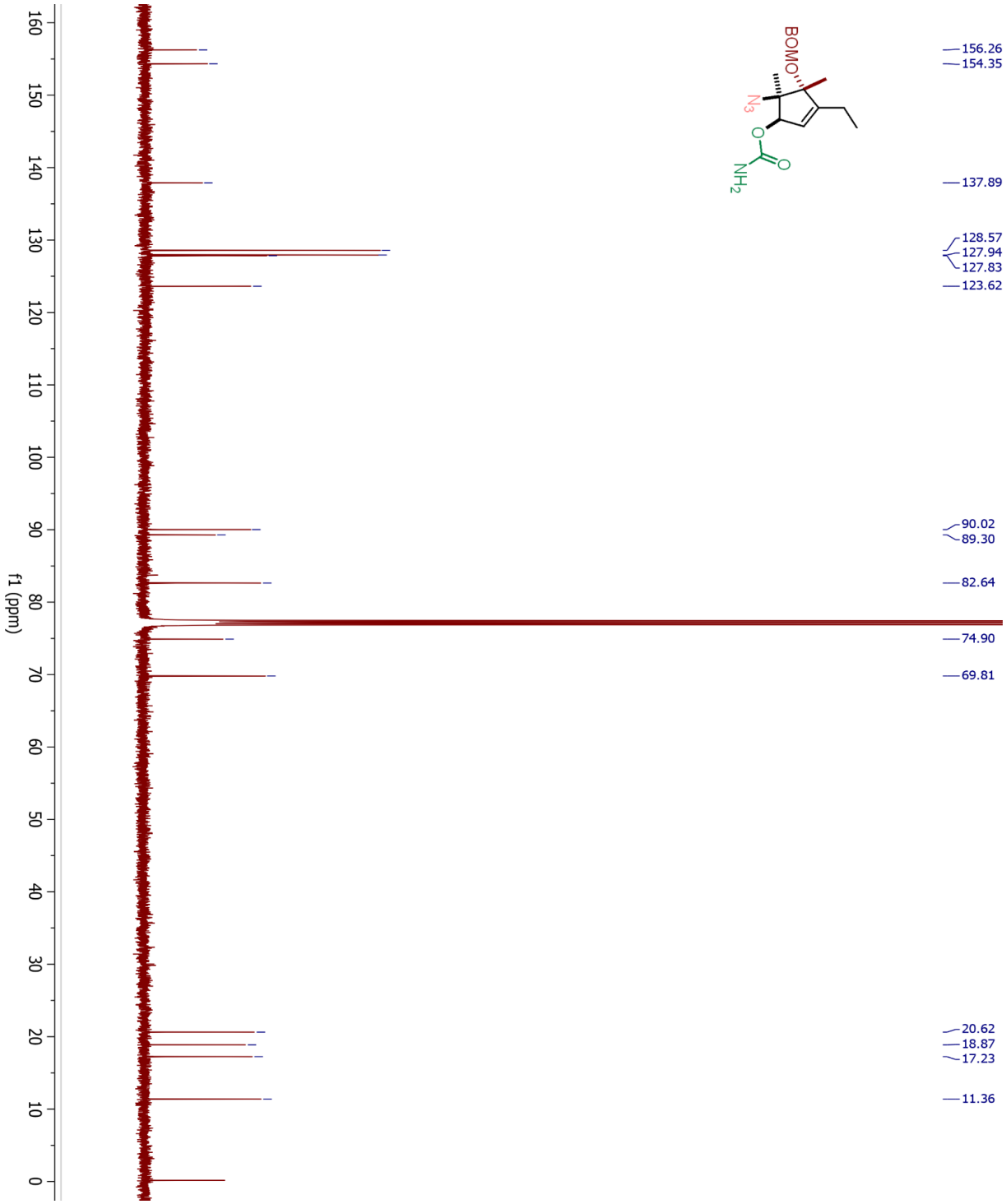
^{13}C NMR (126 MHz, $CDCl_3$) for compound **5.17**



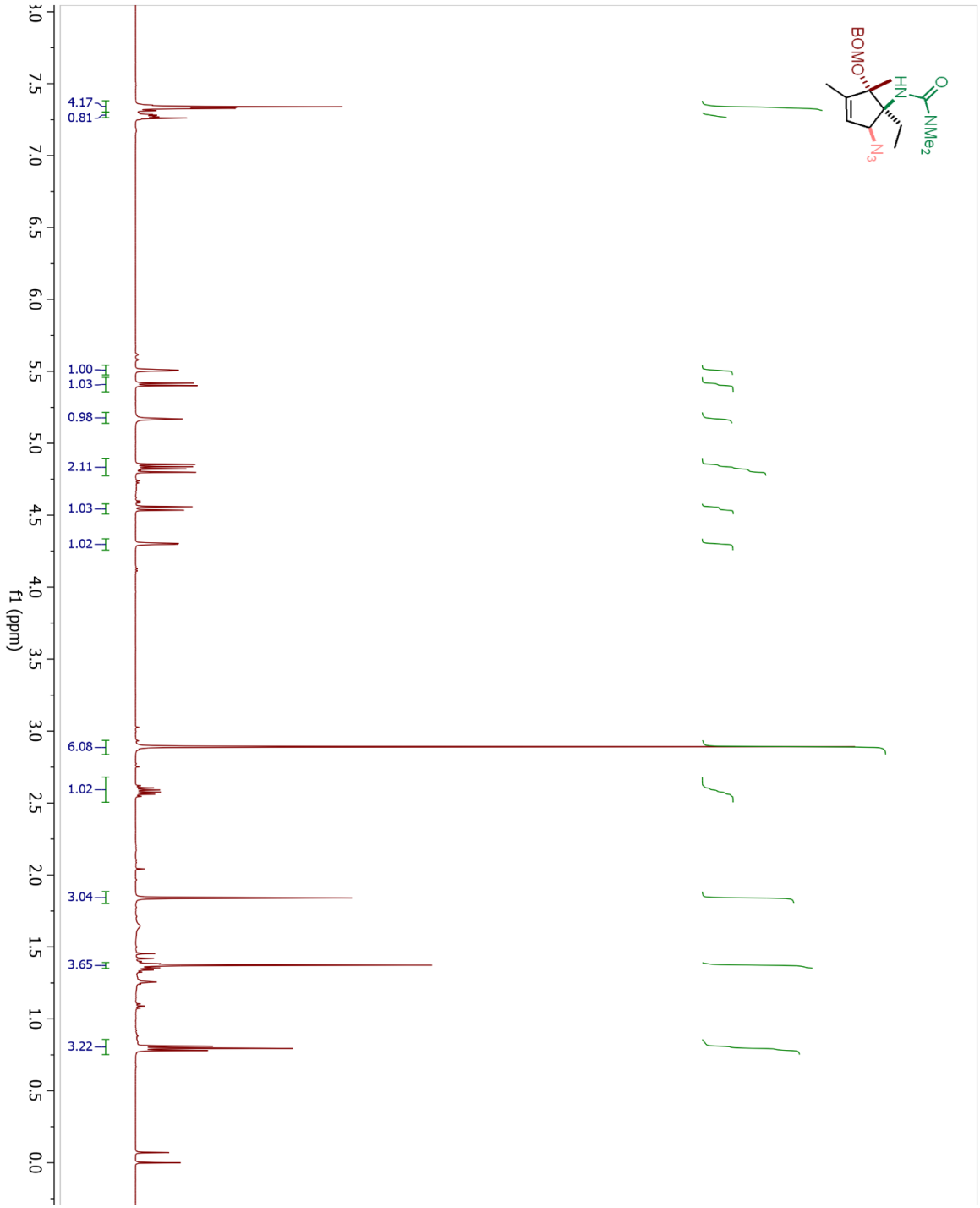
^{1}H NMR (500 MHz, $CDCl_3$) for compound **5.2**



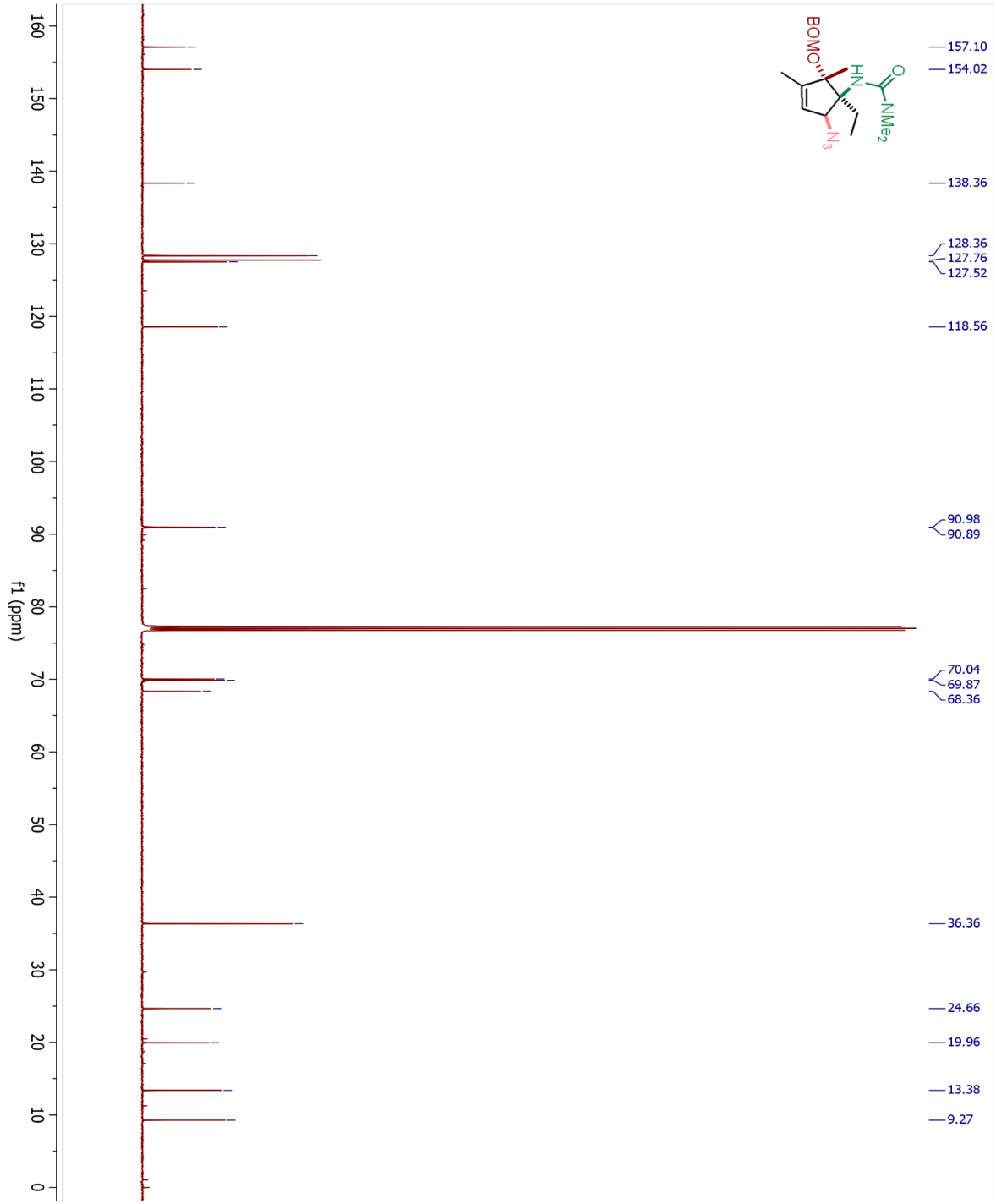
^{13}C NMR (126 MHz, $CDCl_3$) for compound **5.2**



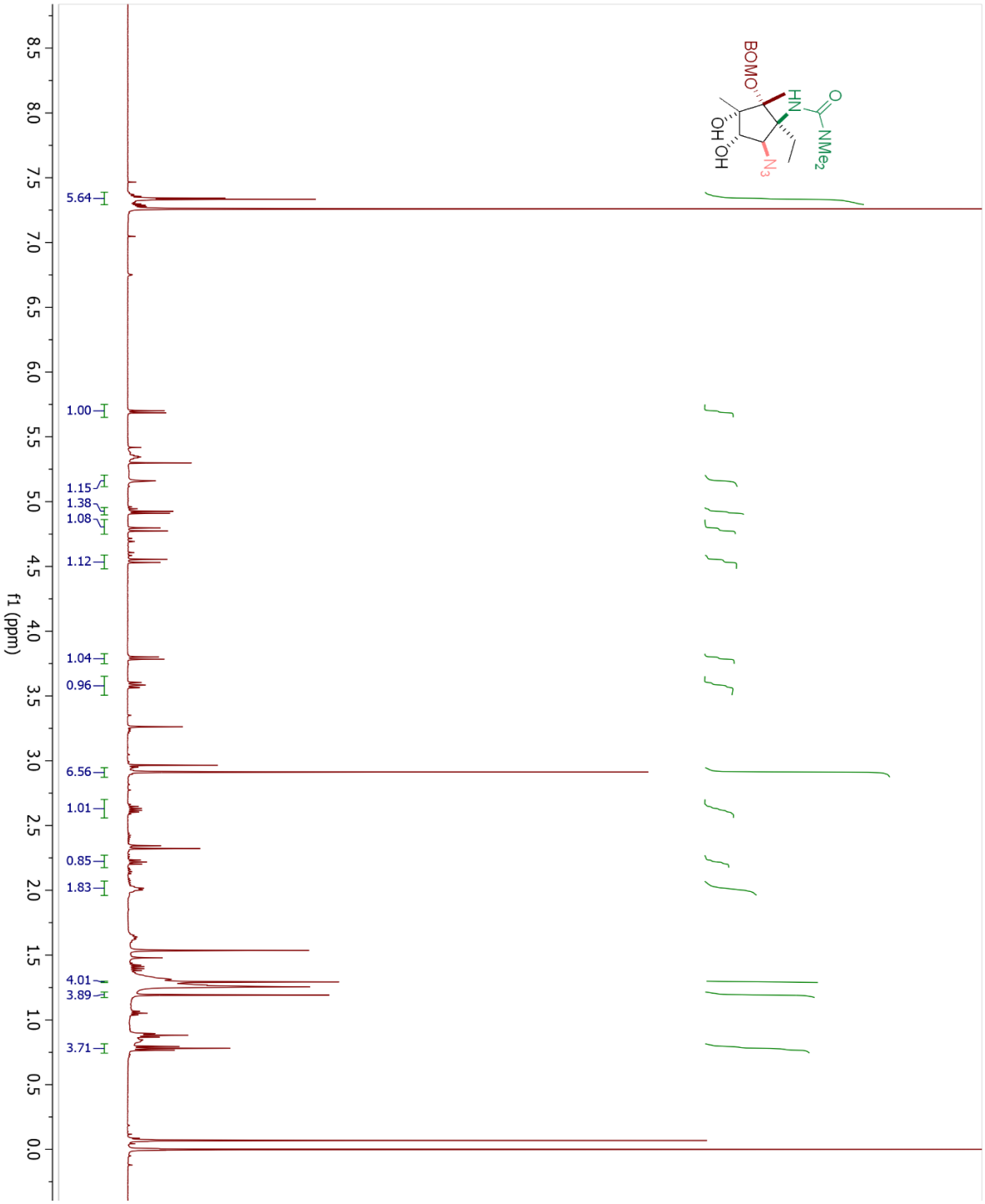
^{1}H NMR (500 MHz, $CDCl_3$) for compound **5.1**



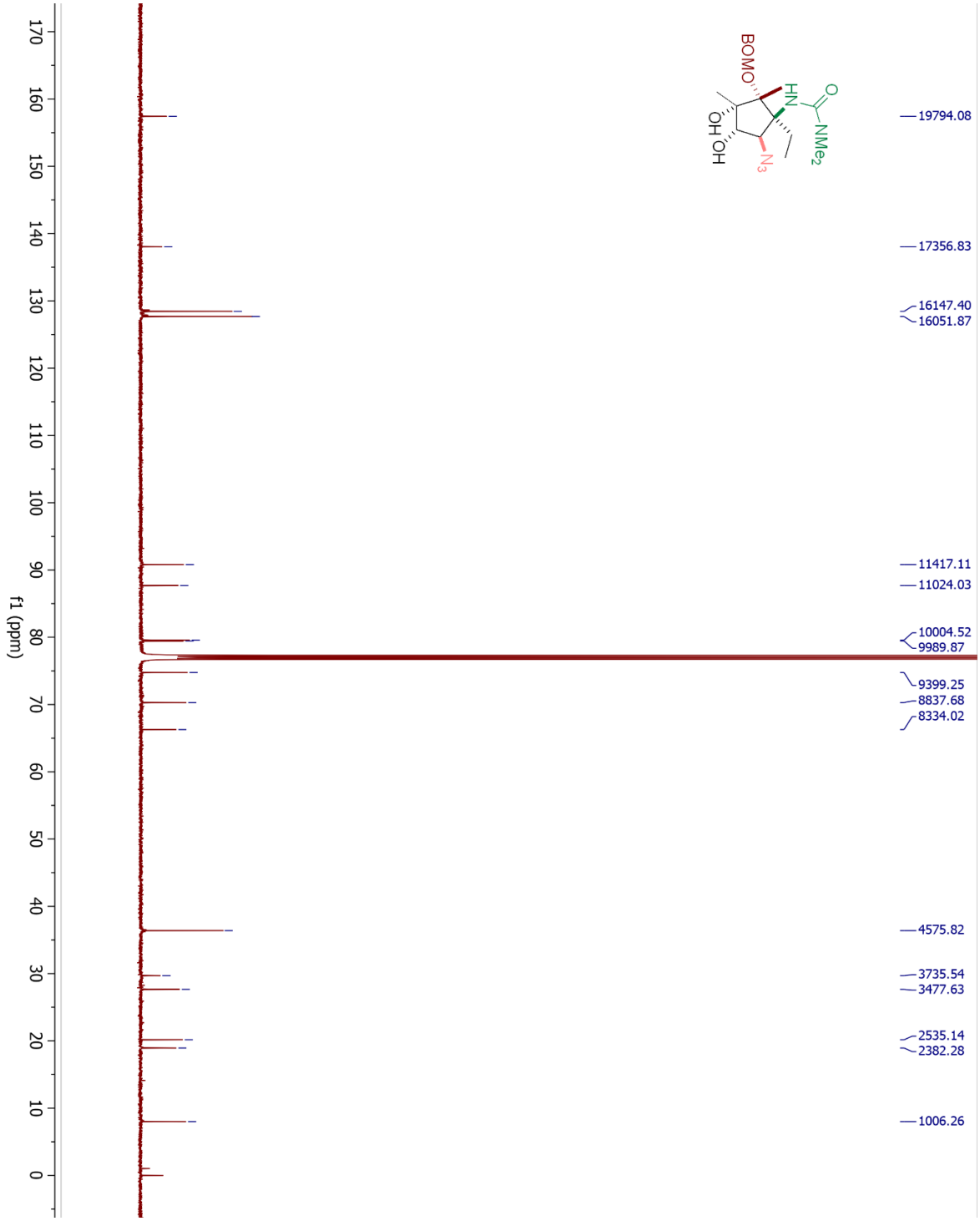
^{13}C NMR (126 MHz, $CDCl_3$) for compound **5.1**



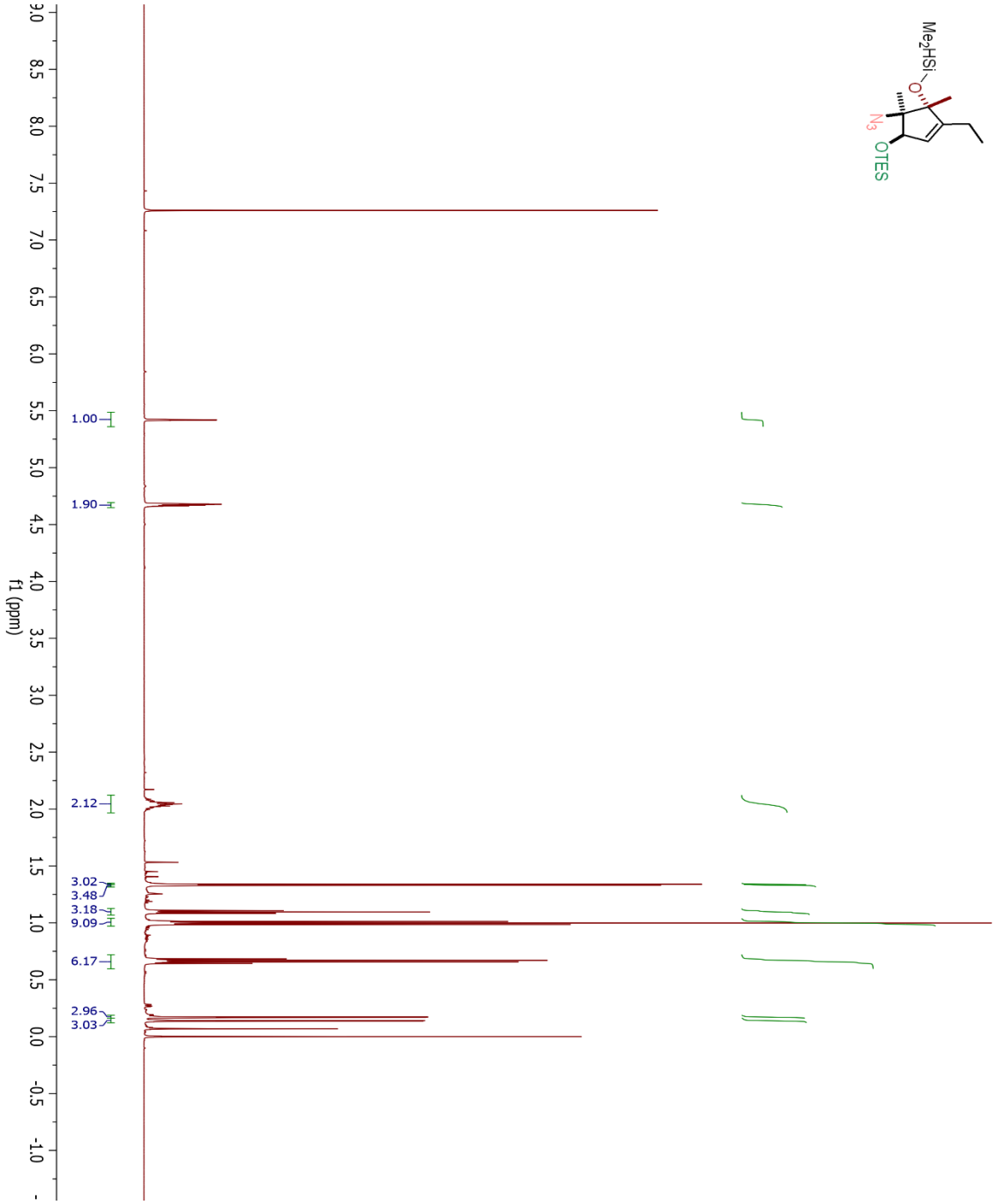
^{1}H NMR (500 MHz, $CDCl_3$) for compound **5.39**



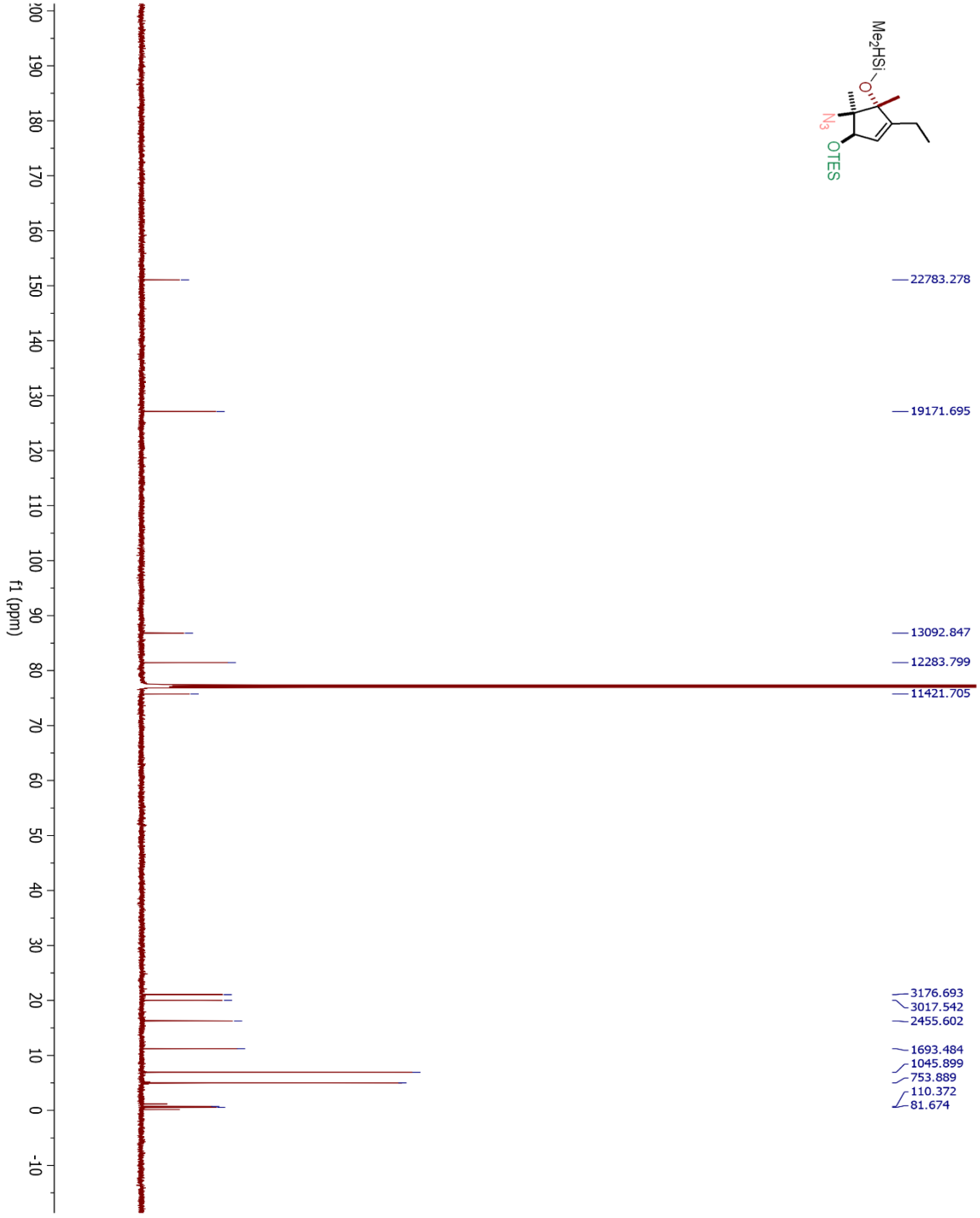
^{13}C NMR (126 MHz, $CDCl_3$) for compound **5.39**



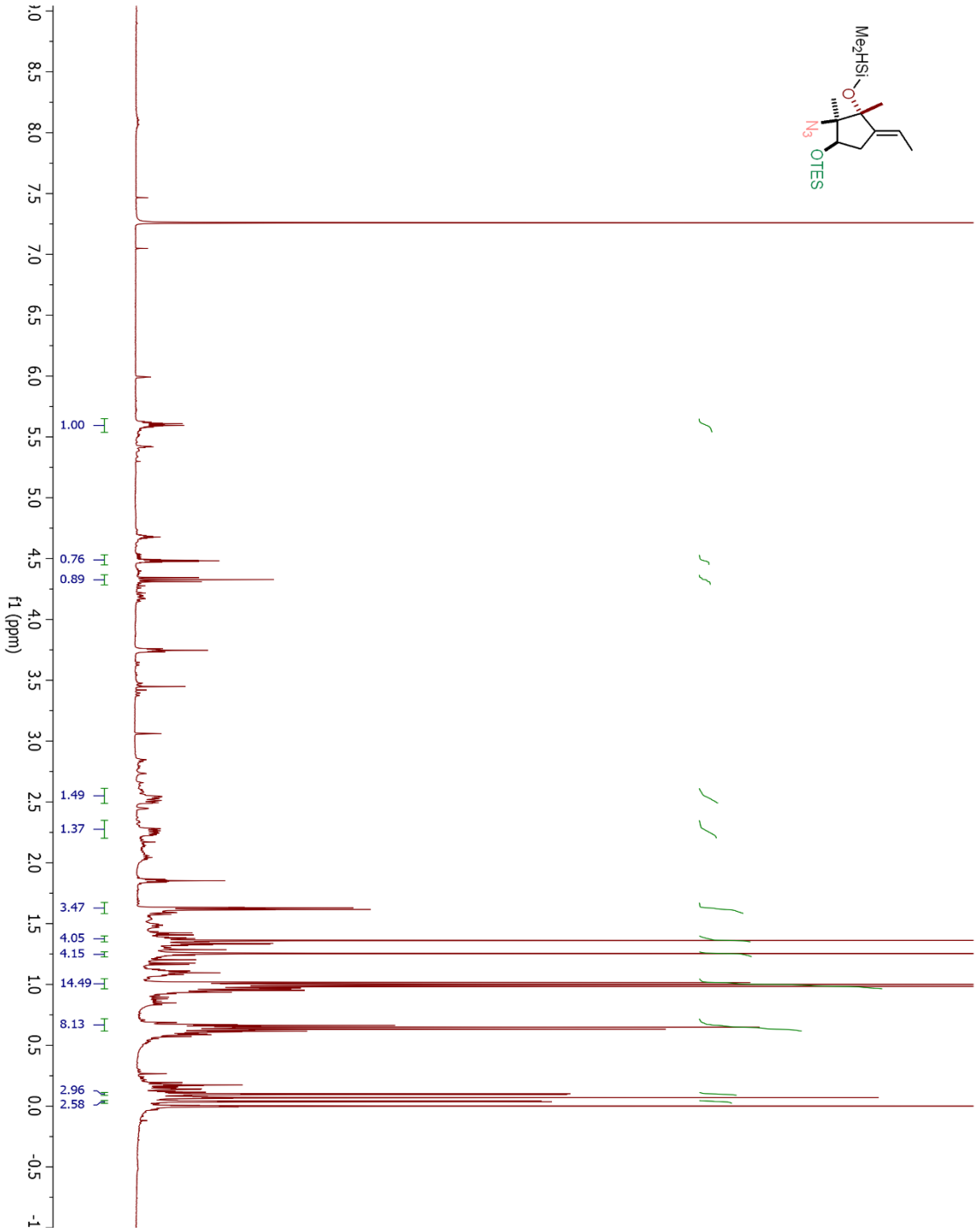
^{1}H NMR (600 MHz, $CDCl_3$) for compound **5.48**



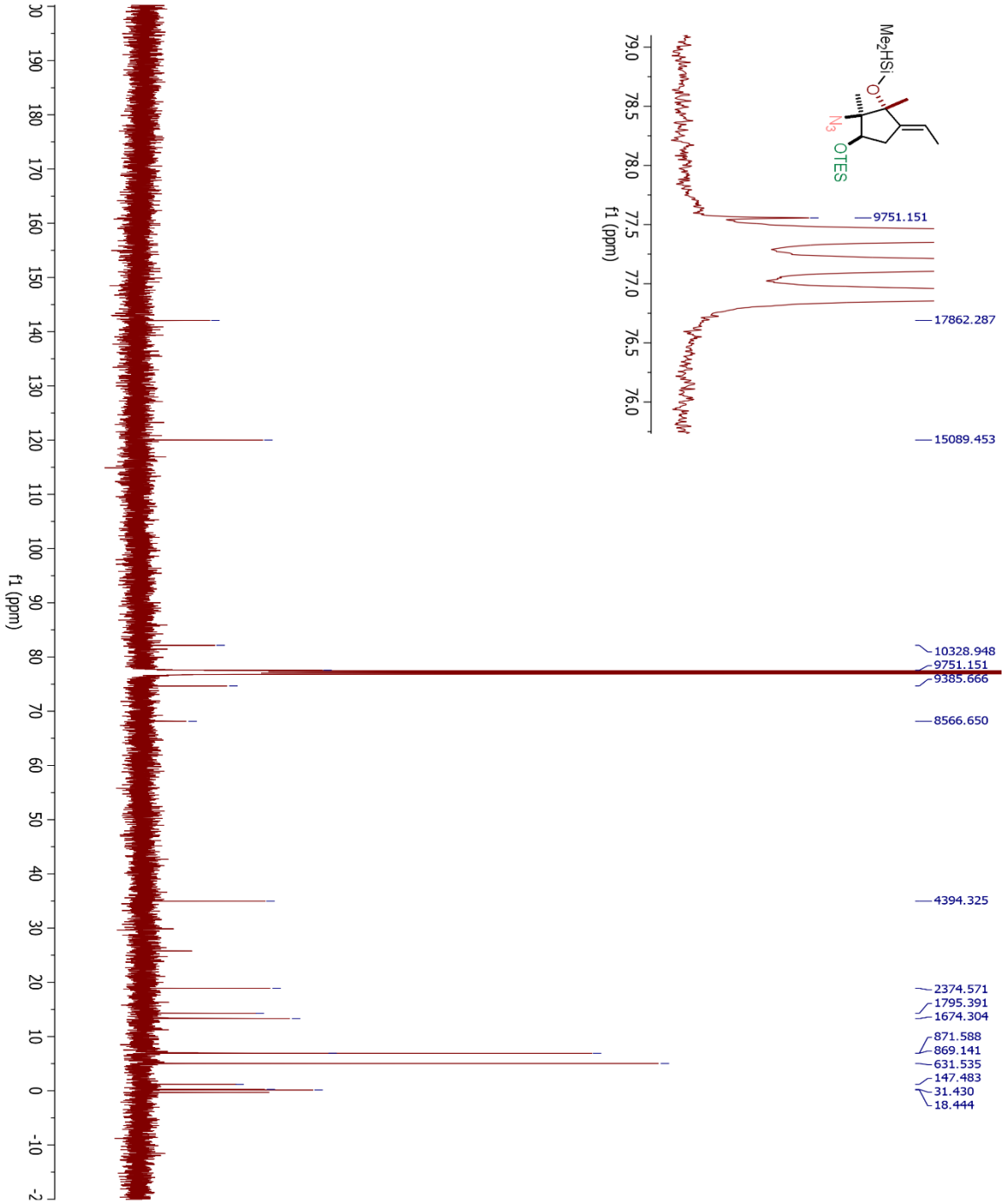
^{13}C NMR (151 MHz, $CDCl_3$) for compound **5.48**



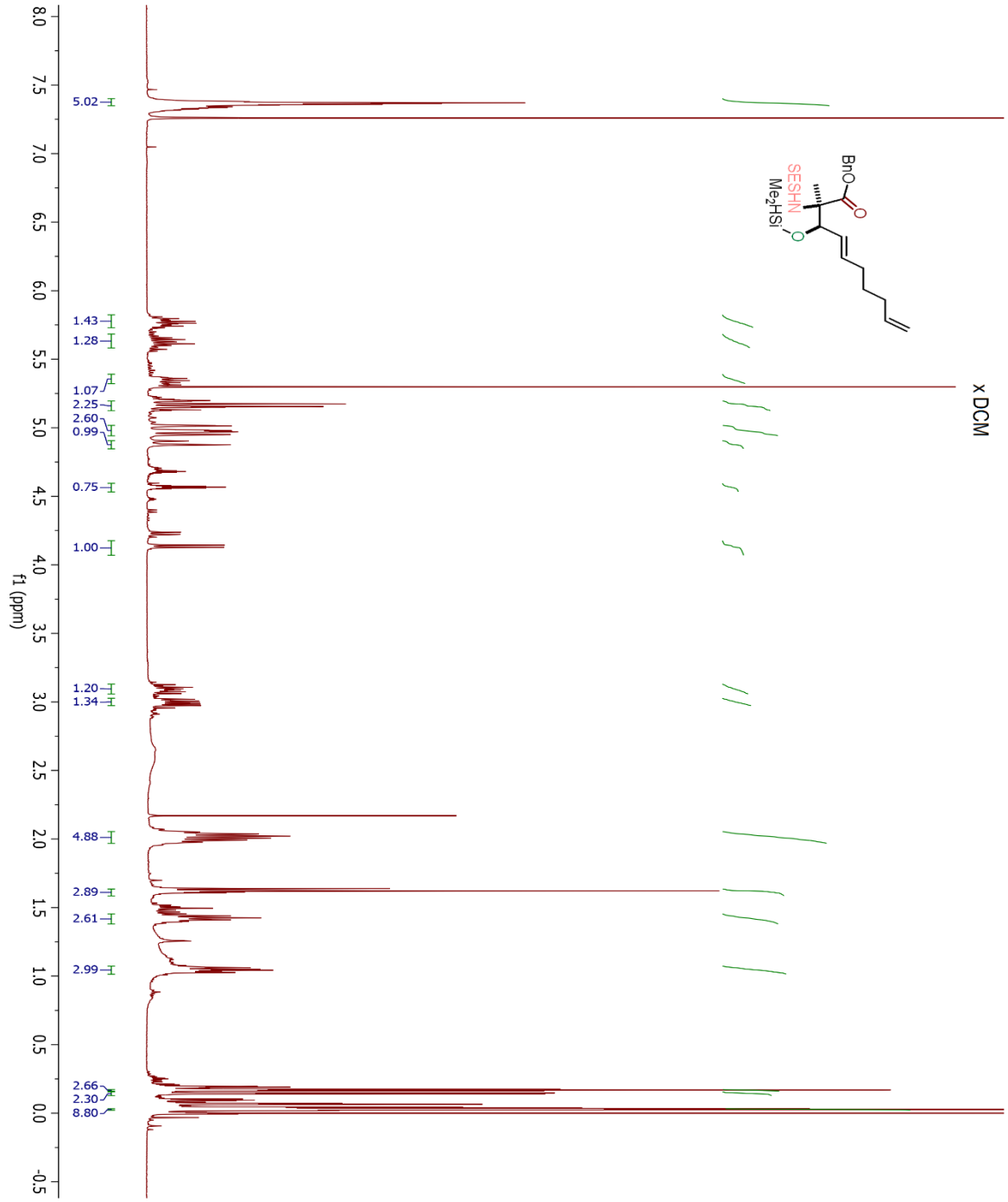
^{1}H NMR (500 MHz, $CDCl_3$) for compound **5.50**



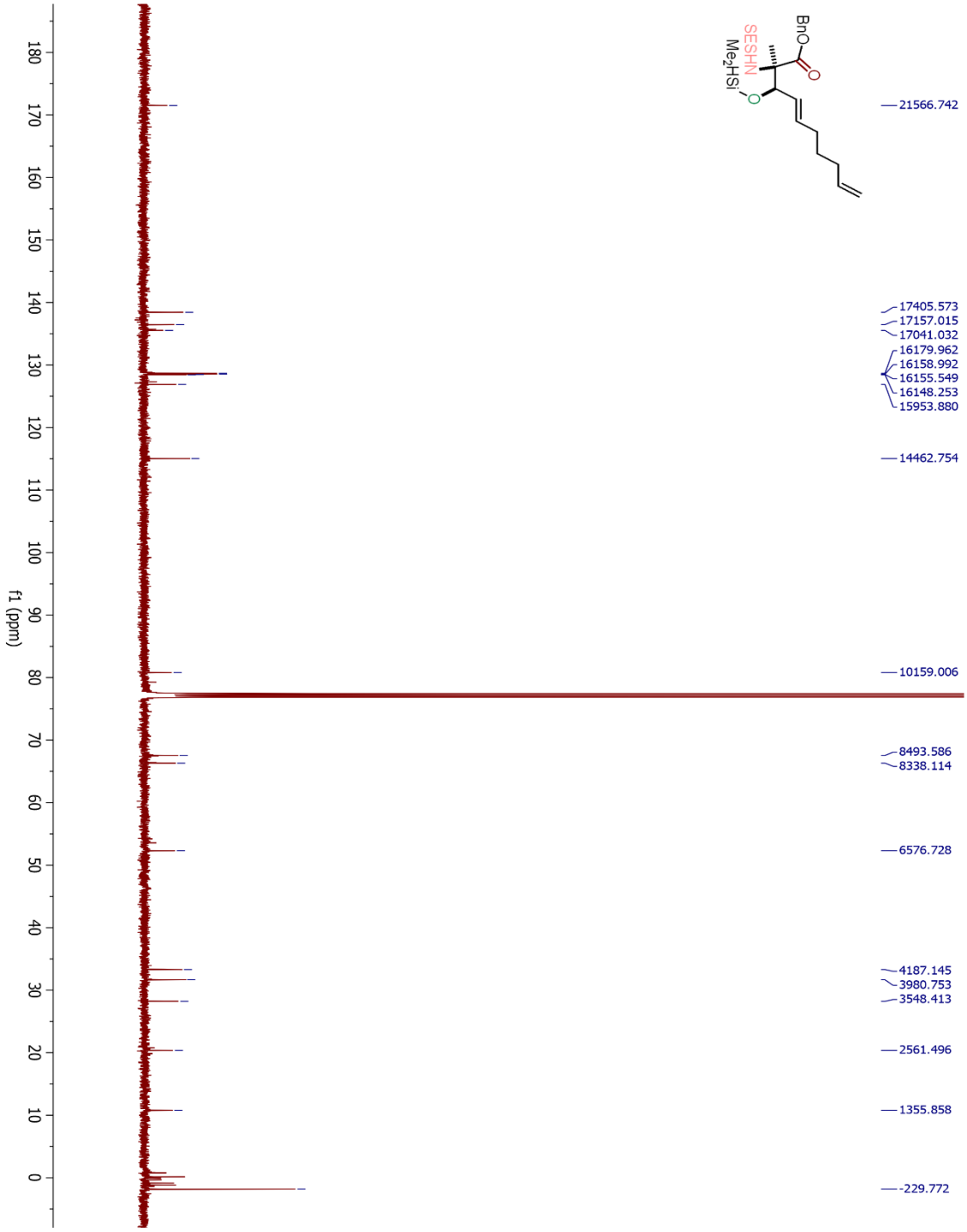
^{13}C NMR (126 MHz, $CDCl_3$) for compound **5.50**



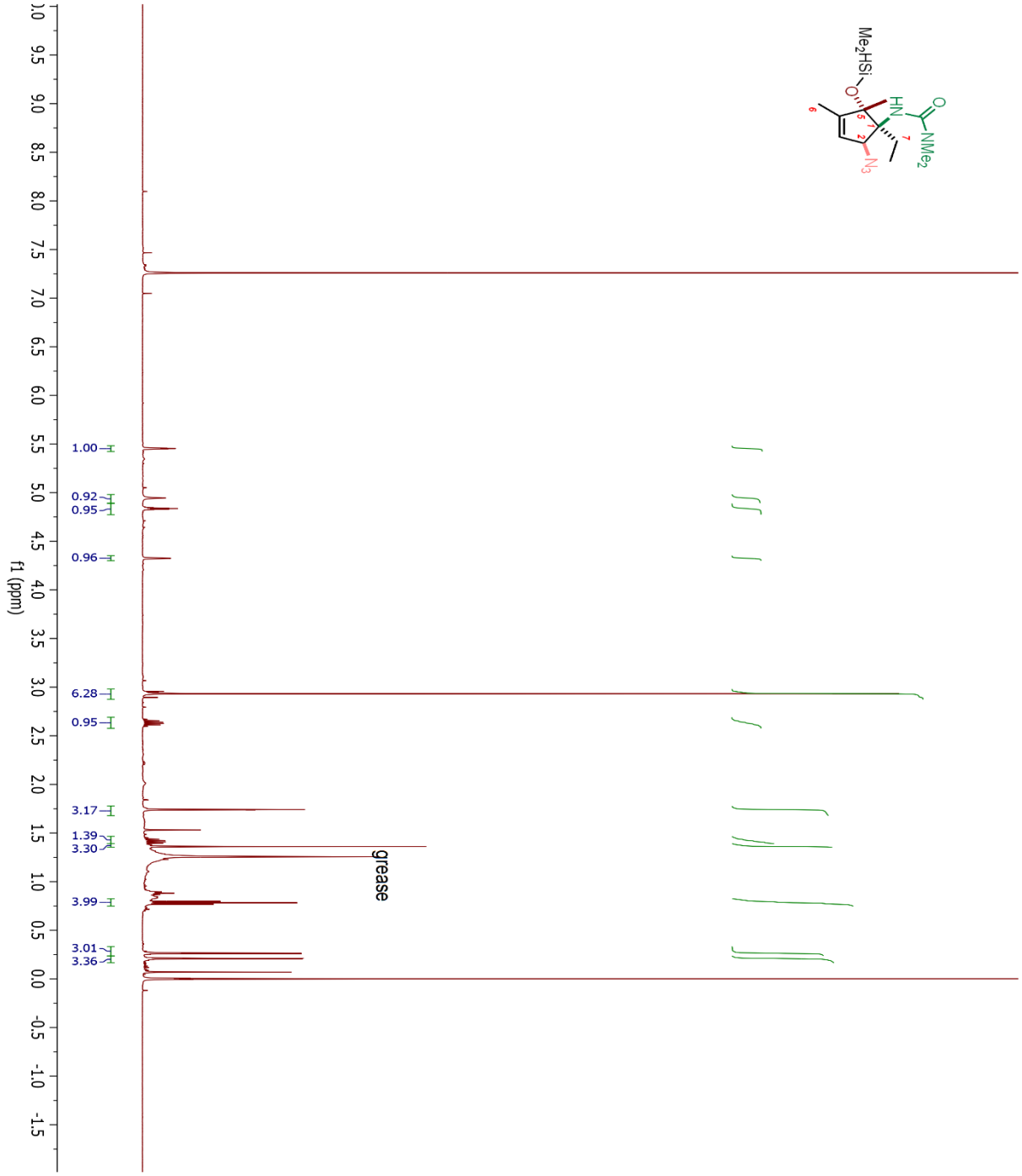
^{1}H NMR (500 MHz, $CDCl_3$) for compound **5.49**



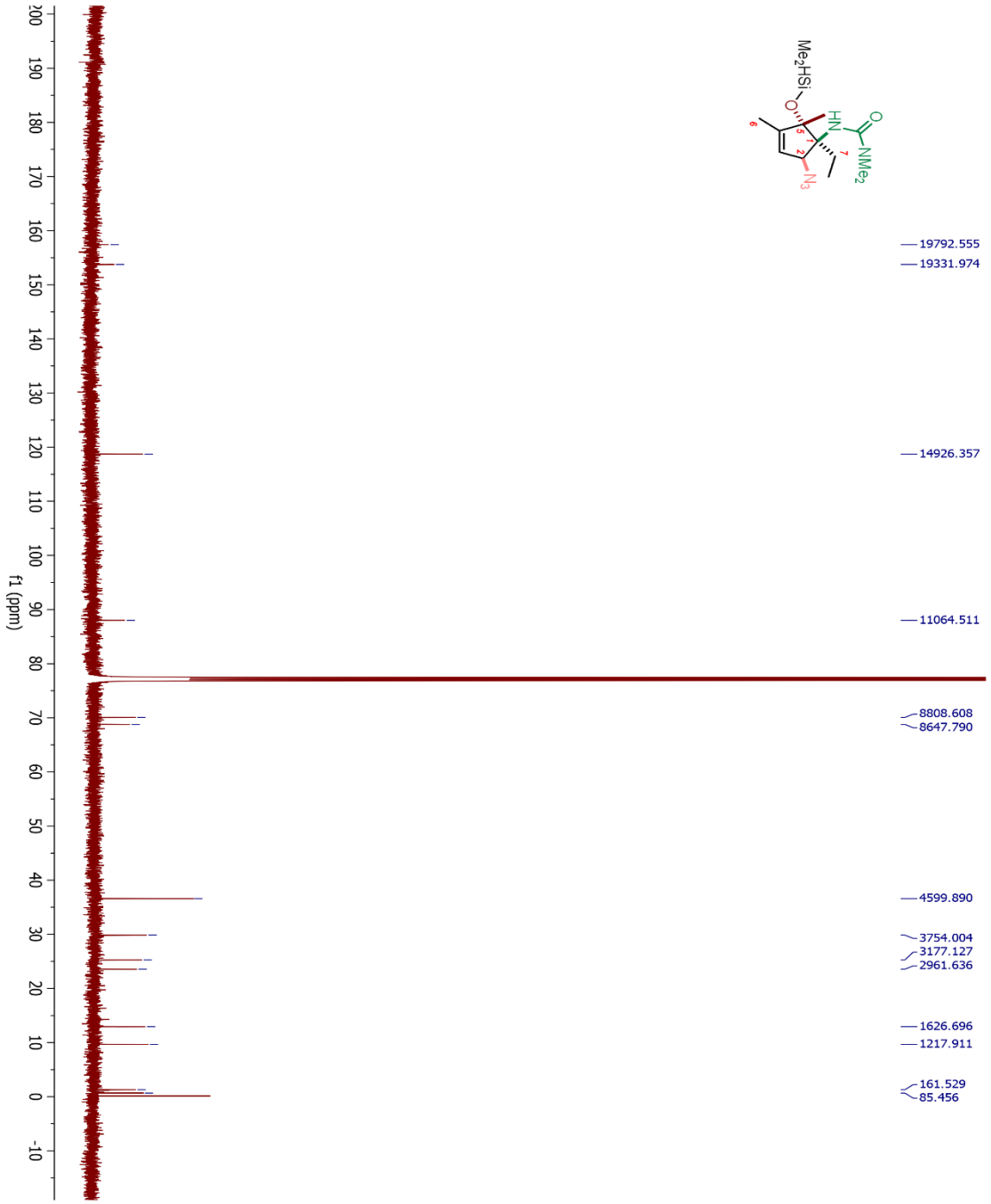
^{13}C NMR (126 MHz, $CDCl_3$) for compound **5.49**



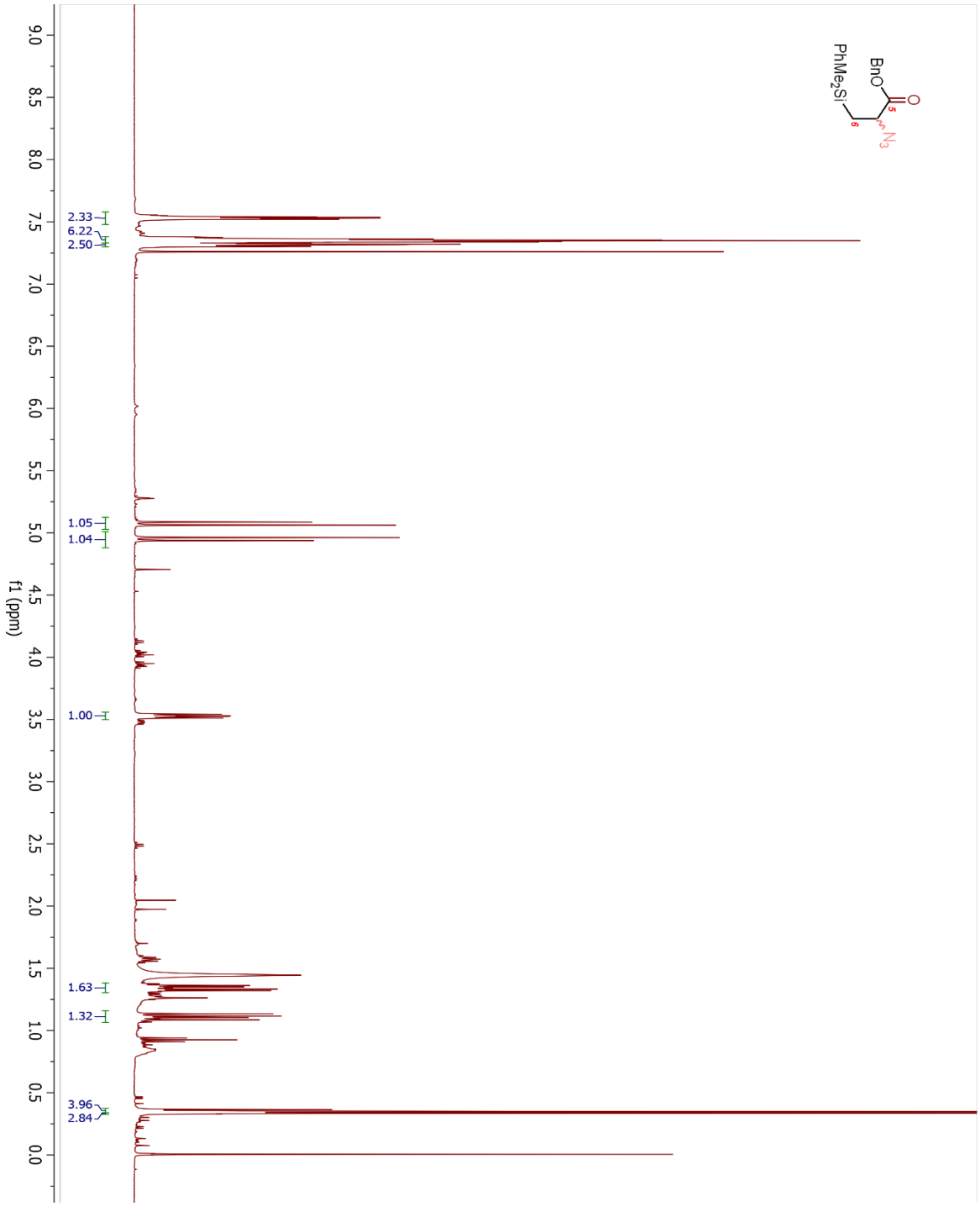
^{1}H NMR (500 MHz, $CDCl_3$) for compound **5.47**



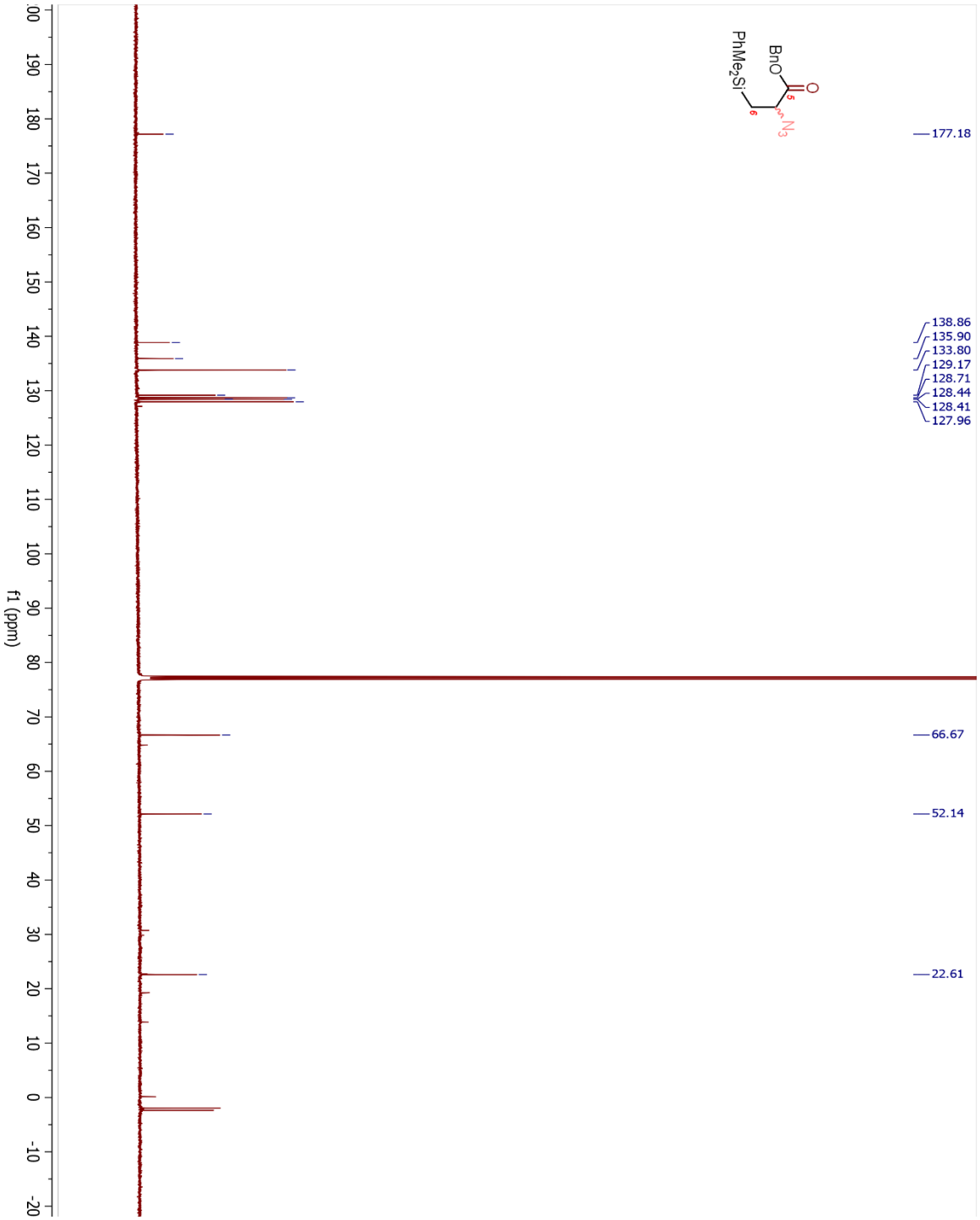
^{13}C NMR (126 MHz, $CDCl_3$) for compound **5.47**



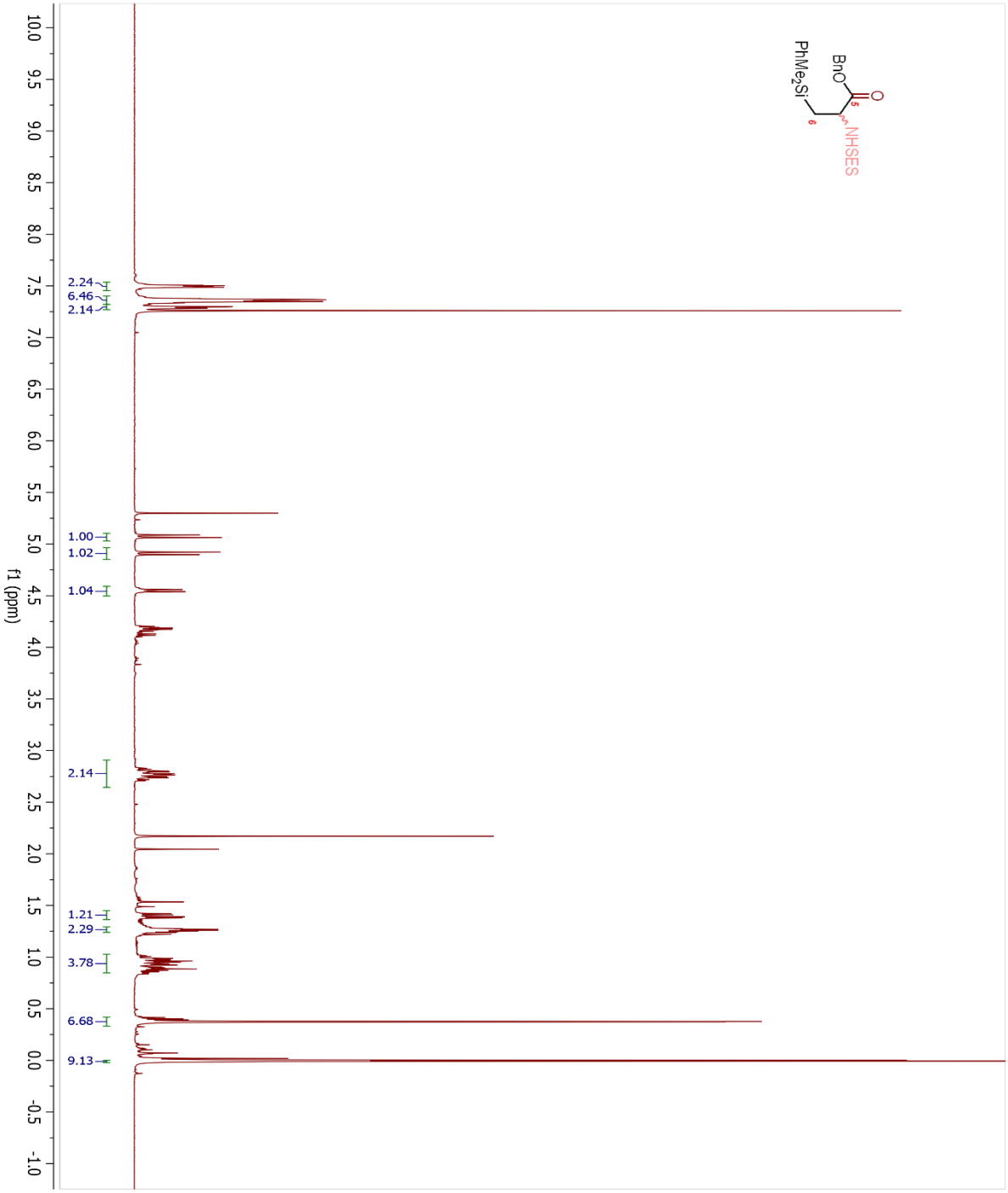
^{1}H NMR (500 MHz, $CDCl_3$) for compound **5.61**



^{13}C NMR (126 MHz, $CDCl_3$) for compound **5.61**



^{1}H NMR (500 MHz, $CDCl_3$) for compound **5.53**



^{13}C NMR (126 MHz, $CDCl_3$) for compound **5.53**

